The genetics of the sexually dimorphic deaths of the *C. elegans* CEM neurons

by

Hillel Tsvi Schwartz

B.S., Biochemistry
University of Washington, 1996

Submitted to the Department of Biology in Partial Fulfillment of the Requirements for the Degree of

DOCTOR OF PHILOSOPHY

at the
MASSACHUSETTS INSTITUTE OF TECHNOLOGY

August 2008

Signature of author_____
Hillel T. Schwartz
August 5, 2008

Certified By_____
H. Robert Horvitz
Professor of Biology
Thesis Supervisor

Accepted by_____
Stephen Bell
Chair of the Graduate Committee
Department of Biology

The genetics of the sexually dimorphic deaths of the *C. elegans* CEM neurons

by

Hillel Tsvi Schwartz

Submitted to the Department of Biology in Partial Fulfillment
of the Requirements for the Degree of DOCTOR OF PHILOSOPHY

The cells of metazoan organisms possess the capability to commit a form of cellular suicide known as programmed cell death or apoptosis. The proper control of this endogenous death program is essential to animal development and to the prevention of disease. To better understand how individual cells are developmentally specified to die, I studied the survival decision of a single cell type in the nematode *Caenorhabditis elegans*, the CEM neurons. The CEMs die during hermaphrodite embryogenesis and survive and function as sensory neurons in males. I identified 144 independent mutant strains in which the CEM neurons of hermaphrodites survive, including 52 mutants in known cell-death genes and 67 mutants generally defective sex determination. Another 29 screen isolates displayed a new defect of transcriptional derepression, the green pharynx phenotype. From these isolates and from additional screens, I defined a set of seven genes that function to prevent inappropriate gene expression.

From the isolates causing CEM survival I identified two new sex-determination proteins, the PLZF-like transcription factor TRA-4 and the F-box protein SEL-10; demonstrated that the neurogenesis genes *vab-3 Pax6* and *cnd-1 NeuroD* are required for aspects of the CEM fate, including CEM death, and likely function together in this process and in other aspects of *C. elegans* development, a cooperative relationship likely to be evolutionarily conserved; and identified the Bar family homeodomain transcription factor gene *ceh-30* as specifically promoting CEM survival.

The CEM neurons of males lacking *ceh-30* inappropriately undergo programmed cell death. In the CEMs of hermaphrodites, *ceh-30* is directly repressed by TRA-1, a transcription factor that acts as the last step in the sex-determination pathway to promote a hermaphrodite identity. The cell-protective function of *ceh-30* is specific to the CEM neurons, and *ceh-30* is expressed in and acts cell-autonomously in the CEMs to promote their survival. Expression of the mouse *ceh-30* homolog *Barhl1* can restore CEM survival to *ceh-30* mutants. In mice lacking *Barhl1*, as in *ceh-30* mutants, a specific class of sensory neuron is generated normally differentiates, but subsequently inappropriately undergoes apoptotic cell death.

Protection of the CEM neurons by *ceh-30* does not require CED-9, the sole member of the multidomain Bcl-2 family in *C. elegans*. By contrast, other regulators of the survival decisions of specific cells in *C. elegans* act through transcriptional control of the CED-9 inhibitor *egl-1*. Mammalian regulation of cell death is similarly almost entirely mediated through members of the multidomain Bcl-2 family. The evolutionarily conserved cell-protective function of *ceh-30* therefore probably defines a previously unknown mechanism capable of promoting cell survival both in nematode development, in the sensory neurons required for hearing in the mouse and likely in humans.

Thesis Advisor: H. Robert Horvitz
Title: Professor of Biology

Acknowledgments

It would be impossible to name every person who made important contributions to my thesis work, and still harder to thank every deserving person appropriately.

I would like to thank in particular those people with whom I have worked in close collaboration. It was a great privilege to work with Dawn Wendell for a summer. It was an enormous privilege, a tremendously rewarding experience, and truly a pleasure to work for an extended period of time with Johanna Varner. A longstanding scientific relationship with Barbara Conradt, involving both collaboration and competition and always collegiality and generosity, has been tremendously valuable to me. I would also like to thank members of the *C. elegans* research community who have provided me with important reagents and information, especially Maureen Barr and Susan Mango.

None of the work in this thesis would have been possible without the guidance, rigor, and dedication to following the biology that I have gotten from my advisor Bob Horvitz, or without the wonderful community that he has assembled in his laboratory. I would especially like to thank for their support, advice, and helpful criticism members of the cell death research group in the Horvitz lab, in particular Scott Cameron, Daniel Denning, Brendan Galvin, Mark Metzstein, Peter Reddien, Gillian Stanfield, and Zheng Zhou, and members of the synMuv research group, in particular Erik Andersen, Craig Ceol, Ewa Davison, and Adam Saffer. I have been fortunate to have excellent colleagues as my baymates in Ignaco Perez de la Cruz, Melissa Harrison, Long Ma, and Daniel Denning. I thank in particular those members of the Horvitz lab who were most helpful and inspirational to me when I was getting started, especially Scott Cameron, Mark Metzstein, Peter Reddien, Liz Speliotes, and Gillian Stanfield, and those lab members on whom I have most relied in recent years, in particular Erik Andersen, Daniel Denning, Brendan Galvin, and Niels Ringstad. I am indebted to Na An for help with strains to Nick Anisimov for his administrative help.

I cannot give enough thanks to my longtime housemates, classmates, and close friends Scott Boyd and Shilpa Joshi. The support and friendship of an excellent group of classmates has been invaluable to me, in particular Audrey Chang, Rebecca Landsberg, Janice Lee, Ryan McQuade, Sheila Menzies, and Elizabeth Reczek

I would never have begun this path without the introduction to and enthusiasm for to learning in general and science in particular that I received from both of my parents, and I could never have pursued it without the encouragement and support I received from my sister. This thesis is dedicated to my grandfather Robert Schwartz, who sadly passed away earlier this year.

Table of contents

Chapter I

Introduction

Cell-specific regulation of programmed cell death in the nematode *C. elegans*

Introduction to programmed cell death

Metazoan organisms exist as organized populations of differentiated cells, each contributing to, or at least not greatly diminishing, the survival of the greater organism. One important aspect of the lives of the cells that make up the larger metazoan organism is the deaths of some of those cells: cells are generated that make no contribution to the organism, and there are circumstances under which the continued survival of certain cells can be deleterious to the organism they inhabit. To ensure that cells die when they no longer serve a purpose or when their survival endangers the organism of which they are a part, cellular programs exist by which the cells can die efficiently and in a manner that minimizes consequences to the host organism. Improper regulation of these cell-death programs, causing the survival of cells that should have died or the deaths of cells that should survive, can impair animal development and health (VAUX and KORSMEYER 1999; LOCKSHIN and ZAKERI 2007).

Reproducible patterns of cell death in animal development were observed early in the modern study of biology, in tissue sculpting during amphibian and insect morphogenesis (reviewed by CLARKE and CLARKE 1996). This reproducible patterns of cell death was termed "programmed cell death" (LOCKSHIN and WILLIAMS 1965). Electron microscopic characterization of cell deaths led to the description of a process, termed 'apoptosis', characterized by contraction of cellular volume, chromatin condensation, and preservation of cytoplasmic organelle integrity (KERR *et al.* 1972). The apoptotic cell undergoes fragmentation into membrane-bounded fragments that rapidly undergo phagocytosis by adjacent cells. This rapid removal of intact cellular fragments of

apoptotic cells has been proposed to prevent an inflammatory response (SAVILL and HASLETT 1995).

Many important discoveries in the field of programmed cell death originated in studies in the nematode *C. elegans*. *C. elegans* offers a powerful platform for experimental genetics: the animals are optically transparent throughout development, permitting the direct observation of cell divisions and cell deaths in the developing animal; *C. elegans* has an invariant somatic cell lineage in which each cell has a described cell fate; and *C. elegans* exist as males and self-fertilizing hermaphrodites that are each capable of generating more than 300 self-progeny, with a three-day generation time (BRENNER 1974; SULSTON 1976; SULSTON and HORVITZ 1977; KIMBLE and HIRSH 1979; SULSTON *et al.* 1983). Examination of the developing ventral nerve cord of *C. elegans* revealed that some cells were generated only to rapidly undergo programmed cell death; lineal equivalents of the same cells at other positions along the anterior-posterior axis survived, leading to the hypothesis that the cell-death fate was used to prune cells the functions of which were not required at a given location (SULSTON 1976).The programmed deaths that occur in the ventral nerve cord of *C. elegans* have ultrastructural characteristics similar to those seen in apoptotic cell death (ROBERTSON and THOMPSON 1982). Determination of the complete somatic cell lineage of *C. elegans* showed that, as part of an invariant pattern of cell divisions, a completely reproducible pattern of somatic cell deaths was observed: of 1090 cells generated in the hermaphrodite, precisely 131 undergo programmed cell death; another 21 cells die in male development that either do not die in hermaphrodite development or are never generated in the hermaphrodite (SULSTON and HORVITZ 1977; KIMBLE and

HIRSH 1979; SULSTON *et al.* 1980; SULSTON *et al.* 1983). This process, in which specific cells are determined by their lineal identity to undergo programmed cell death, after which they are engulfed and degraded by their neighbors, is presented diagrammatically in Figure 1A. The germ cell lineages of *C. elegans* are not invariant, and the germ cells, unlike somatic cells, undergo cell death that cannot be predicted from lineal identity, subject to both stochastic and checkpoint controls (reviewed by STERGIOU and HENGARTNER 2004).

In this Introduction I describe advances in our understanding of the means by which cell identity is coupled to the regulation of cell survival in *C. elegans* and discuss the implications of these findings for our understanding of apoptotic cell death in mammalian development and disease.

Apoptosis is an evolutionarily conserved program of cellular suicide

The gene *ced-3* (*ced*, cell death abnormal) was first identified through mutations that caused the disappearance of persistent cell corpses normally seen in *ced-1* mutant animals defective in the engulfment and removal of dying cells (ELLIS and HORVITZ 1986). In animals lacking *ced-3* function, cells that normally die instead survive and differentiate; as loss of *ced-3* function prevents cells from dying, the cells do not become persistent corpses in *ced-1* mutant animals (ELLIS and HORVITZ 1986). A second gene, *ced-4*, was similarly found to be required for programmed cell death (ELLIS and HORVITZ 1986). The *ced-3* and *ced-4* mutants demonstrated for the first time that genes existed the primary purpose of which was to cause cell death (HORVITZ 2003). The existence of such mutants settled a long-standing question by

demonstrating that cells undergoing programmed cell death were not simply failing to survive; rather, animals possess a genetic program to actively promote programmed cell death. *ced-3* and *ced-4* were shown to act within the dying cells, in a form of cellular suicide (YUAN and HORVITZ 1990).

The first molecularly identified gene shown to regulate apoptotic cell death was the human oncogene *Bcl-2* (MCDONNELL *et al.* 1989; HOCKENBERY *et al.* 1990). Bcl-2 is the founding member of a family of proteins conserved from nematodes to humans. Bcl-2 family members possess one or more of four *Bcl-2* homology domains (BH1, BH2, BH3 and BH4 domains) (reviewed by MERRY and KORSMEYER 1997). *Bcl-2* is subject to translocations that cause it to be overexpressed in B cells, leading to follicular leukemia (TSUJIMOTO *et al.* 1984). Overexpression of *Bcl-2* was found to be a potent inhibitor of apoptotic cell death (VAUX *et al.* 1988; MCDONNELL *et al.* 1989; HOCKENBERY *et al.* 1990). Transgenic overexpression of *Bcl-2* was similarly shown to reduce the number of programmed cell deaths in the nematode *C. elegans* (VAUX *et al.* 1992); this reduction in the number of cell deaths was caused by the survival of cells that in the wild type undergo programmed cell death (HENGARTNER and HORVITZ 1994b). Bcl-2 was therefore demonstrated to promote cell survival by a mechanism evolutionarily conserved between humans and nematodes.

Genetic studies of *C. elegans* identified a gain-of-function mutation defining the gene *ced-9*. Increased *ced-9* function causes the survival of cells normally programmed to die (HENGARTNER *et al.* 1992). Loss-of-function (lf) mutations in *ced-9* have the opposite effect: they cause the inappropriate activation of cell death in cells normally programmed to survive, resulting in lethality (HENGARTNER *et al.* 1992). All defects

associated with loss of *ced-9* function are prevented when programmed cell death is blocked by loss-of-function mutations in *ced-3* or in *ced-4*, demonstrating that *ced-9* acts as an upstream negative regulator of the cellular suicide program (HENGARTNER *et al.* 1992). Molecular identification of *ced-9* showed it to encode the *C. elegans* homolog of the human cell-protective oncogene *Bcl-2* (HENGARTNER and HORVITZ 1994b). Bcl-2 can be substituted for CED-9 in animals lacking *ced-9* function (HENGARTNER and HORVITZ 1994b).

ced-3 encodes a a cysteine protease that cleaves after aspartate, a member of the family of proteins now named caspases (YUAN *et al.* 1993; ALNEMRI *et al.* 1996; XUE *et al.* 1996). The identification of the CED-3 caspase as a critical effector of programmed cell death provided the first molecular mechanism of programmed cell death and prompted the discovery that mammalian caspases perform similar functions in apoptosis (MIURA *et al.* 1993; HORVITZ 2003). Caspase activation is now considered a defining feature of apoptotic cell death (THORNBERRY and LAZEBNIK 1998; NICHOLSON 1999). *ced-4* encodes an adaptor protein that promotes the activity of the CED-3 procaspase in cell-killing in *C. elegans*, when expressed in mammalian cells and *in vitro* (YUAN and HORVITZ 1992; SHAHAM and HORVITZ 1996; CHINNAIYAN *et al.* 1997a; CHINNAIYAN *et al.* 1997b; WU *et al.* 1997; YANG *et al.* 1998). Biochemical reconstitution of the cell-death process in lysates from human HeLa cells identified a counterpart of CED-4, called Apaf-1, that promotes the activation of Caspase 9 (ZOU *et al.* 1997). The antiapoptotic protein CED-9 binds CED-4 and CED-9 inhibits the ability of CED-4 to promote CED-3 activation *in vivo* (SHAHAM and HORVITZ 1996; CHINNAIYAN *et al.* 1997b; SPECTOR *et al.* 1997).

The remaining member of the evolutionarily conserved core pathway for the execution of programmed cell death is the BH3-only protein EGL-1 (CONRADT and HORVITZ 1998). Like *ced-3* and *ced-4*, *egl-1* function is required for essentially all somatic cell deaths in *C. elegans*. Unlike *ced-3* and *ced-4*, *egl-1* acts upstream of *ced-9*: loss of *egl-1* function has no protective effect against programmed cell death in animals lacking *ced-9* function (CONRADT and HORVITZ 1998). Mammalian BH3 proteins, the counterparts of EGL-1, similarly act as upstream inhibitors of the protective functions of members of the multidomain Bcl-2 family (reviewed by WILLIS and ADAMS 2005). EGL-1 is one of two BH3-only proteins known to function in apoptotic cell death in *C. elegans*; the other, CED-13, has been found to function only in the *C. elegans* germline (SCHUMACHER *et al.* 2005). EGL-1 binds CED-9 and disrupts the CED-9-CED-4 interaction (CONRADT and HORVITZ 1998; DEL PESO *et al.* 1998). This core pathway, in which EGL-1 acts to release CED-4 from inhibition by CED-9, whereupon CED-4 promotes CED-3 activation, has been reconstituted *in vitro* using recombinant proteins (YAN *et al.* 2004). The evolutionarily conserved core genetic pathway for the execution of programmed cell death is presented in Figure 1B.

Cell-killing mechanisms supplement the core cell-death execution pathway to achieve a wild-type pattern of programmed cell death in *C. elegans*

In addition to the core pathway for the execution of programmed cell death, a number of genes and cellular processes have been identified that promote programmed cell death in *C. elegans*. These additional activities that promote programmed cell death include the killing function of the bifunctional cell-death regulator *ced-9 Bcl-2*

(HENGARTNER and HORVITZ 1994a), the timing factor *ced-8* (STANFIELD and HORVITZ 2000), the death-promoting activity provided by engulfment of dying cells (HOEPPNER *et al.* 2001; REDDIEN *et al.* 2001), and the killing function provided by a subset of the synthetic multivulva (synMuv) genes (REDDIEN *et al.* 2007). The latter three cell-killing activities are all independent of the Bcl-2 homolog CED-9 and all four are independent of the BH3-only protein EGL-1, which acts upstream of *ced-9* to induce programmed cell death.

Cell-specific regulation of which cells survive could be achieved by regulation of the core pathway for the execution of programmed cell death. Each of these cell-killing functions that supplements the core cell-death-execution pathway offers an additional mechanism for the cell-specific regulation of programmed cell death, other than regulation of the core pathway for the execution of programmed cell death. A central role for one of these additional death-promoting activities in the control of a specific programmed cell death has already been shown for one cell type: mutations that block the engulfment and removal of dying cells by their surviving neighbors cause the survival of both the B.alapaav and B.arapaav cells; normally one member of this pair of cells dies in the development of the *C. elegans* male (SULSTON *et al.* 1980; HEDGECOCK *et al.* 1983). Mutations that block the engulfment of cell corpses can also cause the infrequent survival of ventral cord neurons normally fated to die in the *C. elegans* hermaphrodite (REDDIEN *et al.* 2001).

Regulation of programmed cell death in insects and in vertebrates

In vertebrates, most regulation of apoptotic cell death is transduced through members of the Bcl-2 superfamily. The Bcl-2 superfamily includes pro-survival proteins that contain all four Bcl-2 homology domains; pro-apoptotic proteins that contain the BH1, BH2, and BH3 Bcl-2 homology domains; and the pro-apoptotic BH3-only proteins. The BH3-only proteins promote apoptosis by interaction with multidomain Bcl-2 family members (WANG *et al.* 1996; SATTLER *et al.* 1997). The cell-killing BH3-only proteins of vertebrates are controlled by transcriptional activation, by post-transcriptional modification, and by localization (reviewed by PUTHALAKATH and STRASSER 2002; DANIAL 2007). The human transcription factor p53 has been shown both to activate the transcription of the BH3-only genes *PUMA* and *Noxa* and to directly bind the multidomain Bcl-2 family members Bcl-2 and Bcl-X_L and inhibit their protective functions (ODA *et al.* 2000; NAKANO and VOUSDEN 2001; YU *et al.* 2001; MIHARA *et al.* 2003; CHIPUK *et al.* 2004). The BH3-only protein EGL-1 fills a similar function in the core pathway for the execution of programmed cell death in *C. elegans*.

The multidomain Bcl-2 family members of vertebrates are regulated transcriptionally (GRUMONT *et al.* 1999; MAYO and BALDWIN 2000; CORY and ADAMS 2002) and by post-translational modification (CHANG *et al.* 1997; CHENG *et al.* 1997; YAMAMOTO *et al.* 1999). Although there is no clear evidence for similar regulation of programmed cell death in the *C. elegans* soma, transcriptional and post-translational control of the multidomain Bcl-2 family member CED-9 has been reported in controlling the survival of cells in the *C. elegans* germline. The *Rb* homolog *lin-35* promotes germline cell death by repressing *ced-9* expression and is required for radiation-induced cell death in the *C. elegans* germline (SCHERTEL and CONRADT 2007). The Pax

transcription factor genes *pax-2* and *egl-38* promote Bcl-2 expression and cell survival in the *C. elegans* germline (PARK *et al.* 2006). A Ras/MAPK signaling pathway promotes stochastic cell death in the *C. elegans* germline that is independent of the two BH3-only proteins known to function in *C. elegans* germline cell death but is inhibited by the Bcl-2 homolog CED-9, suggesting that phosphrylation of CED-9 or an unidentified regulator of CED-9 may control cell survival in the *C. elegans* germline (GUMIENNY *et al.* 1999; SCHUMACHER *et al.* 2005).

Another regulatory mechanism, one that does not act through the Bcl-2 superfamily, is the most prominent and extensively characterized death regulatory mechanism not found in *C. elegans*: regulation of apoptosis by the IAP (Inhibitor of Apoptosis) proteins and their inhibitors the IBM (IAP-Binding Motif) proteins (reviewed by YAN and SHI 2005; STELLER 2008). IAP proteins bind to caspases and either inhibit their activity or target them for degradation (SHI 2004). The *Drosophila* IAP gene *DIAP1* is required to prevent lethality caused by ectopic activation of apoptotic caspases (HAY *et al.* 1995; WANG *et al.* 1999). The mammalian IAP proteins XIAP, cIAP1 and cIAP2 block caspase activity *in vitro* and when overexpressed (DEVERAUX *et al.* 1997; ROY *et al.* 1997). The *C. elegans* genome encodes two IAP proteins. Loss-of-function mutations and overexpression of the two *C. elegans* IAP proteins have no demonstrated effect on programmed cell death (SPELIOTES 2000).

IBM proteins are activators of apoptosis that bind directly to the IAP proteins to release caspases from inhibition (reviewed by SHI 2002). The *Drosophila* IBM proteins Hid, Grim, Reaper and Sickle are required for essentially all programmed cell death during *Drosophila* development (reviewed by STELLER 2008). The *Drosophila* IBM

proteins are subject to transcriptional and post-translational control in development and in response to cellular injury (BERGMANN *et al.* 1998; BRODSKY *et al.* 2000; JIANG *et al.* 2000; LOHMANN *et al.* 2002). The mammalian IBM proteins Smac/DIABLO and Omi/HtrA2 promote caspase activation by relieving inhibition by IAP proteins *in vitro* (DU *et al.* 2000; VERHAGEN *et al.* 2000; MARTINS *et al.* 2002; VERHAGEN *et al.* 2002). Studies of knockout mice suggest that members of the Bcl-2 superfamily are critical regulators of apoptotic cell death in mammalian development (MOTOYAMA *et al.* 1995; LINDSTEN *et al.* 2000; WEI *et al.* 2001) but that the IAP and IBM proteins play only minor roles as regulators of apoptotic cell death in mice (HARLIN *et al.* 2001; OKADA *et al.* 2002; JONES *et al.* 2003; POTTS *et al.* 2003; MARTINS *et al.* 2004; CONZE *et al.* 2005; CONTE *et al.* 2006). By contrast, the IAP and IBM proteins of *Drosophila* are required for essentially all apoptosis (WHITE *et al.* 1994; STELLER 2008), but Bcl-2 superfamily members play only minor roles in the regulation of apoptosis in *Drosophila* (SEVRIOUKOV *et al.* 2007). Another mammalian protein, ARTS, similarly acts as an inhibitor of IAP proteins, despite its lacking an IBM motif (LARISCH *et al.* 2000; GOTTFRIED *et al.* 2004). ARTS is frequently lost in cancer (ELHASID *et al.* 2004) and mice with reduced *ARTS* function show upregulation of IAPs and a predisposition to lymphoma (KISSEL *et al.* 2005). There are no known *C. elegans* homologs of the IBM proteins or ARTS.

Cell-specific regulation of non-apoptotic deaths in *C. elegans*

In addition to the apoptotic deaths of cells that normally die in *C. elegans* development, a number of cell deaths that occur only in mutant animals and one specific cell death that occurs in wild-type development have been shown to be

genetically and morphologically distinguishable from normal programmed cell deaths. Many of the non-apoptotic cell deaths that have been described occur only in specific cells, reflecting either cell-specific expression of a toxic gene product or that different cells are differentially sensitive to the activation of these non-apoptotic cell-death programs. Gain-of-function mutations causing channel hyperactivation in neurons can cause those cells to die in a process that has been proposed to be a *C. elegans* model of necrosis or excitotoxicity (DRISCOLL and CHALFIE 1991; SHREFFLER *et al.* 1995; TREININ and CHALFIE 1995; BIANCHI *et al.* 2004). Cell death that occurs by this necrotic mechanism is not affected by loss-of-function mutations of *egl-1*, *ced-4* or *ced-3* or by a gain-of-function mutation of *ced-9*, mutations that prevent essentially all apoptotic cell deaths (CHUNG *et al.* 2000). Mutations in the genes *lin-24*, *lin-33* and *pvl-5* cause the inappropriate deaths of the Pn.p hypodermal blast cells (FERGUSON and HORVITZ 1985; FERGUSON *et al.* 1987; JOSHI and EISENMANN 2004; GALVIN *et al.* 2008). The deaths of the Pn.p cells in these mutants are characterized by morphological changes distinct both from programmed cell deaths and from the neuronal deaths caused by channel hyperactivation (SULSTON and HORVITZ 1977; CHALFIE and SULSTON 1981; GALVIN *et al.* 2008). In a critical difference from apoptotic cell deaths, the deaths of the Pn.p hypodermal blast cells in *pvl-5*, *lin-24*, and *lin-33* mutants are insensitive to loss of function of either of the core cell-killing genes *egl-1* or *ced-4* (JOSHI and EISENMANN 2004; GALVIN *et al.* 2008). Unlike the Pn.p cell deaths of *lin-24* or *lin-33* mutants, the Pn.p cell deaths of *pvl-5* mutants are strongly suppressed by increased *ced-9* function and by loss of *ced-3* function, suggesting that the similar Pn.p death phenotypes of

these mutants may reflect different underlying cell-death mechanisms (JOSHI and EISENMANN 2004; GALVIN *et al.* 2008).

One atypical non-apoptotic cell death has been described that takes place in wild-type *C. elegans* development, the death of the linker cell in male development. Unlike the nonapoptotic cell deaths that have been described as occurring in *C. elegans* mutants, the linker cell dies in wild-type development. The linker cell is specifically generated in male *C. elegans*. The linker cell is part of the somatic gonad, and during larval development the linker cell migrates to lead the extension of the developing gonad. After completing its migration, the linker cell dies in adult *C. elegans* males (KIMBLE and HIRSH 1979; SULSTON *et al.* 1980). The death of the linker cell is not significantly prevented by mutations causing complete loss of *egl-1*, *ced-4* or *ced-3* function or by a mutation causing increased *ced-9* function, mutations that prevent essentially all other somatic cell deaths in *C. elegans* (ABRAHAM *et al.* 2007). The dying linker cell is engulfed in a process independent of the engulfment genes that function in the removal of apoptotic cells (ABRAHAM *et al.* 2007); this is fairly surprising, as the engulfment genes function in the removal both of apoptotic and of necrotic cells and promote the deaths of the Pn.p cells in *lin-24*, *lin-33*, and *pvl-5* mutants (CHUNG *et al.* 2000; JOSHI and EISENMANN 2004; MANGAHAS and ZHOU 2005; GALVIN *et al.* 2008). The death of the linker cell has ultrastructural characteristics that differ from apoptotic cell deaths in *C. elegans* but that may be similar to some neuronal deaths that normally occur in vertebrate development (ABRAHAM *et al.* 2007). The adult-specific death of the male linker cell is strongly blocked by loss of function of the zinc finger transcription

finger gene *lin-29*, which is required for other adult-specific cell fates in *C. elegans* (ROUGVIE and AMBROS 1995; ABRAHAM *et al.* 2007).

Regulation of programmed cell death in specific cells by transcriptional control of the upstream killing gene *egl-1*

The first cell-specific defect in the regulation of programmed cell death to be identified was a gain-of-function (gf) mutant of *egl-1* in which the HSN neurons of hermaphrodites inappropriately died (TRENT *et al.* 1983). The hermaphrodite-specific HSN neurons are required for egg laying by hermaphrodites; in males, the HSN neurons die during embryogenesis (SULSTON *et al.* 1983; TRENT *et al.* 1983). The activation of programmed cell death in the HSN neurons of *egl-1(*gf*)* hermaphrodites results from mutations in an *egl-1* regulatory site that is bound by TRA-1 (*tra*, sexual transformer), a member of the GLI family of transcription factors (ZARKOWER and HODGKIN 1992; CONRADT and HORVITZ 1999). TRA-1 is the final gene in the *C. elegans* sex determination pathway and acts in the hermaphrodite to prevent expression of male sexual characteristics (HODGKIN 2002). As discussed above, the BH3-only killer gene *egl-1* is the first gene in the core pathway for the execution of programmed cell death and is required for essentially all somatic programmed cell deaths that occur in *C. elegans* development; the *egl-1(*gf*)* phenotype indicates that the sexually dimorphic survival of the HSNs is determined by transcriptional control of this upstream cell-killing gene.

Genetic screens seeking suppressors of the HSN death seen in *egl-1(*gf*)* phenotype identified two genes, *eor-1* and *eor-2* (*eor*, *egl-1* suppressor, DiO uptake

defective, *raf* enhancer) (HOEPPNER *et al.* 2004). *eor-1* encodes a zinc finger transcription factor with homology to the human tumor suppressor PLZF; *eor-2* encodes a nuclear protein without recognizeable functional domains but with limited homology to a family of proteins found in fungi and metazoans (HOWARD and SUNDARAM 2002; HOEPPNER *et al.* 2004). The HSN-protective effects of *eor-1* and *eor-2* mutations, like the HSN-protective effects of loss of *egl-1* function, require the function of the Bcl-2 homolog CED-9, and *eor-1* and *eor-2* have been proposed to promote HSN death by transcriptional activation of *egl-1* (HOEPPNER *et al.* 2004). For a schematic of the genetic pathway controlling the deaths of the HSN neurons and the cell-specific pathways controlling other apoptotic cell deaths, see Figure 2.

A series of genetic and molecular studies have identified a pathway for the cell-specific control of the deaths of the lineal sisters of the NSM neurons ("NSM sisters"); again, this pathway controls the deaths of the NSM sisters by regulating transcription of the upstream BH3-only killer gene *egl-1*. The first genes in this pathway to be identified were *ces-1* and *ces-2* (*ces*, cell death specification) (ELLIS and HORVITZ 1991). A gain-of-function mutation in *ces-1* prevents the deaths of the NSM sisters and the sisters of the I2 neurons, cells that die during wild-type development (ELLIS and HORVITZ 1991). Loss of *ces-2* function similarly causes the NSM sisters to survive. When their deaths are prevented, the NSM sisters become serotonergic cells similar to the NSM neurons (ELLIS and HORVITZ 1991; SZE *et al.* 2000; THELLMANN *et al.* 2003). Strikingly, *ces-1* is required for loss of *ces-2* function to protect the NSM sisters; *ces-2* therefore acts upstream of *ces-1* in controlling the deaths of the NSM sisters (ELLIS and HORVITZ 1991). Animals lacking *ces-1* function appear grossly wild-type.

ces-1 and *ces-2* encode transcription factors: CES-1 is a member of the Snail family of transcriptional repressors, and CES-2 is similar to the human bZIP transcription factor HLF (METZSTEIN *et al.* 1996; METZSTEIN and HORVITZ 1999). The *ces-1* gain-of-function mutation alters a site bound by CES-2 *in vitro* (METZSTEIN and HORVITZ 1999), and a *ces-1::yfp* reporter is upregulated in the neuroblast that generates the NSM and NSM sister in animals lacking *ces-2* function (HATZOLD and CONRADT 2008). An *egl-1* transcriptional regulatory region was found to be required for *egl-1* expression in the NSM sisters and for the deaths of the NSM sisters (THELLMANN *et al.* 2003). This region contains four consensus binding sites for members of the Snail family of transcription factors: mutations targeting these sites abolish the ability of loss of *ces-2* function to protect the NSM sister cells, suggesting that in *ces-2* mutants and in *ces-1(*gf*)* mutants CES-1 binds to these *egl-1* regulatory sites and represses *egl-1* transcription to prevent NSM sister death (THELLMANN *et al.* 2003). Consistent with the hypothesis that *ces-1* acts through transcriptional regulation of *egl-1*, increased *ces-1* function has no significant effect on NSM sister survival in animals lacking the Bcl-2 homolog CED-9, the target of EGL-1 (METZSTEIN and HORVITZ 1999). Larger disruptions that target the consensus Snail family binding sites also affect overlapping E-boxes, which are binding sites for bHLH proteins. These mutations that also affect the E-boxes prevent *egl-1* transcription and cell killing in the NSM sisters (THELLMANN *et al.* 2003). Loss of function of either of the bHLH transcription factor genes *hlh-2* or *hlh-3* causes NSM sister cell survival, and a heterodimer of HLH-2 and HLH-3 can bind these *egl-1* regulatory E-boxes *in vitro* (THELLMANN *et al.* 2003). A fifth gene, *dnj-1*, encoding a

member of the MIDA-like family of proteins, acts with *ces-2* to prevent *ces-1* expression in the NSM sister and to promote NSM sister death (HATZOLD and CONRADT 2008).

The deaths of one additional pair of cells have been shown to be regulated by transcriptional control of *egl-1*: loss-of-function mutations in the homeodomain transcription factor genes *mab-5* and *ceh-20* cause survival of the P11.aaap and P12.aaap cells of the ventral nerve cord that die in wild-type development (LIU *et al.* 2006). *mab-5* and *ceh-20* loss-of-function mutations prevent expression of an *egl-1::gfp* reporter in the P11.aaap and P12.aaap cells. Consistent with *mab-5* and *ceh-20* acting to control *egl-1* expression in the P11.aaap cell, a MAB-5-CEH-20 complex binds *in vitro* to an evolutionarily conserved *egl-1* regulatory site required for the death of the P11.aaap cell (LIU *et al.* 2006). Although *mab-5* and *ceh-20* are required for *egl-1::gfp* expression in the P12.aaap cell, this defined MAB-5-CEH-20 binding site is not required for the death of the P12.aaap cell, suggesting that *mab-5* and *ceh-20* function at a different site or act indirectly to promote *egl-1* expression and cell killing in the P12.aaap cell.

Cell-specific control of sensitivity to activation of cell death caused by loss of the protective function of the Bcl-2 homolog CED-9

As discussed above, the Bcl-2 homolog CED-9 provides an essential anti-apoptotic cell-protective function. Loss of *ced-9* function causes ectopic cell death and lethality. Strong loss-of-function mutations in the downstream killing genes *ced-4* or *ced-3* suppress the lethality caused by loss of *ced-9* function. Weak mutations in *ced-4* and *ced-3* have been identified that permit most programmed cell deaths to occur but

can suppress the lethality caused by loss of *ced-9* function (HENGARTNER and HORVITZ 1994a; SHAHAM *et al.* 1999; HERSH 2002; REDDIEN 2002). Animals that lack *ced-9* function and are weakly defective in the downstream killer gene *ced-3* show significant cell death that is restricted almost completely to cells that normally die in the wild type (HENGARTNER and HORVITZ 1994a). Thus, regulation of programmed cell death by developmental lineage can occur independently of *ced-9*. Since loss of *egl-1* function has no effect in the absence of *ced-9* function (CONRADT and HORVITZ 1998), this *ced-9*-independent regulation of cell survival must also be independent of *egl-1* and of its transcriptional regulators.

Loss of *ced-9* causes activation of the cell-death program similar to that caused in cells fated to die by expression of the BH3-only pro-apoptotic protein EGL-1. For example, the HSNs of *ced-9(n1653*lf*)* hermaphrodites and the *egl-1*-expressing HSNs of *egl-1(n1084*gf*)* hermaphrodites undergo programmed cell death (DESAI *et al.* 1988; CONRADT and HORVITZ 1999). Similarly, loss of *ced-9* function and *egl-1* over-expression each cause relocalization of CED-4 from the mitochondria to the nuclear periphery, a proposed early step in programmed cell death (CHEN *et al.* 2000). The *ced-9*-independent regulation of cell death seen in *ced-9(*null*)*; *ced-3(*weak*)* double mutant animals can therefore be considered to be a regulation of sensitivity to an activated cell-death program: cells normally programmed to die are more sensitive to an activated cell-death program than are cells normally programmed to survive.

The first identified mechanism that couples cell identity and *ced-9*-independent regulation of sensitivity to programmed cell death is transcriptional regulation of *ced-3* in the tail spike cell by by the homeodomain transcription factor PAL-1, a homolog of

Drosophila Caudal and mouse Cdx1. Reduced *pal-1* function causes the tail spike cell, which dies in the wild type during embryogenesis, instead to survive, even in animals completely lacking *ced-9* function (MAURER *et al.* 2007). A *ced-3::gfp* reporter is upregulated in the tail spike cell beginning roughly 30 minutes prior to its death; when the death of the tail spike cell is prevented by loss of *ced-3* function, high-level expression of the *ced-3::gfp* reporter persists in the undead tail spike cell through adulthood (MAURER *et al.* 2007). Expression of the *ced-3::gfp* reporter in the tail spike cell requires *pal-1*, and PAL-1 can bind an element within the *ced-3::gfp* reporter required for expression in the tail spike cell. It has therefore been proposed that the tail spike cell contains an activated cell-death program, and that late in the differentiation of the tail spike cell PAL-1 transcriptionally upregulates *ced-3* to render the tail spike cell sensitive to this activated cell-death program (MAURER *et al.* 2007).

I have identified another cell-specific *ced-9*-independent regulator of sensitivity to apoptotic cell death, the Bar homeodomain transcription factor CEH-30. *ceh-30* is required for the male-specific survival of the CEM neurons. In males, the CEM neurons function in the detection of hermaphrodites (CHASNOV *et al.* 2007); the CEM neurons of hermaphrodites die during embryogenesis (SULSTON *et al.* 1983). The Bar homeodomain transcription factor CEH-30 and the Groucho homolog UNC-37 promote CEM survival in males; in the CEM neurons of hermaphrodites, *ceh-30* is transcriptionally repressed by TRA-1 (PEDEN *et al.* 2007; SCHWARTZ and HORVITZ 2007). Sex determination, acting through *ceh-30*, can control CEM survival in animals completely lacking *ced-9* function (SCHWARTZ and HORVITZ 2007). For diagrammatic representation of the pathways controlling tail spike and CEM death, see Figure 2.

There are striking similarities between the death of the tail spike cell and the deaths of the CEM neurons in hermaphrodites. Both the tail spike cell and the CEM neurons are generated some hours before they die and show morphological or ultrastructural signs of differentiation prior to their deaths (J. Sulston and J. White, as cited by HORVITZ *et al.* 1982; SULSTON *et al.* 1983). By contrast, the great majority of cells programmed to die during *C. elegans* development die and are engulfed by their neighbors within 30 minutes of their generation by cell division (SULSTON and HORVITZ 1977; SULSTON *et al.* 1983). Engulfment of a dying cell by its neighbors has been observed to begin even before the division that generates the dying cell is complete (ROBERTSON and THOMPSON 1982). Both the tail spike cell and the CEM neurons are unaffected by the killing function of *ced-9*, and both cell types are only partially protected against cell death by a *ced-9* gain-of-function mutation that almost completely blocks the programmed cell deaths of other cells (HENGARTNER and HORVITZ 1994a; MAURER *et al.* 2007; SCHWARTZ and HORVITZ 2007). Given these similarities, it is tempting to speculate that the *ced-9*-independent mechanisms that control the sensitivity of the tail spike cell and the CEM neurons to their activated cell-death programs might be similar and that both might involve the transcriptional regulation of *ced-3*.

The same *ced-3::gfp* reporters used in studies of the tail spike cell death are expressed not only in cells normally fated to die but also in cells that survive in wild-type development (MAURER *et al.* 2007). *ced-4* is also expressed in most or all cells in *C. elegans* development (CHEN *et al.* 2000). As cell death in animals lacking *ced-9* and weakly defective in *ced-3* is largely restricted to cells that normally die in the wild-type,

these cells must be protected from activation of the cell-death program by loss of *ced-9* function despite their apparently expressing *ced-3* and *ced-4*. It therefore appears likely that mechanisms remain to be identified that function to reduce the sensitivity to programmed cell death of cells normally programmed to survive other than the *ced-3* regulation seen in the tail spike cell. If CEH-30 does not control *ced-3* expression, the transcriptional targets of CEH-30 may determine whether cells that express *ced-3* and *ced-4* are sensitive to the an activated cell-death program

Genes that regulate specific cell survival decisions have additional non-death functions in *C. elegans* development

Nearly every gene that has been found to control the programmed deaths of specific cells also has been found to control aspects of *C. elegans* development other than programmed cell death. The first mutants identified as defective in the deaths of specific cells, *egl-1(*gf*)* and *ces-2(*lf*)*, defined cell-death-regulatory functions of genes that have additional functions in development. *egl-1(*gf*)* mutations that specifically promote HSN death in the hermaphrodite define a role for the transcription factor TRA-1 in directly controlling the sexually dimorphic deaths of the HSN neurons (CONRADT and HORVITZ 1999). This feminizing effect of TRA-1 is not specific to the HSN neurons: TRA-1 is required for all other aspects of the hermaphrodite sexual identity (ZARKOWER and HODGKIN 1992). *ces-2* mutants are defective not only in the deaths of the NSM sisters but also in morphogenesis of the duct cell (WANG and CHAMBERLIN 2002).

As additional genes that control the survival decisions of specific cells in *C. elegans* have been identified, nearly all have been found to be genes already known

to perform other roles in development; for a complete list, see Table 1. These genes and their additional roles in development include EOR-2 and the PLZF homolog EOR-1, which promote the deaths of the HSN neurons and also function in Raf signaling and in neuronal differentiation (HOWARD and SUNDARAM 2002; HOEPPNER *et al.* 2004); the bHLH transcription factor HLH-2, which promotes the deaths of the NSM sister cells and is also an essential gene required during embryogenesis (KRAUSE *et al.* 1997; THELLMANN *et al.* 2003); the homeodomain transcription factors MAB-5 and CEH-20, which promote the deaths of the P11.aaap and P12.aaap neurons and function in patterning of the animal (WANG *et al.* 1993; LIU and FIRE 2000; LIU *et al.* 2006); the Caudal homolog PAL-1, which promotes the death of the tail spike cell and functions in posterior patterning (EDGAR *et al.* 2001; MAURER *et al.* 2007); and UNC-37, a homolog of the transcriptional repressor Groucho, which promotes the survival of the CEM neurons and functions to determine motor neuron identity (PFLUGRAD *et al.* 1997; PEDEN *et al.* 2007). The Bar homeodomain transcription factor CEH-30 is required for CEM neuron survival, and no other defects have been seen in animals lacking *ceh-30* function (PEDEN *et al.* 2007; SCHWARTZ and HORVITZ 2007). Animals lacking both *ceh-30* and its close homolog *ceh-31* display a locomotion defect not seen in animals lacking either one of the two Bar homeodomain transcription factor genes, suggesting that the two related proteins function redundantly in aspects of neuronal development other than promoting the survival of the CEM neurons (see Chapter 2). It seems likely that further studies of specific cell deaths will similarly identify genes that control these survival decisions and have additional functions in *C. elegans* development.

One area of particular interest in the overlap between the regulation of programmed cell death and other aspects of development in *C. elegans* is the generation of cells by asymmetric cell division. Asymmetric cell division is critical to the establishment of cell diversity (HORVITZ and HERSKOWITZ 1992). Asymmetric cell divisions are critical to *C. elegans* development, including the earliest patterning events in the first cell division (reviewed by COWAN and HYMAN 2004). Cells that die in *C. elegans* development are always the products of an asymmetric cell division, with the small daughter being the one that dies (SULSTON and HORVITZ 1977; SULSTON *et al.* 1983). Mutations that disrupt the asymmetric divisions of these neuroblasts can alter the fates of both daughters, including preventing the programmed cell deaths of the daughters normally fated to die (GUENTHER and GARRIGA 1996; FRANK *et al.* 2005; CORDES *et al.* 2006) and causing the deaths of the daughters normally fated to survive (SINGHVI *et al.* 2008). At least two factors have been identified, *ham-1* and *pig-1*, that appear to function only in the divisions of neuroblasts that generate one cell fated to live and one cell fated to die, suggesting that these cell divisions are subjected to special controls (FRANK *et al.* 2005; CORDES *et al.* 2006). The asymmetric cell divisions that generate cells programmed to die are in at least one case closely linked to the transcriptional control of the core pathway for the execution of programmed cell death: CES-1 directly represses *egl-1* expression in the NSM sister and increased *ces-1* function prevents the asymmetry of the neuroblast division that generates the NSM and the NSM sister (HATZOLD and CONRADT 2008). CES-1 homologs in the fruit fly *D. melanogaster* also regulate the asymmetry of cell divisions (ASHRAF and IP 2001; CAI *et al.* 2001).

Genes that regulate the survival decisions of specific cells in *C. elegans* have mammalian homologs that similarly function to control cell survival

In the preceding sections I have described the identification of 13 genes that function to specifically control 13 apoptotic cell deaths in *C. elegans* development. All 13 of these genes encode nuclear proteins, and at least 11 of the 13 encode transcription factors. All have mammalian homologs. Importantly, not only the sequences of these proteins but also their roles as regulators of apoptotic cell death appear to be evolutionarily conserved. In addition to having homologs that have been shown to regulate apoptosis, genes that control specific cell deaths in *C. elegans* have homologs that have been implicated in cancer: genes that promote apoptosis are likely to inhibit tumor progression, and genes that prevent apoptosis are likely to promote tumor progression.

Mice lacking *PLZF*, a homolog of the HSN death-promoting factor *eor-1*, have reduced apoptosis in limb bud development (BARNA *et al.* 2000). The NSM sister-specific death factor HLH-2 (THELLMANN *et al.* 2003) is homologous to the mammalian bHLH transcription factor E2A, which can cause apoptosis when overexpressed in cultured cells (ENGEL and MURRE 1999). Loss of *E2A* function can cause lymphoma (YAN *et al.* 1997), and *E2A* may inhibit tumor development by promoting apoptosis (LIETZ *et al.* 2007). *pal-1* specifically promotes tail spike cell death (MAURER *et al.* 2007) and is homologous to *Cdx2*, which is frequently found to be lost in intestinal tumors (CHAWENGSAKSOPHAK *et al.* 1997; AOKI *et al.* 2003; BONHOMME *et al.* 2003). Gli1, A homolog of the HSN-specific cell-death inhibitor TRA-1 is overexpressed

in the majority of basal cell carcinomas and overexpression of Gli1 can cause epithelial tumor formation (DAHMANE *et al.* 1997).

The best example of conservation of a pathway that controls cell-specific apoptosis in the regulation of apoptotic cell death in mammals is found in the genes that control the deaths of the NSM sister cells, in particular *ces-1* and *ces-2*. The human CES-2 homolog HLF is subject to translocations that cause Acute Lymphoblastic Leukemia (ALL) (INABA *et al.* 1992). As a result of these translocations, a fusion protein is overexpressed in B cells; this fusion protein contains the DNA binding domain from HLF, homologous to the DNA-binding domain of CES-2, but in place of the transcriptional repression domain found in HLF the fusion protein contains a transcriptional activation domain from the transcription factor E2A (INABA *et al.* 1996).This fusion oncogene can therefore increase the expression of targets normally repressed by *HLF* function. Overexpression of this fusion oncogene blocks cell death in pro-B cells, just as loss of *ces-2* function blocks the programmed cell deaths of the the NSM sister cells (ELLIS and HORVITZ 1991; INABA *et al.* 1996; METZSTEIN *et al.* 1996). The E2A-HLF fusion protein that blocks pro-B cell death induces expression of the CES-1 homolog Slug (INUKAI *et al.* 1999); this relationship is analogous to the increased *ces-1* expression in the NSM sisters of animals lacking the HLF homolog CES-2 (HATZOLD and CONRADT 2008). Just as CES-1 binds near and transcriptionally represses the BH3-only killer gene *egl-1*, Slug binds to and represses the transcription of the BH3-only killer gene *Puma* (WU *et al.* 2005). Thus, the entire *ces-2-ces-1-egl-1* pathway that controls the deaths of the NSM sister cells is conserved in the *E2A-HLF-Slug-Puma* pathway. By blocking cell death, the E2A-HLF oncogene causes

ALL, highlighting the importance of this evolutionarily conserved cell-death-regulatory pathway in our understanding of human disease. Another cell-specific regulator of *C. elegans* apoptosis, *ceh-20*, which promotes the deaths of the P11.aaap and P12.aaap cells, encodes a homolog of Pbx1, which like HLF is subject to translocations that give rise to a form of ALL (KAMPS *et al.* 1990; NOURSE *et al.* 1990).

The cell-death regulation function of the Bar homeodomain transcription factor *ceh-30* is also evolutionarily conserved. Mice lacking the *ceh-30* homolog *Barhl1* are born healthy but progressively lose both their sensory cochlear inner ear hair cells and consequently their ability to hear (LI *et al.* 2002). Expression of *Barhl1* in *ceh-30* mutant males restores survival of the CEM neurons, indicating that the target specificity of these Bar homeodomain transcription factors is evolutionarily conserved. Mice lacking *Barhl1* also display defects similar to those seen in mice lacking the neurotrophin survival factor NT-3 (LI *et al.* 2004) as well as increased apoptosis of neurons of the superior colliculus (LI and XIANG 2006). It seems likely that the sensory hair cell neurons of *Barhl1* mutant mice, like the CEM neurons of *ceh-30* mutants, lack protection from apoptotic cell death. An evolutionarily conserved function of the Bar homeodomain transcription factors in regulating the survival of sensory neurons might be particularly notable, because *ceh-30* is able to regulate the survival of the male-specific CEM neurons independently of the Bcl-2 homolog CED-9 (SCHWARTZ and HORVITZ 2007); similar regulation of cell survival by *Barhl1* independently of the Bcl-2 superfamily would yield new insights into the control of apoptosis in mammalian development and disease.

Conclusion

In my thesis work, I have investigated the mechanisms that determine the cell fates and in particular the survival or death decisions of specific neurons in *C. elegans* development. My work began as genetic screens investigating the survival decisions of specific cells and has indeed identified at least one gene that controls programmed cell death in a cell-specific manner. This work has also led to my discovering of mechanisms that control other aspects of the fates of these cells, including genes that determine sexual identity, genes that function to prevent inappropriate gene expression, and a gene that regulates the cell cycle to prevent improper cell division.

In Chapter II, I present genetic screens I performed to identify mutants defective in the hermaphrodite-specific programmed cell deaths of the CEM sensory neurons, and my investigation of the mutants I recovered, mutants that identified genes that function to determine the CEM neuron fate, to establish the sexual identity of the animal, and specifically to control CEM survival.

In Chapter III, I describe my identification of the Bar homeodomain transcription factor gene *ceh-30* as a CEM-specific regulator of CEM survival, and show that *ceh-30* acts by a novel and possibly evolutionarily conserved mechanism independent of the core cell death pathway genes *egl-1* and *ced-9* to promote CEM neuron survival.

In Chapter IV, I describe my characterization of a phenotype of inappropriate gene expression that arose from my screens for mutants defective in CEM neuron death, including additional screens that I performed with undergraduate student Dawn Wendell to recover additional mutants that share this transgene misexpression

phenotype and my cloning of three genes that function to prevent inappropriate gene expression.

In Chapter V, I describe work I did together with undergraduate student Johanna Varner to characterize a mutant I isolated in screens I had performed to investigate the programmed death of a different cell, the sister of the PVD neuron. This work demonstrated a highly cell-specific function of the mitotic exit network gene *cdc-14*.

In Chapter VI, I describe a collaboration with Sibylle Jager and Barbara Conradt to characterize an altered-function mutant of the protein degradation factor *sel-10*. This work demonstrated that *sel-10* functions to promote feminization and led to our proposing a molecular mechanism for the action of *sel-10* in determining sexual identity.

In five Appendices, I describe possible future directions for work to extend some of the results presented in this thesis; present the complete details of screens that I and undergraduate students working with me performed, highlighting some mutants and phenomena of particular interest that have not been substantially pursued; and include a review I wrote describing methods for the analysis of programmed cell death and two papers to which I made minor contributions.

Acknowledgments

I thank Daniel Denning, Brendan Galvin, and Niels Ringstad for their comments concerning this chapter.

References

ABRAHAM, M. C., Y. LU and S. SHAHAM, 2007 A morphologically conserved nonapoptotic program promotes linker cell death in *Caenorhabditis elegans*. Dev Cell **12:** 73-86.

ALNEMRI, E. S., D. J. LIVINGSTON, D. W. NICHOLSON, G. SALVESEN, N. A. THORNBERRY *et al.*, 1996 Human ICE/CED-3 protease nomenclature. Cell **87:** 171.

AOKI, K., Y. TAMAI, S. HORIIKE, M. OSHIMA and M. M. TAKETO, 2003 Colonic polyposis caused by mTOR-mediated chromosomal instability in *Apc*+/Delta716 *Cdx*2+/– compound mutant mice. Nat Genet **35:** 323-330.

ASHRAF, S. I., and Y. T. IP, 2001 The Snail protein family regulates neuroblast expression of inscuteable and string, genes involved in asymmetry and cell division in *Drosophila*. Development **128:** 4757-4767.

BARNA, M., N. HAWE, L. NISWANDER and P. P. PANDOLFI, 2000 Plzf regulates limb and axial skeletal patterning. Nat Genet **25:** 166-172.

BERGMANN, A., J. AGAPITE, K. MCCALL and H. STELLER, 1998 The *Drosophila* gene *hid* is a direct molecular target of Ras-dependent survival signaling. Cell **95:** 331-341.

BIANCHI, L., B. GERSTBREIN, C. FROKJAER-JENSEN, D. C. ROYAL, G. MUKHERJEE *et al.*, 2004 The neurotoxic MEC-4(d) DEG/ENaC sodium channel conducts calcium: implications for necrosis initiation. Nat Neurosci **7:** 1337-1344.

BONHOMME, C., I. DULUC, E. MARTIN, K. CHAWENGSAKSOPHAK, M. P. CHENARD *et al.*, 2003 The *Cdx2* homeobox gene has a tumour suppressor function in the distal colon in addition to a homeotic role during gut development. Gut **52:** 1465-1471.

BRENNER, S., 1974 The genetics of *Caenorhabditis elegans*. Genetics **77:** 71-94.

BRODSKY, M. H., W. NORDSTROM, G. TSANG, E. KWAN, G. M. RUBIN *et al.*, 2000 *Drosophila* p53 binds a damage response element at the reaper locus. Cell **101:** 103-113.

CAI, Y., W. CHIA and X. YANG, 2001 A family of snail-related zinc finger proteins regulates two distinct and parallel mechanisms that mediate *Drosophila* neuroblast asymmetric divisions. Embo J **20:** 1704-1714.

CHALFIE, M., and J. SULSTON, 1981 Developmental genetics of the mechanosensory neurons of *Caenorhabditis elegans*. Dev Biol **82:** 358-370.

CHANG, B. S., A. J. MINN, S. W. MUCHMORE, S. W. FESIK and C. B. THOMPSON, 1997 Identification of a novel regulatory domain in Bcl-X(L) and Bcl-2. Embo J **16:** 968-977.

CHASNOV, J. R., W. K. SO, C. M. CHAN and K. L. CHOW, 2007 The species, sex, and stage specificity of a *Caenorhabditis* sex pheromone. Proc Natl Acad Sci U S A **104:** 6730-6735.

CHAWENGSAKSOPHAK, K., R. JAMES, V. E. HAMMOND, F. KONTGEN and F. BECK, 1997 Homeosis and intestinal tumours in *Cdx2* mutant mice. Nature **386:** 84-87.

CHEN, F., B. M. HERSH, B. CONRADT, Z. ZHOU, D. RIEMER *et al.*, 2000 Translocation of *C. elegans* CED-4 to nuclear membranes during programmed cell death. Science **287:** 1485-1489.

CHENG, E. H., D. G. KIRSCH, R. J. CLEM, R. RAVI, M. B. KASTAN *et al.*, 1997 Conversion of Bcl-2 to a Bax-like death effector by caspases. Science **278:** 1966-1968.

CHINNAIYAN, A. M., D. CHAUDHARY, K. O'ROURKE, E. V. KOONIN and V. M. DIXIT, 1997a Role of CED-4 in the activation of CED-3. Nature **388:** 728-729.

CHINNAIYAN, A. M., K. O'ROURKE, B. R. LANE and V. M. DIXIT, 1997b Interaction of CED-4 with CED-3 and CED-9: a molecular framework for cell death. Science **275:** 1122-1126.

CHIPUK, J. E., T. KUWANA, L. BOUCHIER-HAYES, N. M. DROIN, D. D. NEWMEYER *et al.*, 2004 Direct activation of Bax by p53 mediates mitochondrial membrane permeabilization and apoptosis. Science **303:** 1010-1014.

CHUNG, S., T. L. GUMIENNY, M. O. HENGARTNER and M. DRISCOLL, 2000 A common set of engulfment genes mediates removal of both apoptotic and necrotic cell corpses in *C. elegans*. Nat Cell Biol **2:** 931-937.

CLARKE, P. G., and S. CLARKE, 1996 Nineteenth century research on naturally occurring cell death and related phenomena. Anat Embryol (Berl) **193:** 81-99.

CONRADT, B., and H. R. HORVITZ, 1998 The *C. elegans* protein EGL-1 is required for programmed cell death and interacts with the Bcl-2-like protein CED-9. Cell **93:** 519-529.

CONRADT, B., and H. R. HORVITZ, 1999 The TRA-1A sex determination protein of *C. elegans* regulates sexually dimorphic cell deaths by repressing the *egl-1* cell death activator gene. Cell **98:** 317-327.

CONTE, D., M. HOLCIK, C. A. LEFEBVRE, E. LACASSE, D. J. PICKETTS *et al.*, 2006 Inhibitor of apoptosis protein cIAP2 is essential for lipopolysaccharide-induced macrophage survival. Mol Cell Biol **26:** 699-708.

CONZE, D. B., L. ALBERT, D. A. FERRICK, D. V. GOEDDEL, W. C. YEH *et al.*, 2005 Posttranscriptional downregulation of c-IAP2 by the ubiquitin protein ligase c-IAP1 in vivo. Mol Cell Biol **25:** 3348-3356.

CORDES, S., C. A. FRANK and G. GARRIGA, 2006 The *C. elegans* MELK ortholog PIG-1 regulates cell size asymmetry and daughter cell fate in asymmetric neuroblast divisions. Development **133:** 2747-2756.

CORY, S., and J. M. ADAMS, 2002 The Bcl2 family: regulators of the cellular life-or-death switch. Nat Rev Cancer **2:** 647-656.

COWAN, C. R., and A. A. HYMAN, 2004 Asymmetric cell division in *C. elegans*: cortical polarity and spindle positioning. Annu Rev Cell Dev Biol **20:** 427-453.

DAHMANE, N., J. LEE, P. ROBINS, P. HELLER and A. RUIZ I ALTABA, 1997 Activation of the transcription factor Gli1 and the Sonic hedgehog signalling pathway in skin tumours. Nature **389:** 876-881.

DANIAL, N. N., 2007 BCL-2 family proteins: critical checkpoints of apoptotic cell death. Clin Cancer Res **13:** 7254-7263.

DEL PESO, L., V. M. GONZALEZ and G. NUNEZ, 1998 *Caenorhabditis elegans* EGL-1 disrupts the interaction of CED-9 with CED-4 and promotes CED-3 activation. J Biol Chem **273:** 33495-33500.

DESAI, C., G. GARRIGA, S. L. MCINTIRE and H. R. HORVITZ, 1988 A genetic pathway for the development of the *Caenorhabditis elegans* HSN motor neurons. Nature **336:** 638-646.

DEVERAUX, Q. L., R. TAKAHASHI, G. S. SALVESEN and J. C. REED, 1997 X-linked IAP is a direct inhibitor of cell-death proteases. Nature **388:** 300-304.

DRISCOLL, M., and M. CHALFIE, 1991 The *mec-4* gene is a member of a family of *Caenorhabditis elegans* genes that can mutate to induce neuronal degeneration. Nature **349:** 588-593.

DU, C., M. FANG, Y. LI, L. LI and X. WANG, 2000 Smac, a mitochondrial protein that promotes cytochrome c-dependent caspase activation by eliminating IAP inhibition. Cell **102:** 33-42.

EDGAR, L. G., S. CARR, H. WANG and W. B. WOOD, 2001 Zygotic expression of the caudal homolog *pal-1* is required for posterior patterning in *Caenorhabditis elegans* embryogenesis. Dev Biol **229:** 71-88.

ELHASID, R., D. SAHAR, A. MERLING, Y. ZIVONY, A. ROTEM *et al.*, 2004 Mitochondrial pro-apoptotic ARTS protein is lost in the majority of acute lymphoblastic leukemia patients. Oncogene **23:** 5468-5475.

ELLIS, H. M., and H. R. HORVITZ, 1986 Genetic control of programmed cell death in the nematode *C. elegans*. Cell **44:** 817-829.

ELLIS, R. E., and H. R. HORVITZ, 1991 Two *C. elegans* genes control the programmed deaths of specific cells in the pharynx. Development **112:** 591-603.

ENGEL, I., and C. MURRE, 1999 Ectopic expression of E47 or E12 promotes the death of E2A-deficient lymphomas. Proc Natl Acad Sci U S A **96:** 996-1001.

FERGUSON, E. L., and H. R. HORVITZ, 1985 Identification and characterization of 22 genes that affect the vulval cell lineages of the nematode *Caenorhabditis elegans*. Genetics **110:** 17-72.

FERGUSON, E. L., P. W. STERNBERG and H. R. HORVITZ, 1987 A genetic pathway for the specification of the vulval cell lineages of Caenorhabditis elegans. Nature **326:** 259-267.

FRANK, C. A., N. C. HAWKINS, C. GUENTHER, H. R. HORVITZ and G. GARRIGA, 2005 *C. elegans* HAM-1 positions the cleavage plane and regulates apoptosis in asymmetric neuroblast divisions. Dev Biol **284:** 301-310.

GALVIN, B. D., S. KIM and H. R. HORVITZ, 2008 *Caenorhabditis elegans* genes required for the engulfment of apoptotic corpses function in the cytotoxic cell deaths induced by mutations in *lin-24* and *lin-33*. Genetics **179:** 403-417.

GOTTFRIED, Y., A. ROTEM, R. LOTAN, H. STELLER and S. LARISCH, 2004 The mitochondrial ARTS protein promotes apoptosis through targeting XIAP. Embo J **23:** 1627-1635.

GRUMONT, R. J., I. J. ROURKE and S. GERONDAKIS, 1999 Rel-dependent induction of *A1* transcription is required to protect B cells from antigen receptor ligation-induced apoptosis. Genes Dev **13:** 400-411.

GUENTHER, C., and G. GARRIGA, 1996 Asymmetric distribution of the *C. elegans* HAM-1 protein in neuroblasts enables daughter cells to adopt distinct fates. Development **122:** 3509-3518.

GUMIENNY, T. L., E. LAMBIE, E. HARTWIEG, H. R. HORVITZ and M. O. HENGARTNER, 1999 Genetic control of programmed cell death in the *Caenorhabditis elegans* hermaphrodite germline. Development **126:** 1011-1022.

HARLIN, H., S. B. REFFEY, C. S. DUCKETT, T. LINDSTEN and C. B. THOMPSON, 2001 Characterization of XIAP-deficient mice. Mol Cell Biol **21:** 3604-3608.

HATZOLD, J., and B. CONRADT, 2008 Control of apoptosis by asymmetric cell division. PLoS Biol **6:** e84.

HAY, B. A., D. A. WASSARMAN and G. M. RUBIN, 1995 *Drosophila* homologs of baculovirus inhibitor of apoptosis proteins function to block cell death. Cell **83:** 1253-1262.

HEDGECOCK, E. M., J. E. SULSTON and J. N. THOMSON, 1983 Mutations affecting programmed cell deaths in the nematode *Caenorhabditis elegans*. Science **220:** 1277-1279.

HENGARTNER, M. O., R. E. ELLIS and H. R. HORVITZ, 1992 *Caenorhabditis elegans* gene *ced-9* protects cells from programmed cell death. Nature **356:** 494-499.

HENGARTNER, M. O., and H. R. HORVITZ, 1994a Activation of *C. elegans* cell death protein CED-9 by an amino-acid substitution in a domain conserved in Bcl-2. Nature **369:** 318-320.

HENGARTNER, M. O., and H. R. HORVITZ, 1994b *C. elegans* cell survival gene *ced-9* encodes a functional homolog of the mammalian proto-oncogene *bcl-2*. Cell **76:** 665-676.

HERSH, B. M., 2002 C. elegans apoptosis: CED-4 translocation and involvement in a model of Mucolipidosis Type IV human lysosomal storage disorder. Ph. D. Thesis, Massachusetts Institute of Technology, Cambridge, MA.

HOCKENBERY, D., G. NUNEZ, C. MILLIMAN, R. D. SCHREIBER and S. J. KORSMEYER, 1990 Bcl-2 is an inner mitochondrial membrane protein that blocks programmed cell death. Nature **348:** 334-336.

HODGKIN, J., 2002 Exploring the envelope. Systematic alteration in the sex-determination system of the nematode *Caenorhabditis elegans*. Genetics **162:** 767-780.

HOEPPNER, D. J., M. O. HENGARTNER and R. SCHNABEL, 2001 Engulfment genes cooperate with *ced-3* to promote cell death in *Caenorhabditis elegans*. Nature **412:** 202-206.

HOEPPNER, D. J., M. S. SPECTOR, T. M. RATLIFF, J. M. KINCHEN, S. GRANAT *et al.*, 2004 *eor-1* and *eor-2* are required for cell-specific apoptotic death in *C. elegans*. Dev Biol **274:** 125-138.

HORVITZ, H. R., 2003 Worms, life, and death (Nobel lecture). Chembiochem **4:** 697-711.

HORVITZ, H. R., H. M. ELLIS and P. W. STERNBERG, 1982 Programmed cell death in nematode development. Neuroscience Commentaries **1:** 56-65.

HORVITZ, H. R., and I. HERSKOWITZ, 1992 Mechanisms of assymetric cell division: two Bs or not two Bs, that is the question. Cell **68:** 237-255.

HOWARD, R. M., and M. V. SUNDARAM, 2002 *C. elegans* EOR-1/PLZF and EOR-2 positively regulate Ras and Wnt signaling and function redundantly with LIN-25 and the SUR-2 Mediator component. Genes Dev **16:** 1815-1827.

INABA, T., T. INUKAI, T. YOSHIHARA, H. SEYSCHAB, R. A. ASHMUN *et al.*, 1996 Reversal of apoptosis by the leukaemia-associated E2A-HLF chimaeric transcription factor. Nature **382:** 541-544.

INABA, T., W. M. ROBERTS, L. H. SHAPIRO, K. W. JOLLY, S. C. RAIMONDI *et al.*, 1992 Fusion of the leucine zipper gene HLF to the E2A gene in human acute B-lineage leukemia. Science **257:** 531-534.

INUKAI, T., A. INOUE, H. KUROSAWA, K. GOI, T. SHINJYO *et al.*, 1999 *SLUG*, a *ces-1*-related zinc finger transcription factor gene with antiapoptotic activity, is a downstream target of the E2A-HLF oncoprotein. Mol Cell **4:** 343-352.

JIANG, C., A. F. LAMBLIN, H. STELLER and C. S. THUMMEL, 2000 A steroid-triggered transcriptional hierarchy controls salivary gland cell death during *Drosophila* metamorphosis. Mol Cell **5:** 445-455.

JONES, J. M., P. DATTA, S. M. SRINIVASULA, W. JI, S. GUPTA *et al.*, 2003 Loss of Omi mitochondrial protease activity causes the neuromuscular disorder of *mnd2* mutant mice. Nature **425:** 721-727.

JOSHI, P., and D. M. EISENMANN, 2004 The *Caenorhabditis elegans pvl-5* gene protects hypodermal cells from *ced-3*-dependent, *ced-4*-independent cell death. Genetics **167:** 673-685.

KAMPS, M. P., C. MURRE, X. H. SUN and D. BALTIMORE, 1990 A new homeobox gene contributes the DNA binding domain of the t(1;19) translocation protein in pre-B ALL. Cell **60:** 547-555.

KERR, J. F. R., A. H. WYLLIE and A. R. CURRIE, 1972 Apoptosis: a basic biological phenomenon with wide-ranging implications in tissue kinetics. Br J Cancer **26:** 239-257.

KIMBLE, J., and D. HIRSH, 1979 The postembryonic cell lineages of the hermaphrodite and male gonads in *Caenorhabditis elegans*. Dev Biol **70:** 396-417.

KISSEL, H., M. M. GEORGESCU, S. LARISCH, K. MANOVA, G. R. HUNNICUTT *et al.*, 2005 The *Sept4* septin locus is required for sperm terminal differentiation in mice. Dev Cell **8:** 353-364.

KRAUSE, M., M. PARK, J. M. ZHANG, J. YUAN, B. HARFE *et al.*, 1997 A *C. elegans* E/Daughterless bHLH protein marks neuronal but not striated muscle development. Development **124:** 2179-2189.

LARISCH, S., Y. YI, R. LOTAN, H. KERNER, S. EIMERL *et al.*, 2000 A novel mitochondrial septin-like protein, ARTS, mediates apoptosis dependent on its P-loop motif. Nat Cell Biol **2:** 915-921.

LI, S., S. M. PRICE, H. CAHILL, D. K. RYUGO, M. M. SHEN *et al.*, 2002 Hearing loss caused by progressive degeneration of cochlear hair cells in mice deficient for the *Barhl1* homeobox gene. Development **129:** 3523-3532.

LI, S., F. QIU, A. XU, S. M. PRICE and M. XIANG, 2004 *Barhl1* regulates migration and survival of cerebellar granule cells by controlling expression of the neurotrophin-3 gene. J Neurosci **24:** 3104-3114.

LI, S., and M. XIANG, 2006 Barhl1 is required for maintenance of a large population of neurons in the zonal layer of the superior colliculus. Dev Dyn **235:** 2260-2265.

LIETZ, A., M. JANZ, M. SIGVARDSSON, F. JUNDT, B. DORKEN *et al.*, 2007 Loss of bHLH transcription factor E2A activity in primary effusion lymphoma confers resistance to apoptosis. Br J Haematol **137:** 342-348.

LINDSTEN, T., A. J. ROSS, A. KING, W. X. ZONG, J. C. RATHMELL *et al.*, 2000 The combined functions of proapoptotic Bcl-2 family members bak and bax are essential for normal development of multiple tissues. Mol Cell **6:** 1389-1399.

LIU, H., T. J. STRAUSS, M. B. POTTS and S. CAMERON, 2006 Direct regulation of *egl-1* and of programmed cell death by the Hox protein MAB-5 and by CEH-20, a *C. elegans* homolog of Pbx1. Development **133:** 641-650.

LIU, J., and A. FIRE, 2000 Overlapping roles of two Hox genes and the *exd* ortholog *ceh-20* in diversification of the *C. elegans* postembryonic mesoderm. Development **127:** 5179-5190.

LOCKSHIN, R. A., and C. M. WILLIAMS, 1965 Programmed Cell Death--I. Cytology of Degeneration in the Intersegmental Muscles of the Pernyi Silkmoth. J Insect Physiol **11:** 123-133.

LOCKSHIN, R. A., and Z. ZAKERI, 2007 Cell death in health and disease. J Cell Mol Med **11:** 1214-1224.

LOHMANN, I., N. MCGINNIS, M. BODMER and W. MCGINNIS, 2002 The *Drosophila Hox* gene *deformed* sculpts head morphology via direct regulation of the apoptosis activator *reaper*. Cell **110:** 457-466.

MANGAHAS, P. M., and Z. ZHOU, 2005 Clearance of apoptotic cells in *Caenorhabditis elegans*. Semin Cell Dev Biol **16:** 295-306.

MARTINS, L. M., I. IACCARINO, T. TENEV, S. GSCHMEISSNER, N. F. TOTTY *et al.*, 2002 The serine protease Omi/HtrA2 regulates apoptosis by binding XIAP through a reaper-like motif. J Biol Chem **277:** 439-444.

MARTINS, L. M., A. MORRISON, K. KLUPSCH, V. FEDELE, N. MOISOI *et al.*, 2004 Neuroprotective role of the Reaper-related serine protease HtrA2/Omi revealed by targeted deletion in mice. Mol Cell Biol **24:** 9848-9862.

MAURER, C. W., M. CHIORAZZI and S. SHAHAM, 2007 Timing of the onset of a developmental cell death is controlled by transcriptional induction of the *C. elegans ced-3* caspase-encoding gene. Development **134:** 1357-1368.

MAYO, M. W., and A. S. BALDWIN, 2000 The transcription factor NF-kappaB: control of oncogenesis and cancer therapy resistance. Biochim Biophys Acta **1470:** M55-62.

MCDONNELL, T. J., N. DEANE, F. M. PLATT, G. NUNEZ, U. JAEGER *et al.*, 1989 *bcl-2*-immunoglobulin transgenic mice demonstrate extended B cell survival and follicular lymphoproliferation. Cell **57:** 79-88.

MERRY, D. E., and S. J. KORSMEYER, 1997 Bcl-2 gene family in the nervous system. Annu Rev Neurosci **20:** 245-267.

METZSTEIN, M. M., M. O. HENGARTNER, N. TSUNG, R. E. ELLIS and H. R. HORVITZ, 1996 Transcriptional regulator of programmed cell death encoded by *Caenorhabditis elegans* gene *ces-2*. Nature **382:** 545-547.

METZSTEIN, M. M., and H. R. HORVITZ, 1999 The *C. elegans* cell death specification gene *ces-1* encodes a snail family zinc finger protein. Mol Cell **4:** 309-319.

MIHARA, M., S. ERSTER, A. ZAIKA, O. PETRENKO, T. CHITTENDEN *et al.*, 2003 p53 has a direct apoptogenic role at the mitochondria. Mol Cell **11:** 577-590.

MIURA, M., H. ZHU, R. ROTELLO, E. A. HARTWIEG and J. YUAN, 1993 Induction of apoptosis in fibroblasts by IL-1 beta-converting enzyme, a mammalian homolog of the *C. elegans* cell death gene *ced-3*. Cell **75:** 653-660.

MOTOYAMA, N., F. WANG, K. A. ROTH, H. SAWA, K. NAKAYAMA *et al.*, 1995 Massive cell death of immature hematopoietic cells and neurons in Bcl-x-deficient mice. Science **267:** 1506-1510.

NAKANO, K., and K. H. VOUSDEN, 2001 *PUMA*, a novel proapoptotic gene, is induced by p53. Mol Cell **7:** 683-694.

NICHOLSON, D. W., 1999 Caspase structure, proteolytic substrates, and function during apoptotic cell death. Cell Death Differ **6:** 1028-1042.

NOURSE, J., J. D. MELLENTIN, N. GALILI, J. WILKINSON, E. STANBRIDGE *et al.*, 1990 Chromosomal translocation t(1;19) results in synthesis of a homeobox fusion mRNA that codes for a potential chimeric transcription factor. Cell **60:** 535-545.

ODA, E., R. OHKI, H. MURASAWA, J. NEMOTO, T. SHIBUE *et al.*, 2000 Noxa, a BH3-only member of the Bcl-2 family and candidate mediator of p53-induced apoptosis. Science **288:** 1053-1058.

OKADA, H., W. K. SUH, J. JIN, M. WOO, C. DU *et al.*, 2002 Generation and characterization of Smac/DIABLO-deficient mice. Mol Cell Biol **22:** 3509-3517.

PARK, D., H. JIA, V. RAJAKUMAR and H. M. CHAMBERLIN, 2006 Pax2/5/8 proteins promote cell survival in *C. elegans*. Development **133:** 4193-4202.

PEDEN, E., E. KIMBERLY, K. GENGYO-ANDO, S. MITANI and D. XUE, 2007 Control of sex-specific apoptosis in *C. elegans* by the BarH homeodomain protein CEH-30 and the transcriptional repressor UNC-37/Groucho. Genes Dev **21:** 3195-3207.

PFLUGRAD, A., J. Y. MEIR, T. M. BARNES and D. M. MILLER, 3RD, 1997 The Groucho-like transcription factor UNC-37 functions with the neural specificity gene *unc-4* to govern motor neuron identity in *C. elegans*. Development **124:** 1699-1709.

POTTS, P. R., S. SINGH, M. KNEZEK, C. B. THOMPSON and M. DESHMUKH, 2003 Critical function of endogenous XIAP in regulating caspase activation during sympathetic neuronal apoptosis. J Cell Biol **163:** 789-799.

PUTHALAKATH, H., and A. STRASSER, 2002 Keeping killers on a tight leash: transcriptional and post-translational control of the pro-apoptotic activity of BH3-only proteins. Cell Death Differ **9:** 505-512.

REDDIEN, P. W., 2002 Phagocytosis promotes programmed cell death and is controlled by Rac signaling pathway in *C. elegans*. Ph. D. Thesis, Massachusetts Institute of Technology, Cambridge, MA.

REDDIEN, P. W., E. C. ANDERSEN, M. C. HUANG and H. R. HORVITZ, 2007 DPL-1 DP, LIN-35 Rb and EFL-1 E2F act with the MCD-1 zinc-finger protein to promote programmed cell death in *Caenorhabditis elegans*. Genetics **175:** 1719-1733.

REDDIEN, P. W., S. CAMERON and H. R. HORVITZ, 2001 Phagocytosis promotes programmed cell death in *C. elegans*. Nature **412:** 198-202.

ROBERTSON, A. M. G., and J. N. THOMPSON, 1982 Ultrastructural study of cell death in *Caenorhabditis elegans*. J Embryol Exp Morphol **67:** 89-100.

ROUGVIE, A. E., and V. AMBROS, 1995 The heterochronic gene *lin-29* encodes a zinc finger protein that controls a terminal differentiation event in *Caenorhabditis elegans*. Development **121:** 2491-2500.

ROY, N., Q. L. DEVERAUX, R. TAKAHASHI, G. S. SALVESEN and J. C. REED, 1997 The c-IAP-1 and c-IAP-2 proteins are direct inhibitors of specific caspases. Embo J **16:** 6914-6925.

SATTLER, M., H. LIANG, D. NETTESHEIM, R. P. MEADOWS, J. E. HARLAN *et al.*, 1997 Structure of Bcl-xL-Bak peptide complex: recognition between regulators of apoptosis. Science **275:** 983-986.

SAVILL, J., and C. HASLETT, 1995 Granulocyte clearance by apoptosis in the resolution of inflammation. Semin Cell Biol **6:** 385-393.

SCHERTEL, C., and B. CONRADT, 2007 *C. elegans* orthologs of components of the RB tumor suppressor complex have distinct pro-apoptotic functions. Development **134:** 3691-3701.

SCHUMACHER, B., C. SCHERTEL, N. WITTENBURG, S. TUCK, S. MITANI *et al.*, 2005 *C. elegans ced-13* can promote apoptosis and is induced in response to DNA damage. Cell Death Differ **12:** 153-161.

SCHWARTZ, H. T., and H. R. HORVITZ, 2007 The *C. elegans* protein CEH-30 protects male-specific neurons from apoptosis independently of the Bcl-2 homolog CED-9. Genes Dev **21**.

SEVRIOUKOV, E. A., J. BURR, E. W. HUANG, H. H. ASSI, J. P. MONSERRATE *et al.*, 2007 *Drosophila* Bcl-2 proteins participate in stress-induced apoptosis, but are not required for normal development. Genesis **45:** 184-193.

SHAHAM, S., and H. R. HORVITZ, 1996 Developing *Caenorhabditis elegans* neurons may contain both cell-death protective and killer activities. Genes Dev **10:** 578-591.

SHAHAM, S., P. W. REDDIEN, B. DAVIES and H. R. HORVITZ, 1999 Mutational analysis of the *Caenorhabditis elegans* cell-death gene *ced-3*. Genetics **153:** 1655-1671.

SHI, Y., 2002 Mechanisms of caspase activation and inhibition during apoptosis. Mol Cell **9:** 459-470.

SHI, Y., 2004 Caspase activation, inhibition, and reactivation: a mechanistic view. Protein Sci **13:** 1979-1987.

SHREFFLER, W., T. MAGARDINO, K. SHEKDAR and E. WOLINSKY, 1995 The *unc-8* and *sup-40* genes regulate ion channel function in *Caenorhabditis elegans* motorneurons. Genetics **139:** 1261-1272.

SINGHVI, A., C. A. FRANK and G. GARRIGA, 2008 The T-Box Gene *tbx-2*, the Homeobox Gene *egl-5* and the Asymmetric Cell Division Gene *ham-1* Specify Neural Fate in the HSN/PHB Lineage. Genetics **179:** 887-898.

SPECTOR, M. S., S. DESNOYERS, D. J. HOEPPNER and M. O. HENGARTNER, 1997 Interaction between the C. elegans cell-death regulators CED-9 and CED-4. Nature **385:** 653-656.

SPELIOTES, E. K., 2000 *C. elegans* BIR-1 acts with the Aurora-like kinase AIR-2 to affect chromosomes and the spindle midzone. Ph. D. Thesis, Massachusetts Institute of Technology, Cambridge, MA.

STANFIELD, G. M., and H. R. HORVITZ, 2000 The *ced-8* gene controls the timing of programmed cell deaths in *C. elegans*. Mol Cell **5:** 423-433.

STELLER, H., 2008 Regulation of apoptosis in *Drosophila*. Cell Death Differ **15:** 1132-1138.

STERGIOU, L., and M. O. HENGARTNER, 2004 Death and more: DNA damage response pathways in the nematode *C. elegans*. Cell Death Differ **11:** 21-28.

SULSTON, J. E., 1976 Post-embryonic development in the ventral cord of *Caenorhabditis elegans*. Philos Trans R Soc Lond B Biol Sci **275:** 287-297.

SULSTON, J. E., D. G. ALBERTSON and J. N. THOMSON, 1980 The *Caenorhabditis elegans* male: postembryonic development of nongonadal structures. Dev Biol **78:** 542-576.

SULSTON, J. E., and H. R. HORVITZ, 1977 Post-embryonic cell lineages of the nematode, *Caenorhabditis elegans*. Dev Biol **56:** 110-156.

SULSTON, J. E., E. SCHIERENBERG, J. G. WHITE and J. N. THOMSON, 1983 The embryonic cell lineage of the nematode *Caenorhabditis elegans*. Dev Biol **100:** 64-119.

SZE, J. Y., M. VICTOR, C. LOER, Y. SHI and G. RUVKUN, 2000 Food and metabolic signalling defects in a *Caenorhabditis elegans* serotonin-synthesis mutant. Nature **403:** 560-564.

THELLMANN, M., J. HATZOLD and B. CONRADT, 2003 The Snail-like CES-1 protein of *C. elegans* can block the expression of the BH3-only cell-death activator gene *egl-1* by antagonizing the function of bHLH proteins. Development **130:** 4057-4071.

THORNBERRY, N. A., and Y. LAZEBNIK, 1998 Caspases: enemies within. Science **281:** 1312-1316.

TREININ, M., and M. CHALFIE, 1995 A mutated acetylcholine receptor subunit causes neuronal degeneration in *C. elegans*. Neuron **14:** 871-877.

TRENT, C., N. TSUING and H. R. HORVITZ, 1983 Egg-laying defective mutants of the nematode *Caenorhabditis elegans*. Genetics **104:** 619-647.

TSUJIMOTO, Y., L. R. FINGER, J. YUNIS, P. C. NOWELL and C. M. CROCE, 1984 Cloning of the chromosome breakpoint of neoplastic B cells with the t(14;18) chromosome translocation. Science **226:** 1097-1099.

VAUX, D. L., S. CORY and J. M. ADAMS, 1988 *Bcl-2* gene promotes haemopoietic cell survival and cooperates with c-myc to immortalize pre-B cells. Nature **335:** 440-442.

VAUX, D. L., and S. J. KORSMEYER, 1999 Cell death in development. Cell **96:** 245-254.

VAUX, D. L., I. L. WEISSMAN and S. K. KIM, 1992 Prevention of programmed cell death in *Caenorhabditis elegans* by human *bcl-2*. Science **258:** 1955-1957.

VERHAGEN, A. M., P. G. EKERT, M. PAKUSCH, J. SILKE, L. M. CONNOLLY *et al.*, 2000 Identification of DIABLO, a mammalian protein that promotes apoptosis by binding to and antagonizing IAP proteins. Cell **102:** 43-53.

VERHAGEN, A. M., J. SILKE, P. G. EKERT, M. PAKUSCH, H. KAUFMANN *et al.*, 2002 HtrA2 promotes cell death through its serine protease activity and its ability to antagonize inhibitor of apoptosis proteins. J Biol Chem **277:** 445-454.

WANG, B. B., M. M. MULLER-IMMERGLUCK, J. AUSTIN, N. T. ROBINSON, A. CHISHOLM *et al.*, 1993 A homeotic gene cluster patterns the anteroposterior body axis of *C. elegans*. Cell **74:** 29-42.

WANG, K., X. M. YIN, D. T. CHAO, C. L. MILLIMAN and S. J. KORSMEYER, 1996 BID: a novel BH3 domain-only death agonist. Genes Dev **10:** 2859-2869.

WANG, S. L., C. J. HAWKINS, S. J. YOO, H. A. MULLER and B. A. HAY, 1999 The *Drosophila* caspase inhibitor DIAP1 is essential for cell survival and is negatively regulated by HID. Cell **98:** 453-463.

WANG, X., and H. M. CHAMBERLIN, 2002 Multiple regulatory changes contribute to the evolution of the *Caenorhabditis lin-48 ovo* gene. Genes Dev **16:** 2345-2349.

WEI, M. C., W. X. ZONG, E. H. CHENG, T. LINDSTEN, V. PANOUTSAKOPOULOU *et al.*, 2001 Proapoptotic BAX and BAK: a requisite gateway to mitochondrial dysfunction and death. Science **292:** 727-730.

WHITE, K., M. E. GRETHER, J. M. ABRAMS, L. YOUNG, K. FARRELL *et al.*, 1994 Genetic control of programmed cell death in *Drosophila*. Science **264:** 677-683.

WILLIS, S. N., and J. M. ADAMS, 2005 Life in the balance: how BH3-only proteins induce apoptosis. Curr Opin Cell Biol **17:** 617-625.

WU, D., H. D. WALLEN, N. INOHARA and G. NUNEZ, 1997 Interaction and regulation of the *Caenorhabditis elegans* death protease CED-3 by CED-4 and CED-9. J Biol Chem **272:** 21449-21454.

WU, W. S., S. HEINRICHS, D. XU, S. P. GARRISON, G. P. ZAMBETTI *et al.*, 2005 Slug antagonizes p53-mediated apoptosis of hematopoietic progenitors by repressing *puma*. Cell **123:** 641-653.

XUE, D., S. SHAHAM and H. R. HORVITZ, 1996 The *Caenorhabditis elegans* cell-death protein CED-3 is a cysteine protease with substrate specificities similar to those of the human CPP32 protease. Genes Dev **10:** 1073-1083.

YAMAMOTO, K., H. ICHIJO and S. J. KORSMEYER, 1999 BCL-2 is phosphorylated and inactivated by an ASK1/Jun N-terminal protein kinase pathway normally activated at G(2)/M. Mol Cell Biol **19:** 8469-8478.

YAN, N., J. CHAI, E. S. LEE, L. GU, Q. LIU *et al.*, 2004 Structure of the CED-4–CED-9 complex provides insights into programmed cell death in *Caenorhabditis elegans*. Nature **437:** 831-837.

YAN, N., and Y. SHI, 2005 Mechanisms of apoptosis through structural biology. Annu Rev Cell Dev Biol **21:** 35-56.

YAN, W., A. Z. YOUNG, V. C. SOARES, R. KELLEY, R. BENEZRA *et al.*, 1997 High incidence of T-cell tumors in E2A-null mice and E2A/Id1 double-knockout mice. Mol Cell Biol **17:** 7317-7327.

YANG, X., H. Y. CHANG and D. BALTIMORE, 1998 Essential role of CED-4 oligomerization in CED-3 activation and apoptosis. Science **281:** 1355-1357.

YU, J., L. ZHANG, P. M. HWANG, K. W. KINZLER and B. VOGELSTEIN, 2001 PUMA induces the rapid apoptosis of colorectal cancer cells. Mol Cell **7:** 673-682.

YUAN, J., and H. R. HORVITZ, 1992 The *Caenorhabditis elegans* cell death gene *ced-4* encodes a novel protein and is expressed during the period of extensive programmed cell death. Development **116:** 309-320.

YUAN, J., S. SHAHAM, S. LEDOUX, H. M. ELLIS and H. R. HORVITZ, 1993 The *C. elegans* cell death gene *ced-3* encodes a protein similar to mammalian interleukin-1 beta-converting enzyme. Cell **75:** 641-652.

YUAN, J. Y., and H. R. HORVITZ, 1990 The *Caenorhabditis elegans* genes *ced-3* and *ced-4* act cell autonomously to cause programmed cell death. Dev Biol **138:** 33-41.

ZARKOWER, D., and J. HODGKIN, 1992 Molecular analysis of the *C. elegans* sex-determining gene *tra-1*: a gene encoding two zinc finger proteins. Cell **70:** 237-249.

ZOU, H., W. J. HENZEL, X. LIU, A. LUTSCHG and X. WANG, 1997 Apaf-1, a human protein homologous to *C. elegans* CED-4, participates in cytochrome c-dependent activation of caspase-3. Cell **90:** 405-413.

Table 1. Regulators of specific programmed cell deaths in *C. elegans*

Cell(s)	gene	Homolog	Function in cell death	Other functions	Ref
HSN neurons	*tra-1*	GLI3	Inhibits HSN death. Regulates *egl-1*.	Sex determination	**1,2**
HSN neurons	*eor-1*	PLZF	Promotes HSN death. Likely regulates *egl-1*.	Ras and Wnt signaling. Neuronal development.	**3,4**
HSN neurons	*eor-2*	KIAA1205	Promotes HSN death. Likely regulates *egl-1*.	Ras and Wnt signaling. Neuronal development.	**3,4**
NSM, I2 sisters	*ces-1*	Slug	Inhibits NSM and I2 sister death. Regulates *egl-1*.	Asymmetric cell division	**5,6, 7,8**
NSM sisters	*ces-2*	HLF	Promotes NSM sister cell death. Inhibits *ces-1*.	Duct cell morphogenesis. Asymmetric cell division.	**5,6,8 9,10**
NSM sisters	*dnj-11*	MIDA1	Promotes NSM sister cell death. Inhibits *ces-1*.	Asymmetric cell division. Morphogenesis, viability.	**8**
NSM sisters	*hlh-2*	Daughterless	Promotes NSM sister cell death. Regulates *egl-1*.	Embryogenesis	**7,11**
NSM sisters	*hlh-3*	Achaete-scute	Promotes NSM sister cell death. Regulates *egl-1*.	Unknown	**7**
P11,P12.a aap	*mab-5*	Hox genes	Promotes P11,P12.aaap death. Regulates *egl-1*.	Posterior cell fates	**12, 13**
P11,P12.a aap	*ceh-20*	Pbx1	Promotes P11,P12.aaap death. Regulates *egl-1*.	Mesoderm patterning	**12, 14**
Tail spike cell	*pal-1*	Caudal	Promotes tail spike cell death. Regulates *ced-3*.	Posterior cell fates	**15, 16**
CEM neurons	*ceh-30*	Barhl1	Promotes CEM survival. Does not require *ced-9*.	Unknown	**17, 18**
CEM neurons	*unc-37*	Groucho	Promotes CEM survival	Motor neuron identity	**18, 19**
Linker cell	*lin-29*	Zinc finger txn. factors	Promotes adult-specific linker cell death	Promotes adult cell fates	**20, 21**

A list of genes known to regulate specific programmed cell deaths in *C. elegans*. Homologs, functions in the regulation of cell death, and other known functions are indicated. References are: **1** (CONRADT and HORVITZ 1999), **2** (ZARKOWER and HODGKIN 1992); **3** (HOEPPNER *et al.* 2004); **4** (HOWARD and SUNDARAM 2002); **5** (ELLIS and HORVITZ 1991); **6** (METZSTEIN and HORVITZ 1999); **7** (THELLMANN *et al.* 2003); **8** (HATZOLD and CONRADT 2008); **9** (METZSTEIN *et al.* 1996); **10** (WANG and CHAMBERLIN 2002); **11** (KRAUSE *et al.* 1997); **12** (LIU *et al.* 2006); **13** (WANG *et al.* 1993); **14** (LIU and FIRE 2000); **15** (MAURER *et al.* 2007); **16** (EDGAR *et al.* 2001); **17** (SCHWARTZ and

HORVITZ 2007); **18** (PEDEN *et al.* 2007); **19** (PFLUGRAD *et al.* 1997); **20** (ABRAHAM *et al.* 2007), **21** (ROUGVIE and AMBROS 1995)

Figure legends

Figure 1

An evolutionarily conserved core pathway for the execution of programmed cell death. A. Programmed cell death can be broken into four conceptually separate steps: a healthy cell I specified to undergo programmed cell death, the cell is killed in the execution phase of programmed cell death, the dying cell is engulfed by its neighbors, and the engulfed cell is degraded. B. The evolutionarily conserved core pathway for the execution of programmed cell death. The BH3-only protein EGL-1 binds the Bcl-2 homolog CED-9 and inhibits its protective function. Released from inhibition by CED-9, the adaptor protein CED-4, a homolog of Apaf-1, promotes the activation of the caspase CED-3. Active CED-3 performs the cell-killing function.

Figure 2

Genetic pathways reflecting the current models of how genes control specific apoptotic deaths in *C. elegans*. Note that in the majority of these cells the identified cell-specific regulators act as regulators of the upstream cell-killing gene *egl-1*. In the tail spike cell, *pal-1* acts downstream of *egl-1* and *ced-9* by direct transcriptional regulation of *ced-3*. In the CEM neurons, *ceh-30* acts downstream of *egl-1* and *ced-9*; because the cell-death target of *ceh-30* is not known, dotted lines are drawn from *ceh-30* to *ced-4*, to *ced-3*, and independently of both *ced-4* and *ced-3* directly to cell death. See text for details.

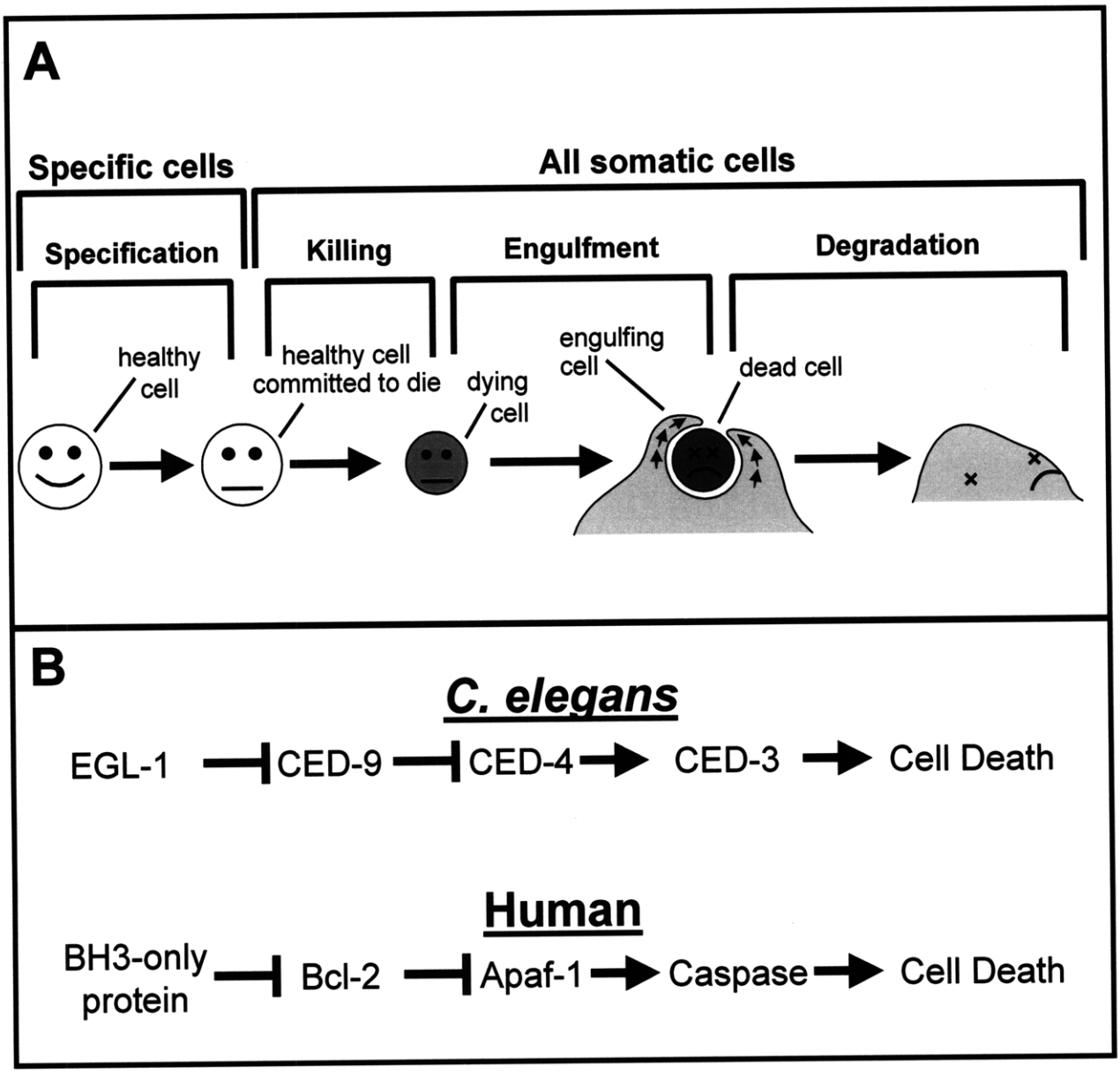
A
Specific cells
All somatic cells
Specification
Killing
Engulfment
Degradation
healthy cell
healthy cell committed to die
dying cell
engulfing cell
dead cell
B
C. elegans
EGL-1
CED-9
CED-4
CED-3
Cell Death
Human
BH3-only protein
Bcl-2
Apaf-1
Caspase
Cell Death

Figure 1

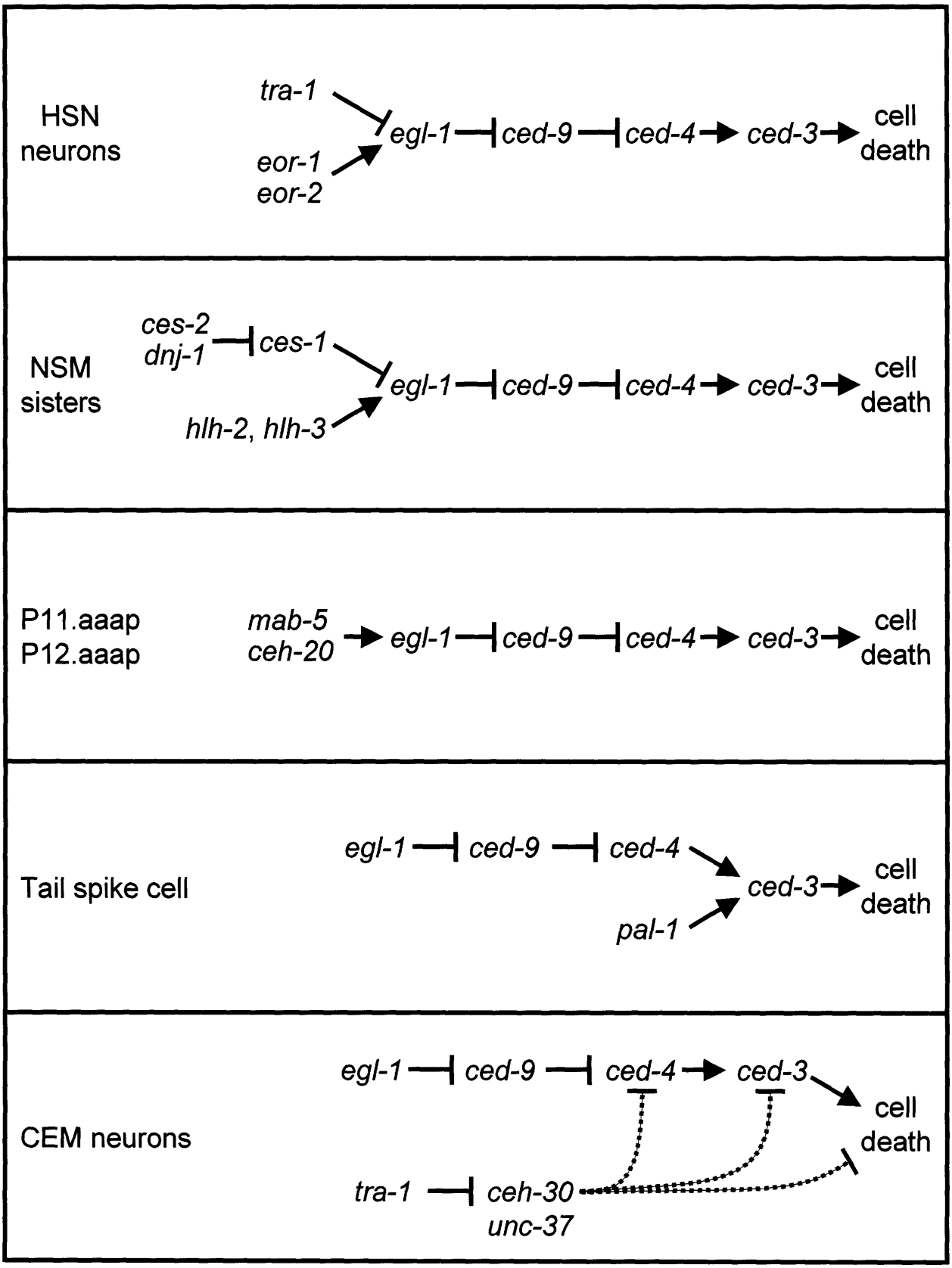
HSN neurons
tra-1
eor-1
eor-2
egl-1
ced-9
ced-4
ced-3
cell death
NSM sisters
ces-2
dnj-1
ces-1
hlh-2, hlh-3
egl-1
ced-9
ced-4
ced-3
cell death
P11.aaap
P12.aaap
mab-5
ceh-20
egl-1
ced-9
ced-4
ced-3
cell death
Tail spike cell
egl-1
ced-9
ced-4
ced-3
pal-1
cell death
CEM neurons
egl-1
ced-9
ced-4
ced-3
cell death
tra-1
ceh-30
unc-37

Figure 2

Chapter II

A genetic pathway that controls the sexually dimorphic cell deaths of the *C. elegans* CEM neurons

Hillel T. Schwartz and H. Robert Horvitz

Abstract

The male-specific CEM sensory neurons of *C. elegans* function in the detection of hermaphrodites. The homologous cells in hermaphrodites undergo programmed cell death. To understand how the sexually dimorphic CEM neurons are determined to follow their proper developmental program, establish their sexual identity, and specifically undergo programmed cell death in hermaphrodites, we screened for mutant hermaphrodites in which the CEM neurons inappropriately survive. We identified 144 independent mutations that cause the presence of CEMs in hermaphrodites. Of these mutations, 52 are alleles of genes known to function in the execution of all programmed cell deaths and at least 67 cause masculinization of hermaphrodites. Four mutations defined the gene *tra-4*, which encodes a zinc-finger transcription factor required for complete masculinization. Three gain-of-function mutations defined the Bar homeodomain transcription factor gene *ceh-30*, a critical regulator of CEM survival. Five isolates carried mutations in genes that determine neuronal fates, *vab-3 Pax6* and *cnd-1 NeuroD*, which specify multiple aspects of the CEM neuron identity and act together in the establishment of head morphology. Based on our studies, we propose a genetic pathway for the control of the sexually dimorphic deaths of the CEM neurons.

Introduction

Cells generated during animal development adopt specific fates. One important cell-fate decision that cells make is whether to survive or to undergo a controlled process of programmed cell death called apoptosis. When the proper developmental control of apoptosis is lost, excessive or insufficient apoptosis can occur, resulting in pathological consequences. In humans, excessive cell death is associated with immunodeficiency and with neurodegenerative diseases (RATHMELL and THOMPSON 2002; YEO and GAUTIER 2004). Conversely, the failure of cells to properly undergo apoptosis is a hallmark of some autoimmune disorders and of cancer (WEAVER and CLEVELAND 2005; BIDERE *et al.* 2006).

Cells specified to die undergo a process of cell death that is evolutionarily conserved from nematodes to mammals. Key insights into the core pathway for the execution of programmed cell death came from genetic studies of *C. elegans* (METZSTEIN *et al.* 1998). In *C. elegans*, the cell-death process is initiated by the expression of the BH3-only killer gene *egl-1* (*egl*, egg-laying defective) (CONRADT and HORVITZ 1998). EGL-1 binds to CED-9 (*ced*, cell death abnormal), the sole multidomain Bcl-2 family member in *C. elegans* (HENGARTNER and HORVITZ 1994b). CED-9 provides an essential cell-protective function and a secondary function that can promote cell killing (HENGARTNER *et al.* 1992; HENGARTNER and HORVITZ 1994a). Binding of CED-9 by EGL-1 inhibits the cell-protective function of *ced-9* and activates the adaptor molecule CED-4 Apaf-1 (YUAN and HORVITZ 1992; CHEN *et al.* 2000; YAN *et al.* 2004). CED-4, like its mammalian homolog Apaf-1 (ZOU *et al.* 1997), promotes the cell-killing activity of cysteine proteases known as caspases (SHAHAM and HORVITZ 1996; YANG *et al.* 1998).

The *C. elegans* caspase activated by CED-4 is encoded by *ced-3* (YUAN *et al.* 1993), the most downstream gene in the core pathway for cell killing.

In contrast to the wealth of information about how cells committed to die progress through apoptosis, little is known about the developmental mechanisms that specify whether cells are to survive or to die. In mammals, the protection of developing neurons by neurotrophic signals and the induction of apoptosis in immune system cells that recognize self-antigens have been described (WEAVER and CLEVELAND 2005; BIDERE *et al.* 2006). In *C. elegans*, 1090 somatic cells are generated in the hermaphrodite, of which 131 undergo programmed cell death (SULSTON and HORVITZ 1977; KIMBLE and HIRSH 1979; SULSTON *et al.* 1983). Another 21 somatic cells that either do not die or are never generated during hermaphrodite development die during male development. Fourteen genes that exert cell-specific control over fourteen of these 152 cell deaths have been described; all are believed to encode transcription factors (ELLIS and HORVITZ 1991; METZSTEIN *et al.* 1996; CONRADT and HORVITZ 1999; METZSTEIN and HORVITZ 1999; THELLMANN *et al.* 2003; HOEPPNER *et al.* 2004; LIU *et al.* 2006; ABRAHAM *et al.* 2007; MAURER *et al.* 2007; PEDEN *et al.* 2007; SCHWARTZ and HORVITZ 2007; HATZOLD and CONRADT 2008). Mutations in mammalian homologs of many of these cell-specific regulators of apoptosis can contribute to disease. For example, *ces-1* and *ces-2* (*ces*, cell death specification), *C. elegans* genes that specifically regulate the deaths of the sister cells of the NSM neurons (ELLIS and HORVITZ 1991; METZSTEIN *et al.* 1996; METZSTEIN and HORVITZ 1999), have human homologs that can regulate B cell survival in humans, and translocations altering the *ces-2* homolog *HLF* cause Acute Lymphoblastic Leukemia (INABA *et al.* 1996; WU *et al.* 2005).

To better understand the control of the survival decisions of specific cells and the interactions between this decision and other aspects of the cell-fate decision, we performed large-scale genetic screens for mutants defective in the specification of four cell deaths, those of the CEM neurons of hermaphrodites, and examined the contributions of known regulators of programmed cell death to this decision. The CEM neurons are generated in both males and hermaphrodites and in hermaphrodites but not in males undergo programmed cell death during embryogenesis; the CEM sensory neurons of males survive and function in the detection of mating partners (SULSTON *et al.* 1983; CHASNOV *et al.* 2007). We describe studies that led to our identification of two genes, the *CDC4* homolog *sel-10* and the *PLZF* homolog *tra-4*, that function to establish sexual identity of the CEM neurons and of the entire animal; two genes, the *Pax6* homolog *vab-3* and the *NeuroD* homolog *cnd-1*, that function to establish multiple aspects of the CEM identity and that cooperate in head morphogenesis. We also expand our characterization of the *Barhl1* homolog *ceh-30*, which we previously identified as a CEM-specific survival factor in work arising from the screens we describe here (SCHWARTZ and HORVITZ 2007) and which we now report acts redundantly with its close homolog *ceh-31* in the establishment of CEM identity. We find that genes that regulate the survival decision of the CEM neurons are also required to specify other aspects of the CEM neuron identity. Finally, we propose a pathway for the survival decision of the CEM neurons.

Results

Genetic screens for mutant hermaphrodites with surviving CEMs

To identify genes that control the fate determination and the sex-specific apoptotic deaths of the CEM neurons, we performed genetic screens for mutant hermaphrodites in which the normally male-specific CEM neurons had failed to die. To facilitate these screens, we used the cell-fate reporter *pkd-2::gfp*, which expresses in the CEM neurons of males and in selected neurons of the male tail that are not generated in hermaphrodites (BARR and STERNBERG 1999). The *pkd-2::gfp* reporter expresses in the surviving CEMs of partially masculinized hermaphrodites and in the undead CEMs of hermaphrodites defective in programmed cell death (Figure 1) (SCHWARTZ and HORVITZ 2007). Using three *pkd-2::gfp* reporter transgenes, each integrated on a different chromosome, we screened more than 150,000 hermaphrodite F_2 progeny of EMS-mutagenized animals (at least 75,000 mutagenized haploid genomes). On the basis of their arising from different pools of independently mutagenized P_0s, their differing mutant phenotypes, and the results of complementation tests, mapping experiments, and DNA sequences (see below), 189 strains were identified as containing independent mutations causing *pkd-2::gfp* expression or autofluorescence in hermaphrodites and were saved for further analysis. Of these 189 screen isolates, 45 had *pkd-2::gfp* expression in hermaphrodites but did not contain apparent surviving CEM neurons or had autofluorescence independent of the *pkd-2::gfp* reporter; these isolates are described in Chapter IV and in Appendix II. The 144 independent isolates that displayed apparent CEM survival are listed in Table 1.

Isolates that showed apparent CEM neuron survival in hermaphrodites were examined for gross phenotypes consistent with a sexual transformation from a hermaphrodite to a male sexual identity. Fifty isolates showed partially penetrant CEM

survival in hermaphrodites and segregated a substantial proportion of male progeny (roughly one in four). These 50 isolates were therefore classified as likely to be carrying heterozygous mutations dominantly causing weak masculinization, including CEM neuron survival, and recessively causing essentially complete masculinization. Such dominant weak masculinization and recessive strong masculinization is caused by strong loss-of-function mutations in the sex determination genes *tra-1* and *tra-2* (*tra*, sexual transformer), genes that are required for the hermaphrodite sexual identity (HODGKIN 2002); such haploinsufficiency for complete expression of the hermaphrodite sexual identity has been previously observed for the sexually dimorphic survival of the HSN neurons in animals heterozygous for the strong *tra-2* loss-of-function mutation *n196* (TRENT *et al.* 1983; DESAI and HORVITZ 1989). Twelve additional isolates did not segregate completely masculinized progeny but did have other gross phenotypic defects consistent with a partial masculinization: the isolates possessed *pkd-2::gfp*-expressing cells in the tail and/or expressed a Pvl (protruding vulva) phenotype similar to that seen for intersex animals (date not shown).

Isolates that had apparent surviving CEM neurons in hermaphrodites and did not show gross indications of sexual transformation were tested for complementation with loss-of-function mutations in the cell-death genes *egl-1*, *ced-4*, and *ced-3*. From these and other experiments (see below), 48 isolates were identified as being alleles of *ced-3* or *ced-4*. The remaining 34 isolates – those that did not show obvious signs of sexual transformation and that by complementation did not appear to be alleles the programmed cell death genes *ced-3* and *ced-4* - were examined for the penetrance of their CEM survival phenotype, their anterior pharynxes were scored for the

inappropriate survival of cells that should normally undergo programmed cell death, and the sizes and morphology of their B cells in L1 larvae were examined. The B cells provide an easy assay with which to detect somatic masculinization: the B cells of of male L1 larvae are larger than those of L1 hermaphrodites and have a distinctive morphology (see Materials and Methods). Seventeen of the remaining screen isolates were selected for further analysis because they had strong CEM survival phenotypes, had been mapped to positions distinct from any genes known to function in programmed cell death or in sex determination, or in the case of three allelic isolates because additional defects indicative of a motor neuron defect suggested broadly acting functions in neuronal differentiation or survival. These 17 isolates were found to contain mutations in the genes *ced-9*, *sel-10*, *tra-4*, *ceh-30*, *cnd-1*, and *vab-3*. A list of all molecularly identified mutations isolated in the *pkd-2::gfp* screens for hermaphrodites with surviving CEM neurons is shown in Table 2. A partial characterization of the remaining unidentified mutations that did not cause apparent defects in programmed cell death and did not cause obvious defects in sexual identity is shown in Table 3.

ced-3 mutations define a common allelic series in the CEM neurons and in other tissues

One *ced-3* allele recovered in the screens, *ced-3(n4707)*, was found not to contain any detectable mutation in the *ced-3* coding sequence, splice junctions, or within the 2,359 bp upstream of the *ced-3* start codon. *ced-3(n4707)* failed to complement *ced-3(n717)* and mapped to a ~373 kb interval containing *ced-3* (see Materials and Methods). Because *ced-3(n4707)* did not alter the *ced-3* coding

sequence, it was possible that in this mutant the expression of *ced-3* might be affected in a specific subset of cells fated to undergo programmed cell death, including the CEM neurons. To address this issue, the strength of the cell-death defect caused by *ced-3(n4707)* was examined in three assays (Table 4): survival of the CEM neurons of hermaphrodites; suppression of the Egl phenotype caused by inappropriate HSN death in *egl-1(n1084*gf*)* hermaphrodites; and survival of additional cells in the anterior pharynx, a tissue that can contain up to 16 surviving cells possessing at least ten distinguishable cell fates (HENGARTNER and HORVITZ 1994a). The strength of the *ced-3(n4707)* killing defect in these assays was compared to a series of *ced-3* missense mutations associated with intermediate defects in cell killing: *ced-3(n2436*, *n2438*, *n2877*, and *n2921)* (Table 4). It was found that in each of the three tissues tested, these five partial-loss-of-function alleles of *ced-3* could be ordered in the same allelic series. As the four additional *ced-3* partial-loss-of-function alleles caused changes in the CED-3 protein sequences that would similarly affect CED-3 in all cell types, it is likely that the apparent noncoding mutation *ced-3(n4707)* affects the level of *ced-3* expression similarly in multiple tissues or in all tissues, rather than in a specific subset of cells that includes the CEM neurons.

The noncoding *egl-1* allele *n4908*Δ specifically affects the deaths of the CEM neurons

The *egl-1* allele *n4908*Δ is a noncoding 309 bp deletion that was recovered as a targeted deletion that spans a site required for *egl-1* cell-killing function in the Pn.aap lineage (B. Galvin and H.R.H., personal communication). We found that the

egl-1(n4908Δ) mutant does not affect all programmed cell deaths: specifically, *egl-1(n4908Δ)* does not cause the survival of extra cells in the anterior pharynx (Table 5A). No protective effect of *egl-1(n4908Δ)* was seen in this tissue even in *ced-3(n2427)* animals weakly defective in programmed cell death, a sensitized genetic background previously shown to facilitate the detection of extremely weak defects in cell killing (STANFIELD and HORVITZ 2000; REDDIEN *et al.* 2001; REDDIEN *et al.* 2007). We found that the *egl-1* noncoding deletion *n4908Δ* blocked the deaths of the CEM neurons in hermaphrodites and in males specifically defective in CEM neuron survival (Table 5B). The BH3-only protein EGL-1 has previously been shown to promote programmed cell death in a process dependent on the cell-protective Bcl-2 homolog CED-9 (CONRADT and HORVITZ 1998). As would be expected for a mutation affecting *egl-1* function, the protection of the CEMs by *n4908Δ* was entirely dependent on *ced-9* function (Table 5C). *egl-1(n4908Δ)* therefore disrupts *egl-1* function in a limited number of cell types that includes the Pn.aap cells and the CEM neurons but not the cells of the anterior pharynx. Because *egl-1(n4908Δ)* is a noncoding mutation, it seems likely this deletion removes a site required for the binding of the *egl-1* locus by an unidentified factor that promotes *egl-1* expression in the CEM neurons. A single nucleotide change within the same region that prevents the deaths of the Pn.aap neurons (B. Galvin and H.R.H., unpublished results) does not affect CEM survival, suggesting that two different sites with in the region deleted by *n4908Δ* function to controls these two programmed cell deaths.

New *ced-9(gf)* mutations affecting the EGL-1-interacting surface of CED-9 prevent the deaths of cells programmed to die

Four of our mutations – *n4081*, *n4698*, *n4700*, and *n4713* – semidominantly caused partial CEM survival in hermaphrodites and were not identified as being allelic with loss-of-function mutations in the cell-death genes *ced-3*, *ced-4*, or *egl-1* by complementation tests. We found that each of these four mutations semidominantly caused survival of extra cells in the anterior pharynx and caused survival of Pn.aap neurons fated to die in the developing ventral nerve cord (Table 6 and data not shown). Each of these four mutations mapped close to the right of *unc-32 III*, a position consistent with that of the cell-death protective gene *ced-9* (data not shown). We determined the DNA sequence of *ced-9* in these mutants and identified a predicted G169R missense mutation in *n4700* and identical lesions, each causing a predicted G173D missense mutation, in the independently isolated mutations *n4081*, *n4698*, and *n4713*. The published crystal structure of the CED-9-EGL-1 protein interaction interface (YAN *et al.* 2004) indicates that these mutations could have effects very similar to those of the canonical *ced-9* gain-of-function (gf) mutation, *n1950*, which causes the change G169E (HENGARTNER and HORVITZ 1994a) and disrupts the interaction surface for binding between the BH3-only cell-killing protein EGL-1 and the Bcl-2 homolog CED-9 (DEL PESO *et al.* 2000; YAN *et al.* 2004).

In addition to the assays shown in Table 6, *ced-9(n4700*gf*)* and *ced-9(n4713*gf*)* completely suppressed the egg-laying defect caused by inappropriate HSN neuron cell death in *egl-1(n1084*gf*)* hermaphrodites (data not shown) and suppressed the presence of persistent cell corpses in the heads of newly hatched *ced-1(e1875)* larvae defective

in the engulfment and removal of cell corpses (5.3 ± 1.7 corpses for *ced-1*; *ced-9(n4700*gf*)* and 2.8 ± 1.4 corpses for *ced-1*; *ced-9(n4713*gf*)*, compared to 25.8 ± 2.1 corpses for *ced-1*; error is standard deviation, n = 10). *ced-9(n4700*gf*)* and *ced-9(n4713*gf*)* therefore prevent the majority of programmed cell deaths. Despite preventing most programmed cell deaths, *ced-9(n4700*gf*)* and *ced-9(n4713*gf*)* cause only partial survival of the CEM neurons (Table 6). Similarly, although in most tissues the canonical *ced-9* gain-of-function allele *n1950* causes a defect in programmed cell death similar to those caused by strong loss-of-function mutations in *egl-1*, *ced-3* or *ced-4* (HENGARTNER and HORVITZ 1994a; CONRADT and HORVITZ 1998), *ced-9(n1950*gf*)* causes only partial protection of the CEM neurons of hermaphrodites, significantly weaker than that caused by loss of *egl-1*, *ced-3* or *ced-4* (SCHWARTZ and HORVITZ 2007).

Only some contributors to cell killing function in the programmed deaths of the CEM neurons

We tested mutations in genes previously shown to contribute to the cell-killing process in *C. elegans* to determine whether they similarly contribute to the deaths of the CEM neurons in hermaphrodites. One such function is provided by the *Bcl-2* homolog *ced-9*, which in addition to its essential function as a negative regulator of programmed cell death also has a secondary function as a weak activator of programmed cell death (HENGARTNER and HORVITZ 1994a). As previously reported (SCHWARTZ and HORVITZ 2007), loss of the bifunctional cell-death regulator *ced-9* caused by the null mutation *ced-9(n2812)* did not enhance the cell-killing defect caused by the weak *ced-3*

loss-of-function mutation *n2427* in the CEM neurons (Table 7). We observed similar results with another null allele of *ced-9* and with other weak alleles of *ced-3* (data not shown). Thus, although *ced-9* has a killing function in other programmed cell deaths and *ced-9(gf)* mutations block most cell deaths, in the CEM neurons the *ced-9* killing function is not detected and *ced-9(gf)* mutations are only partially effective in protecting the CEM neurons of hermaphrodites. Thus, *ced-9* mutations behave differently in the deaths of the CEM neurons than in most programmed cell deaths.

A set of genes that includes members of the synMuv (synthetic Multivulva) genes, which encode transcriptional regulators, contribute to programmed cell death in multiple tissue types (REDDIEN *et al.* 2007). We tested mutations in two of these genes, the DP homolog *dpl-1* and the zinc-finger gene *mcd-1*, and found that loss-of-function mutations in neither *dpl-1* nor *mcd-1* enhanced the partial CEM survival caused by the weak *ced-3* loss-of-function mutation *n2427* (Table 7). We combined the *ced-9* null mutation *n2812* with either the *dpl-1* loss-of-function mutation or the *mcd-1* loss-of-function mutation, thereby generating mutant strains defective in two mechanisms shown to promote cell killing and to act independently of and additively with each other in other cell types (REDDIEN *et al.* 2007). No enhancement of the weak cell-killing defect caused by *ced-3(n2427)* in the CEM neurons of hermaphrodites was observed in these multiply mutant strains (data not shown). We tested two other mechanisms previously shown to provide minor roles in cell killing, the timing factor *ced-8* XK (STANFIELD and HORVITZ 2000) and the cell-corpse engulfment gene *ced-7 ABC1* (HOEPPNER *et al.* 2001; REDDIEN *et al.* 2001). As seen in other tissues,

these two mechanisms contributed to the programmed cell deaths of the CEM neurons of hermaphrodites (Table 7).

In addition to *egl-1*, a second BH3-only gene, *ced-13*, has been identified and observed to promote programmed cell death in the germline of *C. elegans* (SCHUMACHER *et al.* 2005). We tested whether *ced-13* contributes to the deaths of the CEM neurons (Table 8). To maximize our ability to detect the contribution of an EGL-1 family member in CEM death, we performed these assays in *ceh-30(n4289Δ)* males, which are sensitized such that significant protection of the CEM neurons can be observed in animals that lack a single copy of *egl-1*, i.e. in animals heterozygous for the *egl-1* loss-of-function mutation *n1084 n3082*. In this genetic background, no protective effect was seen to be caused by a deletion of *ced-13*, even in animals heterozygous for *egl-1(n1084 n3082)*, indicating that the BH3-only gene *ced-13* does not contribute to the deaths of the CEM neurons.

In short, we find a sharply reduced role for *ced-9* in the regulation of CEM neuron survival, including a complete absence of the *ced-9* killing activity seen in other cell types; that the cell-killing activity provided by members of the synMuv genes in other cell types has no apparent effect role in the CEM neurons; and that the *ced-8* and engulfment-mediated cell-killing activities that contribute to other programmed cell deaths similarly promote CEM neuron death.

sel-10(gf) and the new gene *tra-4* control CEM programmed cell death by acting within the sex determination pathway

One of our isolates, *n3717*, semidominantly caused both CEM neuron survival and a strong defect in egg laying in hermaphrodites. *n3717* mapped to LGV between *rol-4* and *par-1* (data not shown). Epistasis experiments showed that null mutations in *fem-1*, *fem-2*, and *fem-3* (*fem*, feminization), genes required for masculinization, completely suppressed the masculinization caused by *n3717* (Table 9) (JAGER *et al.* 2004). A null mutation in *her-1*, a gene required for masculinization that acts upstream of the *fem* genes, did not affect the CEM survival caused by *n3717* (Table 9) (JAGER *et al.* 2004). These results suggested that *n3717* causes CEM survival by acting within the sex determination pathway, downstream of *her-1* and upstream of the *fem* genes. The masculinization caused by *n3717* was subtle and gross defects were limited to CEM survival and a defect in egg laying, so that *n3717* was not identified early in the examination of screen isolates as being defective in sex determination and consequently was not set aside. Further mapping, complementation, and sequencing experiments identified *n3717* as a mutation in *sel-10* (*sel*, suppressor or enhancer of *lin-12*), a gene also known as *egl-41*. The subsequent characterization of SEL-10 in sex determination has been described elsewhere (JAGER *et al.* 2004).

n3715, *n3716*, *n4724*, and *n4726* are allelic mutations that caused a strong, recessive CEM survival phenotype and a severe egg-laying defect in hermaphrodites (Table 10A and data not shown). We mapped this locus on LGX between the markers *unc-2* and *lon-2*, distinct from any gene previously identified as functioning in sex determination or as a regulator of programmed cell death. The CEM survival caused by *n3715* and *n3716* was suppressed by *mnDp57* and by *yDp14*, genomic duplications that include sequence from this interval (data not shown). Epistasis experiments with null

mutations of genes required for masculinization (*her-1*, *fem-1*, *fem-2*, and *fem-3*) indicated that the CEM survival in *n3715* and *n3716* hermaphrodites was independent of *her-1* and was suppressed by loss of *fem-1*, *fem-2* or *fem-3* function (Table 10B), suggesting that the gene defined by *n3715* acts downstream of *her-1* and upstream of the *fem* genes, within the sex determination pathway. Consistent with their causing a partial defect in sex determination, both alleles enhanced the partially masculinized phenotypes caused by the weak sex determination mutations *tra-2(e1875)*, *tra-2(n1106)*, and *tra-3(e2333)* (data not shown). Similarly to *sel-10(n3717)*, the masculinization caused by *n3715* and *n3716* was subtle and gross defects were limited to CEM survival and a defect in egg laying, so that *n3715* and *n3716* were not identified early in the examination of screen isolates as being grossly defective in sex determination. GROTE and CONRADT (2006) independently performed genetic screens for mutations causing CEM survival in hermaphrodites and identified mutations allelic with *n3715*. Together with Grote and Conradt, we agreed to have the locus named *tra-4*.

tra-4 encodes a C2H2 transcription factor required for complete feminization

We identified a ~119 kb interval containing *tra-4(n3715)* by polymrphism mapping (see Materials and Methods). All five transgenic lines generated from a pool containing two cosmids within this interval, F53B1 and F58G12, rescued the CEM survival phenotype of *n3715*. These two cosmids are predicted to contain seven genes (http://ws190.wormbase.org); a transgene containing the single predicted gene *F53B1.1* rescued the CEM survival phenotype of *n3715* (see Materials and Methods). We

identified missense mutations in *F53B3.1* for each of the four alleles *n3715*, *n3716*, *n4724*, and *n4726* by DNA sequence determination (Table 2 and Figure 2).

tra-4 is predicted to encode a 543 amino acid protein with seven zinc finger domains (FINN *et al.* 2006). As initially noted by GROTE and CONRADT (2006), TRA-4 is related to the human proto-oncoprotein transcription factor PLZF, possessing homology to the zinc fingers and the N-terminal RD2 repressor domain of hPLZF (see Figure 2). hPLZF is a transcription factor that binds DNA and recruits transcriptional repressor complexes; translocations that fuse hPLZF to the retinoic acid receptor cause acute promyelotic leukemia (ZELENT *et al.* 2001; reviewed by KELLY and DANIEL 2006). Two of the four *tra-4* missense alleles, *n3715* and *n4724*, disrupt residues in the zinc finger consensus sequences that are conserved with human PLZF (Figure 2). The other missense alleles, *n3716* and *n4726*, each mutate an amino acid within a TRA-4 region that is not part of any predicted motif and not conserved in PLZF (Figure 2). *n3716* and *n4726* might disrupt protein stability rather than interfering with the function of a particular domain or might affect a functional domain not recognized by current motif identification algorithms.

Control of CEM survival and CEM identity by the Bar homeodomain transcription factor genes *ceh-30* and *ceh-31*

As we have previously reported (SCHWARTZ and HORVITZ 2007), three of the screen isolates, *n3713*, *n3714*, and *n3720*, defined the gene *ceh-30*. These mutations cause increased *ceh-30* function in hermaphrodites by disrupting a regulatory binding site for TRA-1, a transcriptional repressor that acts in hermaphrodites to prevent

masculinization (HODGKIN 1987). *ceh-30* encodes a Bar family homeodomain transcription factor specifically required for CEM survival in males and can protect the CEM neurons of animals completely lacking the function of the *Bcl-2* homolog *ced-9*. We proposed that *ceh-30* acts downstream of or in parallel to *ced-9* to control whether the CEM neurons are sensitive to the activation of programmed cell death (SCHWARTZ and HORVITZ 2007).

Although animals completely lacking *ceh-30* function are strongly defective in CEM neuron survival in males, these animals retain some sexual dimorphism for CEM survival, with 17% of *ceh-30(n4289Δ)* males and 0% of *ceh-30(n4289Δ)* hermaphrodites possessing surviving CEMs (n = 71 and 60, respectively; see Table 11). One candidate to provide the remaining protective function in the CEM neurons of *ceh-30* loss-of-function (lf) males is *ceh-31*, which encodes the only other predicted Bar family homeodomain protein in *C. elegans*. *ceh-31* is adjacent to *ceh-30* in the genome: their coding regions are separated by less than 5 kb, an interval that contains no predicted genes. CEH-31 is closely related to CEH-30, with 52% identity across the entire predicted proteins and a homeodomain differing by only one amino acid (of glutamatic acid for aspartic acid). CEH-30 is more closely related to CEH-31 than either is to Bar homeodomain proteins in non-nematodes. We isolated two deletion alleles: the 1240 bp deletion *ceh-31(n4893Δ)*, which removes the entire predicted *ceh-31* homeodomain of *ceh-31* and is likely a null allele; and a 7771 bp deletion, *nDf65*, which removes the coding regions of both *ceh-30* and *ceh-31* and is not predicted to affect any other identified genes (see Materials and Methods). Loss of *ceh-31* function did not prevent

CEM neuron survival in males and did not promote CEM neuron survival in hermaphrodites (Table 11).

Males lacking both *ceh-30* and *ceh-31* were less likely to contain *pkd-2::gfp*-expressing CEM neurons than were males lacking *ceh-30* and retaining *ceh-31* function (Table 11B and data not shown). Unlike the CEM neurons of animals lacking *ceh-30*, the CEM neurons of animals lacking both *ceh-30* and *ceh-31* were not completely restored by blocking programmed cell death using loss-of-function mutations in *ced-3*, *ced-4*, or *egl-1*: 8-10% of cell-death-defective *nDf65* males were missing CEM neurons (Tables 11 and S1). *ceh-30* can act in parallel to *ced-9 Bcl-2* to promote CEM survival, and although *ced-3* is normally required for CEM death it is possible that *ceh-30* acts downstream of or in parallel to *ced-3* to promote CEM survival (SCHWARTZ and HORVITZ 2007). If this were the case, animals doubly mutant for *ceh-30* and *ceh-31* and defective in programmed cell death might be missing some CEMs because of a *ced-3*-independent cell death mechanism derepressed in the CEM neurons of animals lacking both *ceh-30* and *ceh-31*. To determine whether the CEM neurons of *ceh-30 ceh-31* double mutant animals might be dying by a *ced-3*-independent mechanism, we examined *ced-1(e1875)*; *ced-3(n717)*; *nDf65* larvae defective both in programmed cell death and in the engulfment and removal of cell corpses. We examined hermaphrodites, as at least 80% of cell-death-defective *nDf65* hermaphrodites were missing CEM neurons, compared to fewer than 20% of cell-death defective hermaphrodites possessing wild-type copies of *ceh-30* or *ceh-31* (Tables 11 and S1). Newly hatched *ced-1(e1875)*; *ced-3(n717)*; *nDf65* larvae did not have an increased number of cell corpses compared to *ced-1(e1875)*; *ced-3(n717)* larvae

(0.3 ± 0.5 and 0.2 ± 0.4 corpses, respectively; mean ± SD, n = 10). Because no extra *ced-3*-independent cell corpses were seen in animals lacking both *ceh-30* and *ceh-31*, suggesting that the missing CEM neurons were not dying independently of *ced-3*, we propose that the CEM neurons of *ceh-30 ceh-31* double mutants were not properly generated. The missing CEMs of cell-death-defective *ced-3(n717)*; *nDf65* animals were restored by a transgene containing a wild-type copy of *ceh-30* (Table 11A), suggesting that this defect of CEM fate determination is caused by the loss of *ceh-30* and *ceh-31* rather than by a separate linked mutation.

***vab-3 Pax6* and *cnd-1 NeuroD* are required for CEM death in hermaphrodites and for other aspects of CEM fate determination**

Two complementation groups were defined by mutations that caused the presence of *pkd-2::gfp*-expressing neurons in the heads of approximately 50% of hermaphrodites: *n3721* and *n3723* on LGX; and *n3786*, *n3787*, and *n4744* on LGIII (Table 12A). The nuclear positions of the *pkd-2::gfp* expressing cells of these mutant hermaphrodites and their process morphologies were more variable than those of the CEM neurons of hermaphrodites defective in programmed cell death or the CEM neurons of *ceh-30(n3714*gf*)* hermaphrodites specifically defective in CEM death (data not shown). If the *pkd-2::gfp*-expressing cells of these mutants were cells other than the CEMs ectopically expressing the *pkd-2::gfp* reporter as a result of a cell-fate transformation, it might be expected that in males or in *ced-3(n717)* hermaphrodites both the CEMs and the transformed cells would express the *pkd-2::gfp* reporter. Examination of mutant males and of double mutants between *ced-3(n717)* and *n3721*,

n3723, or *n3786* did not show the presence of supernumerary *pkd-2::gfp*-expressing cells (data not shown). The extra *pkd-2::gfp*-expressing cells in these mutant hermaphrodites were therefore surviving CEM neurons.

We mapped *n3721* to a 258 kb interval on LGX (see Materials and Methods). Both the *n3721* and the *n3723* mutant strains caused a defect in head morphology at very low penetrance, reminiscent of the defects caused by loss-of-function of the *C. elegans Pax6* homolog *vab-3*, which lies within the same interval. The canonical allele *vab-3(e648)*, believed to be a null mutation (CINAR and CHISHOLM 2004), caused weak CEM survival in hermaphrodites similar to that in *n3721* and *n3723* animals (Table 12A). *n3721* and *n3723* failed to complement *vab-3(e648)* for CEM survival (data not shown). As part of a survey of *vab-3* alleles, CINAR and CHISHOLM (2004) identified *vab-3* mutations in both *n3721* and *n3723*: *n3721* is a mutation in the fifth splice donor site, and *n3721* is a mutation in the third splice donor site (Table 2).

vab-3 mutants were originally isolated on the basis of defect in head morphology and transformation of neuronal cell fates (LEWIS and HODGKIN 1977). *vab-3* was subsequently found to specify cell fates in sensory organs (ZHANG and EMMONS 1995) and in the rectal epidermis (CHAMBERLIN and STERNBERG 1995) and to be required for the proper migration of gonadal precursors (NISHIWAKI 1999) and for proper axonal migration (ZALLEN *et al.* 1999). Molecular characterization of *vab-3* revealed that it encodes the *C. elegans* homolog of the mammalian gene *Pax6* and the *D. melanogaster* gene *eyeless* (CHISHOLM and HORVITZ 1995). The Pax6 family of transcription factors were first identified as functioning to specify the developing eye in *Drosophila* and in mice, but in both organisms family members are broadly expressed in

the central nervous system and play numerous roles in the establishment of neuronal cell fate and, in mammals, in pancreatic development (SIMPSON and PRICE 2002).

We mapped *n3786* and *n3787* to LGIII between *dpy-17* and *lon-1*. In addition to causing CEM survival in hermaphrodites, these mutations caused a fully penetrant recessive reverse kinker Unc (*unc*, uncoordinated locomotion) defect. A pool of three cosmids rescued the Unc phenotype caused by *n3786* (see Materials and Methods). The genes on these cosmids include the *NeuroD* homolog *cnd-1*. The canonical allele *cnd-1(ju29)* caused CEM survival and locomotion defects similar to those caused by *n3786* and *n3787* and failed to complement both alleles for locomotion and for CEM survival (Table 12A and data not shown). Determination of DNA sequences identified mutations in *cnd-1* in *n3786*, *n3787*, and *n4744* mutant animals (Table 2). We also identified the canonical *unc-131* mutation *jd19*, which was reported to map to a position overlapping with *cnd-1* (K. Oomen and W. Walthall, personal communication), as failing to complement *cnd-1(ju29)*. Through determination of DNA sequences we identified *jd19* as being a predicted R17opal nonsense mutation in *cnd-1*.

cnd-1 and its mammalian homolog *NeuroD* encode bHLH transcription factors (LEE *et al.* 1995a; HALLAM *et al.* 2000). NeuroD was initially identified as a mammalian bHLH cDNA able to transform nonneuronal ectodermal cells to neurons when expressed in *Xenopus* embryos (LEE *et al.* 1995a). Further work has shown that *NeuroD* is required for pancreas development and acts broadly in neuronal development (reviewed by CHAE *et al.* 2004). The *C. elegans* NeuroD homolog CND-1 is expressed in neuroblasts and developing neurons, and *cnd-1* mutants have numerous motor neuron defects, including in the motor neuron number, cell-fate marker expression and

process morphology (HALLAM *et al.* 2000). CND-1 and NeuroD share a conserved bHLH domain and an additional 42 amino acid motif C-terminal of the bHLH domain (LEE *et al.* 1995b; HALLAM *et al.* 2000); the bHLH motif is the only domain in CND-1 that is recognized by domain prediction software (FINN *et al.* 2006). The missense mutation *cnd-1(n4744)*, which caused a CEM survival phenotype as strong as those of the predicted *cnd-1* null alleles *n3786* and *jd19* (Table 12A), is predicted to cause the amino acid change L42F, altering a residue in the first helix of the bHLH motif that is conserved between *C. elegans* CND-1 and its mouse homolog NeuroD.

In addition to causing CEM survival in hermaphrodites, both *vab-3* mutant males and *cnd-1* mutant males were missing CEMs (Table 12B). The defect in these mutant males is not one of CEM survival, as the CEM neurons of these mutant males were not restored when programmed cell death was blocked by the mutation *ced-3(n717)* (Table 12B). Similarly, *ced-3(n717)* hermaphrodites defective in programmed cell death and mutant for either *vab-3* or *cnd-1* possessed fewer CEM neurons than hermaphrodites defective in programmed cell death normally do (Tables 11A, 12A). Thus, in addition to having CEMs that often failed to die in hermaphrodites and having CEMs apparently defective in nuclear position and process morphology, these mutants often failed to have *pkd-2::gfp*-expressing CEMs at all. The CEM neurons of both *vab-3* and *cnd-1* mutants thus showed a number of partially expressive defects in the establishment of their cell fates: they were often not generated, or at least not detectable using *pkd-2::gfp*, and, when present, the CEM neurons of both *vab-3* and *cnd-1* mutants were often defective in nuclear position, process morphology and cell death.

vab-3 Pax6 and *cnd-1 NeuroD* act together in the establishment of head morphology

We observed that animals lacking *cnd-1 NeuroD* had a weakly penetrant defect in head morphology reminiscent of the defects seen in *vab-3* mutants (Table 13 and Figure 3). The weak *vab-3* alleles *n3721* and *n3723* caused similar defects in head morphology at low penetrance (Table 13). Loss of *cnd-1* strongly enhanced the head morphology defects caused by weak alleles of *vab-3*. For example, 1% of *cnd-1(n3786)* and 6% of *vab-3(n3723)* animals were Vab, but 53% of *cnd-1(n3786)*; *vab-3(n3723)* double mutants were Vab (n>100; see Table 13). We did not observe similar enhancement of weak *vab-3* morphology defects when these weak *vab-3* alleles were combined with mutations in a number of other genes, including mutations causing defects in locomotion, in body size or in CEM fate determination (data not shown).

vab-3 Pax6 and *cnd-1 NeuroD* function in parallel to *ceh-30* to inhibit CEM neuron survival

The survival of CEM neurons in hermaphrodites caused by loss of *vab-3* function was not affected by loss of any of the *fem* genes, and the survival of CEM neurons in hermaphrodites caused by loss of *cnd-1* function was not affected by loss of *fem-2* (Table 14A and data not shown); the *fem* genes are the most downstream genes required for masculinization (HODGKIN 2002). Both *cnd-1* and *vab-3* mutations protected the CEM neurons of hermaphrodites completely lacking the function of the *Bcl-2* homolog *ced-9* (Table 14B). Because loss of *ced-9* function causes ectopic cell death

and lethality, the *ced-9(lf)* animals examined were homozygous for the extremely weak cell-death-execution mutation *ced-3(n2923)* (SHAHAM *et al.* 1999). Although it permits most programmed cell death to occur normally (SHAHAM *et al.* 1999), *ced-3(n2923)* suppressed the lethality caused by loss of *ced-9 Bcl-2* function, permitting the maintenance and examination of strains completely lacking *ced-9*. *ced-3(n2923)* caused a very low baseline level of CEM neuron survival (Table 14B). The CEM survival caused by *vab-3* and *cnd-1* mutations was weaker in animals lacking *ced-9* function than in a wild-type genetic background (Tables 12A and 14B and data not shown), which suggests that a portion of the cell-protective effect of *vab-3* and *cnd-1* mutations is lost in animals lacking *ced-9 Bcl-2*. Thus, *vab-3* and *cnd-1* act downstream of or in parallel to sex determination and act at least partly in parallel to *ced-9 Bcl-2* to promote CEM death in hermaphrodites.

Because *cnd-1* and *vab-3* mutants had similar defects in the CEM neurons and caused similar levels of CEM survival in hermaphrodites, the two genes might act at a similar point within the pathway for CEM cell death. Reduction of *vab-3* function did not enhance the survival of CEM neurons of hermaphrodites completely lacking *cnd-1* function (Table 12A). The lack of enhancement in double mutants might suggest that the two genes act in a common pathway. However, tests for dependence of the CEM survival phenotypes caused by mutations in *vab-3* and *cnd-1* on the CEM-specific cell-survival factor *ceh-30* revealed a significant difference between *vab-3* and *cnd-1*: the survival of CEM neurons conferred by reduction of *vab-3* function was completely unaffected by loss of *ceh-30* function, while the survival conferred by complete loss of *cnd-1* function was greatly reduced in animals lacking *ceh-30* function (Table 14C).

*cnd-1(*lf*)*; *ceh-30(*lf*)* double mutant hermaphrodites showed significantly more CEM survival than either wild-type or *ceh-30(*lf*)* hermaphrodites, but the CEM survival phenotype caused by loss of *cnd-1* function was not as cleanly epistatic to *ceh-30* for CEM survival as is the *vab-3* phenotype.

Discussion

Large-scale genetic screens identifed mutants defective in the deaths of the CEM neurons

From our screens, we identified 144 independent mutations causing CEM survival in hermaphrodites. Through complementation tests, mapping, and DNA sequence determination, we identified 52 alleles of genes known to function in all programmed cell deaths in *C. elegans*: 32 alleles of *ced-3*, 16 alleles of *ced-4*, and four gain-of-function alleles of *ced-9*. The recovery of multiple *ced-3* alleles, *ced-4* alleles, and *ced-9(*gf*)* mutations indicates that these screens were done on a scale sufficient to recover mutations in most genes required to prevent CEM survival in hermaphrodites. However, the screen failed to isolate any alleles of *egl-1*, a gene required for CEM death in hermaphrodites. *egl-1*, which encodes a protein only 106 amino acids in length, presents a small target for mutagenesis. Although the recovery of four gain-of-function mutations of *ced-9* indicates that mutations altering at least one small target were repeatedly recovered, genes that like *egl-1* that present small targets or are not easily mutated by EMS could easily have been missed.

Some mutations causing CEM neuron survival in hermaphrodites might not have been recovered in these screens because of the screen design. If the

maternally-provided function of a gene required for CEM death were sufficient to rescue the defect caused by zygotic loss of gene function, no mutations would have been recovered. Mutations that recessively caused CEM survival in hermaphrodites but also caused additional defects resulting in sterility or maternal-effect lethality also could not be recovered, as the candidate would not have generated viable progeny. Mutations that altered the fates of the CEM neurons so as both to prevent their programmed cell deaths and to block their expression of the cell-fate reporter *pkd-2::gfp* similarly could not be recovered. Importantly, screen isolates defined five genes that had not been previously molecularly characterized or that were not previously known to function in the establishment of sexual identity or the determination of the CEM neuron fate: *sel-10 CDC4*, *tra-4 PLZF*, *ceh-30 Barhl1*, *vab-3 Pax6*, and *cnd-1 NeuroD*.

A pathway for the control of CEM survival by determination of the CEM cell fate and establishment of sexual identity

We propose that there are at least four major categories of genes that affect the deaths of the CEM neurons: genes that function in the establishment of sexual identity, genes that establish the identity of the CEM neurons, and genes that function within the cell death program to cause cell killing, and genes that function in a cell-specific fashion to determine whether the CEM neurons are sensitive to an activated cell-death program (see Figure 4A). Below we discuss the genes that function to determine the sexually dimorphic survival of the CEM neurons, place them into these four major categories, and propose a pathway for the regulation of CEM neuron survival (Figure 4B).

A subset of mechanisms that promote somatic cell death in *C. elegans* function in the deaths of the CEM neurons

The genes regulating the process of programmed cell death in *C. elegans* have been extensively studied (reviewed in METZSTEIN *et al.* 1998; LETTRE and HENGARTNER 2006). The deaths of the CEM neurons are in many ways identical to other cell deaths in the soma of *C. elegans*; in particular, the core pathway of genes that function in the execution of programmed cell death is required for the deaths of hermaphrodites' CEM neurons (SCHWARTZ and HORVITZ 2007). We found that partial-loss-of-function mutations in *ced-3* impaired the deaths of the CEM neurons to degrees that corresponded to their defects in other cell types. As reported for other programmed somatic cell deaths, the deaths of the CEM neurons required the BH3-only killer gene *egl-1* but not the *egl-1* homolog *ced-13*.

egl-1 is required for the deaths of the CEM neurons, indicating that *egl-1* is expressed in the CEMs. Because sex determination and *ceh-30* can regulate CEM survival in parallel to *egl-1* and *ced-9*, *egl-1* expression in the CEMs need not be sexually dimorphic to achieve sex-specific death of the CEM neurons. If *egl-1* expression in the CEMs is sexually dimorphic – if *egl-1* is not normally expressed in males – then this downregulation of *egl-1* expression in male CEMs must be dependent on *ceh-30* function to explain the *egl-1*-dependent CEM death seen in males lacking *ceh-30* function; this possible regulation is indicated with a dotted line in Figure 4A. The first clue towards the identification of additional factors regulating *egl-1* expression in the CEM neurons comes from the noncoding mutation *egl-1(n4908Δ)*. *egl-1(n4908Δ)* removes a site specifically required for the deaths of the Pn.aap cells (B. Galvin and

H.R.H., unpublished results) and causes a CEM-specific death defect, suggesting that the deleted sequence includes a binding site for a factor that promotes *egl-1* expression specifically in the CEM neurons or in a subset of dying cells including the CEM neurons.

Despite the similarities between the programmed cell deaths of the CEM neurons in hermaphrodites and other previously studied somatic cell deaths in *C. elegans*, the programmed deaths of the CEM neurons are distinctive in several ways: the CEM deaths occur hours after the CEMs are generated by cell division (SULSTON *et al.* 1983), after the CEMs have migrated and shown signs of differentiation (HORVITZ *et al.* 1982 and references therein). By contrast, most cells fated to die in *C. elegans* adopt a corpse-like morphology and are removed within an hour of the cell division that created them (SULSTON and HORVITZ 1977; ROBERTSON and THOMPSON 1982; SULSTON *et al.* 1983); engulfment of a cell by its neighbors can even begin before the division that generates the dying cell is complete (ROBERTSON and THOMPSON 1982). One other programmed cell death in *C. elegans*, that of the tail spike cell, bears some striking similarities to the deaths of the CEM neurons: like the deaths of the CEMs, the death of the tail spike cell occurs hours after the tail spike cell is generated, shows no evidence of the killing function of *ced-9 Bcl-2* and is only partially prevented by the *ced-9* gain-of-function *n1950* (MAURER *et al.* 2007). It has been proposed that the tail spike cell death is caused by temporally controlled transcriptional upregulation of the cell-killing gene *ced-3* (MAURER *et al.* 2007); similarly, *ceh-30* might promote CEM neuron survival by cell-specific transcriptional repression of *ced-3*.

In addition to the core pathway of genes required for all programmed cell death in *C. elegans*, at least four separate classes of genes have been identified that provide

functions contributing to, but not required for, the programmed deaths of most or all cells. These include the cell-killing function of the bifunctional cell-death gene *ced-9* (HENGARTNER and HORVITZ 1994a), the cell-death-promoting factor *ced-8* (STANFIELD and HORVITZ 2000), engulfment-mediated cell killing (HOEPPNER *et al.* 2001; REDDIEN *et al.* 2001) and the promotion of cell killing by selected members of the synMuv genes (REDDIEN *et al.* 2007). Although each of these mechanisms has been shown to cause defects in a broad range of cells that normally die, the factors determining whether and to what degree cells are susceptible to their killing functions have not been widely explored. We found that loss of the timing factor *ced-8* or of the cell-corpse engulfment gene *ced-7* enhanced a weak cell-death defect in the CEM neurons, consistent with these genes acting to promote the deaths of the CEM neurons. As each of the death-promoting functions of *ced-8* and the engulfment genes have been shown to promote cell killing independently of *ced-9 Bcl-2* function (STANFIELD and HORVITZ 2000; REDDIEN *et al.* 2001), we propose that these genes act similarly in the control of CEM neuron survival (Figure 4B).

As we have previously reported (SCHWARTZ and HORVITZ 2007), the cell-killing function of the bifunctional cell-death regulator *ced-9 Bcl-2* does not appear to contribute to the deaths of the CEM neurons. Similarly, we observed no cell-killing function for the synMuv genes in the CEM neurons. The cell-killing functions of *ced-9* and of the synMuv genes have previously been observed to contribute to the programmed deaths of several cell types in the anterior pharynx, of the Pn.aap cells of the ventral nerve cord and the sisters of the PVD neurons in the postdeirid sensory structure (REDDIEN *et al.* 2001; REDDIEN 2002; REDDIEN *et al.* 2007).

The mechanisms underlying the differences between the programmed deaths of the CEM neurons of hermaphrodites and the deaths of other cell types are not understood. Given that certain mechanisms known to contribute to cell killing in other tissues of *C. elegans* apparently do not function in the CEMs, further examination of cell death of the CEM neurons and of other previously unexamined cell types might similarly reveal new contributors to the process of cell killing.

sel-10 CDC4 and *tra-4 PLZF* contribute to the determination of sexual identity

The largest single class of mutants with surviving CEM neurons in hermaphrodites comprised the 67 isolates in which the CEM neuron survival was associated with other indications of partial sexual transformation of multiple somatic tissues from a hermaphrodite to a male sexual identity. Of these isolates, 50 showed dominant CEM survival in hermaphrodites, with recessive complete or nearly complete masculinization, a phenomenon seen for strong loss-of-function alleles of *tra-1* and previously observed for strong loss-of-function alleles of *tra-2* (TRENT *et al.* 1983; DESAI and HORVITZ 1989). Five screen isolates defined two genes, *sel-10* and *tra-4*, which had not previously been established to have roles in sex determination. Loss of function of either either *sel-10* or *tra-4* causes weak masculinization of both the soma and the germline (JAGER *et al.* 2004; GROTE and CONRADT 2006 and see Results), and mutants in either *sel-10* or *tra-4* cause synthetic masculinization when combined with weak mutants in the canonical sex-determination genes *tra-2* and *tra-3*. Further investigation of *tra-4* by GROTE and CONRADT (2006) revealed the existence of an entire class of genes providing a weak contribution to the establishment of the hermaphrodite identity,

and it seems likely that additional genes exist, similar to *sel-10* and *tra-4*, that weakly contribute to the establishment of sexual identity in *C. elegans*.

The masculinized phenotypes of *sel-10* and *tra-4* mutants are independent of *her-1* and are completely suppressed by loss of the *fem* genes. Based on these genetic interactions and on molecular data suggesting that SEL-10 directly regulates the stability of FEM-1 and FEM-3, we proposed that *sel-10* acts genetically upstream of *fem-1* and *fem-3* (JAGER *et al.* 2004). The placement of *tra-4* within the sex determination pathway is less clear. GROTE and CONRADT (2006), in their independent cloning and characterization of *tra-4*, obtained similar epistasis data with *her-1* and the *fem* genes, and additionally observed that loss of *tra-4* can enhance the mating efficiency of animals completely lacking *tra-1* function. On the basis of this observation, Grote and Conradt proposed that *tra-4* acts downstream of the *fem* genes and in parallel to *tra-1* to promote female development and further proposed that the observed suppression of the *tra-4* mutant phenotype in *fem* mutants is a consequence of increased *tra-1* function in these feminized animals (GROTE and CONRADT 2006).

The enhancement of the masculinized phenotype of a *tra-1* null mutant by loss of *tra-4* reported by GROTE and CONRADT (2006) is highly salient and their resulting model is certainly plausible. However, it has long been known that elements placed in the sex determination pathway upstream of *tra-1* also act in parallel to *tra-1* to prevent complete masculinization, including the X-chromosome dosage gene *xol-1* (HODGKIN 1980; HODGKIN 2002). TRA-1 and TRA-2 can physically interact, and this interaction has been proposed to suggest the existence of feminizing activity within the sex-determination pathway that circumvents the normal role within that pathway of the *fem* genes (LUM *et*

al. 2000). These observations have led to the proposal that subsidiary mechanisms exist by which genes acting upstream within the sex determination pathway can promote feminization in parallel to *tra-1* (HODGKIN 2002). Despite these proposals for additional functions in sex determination, the core sex determination pathway has continued to be drawn in accordance with the main genetic interactions of sex determination mutants and not their subsidiary relationships. Considered similarly, *tra-4* would be regarded as principally acting within the sex determination pathway, upstream of the *fem* genes (Figure 4B).

The CEM cell survival regulator *ceh-30 Barhl1* promotes CEM survival and acts redundantly with its homolog *ceh-31* in CEM fate determination

In previously published work arising from the screens reported here (SCHWARTZ and HORVITZ 2007), we identified the Bar family homeodomain transcription factor *ceh-30 Barhl1* as a regulator of CEM survival. *ceh-30* specifically controls the survival decisions of the CEM neurons, acting downstream of sex determination and upstream of the execution of programmed cell death. *ceh-30* therefore occupies a central role within the genetic pathway for the control of CEM survival (Figure 4V).

Males lacking *ceh-30* function were strongly defective in CEM survival, but *ceh-30(n4289Δ)* animals retained significant sexual dimorphism for CEM survival. One candidate to provide the remaining CEM survival function in *ceh-30(n4289Δ)* males is the *ceh-30* homolog *ceh-31*, encoding the only other Bar family homeodomain protein predicted in *C. elegans*. CEH-31 has a predicted homeodomain almost identical to that of CEH-31, suggesting that CEH-30 and CEH-31 may share transcriptional targets.

Loss of *ceh-31* function did not affect CEM survival either in hermaphrodites or in males, but we found that males lacking both *ceh-30* and *ceh-31* displayed a loss of CEM neurons more severe than that of males lacking only *ceh-30*. Unlike the missing CEM neurons of *ceh-30(lf)* males, however, the CEMs lost in *ceh-30 ceh-31* double mutants were not completely restored by blocking programmed cell death. The CEM neuron deaths of animals lacking *ceh-30* required *egl-1* and *ced-3* function, indicating that *egl-1* and *ced-3* act downstream of or in parallel to *ceh-30* to promote CEM death. However, loss of *egl-1* had no effect on CEM survival in animals lacking both *ced-9* and *ceh-30*. Thus, *ceh-30* acts in parallel to *egl-1* (and to *ced-9*), and not upstream of *egl-1*. No similar mutant background exists that could permit us to determine whether *ceh-30* might also act in parallel to *ced-3*, so it is possible that the CEM neurons of *ceh-30 ceh-31* animals die in a *ced-3*-independent manner. However, no persistent cell corpses were seen in animals that lacked both *ceh-30* and *ceh-31* and also lacked both the cell-killing gene *ced-3* and the cell-corpse engulfment gene *ced-1*. This suggests that the CEM neurons of the *ceh-30 ceh-31* double mutants did not die independently of *ced-3*, although it remains possible that the CEMs of *ceh-30 ceh-31* double mutants died independently of *ced-3* and then became cell corpses that did not possess the distinctive Nomarski morphologies of cells killed by *ced-3* or of cells killed by other known mechanisms in *C. elegans* (ELLIS *et al.* 1991; CHUNG *et al.* 2000; JOSHI and EISENMANN 2004). We propose that the Bar homeodomain transcription factor gene *ceh-30* acts to promote CEM neuron survival in males and we additionally propose that *ceh-30* acts redundantly with the homologous gene *ceh-31* to promote other aspects of the CEM neuron identity. Thus, the CEM neurons of males lacking *ceh-30* failed to

survive, and some CEM neurons of animals lacking both *ceh-30* and *ceh-31* failed to properly differentiate.

The deletion removing both *ceh-30* and *ceh-31* is associated with a weak kinker Unc phenotype (data not shown). This locomotion defect is similar to locomotion defects seen in animals defective in specification of motor neuron identity (MILLER *et al.* 1992) or in the development of neuronal lineages (PRASAD *et al.* 1998; HALLAM *et al.* 2000; CAMERON *et al.* 2002), and is not seen in animals that retain the function either of *ceh-30* or of *ceh-31*. We previously observed expression of a rescuing *ceh-30::gfp* reporter in neurons other than the CEMs (SCHWARTZ and HORVITZ 2007). The kinker Unc phenotype of *nDf65* animals might indicate that *ceh-30* and *ceh-31* act redundantly to establish the fates of neurons in addition to the CEMs. Other genes that have been identified as controlling specific cell death decisions in *C. elegans* also perform additional functions in other tissues: *ces-2*, *egl-20*, *eor-1*, *eor-2*, *hlh-2*, *hlh-3*, *mab-5*, *pal-1*, and *tra-1* both regulate specific cell deaths and also act in the differentiation other cells (METZSTEIN *et al.* 1996; CONRADT and HORVITZ 1999; HOWARD and SUNDARAM 2002; WANG and CHAMBERLIN 2002; THELLMANN *et al.* 2003; HOEPPNER *et al.* 2004; LIU *et al.* 2006; MAURER *et al.* 2007). As all of these genes encode transcription factors, their possessing multiple functions in multiple tissues is not surprising.

Of the two Bar homeodomain transcription factors in *C. elegans*, only *ceh-30* is required to promote the survival of the CEM neurons. This difference might result from differences in the expression of *ceh-30* and *ceh-31* during CEM neuron development. Animals lacking *ceh-30* and animals lacking both *ceh-30* and *ceh-31* retain a CEM sexual dimorphism, even when programmed cell death was blocked by loss of *ced-3*

function. Therefore, there must exist a factor in addition to the Bar homeodomain proteins that acts in a sexually dimorphic fashion to regulate CEM differentiation or to regulate CEM survival independently of *ced-3*. One candidate is the *Groucho* homolog *unc-37*, which functions with *ceh-30* to promote CEM survival in males (PEDEN *et al.* 2007). We similarly find that males with reduced *unc-37* function show a weak reduction in the number of surviving CEM neurons, and that the missing CEMs of *unc-37* mutant males are restored when a *ced-3(n717)* mutation is added to block programmed cell death (Table S2). PEDEN *et al.* (2007) showed that UNC-37 can physically interact with CEH-30, likely via the N-terminal FIL motif of CEH-30; homeodomain proteins in other organisms have been shown to recruit transcriptional repression complexes, including Groucho (CHOI *et al.* 1999; JIMENEZ *et al.* 1999).

vab-3 Pax6 and *cnd-1 NeuroD* function in CEM fate determination and cooperate in the establishment of head morphology

From our screen, we identified the previously characterized genes *vab-3 Pax6* and *cnd-1 NeuroD* as functioning to promote CEM death. Animals defective in *vab-3* or in *cnd-1* each displayed a range of defects in the CEM neurons: the neurons were often not present; when present, they were frequently mispositioned or showed aberrant process morphology; and they often failed to die appropriately in hermaphrodites. We propose that *vab-3* and *cnd-1* mutants are weakly defective in the establishment of CEM cell identity. Both *vab-3* and *cnd-1* function in a range of neuronal cell-fate decisions in *C. elegans* development (ZHANG and EMMONS 1995; ZALLEN *et al.* 1999; HALLAM *et al.* 2000), and both genes have mammalian homologs that function broadly in

the establishment of cell fates in the central nervous system (CHAE *et al.* 2004; OSUMI *et al.* 2008). Because *vab-3* and *cnd-1* mutants showed similar phenotypes, because both *vab-3* and *cnd-1* functioned downstream of or in parallel to both *ced-9* and *ceh-30* to promote CEM neuron death, and because hermaphrodites mutant for both *vab-3* and *cnd-1* possessed defects in the CEM neuron identity that were not enhanced beyond those seen in either single mutant, including a similar degree of CEM survival in hermaphrodites, we propose that *vab-3* and *cnd-1* work together in establishing CEM identity.

Other aspects of the *vab-3* and *cnd-1* mutant phenotypes also suggest that the two genes cooperate in *C. elegans* development. Animals lacking *cnd-1* function displayed at low penetrance a variable defect in head morphology reminiscent of the defect seen at high penetrance in animals completely lacking *vab-3* function. Loss of *cnd-1* function strongly enhanced the head morphology defects of animals weakly defective in *vab-3* function. Conversely, the strong loss-of-function allele *vab-3(e648)*, an early nonsense mutation proposed to completely abolish *pax-6* function (CHISHOLM and HORVITZ 1995; CINAR and CHISHOLM 2004), was associated with a weak kinker Unc phenotype in outcrossed strains, a defect perhaps related to the strong kinker Unc phenotype seen in animals lacking *cnd-1* function (data not shown). *vab-3* and *cnd-1* are therefore likely to provide similar and mutually redundant functions in multiple aspects of *C. elegans* development. In this context, it is noteworthy that some aspects of the mutant phenotypes of mice lacking the *vab-3* homolog *Pax6* and of mice lacking the *cnd-1* homolog *NeuroD* are strikingly similar, in particular the defects in pancreas

development and insulin production observed in mice lacking either *Pax6* or *NeuroD* (NAYA *et al.* 1997; SANDER *et al.* 1997).

Genes that function to determine CEM neuron identity might also directly control CEM survival

In addition to the genes that we and others have identified as controlling CEM survival, genes have been identified that are required to establish the CEM neuron identity. The POU domain transcription factor gene *unc-86* functions in the establishment of numerous neuronal cell identities in *C. elegans*, including those of the CEM neurons (FINNEY and RUVKUN 1990; SHAHAM and BARGMANN 2002). PEDEN *et al.* (2007) reported that UNC-86 might directly bind the *ceh-30* locus and promote *ceh-30* expression in the CEM neurons. Loss-of-function mutants of the helix-loop-helix transcription gene *lin-32*, which functions to establish the identities of multiple neurons in *C. elegans*, frequently lack CEM neurons (ZHAO and EMMONS 1995; SHAHAM and BARGMANN 2002).

Both mutants defective in CEM fate determination and mutants more specifically defective in CEM survival, such as *ceh-30* or *unc-37*, cause the absence of CEM neurons in males and in masculinized hermaphrodites. The two classes can be distinguished because in mutants of the latter class the CEM neurons can be restored by the addition of mutations that prevent programmed cell death. With the identification and characterization of genes that function to control the deaths of the CEM neurons, significant overlaps appear between the genes that control CEM survival and genes that function to determine CEM identity. *vab-3* and *cnd-1* mutants are weakly defective in

multiple aspects of the CEM fate, such that the CEM neurons are often not properly generated in these mutants, and when generated often fail to properly die in hermaphrodites. *ceh-30* mutants appear to be specifically defective in the survival of the CEM neurons, but animals lacking both *ceh-30* and the homologous gene *ceh-31* show additional defects in the establishment of CEM identity, and might show broader defects in neuronal development. UNC-86, which is required for the presence of *pkd-2::gfp*-expressing CEM neurons in *ceh-30(*gf*)* hermaphrodites and in animals defective in programmed cell death (data not shown), might directly regulate *ceh-30* to promote its CEM-protective function (PEDEN *et al.* 2007). Some of these overlapping relationships might be evolutionarily conserved; for example, the mouse *ceh-30* homolog *Barhl1* is required for the survival of sensory neurons in the inner ear (LI *et al.* 2002), and the mouse *cnd-1* homolog *NeuroD* is required for the proper generation and survival of sensory neurons in the inner ear (KIM *et al.* 2001). As further relationships are established among genes that control the survival of the CEM neurons and between these genes and the genes that function to establish CEM neuron identity, similar gene networks might well be found that act to control neuronal identity, function, and survival in mammals.

Materials and Methods

C. elegans genetics

C. elegans strains were derived from the wild-type strain N2 (Bristol, England) and cultured using standard conditions (BRENNER 1974), except that the bacterial strain HB101 was provided as a food source. A list of mutations used is given below. The following mutations were used and are described by (RIDDLE *et al.* 1997) unless otherwise noted: LGI *cfi-1(ky651)* (SHAHAM and BARGMANN 2002), *dpy-5(e61)*, *unc-37(e262)*; LGII *dpl-1(n3380)*, *dpy-10(e128)*, *mcd-1(n4005Δ)* (REDDIEN *et al.* 2007), *rol-6(e187)*, *unc-4(e120)*, *tra-2(e1875, n1106)*, *unc-52(e444)*; LGIII *ced-4(n1162)*, *ced-7(n1892)*, *ced-9(n2812)*, *ced-9(n3400)* (SCHWARTZ and HORVITZ 2007), *cnd-1(ju29)* (HALLAM *et al.* 2000), *dpy-1(s2171)*, *dpy-17(e164)*, *dpy-18(e364)*, *fem-2(e2105)*, *lon-1(e43, e185)*, *tra-1(e1099)*, *unc-32(e189)*, *unc-49(e382)*, *unc-69(e587)*, *unc-86(n846)*, *unc-131(jd19)* (K. Oomen and W. Walthall, personal communication); LGIV *unc-5(e53)*, *fem-1(e1965)*, *fem-3(e1996)*; *ced-3(n717, n2427, n2438, n2443, n2436, n2877, n2921)* (SHAHAM *et al.* 1999), *tra-3(e2333)*; LGV *dpy-11(e224)*, *egl-1(n1084)*, *egl-1(n1084 n3082)* (CONRADT and HORVITZ 1998), *egl-1(n4908Δ)* (B. Galvin and H.R.H., unpublished results), *her-1(hv1 y101)*, *him-5(e1467)*, *par-1(b274)*, *rol-4(sc8)*, *unc-76(e911)*; and LGX *ced-8(n1891)*, *ced-13(tm536)* (SCHUMACHER *et al.* 2005), *ceh-30(n4289Δ)* (SCHWARTZ and HORVITZ 2007), *dpy-3*(e27), *dpy-6(e14)*, *lin-15(n765)*, *lon-2(e678)*, *unc-2(e55)*, *unc-9(e101)*, *unc-18(e81)*, *vab-3(k121, k143, e648)* (NISHIWAKI 1999), *nIs106* [*lin-11::gfp*] (REDDIEN *et al.* 2001). The extrachromosomal *ceh-30* rescuing transgene *nEx1165* has been previously described, as "*ceh-30* genomic locus" (SCHWARTZ and HORVITZ 2007). The translocation *nT1* [IV; V]

with the dominant marker *deg-3(n754)* (TREININ and CHALFIE 1995) or *qIs51* (SIEGFRIED *et al.* 2004) was used to balance *fem-1* and *fem-3*. The balancer chromosome *sC1* with the recessive marker *dpy-1(s2171)* (PILGRIM *et al.* 1995) was used to balance *fem-2*. The balancer chromosome *mnC1* with the recessive markers *dpy-10(e128)* and *unc-52(e444)* (HERMAN 1978) was used in some strain constructions. The chromosomal duplications *mnDp57* (X:I) and *yDp14* (X:I) (MENEELY and NORDSTROM 1988; AKERIB and MEYER 1994) both span *tra-4*. The genomic deficiency *sDf23* (REINER *et al.* 1995) failed to complement *cnd-1(n3786)* for CEM survival and for locomotion, and the genomic duplications *nDp2* and *sDp3* (ROSENBLUTH *et al.* 1985; FINNEY *et al.* 1988) complemented *cnd-1(n3786)* for both its locomotion and CEM survival defects (data not shown).

Polymorphism mapping was performed essentially as described (WICKS *et al.* 2001). *ced-3(n4707)* was mapped to the right of *unc-30* on LGIV using visible markers and using polymorphisms to the right of 1231 on K10D11 and left of 25818 on W02A2, a ~373 kb interval that includes the *ced-3* locus. The mapping of *sel-10(n3717)* has been described (JAGER *et al.* 2004). *tra-4(n3715)* was mapped to the right of *unc-2* and the left of *lon-2* on LGX using visible markers and polymorphisms to the right of 12743 on F55F1 and to the left of 24830 on F53B3, a ~93 kb interval. The mapping of *ceh-30* mutations has been described (SCHWARTZ and HORVITZ 2007). *vab-3(n3721)* was mapped to the right of *dpy-6* and the left of *unc-9* using visible markers and using polymorphisms to the right of 10699 on R07E3 and to the left of 16547 on F57C7, an interval of ~258 kb that contains the *vab-3* locus. *cnd-1(n3786)* was mapped between the visible markers *dpy-17* and *lon-1*, an interval of approximately 370 kb.

Transgenesis and generation of integrated *pkd-2::gfp* reporters

Germline transformation was performed as described (MELLO *et al.* 1991). Two cosmid pools were injected to attempt rescue of the Unc phenotype of *cnd-1(n3786)*: F21H11, K10D2, and ZC155; and ZC155, C34E10, and ZC395. The second pool gave a single line that showed rescue of the Unc phenotype of *cnd-1(n3786)*. Two cosmid pools were injected to attempt rescue of the CEM survival phenotype of *tra-4(n3715)*: F55F1 and C14A11; and F58H12, F53B3, and C15D2. The second pool gave five lines that rescued the CEM survival phenotype caused by *tra-4(n3715)*. Cosmids were injected at 5 ng/μl each for rescue of *cnd-1(n3786)*. Cosmids were injected at 25 ng/μl each for rescue of *tra-4(n3715)* with 50 ng/μl P76-16B (BLOOM and HORVITZ 1997) as a co-injection marker. The plasmid ppkd-2::gfp1 (BARR and STERNBERG 1999) was injected at a concentration of 100 ng/μl together with the *lin-15*-rescuing co-injection marker pL15EK (CLARK *et al.* 1994) at a concentration of 50 ng/μl into a *lin-15(n765)* strain. A suitable transgenic line was chosen, and integrated using an established protocol (SHAHAM and HORVITZ 1996) using approximately 900 F_1 progeny. From this, seven independent chromosomally integrated versions of the *pkd-2::gfp* transgene were recovered: *nIs125 X*, *nIs128 II*, *nIs129 IV*, *nIs130 IV*, *nIs131 III*, *nIs132 X*, and *nIs133 I*. *nIs125 X* could not be separated from a linked mutation causing a recessive kinker Unc phenotype. Each of the five autosomal integrated transgenes showed tight linkage to a marker used in their mapping (*dpy-5 I*, *rol-6 II*, *unc-32 III*, or *unc-5 IV*) such that recombinants could not be readily obtained between them; it is therefore possible that

each suppresses recombination on parts of their respective chromosomes, including the cluster-linked markers used in their mapping.

Genetic screens and initial classification of screen isolates

We performed three screens, each of approximately 20,000 mutagenized haploid genomes. Each screen used a different one of three *pkd-2::gfp* integrants: *nIs133 I*, *nIs128 II*, or *nIs130 IV*. In these screens, hermaphrodites were mutagenized with EMS according to standard methods (BRENNER 1974). Mutagenized P_0 animals were placed on Petri plates containing NGM agar seeded with HB101 bacteria as a food source: four animals on a seeded 6 cm plate or 32 animals on a seeded 10 cm plate. After 6 days at 20°C, the plates were bleached for approximately 11 minutes with periodic gentle vortexing in 2M NaOH with 12.5% HOCl solution (from a stock with 5% available chlorine) to recover F_2 eggs, which were then allowed to hatch in S medium in the absence of food. One aliquot of 300-400 animals from each 6 cm plate or six such aliquots from each 10 cm plate were put on seeded 6 cm plates and grown at 22.5°C for four days before screening. All isolates were labeled to identify the group of mutagenized P_0s from which they originated. 189 independently mutagenized pools of mutagenized animals were screened, and mutants were isolated from 105 of these pools. All screen isolates were maintained at 22.5°C by picking three phenotypic hermaphrodites in each generation from which to obtain the next generation and were maintained in this fashion until frozen stocks had been established and confirmed by test thaws. After isolates had been assigned to phenotypic classes and subjected to complementation tests and mapping experiments (see below), 52 isolates had mutant

phenotypes and/or complementation data indistinguishable from those of another isolate recovered from the same group of mutagenized P_0s. In such cases, only one of these redundant strains from each P_0 group was retained, leaving 189 independent screen isolates.

Of the 189 final screen isolates, 45 had phenotypes recognizably distinct from CEM survival (see Appendix II). The remaining 144 with phenotypes consistent with CEM survival were examined using a fluorescence-equipped dissecting microscope for defects typical of masculinization of hermaphrodites: mutations dominantly causing CEM survival and recessively causing essentially complete masculinization, mutations causing the presence of *pkd-2::gfp*-expressing cells in the tail or other tail masculinization, mutations causing a Pvl (protruding vulva) phenotype. Egl and Dpy phenotypes, which can result from partial defects in sex determination or dosage compensation, were not considered necessarily to be indicators of sexual transformation. Isolates that displayed CEM survival in hermaphrodites but did not show such gross defects indicative of sexual transformation were classified as candidates to be defective in programmed cell death, weakly defective in sex determination or defective either in the determination of the CEM fate or the specification of CEM cell death. These isolates were mated with males homozygous for the *pkd-2::gfp* transgene used in their isolation, and the F_1 males resulting from these crosses were mated with three *dpy-5*; *nIs128* strains, each homozygous for *ced-3(n717)*, *ced-4(n1162)*, or *egl-1(n1084 n3082)*. A minimum of 16 cross-progeny hermaphrodites from each cross were examined for CEM survival using *pkd-2::gfp*. When complementation tests with an isolate appeared to show failure to complement either none or more than one of the

three cell-death genes tested, the tests were repeated at least once. Isolates with ambiguous complementation results and isolates for which F_1 cross-progeny males were unable to mate were examined for the presence of extra neurons in the anterior pharynx using Nomarski microscopy as described below; eight Ced isolates were identified in this fashion and were later determined to be four gain-of-function alleles of *ced-9*, three alleles of *ced-3*, and one allele of *ced-4* that had initially escaped detection. Remaining isolates were considered candidates to be specifically defective in the deaths of the CEM neurons, and those with a suitably high penetrance of CEM survival were mapped against cluster-linked markers. This mapping necessarily used markers for only five of the six *C. elegans* chromosomes, excluding the chromosome on which was integrated the transgene used in isolating the mutant, as the integrated transgenes used in these screens were found not to readily recombine with cluster-linked markers on their respective chromosomes, making the inclusion of such markers in the mapping impractical. Isolates mapping to LGI and isolates with *pkd-2::gfp*-expressing neurons in positions more consistent with those of the URA neurons than the CEM neurons were tested for their ability to complement *cfi-1(ky651) I*; loss of *cfi-1* function causes the URA neurons to adopt morphology similar to that of the CEM neurons and to express the *pkd-2::gfp* cell fate reporter (SHAHAM and BARGMANN 2002). Candidates were selected from among the remaining isolates on the basis of their phenotypic strength, their map positions, and interesting pleiotropies associated with them and were subjected to additional analysis to identify the genes mutated in these isolates. Isolates that were not assigned to any identified gene were examined for the morphology of their B cells in L1 larvae (see below).

Determination of DNA sequences and DNA manipulation

DNA sequences were determined using an ABI DNA Sequencer model 377, an ABI Genetic Analyzer 3100, and by Gene Gateway (Hayward, CA). For single-gene rescue of *tra-4(n3715)*, genomic DNA corresponding to nucleotides 4096 through 12003 of F53B3 was amplified by PCR genomic (Advantage cDNA; BD Biosciences) from proteinase K-treated N2 animals. This fragment contains the single gene *F53B3.1*, including 2654 bp 5' of the predicted start codon and 1958 bp 3' of the predicted stop codon.

Isolation of deletion mutations

A library of mutagenized *C. elegans* was screened for deletions as previously described (JANSEN *et al.* 1997). Two deletions were isolated: *ceh-31(n4893Δ)*, which removes from 22645 to 27984 of cosmid C33D12 (all references to cosmid C33D12 sequence refer to nucleotides of accession number U64600), and *nDf65*, which removes from 21388 of cosmid C33D12 to 1119 of cosmid F52E4 (accession number U56964). *ceh-31(n4893Δ)* removes part of the first exon and the entire second exon of *ceh-31*, including the predicted homeobox and BARC domains. *nDf65* removes the complete coding sequences of both *ceh-30* and *ceh-31* but not any other predicted genes. We used PCR to confirm that sequences present in the wild type are missing in *ceh-31(n4893Δ)* and *nDf65* homozygotes. *ceh-31(n4893Δ)* and *nDf65* were each outcrossed at least two times for the X chromosome and four times for the autosomal genome prior to strain construction and analysis.

Determination of *C. elegans* phenotypes

Animals were examined for gross developmental defects using dissecting and Nomarski microscopy. Programmed cell death in the anterior pharynx was quantified using Nomarski microscopy as described (SCHWARTZ 2007); at least ten animals were examined for each genotype. Survival of Pn.aap cells was quantified using the *lin-11::gfp* reporter *nIs106* as described (REDDIEN *et al.* 2001). Corpse number in the heads of L1 larvae was determined as described (YUAN and HORVITZ 1992). The Vab defect of abnormal head morphology was scored in mixed-stage young larvae under 500x magnification using a dissecting microscope. The size and morphology of the B cells of L1 larvae were examined using Nomarski microscopy (SULSTON and HORVITZ 1977). The B cells of males and of masculinized L1 larvae are significantly larger than those of hermaphrodites and, unlike the B cells of hermaphrodites, contain a single large nucleolus when seen using Nomarski microscopy. This difference in B cell nuclear size and morphology corresponds with sexual dimorphism of the B cell fate: the hermaphrodite B cell does not divide, while the male B cell is a blast cell that, through seven rounds of cell division, generates 47 cells (SULSTON and HORVITZ 1977). The B cells of *ced-9(*gf*)*, *ceh-30(*gf*)*, *cnd-1(*lf*)*, and *vab-3(*lf*)* L1 larvae did not display morphology abnormal for L1 hermaphrodites (data not shown). Programmed cell death in the CEM lineage was assessed using a fluorescence-equipped dissecting microscope (M^2BIO; Kramer Scientific, Valley Cottage, NY) to detect *pkd-2::gfp* expression in the cell bodies of CEM neurons or by using Nomarski microscopy as described (SCHWARTZ 2007).

Acknowledgments

We Brendan Galvin and Niels Ringstad for comments about the manuscript; Beth Castor, Shannon McGonagle, and Elissa Murphy for assistance with determination of DNA sequences and for the identification of candidate deletions; Na An for help with strains; Brendan Galvin for the unpublished allele *egl-1(n4908Δ)*; Bill Walthall for *unc-131(jd19)*; Kiyoji Nishiwaki for *vab-3(k121)* and *vab-3(k143)*; Yishi Jin for *cnd-1(ju29)* and for unpublished information about the *cnd-1* defect in head morphology; Nese Cinar and Andrew Chisholm for identification of the *vab-3* mutations in *n3721* and *n3723*; Alan Coulson for cosmid clones; the *Caenorhabditis* Genetics Center, which is funded by the NIH National Center for Research Resources (NCRR), for strains; Maureen Barr and Paul Sternberg for ppkd-2::gfp1; and the *C. elegans* Genome Sequencing Consortium and the Genome Sequencing Center at Washington University in St. Louis for genomic sequence and for the identification of polymorphisms in CB4856. This work was supported by the Howard Hughes Medical Institute. H.T.S. was supported in part by a David H. Koch Graduate Fellowship. H.R.H. is an Investigator of the Howard Hughes Medical Institute and is David H. Koch Professor of Biology at MIT.

References

ABRAHAM, M. C., Y. LU and S. SHAHAM, 2007 A morphologically conserved nonapoptotic program promotes linker cell death in *Caenorhabditis elegans*. Dev Cell **12:** 73-86.

AKERIB, C. C., and B. J. MEYER, 1994 Identification of X chromosome regions in *Caenorhabditis elegans* that contain sex-determination signal elements. Genetics **138:** 1105-1125.

BARR, M. M., and P. W. STERNBERG, 1999 A polycystic kidney-disease gene homologue required for male mating behaviour in *C. elegans*. Nature **401:** 386-389.

BIDERE, N., H. C. SU and M. J. LENARDO, 2006 Genetic disorders of programmed cell death in the immune system. Annu Rev Immunol **24:** 321-352.

BLOOM, L., and H. R. HORVITZ, 1997 The *Caenorhabditis elegans* gene *unc-76* and its human homologs define a new gene family involved in axonal outgrowth and fasciculation. Proc Natl Acad Sci U S A **94:** 3414-3419.

BRENNER, S., 1974 The genetics of *Caenorhabditis elegans*. Genetics **77:** 71-94.

CAMERON, S., S. G. CLARK, J. B. MCDERMOTT, E. AAMODT and H. R. HORVITZ, 2002 PAG-3, a Zn-finger transcription factor, determines neuroblast fate in *C. elegans*. Development **129:** 1763-1774.

CHAE, J. H., G. H. STEIN and J. E. LEE, 2004 NeuroD: the predicted and the surprising. Mol Cells **18:** 271-288.

CHAMBERLIN, H. M., and P. W. STERNBERG, 1995 Mutations in the *Caenorhabditis elegans* gene *vab-3* reveal distinct roles in fate specification and unequal cytokinesis in an asymmetric cell division. Dev Biol **170:** 679-689.

CHASNOV, J. R., W. K. SO, C. M. CHAN and K. L. CHOW, 2007 The species, sex, and stage specificity of a *Caenorhabditis* sex pheromone. Proc Natl Acad Sci U S A **104:** 6730-6735.

CHEN, F., B. M. HERSH, B. CONRADT, Z. ZHOU, D. RIEMER *et al.*, 2000 Translocation of *C. elegans* CED-4 to nuclear membranes during programmed cell death. Science **287:** 1485-1489.

CHISHOLM, A. D., and H. R. HORVITZ, 1995 Patterning of the *Caenorhabditis elegans* head region by the *Pax-6* family member *vab-3*. Nature **377:** 52-55.

CHOI, C. Y., Y. H. KIM, H. J. KWON and Y. KIM, 1999 The homeodomain protein NK-3 recruits Groucho and a histone deacetylase complex to repress transcription. J Biol Chem **274:** 33194-33197.

CHUNG, S., T. L. GUMIENNY, M. O. HENGARTNER and M. DRISCOLL, 2000 A common set of engulfment genes mediates removal of both apoptotic and necrotic cell corpses in *C. elegans*. Nat Cell Biol **2:** 931-937.

CINAR, H. N., and A. D. CHISHOLM, 2004 Genetic analysis of the *Caenorhabditis elegans pax-6* locus: roles of paired domain-containing and nonpaired domain-containing isoforms. Genetics **168:** 1307-1322.

CLARK, S. G., X. LU and H. R. HORVITZ, 1994 The *Caenorhabditis elegans* locus *lin-15*, a negative regulator of a tyrosine kinase signaling pathway, encodes two different proteins. Genetics **137:** 987-997.

CONRADT, B., and H. R. HORVITZ, 1998 The *C. elegans* protein EGL-1 is required for programmed cell death and interacts with the Bcl-2-like protein CED-9. Cell **93:** 519-529.

CONRADT, B., and H. R. HORVITZ, 1999 The TRA-1A sex determination protein of *C. elegans* regulates sexually dimorphic cell deaths by repressing the *egl-1* cell death activator gene. Cell **98:** 317-327.

DEL PESO, L., V. M. GONZALEZ, N. INOHARA, R. E. ELLIS and G. NUNEZ, 2000 Disruption of the CED-9.CED-4 complex by EGL-1 is a critical step for programmed cell death in *Caenorhabditis elegans*. J Biol Chem **275:** 27205-27211.

DESAI, C., and H. R. HORVITZ, 1989 *Caenorhabditis elegans* mutants defective in the functioning of the motor neurons responsible for egg laying. Genetics **121:** 703-721.

ELLIS, R. E., and H. R. HORVITZ, 1991 Two *C. elegans* genes control the programmed deaths of specific cells in the pharynx. Development **112:** 591-603.

ELLIS, R. E., D. M. JACOBSON and H. R. HORVITZ, 1991 Genes required for the engulfment of cell corpses during programmed cell death in *Caenorhabditis elegans*. Genetics **129:** 79-94.

FINN, R. D., J. MISTRY, B. SCHUSTER-BOCKLER, S. GRIFFITHS-JONES, V. HOLLICH *et al.*, 2006 Pfam: clans, web tools and services. Nucleic Acids Res **34:** D247-251.

FINNEY, M., and G. RUVKUN, 1990 The *unc-86* gene product couples cell lineage and cell identity in *C. elegans*. Cell **63:** 895-905.

FINNEY, M., G. RUVKUN and H. R. HORVITZ, 1988 The *C. elegans* cell lineage and differentiation gene *unc-86* encodes a protein with a homeodomain and extended similarity to transcription factors. Cell **55:** 757-769.

GROTE, P., and B. CONRADT, 2006 The PLZF-like Protein TRA-4 Cooperates with the Gli-like Transcription Factor TRA-1 to Promote Female Development in *C. elegans*. Dev Cell **11:** 561-573.

HALLAM, S., E. SINGER, D. WARING and Y. JIN, 2000 The *C. elegans* NeuroD homolog *cnd-1* functions in multiple aspects of motor neuron fate specification. Development **127:** 4239-4252.

HATZOLD, J., and B. CONRADT, 2008 Control of apoptosis by asymmetric cell division. PLoS Biol **6:** e84.

HENGARTNER, M. O., R. E. ELLIS and H. R. HORVITZ, 1992 *Caenorhabditis elegans* gene *ced-9* protects cells from programmed cell death. Nature **356:** 494-499.

HENGARTNER, M. O., and H. R. HORVITZ, 1994a Activation of *C. elegans* cell death protein CED-9 by an amino-acid substitution in a domain conserved in Bcl-2. Nature **369:** 318-320.

HENGARTNER, M. O., and H. R. HORVITZ, 1994b *C. elegans* cell survival gene *ced-9* encodes a functional homolog of the mammalian proto-oncogene *bcl-2*. Cell **76:** 665-676.

HERMAN, R. K., 1978 Crossover suppressors and balanced recessive lethals in *Caenorhabditis elegans*. Genetics **88:** 49-65.

HODGKIN, J., 1980 More sex-determination mutants of *Caenorhabditis elegans*. Genetics **96:** 649-664.

HODGKIN, J., 1987 A genetic analysis of the sex-determining gene, *tra-1*, in the nematode *Caenorhabditis elegans*. Genes Dev **1:** 731-745.

HODGKIN, J., 2002 Exploring the envelope. Systematic alteration in the sex-determination system of the nematode *Caenorhabditis elegans*. Genetics **162:** 767-780.

HOEPPNER, D. J., M. O. HENGARTNER and R. SCHNABEL, 2001 Engulfment genes cooperate with *ced-3* to promote cell death in *Caenorhabditis elegans*. Nature **412:** 202-206.

HOEPPNER, D. J., M. S. SPECTOR, T. M. RATLIFF, J. M. KINCHEN, S. GRANAT *et al.*, 2004 *eor-1* and *eor-2* are required for cell-specific apoptotic death in *C. elegans*. Dev Biol **274:** 125-138.

HORVITZ, H. R., H. M. ELLIS and P. W. STERNBERG, 1982 Programmed cell death in nematode development. Neuroscience Commentaries **1:** 56-65.

HOWARD, R. M., and M. V. SUNDARAM, 2002 *C. elegans* EOR-1/PLZF and EOR-2 positively regulate Ras and Wnt signaling and function redundantly with LIN-25 and the SUR-2 Mediator component. Genes Dev **16:** 1815-1827.

INABA, T., T. INUKAI, T. YOSHIHARA, H. SEYSCHAB, R. A. ASHMUN *et al.*, 1996 Reversal of apoptosis by the leukaemia-associated E2A-HLF chimaeric transcription factor. Nature **382:** 541-544.

JAGER, S., H. T. SCHWARTZ, H. R. HORVITZ and B. CONRADT, 2004 The *Caenorhabditis elegans* F-box protein SEL-10 promotes female development and may target FEM-1 and FEM-3 for degradation by the proteasome. Proc Natl Acad Sci U S A **101:** 12549-12554.

JANSEN, G., E. HAZENDONK, K. L. THIJSSEN and R. H. PLASTERK, 1997 Reverse genetics by chemical mutagenesis in *Caenorhabditis elegans*. Nat Genet **17:** 119-121.

JIMENEZ, G., C. P. VERRIJZER and D. ISH-HOROWICZ, 1999 A conserved motif in goosecoid mediates groucho-dependent repression in *Drosophila* embryos. Mol Cell Biol **19:** 2080-2087.

JOSHI, P., and D. M. EISENMANN, 2004 The *Caenorhabditis elegans pvl-5* gene protects hypodermal cells from *ced-3*-dependent, *ced-4*-independent cell death. Genetics **167:** 673-685.

KELLY, K. F., and J. M. DANIEL, 2006 POZ for effect – POZ-ZF transcription factors in cancer and development. Trends Cell Biol **16:** 578-587.

KIM, W. Y., B. FRITZSCH, A. SERLS, L. A. BAKEL, E. J. HUANG *et al.*, 2001 NeuroD-null mice are deaf due to a severe loss of the inner ear sensory neurons during development. Development **128**.

KIMBLE, J., and D. HIRSH, 1979 The postembryonic cell lineages of the hermaphrodite and male gonads in *Caenorhabditis elegans*. Dev Biol **70:** 396-417.

LEE, J. E., S. M. HOLLENBERG, L. SNIDER, D. L. TURNER, N. LIPNICK *et al.*, 1995a Conversion of *Xenopus* ectoderm into neurons by *NeuroD*, a basic helix-loop-helix protein. Science **268:** 836-844.

LEE, J. E., S. M. HOLLENBERG, L. SNIDER, D. L. TURNER, N. LIPNICK *et al.*, 1995b Conversion of *Xenopus* ectoderm into neurons by NeuroD, a basic helix-loop-helix protein. Science **268:** 836-844.

LETTRE, G., and M. O. HENGARTNER, 2006 Developmental apoptosis in *C. elegans*: a complex CEDnario. Nat Rev Mol Cell Biol **7:** 97-108.

LEWIS, J. A., and J. A. HODGKIN, 1977 Specific neuroanatomical changes in chemosensory mutants of the nematode *Caenorhabditis elegans*. J Comp Neurol **172:** 489-510.

LI, S., S. M. PRICE, H. CAHILL, D. K. RYUGO, M. M. SHEN *et al.*, 2002 Hearing loss caused by progressive degeneration of cochlear hair cells in mice deficient for the *Barhl1* homeobox gene. Development **129:** 3523-3532.

LIU, H., T. J. STRAUSS, M. B. POTTS and S. CAMERON, 2006 Direct regulation of *egl-1* and of programmed cell death by the Hox protein MAB-5 and by CEH-20, a *C. elegans* homolog of Pbx1. Development **133:** 641-650.

LUM, D. H., P. E. KUWABARA, D. ZARKOWER and A. M. SPENCE, 2000 Direct protein-protein interaction between the intracellular domain of TRA-2 and the transcription factor TRA-1A modulates feminizing activity in *C. elegans*. Genes Dev **14:** 3153-3165.

MAURER, C. W., M. CHIORAZZI and S. SHAHAM, 2007 Timing of the onset of a developmental cell death is controlled by transcriptional induction of the *C. elegans ced-3* caspase-encoding gene. Development **134:** 1357-1368.

MELLO, C. C., J. M. KRAMER, D. STINCHCOMB and V. AMBROS, 1991 Efficient gene transfer in *C.elegans*: extrachromosomal maintenance and integration of transforming sequences. Embo J **10:** 3959-3970.

MENEELY, P. M., and K. D. NORDSTROM, 1988 X chromosome duplications affect a region of the chromosome they do not duplicate in *Caenorhabditis elegans*. Genetics **119:** 365-375.

METZSTEIN, M. M., M. O. HENGARTNER, N. TSUNG, R. E. ELLIS and H. R. HORVITZ, 1996 Transcriptional regulator of programmed cell death encoded by *Caenorhabditis elegans* gene *ces-2*. Nature **382:** 545-547.

METZSTEIN, M. M., and H. R. HORVITZ, 1999 The *C. elegans* cell death specification gene *ces-1* encodes a snail family zinc finger protein. Mol Cell **4:** 309-319.

METZSTEIN, M. M., G. M. STANFIELD and H. R. HORVITZ, 1998 Genetics of programmed cell death in *C. elegans*: past, present and future. Trends Genet **14:** 410-416.

MILLER, D. M., M. M. SHEN, C. E. SHAMU, T. R. BURGLIN, G. RUVKUN *et al.*, 1992 *C. elegans unc-4* gene encodes a homeodomain protein that determines the pattern of synaptic input to specific motor neurons. Nature **355:** 841-845.

NAYA, F. J., H. P. HUANG, Y. QIU, H. MUTOH, F. J. DEMAYO *et al.*, 1997 Diabetes, defective pancreatic morphogenesis, and abnormal enteroendocrine differentiation in BETA2/neuroD-deficient mice. Genes Dev **11:** 2323-2334.

NISHIWAKI, K., 1999 Mutations affecting symmetrical migration of distal tip cells in *Caenorhabditis elegans*. Genetics **152:** 985-997.

OSUMI, N., H. SHINOHARA, K. NUMAYAMA-TSURUTA and M. MAEKAWA, 2008 Pax6 Transcription Factor Contributes to Both Embryonic and Adult Neurogenesis as a Multifunctional Regulator. Stem Cells.

PEDEN, E., E. KIMBERLY, K. GENGYO-ANDO, S. MITANI and D. XUE, 2007 Control of sex-specific apoptosis in *C. elegans* by the BarH homeodomain protein CEH-30 and the transcriptional repressor UNC-37/Groucho. Genes Dev **21:** 3195-3207.

PILGRIM, D., A. MCGREGOR, P. JACKLE, T. JOHNSON and D. HANSEN, 1995 The *C. elegans* sex-determining gene *fem-2* encodes a putative protein phosphatase. Mol Biol Cell **6:** 1159-1171.

PRASAD, B. C., B. YE, R. ZACKHARY, K. SCHRADER, G. SEYDOUX *et al.*, 1998 *unc-3*, a gene required for axonal guidance in *Caenorhabditis elegans*, encodes a member of the O/E family of transcription factors. Development **125:** 1561-1568.

RATHMELL, J. C., and C. B. THOMPSON, 2002 Pathways of apoptosis in lymphocyte development, homeostasis, and disease. Cell **109 Suppl:** S97-107.

REDDIEN, P. W., 2002 Phagocytosis promotes programmed cell death and is controlled by Rac signaling pathway in *C. elegans*. Ph. D. Thesis, Massachusetts Institute of Technology, Cambridge, MA.

REDDIEN, P. W., E. C. ANDERSEN, M. C. HUANG and H. R. HORVITZ, 2007 DPL-1 DP, LIN-35 Rb and EFL-1 E2F act with the MCD-1 zinc-finger protein to promote programmed cell death in *Caenorhabditis elegans*. Genetics **175:** 1719-1733.

REDDIEN, P. W., S. CAMERON and H. R. HORVITZ, 2001 Phagocytosis promotes programmed cell death in *C. elegans*. Nature **412:** 198-202.

REINER, D. J., D. WEINSHENKER and J. H. THOMAS, 1995 Analysis of dominant mutations affecting muscle excitation in *Caenorhabditis elegans*. Genetics **141:** 961-976.

RIDDLE, D. L., T. BLUMENTHAL, B. J. MEYER and J. R. PRIESS, 1997 *C. elegans* II (Cold Spring Harbor Laboratory Press, Cold Spring Harbor, New York).

ROBERTSON, A. M. G., and J. N. THOMPSON, 1982 Ultrastructural study of cell death in *Caenorhabditis elegans*. J Embryol Exp Morphol **67:** 89-100.

ROSENBLUTH, R. E., C. CUDDEFORD and D. L. BAILLIE, 1985 Mutagenesis in *Caenorhabditis elegans*. II. A spectrum of mutational events induced with 1500 r of gamma-radiation. Genetics **109:** 493-511.

SANDER, M., A. NEUBUSER, J. KALAMARAS, H. C. EE, G. R. MARTIN *et al.*, 1997 Genetic analysis reveals that PAX6 is required for normal transcription of pancreatic hormone genes and islet development. Genes Dev **11:** 1662-1673.

SCHUMACHER, B., C. SCHERTEL, N. WITTENBURG, S. TUCK, S. MITANI *et al.*, 2005 *C. elegans ced-13* can promote apoptosis and is induced in response to DNA damage. Cell Death Differ **12:** 153-161.

SCHWARTZ, H. T., 2007 A protocol describing pharynx counts and a review of other assays of apoptotic cell death in the nematode worm *Caenorhabditis elegans*. Nature Protocols **2:** 705-714.

SCHWARTZ, H. T., and H. R. HORVITZ, 2007 The *C. elegans* protein CEH-30 protects male-specific neurons from apoptosis independently of the Bcl-2 homolog CED-9. Genes Dev **21:** 3181-3194.

SHAHAM, S., and C. I. BARGMANN, 2002 Control of neuronal subtype identity by the *C. elegans* ARID protein CFI-1. Genes Dev **16:** 972-983.

SHAHAM, S., and H. R. HORVITZ, 1996 Developing *Caenorhabditis elegans* neurons may contain both cell-death protective and killer activities. Genes Dev **10:** 578-591.

SHAHAM, S., P. W. REDDIEN, B. DAVIES and H. R. HORVITZ, 1999 Mutational analysis of the *Caenorhabditis elegans* cell-death gene *ced-3*. Genetics **153:** 1655-1671.

SIEGFRIED, K. R., A. R. KIDD, 3RD, M. A. CHESNEY and J. KIMBLE, 2004 The *sys-1* and *sys-3* genes cooperate with Wnt signaling to establish the proximal-distal axis of the *Caenorhabditis elegans* gonad. Genetics **166:** 171-186.

SIMPSON, T. I., and D. J. PRICE, 2002 Pax6; a pleiotropic player in development. Bioessays **24:** 1041-1051.

STANFIELD, G. M., and H. R. HORVITZ, 2000 The *ced-8* gene controls the timing of programmed cell deaths in *C. elegans*. Mol Cell **5:** 423-433.

SULSTON, J. E., and H. R. HORVITZ, 1977 Post-embryonic cell lineages of the nematode, *Caenorhabditis elegans*. Dev Biol **56:** 110-156.

SULSTON, J. E., E. SCHIERENBERG, J. G. WHITE and J. N. THOMSON, 1983 The embryonic cell lineage of the nematode *Caenorhabditis elegans*. Dev Biol **100:** 64-119.

THELLMANN, M., J. HATZOLD and B. CONRADT, 2003 The Snail-like CES-1 protein of *C. elegans* can block the expression of the BH3-only cell-death activator gene *egl-1* by antagonizing the function of bHLH proteins. Development **130:** 4057-4071.

TREININ, M., and M. CHALFIE, 1995 A mutated acetylcholine receptor subunit causes neuronal degeneration in *C. elegans*. Neuron **14:** 871-877.

TRENT, C., N. TSUING and H. R. HORVITZ, 1983 Egg-laying defective mutants of the nematode *Caenorhabditis elegans*. Genetics **104:** 619-647.

WANG, X., and H. M. CHAMBERLIN, 2002 Multiple regulatory changes contribute to the evolution of the *Caenorhabditis lin-48 ovo* gene. Genes Dev **16:** 2345-2349.

WEAVER, B. A., and D. W. CLEVELAND, 2005 Decoding the links between mitosis, cancer, and chemotherapy: The mitotic checkpoint, adaptation, and cell death. Cancer Cell **8:** 7-12.

WICKS, S. R., R. T. YEH, W. R. GISH, R. H. WATERSTON and R. H. PLASTERK, 2001 Rapid gene mapping in *Caenorhabditis elegans* using a high density polymorphism map. Nat Genet **28:** 160-164.

WU, W. S., S. HEINRICHS, D. XU, S. P. GARRISON, G. P. ZAMBETTI *et al.*, 2005 Slug antagonizes p53-mediated apoptosis of hematopoietic progenitors by repressing *puma*. Cell **123:** 641-653.

YAN, N., L. GU, D. KOKEL, J. CHAI, W. LI *et al.*, 2004 Structural, Biochemical, and Functional Analyses of CED-9 Recognition by the Proapoptotic Proteins EGL-1 and CED-4. Mol Cell **15:** 999-1006.

YANG, X., H. Y. CHANG and D. BALTIMORE, 1998 Essential role of CED-4 oligomerization in CED-3 activation and apoptosis. Science **281:** 1355-1357.

YEO, W., and J. GAUTIER, 2004 Early neural cell death: dying to become neurons. Dev Biol **274:** 233-244.

YUAN, J., and H. R. HORVITZ, 1992 The *Caenorhabditis elegans* cell death gene *ced-4* encodes a novel protein and is expressed during the period of extensive programmed cell death. Development **116:** 309-320.

YUAN, J., S. SHAHAM, S. LEDOUX, H. M. ELLIS and H. R. HORVITZ, 1993 The *C. elegans* cell death gene *ced-3* encodes a protein similar to mammalian interleukin-1 beta-converting enzyme. Cell **75:** 641-652.

ZALLEN, J. A., S. A. KIRCH and C. I. BARGMANN, 1999 Genes required for axon pathfinding and extension in the *C. elegans* nerve ring. Development **126:** 3679-3692.

ZELENT, A., F. GUIDEZ, A. MELNICK, S. WAXMAN and J. D. LICHT, 2001 Translocations of the RARalpha gene in acute promyelocytic leukemia. Oncogene **20:** 7186-7203.

ZHANG, Y., and S. W. EMMONS, 1995 Specification of sense-organ identity by a *Caenorhabditis elegans Pax-6* homologue. Nature **377:** 55-59.

ZHAO, C., and S. W. EMMONS, 1995 A transcription factor controlling development of peripheral sense organs in *C. elegans*. Nature **373:** 74-78.

ZOU, H., W. J. HENZEL, X. LIU, A. LUTSCHG and X. WANG, 1997 Apaf-1, a human protein homologous to *C. elegans* CED-4, participates in cytochrome c-dependent activation of caspase-3. Cell **90:** 405-413.

Table 1. Screen isolates with surviving *pkd-2::gfp*-expressing CEM neurons in the hermaphrodite

Class	Gene(s)	Isolates	Alleles
Cell death	*ced-3*	32	*n3452*[a], *n3453*[a], *n3454*[a], *n3458*[c], *n3534*[a], *n3546*[b], *n3547*[b], *n3548*[b], *n3549*[b], *n3570*[b], *n3571*[b], *n3574*[b], *n3575*[c], *n3576*[c], *n3577*[c], *n3578*[c], *n3579*[a], *n3580*[a], *n3612*[b], *n3614*[c], *n3615*[c], *n3616*[c], *n3618*[a], *n3619*[a], *n3695*[c], *n3820*[a], *n3821*[c], *n4079*[b], *n4699*[c], *n4706*[c], *n4707*[c], *n4727*[c]
Cell death	*ced-4*	16	*n3455*[a], *n3456*[a], *n3457*[a], *n3459*[c], *n3460*[c], *n3532*[c], *n3533*[a], *n3550*[b], *n3551*[c], *n3572*[b], *n3573*[b], *n3613*[b], *n3617*[c], *n3620*[a], *n3621*[b], *n4080*[a]
Cell death	*ced-9*	4	*n4081*[a], *n4698*[c], *n4700*[b], *n4713*[b]
CEM fate	*cnd-1*	3	*n3786*[a], *n3787*[a], *n4744*[b]
CEM fate	*vab-3*	2	*n3721*[a], *n3723*[a]
CEM-specific survival	*ceh-30*	3	*n3713*[c], *n3714*[c], *n3720*[a]
Sex determination	*sel-10*	1	*n3717*[c]
Sex determination	*tra-4*	4	*n3715*[c], *n3716*[c], *n4724*[b], *n4726*[b]
Sex determination	N.D.	62	*n3819*[a,d], *n4084*[a,e], *n4085 II*[a,e], *n4657*[a,e], *n4658*[b,e], *n4659*[b,e], *n4660*[b,e], *n4661*[b,e], *n4662*[b,e], *n4663*[b,e], *n4664*[b,e], *n4665*[b,e], *n4667*[b,e], *n4668*[b,e], *n4669*[b,e], *n4680*[a,e], *n4681*[a,e], *n4682*[a,e], *n4683*[a,e], *n4684*[a,e], *n4686*[a,e], *n4687*[a,e], *n4688*[a,e], *n4689*[b,e], *n4690*[b,e], *n4691*[b,e], *n4692*[c,e], *n4693*[c,e], *n4694*[c,e], *n4695*[c,e], *n4701*[a,e], *n4702 II*[c,e], *n4703*[b,e], *n4704*[a,d], *n4708*[c,e], *n4709*[c,e], *n4710*[c,d], *n4714*[c,e], *n4715*[c,e], *n4717*[a,e], *n4718*[a,e], *n4719*[c,e], *n4720*[c,e], *n4721*[c,e], *n4722*[a,d], *n4723*[c,d], *n4728*[c,e], *n4730*[a,d], *n4731*[c,d], *n4732*[c,d], *n4733*[a,e], *n4734*[b,e], *n4735*[c,e], *n4736*[c,e], *n4737*[a,d], *n4738*[a,d], *n4739*[b,e], *n4742*[c,d], *n4745*[c,e], *n4746*[a,e], *n4755*[b,e], *n4758*[a,d]
Undetermined	N.D.	17	*n3788*[b], *n3793 I*[c], *n4082*[a], *n4083*[b], *n4679 V*[a], *n4685*[c], *n4697*[b], *n4711*[c], *n4712*[b], *n4740*[a], *n4741*[b], *n4748*[b], *n4749*[a], *n4750*[c], *n4752*[a], *n4756*[b], *n4757*[a]

[a] Isolated in a MT10729 *nIs128 II* background.
[b] Isolated in a MT10739 *nIs130 IV* background.
[c] Isolated in a MT10742 *nIs133 I* background.
[d] Likely intersex (one or more of the following additional phenotypes observed in the mutant strain: *pkd-2::gfp*-expressing neurons in the tail, Pvl, Egl, Dpy)
[e] Mutation apparently dominantly causes CEM survival in hermaphrodites and recessively causes essentially complete masculinization.

A complete list of mutations causing apparent survival of the CEM neurons in hermaphrodites isolated in our screens. Mutations are organized by class: mutations affecting all programmed cell deaths, mutations affecting multiple aspects of the CEM

identity, mutations specifically affecting the CEM survival decision, mutations affecting multiple aspects of sex determination, and mutations whose defects have not been determined. Mutations are assigned to specific genes where possible. N.D., not determined. The mutations that were molecularly identified are detailed in Table 2. The 17 mutations in the 'undetermined' class are described in more detail in Table 3.

Table 2. Molecularly identified mutations from the *pkd-2::gfp* screen for CEM survival

Gene	Allele	Position	DNA Sequence		Substitution or aberration
			Wild-type	Mutant	
ced-3	*n4699*	6825	AGgtactt	AGatactt	Exon 7 splice donor
ced-3	*n4727*	7007	GCT	GTT	A423V
ced-9	*n4081*gf *n4698*gf *n4713*gf	12134	GGT	GAT	G173D
ced-9	*n4700*gf	11590	GGA	AGA	G169R
sel-10	*n3717*	12613	GGA	GAA	G567E
tra-4	*n3715*	7380	CAT	TAT	H345Y
tra-4	*n3716*	7290	CAC	TAC	H375Y
tra-4	*n4724*	6750	TGT	TAT	C418Y
tra-4	*n4726*	7283	TGT	TAT	C377Y
ceh-30	*n3713*gf *n3714*gf *n3720*gf	22027	gggtggtc	gagtggtc	disrupts TRA-1 binding site
cnd-1	*n3786*	15172	CGA	TGA	R20opal
cnd-1	*n3787*	14667	CAA	TAA	Q76ochre
cnd-1	*n4744*	15106	CTC	TTC	L42F
vab-3	*n3721*	15993	AGCgtgagt	AGCgtgaat	Exon 5 splice donor
vab-3	*n3723*	14340	CGGgtaagt	CGGataagt	Exon 3 splice donor

Position refers to nucleotides in the DNA sequence of the cosmid on which the gene resides (in order of gene appearance, with accession numbers: C48D1 Z81049, T07C4 Z29443, F55B12 Z79757, C33D12 U64600, C34E10 U10402, and F14F3 Z49937). Sequences from the coding strands from wild-type and mutant animals are shown, with the affected nucleotide underlined; for missense and stop mutations, the wild-type and mutant sequences of the relevant codon are shown. Coding nucleotides are shown in uppercase, and noncoding nucleotides are shown in lowercase.

Table 3. Phenotypes associated with unidentified mutations affecting CEM survival.

Isolate	Extra cells in anterior pharynx (n)	Large B cells	CEM survival in hermaphrodites (%) None	D OR V	D AND V	n
n3788	0.1 ± 0.3 (30)	No (0/14)	56	42	2	60
n3793 I	0 ± 0 (12)	**Yes** (11/20)	17	44	38	63
n4082	0 ± 0 (10)	**Yes** (13/15)	54	46	0	67
n4083	0 ± 0 (10)	No (0/15)	53	46	1	68
n4679 V	0 ± 0 (10)	No (0/15)	75	24	1	80
n4685	0 ± 0 (10)	**Yes** (7/15)	88	10	1	67
n4697	0 ± 0 (10)	**Yes** (12/15)	85	14	1	85
n4711	0 ± 0 (10)	**Yes** (7/15)	85	13	2	85
n4712	0 ± 0 (10)	No (0/15)	72	25	3	68
n4740	0 ± 0 (10)	**Yes** (8/15)	75	24	1	67
n4741	0 ± 0 (10)	No (0/15)	78	22	0	60
n4748	0 ± 0 (10)	**Yes** (11/15)	78	21	2	63
n4749	0 ± 0 (10)	**Yes** (11/15)	69	30	1	70
n4750	0 ± 0 (10)	**Yes** (13/15)	72	22	5	59
n4752	0 ± 0 (10)	No (0/15)	88	12	0	60
n4756	0 ± 0 (12)	**Yes** (10/15)	87	13	0	90
n4757	0 ± 0 (10)	**Yes** (10/15)	55	42	3	64

In this and other tables, CEM survival was scored using a *pkd-2::gfp* reporter as described in Materials and Methods. When CEM survival was scored using a dissecting microscope, the left and right ventral CEMs could not readily be distinguished from each other and the left and right dorsal CEMs could not readily be distinguished from each other; CEM survival was therefore assessed for ventral CEMs and for dorsal CEMs. The resulting numbers were found to be reproducible and sensitive to changes in the degree of CEM death or survival. In this and in other tables, D OR V denotes animals in which dorsal or ventral CEMs, but not both, were observed and indicates animals displaying only weak CEM survival; D AND V denotes animals in which both dorsal and ventral CEMs were observed and indicates animals showing strong CEM survival. All strains were homozygous for the *pkd-2::gfp* reporter transgene used in their isolation (for a list, see Table 1). The strain containing *n3793* was outcrossed twice and was homozygous

for *lon-2(e678)*. The other strains were not outcrossed. Number of extra cells in the anterior pharynx, B cell morphology, and CEM survival were assessed as described in Materials and Methods.

Table 4. *ced-3* alleles affect cell death to corresponding degrees in different tissues

ced-3 allele	Extra cells in anterior pharynx ± SD (n)	Suppression of *egl-1(n1084*gf*)*	CEM survival in herm. (%)		
			none	D OR V	D AND V
wild-type	0.0 ± 0.0 (10)	0% (n=68)	98	1	0
n2438	0.8 ± 0.8 (16)	22% (n=60)	62	38	0
n4707	4.4 ± 0.7 (15)	53% (n=100)	34	50	16
n2436	6.1 ± 1.9 (15)	100% (n=82)	14	58	28
n2877	7.0 ± 1.5 (10)	100% (n=73)	0	22	78
n2921	7.9 ± 2.3 (10)	100% (n=72)	0	42	58
n717	12.0 ± 1.1 (20)	100% (n=60)	0	0	100

Numbers of extra cells in the anterior pharynx for *n2877* and for *n2921* are taken from SHAHAM *et al.* (1999). Suppression of *egl-1(n1084)* was determined as percent non-Egl at 24 hours post-L4. CEM neuron survival in hermaphrodites was scored as described in animals homozygous for the *pkd-2::gfp* reporter *nIs133* using at least 50 animals per genotype. Herm., hermaphrodites.

Table 5. The noncoding mutation *egl-1(n4908Δ)* specifically controls the survival of the CEM neurons.

A. *egl-1(n4908Δ)* does not affect the number of programmed cell deaths in the anterior pharynx

Genotype	Extra cells in anterior pharynx ± SD
wild-type	0.0 ± 0.0
egl-1(n4908Δ)	0.1 ± 0.0
ced-3(n2427)	1.6 ± 1.4
ced-3(n2427); *egl-1(n4908Δ)*	1.2 ± 0.9

B. *egl-1(n4908Δ)* prevents the deaths of the CEM neurons in hermaphrodites and protects male CEMs lacking the protective function of *ceh-30*.

		Animals with CEM survival (%)			
Genotype	Sex	None	D OR V	D AND V	n
wild-type	Herm.	100	0	0	60
egl-1(n1084 n3082)	Herm.	0	7	93	60
egl-1(n4908Δ)	Herm.	0	17	83	77
wild-type	Male	0	0	100	60
ceh-30(n4289Δ)	Male	79	21	0	48
egl-1(n1084 n3082); *ceh-30(n4289Δ)*	Male	0	0	100	63
egl-1(n4908Δ); *ceh-30(n4289Δ)*	Male	0	0	100	60

C. Control of CEM survival by *egl-1(n4908Δ)* requires the function of *ced-9 Bcl-2*.

Genotype in the presence of		Animals with CEM survival (%)			
nIs133; *ced-9(n2812)*; *ced-3(n2427)*	Sex	None	D OR V	D AND V	n
wild-type	Herm.	75	25	0	60
egl-1(n4908Δ)	Herm.	70	30	0	63
wild-type	Male	0	18	82	60
egl-1(n4908Δ)	Male	0	23	77	48
ceh-30(n4289Δ)	Male	25	60	15	60
egl-1(n4908Δ); *ceh-30(n4289Δ)*	Male	18	78	3	61

A. Number of extra cells in the anterior pharynx was determined as described in Materials and Methods. Error, standard deviation. Ten animals of each genotype were examined. Genotypes were as listed. If *egl-1(n4908Δ)* interfered with programmed cell death in all cells, it would be expected to cause the presence of extra cells in the anterior pharynx, especially in a genetic background sensitized by the weak cell-killing mutant *ced-3(n2427)*.

B. Animals were homozygous for the *pkd-2::gfp* reporter *nIs133*. Animals mutant for *egl-1* were homozygous for *him-8(e1489)*. Other animals were homozygous for *him-5(e1467)*. Genotypes were otherwise as listed. Herm., hermaphrodite.

C. Animals were homozygous for the *pkd-2::gfp* reporter *nIs133*. Animals containing *egl-1(n4908Δ)* were homozygous for *him-8(e1489)*. Other animals were homozygous for *him-5(e1467)*. Genotypes were otherwise as listed. Herm., hermaphrodite.

Table 6. New *ced-9* gain-of-function mutations block programmed cell death in multiple tissue types.

ced-9 genotype	extra cells in anterior pharynx	Extra surviving Pn.aap cells (n)	CEM survival in herm. (%)			
			none	D OR V	D AND V	n
wild-type	0.0 ± 0.0	0.0 ± 0.0 (40)	99	1	0	70
*n4700*gf/+	4.3 ± 1.3	4.9 ± 0.3 (40)	30	69	1	71
*n4700*gf	10.2 ± 0.9	4.9 ± 0.4 (40)	6	87	7	85
*n4713*gf/+	6.6 ± 1.3	4.8 ± 0.4 (54)	18	82	0	65
*n4713*gf	11.0 ± 1.4	4.9 ± 0.3 (40)	0	68	32	77

Assays were performed as described in Materials and Methods. The new *ced-9(*gf*)* alleles *n4698* and *n4081* are not included in the table as each causes a mutation identical to that caused by *ced-9(n4713*gf*)*. Ten animals of each genotype were scored for the number of extra cells in the anterior pharynx. Animals heterozygous for *ced-9(*gf*)* were also heterozygous for *dpy-11(e224) unc-76(e911)* (anterior pharynx assay), for *unc-76(e911)* (Pn.aap assay), or for *unc-49(e382)* (CEM assay). Animals scored for Pn.aap survival were homozygous for the *lin-11::gfp* reporter *nIs106*. Animals scored for CEM neuron survival were homozygous for the *pkd-2::gfp* reporter *nIs130*. Genotypes were otherwise as indicated. Error, standard deviation. Herm., hermaphrodites.

Table 7. Testing known contributors to cell killing for a role in CEM neuron death

ced-3 genotype	*ced-3* enhancer mutation	CEM survival in hermaphrodites (%)			
		none	D OR V	D AND V	n
wild-type	none	100	0	0	100
ced-3(n2427)	none	62	38	0	128
ced-3(n2427)	*ced-9(n2812)*	64	35	1	136
ced-3(n2427)	*dpl-1(n3380)*	67	33	0	117
ced-3(n2427)	*mcd-1(n4005)*	67	33	0	126
ced-3(n2427)	*ced-8(n1891)*	27	73	1	109
ced-3(n2427)	*ced-7(n1892)*	13	83	4	112

Animals were homozygous for the *pkd-2::gfp* reporter *nIs133*. Genotypes were otherwise as indicated.

Table 8. The EGL-1 homolog CED-13 does not contribute to the deaths of the CEM neurons.

Genotype	CEM survival in males (%)			
	None	D OR V	D AND V	n
wild-type	0	0	100	50
ceh-30(n4289Δ)	80	20	0	99
ceh-30(n4289Δ) ced-13(tm536Δ)	86	14	0	78
egl-1(n1084 n3082/+); ceh-30(n4289Δ)	53	36	10	58
egl-1(n1084 n3082/+); ceh-30(n4289Δ) ced-13(tm536Δ)	54	37	10	114
egl-1(n1084 n3082); ceh-30(n4289Δ)	0	0	100	52
egl-1(n1084 n3082); ceh-30(n4289Δ) ced-13(tm536Δ)	0	0	100	51

All animals were homozygous for the *pkd-2::gfp* reporter *nIs133*. Animals wild-type for *egl-1* were homozygous for *him-5(e1467)*. Animals heterozygous for *egl-1(n1084 n3082)* were heterozygous for both *him-5(e1467)* and *him-8(e1489)*. Animals homozygous for *egl-1(n1084 n3082)* were homozygous for *him-8(e1489)*. Genotypes were otherwise as indicated.

Table 9. *sel-10* acts within the sex determination pathway to promote CEM survival.

Genotype	CEM survival in hermaphrodites (%)			
	None	D OR V	D AND V	n
wild-type	99	1	0	152
sel-10(n3717)	0	2	98	122
her-1(hv1 y101)	99	1	0	174
her-1(hv1 y101) sel-10(n3717)	2	8	90	136
fem-1(e1965)	100	0	0	110
fem-1(e1965); sel-10(n3717)	98	2	0	165
fem-2(e2105)	99	1	0	142
fem-2(e2105); sel-10(n3717)	99	1	0	133
fem-3(e1996)	99	1	0	131
fem-3(e1996); sel-10(n3717)	92	8	0	131

All animals were homozygous for the *pkd-2::gfp* reporter *nIs133*. Genotypes were otherwise as indicated. The *fem-1(e1965)* and *fem-3(e1996)* homozygotes scored were the progeny of crosses between *femInT1 [qIs51]* males and *fem* homozygous females; thus, half were XX females, and half were X0 females. *fem-2(e2105)* homozygotes scored were the self-progeny of maternally-rescued *fem-2(e2105)* mothers.

Table 10. *tra-4* acts within the sex determination pathway to control CEM neuron survival.

A. *tra-4* acts recessively to prevent CEM neuron survival. in hermaphrodites.

		CEM survival in hermaphrodites (%)			
Genotype	Maternal genotype	None	D OR V	D AND V	n
wild-type	wild-type	99	1	0	77
tra-4(n3715/+)	wild-type	99	1	0	74
tra-4(n3716/+)	wild-type	98	2	0	88
tra-4(n3715/+)	*tra-4(n3715)*	48	44	8	79
tra-4(n3716/+)	*tra-4(n3716)*	71	27	2	45
tra-4(n3715)	*tra-4(n3715)*	0	22	78	65
tra-4(n3716)	*tra-4(n3716)*	0	22	78	74
tra-4(n4724)	*tra-4(n4724)*	0	11	89	71
tra-4(n4726)	*tra-4(n4726)*	0	23	77	79
tra-4(n3715/n3716)	*tra-4(n3716)*	0	20	80	106
tra-4(n4724/n3716)	*tra-4(n3716)*	0	19	81	59
tra-4(n4726/n3716)	*tra-4(n3716)*	0	20	80	71

B. *tra-4* acts within the sex determination pathway to control CEM neuron survival.

	CEM survival in hermaphrodites (%)			
Genotype	None	D OR V	D AND V	n
her-1(hv1 y101); *tra-4(n3715)*	1	28	71	68
her-1(hv1 y101); *tra-4(n3716)*	0	41	59	69
fem-1(e1965); *tra-4(n3715)*	95	5	0	38
fem-1(e1965); *tra-4(n3716)*	100	0	0	111
fem-2(e2105); *tra-4(n3715)*	98	2	0	81
fem-2(e2105); *tra-4(n3716)*	97	3	0	79
fem-3(e1996); *tra-4(n3715)*	100	0	0	69
fem-3(e1996); *tra-4(n3716)*	100	0	0	107

A. Animals contained the *pkd-2::gfp* reporters *nIs130* or *nIs133*. Heterozygous animals were also heterozygous for *unc-76(e911)*. Genotypes were otherwise as indicated.

B. Animals were homozygous for the *pkd-2::gfp* reporter *nIs133*. Genotypes were otherwise as indicated. The *fem-1(e1965)* and *fem-3(e1996)* homozygotes scored were the progeny of crosses between *fem/nT1 [qIs51]* males and *fem* homozygous females; thus, half were XX females, and half were X0 females. *fem-2(e2105)* homozygotes scored were the progeny of maternally-rescued *fem-2(e2105)* homozygotes.

Table 11. *ceh-30* and *ceh-31* act synthetically in CEM fate determination.

A. *ceh-30 ceh-31* double mutants are defective in CEM differentiation in hermaphrodites

Genotype	CEM survival in hermaphrodites (%) None	D OR V	D AND V	n
wild-type	100	0	0	60
ceh-30(n3714gf)	3	29	68	63
ceh-30(n4111 n3714lf)	97	3	0	116
ceh-30(n4289Δ)	100	0	0	60
ceh-31(n4893Δ)	100	0	0	65
nDf65	100	0	0	60
ced-3(n717)	0	12	88	60
ced-3(n717); ceh-30(n4111 n3714lf)	0	10	90	60
ced-3(n717); ceh-30(n4289Δ)	0	5	95	60
ced-3(n717); ceh-31(n4893Δ)	0	18	82	63
ced-3(n717); nDf65	2	81	17	63
ced-3(n717); nDf65; Ex[ceh-30(+)]	2	18	80	60

B. *ceh-30 ceh-31* double mutants are weakly defective in CEM differentiation in males

Genotype	CEM survival in males (%) None	D OR V	D AND V	n
wild-type	0	0	100	60
ceh-30(n3714gf)	0	0	100	61
ceh-30(n4111 n3714lf)	44	33	23	66
ceh-30(n4289Δ)	83	14	3	71
ceh-31(n4893Δ)	0	0	100	52
nDf65	92	8	0	49
ced-3(n717)	0	0	100	60
ced-3(n717); ceh-30(n4111 n3714lf)	0	0	100	60
ced-3(n717); ceh-30(n4289Δ)	0	0	100	60
ced-3(n717); ceh-31(n4893Δ)	0	0	100	60
ced-3(n717); nDf65	0	10	90	60

A. The deficiency *nDf65* removes *ceh-30* and *ceh-31*. All animals were homozygous for *nIs133* and for *him-5(e1467)*. Animals containing the *ceh-30(+)* transgene *nEx1165* were also homozygous for *unc-76(e911)*, complemented by the transgene. Genotypes were otherwise as indicated. Similar data obtained with the cell-death-defective mutants *egl-1(n1084 n3082)* and *ced-4(n1162)* are presented in Table S1.

B. The deficiency *nDf65* removes *ceh-30* and *ceh-31*. All animals were homozygous for *nIs133* and for *him-5(e1467)*. Genotypes were otherwise as indicated. Similar data

obtained with the cell-death-defective mutants *egl-1(n1084 n3082)* and *ced-4(n1162)* are presented in Table S1.

Table 12. *vab-3 Pax6* and *cnd-1 NeuroD* promote CEM differentiation and CEM death.

A. *cnd-1 NeuroD* and *vab-3 Pax6* mutations cause CEM survival in hermaphrodites.

	CEM survival in hermaphrodites (%)			
Genotype	None	D OR V	D AND V	n
wild-type	100	0	0	60
cnd-1(n3786)	57	41	1	75
cnd-1(n3787)	56	44	0	77
cnd-1(n4744)	56	44	0	72
cnd-1(jd19)	54	44	1	68
cnd-1(ju29)	61	39	0	72
vab-3(n3721)	58	42	0	72
vab-3(n3723)	36	64	0	80
vab-3(e648)	53	45	2	64
cnd-1(n3786); vab-3(n3721)	54	45	1	76
cnd-1(n3786); vab-3(n3723)	48	48	4	75
cnd-1(n3787); vab-3(n3721)	60	40	0	90
cnd-1(n3787); vab-3(n3723)	52	45	3	75
cnd-1(n3786); ced-3(n717)	0	31	69	55
cnd-1(n3787); ced-3(n717)	0	35	65	74
ced-3(n717); vab-3(n3721)	0	22	78	72
ced-3(n717); vab-3(n3723)	0	34	66	70

B. *cnd-1 NeuroD* and *vab-3 Pax6* males fail to properly generate CEM neurons.

	CEM presence in males (%)			
Genotype	None	D OR V	D AND V	n
wild-type	0	0	100	60
ced-3(n717)	0	0	100	60
cnd-1(n3786)	0	28	72	60
cnd-1(n3786); ced-3(n717)	0	25	75	57
cnd-1(n3787)	0	32	68	84
cnd-1(n3787); ced-3(n717)	0	32	68	74
cnd-1(jd19)	0	38	62	60
vab-3(n3721)	0	6	94	103
ced-3(n717); vab-3(n3721)	0	4	96	48
vab-3(n3723)	0	19	81	68
ced-3(n717); vab-3(n3723)	0	20	80	46
vab-3(e648)	9	64	27	66

A. All animals were homozygous for the *pkd-2::gfp* reporter *nIs128*, *nIs130*, or *nIs133*. Animals homozygous for *cnd-1(jd19)* were also homozygous for *lon-1(e43)*. Some animals contained *him-5(e1467)* or *him-8(e1489)*. Genotypes were otherwise as indicated.

B. All animals were homozygous for the *pkd-2::gfp* reporter *nIs128* or *nIs133*. Some animals contained *him-5(e1467)* or *him-8(e1489)*. Genotypes were otherwise as indicated.

Table 13. Loss-of-function mutations in *cnd-1 NeuroD* strongly enhance the head morphology defect caused by weak mutations in *vab-3 Pax6*

	vab-3(+)	*vab-3(n3721)*	*vab-3(n3723)*
cnd-1(+)	0% (300)	1% (125)	6% (264)
cnd-1(n3786)	1% (142)	23% (120)	53% (135)
cnd-1(n3787)	3% (115)	17% (119)	54% (139)
cnd-1(jd19)	7% (173)	16% (154)	49% (124)

Percentages indicate penetrance of abnormal morphology of the heads of larvae examined at 500x magnification using a dissecting microscope. The number of larvae examined for each genotype is indicated in parentheses. All animals were homozygous for the *pkd-2::gfp* reporter *nIs128*. *cnd-1(jd19)* animals were homozygous for *lon-1(e43)*. Genotypes were otherwise as indicated by the labels on the rows and columns.

Table 14. *vab-3 Pax6* and *cnd-1 NeuroD* function in parallel to *ceh-30* and to *ced-9*.

A. *cnd-1 NeuroD* and *vab-3 Pax6* act downstream of or in parallel to sex determination to promote CEM death.

Genotype	CEM survival in hermaphrodites (%)			
	None	D OR V	D AND V	n
cnd-1(n3786)	59	36	4	76
fem-2(e2105) cnd-1(n3786)	54	46	0	79
vab-3(n3721)	43	54	3	139
fem-2(e2105); vab-3(n3721)	55	44	2	130
vab-3(n3723)	48	52	0	103
fem-2(e2105); vab-3(n3723)	47	53	0	46

B. *cnd-1 NeuroD* and *vab-3 Pax6* act downstream of or in parallel to *ced-9* to promote CEM death.

Genotype	CEM survival in hermaphrodites (%)			
	None	D OR V	D AND V	n
wild type	99	1	0	100
ced-3(n2923)	98	2	0	159
ced-9(n2812); ced-3(n2923)	98	2	0	200
cnd-1(n3786) ced-9(n2812); ced-3(n2923)	86	13	1	300
ced-9(n2812); ced-3(n2923); vab-3(n3723)	83	17	0	214

C. *cnd-1 NeuroD* and *vab-3 Pax6* acts downstream of or in parallel to *ceh-30* to promote CEM death.

Genotype	CEM survival in hermaphrodites (%)			
	None	D OR V	D AND V	n
wild-type	99	1	0	100
cnd-1(n3786)	61	38	1	181
cnd-1(n3786); ceh-30(n4111 n3714)	88	12	0	68
cnd-1(n3786); ceh-30(n4289Δ)	98	2	0	80
cnd-1(jd19)	52	48	1	164
cnd-1(jd19); ceh-30(n4111 n3714)	92	8	0	170
cnd-1(jd19); ceh-30(n4289Δ)	87	13	0	78
vab-3(n3723)	34	58	8	95
ceh-30(n4111 n3714) vab-3(n3723)	52	44	4	77
nDf65 vab-3(n3723)	54	45	1	102
vab-3(e648)	43	53	4	171
ceh-30(n4111 n3714) vab-3(e648)	54	41	6	69
ceh-30(n4289Δ) vab-3(e648)	50	47	3	248

A. All animals were homozygous for the *pkd-2::gfp* reporter *nIs128*. *fem-2(e2105)* animals were the self-progeny of maternally rescued *fem-2(e2105)* homozygotes. Genotypes were otherwise as indicated.

B. All animals were homozygous for the *pkd-2::gfp* reporter *nIs133*. Genotypes were otherwise as indicated.

C. All animals were homozygous for the *pkd-2::gfp* reporter *nIs133*. *cnd-1(jd17)* animals were homozygous for *lon-1(e43)*. All *cnd-1* mutant animals were homozygous for *him-5(e1467)*. All animals homozygous for *ceh-30(n4111 n3714)* were homozygous for *lon-2(e678)*. Genotypes were otherwise as indicated.

Table S1. *ceh-30* and *ceh-31* act synthetically in CEM fate determination.

A. *ceh-30 ceh-31* double mutants are defective in CEM differentiation in hermaphrodites.

	CEM survival in hermaphrodites (%)			
Genotype	None	D OR V	D AND V	n
egl-1(n1084 n3082)	0	7	93	60
egl-1(n1084 n3082); ceh-30(n4111 n3714lf)	0	22	78	67
egl-1(n1084 n3082); ceh-30(n4289Δ)	0	14	86	66
egl-1(n1084 n3082); ceh-31(n4893Δ)	0	27	73	67
egl-1(n1084 n3082); nDf65	2	87	11	63
ced-4(n1162)	0	6	94	63
ced-4(n1162); ceh-30(n4111 n3714lf)	0	16	84	62
ced-4(n1162); ceh-30(n4289Δ)	0	13	87	61
ced-4(n1162); ceh-31(n4893Δ)	0	14	86	63
ced-4(n1162); nDf65	2	81	17	63

B. *ceh-30 ceh-31* double mutants are weakly defective in CEM differentiation in males.

	CEM survival in males (%)			
Genotype	None	D OR V	D AND V	n
egl-1(n1084 n3082)	0	0	100	62
egl-1(n1084 n3082); ceh-30(n4111 n3714lf)	0	0	100	65
egl-1(n1084 n3082); ceh-30(n4289Δ)	0	0	100	63
egl-1(n1084 n3082); ceh-31(n4893Δ)	0	0	100	60
egl-1(n1084 n3082); nDf65	0	9	91	67
ced-4(n1162)	0	0	100	60
ced-4(n1162); ceh-30(n4111 n3714lf)	0	0	100	60
ced-4(n1162); ceh-30(n4289Δ)	0	0	100	60
ced-4(n1162); ceh-31(n4893Δ)	0	0	100	60
ced-4(n1162); nDf65	0	8	92	60

A. The deficiency *nDf65* removes *ceh-30* and *ceh-31*. All animals were homozygous for *nIs133*. Animals homozygous for *egl-1(n1084 n3082)* were homozygous for *him-8(e1489)*. Animals homozygous for *ced-4(n1162)* were homozygous for *him-5(e1467)*. Genotypes were otherwise as indicated.

B. The deficiency *nDf65* removes *ceh-30* and *ceh-31*. All animals were homozygous for *nIs133*. Animals homozygous for *egl-1(n1084 n3082)* were homozygous for *him-8(e1489)*. Animals homozygous for *ced-4(n1162)* were homozygous for *him-5(e1467)*. Genotypes were otherwise as indicated.

Table S2. Loss of *unc-37* function causes the inappropriate deaths of CEM neurons in males.

Genotype	Sex	Animals with CEM survival (%)			
		None	D OR V	D AND V	n
wild-type	Herm.	100	0	0	50
unc-37(e262)	Herm.	100	0	0	103
ced-3(n717)	Herm.	0	4	96	73
unc-37(e262); ced-3(n717)	Herm.	0	3	97	100
wild-type	Male	0	0	100	50
unc-37(e262)	Male	0	12	88	101
ced-3(n717)	Male	0	0	100	50
unc-37(e262); ced-3(n717)	Male	0	0	100	100

Animals were homozygous for the *pkd-2::gfp* reporter *nIs128* and for *him-8(e1489)*.

Genotypes were otherwise as listed. Herm., hermaphrodite.

Figure Legends

Figure 1

pkd-2::gfp is expressed in the "undead" CEM neurons of hermaphrodites when their deaths are prevented by a defect in programmed cell death. (A) There is no strong expression of *pkd-2::gfp* in the head of a wild-type hermaphrodite. (B) Strong *pkd-2::gfp* expression is observed in the CEM neurons of *ced-3(n717)* hermaphrodites defective in programmed cell death. The heads of transgenic animals are shown, using composite images that combine multiple focal planes of fluorescence and visible-light micrographs. Anterior is to the left, and ventral is down.

Figure 2

TRA-4 is a conserved protein possessing homology to the human transcription factor PLZF. Each pair of residues identical between the two proteins is surrounded with a black box. Each pair of residues similar between the two proteins is surrounded with a dark gray box. A light gary box indicates the position of the N-terminal RD2 domain of hPLZF. Black lines under the protein sequence indicate the positions of the seven predicted zinc fingers. The positions and natures of the identified *tra-4* missense mutations are shown. This figure is modified from Figure 1D of GROTE and CONRADT (2006).

Figure 3

Loss of *cnd-1* causes a weak head morphology defect that is enhanced by weak loss-of-function mutations in *vab-3*. Images are Nomarski micrographs of the heads of

young larvae, showing examples of the variable and severe defects in head morphology seen at low penetrance for animals lacking *cnd-1* function or weakly defective in *vab-3* function, and at high penetrance for animals strongly defective in *vab-3* function or animals doubly homozygous for a strong loss-of-function mutation in *cnd-1* and a weak loss-of-function mutation in *vab-3*. Genotypes were as indicated within the panel, except that animals were also homozygous for the *pkd-2::gfp* cell-fate reporter *nIs128*.

Figure 4

Developmental and genetic pathways for the sexually dimorphic survival decision of the CEM neurons. See Discussion for more information. (A) The survival decision of the CEM neurons can be expressed as the result of four processes: establishment of CEM identity, determination of sexual identity, the execution of programmed cell death, and the determination of whether the cells are sensitive to an activated cell death program. The CEM neuron identity establishes both that the cells will contain an activated cell death program and that the cells possess a program that responds to sexual identity to determine whether the cells are sensitive to activation of programmed cell death. (B) A genetic pathway for the sexually dimorphic survival decision of the CEM neurons. Genes mutated in screen isolates described in this work are highlighted in red. As part the CEM neuron identity, the cell-death execution pathway is activated; this CEM-specific activation is caused by a factor that binds within the site deleted by *egl-1(n4908Δ)* to cause transcriptional activation of the BH3-only killer gene *egl-1*. CEM neuron identity separately acts through *unc-86*, *vab-3* and *cnd-1* to promote the possession of a program that responds to sexual identity to control whether the CEM

neurons are sensitive to this activated cell-death program. This program is controlled by the CEM-specific survival factor *ceh-30*. *ceh-30* is also directly controlled by the sex determination pathway. Together, CEM neuron identity and sexual identity act through *ceh-30* to regulate CEM survival independently of *egl-1 BH3-only* and *ced-9 Bcl-2* function, by controlling sensitivity to the activation of programmed cell death. If *egl-1* is inactive in the CEMs of males, this sex-specific repression of *egl-1* is controlled by *ceh-30*; alternatively, *egl-1* could be expressed both in the CEMs of hermaphrodites and of males, and sexual dimorphism of CEM neuron survival could be achieved by *ceh-30* acting independently of *egl-1* and *ced-9*.

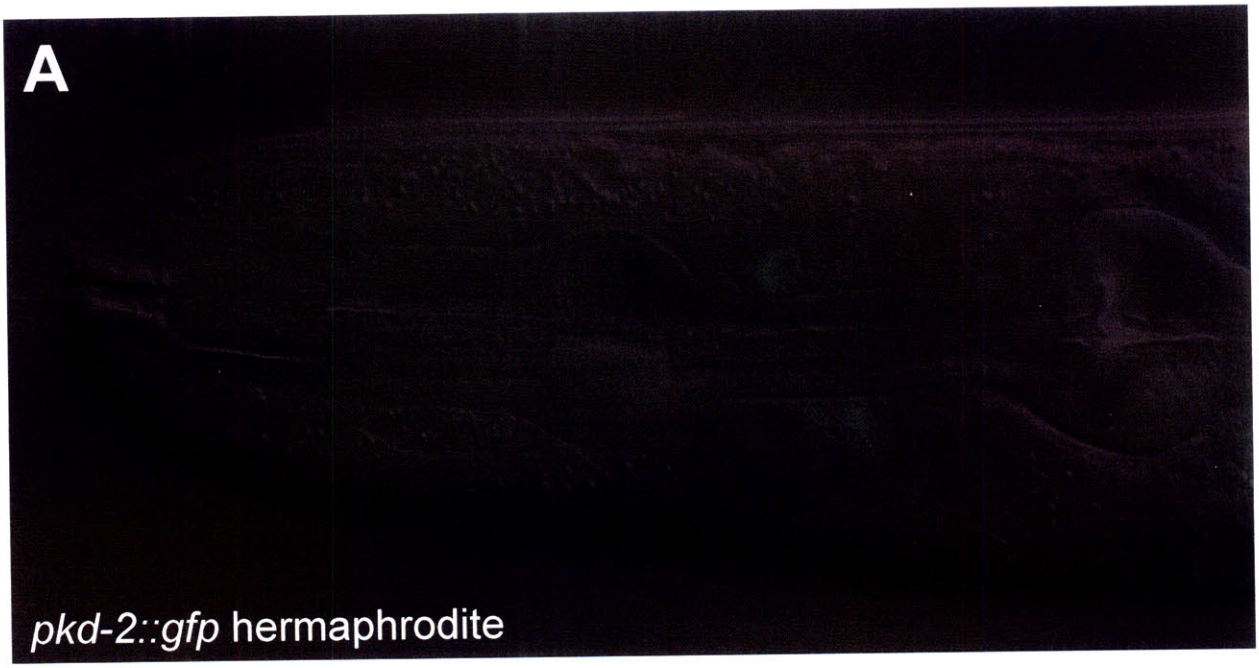
A
pkd-2::gfp hermaphrodite


B
ced-3(n717); *pkd-2::gfp* hermaphrodite

Figure 1

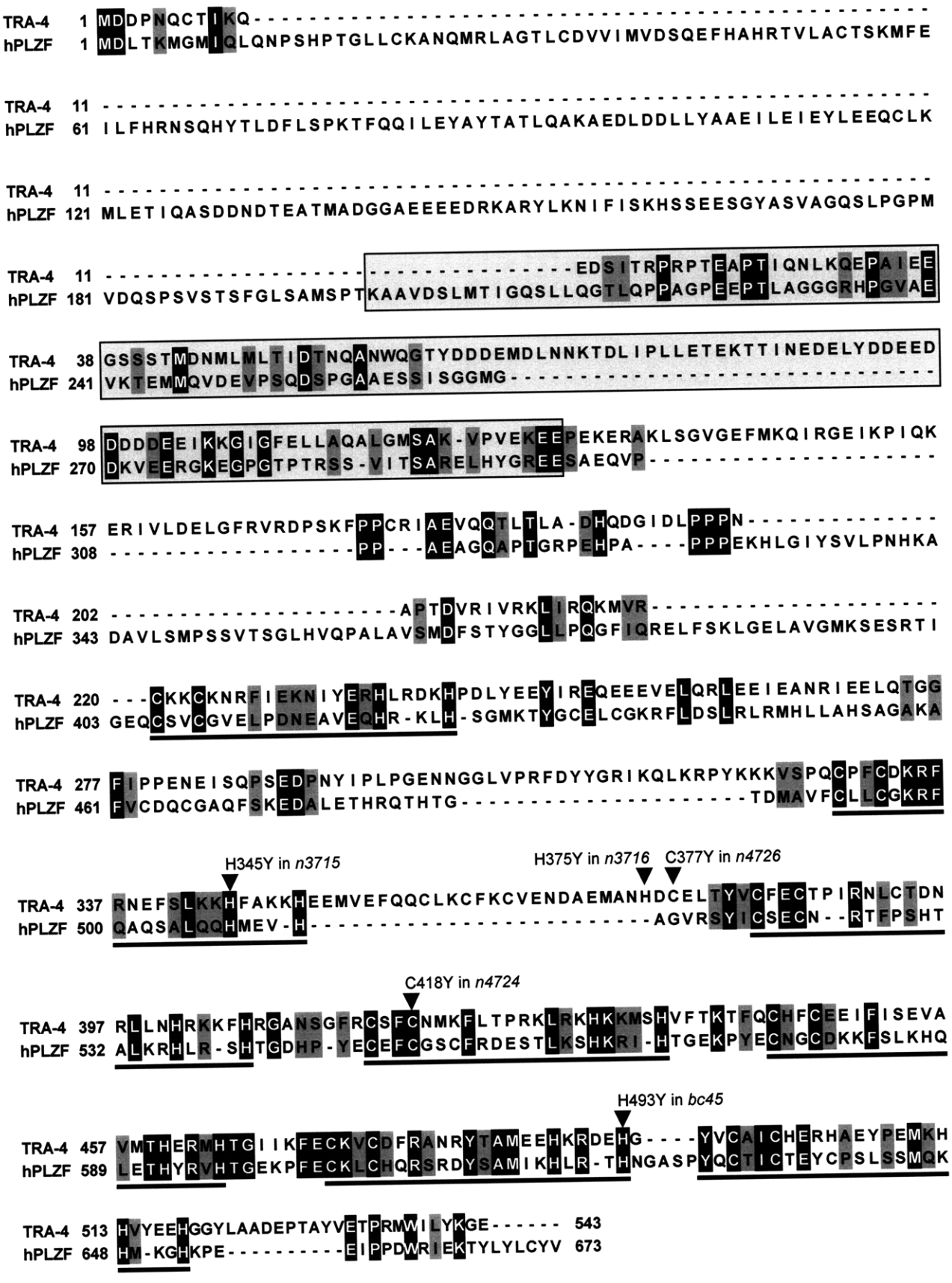
TRA-4 1 MDDPNQCTIKQ
hPLZF 1 MDLTKMGMIQLQNPSHPTGLLCKANQMRLAGTLCDVVIMVDSQEFHAHRTVLACTSKMFE
TRA-4 11
hPLZF 61 ILFHRNSQHYTLDFLSPKTFQQILEYAYTATLQAKAEDLDDLLYAAEILEIEYLEEQCLK
TRA-4 11
hPLZF 121 MLETIQASDDNDTEATMADGGAEEEEDRKARYLKNIFISKHSSEESGYASVAGQSLPGPM
TRA-4 11 EDSITRPRPTEAPTIQNLKQEPAIEE
hPLZF 181 VDQSPSVSTSFGLSAMSPTKAAVDSLMTIGQSLLQGTLQPPAGPEEPTLAGGGRHPGVAE
TRA-4 38 GSSSTMDNMLMLTIDTNQANWQGTYDDDEMDLNNKTDLIPLLETEKTTINEDELYDDEED
hPLZF 241 VKTEMMQVDEVPSQDSPGAAESSISGGMG
TRA-4 98 DDDDEEIKKGIGFELLAQALGMSAK-VPVEKEEPEKERAKLSGVGEFMKQIRGEIKPIQK
hPLZF 270 DKVEERGKEGPGTPTRSS-VITSARELHYGREESAEQVP
TRA-4 157 ERIVLDELGFRVRDPSKFPPCRIAEVQQTLTLA-DHQDGIDLPPPN
hPLZF 308 PP---AEAGQAPTGRPEHPA----PPPEKHLGIYSVLPNHKA
TRA-4 202 APTDVRIVRKLIRQKMVR
hPLZF 343 DAVLSMPSSVTSGLHVQPALAVSMDFSTYGGLLPQGFIQRELFSKLGELAVGMKSESRTI
TRA-4 220 ---CKKCKNRFIEKNIYERHLRDKHPDLYEEYIREQEEEVELQRLEEIEANRIEELQTGG
hPLZF 403 GEQCSVCGVELPDNEAVEQHR-KLH-SGMKTYGCELCGKRFLDSLRLRMHLLAHSAGAKA
TRA-4 277 FIPPENEISQPSEDPNYIPLPGENNGGLVPRFDYYGRIKQLKRPYKKKVSPQCPFCDKRF
hPLZF 461 FVCDQCGAQFSKEDALETHRQTHTG-----------TDMAVFCLLCGKRF
H345Y in n3715
H375Y in n3716
C377Y in n4726
TRA-4 337 RNEFSLKKHFAKKHEEMVEFQQCLKCFKCVENDAEMANHDCELTYVCFECTPIRNLCTDN
hPLZF 500 QAQSALQQHMEV-H----------AGVRSYICSECN--RTFPSHT
C418Y in n4724
TRA-4 397 RLLNHRKKFHRGANSGFRCSFCNMKFLTPRKLRKHKKMSHVFTKTFQCHFCEEIFISEVA
hPLZF 532 ALKRHLR-SHTGDHP-YECEFCGSCFRDESTLKSHKRI-HTGEKPYECNGCDKKFSLKHQ
H493Y in bc45
TRA-4 457 VMTHERMHTGIIKFECKVCDFRANRYTAMEEHKRDEHG----YVCAICHERHAEYPEMKH
hPLZF 589 LETHYRVHTGEKPFECKLCHQRSRDYSAMIKHLR-THNGASPYQCTICTEYCPSLSSMQK
TRA-4 513 HVYEEHGGYLAADEPTAYVETPRMWILYKGE------ 543
hPLZF 648 HM-KGHKPE----------EIPPDWRIEKTYLYLCYV 673

Figure 2

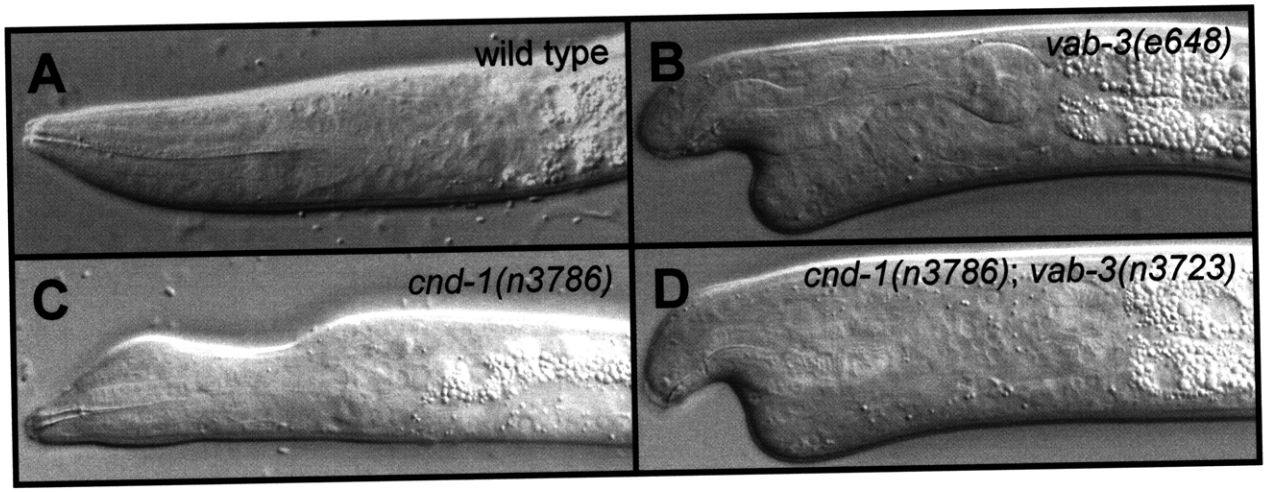

Figure 3

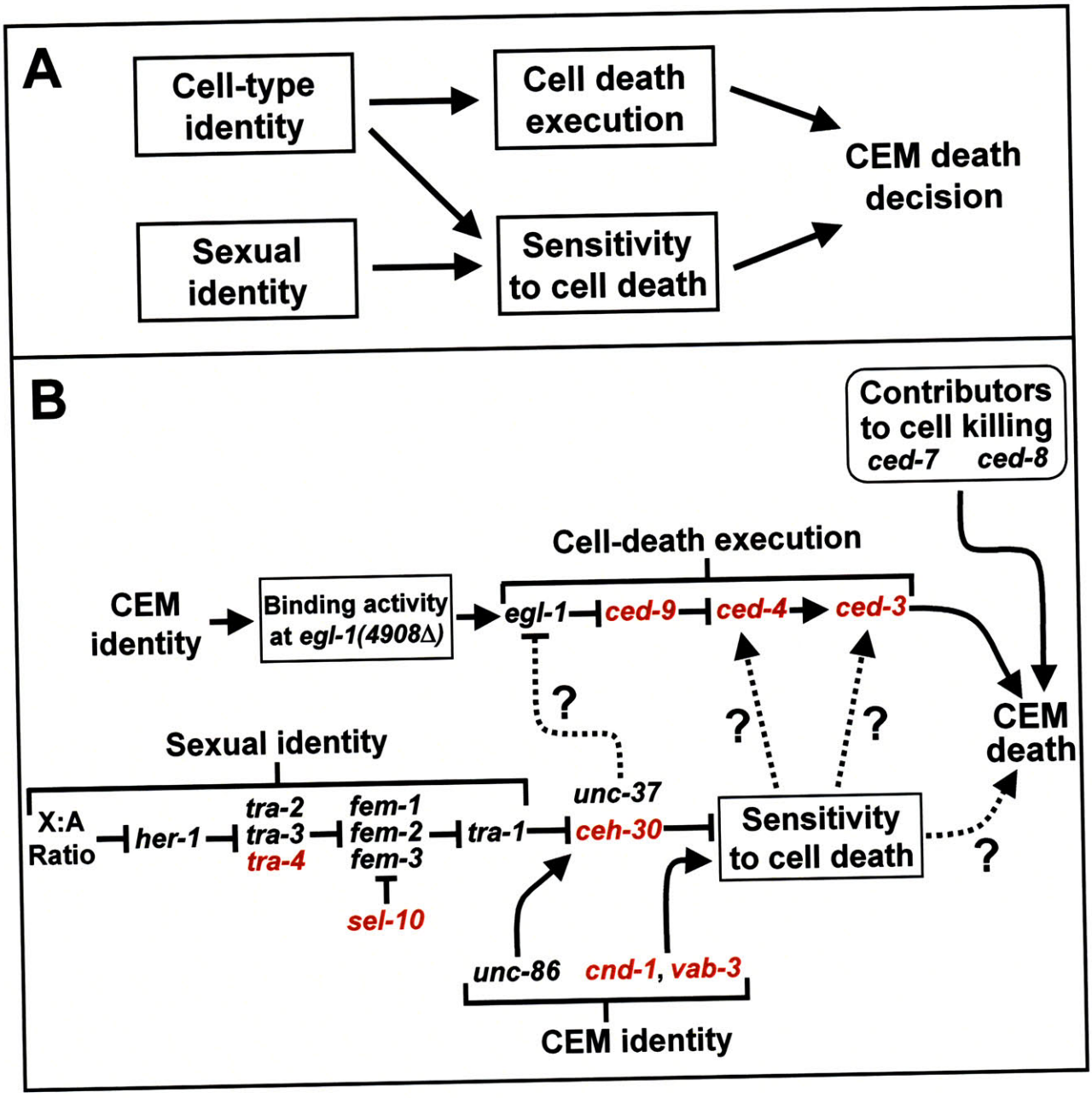
A
Cell-type identity
Cell death execution
CEM death decision
Sexual identity
Sensitivity to cell death
B
Contributors to cell killing
ced-7 ced-8
Cell-death execution
CEM identity
Binding activity at egl-1(4908Δ)
egl-1
ced-9
ced-4
ced-3
?
?
?
CEM death
Sexual identity
X:A Ratio
her-1
tra-2
tra-3
tra-4
fem-1
fem-2
fem-3
tra-1
unc-37
ceh-30
Sensitivity to cell death
?
sel-10
unc-86
cnd-1, vab-3
CEM identity

Figure 4

Chapter III

The *C. elegans* protein CEH-30 protects male-specific neurons from apoptosis independently of the Bcl-2 homolog CED-9

Hillel T. Schwartz and H. Robert Horvitz

Published as Schwartz and Horvitz (2007) *Genes Dev* **21**: 3181-3194

Abstract

The developmental control of apoptosis is fundamental and important. We report that the *Caenorhabditis elegans Bar* homeodomain transcription factor CEH-30 is required for the sexually dimorphic survival of the male-specific CEM sensory neurons; the homologous cells of hermaphrodites undergo programmed cell death. We propose that the cell-type-specific anti-apoptotic gene *ceh-30* is transcriptionally repressed by the TRA-1 transcription factor, the terminal regulator of sexual identity in *C. elegans*, to cause hermaphrodite-specific CEM death. The established mechanism for the regulation of specific programmed cell deaths in *C. elegans* is the transcriptional control of the BH3-only gene *egl-1*, which inhibits the *Bcl-2* homolog *ced-9*; similarly, most regulation of vertebrate apoptosis involves the *Bcl-2* superfamily. By contrast, *ceh-30* acts within the CEM neurons to promote their survival independently of both *egl-1* and *ced-9*. Mammalian *ceh-30* homologs can substitute for *ceh-30* in *C. elegans*. Mice lacking the *ceh-30* homolog *Barhl1* show a progressive loss of sensory neurons and increased sensory-neuron cell death. Based on these observations, we suggest that the function of Bar homeodomain proteins as cell-type-specific inhibitors of apoptosis is evolutionarily conserved.

Introduction

Programmed cell death, or apoptosis, is a widespread feature of animal development. Abnormalities in apoptosis can have pathological consequences. Reduced cell death can cause the survival of unnecessary or unwanted cells, such as neurons that have not made appropriate synaptic connections (reviewed by Yeo and Gautier 2004) or cells that could be dangerous if they were to survive, such as immune cells that recognize self-antigens (Bidere et al. 2006) and cells that have escaped controls on their proliferation (Weaver and Cleveland 2005). Increased programmed cell death is associated with a broad variety of human disorders, including immunodeficiency and neurodegenerative diseases (reviewed by Rathmell and Thompson 2002; Krantic et al. 2005).

A core pathway for the cell-killing step of apoptosis is conserved from nematodes to humans; key insights concerning this pathway have come from investigations of programmed cell death in *C. elegans* (Metzstein et al. 1998). In this core pathway, cells are killed by a cysteine protease called a caspase; in *C. elegans*, this caspase is CED-3 (*ced*, cell death abnormal) (Yuan et al. 1993). Caspase activity is promoted by an adaptor molecule, called CED-4 in *C. elegans* (Yuan and Horvitz 1992; Shaham and Horvitz 1996) and Apaf-1 in mammals (Zou et al. 1997). CED-4 and Apaf-1 activation is regulated by multidomain members of the CED-9 Bcl-2 superfamily. CED-9 is the sole multidomain *Bcl-2* family member in *C. elegans* and provides both anti-apoptotic and, to a lesser extent, pro-apoptotic activities (Hengartner and Horvitz 1994a; Hengartner and Horvitz 1994b). Multidomain members of the Bcl-2 superfamily are regulated by BH3-only proteins; in *C. elegans*, the BH3-only protein EGL-1 (*egl*, egg-laying defective)

is required for essentially all somatic programmed cell deaths (Conradt and Horvitz 1998).

Despite a detailed knowledge of this core pathway for apoptosis, less is known about how cells are developmentally determined to die. In mammals, the regulation of programmed cell death in the developing immune system by recognition of self-antigens (reviewed by Bidere et al. 2006) and in the developing nervous system by neurotrophic signals has been described (reviewed by Weaver and Cleveland 2005). In *C. elegans*, 131 cells die during hermaphrodite development; during male development another 21 cells die that in hermaphrodites either do not die or are never generated (Sulston and Horvitz 1977; Kimble and Hirsh 1979; Sulston et al. 1983). Nine genes that exert cell-specific control over eight of these 152 cell deaths have been described (Ellis and Horvitz 1991; Metzstein et al. 1996; Conradt and Horvitz 1999; Metzstein and Horvitz 1999; Thellmann et al. 2003; Hoeppner et al. 2004; Liu et al. 2006). These nine genes are believed to regulate cell death by cell-specific transcriptional regulation of the BH3-only killer gene *egl-1*, which acts to inhibit the Bcl-2 homolog CED-9. Mutations in human counterparts of these cell-specific regulators of apoptosis can contribute to disease, particularly to cancer. For example, *ces-1* and *ces-2* (*ces*, cell death specification), *C. elegans* genes that specifically regulate the deaths of the sister cells of the NSM neurons, have human homologs that can regulate B cell survival in humans, and translocations altering the *ces-2* homolog *HLF* cause Acute Lymphoblastic Leukemia (Inaba et al. 1996; Wu et al. 2005).

We have studied the survival decision of one of the two classes of neurons sexually dimorphic for programmed cell death in *C. elegans*, the CEM (cephalic male)

neurons. The presumptive CEM neurons die during hermaphrodite embryogenesis but survive in males to become sensory neurons (Sulston et al. 1983; Chasnov et al. 2007). We report that the gene *ceh-30* encodes a cell-type-specific anti-apoptotic homeodomain transcription factor. *ceh-30* is directly regulated by the sex determination pathway to control the sex-specific survival of the CEMs. The anti-apoptotic function of *ceh-30* involves a novel mechanism that is independent of the Bcl-2 homolog CED-9 and the BH3-only cell-killing gene *egl-1*. The anti-apoptotic function of *ceh-30* is conserved in its mammalian counterparts *Barhl1* and *Barhl2*; mice lacking *Barhl1* suffer from progressive deafness, likely because of increased apoptosis of sensory hair cells of the inner ear.

Results

ceh-30 gain-of-function mutations cause CEM neuron survival in hermaphrodites and act downstream of sex determination

The cell-fate reporter *pkd-2::gfp* is expressed in the male-specific CEM neurons as well as in some male-specific tail neurons (Barr and Sternberg 1999) (Figure 1A, B). We found that *pkd-2::gfp* was expressed in hermaphrodite CEM neurons when the programmed deaths of these cells were prevented either by weak masculinization or by a defect in cell death (Figure 1C, D; Table 1A). We used *pkd-2::gfp* as a marker of CEM survival in screens for mutant hermaphrodites in which the CEM neurons survived (H.T.S. and H.R.H., unpublished results). Among the isolates we recovered were three mutations, *n3713*, *n3714*, and *n3720*, each of which semidominantly causes CEM survival in hermaphrodites (Table 1 and Figure 1E). No other defects were seen in

these three mutant strains. The *pkd-2*::*gfp*-expressing CEM neurons of these mutant hermaphrodites more closely resembled those seen in cell-death-defective hermaphrodites than those seen in weakly masculinized hermaphrodites: the intensity of GFP expression and the process morphologies and nuclear positions of the CEMs were more variable in hermaphrodites defective in cell death than in males or in partially masculinized hermaphrodites (data not shown); this latter observation is consistent with previous electron microscopic examination of *ced-3(n717)* hermaphrodites, which found variability in the processes of undead CEM neurons (White et al. 1991). We mapped the three mutations to the left end of a six map unit interval on LGX and found that the three mutations acted similarly (Table 1A and date not shown). We showed that the three mutations are in the same gene, which we later determined to be *ceh-30* (*ceh*, *C. elegans* homeobox) (see below).

We performed gene dosage experiments and concluded that *n3713* and *n3714* are gain-of-function (gf) mutations (Tables 1B and S1). Adding either of two large genomic duplications *mnDp57* and *yDp14*, each of which carries an extra copy of the *ceh-30* region, did not cause increased CEM survival in wild-type hermaphrodites, and adding wild-type *ceh-30* copies to *n3713* or *n3714* mutants neither enhanced nor suppressed their semidominant CEM survival phenotypes. The latter result indicates *n3713* and *n3714* do not cause loss-of-function (lf) or dominant-negative activity and must therefore cause a gain-of-function activity, resulting in either altered or ectopic gene function. Data presented below concerning the wild-type function of *ceh-30* and the nature of the *ceh-30(gf)* mutations are consistent with the hypothesis that the

gain-of-function mutations cause ectopic expression of the wild-type gene product in the CEMs of hermaphrodites.

One way mutations can cause CEM survival in hermaphrodites is by partial masculinization, so that the CEMs adopt their male fate of survival in animals that are nonetheless predominantly hermaphrodites. Unlike the mutation *sel-10(n1077)*, which causes CEM survival by partial masculinization (Desai and Horvitz 1989; Jager et al. 2004), *ceh-30(*gf*)* mutations did not enhance the somatic masculinization caused by the weak *tra-2* (*tra*, sexual transformer) alleles *e1875* and *n1106* (data not shown). Thus, *ceh-30(*gf*)* does not act broadly to promote masculinization. Both *n3713*gf and *n3714*gf protected the CEMs of animals completely feminized by null mutations in the *fem* genes, which are the final genes required for masculinization in the sex determination pathway (Tables 1C and S2) (Hodgkin 2002). Therefore, *ceh-30(*gf*)* mutations act to cause CEM neuron survival downstream of or in parallel to all genes required for masculinization.

Loss of *ceh-30* function causes CEM neurons in males to undergo programmed cell death

We sought intragenic suppressors of *ceh-30(n3714*gf*)* and recovered one mutation, *n4111*, that proved to be an allele of *ceh-30* (Table 2A; see Materials and Methods and below). *ceh-30(n4111 n3714)* caused an effect opposite to that caused by *ceh-30(*gf*)*: whereas *ceh-30(n3714*gf*)* hermaphrodites have normally male-specific CEM neurons, *ceh-30(n4111 n3714)* males lack CEM neurons, as do normal hermaphrodites (Table 2B). The CEM-deficient phenotype of *ceh-30(n4111 n3714)* males is recessive:

*tra-1(*lf); *ceh-30(n4111 n3714/+)* males did not lack CEMs (*tra-1(*lf) can be used to cause animals with two X chromosomes to develop as males), and the CEM-deficient phenotype of *ceh-30(n4111 n3714)* males was complemented by the genomic duplications *mnDp57* and *yDp14* (Table S3 and data not shown). Experiments detailed below demonstrated that *n4111* causes a loss of gene function. The missing CEM neurons of *ceh-30(n4111 n3714)* males were not restored by a null mutation in *tra-1* (Tables 2B and S4). *tra-1* is the most downstream gene in the sex determination pathway (Hodgkin 2002), indicating that *ceh-30* does not act within the sex determination pathway to cause CEMs to adopt their male fate of survival. The missing CEM neurons of *ceh-30(n4111 n3714)* males were completely restored by loss of function of *egl-1*, *ced-4*, or *ced-3*, genes required for programmed cell death (Tables 2B and S4). The missing CEMs of *ceh-30(*lf) males are therefore generated as in wild-type males and then inappropriately undergo programmed cell death.

CEH-30 is an evolutionarily conserved Bar homeodomain transcription factor

We mapped *n3714*gf to a 25 kb interval on the cosmid C33D12 and established an overlapping but less well defined position for *n4111* (see Materials and Methods). *ceh-30(n4111 n3714)* males transformed with the overlapping cosmids C13G6 and C33D12 were rescued for CEM survival (Figure 2A; data not shown). Examination of the genomic sequence corresponding to these cosmids revealed that an intron of the gene *ceh-30* contains a consensus binding site for the transcription factor TRA-1, which is required to repress male sexual fates (Zarkower and Hodgkin 1993) (see Figure 2D). We determined the DNA sequence of *ceh-30* in our mutants and found that

n4111 n3714 animals but not the *n3714* parental strain had a mutation in the predicted *ceh-30* coding sequence, changing codon 21 from glutamine to an ochre stop codon. All three independently isolated *ceh-30(*gf*)* mutants had an identical mutation altering an evolutionarily conserved predicted TRA-1 binding site in the second intron of *ceh-30* (Figure 2D). This mutation is equivalent to one known to prevent TRA-1 from binding to a regulatory site *in vitro* and to prevent transcriptional repression by *tra-1 in vivo* (Conradt and Horvitz 1999). Similarly, we found that TRA-1A could bind the site mutated by *n3714*gf in gel-shift experiments and that this binding was prevented by the addition of excess unlabelled wild-type probe but was very poorly competed by excess unlabelled probe containing the *n3714*gf mutation (Figure 2E). The nature of the *ceh-30* gain-of-function mutations is consistent with the results of our gene-dosage experiments and suggests a model in which the gain-of-function mutations release *ceh-30* from a negative regulation that represses *ceh-30* expression in hermaphrodites.

Our isolation of a *ceh-30* deletion mutation, *n4289*Δ, confirmed that *n4111* causes loss of *ceh-30* gene function. *ceh-30(n4289*Δ*)* removes the second exon, which encodes most of the predicted homeodomain (see below), and is predicted to cause a frameshift after amino acid 61 if the first and third exons are spliced together (Figure 2B). We found that *ceh-30(n4289*Δ*)* caused males to lack CEM neurons (Tables 2B and S4 and Figure 1E) and failed to complement *ceh-30(n4111 n3714)* for CEM survival in *tra-1* XX males (Table S3). The transgene BSK-*ceh-30*, which contains the *ceh-30* genomic locus (see Supplemental Data), complemented the CEM survival defects of both *ceh-30(*lf*)* mutants (Fig. 2A, Table 2C, and data not shown). A version of the rescuing transgene modified to contain the *n3714*gf mutation in the TRA-1 binding site

of *ceh-30* (BSK-*ceh-30(n3714)*) caused CEM survival in hermaphrodites (data not shown).

We performed a *cis-trans* test to confirm our hypothesis that *n3714*gf is an allele of *ceh-30*. Specifically, we asked if the noncoding mutation *n3714*gf causes CEM survival by activating *ceh-30* in *cis*. We found that the *n3714*gf semidominant phenotype of CEM survival in hermaphrodites required only one functional copy of *ceh-30* and that this functional wild-type copy of *ceh-30* must be the copy in *cis* to *n3714*gf: 76% of *n3714*gf/+ and 78% of *n3714*gf/*n4289*Δ hermaphrodites had surviving CEMs, but only 4% of *n4111 n3714*gf/+ hermaphrodites had surviving CEMs (n ≥ 100; Table S5). *n3714*gf therefore affects the same gene as the *ceh-30* loss-of-function mutation *n4111*, proving *n3714*gf is an allele of *ceh-30*.

ceh-30 encodes a homolog of the *Drosophila* homeodomain transcription factors *BarH1* and *BarH2* (Kojima et al. 1991; Higashijima et al. 1992a) and their murine counterparts *Barhl1* and *Barhl2* (Bulfone et al. 2000). The 237 amino acid predicted CEH-30 protein is 64% identical to human Barhl1 from amino acids 85 to 180 of CEH-30 (Figure 2C). This homology includes both the homeodomain, which contains a phenylalanine-to-tyrosine substitution characteristic of the Bar subclass of homeodomains (Kojima et al. 1991), and a 22 amino acid motif immediately C-terminal of the homeodomain; our BLAST searches indicated that homologs of this motif are found only in Bar homeodomain proteins, and we have named it the BARC motif (Bar homeodomain C-terminal motif; see Table S6). A *ceh-30* minigene including *ceh-30* 5' and 3' sequences and 625 bp of *ceh-30* intron 2 (see Supplemental Data) rescued the defect in CEM survival of *ceh-30(n4289Δ)* males as effectively as did the original

genomic construct (Table 2C). We tested whether the protective function of CEH-30 is evolutionarily conserved with that of its mammalian homologs by replacing the *ceh-30* cDNA of this construct with murine *Barhl1* or *Barhl2* cDNAs. Both of the resulting transgenes rescued the CEM survival defect of *ceh-30(n4289Δ)* males (Table 2C).

ceh-30 acts cell-autonomously in the CEM neurons to promote their survival

A *ceh-30* genomic construct into which *gfp* had been inserted (see Supplemental Data) rescued *ceh-30(n4289Δ)* for CEM survival (Table S7) and caused GFP expression in the nuclei of many neurons in the three-fold embryo and in as many as a dozen neurons in larvae. We did not observe GFP expression in the CEMs of male larvae, indicating that any *ceh-30* expression in the CEM neurons is likely to be weak or transient. The ventral CEM neurons of 1.5-fold stage masculinized embryos, which can be identified by their positions within the embryo, expressed *ceh-30::gfp* (see Figure S1). Expression in the dorsal CEMs cannot be as readily examined. We conclude that *ceh-30* is expressed transiently in embryonic CEMs.

We tested whether *ceh-30* acts cell-autonomously in the CEMs to promote their survival by examining animals that developed from zygotes carrying an extrachromosomal *ceh-30(n3714*gf*)* transgene marked with a pan-neuronal *unc-119::mStrawberry* reporter to identify neurons containing the transgene. In males, in which the transgene is not required for CEM neurons to survive, 18.9% (n=477) of CEMs lacked the transgene as a result of mitotic loss. In hermaphrodites, only one of 719 surviving CEMs lacked the transgene, indicating that the CEMs die unless prevented from doing so by a *ceh-30(*gf*)* transgene (the single hermaphrodite CEM that

did not contain the transgene can be explained by the low frequency of spontaneous CEM survival that occurs in wild-type hermaphrodites: in 185 hermaphrodites, one surviving CEM of a possible 740 was seen using *pkd-2::gfp* expression as an assay). Thus, *ceh-30* protected only those CEMs that retained the transgene, indicating that *ceh-30* functions in the CEM neurons.

***ceh-30* acts specifically to control the life vs. death decision of the CEM neurons**

We tested the ability of *ceh-30* mutations to modify the deaths of cells other than CEMs. The partial loss-of-function alleles *ced-4(n3158)* and *ced-3(n2427)* each cause a weak defect in cell death and provide a sensitized genetic background in which weak effects on apoptosis can readily be detected (Reddien et al. 2001). In these sensitized backgrounds, we found no effect of *ceh-30* mutations on programmed cell deaths in the anterior pharynx or of the Pn.aap cells (Table 3A, B). To assess more broadly the extent of cell death in *ceh-30* mutants, we used a *ced-1(*lf*)* mutation to cause persistence of cell corpses (Hedgecock et al. 1983). *ceh-30(*lf*)* did not change the number of persistent cell corpses in the head, while *ceh-30(*gf*)* might have caused a slight reduction in corpse number (Table 3C); a reduction of about one corpse would be consistent with the only effect of *ceh-30(*gf*)* on cell death being that of CEM survival, given that there are four CEM neurons and our observation that *ced-1(*lf*)* causes 24% (n = 10) of embryonic cell deaths to persist into larval development as corpses. The numbers of neurons in the male and hermaphrodite ventral nerve cords were also unaffected by mutations in *ceh-30* (Table 3C). In short, these assays did not demonstrate any function outside the CEM neurons for *ceh-30* in the regulation of either cell death or cell number.

The sex determination pathway and *ceh-30* act independently of *ced-9* Bcl-2 to control CEM neuron survival

To examine how *ceh-30* protects the CEM neurons and, in particular, where *ceh-30* interfaces with the evolutionarily conserved core cell-killing pathway, we tested whether the anti-apoptotic gene *ced-9* is required for CEM survival in *ceh-30(n3714*gf*)* hermaphrodites. Specifically, we asked if the putative null allele *ced-9(n2812)*, a Q46amber mutation (Hengartner and Horvitz 1994b), would suppress the CEM survival caused by *ceh-30(n3714*gf*)*. Loss of *ced-9* Bcl-2 function causes ectopic activation of programmed cell death, resulting in lethality. Mutations that block the cell-death pathway downstream of *ced-9*, such as in the *ced-3* caspase, can suppress this lethality. The weak mutation *ced-3(n2427)*, which suppresses *ced-9(n2812)* lethality and slightly reduces the amount of programmed cell death but allows many programmed cell deaths to occur normally (Hengartner and Horvitz 1994a), can be used to examine the regulation of cell death in strains lacking all *ced-9* Bcl-2 function. We found that in a *ced-9(n2812)*; *ced-3(n2427)* background, the CEMs showed nearly normal sexually dimorphic regulation of their decision to undergo programmed cell death decision: most CEMs survived in males (no males lacked CEMs, and only 23% showed partial CEM survival; n=71), and most CEMs died in hermaphrodites (none showed strong CEM survival, and only 20% showed partial CEM survival; this survival can by attributed to the weak protective effect of *ced-3(n2427)*; n=89) (Table 4 and data not shown). In the absence of *ced-9* function, as in a wild-type background, *ceh-30(n3714*gf*)* caused CEM survival in hermaphrodites (40% showed strong CEM survival and 52% showed partial

CEM survival; n=60), and *ceh-30(lf)* mutations caused the CEM neurons of males to die (22% lacked CEMs and 75% showed only partial CEM survival; n=63). Similar results were observed using a second putative null allele of *ced-9*, *n3400*, and using other weak alleles of *ced-3* (*n2446*, *n2447*, and *n2923*; data not shown). Loss of *egl-1* BH3-only function, which prevents CEM death in wild-type animals, had no effect on CEM death in the absence of *ced-9* function (Table 4). This result is consistent with previous findings indicating that *egl-1* acts through *ced-9* Bcl-2 to perform its cell-killing function (Conradt and Horvitz 1998). The sexually dimorphic control of CEM survival therefore does not require regulation of *ced-9* or of *egl-1*.

Discussion

The Bar-class homeodomain gene *ceh-30* acts as a switch for the sexually dimorphic survival of the CEM neurons

Our studies of the genetic control of the death of the sexually dimorphic CEM sensory neurons of *C. elegans* have identified a novel mechanism by which sex determination regulates specific programmed cell deaths during nervous system development. This regulation depends on the control by sex determination of a previously uncharacterized gene, the evolutionarily conserved Bar homeodomain gene *ceh-30*, that acts as a genetic switch in determining the survival decision of the CEM neurons (shown diagrammatically in Figure 3). *ceh-30* gain-of-function mutations cause the CEMs of hermaphrodites to survive as they do in males. These *ceh-30* gain-of-function mutations disrupt a binding site for TRA-1, the terminal regulator of sexual identity in *C. elegans*, and likely prevent the TRA-1-mediated transcriptional

repression of *ceh-30* in hermaphrodites. A model for how TRA-1 regulates *ceh-30* expression and CEM neuron survival is shown in Figure 3A.

ceh-30 functions in the CEM neurons to promote their survival

We observed expression of a rescuing *ceh-30::gfp* transgene only in neurons. Bar homeodomain proteins in other organisms are similarly expressed primarily in the nervous system (Higashijima et al. 1992b; Saito et al. 1998). Most cells that express *ceh-30* do so only transiently: many more neurons show detectable *ceh-30::gfp* expression in embryos than in larvae or adults. We observed *ceh-30::gfp* expression in the CEMs of embryos, but not in those of larvae, indicating that *ceh-30* expression in the CEMs is transient, and occurs during embryonic development, the stage at which CEM neurons of die.

Consistent with our observation that *ceh-30* is expressed in the CEM neurons, we found strong indications that *ceh-30* functions cell-autonomously in the CEMs: CEM survival in hermaphrodites caused by a *ceh-30* gain-of-function transgene was dependent on the presence of the transgene in the surviving CEMs. The mechanism by which *ceh-30* gain-of-function protects hermaphrodite CEMs conceivably could differ from that by which *ceh-30* normally protects male CEM neurons; experiments to test whether *ceh-30* acts in the CEMs of males were not feasiblebecause of background survival of CEM neurons in *ceh-30(n4289Δ)* males. It seems likely that the requirements for *ceh-30(*gf*)* function in hermaphrodite CEMs are similar to those for normal *ceh-30* function in male CEMs. From these considerations and from our observation of the

expression of *ceh-30* in the CEMs of embryos, we conclude that *ceh-30* likely acts cell-autonomously to cause CEM survival.

ceh-30 acts specifically to control the survival of the CEM neurons

The effects of *ceh-30* on CEM survival could reflect a specific function for *ceh-30* in the CEM neurons or a particular sensitivity of the CEMs to a general defect in the regulation of programmed cell death. We therefore tested for effects of *ceh-30* on other programmed cell deaths, using assays known to be sensitive to subtle defects in programmed cell death and assays that examined the consequences of the generation and survival decisions of a large number of cells (see Table 3). These experiments did not reveal any function for *ceh-30* in the regulation of cell death or cell number other than for the CEM neurons. Nonetheless, *ceh-30::gfp* is expressed in and *ceh-30* might regulate the fates of neurons other than the CEMs, especially if such a role were to be concealed by redundancy. We found no additional defects in *ceh-30* mutants or in animals doubly mutant for *ceh-30* and for *ces-1*, *tra-1*, *eor-1*, or *eor-2*, genes known to regulate other specific programmed cell deaths (Ellis and Horvitz 1991; Conradt and Horvitz 1999; Hoeppner et al. 2004).

The sex determination pathway regulates *ceh-30* to control sensitivity to programmed cell death independently of the Bcl-2 homolog CED-9

Animals lacking the Bcl-2 homolog *ced-9* showed essentially wild-type regulation of the CEM survival decision, specified by sexual identity and mediated by the control of *ceh-30*. This *ced-9*-independent regulation of CEM survival differs from the regulation of

other specific cell deaths in *C. elegans*, which are controlled by the transcriptional regulation of the BH3-only killer gene *egl-1*, which in turn acts through *ced-9* (Conradt and Horvitz 1998; Metzstein and Horvitz 1999; Thellmann et al. 2003; Hoeppner et al. 2004; Liu et al. 2006). Previous results indicated that regulation of programmed cell death can occur independently of *ced-9*: animals lacking *ced-9* function and weakly defective in the downstream killer gene *ced-3* show significant cell death, restricted almost completely to cells that normally die in the wild type (Hengartner and Horvitz 1994a). How cell-specific regulation of programmed cell death can occur independently of *ced-9* has been until very recently completely unknown. Besides *ceh-30*, the only gene demonstrated to act in this process is the transcriptional regulator *pal-1*, recently shown to control the programmed cell death of the tail spike cell (Maurer et al. 2007).

Other evidence indicates that the regulation of CEM neuron survival is atypically independent of *ced-9*. The *ced-9* gain-of-function mutant *n1950*, which in other assays is nearly completely defective in programmed cell death in the soma (Hengartner and Horvitz 1994a), caused only moderate CEM survival (Table S8). Also, the cell-killing function of *ced-9* (Hengartner and Horvitz 1994a; Reddien et al. 2001) appears not to significantly affect CEM survival, as *ced-9(*lf*)* did not enhance the CEM survival caused by any of several weak *ced-3* loss-of-function mutants (Tables 1A and 4 and data not shown).

The *ced-9* Bcl-2-independent inhibition of CEM neuron death by *ceh-30* is unlikely to be mediated by any well-established death regulatory mechanism. In general the regulation of caspase-mediated cell death involves members of the Bcl-2 superfamily (reviewed by Kuwana and Newmeyer 2003). The principal exception is the

regulation of caspases by the IAP (inhibitor of apoptosis) proteins, which directly inhibit caspase function and are themselves regulated by IAP inhibitors such as the *Drosophila* proteins Hid, Grim, and Reaper and the mammalian proteins Smac/DIABLO and ARTS (Bergmann et al. 1998; Wang et al. 1999; Du et al. 2000; Goyal et al. 2000; Verhagen and Vaux 2002; Gottfried et al. 2004). Loss-of-function and overexpression of the two *C. elegans* IAP genes have no apparent effect on cell death (Speliotes 2000), and we found that animals lacking both *C. elegans* IAP genes showed no reduction in the ability of increased *ceh-30* function to prevent the apoptotic deaths of CEM neurons of hermaphrodites (Table S9). Other activities shown to regulate apoptotic cell death independently of the Bcl-2 superfamily, including ligand-mediated activation of caspase 8 and calpain-mediated regulation of caspase 12 (reviewed by Benn and Woolf 2004), have no obvious parallels in *C. elegans*. Another conceivable mechanism to account for *ced-9* Bcl-2-independent regulation of cell death is the cell-cycle regulation of Apaf-1 transcription by the DP-E2F heterodimer (Moroni et al. 2001); however, we found that a loss-of-function mutation in the only DP homolog, *dpl-1*, did not affect CEM survival (data not shown), suggesting that this mechanism is not important for CEM survival. Maurer et al. (2007) recently reported that the programmed death of the tail spike cell in *C. elegans* is effected by transcriptional regulation of the caspase gene *ced-3*. This report, which includes effects of *ced-9* Bcl-2 mutations similar to those we found in the CEM neurons, suggests a mechanism by which *ceh-30* might control CEM survival. We performed experiments using a *ced-3::gfp* reporter similar those of Maurer et al. (2007) and failed to observe up-regulation of *ced-3* in the surviving CEMs of *ced-3(n717)* hermaphrodites (data not shown). We could have missed sexually

dimorphic *ced-3* expression in the CEMs in these experiments because of the developmental stages we examined or because elements necessary for the appropriate transcriptional control of *ced-3* were not included in the reporter construct.

The loss of *ced-9* causes an activation of programmed cell death similar to that caused by expression of the BH3-only pro-apoptotic protein EGL-1. For example, the HSNs of *ced-9(n1653*lf*)* hermaphrodites and the *egl-1*-expressing HSNs of *egl-1(n1084*gf*)* hermaphrodites undergo programmed cell death (Desai et al. 1988; Conradt and Horvitz 1999). Similarly, the *ced-9* loss and *egl-1* over-expression each cause relocalization of CED-4 from the mitochondria to the perinucleus, a proposed early step in programmed cell death (Chen et al. 2000). *ceh-30* therefore protects by rendering cells that have activated programmed cell death less sensitive to this activation. A schematic representation of such a desensitizing effect of CEH-30 is shown in Figure 3C.

A genetic pathway for the regulation of CEM neuron survival

A proposed genetic pathway for the control of CEM neuron death is shown in Figure 3D. First, CEM neuron identity is established; one aspect of this identity is the activation of programmed cell death. The activation of CEM programmed cell death includes expression of the pro-apoptotic BH3-only protein EGL-1, which is required for somatic programmed cell deaths in *C. elegans* (Conradt and Horvitz 1998), including the deaths of the CEMs of hermaphrodites (Table 1A). Sexual identity, established by *tra-1* activity, controls *ceh-30* activity. *ceh-30* then acts downstream of or in parallel to *ced-9 Bcl-2* to establish whether the CEM neurons are sensitive to the activation of

programmed cell death. In other words, *ceh-30* activity defines the sensitivity of the CEM neurons to the initiation of programmed cell death. How *ceh-30* exerts a cell-specific anti-apoptotic function independently of *ced-9 Bcl-2* remains to be determined.

The deaths of the CEM neurons in hermaphrodites normally require *egl-1* function. As described above, we have shown that *ceh-30* protects the CEMs from programmed cell death by acting downstream of or in parallel to *egl-1* and *ced-9*. In addition to the regulation of CEM survival by *ceh-30* downstream of or parallel to *egl-1* and *ced-9*, it is possible that the sexually dimorphic deaths of the CEM neurons are also regulated at the level of *egl-1* transcription, as are other cell-type-specific cell deaths. We could not directly assess *egl-1* expression in the CEM neurons, as our *egl-1::gfp* reporters were not expressed in the CEM neurons of cell-death-defective larvae or in early embryonic CEM neurons (see Supplementary Data). *egl-1* might be expressed equivalently in the CEM neurons of both sexes, in which case the sexual dimorphism of CEM survival is established entirely by the function of *ceh-30* to alter the sensitivity of the CEMs to the death-inducing effects of *egl-1*, as described above. Alternatively, the sex determination pathway might also regulate *egl-1* expression in the CEMs, so that in hermaphrodite CEMs express *egl-1* but in male CEMs do not. Importantly, the CEM neurons of *ceh-30(*lf*)* males died in an *egl-1*-dependent fashion. Thus, *egl-1* is active in the CEMs of *ceh-30(*lf*)* males. If *egl-1* is normally off in male CEMs, repression of *egl-1* expression in male CEMs must be dependent on *ceh-30*. We conclude that the regulation of *egl-1* expression in the CEMs by sexual identity, if it occurs, is performed

by *ceh-30*. We depict this possible regulation of *egl-1* in the CEMs by sexual identity by a dotted line from *ceh-30* to *egl-1* in Figure 3D.

The novel anti-apoptotic function of *ceh-30* is evolutionarily conserved

Parallels exist between the specific apoptotic loss of the *C. elegans* CEM sensory neurons caused by a loss of *ceh-30* function and the reported consequence of deleting the homologous murine gene *Barhl1*: *Barhl1* deletion mice are born healthy and able to hear, but progressively lose both their hearing and their sensory cochlear inner ear hair cells (Li et al. 2002). Similar to the sensory hair cells of *Barhl1* mice, but atypically for *C. elegans* cells that undergo programmed cell death, hermaphrodite CEMs persist for hours and show signs of differentiation (the extension of ciliated processes) prior to their apoptotic deaths (J. Sulston and J. White, as cited by Horvitz et al. 1982). Mice deleted for the *Barhl1* gene also display defectssimilar to those seen in mice lacking the neurotrophin survival factor NT-3 (Li et al. 2004), as well as increased apoptosis of neurons of the superior colliculus (Li and Xiang 2006). It seems likely that the sensory hair cell neurons of *Barhl1* mutant mice, like the CEM neurons of *ceh-30* mutants, lack protection from apoptotic cell death. *Barhl2* has been reported to be a possible positive regulator of cell death in *Xenopus* (Offner et al. 2005), raising the possibility that in different contexts Bar homeodomain proteins might be able to regulate targets involved in apoptosis either to promote or to prevent cell death.

Barhl1 and *Barhl2* transgenes rescued the CEM survival defect of *ceh-30* mutant males. These genes therefore encode proteins that retain the functions and target specificity of CEH-30. We conclude that *C. elegans* and vertebrate Bar homeodomain

proteins likely share a conserved biological role as cell-type-specific regulators of programmed cell death. We suggest that vertebrate Bar proteins act to prevent neurodegeneration of certain neuron types and that the ectopic expression or increased activity of vertebrate Bar proteins might inhibit apoptotic cell death and promote oncogenesis. The novel mechanism by which *ceh-30* acts to prevent CEM neuron death together with the apparent conservation of the role of *ceh-30* in regulating cell survival suggests that further investigation of *ceh-30* and its vertebrate homologs might reveal a new evolutionarily conserved mechanism for the regulation of apoptotic cell death.

Materials and Methods

C. elegans genetics

C. elegans strains were derived from the wild-type strain N2 and cultured using standard conditions (Brenner 1974). The mutations used are listed in Supplemental Material.

We performed two screens using EMS mutagenesis (Brenner 1974) to identify revertants of *n3714*gf. In the first, F_1 progeny of mutagenized *nIs133*; *unc-2 ceh-30(n3714) lon-2* hermaphrodites were placed singly on Petri plates, and the progeny of 523 F_1s were examined for decreased penetrance of the *n3714* phenotype of CEM survival in hermaphrodites. Suppressors were tested for linkage to *n3714* by outcrossing. In the second screen, mutagenized *nIs133*; *unc-2 ceh-30(n3714) lon-2* hermaphrodites were mated with *nIs133*; *him-5* males, 1960 larval hermaphrodite F_1 cross-progeny were placed singly on Petri plates, and their progeny were assessed for CEM survival. The only suppressor closely linked to *n3714*, *n4111*, came from the second screen. Adding a wild-type copy of the locus with the chromosomal duplications *mnDp57* or *yDp14* did not complement *n4111* for suppression of *ceh-30(n3714*gf*)* (data not shown), indicating that *n4111* does not cause loss-of-function in a second locus required to support the *n3714*gf phenotype.

ceh-30(n3713, n3714, and *n3720)* were mapped to the left end of the *unc-2 lon-2* interval on LGX using standard methods. *ceh-30(n3714)* was mapped between nucleotide 3383 on C33D12 (all references to cosmid C33D12 sequence refer to nucleotides of accession number U64600) and 801 on F52E4 (accession number U56964) using 124 Lon recombinants recovered after crossing *nIs133*; *unc-2*

ceh-30(n3714) lon-2 hermaphrodites with males containing LGX from the Hawaiian strain CB4856 (Wicks et al. 2001). *ceh-30(n4111 n3714)* was mapped to the right of 14788 on M02F4 (accession number U41548) using 127 Lon and 86 Unc recombinants recovered after crossing *nIs133*; *unc-2 ceh-30(n4111 n3714) lon-2* hermaphrodites with males containing LGX from the Hawaiian strain and further genotyping those recombinants that had broken left of 22142 on F52E4. None of these recombinant chromosomes contained *n3714*gf in the absence of *n4111*.

Isolation of *ceh-30(n4289)*

A library of mutagenized *C. elegans* was screened for deletions in *ceh-30* as previously described (Jansen et al. 1997). The deletion *n4289*, which removes from 22227 to 22893 of cosmid C33D12, was recovered. We used PCR to determine that sequences present in the wild type are missing in *ceh-30(n4289Δ)* homozygotes. *ceh-30(n4289Δ)* was outcrossed three times for the X chromosome and five times for the autosomal genome prior to strain construction and analysis.

DNA and RNA manipulations and generation of transgenic animals

DNA sequence determination was performed using an ABI DNA Sequencer model 373, an ABI Genetic Analyzer 3100 and by Gene Gateway (Hayward, CA). DNA constructs used are described in Supplemental Data. All germline transformation experiments were performed using the co-injection marker P76-16B (Bloom and Horvitz 1997) at 50 ng/μl as described (Mello et al. 1991). Cosmids and genomic and cDNA constructs were injected at 20 ng/μl, and reporter constructs were injected at

concentrations from 2.5 to 50 ng/μl. Embryonic *ceh-30::gfp* expression was examined using embryos masculinized by *tra-2(n1106)*.

Total RNA from N2 and *him-5* was isolated using Trizol (Invitrogen, Carlsbad, CA). 5' RACE and 3' RACE were performed using appropriate reagents (Invitrogen). RNA ligase-mediated 5' RACE was performed essentially as described (Maruyama and Sugano 1994) using appropriate reagents (Invitrogen; Epicentre, Madison, WI; New England Biolabs, Beverly, MA). The 5' end of the *ceh-30* transcript was also isolated by PCR with *ceh-30*-specific and vector-specific primers from cDNA libraries provided by Shai Shaham and by Zheng Zhou (personal communications). The 5' ends determined using each of these methods were essentially identical and did not contain a splice-leader sequence. The vector BSK-*ceh-30*-Sn (see Supplemental Data) was used to express the *ceh-30* cDNA and to express mouse *Barhl1* and *Barhl2* cDNAs (gifts of Shengguo Li and Mengqing Xiang), and these constructs were used to obtain the data shown in Table 2C.

Gel mobility shifts and competition experiments

Gel mobility shift experiments were performed essentially as described (Zarkower and Hodgkin 1993; Conradt and Horvitz 1999). Probes were generated by PCR using the primers CGTCATCATCAAATTTTCACC and AATGATGTTTTTATGTCGCAACT for *ceh-30* and the primers CTGTTCCAGCTCAAATTTCCA and AACAAGTATCAGGCGGCATC for *egl-1* controls (not shown). TRA-1A protein was generated by *in vitro* transcription and translation of a full-length *tra-1A* cDNA (plasmid pDZ118, a gift from David Zarkower). 1.5 μl of

reticulocyte lysate, 0.5-1 ng of ^{32}P-labeled probe, and 0, 10x, 100x, or 1000x unlabeled competitor were incubated at room temperature for one hour before electrophoresis through 4% acrylamide gels in 0.5X TBE.

Analysis of *C. elegans* phenotypes

Animals were examined for gross developmental defects using dissecting and Nomarski microscopy. In determining cell-autonomy of the CEM survival caused by the pBSK-*ceh-30(n3714*gf*)* transgene, we used animals rescued for the Unc-76 phenotype. Programmed cell death in the anterior pharynx was quantified using Nomarski microscopy as described (Hengartner et al. 1992). Survival of Pn.aap cells was quantified using *lin-11::gfp* as described (Reddien et al. 2001). Corpse number in the heads of L1 hermaphrodites was scored as described (Yuan and Horvitz 1992). The number of neuronal nuclei in a region of the ventral nerve cords of late L4 larvae and young adults was determined following staining with DAPI as described (Sulston and Horvitz 1981; Fixsen 1985). Programmed cell death in the CEM lineage was assessed using a fluorescence-equipped dissecting microscope (M^{2}BIO; Kramer Scientific, Valley Cottage, NY) to detect *pkd-2::gfp* expression in the cell bodies of CEM neurons or by using Nomarski microscopy as described (Schwartz 2007). The ventral CEMs of 1.5-fold stage embryos were identified by reference to Figure 8C of Sulston et al. (1983); the positions of the dorsal CEMs is less distinctive, and these cells were not examined.

Supplemental Materials and Methods

C. elegans genetics

The following mutations were used and are described by Riddle et al. (1997) unless otherwise noted: LGI: *ces-1(n703 n1434)*, *ced-1(e1735)*; LGII: *tra-2(e1875, n1106)*, *dpl-1(n3380)* (Reddien et al. 2007); LGIII: *tra-1(e1099)*, *fem-2(e2105)*, *ced-4(n1162), ced-4(n3158)* (Reddien et al. 2001), *ced-9(n1950*, *n2812*, *n3400)* (Reddien et al. 2007); LGIV: *fem-1(e1965)*, *fem-3(e1996)*; *ced-3(n717*, *n2427*, *n2446*, *n2447*, *n2923)* (Shaham et al. 1999), *him-8(e1489)*, *eor-1(cs28)* (Rocheleau et al. 2002); LGV: *egl-1(n2248*, *n1084 n3082)* (Conradt and Horvitz 1998), *him-5(e1467)*, *unc-76(e911)*, *bir-1(n3329)* (Speliotes 2000), *bir-2(ok104)* (Speliotes 2000); and LGX: *unc-2(e55)*, *ceh-30(n3713, n3714, n3720, n4111*, *n4289)* (this study), *lon-2(e678)*, *eor-2(cs42)* (Rocheleau et al. 2002), *nIs106* (Reddien et al. 2001). *nIs133* I and *nIs128* II are chromosomally integrated versions of *pkd-2::gfp*, each marked with a *lin-15(+)* marker (H.T.S. and H.R.H., unpublished results). *ceh-30(n3713)* and *ceh-30(n3714)* were generated by different mutagenized P_0s of the strain MT10742 *nIs133*, and *ceh-30(n3720)* was isolated after mutagenesis of the strain MT10729 *nIs128*. Each of the chromosomal duplications *mnDp57* (X:I) and *yDp14* (X:I) (Meneely and Nordstrom 1988; Akerib and Meyer 1994) spans *ceh-30*. No reported chromosomal deficiencies eliminate *ceh-30*. *nT1* [IV; V] with the dominant marker *qIs51* (Siegfried et al. 2004) was used to balance *fem-1*, *fem-3*, and *bir-1*. *sC1* (Pilgrim et al. 1995) was used to balance *fem-2*. *qC1* (Austin and Kimble 1989) was used to balance *tra-1*. Strains constructed using the integrated *egl-1::gfp* reporters *bcIs1* and *bcIs37* (Thellmann et al. 2003) were examined for *gfp* expression in the CEMs of wild-type male larvae, cell-death-defective

ced-3(n717) hermaphrodite larvae, *ceh-30(n3714*gf*)* hermaphrodite larvae, cell-death-defective *ced-3(n717)*; *ceh-30(n4289Δ)* male larvae, cell-death-defective *ced-3(n717)* embryos, masculinized *tra-2(n1106)* embryos, masculinized cell-death-defective *tra-2(n1106)*; *ced-3(n717)*; *ceh-30(n4289Δ)* embryos, and *ceh-30(n3714*gf*)* embryos. *egl-1::gfp* expression was not observed in the CEM neurons of larvae or in the CEM neurons of 1.5-fold stage embryos, the stage at which the CEM neurons can readily be identified on the basis of their positions within the embryo.

Generation of DNA constructs

The *ceh-30* rescuing construct pBSK-*ceh-30* contains genomic DNA corresponding to 17761 through 26079 of C33D12, amplified by PCR (Advantage cDNA; BD Biosciences, Mountain View, CA) from proteinase K-treated N2 and cloned using endogenous *Cla*I and *Avr*II sites into a modified Bluescript vector (Stratagene, La Jolla, CA) digested with *Cla*I and *Spe*I. pBSK-*ceh-30* contains 4205 bp of the *ceh-30* locus 5' of the *ceh-30* ATG and 2456 bp of the *ceh-30* locus 3' of the *ceh-30* stop codon. As a control for *ceh-30* rescue, the mutated construct pBSK-*ceh-30*-STOP, with two stop codons inserted at position 22,649 of C33D12, was used. A *Hind*III fragment of pBSK-*ceh-30* was replaced with sequence amplified by PCR from a *ceh-30(n3714)* mutant to generate the construct pBSK-*ceh-30(n3714)*. *Mlu*I and *Pst*I sites were introduced by PCR at sites in pBSK-*ceh-30* corresponding to C33D12 21784, 22029, 22518, 23477, and 23604; a *gfp* cassette with appropriate restriction sites added was amplified from pPD95.02 (provided by Andrew Fire) and cloned into the modified rescuing constructs; the third of these, called *ceh-30::gfp*, rescued *ceh-30(n4289Δ)* for

CEM survival in males and caused GFP expression. *unc-119::mStrawberry* was generated by cloning a PCR product corresponding to 1193 through 3559 of cosmid M142 (accession number Z73428) into a modified PD95.70 (provided by Andrew Fire), the *gfp* cassette of which had been replaced with *mStrawberry* (Shaner et al. 2004). A *ced-3::gfp* reporter containing 2066 bp of promoter sequence was generated by cloning a PCR product corresponding to 11115 through 13189 of cosmid C48D1 into PD95.70.

A version of pBSK-*ceh-30* lacking introns was unable to rescue *ceh-30(n4289)* for CEM survival (data not shown). Successful minigene constructs were made by placing into this intronless version a PCR product containing most of the missing second intron at any of three positions: 1.0 or 2.1 kb downstream of the coding sequence in an *Afl*II site or a *Sna*BI site, respectively, or 0.5 kb upstream in an *Eco*RV site. The addition of this intronic sequence restored the rescuing activity of these constructs; this finding is consistent with data suggesting that sequences in the second intron are required for *ceh-30* function (P. Grote and B. Conradt, personal communication; E. Peden and D. Xue, personal communication). The plasmid with intronic sequence inserted at the *Sna*BI site in the same orientation as in its original position was modified by adding *Spe*I and *Sph*I sites to replace the sequence from just after the second codon of *ceh-30* to just before the last four codons and the stop codon of *ceh-30*. This plasmid, named BSK-*ceh-30*-Sn, was used as an expression vector for *ceh-30*, *mBarhl1*, and *mBarhl2* cDNAs.

Examining embryonic CEM neurons for *ceh-30::gfp* expression

As described in Materials and Methods, The ventral CEMs of 1.5-fold stage embryos can be identified by their stereotyped positions within the embryo with reference to Figure 8C of (Sulston et al. 1983); the positions of the dorsal CEMs are less distinctive, and we did not examine these cells. To test for *ceh-30::gfp* expression in embryonic CEMs, *tra-2(n1106)*; *unc-76(e911)* animals were transformed with *ceh-30::gfp* and the co-transformation marker P76-16B. The *tra-2* mutation *n1106* was used to avoid difficulties in distinguishing male embryos from hermaphrodite embryos. *tra-2(n1106)* causes partial masculinization of hermaphrodites, including a very strong CEM survival phenotype. The CEM survival caused by *tra-2(n1106)* requires *ceh-30* function (data not shown), indicating that in these masculinized animals *ceh-30* must be expressed where its function is required to promote CEM neuron survival. Thus, the *tra-2(n1106)* mutation enabled us to examine *ceh-30* expression in embryos in which the CEM neurons are fated to survive and in which *ceh-30* is functioning to protect these neurons from apoptotic cell death. An example of *ceh-30::gfp* expression in an embryonic ventral CEM can be seen in Figure S1.

Acknowledgments

We thank Niels Ringstad, Brendan Galvin, Scott Boyd, and Shilpa Joshi for comments about this manuscript; Shengguo Li and Mengqing Xiang for *Barhl1* and *Barhl2* cDNAs and for unpublished information regarding *Barhl1* and *Barhl2*; Phillip Grote, Ralda Nehme, and Barbara Conradt for unpublished information about intronic requirements for *ceh-30* expression, for advice about using Nomarski to identify CEM neurons and about TRA-1 gel shift experiments, and for *bcIs1* and *bcIs37*; Erin Peden and Ding Xue for unpublished information about intronic requirements for *ceh-30* expression; Shai Shaham and Zheng Zhou for cDNA libraries; David Zarkower for plasmid pDZ118; Roger Tsien for *mStrawberry*; Andrew Fire for PD95.02 and PD95.70; Na An for help with strains; Beth Castor for DNA sequence determination; Andrew Hellman for the identification of *n4289*; Brad Hersh for DNA sequence of *ced-9(n3400)*; other members of the Horvitz laboratory for discussions and for construction of the deletion library; the *Caenorhabditis* Genetics Center, which is funded by the NIH National Center for Research Resources (NCRR), for strains; and the *C. elegans* Genome Sequencing Consortium and the Genome Sequencing Center at Washington University in St. Louis for genomic sequence of the *ceh-30* locus in *C. elegans*, *C. briggsae*, and *C. remanei*. This work was supported by the Howard Hughes Medical Institute. H.T.S. was supported in part by a David H. Koch Graduate Fellowship. H.R.H. is an Investigator of the Howard Hughes Medical Institute and is David H. Koch Professor of Biology at MIT.

References

Akerib, C.C. and B.J. Meyer. 1994. Identification of X chromosome regions in *Caenorhabditis elegans* that contain sex-determination signal elements. *Genetics* **138**: 1105-25.

Austin, J. and J. Kimble. 1989. Transcript analysis of *glp-1* and *lin-12*, homologous genes required for cell interactions during development of *C. elegans*. *Cell* **58**: 565-71.

Barr, M.M. and P.W. Sternberg. 1999. A polycystic kidney-disease gene homologue required for male mating behaviour in *C. elegans*. *Nature* **401**: 386-9.

Benn, S.C. and C.J. Woolf. 2004. Adult neuron survival strategies - slamming on the brakes. *Nat Rev Neurosci* **5**: 686-700.

Bergmann, A., J. Agapite, K. McCall, and H. Steller. 1998. The *Drosophila* gene *hid* is a direct molecular target of Ras-dependent survival signaling. *Cell* **95**: 331-41.

Bidere, N., H.C. Su, and M.J. Lenardo. 2006. Genetic disorders of programmed cell death in the immune system. *Annu Rev Immunol* **24**: 321-352.

Bloom, L. and H.R. Horvitz. 1997. The *Caenorhabditis elegans* gene *unc-76* and its human homologs define a new gene family involved in axonal outgrowth and fasciculation. *Proc Natl Acad Sci U S A* **94**: 3414-9.

Brenner, S. 1974. The genetics of *Caenorhabditis elegans*. *Genetics* **77**: 71-94.

Bulfone, A., E. Menguzatto, V. Broccoli, A. Marchitiello, C. Gattuso, M. Mariani, G.G. Consalez, S. Martinez, A. Ballabio, and S. Banfi. 2000. *Barhl1*, a gene belonging to a new subfamily of mammalian homeobox genes, is expressed in migrating neurons of the CNS. *Hum Mol Genet* **9**: 1443-1452.

Chasnov, J.R., W.K. So, C.M. Chan, and K.L. Chow. 2007. The species, sex, and stage specificity of a *Caenorhabditis* sex pheromone. *Proc Natl Acad Sci U S A* **104**: 6730-5.

Chen, F., B.M. Hersh, B. Conradt, Z. Zhou, D. Riemer, Y. Gruenbaum, and H.R. Horvitz. 2000. Translocation of *C. elegans* CED-4 to nuclear membranes during programmed cell death. *Science* **287**: 1485-9.

Conradt, B. and H.R. Horvitz. 1998. The *C. elegans* protein EGL-1 is required for programmed cell death and interacts with the Bcl-2-like protein CED-9. *Cell* **93**: 519-29.

-. 1999. The TRA-1A sex determination protein of *C. elegans* regulates sexually dimorphic cell deaths by repressing the *egl-1* cell death activator gene. *Cell* **98**: 317-27.

Desai, C., G. Garriga, S.L. McIntire, and H.R. Horvitz. 1988. A genetic pathway for the development of the *Caenorhabditis elegans* HSN motor neurons. *Nature* **336**: 638-46.

Desai, C. and H.R. Horvitz. 1989. *Caenorhabditis elegans* mutants defective in the functioning of the motor neurons responsible for egg laying. *Genetics* **121**: 703-21.

Du, C., M. Fang, Y. Li, L. Li, and X. Wang. 2000. Smac, a mitochondrial protein that promotes cytochrome c-dependent caspase activation by eliminating IAP inhibition. *Cell* **102**: 33-42.

Ellis, R.E. and H.R. Horvitz. 1991. Two *C. elegans* genes control the programmed deaths of specific cells in the pharynx. *Development* **112**: 591-603.

Fixsen, W. 1985. The genetic control of hypodermal lineages during nematode development. *Ph. D. Thesis, Massachusetts Institute of Technology, Cambridge, MA*.

Gottfried, Y., A. Rotem, R. Lotan, H. Steller, and S. Larisch. 2004. The mitochondrial ARTS protein promotes apoptosis through targeting XIAP. *Embo J* **23**: 1627-35.

Goyal, L., K. McCall, J. Agapite, E. Hartwieg, and H. Steller. 2000. Induction of apoptosis by *Drosophila reaper*, *hid* and *grim* through inhibition of IAP function. *Embo J* **19**: 589-97.

Hedgecock, E.M., J.E. Sulston, and J.N. Thomson. 1983. Mutations affecting programmed cell deaths in the nematode *Caenorhabditis elegans*. *Science* **220**: 1277-9.

Hengartner, M.O., R.E. Ellis, and H.R. Horvitz. 1992. *Caenorhabditis elegans* gene *ced-9* protects cells from programmed cell death. *Nature* **356**: 494-9.

Hengartner, M.O. and H.R. Horvitz. 1994a. Activation of *C. elegans* cell death protein CED-9 by an amino-acid substitution in a domain conserved in Bcl-2. *Nature* **369**: 318-20.

-. 1994b. *C. elegans* cell survival gene *ced-9* encodes a functional homolog of the mammalian proto-oncogene *bcl-2*. *Cell* **76**: 665-76.

Higashijima, S., T. Kojima, T. Michiue, S. Ishimaru, Y. Emori, and K. Saigo. 1992a. Dual *Bar* homeo box genes of *Drosophila* required in two photoreceptor cells, R1 and R6, and primary pigment cells for normal eye development. *Genes Dev* **6**: 50-60.

Higashijima, S., T. Michiue, Y. Emori, and K. Saigo. 1992b. Subtype determination of *Drosophila* embryonic external sensory organs by redundant homeo box genes *BarH1* and *BarH2*. *Genes Dev* **6**: 1005-1018.

Hodgkin, J. 2002. Exploring the envelope. Systematic alteration in the sex-determination system of the nematode *Caenorhabditis elegans*. *Genetics* **162**: 767-80.

Hoeppner, D.J., M.S. Spector, T.M. Ratliff, J.M. Kinchen, S. Granat, S.-C. Lin, S.S. Bhusri, B. Conradt, M.A. Herman, and M.O. Hengartner. 2004. *eor-1* and *eor-2* are required for cell-specific apoptotic death in *C. elegans*. *Dev Biol* **274**: 125-38.

Horvitz, H.R., H.M. Ellis, and P.W. Sternberg. 1982. Programmed cell death in nematode development. *Neuroscience Commentaries* **1**: 56-65.

Inaba, T., T. Inukai, T. Yoshihara, H. Seyschab, R.A. Ashmun, C.E. Canman, S.J. Laken, M.B. Kastan, and A.T. Look. 1996. Reversal of apoptosis by the leukaemia-associated E2A-HLF chimaeric transcription factor. *Nature* **382**: 541-4.

Jager, S., H.T. Schwartz, H.R. Horvitz, and B. Conradt. 2004. The *Caenorhabditis elegans* F-box protein SEL-10 promotes female development and may target FEM-1 and FEM-3 for degradation by the proteasome. *Proc Natl Acad Sci U S A* **101**: 12549-54.

Jansen, G., E. Hazendonk, K.L. Thijssen, and R.H. Plasterk. 1997. Reverse genetics by chemical mutagenesis in *Caenorhabditis elegans*. *Nat Genet* **17**: 119-21.

Kimble, J. and D. Hirsh. 1979. The postembryonic cell lineages of the hermaphrodite and male gonads in *Caenorhabditis elegans*. *Dev Biol* **70**: 396-417.

Kojima, T., S. Ishimaru, S. Higashijima, E. Takayama, H. Akimaru, M. Sone, Y. Emori, and K. Saigo. 1991. Identification of a different-type homeobox gene, *BarH1*, possibly causing Bar (*B*) and *Om(1D)* mutations in *Drosophila*. *Proc Natl Acad Sci U S A* **88**: 4343-7.

Krantic, S., N. Mechawar, S. Reix, and R. Quirion. 2005. Molecular basis of programmed cell death involved in neurodegeneration. *Trends Neurosci* **28**: 670-676.

Kuwana, T. and D.D. Newmeyer. 2003. Bcl-2-family proteins and the role of mitochondria in apoptosis. *Curr Opin Cell Biol* **15**: 691-9.

Li, S., S.M. Price, H. Cahill, D.K. Ryugo, M.M. Shen, and M. Xiang. 2002. Hearing loss caused by progressive degeneration of cochlear hair cells in mice deficient for the *Barhl1* homeobox gene. *Development* **129**: 3523-3532.

Li, S., F. Qiu, A. Xu, S.M. Price, and M. Xiang. 2004. *Barhl1* regulates migration and survival of cerebellar granule cells by controlling expression of the neurotrophin-3 gene. *J Neurosci* **24**: 3104-3114.

Li, S. and M. Xiang. 2006. Barhl1 is required for maintenance of a large population of neurons in the zonal layer of the superior colliculus. *Dev Dyn* **235**: 2260-5.

Liu, H., T.J. Strauss, M.B. Potts, and S. Cameron. 2006. Direct regulation of *egl-1* and of programmed cell death by the Hox protein MAB-5 and by CEH-20, a *C. elegans* homolog of Pbx1. *Development* **133**: 641-650.

Maruyama, H. and S. Sugano. 1994. Oligo-capping: a simple method to replace the cap structure of eukaryotic mRNAs with oligoribonucleotides. *Gene* **138**: 171-174.

Maurer, C.W., M. Chiorazzi, and S. Shaham. 2007. Timing of the onset of a developmental cell death is controlled by transcriptional induction of the *C. elegans ced-3* caspase-encoding gene. *Development* **134**: 1357-68.

Mello, C.C., J.M. Kramer, D. Stinchcomb, and V. Ambros. 1991. Efficient gene transfer in *C.elegans*: extrachromosomal maintenance and integration of transforming sequences. *Embo J* **10**: 3959-70.

Meneely, P.M. and K.D. Nordstrom. 1988. X chromosome duplications affect a region of the chromosome they do not duplicate in *Caenorhabditis elegans*. *Genetics* **119**: 365-75.

Metzstein, M.M., M.O. Hengartner, N. Tsung, R.E. Ellis, and H.R. Horvitz. 1996. Transcriptional regulator of programmed cell death encoded by *Caenorhabditis elegans* gene *ces-2*. *Nature* **382**: 545-7.

Metzstein, M.M. and H.R. Horvitz. 1999. The *C. elegans* cell death specification gene *ces-1* encodes a snail family zinc finger protein. *Mol Cell* **4**: 309-19.

Metzstein, M.M., G.M. Stanfield, and H.R. Horvitz. 1998. Genetics of programmed cell death in *C. elegans*: past, present and future. *Trends Genet* **14**: 410-6.

Moroni, M.C., E.S. Hickman, E. Lazzerini Denchi, G. Caprara, E. Colli, F. Cecconi, H. Muller, and K. Helin. 2001. Apaf-1 is a transcriptional target for E2F and p53. *Nat Cell Biol* **3**: 552-8.

Offner, N., N. Duval, M. Jamrich, and B. Durand. 2005. The pro-apoptotic activity of a vertebrate Bar-like homeobox gene plays a key role in patterning the *Xenopus* neural plate by limiting the number of *chordin*- and *shh*-expressing cells. *Development* **132**: 1807-1818.

Pilgrim, D., A. McGregor, P. Jackle, T. Johnson, and D. Hansen. 1995. The *C. elegans* sex-determining gene *fem-2* encodes a putative protein phosphatase. *Mol Biol Cell* **6**: 1159-71.

Rathmell, J.C. and C.B. Thompson. 2002. Pathways of apoptosis in lymphocyte development, homeostasis, and disease. *Cell* **109 Suppl**: S97-107.

Reddien, P.W., E.C. Andersen, M.C. Huang, and H.R. Horvitz. 2007. DPL-1 DP, LIN-35 Rb and EFL-1 E2F act with the MCD-1 zinc-finger protein to promote programmed cell death in *Caenorhabditis elegans*. *Genetics* **175**: 1719-33.

Reddien, P.W., S. Cameron, and H.R. Horvitz. 2001. Phagocytosis promotes programmed cell death in *C. elegans*. *Nature* **412**: 198-202.

Riddle, D.L., T. Blumenthal, B.J. Meyer, and J.R. Priess. 1997. *C. elegans* II (Cold Spring Harbor Laboratory Press, Cold Spring Harbor, New York).

Rocheleau, C.E., R.M. Howard, A.P. Goldman, M.L. Volk, L.J. Girard, and M.V. Sundaram. 2002. A *lin-45 raf* enhancer screen identifies *eor-1*, *eor-2* and unusual alleles of Ras pathway genes in *Caenorhabditis elegans*. *Genetics* **161**: 121-31.

Saito, T., K. Sawamoto, H. Okano, D.J. Anderson, and K. Mikoshiba. 1998. Mammalian BarH homologue is a potential regulator of neural bHLH genes. *Dev Biol* **199**: 216-225.

Schwartz, H.T. 2007. A protocol describing pharynx counts and a review of other assays of apoptotic cell death in the nematode worm *Caenorhabditis elegans*. *Nature Protocols* **2**: 705-14.

Shaham, S. and H.R. Horvitz. 1996. Developing *Caenorhabditis elegans* neurons may contain both cell-death protective and killer activities. *Genes Dev* **10**: 578-91.

Shaham, S., P.W. Reddien, B. Davies, and H.R. Horvitz. 1999. Mutational analysis of the *Caenorhabditis elegans* cell-death gene *ced-3*. *Genetics* **153**: 1655-71.

Shaner, N.C., R.E. Campbell, P.A. Steinbach, B.N. Giepmans, A.E. Palmer, and R.Y. Tsien. 2004. Improved monomeric red, orange and yellow fluorescent proteins derived from *Discosoma* sp. red fluorescent protein. *Nat Biotechnol* **22**: 1567-1572.

Siegfried, K.R., A.R. Kidd, 3rd, M.A. Chesney, and J. Kimble. 2004. The *sys-1* and *sys-3* genes cooperate with Wnt signaling to establish the proximal-distal axis of the *Caenorhabditis elegans* gonad. *Genetics* **166**: 171-86.

Speliotes, E.K. 2000. *C. elegans* BIR-1 acts with the Aurora-like kinase AIR-2 to affect chromosomes and the spindle midzone. *Ph. D. Thesis, Massachusetts Institute of Technology, Cambridge, MA*.

Sulston, J.E. and H.R. Horvitz. 1977. Post-embryonic cell lineages of the nematode, *Caenorhabditis elegans*. *Dev Biol* **56**: 110-56.

-. 1981. Abnormal cell lineages in mutants of the nematode *Caenorhabditis elegans*. *Dev Biol* **82**: 41-55.

Sulston, J.E., E. Schierenberg, J.G. White, and J.N. Thomson. 1983. The embryonic cell lineage of the nematode *Caenorhabditis elegans*. *Dev Biol* **100**: 64-119.

Thellmann, M., J. Hatzold, and B. Conradt. 2003. The Snail-like CES-1 protein of *C. elegans* can block the expression of the BH3-only cell-death activator gene *egl-1* by antagonizing the function of bHLH proteins. *Development* **130**: 4057-71.

Verhagen, A.M. and D.L. Vaux. 2002. Cell death regulation by the mammalian IAP antagonist Diablo/Smac. *Apoptosis* **7**: 163-6.

Wang, S.L., C.J. Hawkins, S.J. Yoo, H.A. Muller, and B.A. Hay. 1999. The *Drosophila* caspase inhibitor DIAP1 is essential for cell survival and is negatively regulated by HID. *Cell* **98**: 453-63.

Weaver, B.A. and D.W. Cleveland. 2005. Decoding the links between mitosis, cancer, and chemotherapy: The mitotic checkpoint, adaptation, and cell death. *Cancer Cell* **8**: 7-12.

White, J.G., E. Southgate, and J.N. Thomson. 1991. On the nature of undead cells in the nematode *Caenorhabditis elegans*. *Philos Trans R Soc Lond B Biol Sci* **331**: 263-271.

Wicks, S.R., R.T. Yeh, W.R. Gish, R.H. Waterston, and R.H. Plasterk. 2001. Rapid gene mapping in *Caenorhabditis elegans* using a high density polymorphism map. *Nat Genet* **28**: 160-4.

Wu, W.S., S. Heinrichs, D. Xu, S.P. Garrison, G.P. Zambetti, J.M. Adams, and A.T. Look. 2005. Slug antagonizes p53-mediated apoptosis of hematopoietic progenitors by repressing *puma*. *Cell* **123**: 641-653.

Yeo, W. and J. Gautier. 2004. Early neural cell death: dying to become neurons. *Dev Biol* **274**: 233-244.

Yuan, J. and H.R. Horvitz. 1992. The *Caenorhabditis elegans* cell death gene *ced-4* encodes a novel protein and is expressed during the period of extensive programmed cell death. *Development* **116**: 309-20.

Yuan, J., S. Shaham, S. Ledoux, H.M. Ellis, and H.R. Horvitz. 1993. The *C. elegans* cell death gene *ced-3* encodes a protein similar to mammalian interleukin-1 beta-converting enzyme. *Cell* **75**: 641-52.

Zarkower, D. and J. Hodgkin. 1993. Zinc fingers in sex determination: only one of the two *C. elegans* Tra-1 proteins binds DNA *in vitro*. *Nucleic Acids Res* **21**: 3691-8.

Zou, H., W.J. Henzel, X. Liu, A. Lutschg, and X. Wang. 1997. Apaf-1, a human protein homologous to *C. elegans* CED-4, participates in cytochrome c-dependent activation of caspase-3. *Cell* **90**: 405-13.

Table 1. A *ceh-30* gain-of-function mutation causes survival of the sexually dimorphic CEM neurons by acting downstream of or in parallel to the sex determination pathway

A. Mutations in the *ceh-30* locus semidominantly cause CEM survival.

Genotype	Sex	CEM survival (%) None	D OR V	D AND V	n=
wild-type	Herm.	100	0	0	60
wild-type	Male	0	0	100	60
tra-2(n1106)	Intersex	0	8	92	60
egl-1(n1084 n3082)	Herm.	0	7	93	60
ced-4(n1162)	Herm.	0	6	94	63
ced-3(n2427)	Herm.	85	15	0	113
ced-3(n717)	Herm.	0	10	90	60
*ceh-30(n3713*gf)/+	Herm.	22	72	7	60
*ceh-30(n3714*gf)/+	Herm.	22	70	8	60
*ceh-30(n3720*gf)/+	Herm.	25	67	8	60
*ceh-30(n3713*gf)	Herm.	0	47	53	60
*ceh-30(n3714*gf)	Herm.	0	42	58	60
*ceh-30(n3720*gf)	Herm.	0	48	52	60
*ceh-30(n3713*gf/*n3714*gf)	Herm.	0	50	50	60
*ceh-30(n3713*gf/*n3720*gf)	Herm.	2	47	52	60

B. The *ceh-30* mutation *n3714* acts by gain-of-function to cause CEM neuron survival.

Genotype	*ceh-30* locus	CEM survival in hermaphrodites (%) None	D OR V	D AND V	n=
wild-type	+ / +	100	0	0	60
yDp14	+ / + / + / +	100	0	0	60
ceh-30(n3714)/+	gf / +	28	68	3	60
yDp14/+; *ceh-30(n3714)*/+	gf / + / +	30	65	5	60
ceh-30(n3714)	gf / gf	0	48	52	100
yDp14/+; *ceh-30(n3714)*	gf / gf / +	3	53	44	68
yDp14; *ceh-30(n3714)*	gf / gf / + / +	2	57	42	60

C. Gain of *ceh-30* function promotes CEM survival downstream of or parallel to the *fem* genes.

Genotype	CEM survival in hermaphrodites (%) None	D OR V	D AND V	n=
wild-type	100	0	0	60
*ceh-30(n3714*gf)	0	45	55	60
fem-1(e1965)	98	2	0	60
fem-1(e1965); *ceh-30(n3714*gf)	5	55	40	60
fem-2(e2105)	99	1	0	139
fem-2(e2105); *ceh-30(n3714*gf)	3	84	14	110
fem-3(e1996)	100	0	0	60
fem-3(e1996); *ceh-30(n3714*gf)	12	43	45	60

A. In this and other tables, CEM survival was scored using a *pkd-2::gfp* reporter as described in Materials and Methods. When CEM survival was scored using the dissecting microscope, the left and right ventral CEMs could not readily be distinguished from each other and the left and right dorsal CEMs could not readily be distinguished from each other; CEM survival was therefore assessed for ventral CEMs and for dorsal CEMs. The resulting numbers were found to be reproducible and sensitive to changes in the degree of CEM death or survival. In this and in other tables, D OR V denotes animals in which dorsal or ventral CEMs, but not both, were observed and indicates animals displaying only weak CEM survival; D AND V denotes animals in which both dorsal and ventral CEMs were observed and indicates animals showing strong CEM survival. All animals were homozygous for *nIs133*. Otherwise, the genotypes of the animals analyzed were as listed, except for the heterozygotes, which were heterozygous for *unc-2(e55)* and *lon-2(e678)*. Maternal genotype did not affect the results concerning the heterozygotes (data not shown). *tra-2(n1106)* hermaphrodites are weakly masculinized (Desai and Horvitz 1989). *ced-3(n2427)* and *ced-3(n717)* animals are weakly and strongly defective in programmed cell death, respectively (Shaham et al. 1999). Herm., hermaphrodite. *tra-2(n1106)* XX animals are largely hermaphroditic with some male characteristics, including CEM survival.

B. All animals were homozygous for *nIs128*. Otherwise, genotypes were as listed, except that when the chromosomal duplication *yDp14* was present the strain was also homozygous for *unc-2(e55)* and *lon-2(e678)*, and the *ceh-30(n3714)*/+ strain was heterozygous for *unc-2(e55)* and *lon-2(e678)*. *ceh-30* locus, number of wild-type (+) and mutant (gf) copies of the locus in each strain. An expanded version of this table, examining all of the same dosage conditions using the duplication *mnDp57* and using the allele *ceh-30(n3713*gf*)*, is shown in Supplementary Material (Table S1).

C. All animals were homozygous for *nIs133*. Otherwise, the genotypes of the animals analyzed were as listed. The *fem-1(e1965)* and *fem-3(e1996)* homozygotes scored were the progeny of crosses between *fem/nT1*[*qIs51*] males and *fem* homozygous females; thus, half were XX females and half X0 females. *fem-2(e2105)* homozygotes scored were the progeny of maternally-rescued *fem-2(e2105)* homozygotes. An expanded version of this table including similar results obtained using *ceh-30(n3713*gf*)* is shown in Supplementary Material (Table S2).

Table 2. The *BarH* homeodomain gene *ceh-30* protects CEM neurons from apoptosis and this function is evolutionarily conserved.

A. *ceh-30(n4111)* is a linked suppressor of *ceh-30(n3714*gf*)*.

Genotype	CEM survival in hermaphrodites (%) None	D OR V	D AND V	n=
wild-type	98	2	0	100
*ceh-30(n3714*gf*)*	0	33	67	60
ceh-30(n4111 n3714)	98	2	0	60
*ceh-30(n3714*gf*)/+*	15	67	19	81
*ceh-30(n3714*gf*/n4111 n3714)*	13	68	19	120
ceh-30(n4111 n3714)/+	97	3	0	120

B. The CEM neurons of *ceh-30(*lf*)* males inappropriately undergo programmed cell death.

Genotype	CEM survival in males (%) None	D OR V	D AND V	n=
wild-type	0	0	100	60
*ceh-30(n3714*gf*)*	0	0	100	61
*ceh-30(n4111 n3714*lf*)*	44	33	23	66
ceh-30(n4289Δ)	83	14	3	71
tra-1(e1099)	0	0	100	46
tra-1(e1099); *ceh-30(n4111 n3714*lf*)*	51	47	2	45
egl-1(n1084 n3082)	0	0	100	62
egl-1(n1084 n3082); *ceh-30(n4111 n3714*lf*)*	0	0	100	65
ced-3(n717)	0	0	100	60
ced-3(n717); *ceh-30(n4111 n3714*lf*)*	0	0	100	60

C. The CEH-30 homologs mBarhl1 and mBarhl2 can rescue *ceh-30(n4289Δ)* for CEM survival.

ceh-30(n4289Δ) ± transgene:	CEM survival in males (%) None	D OR V	D AND V	n=
No transgene	93	7	0	42
ceh-30 genomic locus	4	19	77	26
No cDNA insert	86	14	0	43
ceh-30 cDNA	0	11	89	36
mBarhl1 cDNA	13	51	36	53
mBarhl2 cDNA	31	40	29	48

A. All animals were homozygous for *nIs133*. Otherwise, the genotypes of the animals analyzed were as listed, except for the heterozygotes, which were heterozygous for *unc-2(e55)* and *lon-2(e678)*.

B. All animals were homozygous for *nIs133*, and all animals not homozygous for *tra-1(e1099)* were homozygous for *him-5(e1467)* or, in the case of strains containing *egl-1(n1084 n3082)*, for *him-8(e1489)*. The genotypes of the animals analyzed were otherwise as listed. *tra-1(e1099)* homozygous animals were the self-progeny of *tra-1(e1099)/qC1* heterozygotes. An expanded version of this table, including *ced-4(n1162)* and *ceh-30(n4289Δ)*, is shown in Supplementary Material (Table S4).

C. All animals were homozygous for *nIs133*, *him-5(e1467)*, and *unc-76(e911)*. Transgenic animals rescued for *unc-76* were scored for CEM survival. Constructs are described in the Supplemental Data. "*ceh-30* genomic locus" is pBSK-*ceh-30*.

Table 3. The cell-death-protective function of *ceh-30* is specific to the CEM neurons.

A. *ceh-30* mutations do not modify programmed cell death in the anterior pharynx.

	Extra cells in the anterior pharynx		
Genotype	wild-type	*ced-3(n2427)*	*ced-4(n3158)*
wild-type	0 ± 0	1.2 ± 0.2	4.2 ± 0.2
*ceh-30(n3714*gf*)*	0 ± 0	1.3 ± 0.2	4.3 ± 0.3
*ceh-30(n4111 n3714*lf*)*	0 ± 0	1.1 ± 0.2	4.1 ± 0.2
ceh-30(n4289Δ)	0 ± 0	1.2 ± 0.2	4.0 ± 0.4

B. *ceh-30* mutations do not modify programmed cell death in the Pn.aap lineage.

	Extra *lin-11::gfp*-expressing cells in the ventral nerve cord		
Genotype	wild-type	*ced-3(n2427)*	*ced-4(n3158)*
wild-type	0 ± 0	2.4 ± 1.1	4.5 ± 0.6
*ceh-30(n3714*gf*)*	0 ± 0	2.5 ± 1.1	4.7 ± 0.6
ceh-30(n4289Δ)	0 ± 0	2.7 ± 0.9	4.6 ± 0.6

C. Persistent cell corpses in a *ced-1* background and cell number in the ventral nerve cord are inconsistent with nonspecific effects of *ceh-30* on cell death.

	Cell corpses in L1 heads	Neurons in the ventral nerve cord	
Genotype	in a *ced-1(e1735)* background	hermaphrodite	male
wild-type	26.1 ± 1.7	56.2 ± 1.1	56.4 ± 1.0
*ceh-30(n3714*gf*)*	24.7 ± 2.7	55.7 ± 0.8	56.4 ± 1.3
ceh-30(n4289Δ)	26.0 ± 2.0	55.9 ± 0.9	57.4 ± 1.7

A. The number of cells in the anterior pharynx was determined as described in Materials and Methods. 20 animals of each genotype were counted. Error is standard deviation. Genotypes were as listed.

B. The number of Pn.aap cells was determined using a modified *nIs106 lin-11::gfp* reporter for the VC neuron cell fate as described in Materials and Methods. 50 animals of each genotype were counted. Error is standard deviation. All animals were homozygous for *nIs106*. Genotypes were otherwise as listed.

C. The numbers of persistent cell corpses in the heads of L1 larvae and of neuronal nuclei in the ventral nerve cords of males and hermaphrodites were determined as described in Materials and Methods. 10 animals of each genotype were counted. Error

is standard deviation. Genotypes are as listed, except that ventral nerve cord neuronal nuclei were counted in animals homozygous for *him-5(e1467)*.

Table 4. *ceh-30* and sexual identity regulate CEM survival downstream of or in parallel to *egl-1* and *ced-9*.

Genotype in the presence of *nIs133*; *ced-9(n2812)*; *ced-3(n2427)*	Sex	CEM survival (%) None	D OR V	D AND V	n=
wild-type	Herm.	80	20	0	89
ceh-30(n3714gf)	Herm.	0	63	37	63
ceh-30(n4289Δ)	Herm.	84	16	0	74
egl-1(n1084 n3082)	Herm.	83	17	0	103
egl-1(n1084 n3082); *ceh-30(n3714gf)*	Herm.	0	73	27	77
egl-1(n1084 n3082); *ceh-30(n4289Δ)*	Herm.	85	15	0	100
wild-type	Male	0	23	77	71
ceh-30(n3714gf)	Male	0	10	90	70
ceh-30(n4289Δ)	Male	22	75	3	63
egl-1(n1084 n3082)	Male	1	14	85	101
egl-1(n1084 n3082); *ceh-30(n3714gf)*	Male	0	7	93	71
egl-1(n1084 n3082); *ceh-30(n4289Δ)*	Male	28	71	1	92

All animals except those containing *egl-1(n1084 n3082)* were homozygous for *him-5(e1467)*. Animals containing *egl-1(n1084 n3082)* were homozygous for *him-8(e1489)*. Genotypes were otherwise as listed. Note that the apparent lessening of the *ceh-30(n4289Δ)* phenotype in these animals is a result of the presence of the defect in cell killing caused by the weak mutation *ced-3(n2427)*. Herm., hermaphrodite.

Table S1. The *ceh-30* alleles *n3713* and *n3714* act by gain-of-function to cause CEM survival.

Genotype	*ceh-30* locus	CEM survival in hermaphrodites (%) None	D OR V	D AND V	n=
wild-type	+ / +	100	0	0	60
yDp14	+ / + / + / +	100	0	0	60
mnDp57	+ / + / + / +	98	2	0	60
ceh-30(n3713)/+	gf / +	27	70	3	60
ceh-30(n3714)/+	gf / +	28	68	3	60
yDp14/+; ceh-30(n3713)/+	gf / + / +	30	63	7	60
yDp14/+; ceh-30(n3714)/+	gf / + / +	30	65	5	60
mnDp57/+; ceh-30(n3713)/+	gf / + / +	23	73	4	91
mnDp57/+; ceh-30(n3714)/+	gf / + / +	23	70	7	60
ceh-30(n3713)	gf / gf	0	48	52	100
ceh-30(n3714)	gf / gf	0	48	52	100
yDp14/+; ceh-30(n3713)	gf / gf / +	2	57	42	60
yDp14/+; ceh-30(n3714)	gf / gf / +	3	53	44	68
mnDp57/+; ceh-30(n3713)	gf / gf / +	3	50	46	68
mnDp57/+; ceh-30(n3714)	gf / gf / +	0	40	60	60
yDp14; ceh-30(n3713)	gf / gf / + / +	2	55	43	60
yDp14; ceh-30(n3714)	gf / gf / + / +	2	57	42	60
mnDp57; ceh-30(n3713)	gf / gf / + / +	0	53	47	60
mnDp57; ceh-30(n3714)	gf / gf / + / +	0	59	41	61

In this and other tables, CEM survival was scored using a *pkd-2::gfp* reporter as described in Materials and Methods. When CEM survival was scored using the dissecting microscope, the left and right ventral CEMs could not readily be distinguished from each other and the left and right dorsal CEMs could not readily be distinguished from each other; CEM survival was therefore assessed for ventral CEMs and for dorsal CEMs, and the resulting numbers were found to be reproducible and sensitive to changes in the degree of CEM death or survival defect. In this and in other tables, D OR V denotes animals in which dorsal or ventral CEMs, but not both, were observed; D AND V denotes animals in which both dorsal and ventral CEMs were observed. This supplementary table is an expanded version of Table 1B and contains the data

presented in that table. All animals were homozygous for *nIs128*; otherwise, genotypes were as listed except that when either duplication was present the strain was also homozygous for *unc-2(e55)* and *lon-2(e678)*, and the *ceh-30(n3713)/+* and *ceh-30(n3714)/+* strains were heterozygous for *unc-2(e55)* and *lon-2(e678)*. *ceh-30* locus, number of wild-type (+) and mutant (gf) copies of the locus in each strain.

Table S2. Gain of *ceh-30* function promotes CEM survival downstream of or parallel to the *fem* genes.

Genotype	CEM survival in hermaphrodites (%) None	D OR V	D AND V	n=
wild-type	100	0	0	60
ceh-30(n3713gf)	2	38	60	60
ceh-30(n3714gf)	0	45	55	60
fem-1(e1965)	98	2	0	60
fem-1(e1965); ceh-30(n3713gf)	5	58	37	60
fem-1(e1965); ceh-30(n3714gf)	5	55	40	60
fem-2(e2105)	99	1	0	139
fem-2(e2105); ceh-30(n3713gf)	3	78	18	125
fem-2(e2105); ceh-30(n3714gf)	3	84	14	110
fem-3(e1996)	100	0	0	60
fem-3(e1996); ceh-30(n3713gf)	12	48	40	60
fem-3(e1996); ceh-30(n3714gf)	12	43	45	60

This supplementary table is an expanded version of Table 1C and contains the data presented in that table. All animals were homozygous for *nIs133*. Otherwise, the genotypes of the animals analyzed were as listed. The *fem-1(e1965)* and *fem-3(e1996)* homozygotes scored were the progeny of crosses between *fem/nT1* [*qIs51*] males and *fem* homozygous females; thus, half were XX and half X0 females. *fem-2(e2105)* homozygotes scored were the progeny of maternally-rescued *fem-2(e2105)* homozygotes.

Table S3. *ceh-30(n4111 n3714)* fails to complement *ceh-30(n4289Δ)* for CEM death in males.

Genotype in a *tra-1(e1099)* background	CEM survival in males (%) None	D OR V	D AND V	n=
wild-type	0	0	100	46
ceh-30(n4111 n3714)/+	0	0	100	28
ceh-30(n4111 n3714)	70	30	0	50
ceh-30(n4289Δ)/+	0	0	100	40
ceh-30(n4289Δ)	88	12	0	78
ceh-30(n4289Δ)/ceh-30(n4111 n3714)	84	16	0	50

All animals were homozygous for *nIs133* and *tra-1(e1099)* and were the progeny of *tra-1(e1099)/qC1* heterozygotes. The genotypes were otherwise as follows, top to bottom: +, *+/unc-2(e55) ceh-30(n4111 n3714) lon-2(e678)*, *unc-2(e55) ceh-30(n4111 n3714) lon-2(e678)*, *ceh-30(n4289)/dpy-6(e14)*, *ceh-30(n4289)*, *ceh-30(n4289)/unc-2(e55) ceh-30(n4111 n3714) lon-2(e678)*.

Table S4. Loss-of-function mutations in *ceh-30* cause CEM death in males

Genotype	CEM survival in males (%)			
	None	D OR V	D AND V	n=
wild-type	0	0	100	60
*ceh-30(n3714*gf*)*	0	0	100	61
*ceh-30(n4111 n3714*lf*)*	44	33	23	66
ceh-30(n4289Δ)	83	14	3	71
tra-1(e1099)	0	0	100	46
tra-1(e1099); *ceh-30(n4111 n3714*lf*)*	51	47	2	45
tra-1(e1099); *ceh-30(n4289Δ)*	88	12	0	43
egl-1(n1084 n3082)	0	0	100	62
egl-1(n1084 n3082); *ceh-30(n4111 n3714*lf*)*	0	0	100	65
egl-1(n1084 n3082); *ceh-30(n4289Δ)*	0	0	100	63
ced-4(n1162)	0	0	100	60
ced-4(n1162); *ceh-30(n4111 n3714*lf*)*	0	0	100	60
ced-4(n1162); *ceh-30(n4289Δ)*	0	0	100	60
ced-3(n717)	0	0	100	60
ced-3(n717); *ceh-30(n4111 n3714*lf*)*	0	0	100	60
ced-3(n717); *ceh-30(n4289Δ)*	0	0	100	60

This supplementary table is an expanded version of Table 2B and contains the data presented in that table. All animals were homozygous for *nIs133*, and all animals not homozygous for *tra-1(e1099)* were homozygous for *him-5(e1467)* or in the case of strains containing *egl-1(n1084 n3082)* for *him-8(e1489)*; the genotypes of the animals analyzed were otherwise as listed. *tra-1(e1099)* homozygous animals were the self-progeny of *tra-1(e1099)/qC1* heterozygotes.

Table S5. The mutation *n3714* causes gain-of-function specifically in *ceh-30*: a *cis/trans* test

Genotype	CEM survival in hermaphrodites (%)			
	None	D OR V	D AND V	n=
wild-type	99	1	0	104
*ceh-30(n3714*gf*)/+*	24	64	12	100
ceh-30(n4111 n3714)/+	96	4	0	115
*ceh-30(n3714*gf*)/ceh-30(n4289Δ)*	24	70	8	102

All animals were homozygous for *nIs133* and heterozygous for *unc-2(e55)* and *lon-2(e678)*. Genotypes were otherwise as indicated.

Table S6. The conserved 22 amino-acid BARC (Bar homeodomain C-terminal) motif is found in only Bar homeodomain proteins

Species	Animal	Protein	Sequence	Accession #
H. sapiens	Human	BARHL1	GLELLAEAGNYSAL-QRMF--PSPY	CAB92439
H. sapiens	Human	BARHL2	GLELLAEAGNYSAL-QRMF--PSPY	Q9NY43
M. musculus	Mouse	Barhl1	GLELLAEAGNYSAL-QRMF--PSPY	EDL08401
M. musculus	Mouse	Barhl2	GLELLAEAGNYSAL-QRMF--PSPY	AAH55789
R. norvegicus	Rat	Barhl1	GLELLAEAGNYSAL-QRMF--PSPY	P63156
R. norvegicus	Rat	Barhl2	GLELLAEAGNYSAL-QRMF--PSPY	O88181
X. laevis	Frog	XBH1	GLELLAEAGNYSAL-QRMF--PSPY	NP_001082021
X. laevis	Frog	XBH2	GLELLAEAGNYSAL-QRMF--PSPY	AAG14451
D. rerio	Zebrafish	Barhl1	GLELLAEAGNYSAL-QRMF--PSPY	XP_682832
D. rerio	Zebrafish	Barhl2	GLELLAEAGNYSAL-QRMF--PSPY	AAH97030
D. rerio	Zebrafish		GLELLAEAGNYSAL-QRMF--PSPY	AAU00059
O. anatinus	Platypus		GLELLAEAGNYSAP-QRMF--PSPY	XP_001507472
S. purpuratus	Sea urchin		GLELLAEAGNYSASMQRLF--APPY	XP_785514
C. intestinalis	Sea squirt		GLELLAETGNYAAL-EQVL--PQTF	BAE06324
D. melanogaster	Fly	BarH1	GLELLAEAGNFAAF-QRLYG-GSPY	AAA28382
D. melanogaster	Fly	BarH2	GLELLAEAGNYAAF-QRLYGGATPY	NP_523386
D. ananassae	Fly	BarH1	GLELLAEAGNFAAF-QRLYG-GSPY	AAA28381
A. aegypti	Mosquito		GLELLAEAGNYAAF-QRLYG-GPPY	EAT39758
C. elegans	Roundworm	CEH-30	GMDLLSEPGNLSAV-QNLIR-SSPY	NP_508524
C. elegans	Roundworm	CEH-31	GMDLLHDAGNMAAV-QQLLR-TNPY	NP_508525
C. briggsae	Roundworm	CBG14125	GMDLLSEPGNLSAV-QNLIR-SSPY	CAE68370
C. briggsae	Roundworm	CBG14126	GMDLLHDAGNMAAV-QQLLR-TNPY	CAE68371
	Consensus:		$G^{LD}_{ME}LLx^{DA}_{EP}GNx^{A}_{S}Ax\text{-}QQ^{N}_{R}{}^{L}_{M}xx\text{-}xxP^{Y}_{F}$	

When a BLASTP search was performed using as its query sequence the Barhl1 peptide GLELLAEAGNYSALQRMFPSPY, the only proteins identified with e-values less than 1 or with homology across the entire peptide contained Bar-subclass homeodomains immediately N-terminal to the sequence homologous to this Barhl1 BARC motif. The BARC motif is not found in the BarX family of transcription factors, which also contain Bar-subclass homeodomains but have a different conserved motif C-terminal to their homeodomains (Jones, F.S., C. Kioussi, D.W. Copertino, P. Kallunki, B.D. Holst, and G.M. Edelman. 1997. *Barx2*, a new homeobox gene of the Bar class, is expressed in neural and craniofacial structures during development. *Proc Natl Acad Sci U S A* **94**: 2632-7); this BarX-specific motif is in turn not found in proteins containing the BARC

motif. 22 distinct Bar homeodomain proteins identified in our BLASTP search are listed and are identified by accession numbers. An alignment of their conserved BARC motifs is shown. A consensus sequence is shown immediately beneath the aligned peptide sequences; in this consensus sequence, the most variable residues are marked as 'x.' All vertebrate proteins identified in these searches, with the exception of one example found in the platypus *O. anatinus*, contained this peptide completely unchanged. To limit redundancy, many identified vertebrate proteins containing a BARC motif are not included in this figure; these include proteins found in the chimpanzee, rhesus monkey, dog, horse, cattle, opossum, chicken, medakafish, and pufferfish.

Table S7. Rescue of *ceh-30(n4289Δ)* CEM death by the *ceh-30* genomic locus and by *ceh-30::gfp*

	CEM survival in males (%)			
ceh-30(n4289Δ) with the transgene:	None	D OR V	D AND V	n=
No transgene	82	15	3	33
ceh-30 genomic locus	4	19	77	26
ceh-30 genomic locus with stop codons	65	22	13	23
ceh-30::gfp	0	23	77	22

All animals were homozygous for *nls133*, *him-5(e1467)*, *unc-76(e911)*, and *ceh-30(n4289Δ)*. Transgenic animals rescued for *unc-76* were scored for CEM survival. Constructs are described in the Supplemental Data; "*ceh-30* genomic locus," pBSK-*ceh-30*. "*ceh-30* genomic locus with stop codons," pBSK-*ceh-30*-STOP.

Table S8. A gain-of-function allele of *ced-9* is a poor protector of CEM neurons

Genotype	Sex	CEM survival (%) None	D OR V	D AND V	n=
wild-type	Herm.	100	0	0	60
ceh-30(n4289Δ)	Herm.	100	0	0	60
ced-9(n1950gf)	Herm.	8	75	17	160
ced-9(n1950gf); *ceh-30(n4289Δ)*	Herm.	9	83	8	90
wild-type	Male	0	0	100	60
ceh-30(n4289Δ)	Male	82	16	1	597
ced-9(n1950gf)	Male	0	0	100	355
ced-9(n1950gf); *ceh-30(n4289Δ)*	Male	0	10	90	280

All animals were homozygous for *nIs133* and *him-5(e1467)*. Otherwise, the genotypes of the animals analyzed were as listed.

Table S9. *ceh-30* does not require the *C. elegans* Inhibitor of Apoptosis (IAP) homologs to protect the CEM neurons

Genotype	CEM survival in hermaphrodites (%)			
	None	D OR V	D AND V	n=
ceh-30(n3714gf)	2	63	35	60
bir-2(ok104Δ); ceh-30(n3714gf)	5	66	30	61
bir-1(n3329Δ) bir-2(ok104Δ); ceh-30(n3714gf)	3	65	32	60

All animals were homozygous for *nIs133*. *bir-1(n3329Δ)* homozygous animals are sterile, and the animals examined were therefore the progeny of heterozygous mothers. Genotypes were otherwise as indicated.

Figure legends

Figure 1

pkd-2::gfp is expressed in the CEM neurons and is a marker of CEM survival. Merged fluorescence and visible light images. (A) Wild-type hermaphrodite. (B) Wild-type male. (C) *tra-2(n1106)* partially masculinized hermaphrodite (D) *ced-3(n717)* cell-death-defective hermaphrodite. (E) *ceh-30(n3714*gf*)* hermaphrodite. (F) *ceh-30(n4289Δ)* male. All strains are homozygous for the *pkd-2::gfp* reporter *nIs133* and *him-5(e1467)*. Genotypes are otherwise as indicated. Anterior is to the left, and ventral is down.

Figure 2

The *ceh-30* locus. (A) High-resolution genetic mapping of *ceh-30* mutations. Scale indicates location on LGX. Arrowheads indicate polymorphisms used to map *ceh-30(n3714*gf*)* and *ceh-30(n4111 n3714*lf*)*. Coding regions for *ceh-30* and nearby genes are shown according to Wormbase (http://WS160.Wormbase.org). The sequenced cosmid M02F4 is similar to the cosmid C13G6. The *ceh-30* genomic rescuing construct is shown as a horizontal bar labeled "BSK-*ceh-30*." The intervals containing *n3714*gf and *n4111*lf are indicated with dotted lines (see Materials and Methods). (B) Genomic organization of the *ceh-30* locus. Locations and natures of *ceh-30* mutations are indicated. The portion of the *ceh-30* locus encoding the homeodomain is indicated by the split dotted box. (C) Alignment of the indicated sections of the predicted CEH-30 protein with its *Drosophila* homologs BarH1 (accession number AAA28382) and BarH2 (accession number M82884) and mouse

homologs mBarhl1 (accession number AAH55731) and mBarhl2 (accession numer AAH55789). On the line labeled "Conserved," Residues identical among all five proteins are named and residues similar among all five proteins indicated with a plus symbol. The PFAM consensus homeobox domain (accession number PH00046) is shown. A black box surrounds the conserved residues that define the BARC motif we have identified as specific to Bar-subclass homeodomain proteins (see Table S6). (D) The putative TRA-1A binding sites of *ceh-30* and *egl-1* in *C. elegans* and related nematodes are shown (http://genome.wustl.edu), with *ceh-30(*gf*)* mutations *n3713*, *n3714*, and *n3720* and the homologous *egl-1(n2248*gf*)* mutation underlined. The core of the TRA-1 consensus binding site (Zarkower and Hodgkin 1993) is indicated. (E) TRA-1A binds to the wild-type but not to the *n3714*gf mutant predicted TRA-1A binding site in the second intron of *ceh-30*. 1 ng of labeled probe was shifted by *in vitro*-translated TRA-1A (lane 2) but not by *in vitro* translation products made without a *tra-1* template (lane 1). This binding was competed by excess unlabelled wild-type probe (lanes 3-5) but only poorly by excess *n3714*gf mutant probe (lanes 6-8).

Figure 3

(A) A model for the regulation of CEM neuron survival by the sex determination pathway and by *ceh-30*. In the wild-type hermaphrodite, TRA-1 is active and binds an intronic regulatory site of *ceh-30*, preventing *ceh-30* transcription and thereby preventing CEM survival. In the wild-type male, TRA-1 is inactive; *ceh-30* is therefore expressed and protects the CEM neurons from programmed cell death. In a *ceh-30* gain-of-function hermaphrodite, TRA-1 is active but is unable to bind the mutated regulatory site, so

ceh-30 is expressed and protects the CEMs. In a *ceh-30* loss-of-function male, *ceh-30* is expressed but is nonfunctional and unable to protect the CEM neurons from programmed cell death. (B) *ceh-30* acts as a genetic switch for CEM neuron survival: if *ceh-30* is active, CEMs live; if *ceh-30* is inactive, CEMs die. Normally, *ceh-30* is on active males and inactive in hermaphrodites. (C) A representation of the sensitivity to programmed cell death controlled by *ceh-30*. In hermaphrodites the CEM neurons express the killer gene *egl-1*, which promotes their deaths. In males, the CEM neurons have *ceh-30* activity,which desensitizes these cells to programmed cell death by acting downstream of or in parallel to *egl-1* and *ced-9*. Such a CEH-30-protected CEM neuron will live even when EGL-1 is expressed. (D) A model for the genetic pathway for the regulation of CEM neuron death by the determination of sexual identity. See text for details.

Figure S1

A rescuing *ceh-30::gfp* transgene is expressed in ventral CEM neurons in embryos. *ceh-30::gfp* expression in a 1.5-fold stage masculinized embryo is shown. Arrowheads indicate GFP expression in the nuclei of the CEMVR neuron and the CEPVR neuron. Other nuclei also visibly contain fluorescence as a result of the *ceh-30::gfp* transgene. (A) Fluorescence micrograph showing *ceh-30::gfp* expression. (B) Nomarski image showing CEMVR and other nearby neurons. A composite image composed of three focal planes was used to maximize visibility of nuclei anterior and posterior of the CEMVR nucleus. (C) Merged image of panels A and B. Anterior is to the left, dorsal is

up. For details, see the section of the Supplemental Materials and Methods titled "Examining embryonic CEM neurons for *ceh 30::gfp* expression."

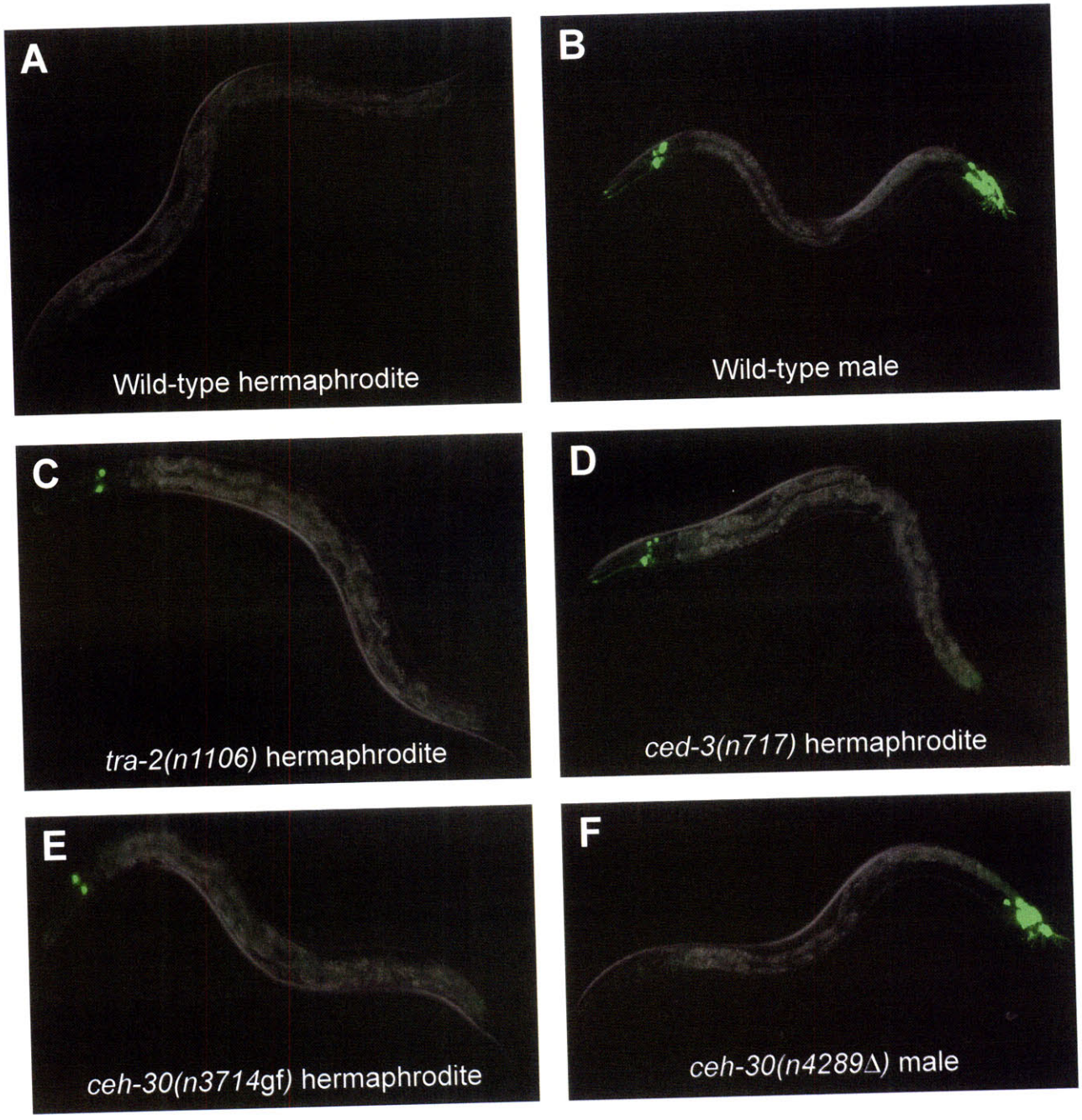
A
Wild-type hermaphrodite
B
Wild-type male
C
tra-2(n1106) hermaphrodite
D
ced-3(n717) hermaphrodite
E
ceh-30(n3714gf) hermaphrodite
F
ceh-30(n4289Δ) male

Figure 1

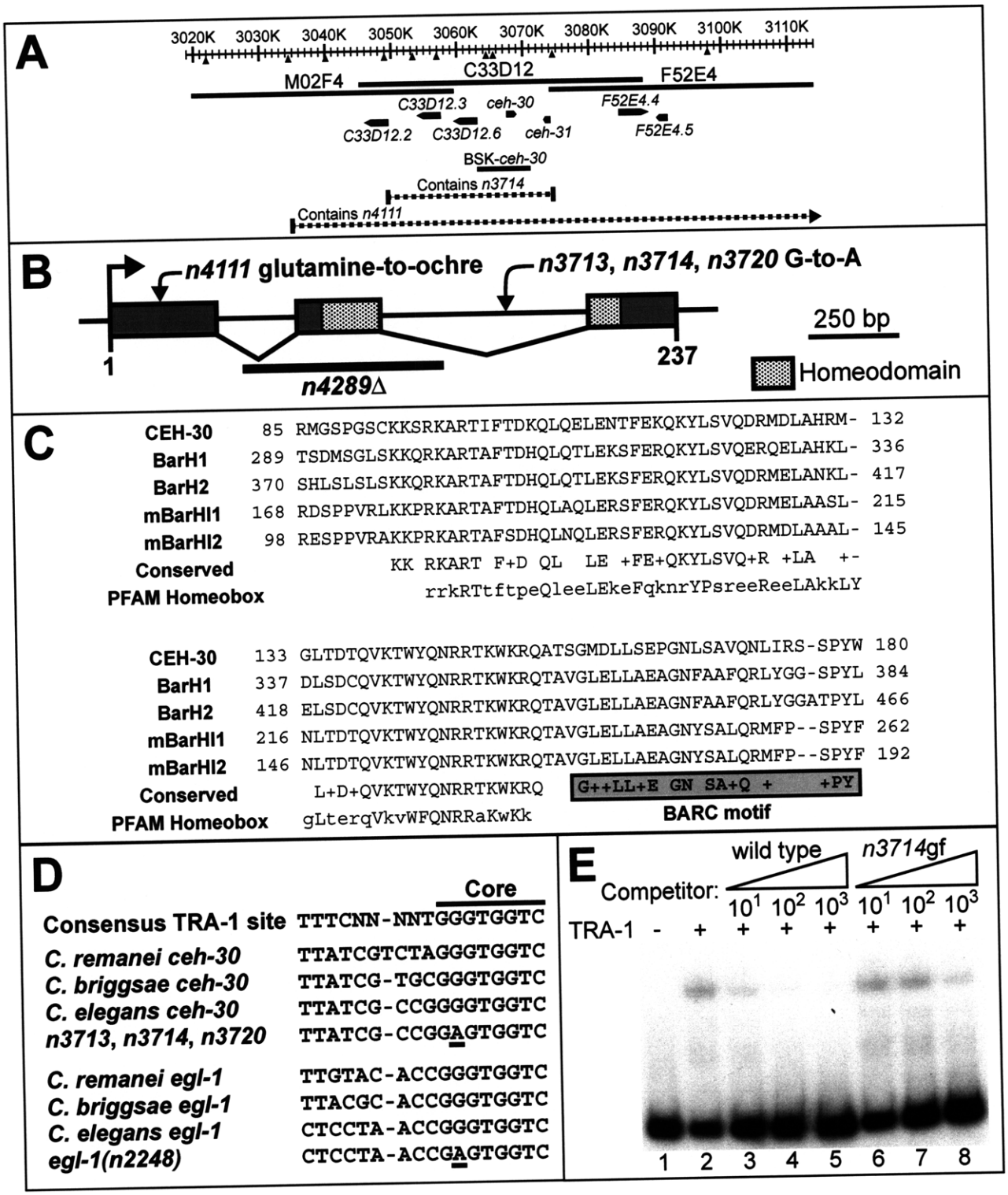
A
3020K 3030K 3040K 3050K 3060K 3070K 3080K 3090K 3100K 3110K
M02F4
C33D12
F52E4
C33D12.3
ceh-30
F52E4.4
C33D12.2
C33D12.6
ceh-31
F52E4.5
BSK-ceh-30
Contains n3714
Contains n4111
B
n4111 glutamine-to-ochre
n3713, n3714, n3720 G-to-A
250 bp
1
237
n4289Δ
Homeodomain
C
CEH-30 85 RMGSPGSCKKSRKARTIFTDKQLQELENTFEKQKYLSVQDRMDLAHRM- 132
BarH1 289 TSDMSGLSKKQRKARTAFTDHQLQTLEKSFERQKYLSVQERQELAHKL- 336
BarH2 370 SHLSLSLSKKQRKARTAFTDHQLQTLEKSFERQKYLSVQDRMELANKL- 417
mBarHl1 168 RDSPPVRLKKPRKARTAFTDHQLAQLERSFERQKYLSVQDRMELAASL- 215
mBarHl2 98 RESPPVRAKKPRKARTAFSDHQLNQLERSFERQKYLSVQDRMDLAAAL- 145
Conserved KK RKART F+D QL LE +FE+QKYLSVQ+R +LA +-
PFAM Homeobox rrkRTtftpeQleeLEkeFqknrYPsreeReeLAkkLY
CEH-30 133 GLTDTQVKTWYQNRRTKWKRQATSGMDLLSEPGNLSAVQNLIRS-SPYW 180
BarH1 337 DLSDCQVKTWYQNRRTKWKRQTAVGLELLAEAGNFAAFQRLYGG-SPYL 384
BarH2 418 ELSDCQVKTWYQNRRTKWKRQTAVGLELLAEAGNFAAFQRLYGGATPYL 466
mBarHl1 216 NLTDTQVKTWYQNRRTKWKRQTAVGLELLAEAGNYSALQRMFP--SPYF 262
mBarHl2 146 NLTDTQVKTWYQNRRTKWKRQTAVGLELLAEAGNYSALQRMFP--SPYF 192
Conserved L+D+QVKTWYQNRRTKWKRQ G++LL+E GN SA+Q + +PY
PFAM Homeobox gLterqVkvWFQNRRaKwKk
BARC motif
D
Core
Consensus TRA-1 site TTTCNN-NNTGGGTGGTC
C. remanei ceh-30 TTATCGTCTAGGGTGGTC
C. briggsae ceh-30 TTATCG-TGCGGGTGGTC
C. elegans ceh-30 TTATCG-CCGGGGTGGTC
n3713, n3714, n3720 TTATCG-CCGGAGTGGTC
C. remanei egl-1 TTGTAC-ACCGGGTGGTC
C. briggsae egl-1 TTACGC-ACCGGGTGGTC
C. elegans egl-1 CTCCTA-ACCGGGTGGTC
egl-1(n2248) CTCCTA-ACCGAGTGGTC
E
wild type
n3714gf
Competitor:
10^1 10^2 10^3 10^1 10^2 10^3
TRA-1 - + + + + + + +
1 2 3 4 5 6 7 8

Figure 2

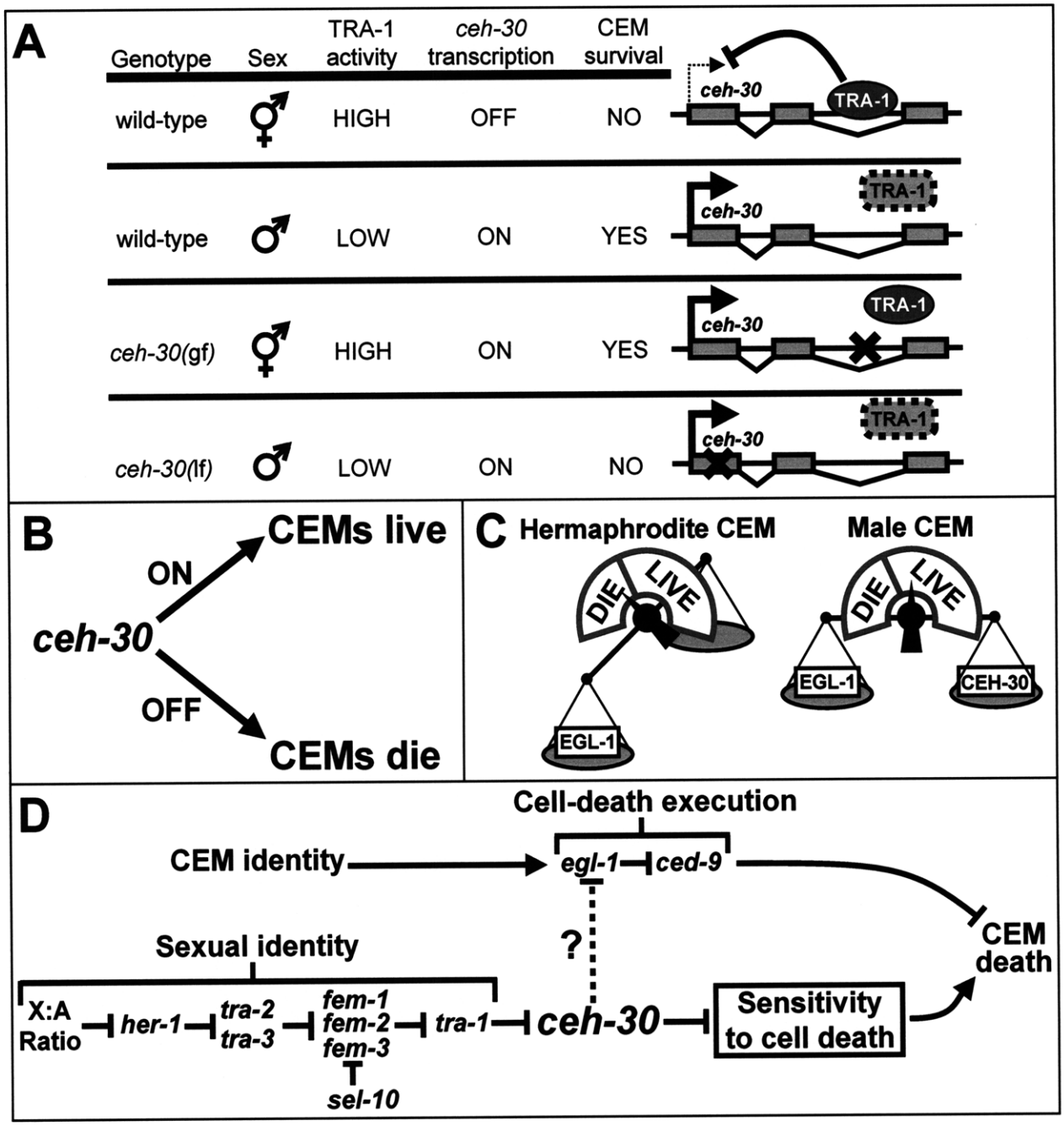
A
Genotype
Sex
TRA-1 activity
ceh-30 transcription
CEM survival
wild-type
HIGH
OFF
NO
ceh-30
TRA-1
wild-type
LOW
ON
YES
ceh-30(gf)
HIGH
ON
YES
ceh-30(lf)
LOW
ON
NO
B
CEMs live
ON
ceh-30
OFF
CEMs die
C
Hermaphrodite CEM
Male CEM
DIE
LIVE
EGL-1
CEH-30
D
Cell-death execution
CEM identity
egl-1
ced-9
CEM death
Sexual identity
?
X:A Ratio
her-1
tra-2
tra-3
fem-1
fem-2
fem-3
sel-10
tra-1
ceh-30
Sensitivity to cell death

Figure 3

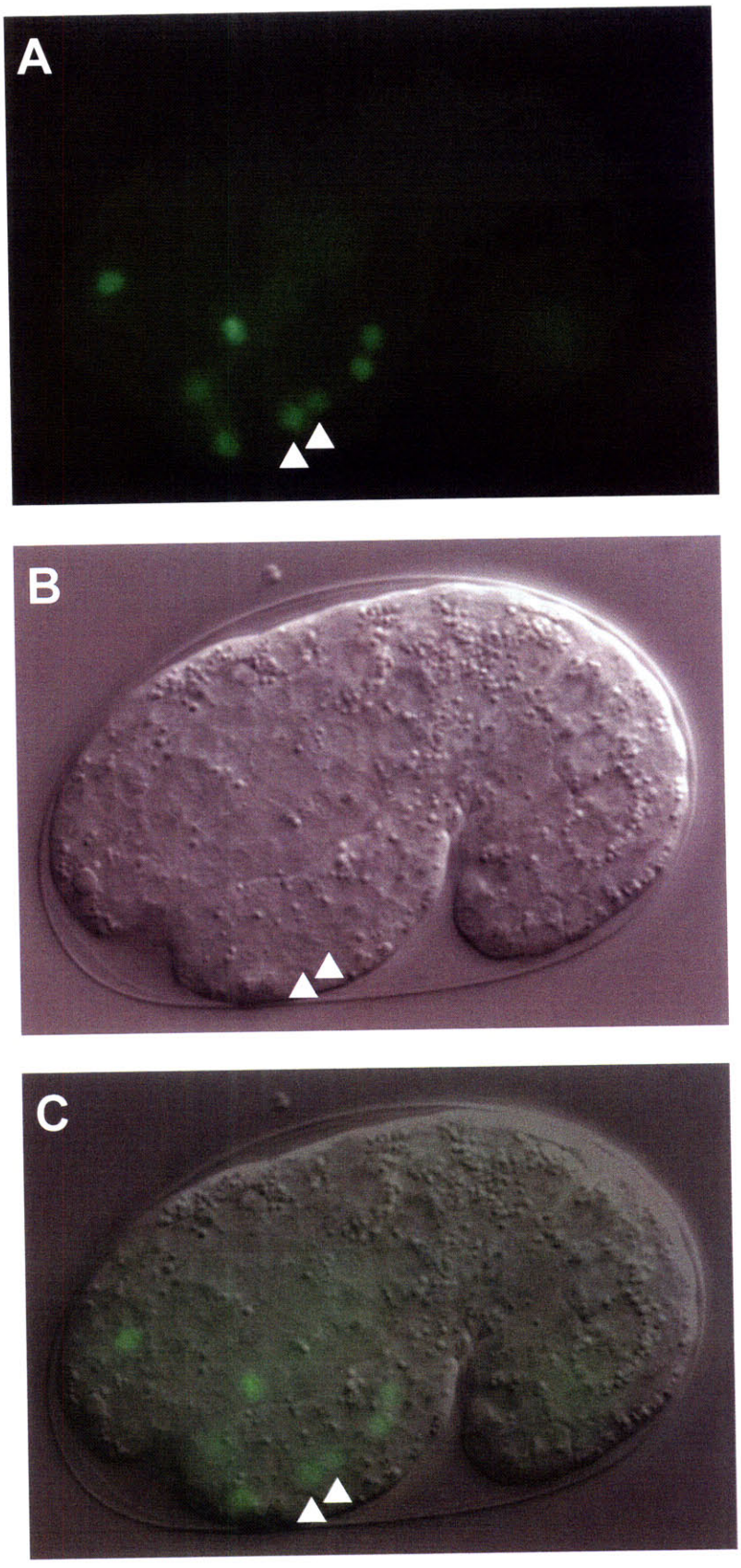

Figure S1

Chapter IV

The green pharynx phenotype of *C. elegans* defines a novel set of genes that function in transcriptional repression

Hillel T. Schwartz, Dawn M. Wendell, and H. Robert Horvitz

As an undergraduate working under my supervision, Dawn Wendell performed the clonal genetic screen for green pharynx mutants, recovering 22 green pharynx mutants and one additional mutant (see Appendix II). Dawn performed complementation tests and mapping experiments concerning many of the 31 green pharynx mutants identified in clonal screens for the green pharynx phenotype. I performed all of the other work presented in this chapter.

Abstract

The *C. elegans* synthetic multivulva (synMuv) genes are grouped in two classes, A and B, that redundantly inhibit vulval induction. Class B synMuv genes encode homologs of mammalian genes involved in chromatin modification and transcriptional regulation. We report that loss of function of any of five synMuv genes - the class A synMuv gene *lin-8* and the class B synMuv genes *gei-4*, *hpl-2 HP1*, *lin-13*, and *lin-61 L3MBT* – can cause a new phenotype of transgene misexpression, resulting in GFP fluorescence in the pharynx, the green pharynx phenotype. This phenotype reflects the loss of a transcriptional repression activity that prevents inappropriate transcriptional activation. The identification of the class A synMuv gene *lin-8* with four class B synMuv genes suggests that these genes can act in a combination that trangresses the previously described synMuv gene classes and that the class A synMuv gene *lin-8* acts in transcriptional repression. From genetic screens, we identified genes that encode the MSP domain protein PAG-6 and the LIN-8 homolog LNES-1, a weak synMuv suppressor, as also mutating to cause the green pharynx phenotype. We propose that the seven green pharynx proteins form a complex that prevents activation driven by nearby sequences in order to ensure proper transcriptional regulation of endogenous genes.

Introduction

The tissue-specific and temporal regulation of transcription is crucial in development and in the prevention of disease: genes must be expressed in the proper tissues, at the proper levels, and at the proper times. Mechanisms must exist that cause genes to be transcribed appropriately. One way that proper transcriptional regulation is achieved is by the establishment and maintenance of repressive and open chromatin structures (WALLACE and FELSENFELD 2007; TAKIZAWA and MESHORER 2008). Chromatin function is critical to cell identity (FISHER 2002), and defects in chromatin are associated with disease (FEINBERG *et al.* 2006; KRIVTSOV and ARMSTRONG 2007; ESTELLER 2008).

Many of the synthetic multivulva (synMuv) genes of *C. elegans* encode regulators of chromatin structure and transcription (reviewed by ANDERSEN and HORVITZ 2007; FAY and YOCHEM 2007). Following the finding that the multivulval (Muv) phenotype of a mutant strain resulted from loss of function of two genes, *lin-8* and *lin-9* (*lin*, abnormal cell lineage) (HORVITZ and SULSTON 1980), two classes of synMuv genes, class A and class B, were identified as being redundantly required to prevent ectopic vulval development (FERGUSON and HORVITZ 1985). Animals lacking the function of a class A gene and a class B gene, but not animals lacking the function of one or more genes of the same class, display a strong vulval phenotype (FERGUSON and HORVITZ 1989; ANDERSEN *et al.* 2008). Genetic screens, RNAi screens and testing of candidate mutants have identified four class A synMuv genes and at least 34 class B synMuv genes (FERGUSON and HORVITZ 1985; LU and HORVITZ 1998; HSIEH *et al.* 1999; VON ZELEWSKY *et al.* 2000; CEOL and HORVITZ 2001; COUTEAU *et al.* 2002; UNHAVAITHAYA *et al.* 2002; THOMAS *et al.* 2003; CEOL and HORVITZ 2004; POULIN *et al.* 2005; CEOL *et al.*

2006; GROTE and CONRADT 2006; ANDERSEN and HORVITZ 2007) (E. Andersen and H.R.H., unpublished results). The class B synMuv genes include homologs of known regulators of chromatin structure and of transcription, including the Rb homolog *lin-35* (LU and HORVITZ 1998), the heterochromatin protein 1 (HP1) homolog *hpl-2* (COUTEAU *et al.* 2002), and members of a DRM and a NuRD-like complex (VON ZELEWSKY *et al.* 2000; UNHAVAITHAYA *et al.* 2002; HARRISON *et al.* 2006). The synMuv genes have been suggested to prevent ectopic vulval induction by transcriptional repression of the EGF-like ligand *lin-3* (CUI *et al.* 2006a). LIN-3 is an inductive signal required for vulval development (HILL and STERNBERG 1992). Further investigation of the synMuv phenotype has led to the identification of synMuv suppressors, genes that provide functions opposed to those of the synMuv genes. Not surprisingly, the synMuv suppressor genes also encode modifiers of chromatin structure and of transcription, including proteins homologous to members of the COMPASS and NURF complexes (ANDERSEN *et al.* 2006; CUI *et al.* 2006b; ANDERSEN and HORVITZ 2007).

In addition to causing a multivulva phenotype when combined with class A synMuv mutations, many class B synMuv mutations cause other defects in the absence of a class A synMuv mutation. Many of the phenotypes associated with subsets of the class B synMuv genes are likely to reflect defects in transcriptional regulation. Some class B synMuv mutants, including *lin-35 Rb*, show the Tam (tandem array modification) phenotype of reduced expression from repetitive transgenes (HSIEH *et al.* 1999; TSENG *et al.* 2007). SynMuv single mutants have also been found to be associated with derepression of germline-specific gene expression, specifically *pgl-1* in the soma (UNHAVAITHAYA *et al.* 2002; WANG *et al.* 2005; LEHNER *et al.* 2006). Because repetitive

transgenes are transcriptionally repressed in the *C. elegans* germline (KELLY *et al.* 1997), it has been proposed that the Tam and *pgl-1* derepression phenotypes reflect a common mechanism of gene repression (WANG *et al.* 2005). A group of genes that includes both class B synMuv and non-synMuv genes has been shown to cause derepression of a *lag-2::gfp* reporter (DUFOURCQ *et al.* 2002; POULIN *et al.* 2005).

We report the identification of a novel set of genes that function to prevent a new phenotype of transgene derepression, the green pharynx phenotype. We propose that transcriptional repression complexes are recruited to transgenes and act to prevent activation driven by nearby cryptic or weak enhancer elements, and that for selected transgenes, a single mechanism, provided by the green pharynx genes, fulfills this function. From testing candidate regulators and through large-scale genetic screens, we identify seven genes that can mutate to cause the green pharynx phenotype. These genes are the class A synMuv gene *lin-8*, the class B synMuv genes *gei-4*, *hpl-2 HP1*, *lin-13*, and *lin-61 L3MBT* and the previously uncharacterized genes *lnes-1* and *pag-6*. We propose that these seven genes function together to ensure proper regulation of gene expression by preventing the inappropriate activation of transcription.

Results

The green pharynx phenotype is likely a defect of transcriptional derepression

In the course of genetic screens using *pkd-2::gfp* (*gfp*, green fluorescent protein) cell-fate reporters, which normally are strongly expressed only in male-specific neurons (BARR and STERNBERG 1999), intended to identify mutant hermaphrodites with *pkd-2::gfp*-expressing CEM neurons (see Chapter II and Appendix II), we isolated 29

mutations causing expression from integrated *pkd-2* transgenes in the posterior pharynx, a tissue than normally does not express this transgene (see Figure 1A). Because of the inappropriate expression of these *gfp* reporter transgenes causes green fluorescence in the posterior pharynx, we refer to this phenotype as the green pharynx phenotype.

We deduced the first clues to the biological defect underlying the green pharynx phenotype from the transgene requirements of the green pharynx phenotype. We initially observed the green pharynx phenotype in screen isolates after mutagenesis of strains containing three different versions of the *pkd-2::gfp* reporter, each integrated on a different chromosome: *nIs133 I*, *nIs128 II*, and *nIs130 IV*. We observed the green pharynx phenotype in a green pharynx mutant containing an extrachromosomal *pkd-2::gfp* reporter transgene and with *pkd-2::gfp* transgenes containing a *lin-15(+)* or an *unc-119(+)* co-injection marker (see Materials and Methods). The phenotype was thus not dependent on chromosomal integration, let alone on particular sites of chromosomal integration, nor was it dependent on one particular co-injection marker. Using microparticle bombardment (PRAITIS *et al.* 2001), we generated two integrated *pkd-2::gfp* transgenes likely to be of low copy number and found that these transgenes could also lead to the green pharynx phenotype. Finally, of several other reporter transgenes tested (see Materials and Methods), three, the modified *lin-11::gfp* reporter *nIs106* (REDDIEN *et al.* 2001), the *flp-15::gfp* reporter *ynIs45* (KIM and LI 2004), and the *lag-2::gfp* reporter *qIs56* (SIEGFRIED and KIMBLE 2002), also had inappropriate *gfp* expression in the posterior pharynx in green pharynx mutants not seen in a wild-type

genetic background. The phenomenon of the green pharynx phenotype is therefore not unique to strains containing a *pkd-2::gfp* reporter.

Following an insightful suggestion by Susan Mango (personal communication), who had previously observed the presence of cryptic pharyngeal enhancer activity provided by the common plasmid backbone of the vectors developed by Andrew Fire (A. Fire, personal communication) and commonly used in the construction of *gfp* reporter constructs, particularly when little or no promoter sequence had been inserted into the multiple cloning site, we found that green pharynx mutants containing an extrachromosomal *pkd-2::gfp* reporter transgene that lacked the vector backbone (see Materials and Methods) showed expression specific to *pkd-2* but did not show the green pharynx phenotype. These results, which are summarized in Figure 1B, suggested that the ectopic expression seen in the green pharynx phenotype was caused by the cryptic pharyngeal enhancer present in the vector backbone and that in green pharynx mutants carrying the *pkd-2::gfp* reporter there was a defect in a mechanism that would normally prevent expression driven by this cryptic enhancer. The pharyngeal expression from which the green pharynx phenotype acquires its name therefore likely comes from the pharynx-specific nature of the cryptic promoter coupled with a broader defect in transcriptional repression and not from transcriptional derepression specific to the pharynx.

Identification of synMuv mutants causing a green pharynx phenotype

Of the initial 29 green pharynx screen isolates, one, the strain containing the green pharynx mutation *n3605*, showed a multivulva phenotype similar to that seen in

class A synMuv; class B synMuv double mutants. Many synMuv genes were known to encode proteins homologous to regulators of gene expression and chromatin structure (reviewed by ANDERSEN and HORVITZ 2007; FAY and YOCHEM 2007), and it was known that animals lacking the function of any of several class B synMuv genes displayed alterations in transgene expression (HSIEH *et al.* 1999; DUFOURCQ *et al.* 2002; UNHAVAITHAYA *et al.* 2002). We tested every known synMuv gene for which mutant alleles were available for the ability to cause the green pharynx phenotype (see Table 1). We also performed feeding-RNAi treatment targeting the candidate class B synMuv genes *E01A2.4 NKAP* and *W01G7.3 RPB11*; neither treatment caused the green pharynx phenotype (data not shown). We additionally tested alleles of selected genes believed to function together with, in opposition to or in parallel with the synMuv genes (see Table S1). Loss-of-function mutations in of any of four synMuv genes of 36 tested caused the green pharynx phenotype. One of the four genes is the class A synMuv gene *lin-8*, which encodes a novel protein (FERGUSON and HORVITZ 1989; DAVISON *et al.* 2005). The other three are class B synMuv genes: *lin-13*, which encodes a protein with 24 zinc finger motifs (MELENDEZ and GREENWALD 2000); *hpl-2*, which encodes a protein with homology to mammalian heterochromatin protein 1 (COUTEAU *et al.* 2002); and *lin-61*, which encodes an MBT (Malignant Brain Tumor) repeat-containing protein with similarity to the chromatin remodeling factor L3MBTL1 (HARRISON *et al.* 2007). The green pharynx phenotype is the first phenotype reported to be caused by both class A and class B synMuv mutations (see Discussion). The original Muv green pharynx isolate was found to contain two separate synMuv mutations, the *lin-8* allele *n3605* (see Tables 2, 3) and an unidentified class B synMuv mutation on LGIII

(C. Ceol and H.R.H., unpublished observations). No other synMuv, synMuv-related, or chromatin factor mutation tested, nor any of the many dozens of other previously characterized mutations used in the course of building strains containing reporter transgenes, have been found to cause the green pharynx phenotype (Tables 1 and S1 and data not shown).

A clonal screen for mutations causing the green pharynx phenotype

From the initial screens intended to recover hermaphrodites with *pkd-2::gfp*-expressing CEM neurons, we had recovered 29 green pharynx mutants. These 29 mutations included 24 alleles of *lin-8*, one allele of *lin-13*, and four alleles of two previously uncharacterized genes, now named *lnes-1* and *pag-6* (see below). We performed additional, clonal screens in which we looked for expression of the *pkd-2::gfp* reporter in the pharynges of late embryos and young larvae trapped within egg-laying-defective mothers. These mothers also contained the heterozygous and wild-type siblings of the phenotypic animals, permitting the recovery of mutations that cause sterility or lethality (see Materials and Methods). From these screens, we recovered 31 green pharynx mutants. An additional twelve green pharynx mutants were recovered as incidental isolates in screens that made use of *pkd-2::gfp* transgenes but were not intended to identify mutations causing the green pharynx phenotype: four green pharynx isolates from a screen for suppressors of *tra-2(n1106)*-induced CEM neuron survival (H.T.S. and H.R.H., unpublished results); four green pharynx isolates from a screen for suppressors of the Unc phenotype of *cnd-1(n3786)* (H.T.S. and H.R.H., unpublished results); and four green pharynx isolates from screens for

suppressors of *ceh-30(n3714*gf*)*-induced CEM neuron survival (J. Varner, H.T.S., and H.R.H., unpublished results). Two additional green pharynx mutations were discovered in the course of strain constructions as previously unnoticed mutations in strains from the Horvitz laboratory strain collection. In all, we recovered 74 independent isolates (Table 2).

The 74 green pharynx isolates include 57 alleles of known synMuv green pharynx genes: 44 *lin-8* alleles, four *lin-61* alleles, and nine *lin-13* alleles, including five *lin-13* mutations causing recessive sterility. Fourteen mutations defined the new gene *lnes-1* (see below). An additional two mutations, *n4319* and *n3599*, were the first known mutations in the genes *gei-4* and *pag-6*, respectively (see below). One additional mutation, *n3841 I*, caused a weak and impenetrant green pharynx phenotype and has not been assigned to a gene (see Materials and Methods). No alleles of *hpl-2* were recovered.

Molecular identification of synMuv- and green pharynx-specific alleles of *lin-8*

The molecular lesions in nine loss-of-function mutations of *lin-8* have previously been reported (DAVISON *et al.* 2005). We determined the molecular lesion in every known allele of *lin-8* (see Table 3). Twenty-three *lin-8* alleles have been isolated on the basis of their ability to cause a class A synMuv phenotype (A. Saffer, J. Doll, and H.R.H., unpublished results) (FERGUSON and HORVITZ 1989; THOMAS *et al.* 2003). We tested these 23 alleles for their ability to cause the green pharynx phenotype and found that 22 caused the green pharynx phenotype. The one allele from among these 23 that did not cause a green pharynx phenotype is the missense mutation *lin-8(n2376)*, which

causes the amino acid substitution E148K. *lin-8(n2376)* causes a class A synMuv phenotype as strong as those caused by likely null mutations in *lin-8* (DAVISON *et al.* 2005).

We tested the 44 *lin-8* alleles recovered based on their green pharynx phenotypes to determine whether they were synthetically Muv in combination with the class B synMuv mutation *lin-36(n766)* (see Materials and Methods). *lin-36(n766)* was chosen for these tests of class A synMuv activity as it is a class B synMuv mutation that was known not to cause the Tam phenotype of altered transgene expression (HSIEH *et al.* 1999) and because *lin-36(n766)* did not cause synthetic lethality in combination with the green pharynx mutation *pag-6(n3599)* (see below). Of these 44 *lin-8* alleles, 32 caused a strong Muv phenotype in combination with *lin-36(n766)*, ten were never observed to cause a synMuv phenotype and two caused only a weakly penetrant and weakly expressive Muv phenotype in combination with *lin-36(n766)* (see Table 3). DNA sequence determination of the *lin-8* alleles revealed that, of the ten alleles that did not cause an apparent synMuv phenotype and the two alleles that were only weakly synMuv, nine were missense mutations, including two pairs of identical mutations; two affected splice sites; and one was a single base-pair change 12 nucleotides before the start of translation.

Loss of the *lin-8* homolog *lnes-1* causes the green pharynx phenotype and weakly suppresses the synMuv phenotype

Fourteen green pharynx mutations were assigned to a complementation group defined by the allele *n3688*. Mapping placed *n3688* in a 78 kb interval that contains

seven genes, including *lin-8* and the *lin-8* homologous gene *B0454.9*, which we named *lnes-1* (*lnes*, LIN-EIGHT similarity) (see Materials and Methods). *lnes-1* encodes the closest of 16 identified homologs of LIN-8 in *C. elegans* (DAVISON *et al.* 2005). Determination of DNA sequences showed that the gene affected by these green pharynx mutations is *lnes-1*. Eight of the 14 alleles are nonsense mutations, two alter splice acceptor sites, one is a 81 base-pair deletion that removes a splice acceptor site, and two independently isolated mutations cause an identical nucleotide change, resulting in the predicted missense change R119C (see Table 4). The remaining mutation, *n3814*, complemented *lin-8(n3686Δ)* and failed to complement *lnes-1(n3688)*; however, no coding mutation was found in *lnes-1* in *n3814* animals. A transgene containing the single gene *lnes-1* (see Figure 2A and see Materials and Methods) rescued the green pharynx phenotype of *lnes-1(n3917Δ)* mutants. GFP-tagged versions of this transgene (see Materials and Methods) rescued the green pharynx phenotype of *lnes-1(n3917Δ)* mutants and caused the accumulation of green fluorescent LNES-1 fusion protein in the nuclei of most or all cells (see Figure S1).

Like LNES-1, LIN-8 is found in the nuclei of most or all cells (DAVISON *et al.* 2005). Like other members of this family, LNES-1 and LIN-8 share extensive homology in their N- and C-termini, with a more divergent core region (see Figure 2B). No biological function has been associated with this divergent core domain, but biochemical studies indicate that it is capable of interacting with the class B synMuv protein LIN-35 Rb *in vitro* (DAVISON *et al.* 2005). The identified missense mutations in LIN-8 and the single missense mutation identified in LNES-1 are shown in Figure 2B. The single missense mutation identified in *lnes-1*, caused by both *n3604* and *n3689*, results in the

change R119C; the corresponding residue is mutated in the *lin-8(lf)* alleles *n3585* and *n3598*, suggesting that this arginine residue is important for the functions of both *lin-8* and *lnes-1*. This arginine residue is not conserved in other members of the *C. elegans* LIN-8 family (DAVISON *et al.* 2005).

Because *lnes-1* shares a function in the green pharynx phenotype with several synMuv genes, and because the protein LNES-1 is so closely related to the class A synMuv protein LIN-8, we tested whether loss of *lnes-1* function might similarly cause, or at least modify a synMuv phenotype. When the putative null allele *lnes-1(n3917)* or the missense allele *lnes-1(n3604)* were combined in double mutants with the strong class A synMuv mutant *lin-15A(n767)* or the strong class B synMuv mutant *lin-15B(n744)*, no synthetic Muv phenotype was observed (Table 5), even at higher temperatures previously shown to sensitize the synMuv phenotype (FERGUSON and HORVITZ 1989). Under temperature conditions sensitized to cause partially penetrant synMuv phenotypes, the putative null allele *lnes-1(n3917)* caused a small but reproducible reduction in the strength of the synMuv phenotypes of either of two partial loss-of-function *lin-15AB* double mutants, *lin-15AB(n765*ts*)* and *lin-15(n2993 n433)* (Table 5 and data not shown). The synMuv suppression caused by loss of *lnes-1* function was weak compared to the suppression seen for strong synMuv suppressors, such as loss of *isw-1* function (ANDERSEN *et al.* 2006), but was comparable to the effects of other established synMuv suppressors (CUI *et al.* 2006b).

The green pharynx mutation *n4319* is an allele of the class B synMuv gene *gei-4*

We mapped the green pharynx mutation *n4319* to the far left end of LGIII. Further mapping placed *n4319* within the first 527 kb of LGIII, a region that showed very little or no recombination between the wild-type strain N2 and the polymorphic Hawaiian strain CB4856 (see Materials and Methods). *n4319* causes a weakly semidominant green pharynx phenotype. Transformation rescue experiments using cosmids representing ~363 kb of this 527 kb interval showed that a transgene containing the cosmids W07B3 and K10F12, but not transgenes containing any of the other cosmids tested, was capable of rescuing the green pharynx phenotype caused by *n4319* (see Materials and Methods). DNA sequence determination of candidate genes on the two cosmids identified a late nonsense mutation in the gene *gei-4* (*gei*, GEX interacting molecule), causing the predicted change Q505ochre. Transgenes containing the single gene *gei-4* could rescue the green pharynx phenotype caused by *gei-4(n4319)* (see Materials and Methods).

gei-4 is predicted to encode a 545 amino acid protein that contains a coiled-coil domain (FINN *et al.* 2006). GEI-4 has previously been identified as a possible physical interactor with GEX-2 (TSUBOI *et al.* 2002), an evolutionarily conserved protein required for cell morphology and migration in *C. elegans* embryonic development (SOTO *et al.* 2002). GEX-2 is a homolog of the human protein Sra-1, which interacts with an activated form of the GTPase Rac (KOBAYASHI *et al.* 1998). The significance of this reported physical interaction is not clear. Using BLAST searches with GEI-4, we identified proteins in other organisms similarly predicted to contain coiled-coil domains, but we detected no homology with other proteins outside of the predicted coiled-coil domain, and no other conserved domains were identifiable within GEI-4.

gei-4 has previously been identified in a genome-wide RNAi-feeding study as a class B synMuv gene (POULIN *et al.* 2005). Injection of dsRNA targeting *gei-4* for RNAi caused early embryonic lethality, and the rare viable escapers possessed a green pharynx phenotype but did not display a synMuv phenotype (data not shown). To further examine the effects of *gei-4(*RNAi*)*, we performed zygotic RNAi. Briefly, we injected dsRNA into RNAi-defective *rde-1(ne219)* hermaphrodites. The injected animals were then mated with males wild-type for *rde-1*, such that RNAi would become effective only after the onset of zygotic gene expression (HERMAN 2001). As was previously seen for RNAi-feeding targeting *gei-4*, zygotic RNAi targeting *gei-4* caused a strong class B synMuv phenotype (Table 6A).

The green pharynx allele *gei-4(n4319)*, which causes a variably penetrant and semidominant green pharynx phenotype, did not cause a synMuv defect in combination with either the strong class A synMuv mutation *lin-15A(n767)* or the strong class B synMuv mutation *lin-15B(n744)* (Table 6A). *gei-4(n4319)* did increase both the penetrance and the expressivity of the Muv phenotype of the synMuv double mutant *lin-15AB(n2993 n433)* (Table 6B and data not shown). These results suggest that *gei-4* is, as previously reported, a class B synMuv gene, and that the semidomonantly acting mutation *n4319* either causes a defect in GEI-4 function largely specific to the green pharynx phenotype or, more likely, causes a weak dominant-negative activity insufficient to cause a synMuv phenotype.

***pag-6(n3599)* causes altered function of *Y015C5B.19*, which encodes a nuclear protein with an MSP domain and a C-terminal domain homologous to *C. elegans* proteins**

The green pharynx mutation *n3599* defined the gene *pag-6* (*pag*, pattern of reporter gene expression abnormal). *pag-6(n3599)* animals had a fully penetrant recessive green pharynx phenotype and were severely egg-laying defective (data not shown). We mapped *pag-6(n3599)* to a 103 kb interval at the far right end of LGIV (see Figure 3A and Materials and Methods). This interval is predicted to contain 13 genes that encode proteins and at least 165 noncoding RNAs. A 9.1 kb PCR product containing the single gene *Y105C5B.19*, but not PCR products containing *Y105C5B.20* or *Y105C5B.21*, rescued the green pharynx phenotype of *pag-6(n3599).* DNA sequence determination of *n3599* mutant animals identified a missense mutation causing the predicted amino acid change E425K in the 484 amino acid protein Y105C5B.19, now named PAG-6.

The single green pharynx allele of *pag-6*, *n3599*, recessively caused a green pharynx phenotype. Heterozygotes between *pag-6(n3599)* and the chromosomal deficiency *sDf23* resembled *pag-6(n3599)* homozygotes. The green pharynx phenotype caused by *pag-6(n3599)* could be rescued by a transgene containing a wild-type copy of *pag-6*. All of these observations are consistent with *n3599* causing reduction of gene function. However, when *pag-6* was targeted for RNAi using dsRNAs targeting exon 1 or targeting exons 5 through 7 of *pag-6*, no resulting green pharynx phenotype was observed. On the contrary, RNAi of *pag-6* completely suppressed the green pharynx phenotype of *pag-6(n3599)*, and also suppressed the Egl and scrawny phenotypes

associated with *pag-6(n3599)* (see below). Similarly, the green pharynx, Egl, and scrawny phenotypes associated with *pag-6(n3599)* were all suppressed by a loss-of-function mutation in *pag-6*, *n5161*. We identified *n5161* as a spontaneously arising mutation in the *pag-6(n3599)* background and found *n5161* to be a single-nucleotide deletion causing a predicted frameshift early in the *pag-6* open reading frame, after codon 83 (see Figure 3B and see Materials and Methods). As would be expected based on the green pharynx phenotype seen in *pag-6(n3599)/sDf23* heterozygotes, the *pag-6* loss-of-function allele *pag-6(n3599 n5161lf)* failed to complement *pag-6(n3599)* for the green pharynx phenotype. These results strongly suggested that the *n3599* mutation causes altered gene function that is antagonized by the presence of wild-type *pag-6* function. Reinforcing this hypothesis, a multicopy transgene containing a version of the *pag-6* rescuing fragment modified to include the missense mutation *n3599* could cause the green pharynx phenotype (data not shown).

The predicted protein PAG-6 is 484 amino acids long and contains only one recognizable domain, an N-terminal MSP (major sperm protein) domain (Figure 3B). The C-terminus of PAG-6, which contains the missense mutation *n3599*, is closely related to three other predicted *C. elegans* proteins that are homologous across the length of this C-terminal domain (see Figure 3C) and more distantly related to two other *C. elegans* proteins; of these proteins with C-terminal homology, one, M199.2, is also predicted to contain an MSP domain. RNAi targeting the first exon of *pag-6* and the *pag-6* frameshift mutation *n5161*, which occurs early within the MSP domain, each suppressed the green pharynx phenotype caused by *pag-6(n3599)*, demonstrating that *pag-6* is indeed encoded by a single transcript containing both the N-terminal MSP

domain and the conserved C-terminus mutated by *n3599*. There are no identifiable non-nematode homologs of the PAG-6 C-terminus.

Nematode proteins containing MSP domains have been suggested to act in cytoskeletal analogs of actin filaments (ROBERTS and KING 1991) or as secreted ligands in ephrin signaling (MILLER *et al.* 2001; MILLER *et al.* 2003). The function of MSP domain proteins as secreted ligands in ephrin signaling is evolutionarily conserved from nematodes to mammals (TSUDA *et al.* 2008). The vertebrate proteins that contain MSP domains belong to the VAP (VAMP-Associated Protein) family. In addition to their MSP domains, members of the VAP protein family also contain coiled-coil and transmembrane domains, which are not found in PAG-6. The VAP family is broadly conserved in eukaryotes, from the fission yeast *S. cerevisiae* Scs2p to vertebrate VAP-33, including the predicted *C. elegans* protein VPR-1 (NIKAWA *et al.* 1995; SKEHEL *et al.* 1995; WEIR *et al.* 1998; NISHIMURA *et al.* 1999; PENNETTA *et al.* 2002; TSUDA *et al.* 2008). The VAP proteins have been implicated in a number of functions, including endoplasmic reticulum organization (PERRY and RIDGWAY 2006), vesicular transport (SKEHEL *et al.* 1995; FOSTER *et al.* 2000), and fatty acid metabolism (PERRY and RIDGWAY 2006). Despite these non-nuclear functions of MSP proteins in nematodes and of the VAP family proteins and consistent with the likely role of *pag-6* in regulating transcription, fluorescence from a translational *pag-6::gfp* fusion transgene capable of rescuing the green pharynx phenotype caused by *pag-6(n3599)* was tightly localized within the nucleus, with expression seen in most or all cells (Figure S2 and data not shown).

The green pharynx mutation *pag-6(n3599)* causes a class B synMuv phenotype and is synthetically lethal with loss-of-function mutations in selected synMuv genes

The *pag-6* altered function mutation *n3599* did not cause a synMuv phenotype in combination with any class B synMuv mutant tested (Table 8A and data not shown). A weak synthetic Muv phenotype was observed in double mutants between *pag-6(n3599)* and the class A synMuv mutant *lin-15A(n767)* and in double mutants between *pag-6(n3599)* and the class A synMuv mutant *lin-38(n751)*, mostly at higher temperatures (Table 7A and data not shown). The synthetic Muv phenotypes of *pag-6(n3599)*; *lin-15A(n767)* and in *lin-38(n751)*; *pag-6(n3599)* double mutants were only partially penetrant, and the ectopic vulval protrusions of the Muv animals were small when compared to those seen in most class A synMuv; class B synMuv double mutants (data not shown). The *pag-6* loss-of-function mutant *n3599 n5161* did not cause a synMuv phenotype in combination with the strong class A synMuv mutation *lin-15A(n767)* or the strong class B synMuv mutation *lin-15B(n744)* (Table 7B) and did not modify the synMuv phenotypes even of the highly sensitized synMuv double mutants *lin-15AB(n765*ts*)* or *lin-15AB(n2993 n433)* (Table 7C).

While testing whether *pag-6(n3599)* causes a synMuv phenotype, we found that double mutants between *pag-6(n3599)* and selected class B synMuv mutants displayed a larval arrest phenotype, with rare escapers becoming sterile adults or very occasionally producing one or two progeny that arrested during embryogenesis. This synthetic-lethal phenotype was not seen with the *pag-6* loss-of-function mutant *pag-6(n3599 n5161)*, and the synthetic lethality seen in *lin-35(n745)*; *pag-6(n3599)*

animals was suppressed by RNAi of *pag-6*. The class B synMuv mutants with which *pag-6(n3599)* is synthetically inviable include the *Rb* homolog *lin-35* and the *DP* homolog *dpl-1*. Both of these genes are predicted to function in transcriptional modification regulation and remodeling. A complete list of synMuv and synMuv-related mutations tested for synthetic lethality with *pag-6(n3599)* is shown in Table 8.

Viable or conditionally viable mutants in *fzr-1*, *mcd-1*, *pha-1*, *psa-1*, *spr-1*, *ubc-18*, and *xnp-1* have been described that are synthetically inviable when combined with loss-of-function in *lin-35*, a Slr (*slr*, synthetic lethality with loss of *lin-35 Rb*) phenotype (FAY *et al.* 2002; FAY *et al.* 2003; BENDER *et al.* 2004; CUI *et al.* 2004; FAY *et al.* 2004; CARDOSO *et al.* 2005; CHESNEY *et al.* 2006; BENDER *et al.* 2007; REDDIEN *et al.* 2007). In each case, additional defects have been observed either in the *slr* mutant animals or in the *lin-35*; *slr* double mutant animals. Unlike the result reported for *ubc-18* and *pha-1* mutants (FAY *et al.* 2003), the lethality of *lin-35*; *pag-6(n3599)* double mutants was not associated with a defect in pharyngeal morphogenesis. Additionally, unlike the synthetic lethality of *lin-35*; *ubc-18* or *lin-35*; *pha-1* double mutants (FAY *et al.* 2004), the synthetic lethality of *lin-35*; *pag-6(n3599)* animals was not suppressed by mutations in *sup-36* or *sup-37* (data not shown). Another class of Slr mutants, exemplified by *psa-1* and *xnp-1*, is typified by a polarity defect in the development of the T lineage (BENDER *et al.* 2004; CUI *et al.* 2004), which can readily be assessed by testing for dye-filling defects in the phasmid neurons. As seen for *psa-1* and *xnp-1* mutants, *pag-6(n3599)* animals have a defect in phasmid development: some phasmids failed to fill with dye in *pag-6(n3599)* mutants (10%; n = 266), as compared with none for the wild type (0%; n = 40). This defect was not further enhanced by loss of *lin-35*

function (6% of phasmids of *lin-35(n745)*; *pag-6(n3599)* animals failed to fill; n = 36). This failure of a *lin-35* mutation to enhance the weak phasmid defect caused by *pag-6(n3599)* is similar to what has been reported for the *lin-35* synthetic lethal mutation *xnp-1(fd2)* (BENDER *et al.* 2004), although different from the result reported for the *lin-35* synthetic lethal mutation *psa-1(ku355)*, the phasmid defect of which is enhanced by loss of *lin-35* function (CUI *et al.* 2004). It therefore seems plausible that *pag-6(n3599)* animals have a defect similar to that seen in animals mutant for *psa-1* and particularly similar to that seen in animals mutant for *xnp-1*. *psa-1* and *xnp-1* encode members of a proposed *C. elegans* SWI/SNF transcriptional regulation complex (BENDER *et al.* 2004; CUI *et al.* 2004; CARDOSO *et al.* 2005). By analogy to *psa-1* and *xnp-1*, the defect in *pag-6(n3599)* animals is likely to be one of transcriptional regulation.

Discussion

The green pharynx phenotype likely indicates a defect in transcriptional repression

We propose that using the green pharynx phenotype we have identified animals that lack a mechanism that functions to modify chromatin and prevent inappropriate transcription driven by nearby enhancer sequences. This defect in repression is independent of chromosomal integration and is not limited to a single reporter transgene, as we identified transgenic reporters for four genes that can support the green pharynx phenotype. Elements within the vector backbone of the plasmid containing the *gfp* reporter construct are required for pharyngeal expression, and the vector backbone has been observed to contain sequences capable of driving

pharyngeal expression in a wild-type genetic background (Susan Mango, personal communication). All green pharynx genes for which an expression pattern has been reported are believed to be expressed in most or all cells (MELENDEZ and GREENWALD 2000; COUTEAU *et al.* 2002; DAVISON *et al.* 2005; COUSTHAM *et al.* 2006; HARRISON *et al.* 2007). Given the apparently ubiquitous expression of the green pharynx genes coupled with the pharyngeal enhancer element within the *gfp* transgenes, it seems likely that the green pharynx genes provide a repressive function in all cells, and the distinctive pharyngeal reporter expression that gives the green pharynx phenotype its name is a consequence not of a pharynx-specific defect in transcriptional repression, but of a global defect in repression coupled with elements weakly driving pharyngeal expression. Despite the artifactual nature of the green pharynx phenotype that we use as a readout of gene function, the green pharynx genes we have identified are part of the endogenous biology of *C. elegans*, and we believe that the green pharynx genes function to control the expression of endogenous genes.

Identification of a set of genes that function to prevent inappropriate gene expression

The initial set of 29 green pharynx isolates and the four isolates later recovered in nonclonal screens provided an incomplete and highly skewed set, including only a single allele of *lin-13* and no alleles of *lin-61*, even though animals completely lacking *lin-61* function are viable and have a green pharynx phenotype. Of the 74 total green pharynx isolates, 41 were isolated in clonal screens or as previously undetected mutations in strains from the Horvitz laboratory strain collection, including 31 recovered

in screens designed to target the green pharynx phenotype. These clonal screens generated a set of green pharynx mutants that was far more representative of the genes that function to prevent the green pharynx phenotype than was the set of green pharynx mutants generated from nonclonal screens. Four of the seven green pharynx genes were represented by loss-of-function alleles: the class A synMuv gene *lin-8*, the *lin-8* homolog *lnes-1*, and the class B synMuv genes *lin-13* and *lin-61*. The least represented among these was *lin-61*, with four alleles. As multiple isolates were isolated for each of these genes, including five *lin-13* alleles causing recessive sterility, it seems likely these screens have identified every gene for which a loss-of-function mutation will cause a green pharynx phenotype in the F_2 generation following EMS mutagenesis.

The screens did not identify every gene that can mutate to cause the green pharynx phenotype. In particular, none of the screen isolates were alleles of *hpl-2 HP1*. *hpl-2* loss-of-function homozygotes produced by heterozygous mothers are maternally rescued for the green pharynx phenotype, and therefore could not be identified in most of the screens that were performed. The two remaining green pharynx genes, *gei-4* and *pag-6*, were each represented by a single allele. The green pharynx mutation *pag-6(n3599)* causes altered gene function, and loss of *pag-6* function does not cause a green pharynx phenotype. The single green pharynx allele *gei-4(n4319)* likely causes weak dominant-negative function: it is not completely recessive, and its green pharynx phenotype can be reproduced by RNAi targeting *gei-4*. No mutations in *gei-4* have previously been reported, even from large-scale genetic screens designed to recover mutations causing a synMuv phenotype (FERGUSON and HORVITZ 1989; THOMAS *et al.* 2003) or from synMuv screens that permitted the recovery of mutations causing a

synMuv phenotype and sterility (CEOL *et al.* 2006). Mutations causing loss of *gei-4* function might not be recoverable in synMuv or green pharynx screens, either because a lethal phenotype does not permit scoring of either phenotype or because *gei-4* might be subject to maternal rescue for these phenotypes. Additional large-scale genetic screens might serve to identify additional genes that, like *pag-6* and apparently *gei-4*, can be identified only through rare alleles. Screens of the F_3 generation from mutagenized animals might identify genes that, like *hpl-2*, are maternally rescued for the green pharynx phenotype. Given the scale of the screens already performed, it seems likely that any remaining unidentified green pharynx genes might more readily be found using alternative approaches, such as detection of biochemical interactions or whole-genome RNAi screens.

Different combinations of synMuv genes act in different biological processes

Although most of the synMuv genes have initially been identified on the basis of the ectopic vulval induction seen in animals double mutant for a class A and a class B synMuv gene, many additional defects have been identified in synMuv single mutants. Beyond the finding that one class A synMuv gene and 14 class B synMuv genes are required for viability, subsets of the class B synMuv genes have been shown to function in expression of repetitive transgenes (HSIEH *et al.* 1999), cell cycle regulation (BOXEM and VAN DEN HEUVEL 2001; BOXEM and VAN DEN HEUVEL 2002), meiotic chromosome segregation (REDDY and VILLENEUVE 2004), downregulation of RNA-mediated gene interference (WANG *et al.* 2005), feminization (GROTE and CONRADT 2006), promotion of programmed cell death in the soma (REDDIEN *et al.* 2007), and promotion of

programmed cell death in the germline (SCHERTEL and CONRADT 2007), among other functions. Although these previous findings have identified synMuv genes as acting in a variety of biological processes independently of other synMuv genes, the set of genes that functions to prevent the green pharynx phenotype is strikingly different in that this set does not merely make use of a subset of the class B synMuv genes, but rather combines a subset of the class B synMuv genes with a member of the class A synMuv genes and even a weak synMuv suppressor. It seems likely that additional processes will be found that, like the process controlled by the green pharynx genes, use combinations of the synMuv genes that fundamentally differ from the combinations seen for the synMuv genes in repression of vulval induction and in other processes studied to date.

hpl-2 HP1 functions to prevent transgene misexpression independently of the histone methyltransferase genes *met-1* and *met-2*

Examination of the mutants isolated on the basis of their green pharynx phenotypes and testing of candidate genes identified five synMuv genes that are each required to prevent the inappropriate reporter gene expression seen in the green pharynx phenotype. As mutation of any of the green pharynx genes causes a similar phenotype of transgene derepression in the pharynx, it seems likely that the green pharynx proteins all work together to contribute to a shared function of transcriptional repression. At least two of these five green pharynx synMuv genes encode proteins very likely to function in chromatin modification and in the regulation of transcription: *lin-61* encodes the *C. elegans* homolog of L3MBTL1, a human protein that

binds methylated histones and maintains a compacted and repressive chromatin structure (TROJER *et al.* 2007), and *hpl-2* encodes one of two *C. elegans* homologs of heterochromatin protein 1 (HP1), a protein that binds methylated histones to epigenetically maintain heterochromatin, a compacted and repressive chromatin structure, through meiosis and mitosis (EISSENBERG *et al.* 1990; EISSENBERG *et al.* 1992; FISCHLE *et al.* 2003; HORN and PETERSON 2006; LOMBERK *et al.* 2006).

Animals lacking *hpl-1* function display a green pharynx phenotype, but animals lacking the function of the histone methyltransferase *met-1* or the histone methyltransferase *met-2* do not. *met-1* encodes a homolog of *S. cerevisiae* Set2 and *met-2* encodes a homolog of human SETDB1. *met-1* and *met-2* are required for trimethylation of *C. elegans* histones at lysines 9 and 36 (ANDERSEN and HORVITZ 2007). Like animals lacking *met-1* or *met-2*, animals lacking both *met-1* and *met-2* do not display a green pharynx phenotype. Histone trimethylation recruits HP1, which promotes methylation-dependent transcriptional repression (HEDIGER and GASSER 2006). *hpl-2* has been shown to act together with and also independently of *met-1* and *met-2* in the regulation of vulval cell fates (ANDERSEN and HORVITZ 2007). If HPL-2 is recruited to DNA to maintain a repressive chromatin structure in the transcriptional repression seen in the green pharynx phenotype, a mechanism other than binding to histones trimethylated by MET-1 and MET-2 must be involved. One possible mechanism for this histone-methylation-independent recruitment of HPL-2 in prevention of the green pharynx phenotype can be inferred from reports that HPL-2 can physically interact with the zinc finger protein LIN-13, which like HPL-2 is the product of a synMuv green pharynx gene (COUSTHAM *et al.* 2006). Both LIN-13 and HPL-2 fusion proteins

have been reported to localize to foci within nuclei (MELENDEZ and GREENWALD 2000; COUTEAU *et al.* 2002); these expression patterns within nuclei overlap, and HPL-2::RFP localization to these foci depends on *lin-13* function (COUSTHAM *et al.* 2006). LIN-13 is a 2248 amino acid protein containing 24 zinc fingers, suggesting that it might bind DNA (MELENDEZ and GREENWALD 2000). LIN-13 might therefore function in parallel to histone methylation to promote HPL-2 localization and maintain a repressive chromatin structure. Alternatively, HPL-2 might be recruited by histone methylation provided by a different histone methyltransferase, or HPL-2 might bind DNA or nucleosome indirectly of histone tails (ZHAO *et al.* 2000; ANDERSEN and HORVITZ 2007).

The class A synMuv protein LIN-8 likely functions to regulate transcription

No known class A synMuv gene has a homolog of known molecular function or even an identifiable non-nematode homolog (CLARK *et al.* 1994; HUANG *et al.* 1994; DAVISON *et al.* 2005) (E. Davison, A. Saffer, and H.R.H., personal communication). In the prevention of ectopic vulval induction, the class A synMuv genes act in parallel to the class B synMuv genes. Transcript levels of *lin-3*, which encodes an EGF-like ligand that induces vulval development (HILL and STERNBERG 1992), are increased in class A synMuv; class B synMuv double mutant animals (CUI *et al.* 2006a). This latter result provides the best evidence to date that the class A synMuv genes act in transcriptional regulation. We have now found that *lin-8* single mutants, rather than animals doubly mutant for *lin-8* and for another gene, show a defect of transcriptional repression, the green pharynx phenotype. *lin-8* shares this defect with mutants in genes that encode known regulators of transcription. It therefore seems likely that the normal function of

the class A synMuv protein LIN-8 is to regulate transcription. similarly, it seems likely that other members of the LIN-8 protein family and other members of the class A synMuv genes also function as regulators of transcription.

Separable synMuv and green pharynx functions of LIN-8

Of 67 *lin-8* alleles, there are 48 distinct mutations, including 20 different missense mutations. None of the missense mutations alters residues of the core domain of LIN-8, a domain that has been shown to be capable of interacting with the Rb homolog LIN-35 and is not conserved in other members of the large LIN-8 family of proteins in *C. elegans* (DAVISON *et al.* 2005). The failure to identify either synMuv or green pharynx alleles that alter residues within this interaction domain suggests that the interaction of LIN-8 with LIN-35 might not be important to the prevention of the green pharynx or synMuv phenotypes.

Of the 23 *lin-8* alleles identified in screens for animals with ectopic vulval induction, one, *lin-8(n2376)*, did not cause a green pharynx phenotype. The E148K change caused by *lin-8(n2376)* alters a residue conserved in LNES-1 and in most members of the LIN-8 family (DAVISON *et al.* 2005). *lin-8(n2376)* has previously been shown to cause a class A synMuv phenotype stronger than those caused by the *lin-8* mutations *n111* and *n2741* (DAVISON *et al.* 2005); unlike *lin-8(n2376)*, *lin-8(n111)* and *lin-8(n2741)* caused the green pharynx phenotype. LIN-8 protein levels are not strikingly reduced in *lin-8(n2376)* animals (DAVISON *et al.* 2005). It therefore seems likely that the mutant LIN-8 protein produced in *lin-8(n2376)* animals is stable and is specifically

defective in synMuv function but retains the functionality required to prevent the green pharynx phenotype.

Ten *lin-8* mutations show specificity for the green pharynx phenotype. Two of these alter splice sites and one mutates a nucleotide 12 bases before the beginning of the *lin-8* open reading frame. Because these splice site and promoter mutations seem more likely to reduce the total level of *lin-8* expression than to disrupt specific functions of the LIN-8 protein, it seems probable that the green pharynx phenotype is more sensitive to a subtle reduction in *lin-8* function than is the class A synMuv phenotype. The missense mutations that cause a green pharynx phenotype but not a synMuv phenotype might similarly cause a partial reduction in *lin-8* function insufficient to cause a synMuv phenotype; alternatively they might specifically and strongly affect a LIN-8 function required to prevent the green pharynx phenotype but not the synMuv phenotype. In the latter context it is notable that the only missense alleles altering the C-terminus of LIN-8, a domain that is conserved in other members of the LIN-8 family (DAVISON *et al.* 2005), are the green pharynx-specific alleles *n3593* and *n3591*, which cause the predicted amino acid changes R343C and E347K, respectively.

The synMuv protein LIN-8 and the homologous synMuv suppressor LNES-1 are separately required to prevent inappropriate transcriptional activation

LIN-8 is a member of a large family of proteins thus far found only in nematodes (DAVISON *et al.* 2005). Loss-of-function mutations in either *lin-8* or its closest homolog *lnes-1* including likely null mutations, caused a green pharynx phenotype. That the green pharynx phenotype is seen in animals mutant for either *lin-8* or *lnes-1* suggests

that, despite the highly similar sequences of the proteins LIN-8 and LNES-1, the two genes are not redundant for green pharynx function. If the two proteins were interchangeable, then loss of one copy of each gene would presumably be equivalent to the loss of both copies of one gene, or at least equivalent to the loss of both copies of the lower expressed of the two genes. In this case, null alleles of both *lin-8* and of *lnes-1* should fail to complement for the green pharynx phenotype, when in fact the mutations did complement. Further arguing against redundant functions of *lin-8* and *lnes-1*, no additional defects were seen when animals lacking *lin-8* function were treated with RNAi capable of causing loss of *lnes-1* function or when animals lacking *lnes-1* function were treated with RNAi capable of causing loss of *lin-8* function.

It could alternatively be suggested that only one of the two related genes *lin-8* and *lnes-1* normally functions to prevent the green pharynx phenotype but that loss of the other, related protein causes the first protein to be titrated away from its normal functions and into complexes and contexts that normally contain the now-missing second protein. If so, the protein that performs this function must be LIN-8, as multicopy transgenes overexpressing *lin-8* rescued the green pharynx phenotypes of *lin-8* and *lnes-1* mutants; in contrast, multicopy transgenes overexpressing *lnes-1* rescued the green pharynx phenotypes of *lnes-1* mutants but not those of *lin-8* mutants. It therefore might be suggested that only *lin-8* normally functions to prevent the green pharynx phenotype and that loss of *lnes-1* causes LIN-8 to be titrated away from its normal functions and into complexes and contexts that normally contain LNES-1. Contrary to this hypothesis, the green pharynx phenotype caused by the R119C missense mutants *lnes-1(n3604)* and *lnes-1(n3689)* strongly suggests that LNES-1 is normally present in

complexes that prevent the green pharynx phenotype of transgene misexpression. Specifically, multicopy *lnes-1* transgene carrying the R119C missense mutation caused a green pharynx phenotype, an effect not seen for transgenes that overexpressed the *lnes-1* nonsense mutants *lnes-1(n3592)* or *lnes-1(n3917Δ)*. These results suggest that LNES-1(R119C) protein is stable and nonfunctional, and that when it is overexpressed it can compete with wild-type LNES-1 protein and interfere with the function of complexes that can contain LNES-1. Because the R119C missense change caused a green pharynx phenotype in *lnes-1(n3604)* animals that presumably expressed LNES-1(R119C) at normal levels, LNES-1 must normally be included in complexes required to prevent the green pharynx phenotype. Consequently, LNES-1 has a function in preventing the inappropriate gene expression of the green pharynx phenotype that is independent of the function provided by LIN-8.

Identification of a nuclear MSP domain protein that can function to regulate transcription

The green pharynx mutation *n3599* defines the gene *pag-6*, which encodes a protein with an N-terminal MSP domain and a C-terminal domain with homology to other nematode proteins. In addition to the green pharynx phenotype, *pag-6(n3599)* causes synthetic lethality with some class B synMuv mutants, defects in egg laying, slow growth and a weak class B synMuv phenotype. Strikingly, all of these defects are shared, to greater or lesser degrees, with strong loss-of-function mutations of the green pharynx and class B synMuv gene *hpl-2 HP1* (COUSTHAM *et al.* 2006).

The set of class B synMuv mutants synthetically lethal with *pag-6(n3599)* is closely related to the set of class B synMuv mutants observed to be synthetically lethal with loss of function of *mcd-1* (*mcd*, modifier of cell death) (REDDIEN *et al.* 2007). Like *pag-6(n3599)* mutants, *mcd-1* mutants share with a subset of synMuv mutants a defect in a phenotype other than vulval induction; in the case of *mcd-1*, this function is one of promoting programmed cell death (REDDIEN *et al.* 2007). *mcd-1(n4005)* and *pag-6(n3599)* are synthetically lethal with similar sets of class B synMuv mutants and also with each other, suggesting that the synthetic-lethal phenotypes of *mcd-1(n4005)* and *pag-6(n3599)* mutants might result from different defects. *mcd-1(n4005)* and *pag-6(n3599)* acting differently to cause synthetic-lethal phenoypes would be consistent with their different defects in programmed cell death and in reporter expression, respectively. The core set of synMuv mutants synthetically lethal both with *pag-6(n3599)* and with loss of *mcd-1* function may define a group of synMuv genes that cooperate to provide a function redundantly required for animal development or viability, likely a function in transcriptional regulation.

The wild-type function of *pag-6* is not necessarily revealed by the phenotypic defects caused by the altered-function mutation *pag-6(n3599)*. RNAi targeting *pag-6* and the *pag-6* loss-of-function mutation *n5161* do not cause defects similar to those seen in *pag-6(n3599)* mutants. Even in weak synMuv double mutants that act as sensitized genetic backgrounds, loss of *pag-6* function does not alter the penetrance of defects in vulval induction, indicating that loss of *pag-6* function does not cause any significant defect in synMuv gene function. Nonetheless, PAG-6 expression from a rescuing *pag-6::gfp* transgene is nuclearly localized, consistent with a role for PAG-6 in

the regulation of transcription. The *n3599* missense mutation changes the glutamic acid at position 425 in the conserved C-terminal domain to an arginine and results in a sequence that is similar to the most divergent of the proteins with a domain similar to the PAG-6 C-terminus, T27A8.5: T27A8.5 similarly has a basic residue, a lysine, at the homologous position. It is therefore possibly that the mutant PAG-6 produced in *pag-6(n3599)* mutants is altered to possess properties more similar to those of T27A8.5 than those normally seen in PAG-6.

One possible explanation for the recessive action of the *n3599* altered-function mutation is that *n3599* might cause the generation of a stable but nonfunctional PAG-6 protein. The stable, nonfunctional protein is then incorporated into complexes that normally include wild-type PAG-6. In animals homozygous for *pag-6(n3599)*, all of the PAG-6 protein would be nonfunctional, and the incorporation of this nonfunctional protein could then impede the function of these complexes. If no PAG-6 protein is present, the function normally supplied by PAG-6 can instead be provided by another protein, possibly by a protein related to PAG-6. Injection of dsRNAs targeting all *C. elegans* genes predicted to encode proteins homologous to the C-terminus of PAG-6 did not cause a green pharynx phenotype similar to that caused by *pag-6(n3599)* (data not shown); however, it cannot be known whether these multiple-RNAi treatments were effective in targeting the several PAG-6-homologous proteins.

Implications from studies of the green pharynx genes about mechanisms that ensure fidelity of gene expression at endogenous loci

Although expression from four different reporters can lead to the green pharynx phenotype of transgene misexpression, at least six other reporters were tested and did not lead to the green pharynx phenotype, even though they were generated using the same vector backbone. Perhaps the promoter inserts in these other *gfp* reporters recruit multiple systems that prevent inappropriate transcriptional activation caused by enhancer elements in the vector backbone, so that loss of the transcriptional repression activity provided by the green pharynx genes still leaves other repressive activities intact and able to prevent inappropriate gene expression. In this model, in those few reporter transgenes that lead to the green pharynx phenotype the promoter insert recruits a single repressive system, provided by the green pharynx proteins, that prevents inappropriate gene expression. A model for how the green pharynx proteins act to prevent inappropriate reporter expression is shown in Figure 4.

Because the green pharynx phenotype is defined by multicopy transgenes at which the green pharynx genes act to repress transcription, it should be possible to define the elements required within the transgenes that support the green pharynx phenotype for recruitment of transcriptional repression activity and also to identify proteins and chromatin modifications present at such elements. The genes identified by the green pharynx phenotype act together to prevent inappropriate transgene expression, but these genes are part of the normal biology of *C. elegans*, and several of the green pharynx genes have previously been shown to function in *C. elegans* development and to have homologs that modify chromatin in other organisms. That these *C. elegans* genes share a common function in the green pharynx assay strongly

suggests that further investigation will reveal common targets in the *C. elegans* genome at which these genes function to prevent activation by nearby weak enhancer elements.

Materials and Methods

C. elegans genetics

C. elegans strains were derived from the wild-type strain N2 (Bristol, England) and cultured using standard conditions (BRENNER 1974), except that the bacterial strain HB101 was the food source. Mutations isolated in this study on the basis of their green pharynx phenotypes are listed in Table 2. *lin-8* alleles used in this study are listed in Table 3, and references for their isolation are listed therein. Other mutations used are listed below and are described by RIDDLE *et al.* (1997) unless otherwise noted. LGI: *dcp-66(gk370)* (ZHAO *et al.* 2005), *dpy-5(e61)*, *lin-35(n745)*, *lin-53(n833, n3368)* (ANDERSEN *et al.* 2006), *lin-61(sy223, n3442, n3446, n3447, n3624, n3736)* (HARRISON *et al.* 2007), *lin-65(n3441)* (CEOL *et al.* 2006), *mes-3(bn35)*, *met-1(n3628, n4337)* (CEOL *et al.* 2006; ANDERSEN and HORVITZ 2007), *sem-4(n1378)*, *smo-1(ok359)* (BRODAY *et al.* 2004), *unc-13(e1091)*, *xnp-1(fd2)* (BENDER *et al.* 2004); LGII: *dpl-1(n3316, n3380, n3643)* (CEOL and HORVITZ 2001), *fzr-1(ku298)* (FAY *et al.* 2002), *lin-38(n751, tm736)* (A. Saffer and H.R.H., unpublished results), *lin-56(n2728)*, *mcd-1(n4005)* (REDDIEN *et al.* 2007), *mes-2(bn11)*, *rol-6(e187)*, *trr-1(n3630, n3712)* (CEOL and HORVITZ 2004), *unc-4(e120)*, *unc-52(e444)*; LGIII: *dpy-1(e1)*, *dpy-17(e164)*, *dpy-19(e1259)*, *epc-1(n4076)* (CEOL and HORVITZ 2004), *glp-1(q339)*, *hpl-1(n4317)* (ANDERSEN and HORVITZ 2007), *hpl-2(ok916, ok917, tm1489)* (COUSTHAM *et al.* 2006), *hpl-2(n4274)* (E. Andersen and H.R.H., unpublished results), *isw-1(n3294)* (ANDERSEN *et al.* 2006), *lin-9(n112, n942)*, *lin-13(n387, n770, n2238, n2985, ok838)* (THOMAS *et al.* 2003; WANG *et al.* 2005), *lin-36(n766, n3096)* (THOMAS and HORVITZ 1999), *lin-37(n758)*, *lin-52(n771, n3718)* (CEOL *et al.* 2006), *met-2(n4256)* (ANDERSEN and HORVITZ 2007), *ssl-1(n4077)*

(CEOL and HORVITZ 2004), *ubc-9(ju484)* (J. McCleery and Y. Jin, personal communication), *ubc-18(ku354)* (FAY *et al.* 2003), *unc-32(e189)*, *unc-45(e286)*, *unc-119(ed3)*; LGIV: *ark-1(n3701)* (CEOL *et al.* 2006), *dpy-4(e1166)*, *dpy-13(e184)*, *dpy-20(e1282)*, *egl-23(n601)*, *let-60(n1046*gf*)*, *lex-1(gu47)* (TSENG *et al.* 2007), *lin-54(n2231*, *n3423)* (HARRISON *et al.* 2006), *lst-3(n4590)* (E. Andersen and H.R.H., unpublished results), *mep-1(n3680*, *n3703)* (CEOL *et al.* 2006), *mes-6(bn66)*, *pag-6(n3599 n5161)* (this study), *sup-36(e2217)*, *unc-24(e138)*, *unc-26(e205)*, *unc-31(e169)*; LGV: *dpy-11(e224)*, *efl-1(n3318)* (CEOL and HORVITZ 2001), *egl-1(n1084)*, *hda-1(e1795)* (DUFOURCQ *et al.* 2002), *him-5(e1467)*, *let-418(n3536, s1617)* (VON ZELEWSKY *et al.* 2000; CEOL *et al.* 2006), *lin-40(ku285*, *s1593*, *s1669)* (CHEN and HAN 2001), *mes-4(bn23*, *bn67)*, *mys-1(n3681*, *n4075)* (CEOL and HORVITZ 2004), *psa-1(ku355)* (CUI *et al.* 2004), *rde-1(ne219)* (TABARA *et al.* 1999), *spr-1(ar200)* (JARRIAULT and GREENWALD 2002), *sup-37(e2215)*, *tam-1(cc567)* (HSIEH *et al.* 1999), *unc-46(e177)*, *unc-51(n4437)* (H.T.S. and H.R.H., unpublished), *unc-76(e911)*; LGX: *chd-3(eh4)* (VON ZELEWSKY *et al.* 2000), *gap-1(n3535)* (CEOL *et al.* 2006), *lin-15(n433*, *n744*, *n765*, *n767*, *n2994 n433)* (THOMAS *et al.* 2003), *lin(n3542)* (CEOL *et al.* 2006), *lin(n3707)* (C. Ceol and H.R.H., unpublished results), *sli-1(n3538)* (CEOL *et al.* 2006), *tra-4(bc250*, *n3715*, *n3716*, *n4724*, *n4726)* (H.T.S. and H.R.H., manuscript in preparation, and GROTE and CONRADT 2006). The integrated *pkd-2::gfp* reporters *nIs128 II*, *nIs130 IV*, and *nIs133 I* were generated using the cell-fate reporter plasmid ppkd-2::gfp1 (BARR and STERNBERG 1999) and the rescuing *lin-15(+)* plasmid pL15EK (CLARK *et al.* 1994) and are described in more detail in chapter 2. The integrated *lin-11::gfp* reporter *nIs106 X* (REDDIEN *et al.* 2001), the integrated *flp-15::gfp* reporter

ynIs45 (KIM and LI 2004), and the integrated *lag-2::gfp* reporter *qIs56 V* (SIEGFRIED *et al.* 2004) were also used. The translocation *nT1* [IV; V] with the dominant Unc marker *deg-3(n754)* (TREININ and CHALFIE 1995) or the dominant *gfp* marker *qIs51* (SIEGFRIED *et al.* 2004), the translocation *hT2* [I; III] with the dominant *gfp* marker *qIs48* (SIEGFRIED and KIMBLE 2002), the inversion chromosome *mIn1* with the recessive marker *dpy-10(e128)* and the dominant *gfp* marker *mIs14* (EDGLEY and RIDDLE 2001), the modified chromosome *mnC1* (HERMAN 1978) with the recessive markers *dpy-10(e128)* and *unc-52(e444)*, and the modified chromosome *qC1* (AUSTIN and KIMBLE 1989) with the recessive markers *dpy-19(e1259)* and *glp-1(q339)* were used as balancers. *sDf23 IV* (GILCHRIST and MOERMAN 1992) is a chromosomal deficiency that removes the *pag-6* locus. The related free duplications *yDp1 (IV; V; f)* (DELONG *et al.* 1987) and *nDp3 (IV; V; f)* (YUAN and HORVITZ 1990) complement *dpy-4* but do not complement *pag-6(n3599)* (data not shown).

Double mutants homozygous for *pag-6(n3599)* and autosomal mutations were constructed using balancer chromosomes or pairs of linked visible markers to follow the second mutation in *trans*; X-linked mutations were made homozygous by crosses using *pag-6(n3599)*/+ males hemizygous for the mutant X chromosome. *pag-6(n3599)* homozygotes were detected using the recessive green pharynx phenotype caused by *pag-6(n3599)* in animals heterozygous for a *pkd-2::gfp* transgene. Progeny that had lost the *pkd-2::gfp* transgene were then identified, and attempts was made to identify progeny that no longer contained the markers or balancer chromosome that were used to follow the second mutation *in trans*; animals no longer containing these markers or balancer chromosomes would be homozygous for the second mutation. All double

mutants involving *pag-6(n3599)* were built such that the only identified mutations present in the finished strains were *pag-6(n3599)* and the mutation being tested for synthetic viability with *pag-6(n3599)*, with the exception of the double mutant between *lin-8(n2731)* and *pag-6(n3599)*; in this case, *pag-6(n3599)* was marked in *cis* with *dpy-4(e1166)*. Animals mutant both for *lin-8* or *lnes-1* and for *lin-36* were built using a *lin-36(n766)* mutation marked in *cis* with *unc-32(e189)*. Males heterozygous for *lin-8* or *lnes-1* and for the balancer chromosome *qC1* were used in these strain constructions to ensure that the homozygous *unc-32(e189)* chromosome was also homozygous for the linked mutation *lin-36(n766)*. Double mutants between autosomal green pharynx mutations and *lin-15 X* mutations were built by mating males heterozygous for the green pharynx mutation with *lin-15* mutant hermaphrodites, mating the resulting male progeny to *lin-15* mutant hermaphrodites, identifying progeny homozygous for the green pharynx mutation, and then identifying progeny that had lost the heterozygous *pkd-2::gfp* transgene. Alternately, double mutants between autosomal green pharynx mutations and *lin-15 X* mutations were built using an extrachromosomal transgene containing *pkd-2::gfp* marked with a rescuing *unc-119(+)* transgene, *lin-15A(n767)* and *lin-15B(n744)* were placed in *trans* to *lin-15AB(n765)*, and *lin-1A(n767)* or *lin-15B(n744)* homozygoutes were identified by their failure to generate progeny homozygous for *lin-15AB(n765)*, identifiable by their strong Muv phenotype.

Isolation and mapping of alleles of green pharynx genes

Clonal screens for green pharynx mutants were performed using EMS mutagenesis (BRENNER 1974) of *sem-4(n1378)*; *nIs128* and *nIs133*; *egl-1(n1084*gf)

hermaphrodites. Both strains are defective in egg laying, and adult hermaphrodites of either strain can contain late-stage embryos or young larvae in which the green pharynx phenotype can be scored. Following mutagenesis, gravid F_1 progeny were examined to determine whether the F_2 progeny (late-stage embryos and internally hatched progeny) they contained displayed a green pharynx phenotype. The progeny within 4,914 F_1 *sem-4(n1378)*; *nIs128* hermaphrodites and the progeny within 767 F_1 *nIs133*; *egl-1(n1084*gf*)* hermaphrodites were examined, for a total of 11,362 mutagenized haploid genomes. Other mutations causing a green pharynx phenotype were identified incidentally in screens for phenotypes other than the green pharynx phenotype or were discovered in the process of strain construction as previously unnoticed mutations in pre-existing strains. A complete list of mutations isolated based on their having caused a green pharynx phenotype is in Table 2.

Both *nIs133* and *nIs128* appeared to suppress recombination on at least part of their respective chromosomes: we observed no recombination between *nIs133* and *dpy-5*, between *nIs133* and *lin-61* or between *nIs128* and *dpy-10*, and *lin-8* has only recombined away from *nIs128* spontaneously once, from among several dozen strain constructions in which we used *lin-8* mutations linked to *nIs128*, with each strain construction involving many animals.

We mapped the *lnes-1* mutations *n3688*, *n3689*, *n3917*, *n3919*, and *n3921* to LGII at an average distance of approximately 12 map units from *rol-6* using standard methods. Polymorphism mapping using 322 green pharynx progeny of animals heterozygous in *trans* for *lnes-1(n3688)* and chromosomal regions from the Hawaiian strain CB4856 placed *n3688* between ~19,000 on B0454 (all references to B0454

sequence refer to accession number AF025452) and ~55,000 on Y25C1A (accession number AF125459), a 76 kb interval.

We mapped *gei-4(n4319)* to the left end of LGIII using polymorphisms. In further mapping, we screened a total of 786 progeny of animals heterozygous in *trans* for *n4319* and for chromosomal regions derived from the Hawaiian strain CB4856 to identify animals containing chromosomes recombinant between markers at ~17,600 on H10E21 (accession number AF078783) and ~13,200 on Y92C3A (accession number AC024874). We identified animals homozygous for the recombinant chromosomes and tested them for *n4319* and for their genotypes at markers on T17A3, K10F12, T22F7, B0353, W06E11, W02B3, C24A1, T17H7, K02F3, Y22D7AL, and Y39A3CL. These experiments placed *n4319* left of a marker at ~8,700 on B0353 (accession number U23413), within the first 527 kb of LGIII. We found this region of LGIII to be recombinationally suppressed between N2 and CB4856: none of the 28 F_2 progeny identified as recombinant between markers on H10E21 and Y92C3A, an interval of approximately 1,148 kbp, had recombined within the approximately 523 kb of this interval to the left of the marker on B0353. Thirteen cosmids representing ~363 kb of the left end of LGIII were injected in four pools to test for their ability to rescue the green pharynx phenotype caused by *n4319*: H10E21, W05G11, F54C4, and C29F9; T17A3, F40G9, and W10C4; W07B3 and K10F12; and F10C5, F30H5, T22F7, and B0353.

Of 180 Dpy progeny of *nIs128*; *dpy-4(e1166)* +/+ *n3599* heterozygotes, 13 generated green pharynx progeny, indicating a distance of approximately 3.6 map units. Polymorphism mapping placed *pag-6(n3599)* to the right of ~49,900 on Y105C5B and to

the left of ~152,600 on Y105C5B (all references to Y105C5B refer to accession number AL110479), restricting *n3599* to a ~103 kb interval. We determined using DNA polymorphisms between the wild-type and the Hawaiian strain CB4856 that the related free duplications *nDp3* and *yDp1*, the extents of which to the right of *dpy-4* were unknown and therefore might have included the *pag-6* locus, contained sequence derived from LGIV up to ~297,100 on clone Y105C5A (accession number AL117193) but did not contain sequences at or to the right of ~49,900 on clone Y015C5B, and thus these genomic duplications broke to the left of the recombinationally determined left endpoint of *pag-6*. DNA sequence determination revealed the *pag-6(n3599)* suppressor mutation *n5161* to be a single nucleotide deletion within the *pag-6* open reading frame, removing nucleotide 119998 of Y105C5B and causing a predicted frameshift after amino acid 83.

The uncharacterized mutation *n3841*, which causes a weakly penetrant and inconsistent green pharynx phenotype, was mapped to LGIC using SNPs with the Hawaiian strain CB4856. Weak penetrance and possible semidominance made mapping this mutation difficult. The tightest linkage we observed was to a marker on cosmid K04F10, with only one of 22 F_2 green pharynx animals homozygous for the Hawaiian-derived haplotype at this marker. Complementation tests with this weak mutation were inconclusive. No mutations were found in *n3841* animals in the coding sequence of *lin-61*, the only known green pharynx gene on LGI.

DNA and RNA manipulations and generation of transgenic animals

DNA sequences were determined using an ABI DNA Sequencer model 377, an ABI Genetic Analyzer 3100, and by Gene Gateway (Hayward, CA). The *lin-8* allele *n3686* is a large deletion the precise extent of which could not be determined; sequences 5' of nucleotide 38077 and 3' of nucleotide 42872 on B0454 could be amplified from *lin-8(n3686Δ)* animals, while sequences at least from nucleotide 38657 to nucleotide 42872 of B0454 could not. Long PCR (using Advantage cDNA; BD Biosciences, Mountain View, CA) that amplified the sequence corresponding to nucleotides 38024 through 43169 of B0454 from the wild-type strain did not generate a product from *lin-8(n3686Δ)* animals, suggesting that alterations associated with *n3686* prevented amplification of this locus using PCR.

The *pag-6* rescuing construct pBSK-*pag-6* contains DNA corresponding to 116918 through 126022 of Y105C5B, including 5776 bp 5' of the predicted *pag-6* ATG and 1037 bp 3' of the predicted *pag-6* stop codon, amplified by PCR from proteinase K-treated N2 and cloned using endogenous *Kpn*I and *Eco*RV sites into pBSKII+ (Stratagene). The *pag-6(n3599)* phenocopying plasmid pBKS-*pag-6(n3599)* contains DNA amplified by PCR from a *pag-6(n3599)* mutant using the same primers as the *pag-6* rescuing construct and cloned similarly into pBSKII+. The *pag-6::gfp* rescuing construct contains sequence corresponding to 124670 of Y105C5B through the last codon before the stop codon, including 4424 bp 5' to the predicted *pag-6* ATG, cloned into the *gfp* reporter vector pPD95.79 (provided by Andrew Fire), resulting in an in-frame fusion to *gfp* in place of the stop codon of the *pag-6* open reading frame.

The *lin-8* rescuing construct pEMD13 has been previously described (DAVISON *et al.* 2005). The *lnes-1* rescuing construct BKS-*lnes-1* contains DNA corresponding to

34652 through 39126 of B0454, including 4040 bp 5' of the predicted *lnes-1* ATG and 1613 bp 3' of the predicted *lnes-1* stop codon, amplified by PCR and cloned using a *Spe*I site added by a primer and an endogenous *Kpn*I site into pBSKII+. The same primers were used to amplify DNA from *lnes-1* mutants to generate the constructs BKS-*lnes-1(n3592)*, BKS-*lnes-1(n3604)*, and BKS-*lnes-1(n3917)*. Two *lnes-1::gfp* reporters were made by amplifying the *gfp* coding sequence from pPD95.02 (provided by Andrew Fire) using PCR primers that added in-frame *Sph*I and *Pst*I sites and cloning it into modified versions of BKS-*lnes-1* after the first three amino acids (to generate *lnes-1::gfpN::lnes-1*) or before the last two amino acids (to generate *lnes-1::gfpC::lnes-1*). Two *gei-4* rescuing constructs, BKS-*gei-4(Avr*II*)* and BKS-*gei-4(Sna*BI*)*, were generated by cloning subclones of the cosmid W07B3 generated using the indicated enzymes into pBSKII+ cloned with *Spe*I or with *Eco*RV, respectively.

Germline transformation was performed as described (MELLO *et al.* 1991) using the co-injection markers P76-16B (BLOOM and HORVITZ 1997) or pMM016b (MADURO and PILGRIM 1995) at 50 ng/μl. BKS-*pag-6*, *pag-6::gfp*, EMD13, BKS-*lnes-1*, BKS-*lnes-1(n3592)*, BKS-*lnes-1(n3604)*, BKS-*lnes-1(n3917)*, *lnes-1::gfpN::lnes-1*, *lnes-1::gfpC::lnes-1*, BKS-*gei-4(Avr*II*)*, and BKS-*gei-4(Sna*BI*)* were each injected at 20 ng/μl. Injection of BKS-*pag-6(n3599)* at 20 ng/μl or 1 ng/μl did not generate viable transgenic progeny, although inviable green pharynx F_1 embryos were observed. BKS-*pag-6(n3599)* injected at 0.1 ng/μl gave stable transgenic lines with a green pharynx phenotype. The putative low-copy *pkd-2::gfp* integrants *nIs136 V* and *nIs137 I* were generated by microparticle bombardment using 1.0 μm gold particles

prepared with 25 μg pMM016b and 25 μg ppkd-2::gfp1 (BARR and STERNBERG 1999) using a Helios Gene Gun System (Bio-Rad) with advice from Frank Miskevich and adapting a published protocol (PRAITIS *et al.* 2001). ppkd-2::gfp1 was digested with *Sph*I and *Spe*I to remove vector sequence, and the purified *pkd-2::gfp* fragment was injected at 50 ng/μl with the co-injection marker P76-16B.

Transgenic lines containing integrated *gfp* reporters or containing extrachromosomal arrays generated with *gfp* reporter plasmids in combination with the *lin-15(+)* rescuing plasmid pL15EK used as a coinjection marker were tested for the ability of the green pharynx and class A synMuv mutation *lin-8(n111)* to cause a green pharynx phenotype in combination with those reporters. The reporters tested and not found to cause the green pharynx phenotype included *utIs13 [dat-1::gfp]* (T. Ishihara and I. Katsura, personal communication), *unc-86::gfp* (plasmid SA2I; O. Hobert and G. Ruvkun, personal communication), *osm-10::gfp* (plasmid KP#55, A. Hart, personal communication), *ceh-28::gfp* (B. Harfe and A. Fire, personal communication), *cat-2::gfp* (plasmid EM282, R. Lints and S. Emmons, personal communication) and *ayIs9 [egl-17::gfp]* (BRANDA and STERN 2000).

RNAi

RNAi was performed by injection using dsRNA synthesized using as templates PCR products of exonic sequence amplified using primers with T7 sites appended to their 5' ends. *In vitro* transcribed RNA was denatured and allowed to anneal prior to injection. For *pag-6*, PCR products corresponding to 119599 through 120223 or to 117951 through 118374 of Y105C5B were used; for *M199.2*, PCR products

corresponding to 8364 through 8783 or to 9004 through 9496 of M199 (accession number Z81104); for *T27A8.5*, a PCR product corresponding to 19475 through 19821 of T27A8 (Z68134); for *T25D1.1*, a PCR product corresponding to 16364 through 16727 of T25D1 (U41275); for *lin-8*, PCR products corresponding to 40841 through 41086 or to 40273 through 40581 of B0454; for *lnes-1*, PCR products corresponding to 35899 through 36184 or to 35140 through 35351 of B0454; and for *gei-4*, PCR products corresponding to 6845 through 7214 or to 5268 through 5638 of W07B3 were used. Zygotic RNAi was performed as described (HERMAN 2001) by injection of *unc-32(e189)*; *rde-1(ne219)*; *lin-15A(n767)* hermaphrodites followed by mating with *lin-15A(n767)* males or injection of *unc-32(e189)*; *lin-36(n766)*; *rde-1(ne219)* hermaphrodites followed by mating with *lin-36(n766)*; *him-5(e1467)* males. Feeding RNAi was performed as described using clones from the Ahringer RNAi feeding library (KAMATH *et al.* 2003).

Analysis of *C. elegans* phenotypes

The green pharynx phenotype was scored using a fluorescence-equipped dissecting microscope (M^2BIO; Kramer Scientific). The phenotype is most strongly expressed in late embryos and L1 larvae; in most mutants, the phenotype is readily observed in later larvae but is variable in L4 larvae and in adults, and intensity and duration of expression depend on the mutant allele and the strength of the *gfp* transgene. When possible, in testing synMuv mutants for the green pharynx phenotype, the progeny of animals homozygous for the synMuv mutation were examined in case the green pharynx phenotype might be subject to maternal rescue, as is the case for *hpl-2(*lf*)* mutants. The progeny of homozygous animals could not be obtained and

examined when all mutant alleles of a synMuv gene caused sterility; when a synMuv gene was represented both by alleles that did not cause sterility and by stronger alleles that did cause sterility, an allele from each class was tested. The strain *nIs133 lin-61(n3687)*; *lin-8(n2376)* was built and examined to confirm that the synMuv-specific allele *lin-8(n2376)* was not linked to a mutation suppressing the green pharynx phenotype.

The Multivulva phenotype was assessed using dissecting microscopy as described (ANDERSEN and HORVITZ 2007). Egg-laying defects were determined by the accumulation of unlaid eggs and by presence of embryos retained within gravid mothers that had undergone morphogenesis and had reached the threefold stage of embryonic development. Attachment of the pharynx to the anterior intestine was examined using Nomarski microscopy as described (FAY *et al.* 2003). Filling of phasmid neurons with DiO was performed as described (HERMAN and HORVITZ 1994) and scored using a Nomarski microscope equipped with fluorescence optics (AxioSkop, Zeiss).

Synthetic lethality between *pag-6(n3599)* and synMuv mutants was identified as the inability to identify fertile animals that had lost a balancer chromosome or paired linked visible markers in *trans* either to the synMuv mutation or to *pag-6(n3599)*. For mutations followed in *trans* with balancers that did not cause a visible dominant phenotype or followed in *trans* with a linked pair of visible markers, at least 30 eggs laid by balancer heterozygotes were each placed on individual Petri plates to test whether any generated viable progeny that had lost the balancer chromosome or lost both visible markers. For double mutants with *pag-6(n3599)*, *dpl-1* mutants were balanced with *mIn1* [*dpy-10(e128) mIs14*] and *lin-9(n112)* and *lin-37(n758)* mutants were

balanced with *qC1* [*dpy-19(e1259) glp-1(q339)*]. For double mutants with *lin-15B(n744)* or with *mcd-1(n4005)*, *pag-6(n3599)* was balanced with *nT1 [deg-3(n754)]*. A *lin-54(n2231) pag-6(n3599)* recombinant chromosome was built and balanced with *nT1 [deg-3(n754)]*. For double mutants between *lin-35(n745)* and *pag-6(n3599)*, strains were built in which *pag-6(n3599)* was homozygous and *lin-35(n745)* was balanced with *hT2 [qIs48]* and strains were built in which *lin-35(n745)* was homozygous and *pag-6(n3599)* was balanced with *nT1 [deg-3(n754)]* and with *nT1 [qIs51]*.

Acknowledgments

We thank Adam Saffer and Robert Shivers for their comments about this manuscript; Adam Saffer and John Doll for unpublished synMuv alleles of *lin-8*; Johanna Varner for the green pharynx mutations *n4319*, *n4320*, *n4356*, and *n4411*; Susan Mango for helpful comments regarding pharyngeal expression driven by a cryptic enhancer element in the *gfp* vector backbone; Beth Castor for assistance with DNA sequencing; Na An for assistance with strains; Ewa Davison for the *lin-8* rescuing construct EMD13 and for information about *lin-8* mutations; Niels Ringstad for assistance with phasmid dyes; Erik Andersen for *lst-3(n4590)* and *hpl-2(n4274)*; Erik Andersen and Adam Saffer for unpublished information; Craig Ceol for *lin(n3707)* and for mapping the class B synMuv mutation isolated with *lin-8(n3605)*; David Fay for helpful discussions and for *sup-36* and *sup-37* strains; Julie McCleery and Yishi Jin for *ubc-9(ju484)*; the *Caenorhabditis* Genetics Center, which is funded by the NIH National Center for Research Resources (NCRR), for strains; Maureen Barr and Paul Sternberg for the plasmid ppkd-2::gfp1; Morris Maduro and David Pilgrim for the plasmid pMM016b, Andrew Fire for the plasmids pPD95.79 and pPD95.02; Audrey Fraser and the Sanger Institute for cosmid clones, Takeshi Ishihara and Isao Katsura, Oliver Hobert and Gary Ruvkun, Anne Hart, Brian Harfe and Andy Fire, Robyn Lints and Scott Emmons, and Cathy Branda and Michael Stern for providing *gfp* reporters; Frank Miskevich and Martha Constantine-Paton for advice and for use of a Helios gene gun system; and the *C. elegans* Genome Sequencing Consortium and the Genome Sequencing Center at Washington University in St. Louis for the genomic sequence of *C. elegans* and for the identification of polymorphisms in CB4856. This work was

supported by NIH grant GM24663. H.T.S. was supported in part by a David H. Koch Graduate Fellowship. D.M.W. was supported by the Howard Hughes Medical Institute. H.R.H. is an Investigator of the Howard Hughes Medical Institute and is David H. Koch Professor of Biology at MIT.

References

ANDERSEN, E. C., and H. R. HORVITZ, 2007 Two *C. elegans* histone methyltransferases repress *lin-3* EGF transcription to inhibit vulval development. Development **134:** 2991-2999.

ANDERSEN, E. C., X. LU and H. R. HORVITZ, 2006 *C. elegans* ISWI and NURF301 antagonize an Rb-like pathway in the determination of multiple cell fates. Development **133:** 2695-2704.

ANDERSEN, E. C., A. M. SAFFER and H. R. HORVITZ, 2008 Multiple levels of redundant processes inhibit *Caenorhabditis* elegans vulval cell fates. Genetics **In press**.

AUSTIN, J., and J. KIMBLE, 1989 Transcript analysis of *glp-1* and *lin-12*, homologous genes required for cell interactions during development of *C. elegans*. Cell **58:** 565-571.

BARR, M. M., and P. W. STERNBERG, 1999 A polycystic kidney-disease gene homologue required for male mating behaviour in *C. elegans*. Nature **401:** 386-389.

BENDER, A. M., N. V. KIRIENKO, S. K. OLSEN, J. D. ESKO and D. S. FAY, 2007 *lin-35*/Rb and the CoREST ortholog *spr-1* coordinately regulate vulval morphogenesis and gonad development in *C. elegans*. Dev Biol **302:** 448-462.

BENDER, A. M., O. WELLS and D. S. FAY, 2004 *lin-35/Rb* and *xnp-1*/ATR-X function redundantly to control somatic gonad development in *C. elegans*. Dev Biol **273:** 335-349.

BLOOM, L., and H. R. HORVITZ, 1997 The *Caenorhabditis elegans* gene *unc-76* and its human homologs define a new gene family involved in axonal outgrowth and fasciculation. Proc Natl Acad Sci U S A **94:** 3414-3419.

BOXEM, M., and S. VAN DEN HEUVEL, 2001 *lin-35* Rb and *cki-1* Cip/Kip cooperate in developmental regulation of G1 progression in *C. elegans*. Development **128:** 4349-4359.

BOXEM, M., and S. VAN DEN HEUVEL, 2002 *C. elegans* class B synthetic multivulva genes act in G(1) regulation. Curr Biol **12:** 906-911.

BRANDA, C. S., and M. J. STERN, 2000 Mechanisms controlling sex myoblast migration in *Caenorhabditis elegans* hermaphrodites. Dev Biol **226:** 137-151.

BRENNER, S., 1974 The genetics of *Caenorhabditis elegans*. Genetics **77:** 71-94.

BRODAY, L., I. KOLOTUEV, C. DIDIER, A. BHOUMIK, B. P. GUPTA *et al.*, 2004 The small ubiquitin-like modifier (SUMO) is required for gonadal and uterine-vulval morphogenesis in *Caenorhabditis elegans*. Genes Dev **18:** 2380-2391.

CARDOSO, C., C. COUILLAULT, C. MIGNON-RAVIX, A. MILLET, J. J. EWBANK *et al.*, 2005 XNP-1/ATR-X acts with RB, HP1 and the NuRD complex during larval development in *C. elegans*. Dev Biol **278:** 49-59.

CEOL, C. J., and H. R. HORVITZ, 2001 *dpl-1* DP and *efl-1* E2F act with *lin-35* Rb to antagonize Ras signaling in *C. elegans* vulval development. Mol Cell **7:** 461-473.

CEOL, C. J., and H. R. HORVITZ, 2004 A new class of *C. elegans* synMuv genes implicates a Tip60/NuA4-like HAT complex as a negative regulator of Ras signaling. Dev Cell **6:** 563-576.

CEOL, C. J., F. STEGMEIER, M. M. HARRISON and H. R. HORVITZ, 2006 Identification and classification of genes that act antagonistically to *let-60* Ras signaling in *Caenorhabditis elegans* vulval development. Genetics **173:** 709-726.

CHEN, Z., and M. HAN, 2001 Role of *C. elegans lin-40* MTA in vulval fate specification and morphogenesis. Development **128:** 4911-4921.

CHESNEY, M. A., A. R. KIDD, 3RD and J. KIMBLE, 2006 *gon-14* functions with class B and class C synthetic multivulva genes to control larval growth in *Caenorhabditis elegans*. Genetics **172:** 915-928.

CLARK, S. G., X. LU and H. R. HORVITZ, 1994 The *Caenorhabditis elegans* locus *lin-15*, a negative regulator of a tyrosine kinase signaling pathway, encodes two different proteins. Genetics **137:** 987-997.

COUSTHAM, V., C. BEDET, K. MONIER, S. SCHOTT, M. KARALI *et al.*, 2006 The *C. elegans* HP1 homologue HPL-2 and the LIN-13 zinc finger protein form a complex implicated in vulval development. Dev Biol **297:** 308-322.

COUTEAU, F., F. GUERRY, F. MULLER and F. PALLADINO, 2002 A heterochromatin protein 1 homologue in *Caenorhabditis elegans* acts in germline and vulval development. EMBO Rep **3:** 235-241.

CUI, M., J. CHEN, T. R. MYERS, B. J. HWANG, P. W. STERNBERG *et al.*, 2006a SynMuv genes redundantly inhibit *lin-3/EGF* expression to prevent inappropriate vulval induction in *C. elegans*. Dev Cell **10:** 667-672.

CUI, M., D. S. FAY and M. HAN, 2004 *lin-35/Rb* Cooperates With the SWI/SNF Complex to Control *Caenorhabditis elegans* Larval Development. Genetics **167:** 1177-1185.

CUI, M., E. B. KIM and M. HAN, 2006b Diverse chromatin remodeling genes antagonize the Rb-involved SynMuv pathways in *C. elegans*. PLoS Genet **2:** e74.

DAVISON, E. M., M. M. HARRISON, A. J. M. WALHOUT, M. VIDAL and H. R. HORVITZ, 2005 *lin-8*, which antagonizes *Caenorhabditis elegans* Ras-mediated vulval induction, encodes a novel protein that interacts with the LIN-35 Rb protein. Genetics **171:** 1017-1031.

DELONG, L., L. P. CASSON and B. J. MEYER, 1987 Assessment of X chromosome dosage compensation in *Caenorhabditis elegans* by phenotypic analysis of *lin-14*. Genetics **117:** 657-670.

DUFOURCQ, P., M. VICTOR, F. GAY, D. CALVO, J. HODGKIN *et al.*, 2002 Functional requirement for histone deacetylase 1 in *Caenorhabditis elegans* gonadogenesis. Mol Cell Biol **22:** 3024-3034.

EDGLEY, M. L., and D. L. RIDDLE, 2001 LG II balancer chromosomes in *Caenorhabditis elegans*: mT1(II;III) and the mIn1 set of dominantly and recessively marked inversions. Mol Genet Genomics **266:** 385-395.

EISSENBERG, J. C., T. C. JAMES, D. M. FOSTER-HARTNETT, T. HARTNETT, V. NGAN *et al.*, 1990 Mutation in a heterochromatin-specific chromosomal protein is associated with suppression of position-effect variegation in *Drosophila melanogaster*. Proc Natl Acad Sci U S A **87:** 9923-9927.

EISSENBERG, J. C., G. D. MORRIS, G. REUTER and T. HARTNETT, 1992 The heterochromatin-associated protein HP-1 is an essential protein in *Drosophila* with dosage-dependent effects on position-effect variegation. Genetics **131:** 345-352.

ESTELLER, M., 2008 Epigenetics in cancer. N Engl J Med **358:** 1148-1159.

FAY, D. S., S. KEENAN and M. HAN, 2002 *fzr-1* and *lin-35*/Rb function redundantly to control cell proliferation in *C. elegans* as revealed by a nonbiased synthetic screen. Genes Dev **16:** 503-517.

FAY, D. S., E. LARGE, M. HAN and M. DARLAND, 2003 *lin-35/Rb* and *ubc-18*, an E2 ubiquitin-conjugating enzyme, function redundantly to control pharyngeal morphogenesis in *C. elegans*. Development **130:** 3319-3330.

FAY, D. S., X. QIU, E. LARGE, C. P. SMITH, S. MANGO *et al.*, 2004 The coordinate regulation of pharyngeal development in *C. elegans* by *lin-35/Rb*, *pha-1*, and *ubc-18*. Dev Biol **271:** 11-25.

FAY, D. S., and J. YOCHEM, 2007 The SynMuv genes of *Caenorhabditis elegans* in vulval development and beyond. Dev Biol **306:** 1-9.

FEINBERG, A. P., R. OHLSSON and S. HENIKOFF, 2006 The epigenetic progenitor origin of human cancer. Nat Rev Genet **7:** 21-33.

FERGUSON, E. L., and H. R. HORVITZ, 1985 Identification and characterization of 22 genes that affect the vulval cell lineages of the nematode *Caenorhabditis elegans*. Genetics **110:** 17-72.

FERGUSON, E. L., and H. R. HORVITZ, 1989 The multivulva phenotype of certain *Caenorhabditis elegans* mutants results from defects in two functionally redundant pathways. Genetics **123:** 109-121.

FINN, R. D., J. MISTRY, B. SCHUSTER-BOCKLER, S. GRIFFITHS-JONES, V. HOLLICH *et al.*, 2006 Pfam: clans, web tools and services. Nucleic Acids Res **34:** D247-251.

FISCHLE, W., Y. WANG, S. A. JACOBS, Y. KIM, C. D. ALLIS *et al.*, 2003 Molecular basis for the discrimination of repressive methyl-lysine marks in histone H3 by Polycomb and HP1 chromodomains. Genes Dev **17:** 1870-1881.

FISHER, A. G., 2002 Cellular identity and lineage choice. Nat Rev Immunol **2:** 977-982.

FOSTER, L. J., M. L. WEIR, D. Y. LIM, Z. LIU, W. S. TRIMBLE *et al.*, 2000 A functional role for VAP-33 in insulin-stimulated GLUT4 traffic. Traffic **1:** 512-521.

GILCHRIST, E. J., and D. G. MOERMAN, 1992 Mutations in the *sup-38* gene of *Caenorhabditis elegans* suppress muscle-attachment defects in *unc-52* mutants. Genetics **132:** 431-442.

GROTE, P., and B. CONRADT, 2006 The PLZF-like Protein TRA-4 Cooperates with the Gli-like Transcription Factor TRA-1 to Promote Female Development in *C. elegans*. Dev Cell **11:** 561-573.

HARRISON, M. M., C. J. CEOL, X. LU and H. R. HORVITZ, 2006 Some *C. elegans* class B synthetic multivulva proteins encode a conserved LIN-35 Rb-containing complex distinct from a NuRD-like complex. Proc Natl Acad Sci U S A **103:** 16782-16787.

HARRISON, M. M., X. LU and H. R. HORVITZ, 2007 LIN-61, one of two *Caenorhabditis elegans* malignant-brain-tumor-repeat-containing proteins, acts with the DRM and NuRD-like protein complexes in vulval development but not in certain other biological processes. Genetics **176:** 255-271.

HEDIGER, F., and S. M. GASSER, 2006 Heterochromatin protein 1, don't judge the book by its cover! Curr Opin Genet Dev **16:** 143-150.

HERMAN, M., 2001 *C. elegans* POP-1/TCF functions in a canonical Wnt pathway that controls cell migration and in a noncanonical Wnt pathway that controls cell polarity. Development **128:** 581-590.

HERMAN, M. A., and H. R. HORVITZ, 1994 The *Caenorhabditis elegans* gene *lin-44* controls the polarity of asymmetric cell divisions. Development **120:** 1035-1047.

HERMAN, R. K., 1978 Crossover suppressors and balanced recessive lethals in *Caenorhabditis elegans*. Genetics **88:** 49-65.

HILL, R. J., and P. W. STERNBERG, 1992 The gene *lin-3* encodes an inductive signal for vulval development in *C. elegans*. Nature **358:** 470-476.

HORN, P. J., and C. L. PETERSON, 2006 Heterochromatin assembly: a new twist on an old model. Chromosome Res **14:** 83-94.

HORVITZ, H. R., and J. E. SULSTON, 1980 Isolation and genetic characterization of cell-lineage mutants of the nematode *Caenorhabditis elegans*. Genetics **96:** 435-454.

HSIEH, J., J. LIU, S. A. KOSTAS, C. CHANG, P. W. STERNBERG *et al.*, 1999 The RING finger/B-box factor TAM-1 and a retinoblastoma-like protein LIN-35 modulate context-dependent gene silencing in *Caenorhabditis elegans*. Genes Dev **13:** 2958-2970.

HUANG, L. S., P. TZOU and P. W. STERNBERG, 1994 The *lin-15* locus encodes two negative regulators of *Caenorhabditis elegans* vulval development. Mol Biol Cell **5:** 395-411.

JARRIAULT, S., and I. GREENWALD, 2002 Suppressors of the egg-laying defective phenotype of *sel-12* presenilin mutants implicate the CoREST corepressor complex in LIN-12/Notch signaling in *C. elegans*. Genes Dev **16:** 2713-2728.

KAMATH, R. S., A. G. FRASER, Y. DONG, G. POULIN, R. DURBIN *et al.*, 2003 Systematic functional analysis of the *Caenorhabditis elegans* genome using RNAi. Nature **421:** 231-237.

KELLY, W. G., S. XU, M. K. MONTGOMERY and A. FIRE, 1997 Distinct requirements for somatic and germline expression of a generally expressed *Caernorhabditis elegans* gene. Genetics **146:** 227-238.

KIM, K., and C. LI, 2004 Expression and regulation of an FMRFamide-related neuropeptide gene family in *Caenorhabditis elegans*. J Comp Neurol **475:** 540-550.

KOBAYASHI, K., S. KURODA, M. FUKATA, T. NAKAMURA, T. NAGASE *et al.*, 1998 p140Sra-1 (Specifically Rac1-associated Protein) Is a Novel Specific Target for Rac1 Small GTPase. J Biol Chem **273:** 291-295.

KRIVTSOV, A. V., and S. A. ARMSTRONG, 2007 MLL translocations, histone modifications and leukaemia stem-cell development. Nat Rev Cancer **7:** 823-833.

LEHNER, B., A. CALIXTO, C. CROMBIE, J. TISCHLER, A. FORTUNATO *et al.*, 2006 Loss of LIN-35, the *Caenorhabditis elegans* ortholog of the tumor suppressor p105Rb, results in enhanced RNA interference. Genome Biol **7:** R4.

LOMBERK, G., L. WALLRATH and R. URRUTIA, 2006 The Heterochromatin Protein 1 family. Genome Biol **7:** 228.

LU, X., and H. R. HORVITZ, 1998 lin-35 and lin-53, two genes that antagonize a C. elegans Ras pathway, encode proteins similar to Rb and its binding protein RbAp48. Cell **95:** 981-991.

MADURO, M., and D. PILGRIM, 1995 Identification and cloning of *unc-119*, a gene expressed in the *Caenorhabditis elegans* nervous system. Genetics **141:** 977-988.

MELENDEZ, A., and I. GREENWALD, 2000 *Caenorhabditis elegans lin-13*, a member of the LIN-35 Rb class of genes involved in vulval development, encodes a protein with zinc fingers and an LXCXE motif. Genetics **155:** 1127-1137.

MELLO, C. C., J. M. KRAMER, D. STINCHCOMB and V. AMBROS, 1991 Efficient gene transfer in *C.elegans*: extrachromosomal maintenance and integration of transforming sequences. Embo J **10:** 3959-3970.

MILLER, M. A., V. Q. NGUYEN, M. H. LEE, M. KOSINSKI, T. SCHEDL *et al.*, 2001 A sperm cytoskeletal protein that signals oocyte meiotic maturation and ovulation. Science **291:** 2144-2147.

MILLER, M. A., P. J. RUEST, M. KOSINSKI, S. K. HANKS and D. GREENSTEIN, 2003 An Eph receptor sperm-sensing control mechanism for oocyte meiotic maturation in *Caenorhabditis elegans*. Genes Dev **17:** 187-200.

NIKAWA, J., A. MURAKAMI, E. ESUMI and K. HOSAKA, 1995 Cloning and sequence of the *SCS2* gene, which can suppress the defect of *INO1* expression in an inositol auxotrophic mutant of *Saccharomyces cerevisiae*. J Biochem **118:** 39-45.

NISHIMURA, Y., M. HAYASHI, H. INADA and T. TANAKA, 1999 Molecular cloning and characterization of mammalian homologues of vesicle-associated membrane protein-associated (VAMP-associated) proteins. Biochem Biophys Res Commun **254:** 21-26.

PENNETTA, G., P. R. HIESINGER, R. FABIAN-FINE, I. A. MEINERTZHAGEN and H. J. BELLEN, 2002 *Drosophila* VAP-33A directs bouton formation at neuromuscular junctions in a dosage-dependent manner. Neuron **35:** 291-306.

PERRY, R. J., and N. D. RIDGWAY, 2006 Oxysterol-binding protein and vesicle-associated membrane protein-associated protein are required for sterol-dependent activation of the ceramide transport protein. Mol Biol Cell **17:** 2604-2616.

POULIN, G., Y. DONG, A. G. FRASER, N. A. HOPPER and J. AHRINGER, 2005 Chromatin regulation and sumoylation in the inhibition of Ras-induced vulval development in *Caenorhabditis elegans*. Embo J **24:** 2613-2623.

PRAITIS, V., E. CASEY, D. COLLAR and J. AUSTIN, 2001 Creation of low-copy integrated transgenic lines in *Caenorhabditis elegans*. Genetics **157:** 1217-1226.

REDDIEN, P. W., E. C. ANDERSEN, M. C. HUANG and H. R. HORVITZ, 2007 DPL-1 DP, LIN-35 Rb and EFL-1 E2F act with the MCD-1 zinc-finger protein to promote programmed cell death in *Caenorhabditis elegans*. Genetics **175:** 1719-1733.

REDDIEN, P. W., S. CAMERON and H. R. HORVITZ, 2001 Phagocytosis promotes programmed cell death in *C. elegans*. Nature **412:** 198-202.

REDDY, K. C., and A. M. VILLENEUVE, 2004 *C. elegans* HIM-17 links chromatin modification and competence for initiation of meiotic recombination. Cell **118:** 439-452.

RIDDLE, D. L., T. BLUMENTHAL, B. J. MEYER and J. R. PRIESS, 1997 *C. elegans* II (Cold Spring Harbor Laboratory Press, Cold Spring Harbor, New York).

ROBERTS, T. M., and K. L. KING, 1991 Centripetal flow and directed reassembly of the major sperm protein (MSP) cytoskeleton in the amoeboid sperm of the nematode, *Ascaris suum*. Cell Motil Cytoskeleton **20:** 228-241.

SCHERTEL, C., and B. CONRADT, 2007 *C. elegans* orthologs of components of the RB tumor suppressor complex have distinct pro-apoptotic functions. Development **134:** 3691-3701.

SIEGFRIED, K. R., A. R. KIDD, 3RD, M. A. CHESNEY and J. KIMBLE, 2004 The *sys-1* and *sys-3* genes cooperate with Wnt signaling to establish the proximal-distal axis of the *Caenorhabditis elegans* gonad. Genetics **166:** 171-186.

SIEGFRIED, K. R., and J. KIMBLE, 2002 POP-1 controls axis formation during early gonadogenesis in *C. elegans*. Development **129:** 443-453.

SKEHEL, P. A., K. C. MARTIN, E. R. KANDEL and D. BARTSCH, 1995 A VAMP-binding protein from *Aplysia* required for neurotransmitter release. Science **269:** 1580-1583.

SOTO, M. C., H. QADOTA, K. KASUYA, M. INOUE, D. TSUBOI *et al.*, 2002 The GEX-2 and GEX-3 proteins are required for tissue morphogenesis and cell migrations in *C. elegans*. Genes Dev **16:** 620-632.

TABARA, H., M. SARKISSIAN, W. G. KELLY, J. FLEENOR, A. GRISHOK *et al.*, 1999 The *rde-1* gene, RNA interference, and transposon silencing in *C. elegans*. Cell **99:** 123-132.

TAKIZAWA, T., and E. MESHORER, 2008 Chromatin and nuclear architecture in the nervous system. Trends Neurosci.

THOMAS, J. H., C. J. CEOL, H. T. SCHWARTZ and H. R. HORVITZ, 2003 New genes that interact with *lin-35* Rb to negatively regulate the *let-60* ras pathway in *Caenorhabditis elegans*. Genetics **164:** 135-151.

THOMAS, J. H., and H. R. HORVITZ, 1999 The *C. elegans* gene *lin-36* acts cell autonomously in the lin-35 Rb pathway. Development **126:** 3449-3459.

TREININ, M., and M. CHALFIE, 1995 A mutated acetylcholine receptor subunit causes neuronal degeneration in *C. elegans*. Neuron **14:** 871-877.

TROJER, P., G. LI, R. J. SIMS, 3RD, A. VAQUERO, N. KALAKONDA *et al.*, 2007 L3MBTL1, a histone-methylation-dependent chromatin lock. Cell **129:** 915-928.

TSENG, R. J., K. R. ARMSTRONG, X. WANG and H. M. CHAMBERLIN, 2007 The bromodomain protein LEX-1 acts with TAM-1 to modulate gene expression in *C. elegans*. Mol Genet Genomics **278:** 507-518.

TSUBOI, D., H. QADOTA, K. KASUYA, M. AMANO and K. KAIBUCHI, 2002 Isolation of the interacting molecules with GEX-3 by a novel functional screening. Biochem Biophys Res Commun **292:** 697-701.

TSUDA, H., S. M. HAN, Y. YANG, C. TONG, Y. Q. LIN *et al.*, 2008 The Amyotrophic Lateral Sclerosis 8 Protein VAPB Is Cleaved, Secreted, and Acts as a Ligand for Eph Receptors. Cell **133:** 963-977.

UNHAVAITHAYA, Y., T. H. SHIN, N. MILIARAS, J. LEE, T. OYAMA *et al.*, 2002 MEP-1 and a homolog of the NURD complex component Mi-2 act together to maintain germline-soma distinctions in *C. elegans*. Cell **111:** 991-1002.

VON ZELEWSKY, T., F. PALLADINO, K. BRUNSCHWIG, H. TOBLER, A. HAJNAL *et al.*, 2000 The *C. elegans* Mi-2 chromatin-remodelling proteins function in vulval cell fate determination. Development **127:** 5277-5284.

WALLACE, J. A., and G. FELSENFELD, 2007 We gather together: insulators and genome organization. Curr Opin Genet Dev **17:** 400-407.

WANG, D., S. KENNEDY, D. CONTE, JR., J. K. KIM, H. W. GABEL *et al.*, 2005 Somatic misexpression of germline P granules and enhanced RNA interference in retinoblastoma pathway mutants. Nature **436:** 593-597.

WEIR, M. L., A. KLIP and W. S. TRIMBLE, 1998 Identification of a human homologue of the vesicle-associated membrane protein (VAMP)-associated protein of 33 kDa (VAP-33): a broadly expressed protein that binds to VAMP. Biochem J **333 (Pt 2):** 247-251.

YUAN, J. Y., and H. R. HORVITZ, 1990 The *Caenorhabditis elegans* genes *ced-3* and *ced-4* act cell autonomously to cause programmed cell death. Dev Biol **138:** 33-41.

ZHAO, T., T. HEYDUK, C. D. ALLIS and J. C. EISSENBERG, 2000 Heterochromatin protein 1 binds to nucleosomes and DNA *in vitro*. J Biol Chem **275:** 28332-28338.

ZHAO, Z., L. FANG, N. CHEN, R. C. JOHNSEN, L. STEIN *et al.*, 2005 Distinct regulatory elements mediate similar expression patterns in the excretory cell of *Caenorhabditis elegans*. J Biol Chem **280:** 38787-38794.

Table 1. Loss of function of any of four synMuv genes causes the green pharynx phenotype

synMuv	Gene	Homology	Green pharynx?	Allele(s) or treatment tested
Class A	***lin-8***	**LIN-8 family**	**YES**	**See Table 3**
Class A	*lin-15A*	THAP domain	No	*n767*[a]
Class A	*lin-38*	Zinc finger[c]	No	*n751*[b,c], *tm736*[d]
Class A	*lin-56*	THAP domain[e]	No	*n2728*[a,e]
Class B	*ark-1*	Ack	No	*n3701*
Class B	*dpl-1*	DP	No	*n3316*[d], *n3380*[b], *n3643*[b]
Class B	*efl-1*	E2F	No	*n3318*[d]
Class B	*epc-1*	E(Pc)	No	*n4076*[d]
Class B	*gap-1*	Gap	No	*n3535*
Class B	*hda-1*	HDAC1	No	*e1795*[d]
Class B	***hpl-2***	**HP1**	**YES**	***n4274***[a,f]***, ok916, ok917***[a]***, tm1489***[a]
Class B	*let-418*	Mi2	No	*n3536*[b], *s1617*[d]
Class B	*lex-1*	Bromodomain	No	*gu47*
Class B	*lin-9*	Mip130	No	*n112*[b], *n942*[d]
Class B	***lin-13***	**Zinc fingers**	**YES**	***n387***[d]***, n770***[b]***, n2238***[b]***, n2985***[b]***, ok838***[b]
Class B	*lin-15B*	THAP domain	No	*n744*[a]
Class B	*lin-35*	Rb	No	*n745*[a]
Class B	*lin-36*	THAP domain	No	*n766*[a], *n3096*[a]
Class B	*lin-37*	Mip40	No	*n758*[a]
Class B	*lin-52*	dLin-52	No	*n771*[b], *n3718*[d]
Class B	*lin-53*	RbAp48	No	*n833*[b], *n3368*[d]
Class B	*lin-54*	Mip120	No	*n2231*[b], *n3423*[d]
Class B	***lin-61***	**L3MBTL1**	**YES**	***sy223***[a]***, n3442***[a]***, n3446***[a]***, n3447, n3624, n3736***
Class B	*lin-65*	Novel	No	*n3441*[a]
Class B	*lst-3*	CCAR1	No	*n4590*[a,f]
Class B	*mep-1*	Zinc fingers	No	*n3703*[b], *n3680*[d]
Class B	*met-1*	SET2	No	*n3628*, *n4337*[a]
Class B	*met-2*	SETDB1	No	*n4256*[a]
Class B	*mys-1*	HAT	No	*n3681*[b], *n4075*[d]
Class B	*sli-1*	Cbl	No	*n3538*
Class B	*smo-1*	Sumo	No	*ok359*[d]
Class B	*tam-1*	RING finger	No	*cc567*[a]
Class B	*tra-4*	PLZF	No	*bc250*[a], *n3715*, *n3716*, *n4724*, *n4726*
Class B	*trr-1*	TRRAP	No	*n3630*[d], *n3712*[d]

[a] Strong loss-of-function allele, likely a null allele.

[b] Partial loss-of-function allele or altered-function allele of gene required for viability.

[c] Adam Saffer and H.R.H., unpublished results.

[d] Strong loss-of-function allele causing recessive sterility; homozygous animals are the progeny of heterozygous mothers, indicating that maternal rescue of the green pharynx phenotype cannot be excluded.

[e] Ewa Davison and H.R.H., personal communication.

[f] Erik Andersen and H.R.H., personal communication.

SynMuv mutations and RNAi treatments tested for the green pharynx phenotype as described in Materials and Methods. Genes tested are grouped by their synMuv class and then listed in alphabetical order. *tam-1(cc567)* was tested in the presence of the *cis*-marker *unc-46(e177)*. Genotypes were otherwise as indicated.

Table 2. Mutations isolated on the basis of their green pharynx phenotypes

Gene	Isolates: Total (Clonal)	Allele(s)
lin-8	44 (15)	*n3582*[a], *n3583*[a], *n3584*[a], *n3585*[a], *n3586*[a], *n3587*[a], *n3588*[a], *n3589*[a], *n3590*[a], *n3591*[a], *n3593*[a], *n3595*[a], *n3597*[a], *n3598*[a], *n3600*[b], *n3601*[b], *n3602*[b], *n3603*[b], *n3605*[b], *n3606*[b], *n3607*[b], *n3608*[c], *n3609*[c], *n3610*[c], *n3686*[d], *n3761*[e], *n3794*[f], *n3800*[f], *n3808*[f], *n3810*[f], *n3811*[f], *n3812*[f], *n3813*[f], *n3815*[f], *n3816*[f], *n3817*[f], *n3818*[f], *n4032*[g], *n4033*[g], *n4035*[g], *n4320*[h], *n4356*[h], *n4411*[i], *n4656*[e]
lnes-1	14 (10)	*n3592*[a], *n3594*[a], *n3604*[b], *n3688*[d], *n3689*[d], *n3795*[f], *n3796*[f], *n3803*[f], *n3814*[f], *n3822*[f], *n3917*[j], *n3919*[j], *n3921*[j], *n4038*[g],
lin-13	9 (8)	*n3596*[a], *n3797*[f], *n3801*[f,k], *n3802*[f,k], *n3804*[f,k], *n3907*[j,k], *n3918*[j,k], *n3920*[j], *n3989*[j]
lin-61	4 (4)	*n3687*[d], *n3807*[f], *n3809*[f], *n3922*[l]
gei-4	1 (1)	*n4319*[h]
pag-6	1 (0)	*n3599*[a]
hpl-2	none[l]	
Unknown	1 (1)	*n3841*[f,m]

[a] Isolated as an F_2 animal in a *nIs128* screen intended to recover hermaphrodites with surviving CEMs.

[b] Isolated as an F_2 animal in a *nIs130* screen intended to recover hermaphrodites with surviving CEMs.

[c] Isolated as an F_2 animal in a *nIs133* screen intended to recover hermaphrodites with surviving CEMs.

[d] Isolated as F_3 embryos trapped within egg-laying-defective F_2 progeny of mutagenized animals in a screen intended to recover *nIs133*; *tra-2(n1106)* hermaphrodites without surviving CEMs (H.T.S. and H.R.H., unpublished results).

[e] Isolated as a previously unnoticed background mutation in a pre-existing strain.

[f] Isolated as F_2 embryos in a clonal *sem-4(n1378)*; *nIs128* screen intended to recover mutations causing the green pharynx phenotype in embryos and larvae.

[g] Isolated as an F_2 animal in a *nIs128* screen intended to recover suppressors of the Unc phenotype of *cnd-1(n3786)* (H.T.S. and H.R.H., unpublished results).

[h] Isolated by Johanna Varner in a clonal *nIs133* screen intended to recover *ceh-30(n3714*gf*)* hermaphrodites without surviving CEMs (J. Varner, H.T.S., and H.R.H., unpublished results).

[i] Isolated by Johanna Varner in a clonal *nIs128* screen intended to recover *ceh-30(n3714*gf*)* hermaphrodites without surviving CEMs (J. Varner, H.T.S., and H.R.H., unpublished results).

[j] Isolated as F_2 embryos in a clonal *nIs133*; *egl-1(n1084)* screen intended to recover mutations causing the green pharynx phenotype in embryos and larvae.

[k] Mutation recessively causes sterility.

[l] *hpl-2(*lf*)* homozygous progeny of *hpl-2(*lf*)*/+ heterozygous mothers are maternally rescued for the green pharynx phenotype, so that *hpl-2* alleles would not be detected in the F_2 generation. Only nine green pharynx screen isolates were recovered as F_3 progeny of mutagenized animals; none of these was an allele of *hpl-2*.

[m] *n3841* causes a weakly penetrant dominant green pharynx phenotype and by mapping and sequencing is likely not an allele of any known green pharynx gene.

Mutations isolated on the basis of their causing the green pharynx phenotype of transgene misexpression. The origins of each mutation are indicated. For each gene, the total number of isolates and the number of isolates isolated clonally, using methods that would permit the recovery of mutations causing both a green pharynx phenotype and inviability, are indicated.

Table 3. *lin-8* alleles and their synMuv and green pharynx properties

Allele(s)	Position	Sequence wild-type	Sequence mutant	Mutation	synMuv?	green pharynx?
n3761	39127	CCA	CTA	P16L	**No**	Yes
n111[a]	39139	CTG	CCG	L20P	Yes	Yes
n3815[b]	39168	CCG	TCG	P30S	**No**	Yes
n4415[c]	39280	GTG	GGG	V67G	Yes	Yes
n3812[b], *n2741*[a]	39282	GTG	ATG	V68M	Yes	Yes
n3794[b], *n3810*[b]	39307	CCG	CTG	P76L	**No**	Yes
n3582[b]	39355	CCG	CTG	P92L	Yes	Yes
n4033[b]	39363	GCA	ACA	A95T	Yes	Yes
n3800[b], *n4320*	40257	TCG	TTG	S110L	**No**	Yes
n4032[b]	40302	CGG	CAG	R125Q	Yes	Yes
n3585[b], *n3598*[b]	40308	CGC	CAC	R127H	Yes	Yes
n4371[c]	40313	GCA	ACA	A129T	Yes	Yes
n4443[c]	40364	CGC	TGC	R146C	Yes	Yes
n3646[d]	40365	CGC	CAC	R146H	Yes	Yes
n2376[a]	40370	GAG	AAG	E148K	Yes	**No**
n3808[b]	40380	GGC	GTC	G151V	**Weak**	Yes
n2378[a]	40388	CGC	TGC	R154C	Yes	Yes
n2403[a], *n2724*[a], *n3607*, *n3816*[b]	40418	GAG	AAG	E164K	Yes	Yes
n3593[b]	42238	CGT	TGT	R343C	**No**	Yes
n3591[b]	42250	GAG	AAG	E347K	**No**	Yes
n3686	38077-41978[e]			Large deletion[e]	Yes	Yes
n4416[c]	39279	AAAGTG	AAATG	-1 frameshift[f]	Yes	Yes
n2738[a], *n3597*[b]	39316	TGG	TAG	W79amber	Yes	Yes
n3583[b], *n3817*[b], *n3818*[b], *n4373*[c], *n4422*[c]	39317	TGG	TGA	W79opal	Yes	Yes
n2731[a]	40265	CAA	TAA	Q113ochre	Yes	Yes
n4417[c]	40273	TAC	TAA	Y115ochre	Yes	Yes
n3608	40295	AGA	TGA	R123opal	Yes	Yes
n4372[c], *n4414*[c]	40343	CAA	TAA	Q139ochre	Yes	Yes
n3605, *n3811*[b]	40368	TGG	TAG	W147amber	Yes	Yes
n3606, *n4411*[b]	40369	TGG	TGA	W147opal	Yes	Yes
n3603, *n4656*	40397	CGA	TGA	R157opal	Yes	Yes
n3595[b]	40416	TGG	TAG	W163amber	Yes	Yes
n3587[b]	40417	TGG	TGA	W163opal	Yes	Yes
n4356	40469	AGA	TGA	R181opal	Yes	Yes
n3581[d]	40492	AAAGGT	AAAGT	-1 frameshift[g]	Yes	Yes
n3610, *n3813*[b]	40594	TGG	TGA	W222opal	Yes	Yes
n3600	40851	CAA	TAA	Q231ochre	Yes	Yes

n4420[c]	40863	CAA	TAA	Q235ochre	Yes	Yes
n4035[b]	40924 - 40970			47 bp deletion[h]	Yes	Yes
n3609	40995	CAG	TAG	Q279amber	Yes	Yes
n3584[b]	41025	CAG	TAG	Q289amber	Yes	Yes
n4423[c]	41048	CAG	TAG	Q297amber	Yes	Yes
n2739[a]	41070	AGA	TGA	R304opal	Yes	Yes
n3586[b], *n3588*[b]	42229	CAA	TAA	Q340ochre	Yes	Yes
n3590[b]	39069	tgcagaatc	tgcaaaatc	noncoding[i]	**No**	Yes
n3589[b], *n4376*[c]	39403	TAgtgag	TAatgag	Exon 1 donor	Yes	Yes
n3602	40616	GAgtgag	GAgtgaa	Exon 2 donor	**No**	Yes
n3601	40843	ttcagAC	ttcaaAC	Exon 3 acceptor	**Weak**	Yes

[a] Mutation isolated on the basis of a synMuv phenotype. This mutation has previously been described by Davison *et al.* (2005).

[b] Mutation isolated in a *nIs128* background and remains linked to *nIs128*.

[c] Mutation isolated on the basis of a synMuv phenotype by Adam Saffer and H.R.H. (unpublished results).

[d] Mutation isolated on the basis of a synMuv phenotype by John Doll and H.R.H. (unpublished results).

[e] The extent of the *n3686* deletion is not clear; the nucleotides listed describe the minimum missing sequence, and the deletion could be ~1500 bp larger. At least the first three exons of *lin-8* are missing, and the fourth exon may also be missing; for more information, see Materials and Methods.

[f] *n4416* is predicted to cause a frameshift after amino acid 66.

[g] *n3581* is predicted to cause a frameshift after amino acid 191.

[h] The 47 bp deletion *n4035* also has 9 nucleotides inserted at the site of deletion and is predicted to cause a frameshift after amino acid 258.

[i] The noncoding mutation *n3590* alters a residue 12 nucleotides before the open reading frame begins.

A complete list of identified *lin-8* mutations. Missinse mutations are listed first, followed by nonsense mutations and then by noncoding and splice site mutations. Within these categories, mutations are listed in an order determined by their positions within *lin-8*. All alleles listed were isolated as green pharynx isolates and are listed in Table 2 or were isolated in genetic screens for Multivulva animals as indicated with superscripts. Position refers to nucleotides in the sequence of cosmid B0454 (Accession number AF025452). Sequences from wild-type and mutant animals are shown, with the affected nucleotide underlined. For missense, stop, and frameshift mutations, the wild-type and mutant sequences of the relevant codon or codons are shown. For noncoding and splice site mutations, wild-type and mutant sequences are shown with noncoding nucleotides in lowercase and coding nucleotides in uppercase. SynMuv and green pharynx phenotypes were tested as described in Materials and Methods. Alleles described as weakly synMuv caused a low-expressivity Muv phenotype in a minority of animals when combined with the class B synMuv mutation *lin-36(n766)*. All other mutations either caused a strongly expressive synMuv phenotype in all animals when combined with *lin-36(n766)* or were not observed to cause a synMuv phenotype.

Table 4. *lnes-1* alleles

Allele(s)	Position	Sequence		Mutation
		wild-type	mutant	
n3604, *n3689*	36151	CGC	TGC	R119C
n3917	35385 - 35465			81 bp deletion[a]
n3796[b]	36424	CAG	TAG	Q47amber
n3592[b]	36350	TGG	TGA	W71opal
n3795[b]	36089	TGG	TGA	W139opal
n3919	36042	TGG	TAG	W155amber
n3594[b]	36041	TGG	TGA	W155opal
n3822[b]	36016	CAA	TAA	Q164ochre
n4038[b,c]	35912	TGG	TGA	W198opal
n3803[b]	35020	CAG	TAG	Q309amber
n3921	35388	tttcagCC	tttcaaCC	Exon 3 acceptor
n3688	35087	ttgcagAA	ttgcaaAA	Exon 4 acceptor

[a] The deletion *n3917* removes the splice acceptor and first 3 nucleotides of exon 3. There is a second mutation, at 35308, causing the change P230S (CCC to TCC).

[b] Isolated in a *nIs128* background and remains linked to the *nIs128* transgene.

[c] The nonsense mutation *n4038* is linked to a second mutation, at 35409, causing the change R52W (CGG to TGG).

Position refers to nucleotides in the sequence of cosmid B0454. Sequences from wild-type and mutant animals are shown, with the affected nucleotide underlined. For missense and stop mutations, the wild-type and mutant sequences of the relevant codon are shown. For noncoding and splice site mutations, wild-type and mutant sequences are shown with noncoding nucleotides in lowercase and coding nucleotides in uppercase. One isolate, *n3814*, was allelic with *lnes-1* by complementation but did not contain any identifiable mutation in the *lnes-1* coding sequence or in its immediate proximity.

Table 5. synMuv properties of the green pharynx gene *lnes-1*

A. Loss of *lnes-1* function does not cause a synMuv phenotype.

Genotype	% Muv at 20°C (n)	% Muv at 25°C (n)
wild-type	0 100	0 100
lin-15A(n767)	0 100	0 200
lnes-1(n3604); *lin-15A(n767)*	0 100	0 100
lnes-1(n3917); *lin-15A(n767)*	0 100	0 100
lin-15B(n744)	0 105	0 68
lnes-1(n3604); *lin-15B(n744)*	0 103	0 100
lnes-1(n3917); *lin-15B(n744)*	0 100	0 100

B. Loss of *lnes-1* function might weakly suppress the synMuv phenotype in sensitized strains.

Genotype	% Muv at 17.5°C (n)	% Muv at 20°C (n)
wild-type	0 (100)	0 (100)
lin-15AB(n765)	81 (100)	100 (100)
lnes-1(n3917); *lin-15AB(n765)*	28 (101)	100 (100)
lin-15AB(n2993 n433)	3 (100)	28 (100)
lnes-1(n3917); *lin-15AB(n2993 n433)*	0 (100)	4 (104)

Genotypes were as indicated. Muv (Multivulva phenotype) was scored as described in Materials and Methods.

Table 6. synMuv properties of the green pharynx gene *gei-4*

A. *gei-4(*zygotic RNAi*)*, but not *gei-4(n4319)*, causes a class B synMuv phenotype.

Genotype	% Muv at 20°C (n)	% Muv at 25°C (n)
wild-type	0 (100)	0 (100)
lin-15A(n767)	0 (151)	0 (100)
gei-4(n4319); *lin-15A(n767)*	1 (150)	0 (100)
*gei-4(*zygotic RNAi*)*; *lin-15A(n767)*	98 (52)	88 (50)
lin-15B(n744)	0 (105)	0 (68)
gei-4(n4319); *lin-15B(n744)*	0 (100)	0 (100)
lin-36(n766)	0 (100)	0 (100)
*gei-4(*zygotic RNAi*)*; *lin-36(n766)*	0 (21)	0 (30)

B. *gei-4(n4319)* may weakly enhance the synMuv phenotype of a sensitized strain.

Genotype	% Muv at 17.5°C (n)	% Muv at 20°C (n)
wild-type	0 (100)	0 (100)
lin-15AB(n2993 n433)	0 (100)	62 (100)
gei-4(n4319); *lin-15AB(n2993 n433)*	0 (100)	98 (100)

Zygotic RNAi targeting *gei-4* was performed as described in Materials and Methods. Animals treated with zygotic RNAi were heterozygous for *rde-1(ne219)* and for *dpy-11(e224)*. *lin-36(n766)* zygotic RNAi animals were also heterozygous for *him-5(e1467)*. All other genotypes were as indicated. Muv (Multivulva phenotype) was scored as described in Materials and Methods.

Table 7. synMuv properties of the green pharynx gene *pag-6*

A. Altered *pag-6* function causes a weak class B synMuv phenotype.

Genotype	% Muv at 20°C (n)	% Muv at 22.5°C (n)
wild-type	0 (100)	0 (100)
pag-6(n3599)	0 (100)	0 (100)
lin-8(n2731)	0 (100)	0 (100)
lin-8(n2731); *pag-6(n3599)*	12 (100)	26 (100)
lin-15A(n767)	0 (100)	0 (100)
pag-6(n3599); *lin-15A(n767)*	8 (315)	25 (100)
lin-38(n751)	0 (100)	0 (100)
lin-38(n751); *pag-6(n3599)*	14 (100)	30 (100)
lin-56(n2728)	0 (100)	1 (100)
lin-56(n2728); *pag-6(n3599)*	4 (100)	13 (100)
lin-36(n766)	0 (100)	0 (100)
pag-6(n3599); *lin-36(n766)*	0 (100)	0 (100)

B. Loss of *pag-6* function does not cause a synMuv phenotype.

Genotype	% Muv at 20°C (n)	% Muv at 22.5°C (n)
wild-type	0 (100)	0 (100)
*pag-6(n3599 n5161*lf*)*	0 (100)	0 (100)
lin-15A(n767)	0 (100)	0 (100)
*pag-6(n3599 n5161*lf*)*; *lin-15A(n767)*	0 (100)	0 (100)
lin-15B(n744)	0 (100)	0 (100)
*pag-6(n3599 n5161*lf*)*; *lin-15AB(n744)*	0 (100)	0 (100)

C. Loss of *pag-6* function does not modify the synMuv phenotype in sensitized strains.

Genotype	% Muv, 17.5°C (n)	% Muv, 20°C (n)
wild-type	0 (100)	0 (100)
lin-15AB(n765)	66 (111)	100 (50)
*pag-6(n3599 n5161*lf*)*; *lin-15AB(n765)*	67 (103)	100 (50)
lin-15AB(n2993 n433)	0 (102)	69 (91)
*pag-6(n3599 n5161*lf*)*; *lin-15AB(n2993 n433)*	0 (108)	65 (102)

All genotypes were as indicated. Muv was scored as described in Materials and Methods.

Table 8. Synthetic lethality with *pag-6(n3599)*

synMuv class	Gene	Homology	Green pharynx?	*n3599* Synthetic lethality?	Allele(s) tested
A	*lin-8*	LIN-8 family	**YES**	No	*n2731*[a]
A	*lin-15A*	THAP domain	No	No	*n767*[a]
A	*lin-38*	Zinc finger[c]	No	No	*n751*[b,c]
A	*lin-56*	THAP domain	No	No	*n2728*[a]
B	*dpl-1*	DP	No	**YES**	*n2994*[b], *n3380*[b], *n3643*[b]
B	*hpl-2*	HP1	**YES**	No	*tm1489*[a]
B	*let-418*	Mi2	No	No	*n3536*[b]
B	*lin-9*	Mip130	No	**YES**	*n112*[b]
B	*lin-13*	Zinc fingers	**YES**	No	*n770*[b]
B	*lin-15B*	THAP domain	No	**YES**	*n744*[a]
B	*lin-35*	Rb	No	**YES**	*n745*[a]
B	*lin-36*	THAP domain	No	No	*n766*[a]
B	*lin-37*	Mip40	No	**YES**	*n758*[a]
B	*lin-52*	dLin-52	No	No	*n771*[b]
B	*lin-54*	Mip120	No	**YES**	*n2231*[b]
B	*lin-61*	L3MBTL1	**YES**	No	*n3809*[a]
B	*mys-1*	HAT	No	No	*n3681*[b]
N/A	*let-60*	Ras	No	No	*n1046*[d]
N/A	*isw-1*	Isw1p	No	No	*n3294*[b]
N/A	*gei-4*	Coiled coil	**YES**	No	*n4319*[b]
N/A	*lnes-1*	LIN-8 family	**YES**	No	*n3917*[a]
N/A	*mcd-1*	Zinc finger	No	**YES**	*n4005*[c]
N/A	*fzr-1*	Cdh1/Hct1/FZR	No	No	*ku298*[a]
N/A	*psa-1*	SWI3	No	No	*ku355*[b]
N/A	*spr-1*	CoREST	No	No	*ar200*[b]
N/A	*ubc-18*	UBCH7	No	No	*ku354*[b]
N/A	*xnp-1*	SNF2	No	No	*fd2*[b]

[a] Strong loss-of-function allele, likely a null allele.
[b] Partial loss-of-function allele or altered-function allele of gene required for viability.
[c] Mutation causing altered gene function; Adam Saffer and H.R.H., personal communication.
[d] Gain-of-function or altered-function mutation.

A list of synMuv and selected other mutations tested for synthetic lethality with *pag-6(n3599)*. In the case of genes required for fertility, partial loss-of-function mutations that did not cause sterility were used. Non-synMuv mutants that were tested for synthetic lethality with *pag-6(n3599)* are listed as "N/A" for "not applicable" in the

synMuv class column; these mutants include *let-60(n1046*gf*)*, which causes a Muv phenotype; *isw-1(n3294)*, which suppresses the synMuv phenotype; the green pharynx mutant *lnes-1(n3917Δ)*; *gei-4(n4319)*, a viable allele of the green pharynx and class B synMuv gene *gei-4* that causes the green pharynx phenotype but not a synMuv phenotype; and alleles of *mcd-1*, *fzr-1*, *psa-1*, *spr-1*, *ubc-18*, and *xnp-1*, genes required redundantly with *lin-35 Rb* for viability. *lin-8(n2731)* was tested in animals homozygous for *dpy-4(e1166)*; genotypes were otherwise as indicated.

Table S1. Testing genes that interact with the synMuv genes for the green pharynx phenotype

Gene	Homology	Green pharynx?	Allele(s) or treatment tested
lin(n3542)	unknown	No	*n3542*
lin(n3707)	unknown	No	*n3707*
uba-2	Uba2	No	RNAi[a]
ubc-9	Ubc9p	No	*ju484*[b]
ssl-1	p400	No	*n4077*[c]
ruvb-1	RuvB-like 1	No	RNAi[a]
ruvb-2	RuvB-like 2	No	RNAi[a]
dcp-66	p66	No	*gk370*[c]
chd-3	Mi2	No	*eh4*[d]
pcaf-1	PCAF	No	RNAi[a]
ada-2	Ada2b	No	RNAi[a]
lin-40	MTA1	No	*ku285*[b], *s1593*[c], *s1669*[c]
hpl-2	HP1	No	*n4317*[d]
let-60	Ras	No	*n1046*[e]
isw-1	Isw1p	No	*n3294*[b]
mes-2	E(z)	No	*bn11*[d]
mes-3	Novel	No	*bn35*[d]
mes-4	MMSET	No	*bn23*[d], *bn67*[d]
mes-6	Esc	No	*bn66*[b]
mcd-1	Zinc finger	No	*n4005*[f]
fzr-1	Cdh1/Hct1/FZR	No	*ku298*[d]
psa-1	SWI3	No	*ku355*[b]
spr-1	CoREST	No	*ar200*[b]
ubc-18	UBCH7	No	*ku354*[b]
xnp-1	SNF2	No	*fd2*[b]

[a] RNAi was performed by feeding as described in Materials and Methods.

[b] Partial loss-of-function allele or altered-function allele of gene required for viability.

[c] Strong loss-of-function allele causing recessive sterility; homozygous animals are the progeny of heterozygous mothers, indicating that maternal rescue of the green pharynx phenotype cannot be excluded.

[d] Strong loss-of-function allele, likely a null allele.

[e] Mutation causing increased or altered gene function.

[f] Mutation causing altered gene function; Adam Saffer and H.R.H., unpublished results.

A list of synMuv mutations, selected other mutations, and RNAi treatments tested for the green pharynx phenotype as described in Materials and Methods. Genes tested include *lin(n3542)* and *lin(n3707)*, which are linked to *lin-15A(n767)* and either cause Muv phenotypes or cause synthetic Muv phenotypes in a *lin-15A(n767)* background; *uba-2* and *ubc-9*, genes for which RNAi has been reported to cause a Muv phenotype in both a class A and a class B synMuv background; *ssl-1*, *ruvb-1*, *ruvb-2*, *pcaf-1*, and *ada-2*, genes that, on the basis of homology and in some cases similar ectopic expression phenotypes, have been proposed to act with the synMuv genes previously known as class C; *dcp-66*, which has been proposed on the basis of homology and similar ectopic expression phenotypes to act with selected class B synMuv genes; two genes, *chd-3* and *lin-40* (*lin-40* is also known as *egr-1*), for which RNAi treatments, but not available alleles, have been reported to cause a synMuv phenotype; *hpl-1*, which is homologous to and synthetically Muv with the class B synMuv gene *hpl-2*; *let-60(n1046*gf*)*, which causes a Muv phenotype; *mcd-1*, a gene that acts with selected synMuv genes in promoting programmed cell death; *isw-1* and *mes-2*, *-3*, *-4*, and *-6*, genes that encode chromatin factors required for the synMuv phenotype; and *fzr-1*, *psa-1*, *spr-1*, *ubc-18*, and *xnp-1*, genes required redundantly with *lin-35 Rb* for viability. *ubc-9(ju484)* animals were homozygous for the *cis* marker *dpy-13(e184)*. Genotypes were otherwise as indicated.

Figure legends

Figure 1

Model for how misexpression of a *gfp* transgene generates the green pharynx phenotype. (A) Expression of the *pkd-2::gfp* reporter *nIs133* in a wild-type L4 larval hermaphrodite and in a green pharynx mutant, a *lin-8(n2731)* L4 larval hermaphrodite. Images are composites of fluorescence and visible light images. The only strong expression seen in hermaphrodites is that in the posterior bulb of the pharynx of green pharynx mutants. (B) A model for the transgene misexpression causing the green pharynx phenotype. *gfp* reporter transgenes containing vector sequences can cause pharyngeal GFP expression in a wild-type background, shown diagrammatically in the male at right. In a wild-type genetic background, pharyngeal expression can be prevented by the inclusion of genomic sequences capable of driving specific gene expression; as an example, the expression of *pkd-2::gfp* in male-specific sensory neurons is shown diagrammatically. Green pharynx proteins are recruited by these genomic sequences and act to prevent inappropriate reporter expression driven by sequences in the plasmid vector. In green pharynx mutant animals, the specific expression driven by the included genomic sequences is retained and in addition reporter expression is observed in the pharynx. When vector sequences are removed, pharyngeal expression is lost even in green pharynx mutant animals.

Figure 2

The homologous genes *lin-8* and *lnes-1* both function to prevent inappropriate gene expression. (A) Genomic organization of the locus containing both *lin-8* and *lnes-1*. The

lin-8 and *lnes-1* genomic rescuing constructs are shown as horizontal bars respectively labeled "EMD13" and "BSK-*lnes-1*." (B) Alignment of the full-length sequences of LIN-8 and LNES-1. Identical residues are surrounded with black boxes, and similar residues are surrounded with gray boxes. Missense mutations that cause both a green pharynx phenotype and a synMuv phenotype are indicated with black arrowheads. Missense mutations that cause a green pharynx phenotype but do not cause a synMuv phenotype are indicated with green arrowheads. The *lin-8* mutation *n2376*, which causes a synMuv phenotype but does not cause a green pharynx phenotype, is indicated with a blue arrowheads.

Figure 3

A missense mutation in PAG-6 causes the green pharynx phenotype. (A) Genomic organization of the *pag-6* locus. The positions of phenotypic markers and DNA polymorphisms used in mapping *pag-6* are shown. The genomic duplication *yDp1*, which does not complement *pag-6*, ends between polymorphisms at approximately 297 kb on Y105C5A and 50 kb on Y105C5B. The interval into which *pag-6(n3599)* was mapped, between 50 kb and 126 kb on Y105C5B, is shown in greater detail, including the positions and extents of predicted protein-coding genes. The *pag-6* genomic rescuing construct is shown as a horizontal bar labeled "BSK-*pag-6*." (B) Diagrammatic representation of PAG-6. The extents of the MSP domain and of the C-terminal domain conserved in three other *C. elegans* proteins are shown. The positions of the green pharynx missense mutation *n3599* and of the *pag-6* loss-of-function frameshift mutation *n5161* are indicated. (C) The C-terminal domain of PAG-6 (accession number

CAB54365) is aligned with the homologous domains within the predicted *C. elegans* proteins M199.2 (CAB70252), T25D1.1 (AAA82466), and T27A8.5 (CAA92224). A fifth family member, F43D2.2, does not contain homology across the entire domain and is not included. Residues identical among at least three of the four proteins are surrounded with black boxes, and residues similar among at least three of the four proteins are surrounded with gray boxes. The position of the *pag-6* green pharynx missense mutation *n3599* is indicated.

Figure 4

A model for the function of the green pharynx genes in preventing inappropriate gene expression. According to this model, in the green pharynx phenotype as seen using a *gfp* transgene, the green pharynx proteins are recruited to promoter sequences. The green pharynx proteins act to repress pharyngeal transcription driven by a nearby cryptic enhancer element. We propose that the green pharynx proteins act similarly at endogenous genomic loci to prevent weak or fortuitous enhancer elements near genes from altering their patterns of expression.

Figure S1

A rescuing *lnes-1::gfp* transgene gives expression in most or all nuclei. (A) Fluorescence micrograph showing expression of a rescuing *lnes-1::gfpC::lnes-1* transgene in the head of an L4 larva. (B) Nomarski micrograph corresponding to the fluorescence micrograph in panel A. (C) Composite image created by merging panels A and B. Note that GFP is localized to the nuclei of many cells, and that these

lnes-1::gfp-expressing cells can be identified by their positions and their Nomarski morphology as being of multiple different cell types. Anterior is left, ventral is down.

Figure S2

A rescuing *pag-6::gfp* transgene gives expression in most or all nuclei. (A) Fluorescence micrograph showing expression of a rescuing *pag-6::gfp* transgene in the head of an L4 larva. (B) Nomarski micrograph corresponding to the fluorescence micrograph in panel A. (C) Composite image created by merging panels A and B. Note that GFP is tightly localized within the nuclei of many cells, possibly to the nucleolus. The extremely tight localization might reflect normal localization or might be an artifact of overexpression. Note also that these *pag-6::gfp*-expressing cells can be identified by their positions and their Nomarski morphology as being of multiple different cell types. Anterior is left, ventral is down.

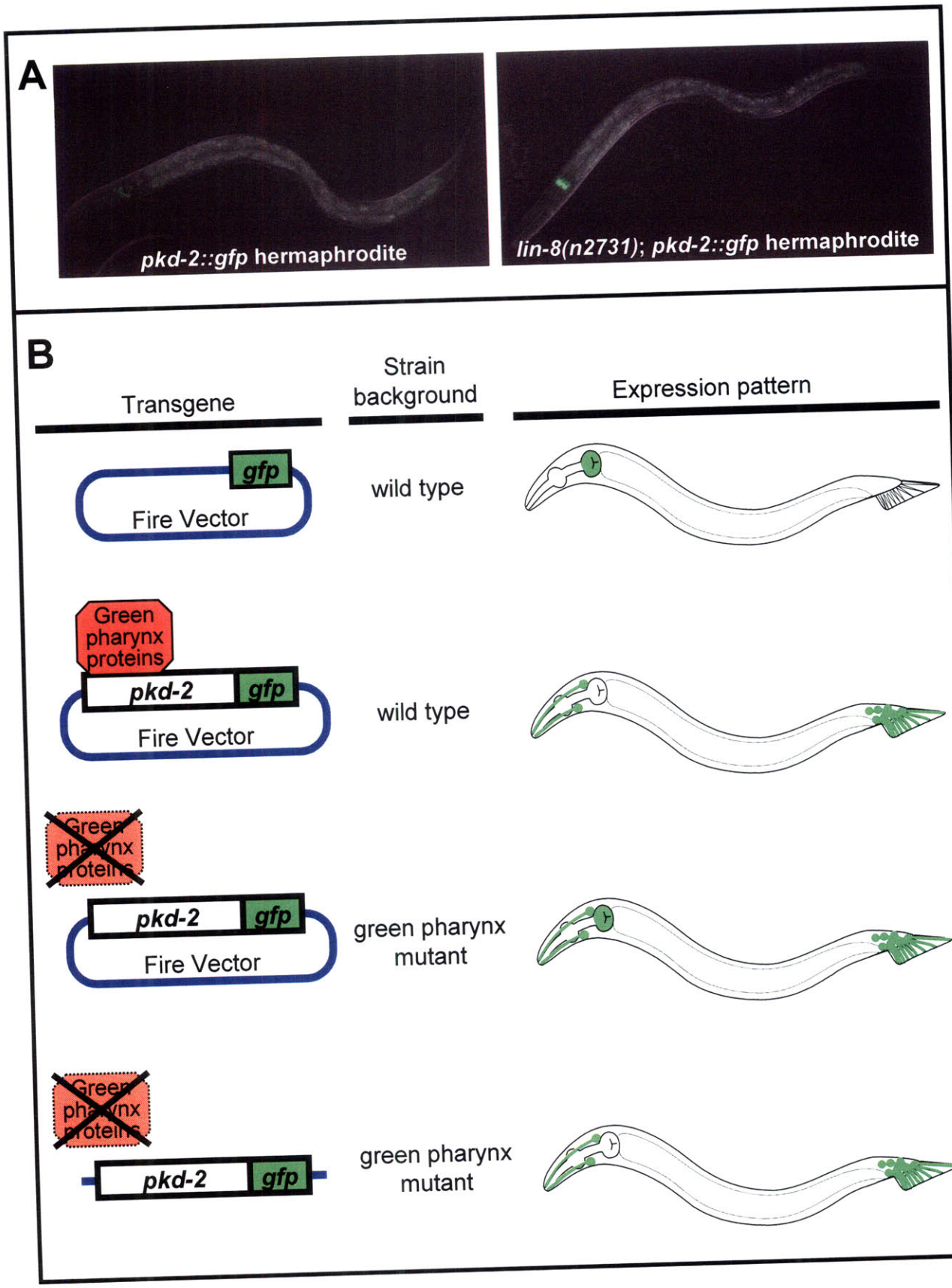
A
pkd-2::gfp hermaphrodite
lin-8(n2731); pkd-2::gfp hermaphrodite
B
Transgene
Strain background
Expression pattern
gfp
Fire Vector
wild type
Green pharynx proteins
pkd-2
gfp
Fire Vector
wild type
pkd-2
gfp
Fire Vector
green pharynx mutant
pkd-2
gfp
green pharynx mutant

Figure 1

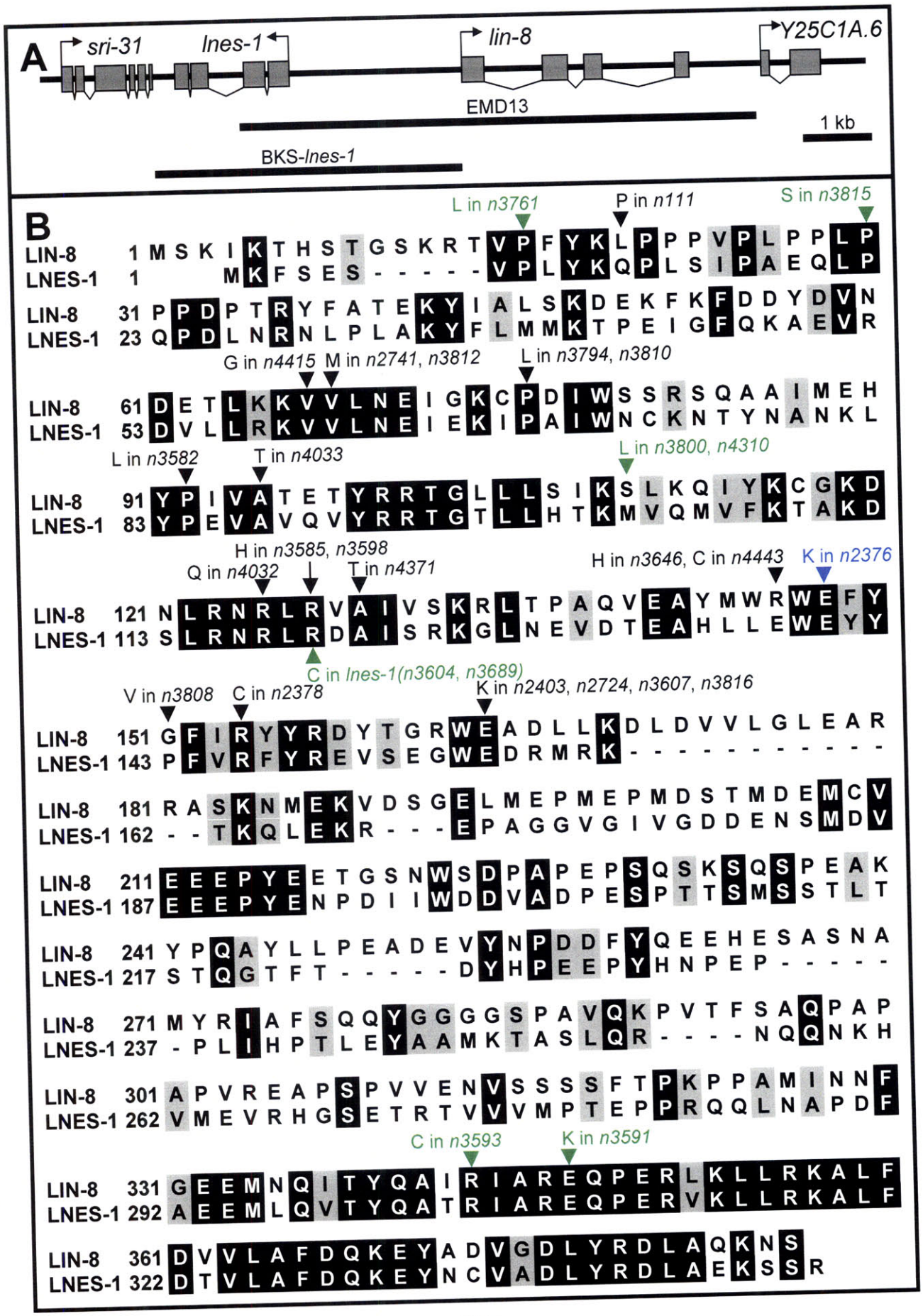
A
sri-31
lnes-1
lin-8
Y25C1A.6
EMD13
1 kb
BKS-lnes-1
B
L in n3761
P in n111
S in n3815
LIN-8 1 M S K I K T H S T G S K R T V P F Y K L P P P V P L P P L P
LNES-1 1 M K F S E S - - - - - V P L Y K Q P L S I P A E Q L P
LIN-8 31 P P D P T R Y F A T E K Y I A L S K D E K F K F D D Y D V N
LNES-1 23 Q P D L N R N L P L A K Y F L M M K T P E I G F Q K A E V R
G in n4415
M in n2741, n3812
L in n3794, n3810
LIN-8 61 D E T L K K V V L N E I G K C P D I W S S R S Q A A I M E H
LNES-1 53 D V L L R K V V L N E I E K I P A I W N C K N T Y N A N K L
L in n3582
T in n4033
L in n3800, n4310
LIN-8 91 Y P I V A T E T Y R R T G L L L S I K S L K Q I Y K C G K D
LNES-1 83 Y P E V A V Q V Y R R T G T L L H T K M V Q M V F K T A K D
H in n3585, n3598
Q in n4032
T in n4371
H in n3646, C in n4443
K in n2376
LIN-8 121 N L R N R L R V A I V S K R L T P A Q V E A Y M W R W E F Y
LNES-1 113 S L R N R L R D A I S R K G L N E V D T E A H L L E W E Y Y
C in lnes-1(n3604, n3689)
V in n3808
C in n2378
K in n2403, n2724, n3607, n3816
LIN-8 151 G F I R Y Y R D Y T G R W E A D L L K D L D V V L G L E A R
LNES-1 143 P F V R F Y R E V S E G W E D R M R K - - - - - - - - - -
LIN-8 181 R A S K N M E K V D S G E L M E P M E P M D S T M D E M C V
LNES-1 162 - - T K Q L E K R - - - E P A G G V G I V G D D E N S M D V
LIN-8 211 E E E P Y E E T G S N W S D P A P E P S Q S K S Q S P E A K
LNES-1 187 E E E P Y E N P D I I W D D V A D P E S P T T S M S S T L T
LIN-8 241 Y P Q A Y L L P E A D E V Y N P D D F Y Q E E H E S A S N A
LNES-1 217 S T Q G T F T - - - - - D Y H P E E P Y H N P E P - - - - -
LIN-8 271 M Y R I A F S Q Q Y G G G G S P A V Q K P V T F S A Q P A P
LNES-1 237 - P L I H P T L E Y A A M K T A S L Q R - - - - N Q Q N K H
LIN-8 301 A P V R E A P S P V V E N V S S S S F T P K P P A M I N N F
LNES-1 262 V M E V R H G S E T R T V V V M P T E P P R Q Q L N A P D F
C in n3593
K in n3591
LIN-8 331 G E E M N Q I T Y Q A I R I A R E Q P E R L K L L R K A L F
LNES-1 292 A E E M L Q V T Y Q A T R I A R E Q P E R V K L L R K A L F
LIN-8 361 D V V L A F D Q K E Y A D V G D L Y R D L A Q K N S
LNES-1 322 D T V L A F D Q K E Y N C V A D L Y R D L A E K S S R

Figure 2

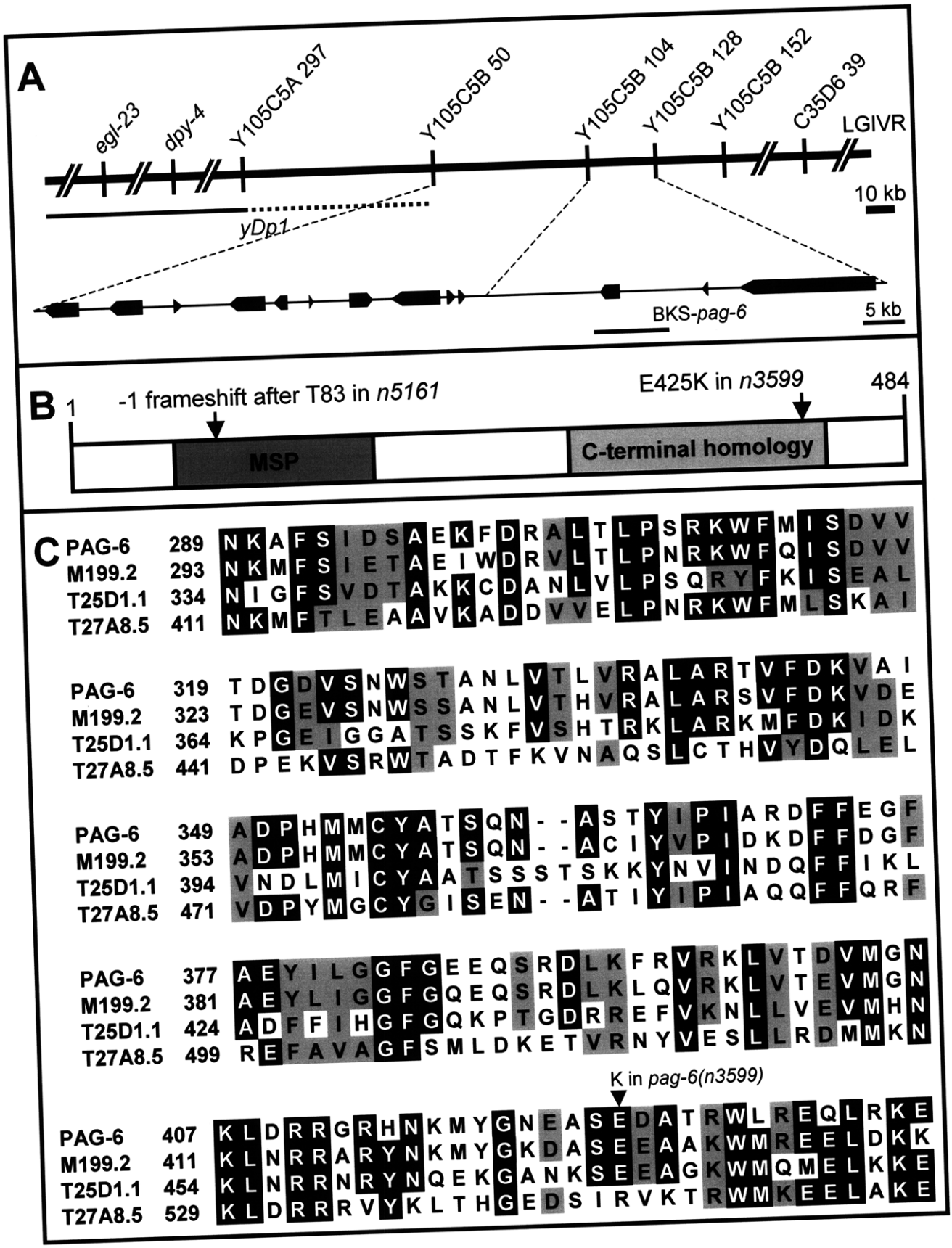
A
egl-23
dpy-4
Y105C5A 297
Y105C5B 50
Y105C5B 104
Y105C5B 128
Y105C5B 152
C35D6 39
LGIVR
10 kb
yDp1
BKS-pag-6
5 kb
B
1
-1 frameshift after T83 in n5161
E425K in n3599
484
MSP
C-terminal homology
C
PAG-6 289 NKAFSIDSAEKFDRALTLPSRKWFMISDVV
M199.2 293 NKMFSIETAEIWDRVLTLPNRKWFQISDVV
T25D1.1 334 NIGFSVDTAKKCDANLVLPSQRYFKISEAL
T27A8.5 411 NKMFTLEAAVKADDVVELPNRKWFMLSKAI
PAG-6 319 TDGDVSNWSTANLVTLVRALARTVFDKVAI
M199.2 323 TDGEVSNWSSANLVTHVRALARSVFDKVDE
T25D1.1 364 KPGEIGGATSSKFVSHTRKLARKMFDKIDK
T27A8.5 441 DPEKVSRWTADTFKVNAQSLCTHVYDQLEL
PAG-6 349 ADPHMMCYATSQN--ASTYIPIARDFFEGF
M199.2 353 ADPHMMCYATSQN--ACIYVPIDKDFFDGF
T25D1.1 394 VNDLMICYAATSSSTSKKYNVINDQFFIKL
T27A8.5 471 VDPYMGCYGISEN--ATIYIPIAQQFFQRF
PAG-6 377 AEYILGGFGEEQSRDLKFRVRKLVTDVMGN
M199.2 381 AEYLIGGFGQEQSRDLKLQVRKLVTEVMGN
T25D1.1 424 ADFFIHGFGQKPTGDRREFVKNLLVEVMHN
T27A8.5 499 REFAVAGFSMLDKETVRNYVESLLRDMMKN
K in pag-6(n3599)
PAG-6 407 KLDRRGRHNKMYGNEASEDATRWLREQLRKE
M199.2 411 KLNRRARYNKMYGKDASEEAAKWMREELDKK
T25D1.1 454 KLNRRNRYNQEKGANKSEEAGKWMQMELKKE
T27A8.5 529 KLDRRRVYKLTHGEDSIRVKTRWMKEELAKE

Figure 3

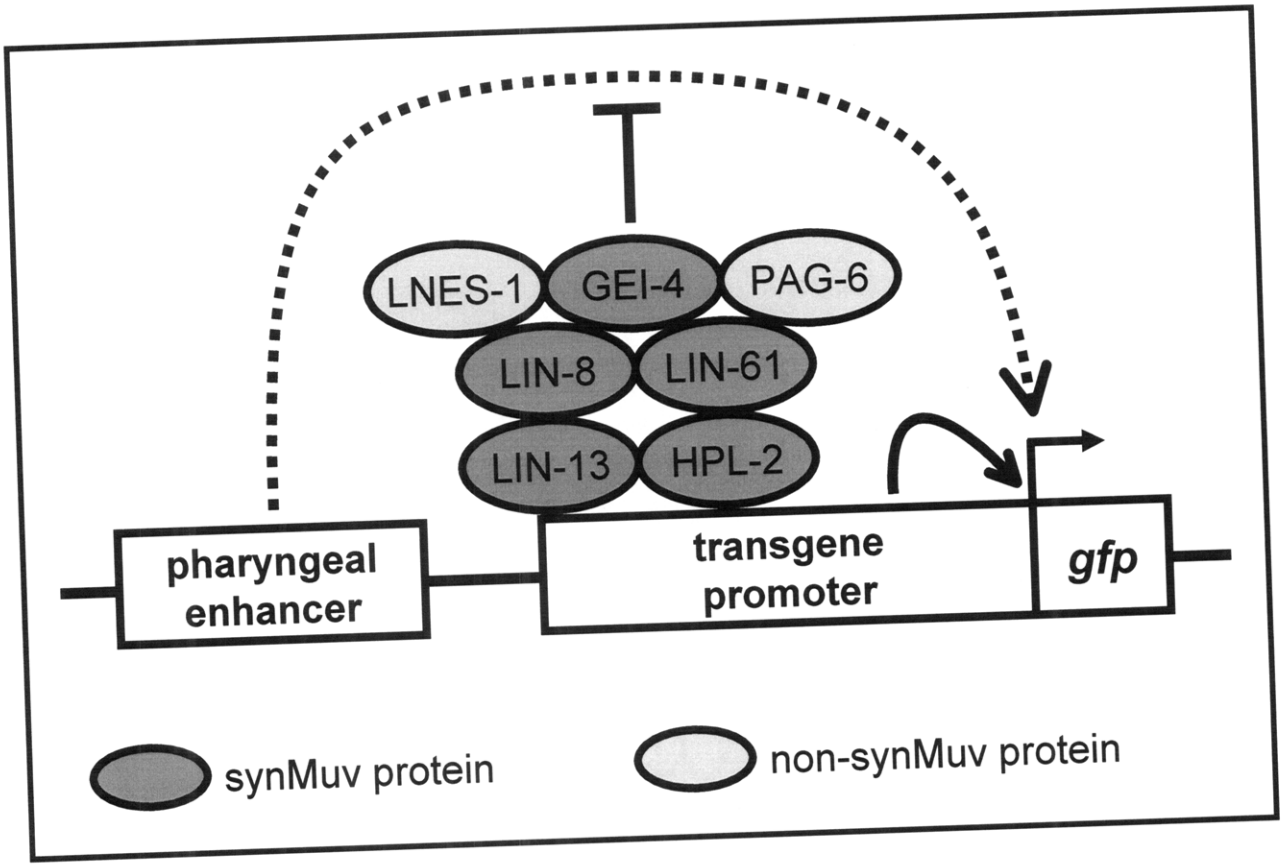
LNES-1
GEI-4
PAG-6
LIN-8
LIN-61
LIN-13
HPL-2
pharyngeal enhancer
transgene promoter
gfp
synMuv protein
non-synMuv protein

Figure 4

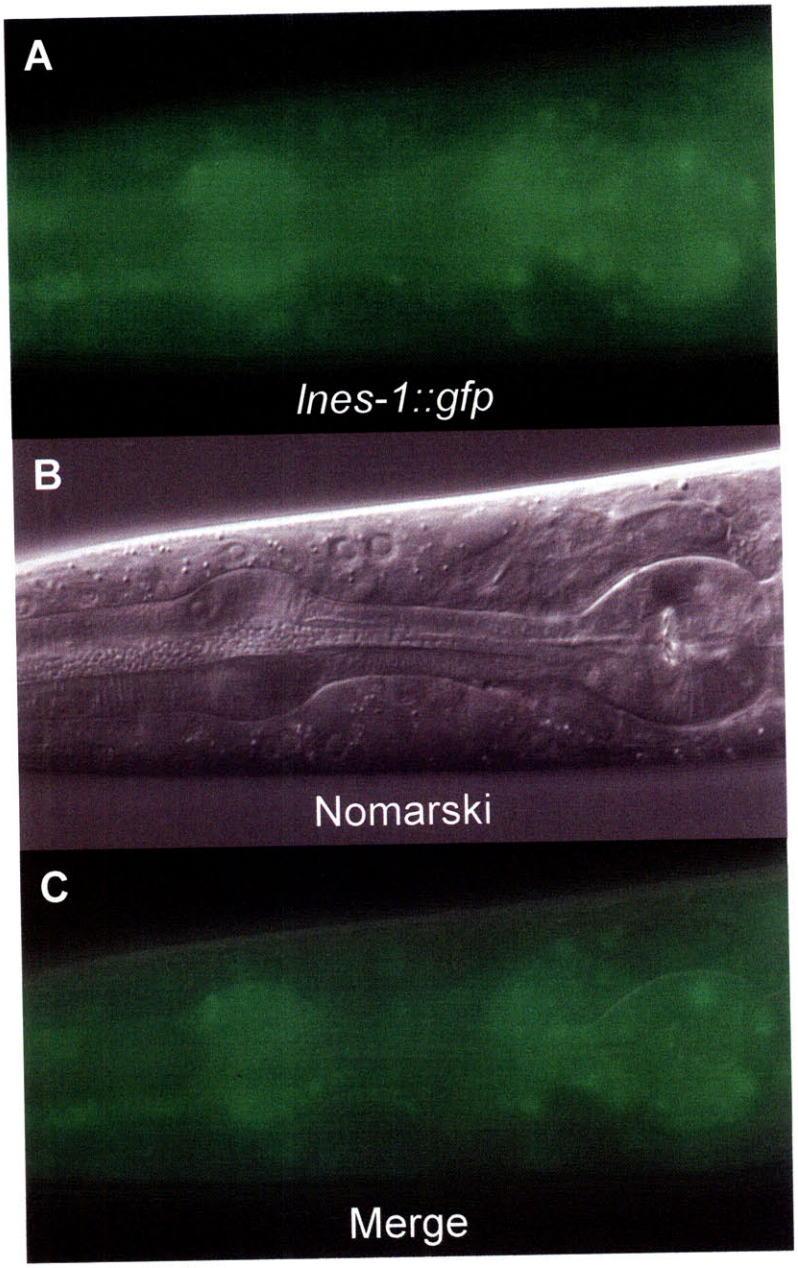

Figure S1

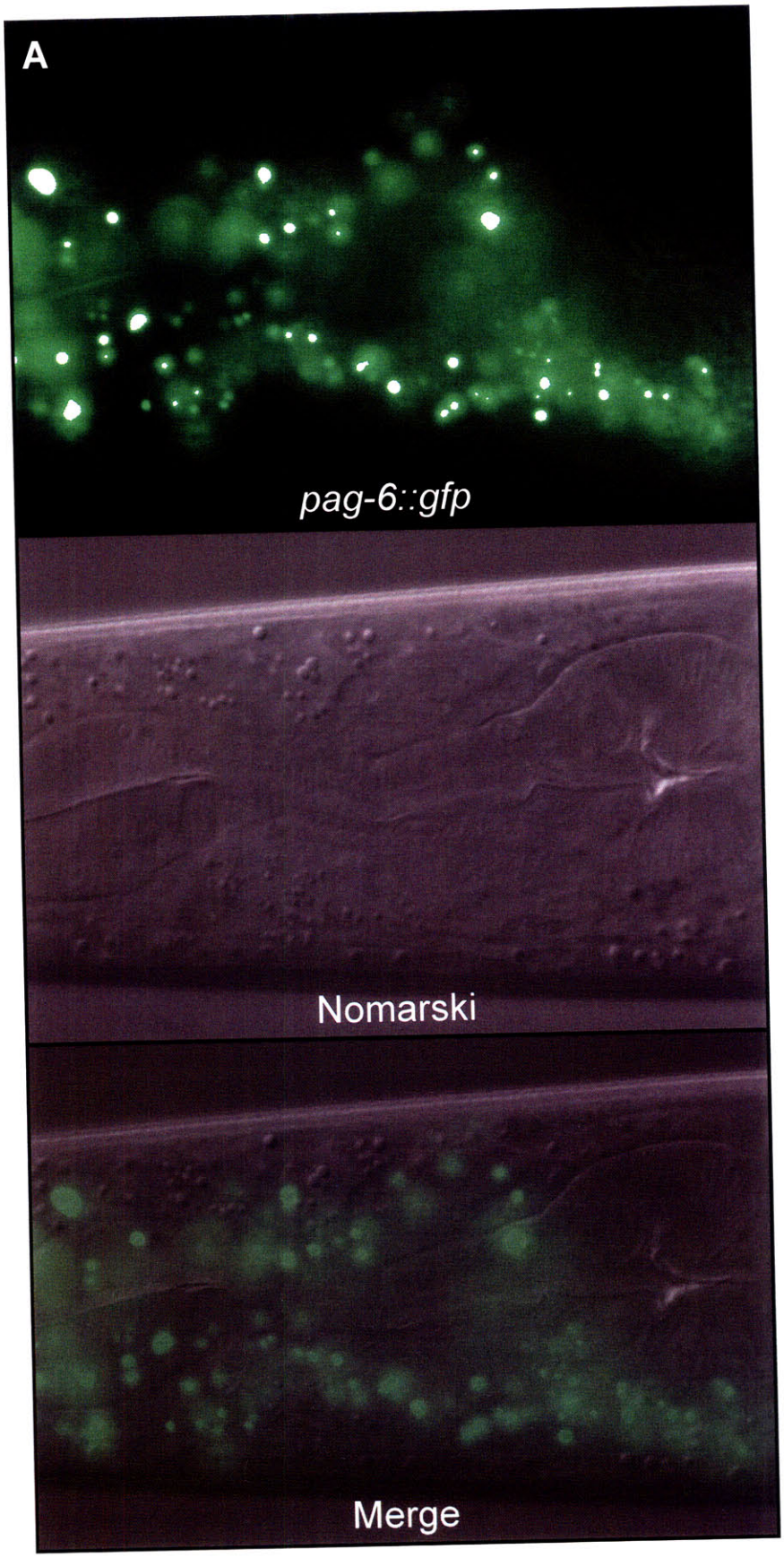

Figure S2

Chapter V

The mitotic exit factor *cdc-14* is required to prevent the divisions of specific cells in *C. elegans*

Johanna Varner[1], Hillel T. Schwartz[1], and H. Robert Horvitz

[1] These authors contributed equally to this work

I developed and performed the genetic screens in which I isolated *n3444* and performed the initial characterization and mapping of *n3444*. As an undergraduate working under my supervision, Johanna Varner refined the mapping of *n3444*, performed cosmid rescue experiments and identified the *cdc-14* mutation in *n3444* animals. Johanna observed the developing postdeirid lineages of *cdc-14(he141Δ)* animals and examined the postdeirids of mutant animals using Nomarski microscopy. I tested expression of additional cell-fate reporters in wild-type and in *cdc-14(he141Δ)* mutant animals.

Abstract

The *S. cerevisiae* phosphatase Cdc14p and its human homolog Cdc14A are essential, share substrate specificity and function in mitosis and cytokinesis. By contrast, *C. elegans* mutants completely lacking *cdc-14* are viable and superficially wild-type. The requirement for *cdc-14* is limited to specific cells in *C. elegans*: as many as 40% of the two presumptive PDE neurons inappropriately divided in animals lacking *cdc-14* function, while lineally related cells were completely unaffected. In animals lacking *cdc-14* function, some specific cells were frequently subject to ectopic cell divisions while other specific cells were never affected. We propose that mechanisms controlling the specification of cell fates determine the relative importance of mechanisms regulating the cell cycle machinery in *C. elegans*.

Introduction

Entry into and exit from the cell cycle are tightly regulated processes in development (Fay 2005), and misregulation of the cell cycle is a major feature of cancer (Malumbres and Barbacid 2007). The nematode *Caenorhabditis elegans* offers an excellent organism for the study of the genetics of the cell cycle in a developing metazoan. The pattern of somatic cell division and cell fate that occurs during *C. elegans* development is essentially invariant and completely known (Sulston and Horvitz 1977; Kimble and Hirsh 1979; Sulston et al. 1983). Many genes have been identified that perturb the normal pattern of cell division and cell fate (Horvitz and Sulston 1980; Ferguson and Horvitz 1985; Sternberg 1990; Sarin et al. 2007). One such gene is the cell cycle gene *cdc-14*, a member of the Cdc14 family (Saito et al. 2004).

In *Saccharomyces cerevisiae CDC14* is required for exit from mitosis in *S. cerevisiae* (reviewed by Stegmeier and Amon 2004; D'Amours and Amon 2007). Overexpression and RNA interference (RNAi) studies indicate that one of two homologs of Cdc14p in humans, hCdc14A, plays an essential role in mitosis and cytokinesis (Kaiser et al. 2002; Mailand et al. 2002). The second human homolog, the nucleolar protein hCdc14b, is not required for mitosis (Berduogo et al. 2008). Cdc14 proteins are highly conserved across evolution. Both human homologs are able to rescue the cell cycle defects of *S. cerevisiae cdc14* mutants and the cytokinesis defects of *Schizosaccharomyces pombe* lacking the *CDC14* homolog *FLP1* (Li et al. 1997; Vazquez-Novelle et al. 2005); also, yeast Cdc14p and its human homologs share substrate specificities (Visintin et al. 1998; Trautmann et al. 2001; Kaiser et al. 2002).

Similarly to *S. cerevisiae CDC14*, *C. elegans cdc-14* promotes exit from mitosis (Saito et al. 2004). Saito and colleagues found that *cdc-14* functions to promote cell-cycle arrest in multiple tissues but that *cdc-14* is not required for viability. They also reported that although *cdc-14* is broadly expressed and functions in multiple tissues, some tissues do not show ectopic divisions or cell reduplication in animals lacking *cdc-14* function: extra divisions in the mesoblast muscle-precursor lineage were very rare, and extra distal tip cells were never observed (Saito et al. 2004). Thus, the cells of different tissue types were affected differently by loss of *cdc-14* function.

We similarly find that loss of *cdc-14* affects selected cell types. However, our observations extend beyond the previous observation that cells belonging to different types of tissues are differingly sensitive to loss of *cdc-14* function. We find that when individual neurons are examined in animals lacking *cdc-14* function, only a small subset of specific neurons are subject to extra cell divisions. In particular, the PDE neuron is strongly affected, while cells closely related to the PDE by lineage and cells with fates very similar to those of the PDE neurons are completely unaffected. We propose that mechanisms that determine specific cell fates within a developing cell lineage determine whether specific cells require the CDC-14 phosphatase to limit their cell divisions.

Results and Discussion

cdc-14 functions in the postdeirid lineage of *C. elegans*

The postdeirid is a sensory structure generated from the V5.pa blast cell during the second larval stage of *C. elegans* development. The V5.pa blast cell undergoes three rounds of division to generate five cells: the two glia-like cells PDEso and PDEsh,

the dopaminergic PDE neuron, the PVD neuron, and a cell that undergoes programmed cell death (see Figure 1) (Sulston et al. 1975; Sulston and Horvitz 1977). When programmed cell death is blocked by loss-of-function mutations in the cell-killing caspase gene *ced-3* (*ced*, cell death abnormal), 50% (n=135) of "undead" PVD sisters contain dopamine as their lineal "aunts" the PDE neurons normally do (Ellis and Horvitz 1986). Cells developmentally programmed to contain dopamine can be identified using a transgenic reporter for the tyrosine hydroxylase gene *cat-2*; the tyrosine hydroxylase CAT-2 is required in dopamine synthesis to convert L-DOPA to dopamine (Lints and Emmons 1999). Genetic screens using the *cat-2::gfp* dopaminergic cell-fate reporter (see Appendix II) identified a mutation, *n3444*, that caused the generation of extra *cat-2::gfp*-expressing cells in the postdeirid. This mutation quantitatively resembled cell-death-defective mutants for the number of *cat-2::gfp* expressing cells in the postdeirid: 43% of *n3444* mutant postdeirids contained an extra *cat-2::gfp* expressing cell similar in appearance, process morphology, and location to the PDE neuron (n = 37). *n3444* recessively caused the presence of extra *cat-2::gfp*-expressing cells and complemented *ced-3(n717)*, *ced-4(n1162)*, and *egl-1(n1084 n3082)* mutants defective in programmed cell death for the number of *cat-2::gfp*-expressing cells in the postdeirid, indicating that *n3444* was not an allele of a known cell-death gene. We mapped *n3444* to LGII, away from the positions of any genes required for programmed cell death and from any genes known to prevent the generation of extra dopaminergic neurons.

The PDE dopaminergic neurons of the postdeirid are one of four bilaterally symmetric pairs of dopaminergic neurons in *C. elegans*; the others are the CEPV,

CEPD, and ADE neurons (Sulston et al. 1975). The ADE neurons are part of an anterior lateral sensory structure ultrastructurally similar to the postdeirid (Sulston et al. 1975; Ward et al. 1975; White et al. 1986) and subject to similar developmental control by genes specifying cell lineage, including the transcription factor genes *lin-32* and *unc-86*, which are required to generate and to control the numbers of both ADE and PDE neurons, respectively (Finney and Ruvkun 1990; Zhao and Emmons 1995). In mutants defective in programmed cell death, the undead lineal sisters of the CEPV neurons, like the undead lineal nieces of the PDE neurons, can contain dopamine (Ellis and Horvitz 1986). Unlike these cell-lineage and cell-death mutants, *n3444* was not observed to affect the number of *cat-2::gfp*-expressing dopaminergic neurons other than the PDEs (n = 80).

We used visible markers and DNA polymorphisms to map *n3444* to a 118 kb interval on LGII. We performed transformation rescue experiments (Mello and Fire 1995) with cosmids corresponding to this interval. We found that transgenes containing either of two overlapping cosmids, C12A7 and C17G10, complemented the *cat-2::gfp* expression phenotype of *n3444* and restored the normal number of *cat-2::gfp*-expressing cells to the postdeirids of *n3444* mutants. We examined the overlapping region between the two cosmids and determined the DNA sequences of genes in the region. In this way we identified *n3444* as a mutation in *cdc-14*, predicted to change codon 349 from a tryptophan to an opal stop codon.

Although the *S. cerevisiae* and human homologs of CDC-14 are essential, animals homozygous for *cdc-14(n3444)*, for the deletion *cdc-14(he141Δ)* (Saito et al. 2004), or for the Q446ochre nonsense mutation *cdc-14(he118)* (Saito et al. 2004) are

viable and do not show gross phenotypic abnormalities. *cdc-14(he141Δ)* caused a *cat-2::gfp* expression phenotype identical to that caused by *cdc-14(n3444)* and failed to complement *cdc-14(n3444)* for *cat-2::gfp* expression in the postdeirid (data not shown). RNAi targeting *cdc-14* similarly phenocopied *n3444*: in *rrf-3(pk1426)* animals hypersensitive to RNAi (Simmer et al. 2002), 32% of postdeirids contained two *cat-2::gfp*-expressing cells (n=72).

Loss of *cdc-14* function specifically causes an extra division of the PDE neuron

To determine the defect that gives rise to the presence of two *cat-2::gfp*-expressing cells in the postdeirids of animals lacking *cdc-14* function, we observed the developing lineages of *cdc-14(he141Δ)* animals. Starting at various points within the generation of the postdeirid, 39 developing postdeirid lineages were examined until cell divisions had ceased. Animals were allowed to develop to adulthood, and the postdeirids were examined for *cat-2::gfp* expression (see Figure 2 and Materials and Methods). Of the 39 lineages observed, 26 were wild-type in their cell division pattern and for *cat-2::gfp* expression in the PDE. In the other 13 lineages the presumptive PDE neuron inappropriately divided once, and both daughter cells expressed the *cat-2::gfp* dopaminergic cell fate reporter. No other defects in the developing postdeirid lineage were observed. We used Nomarski and fluorescence optics to examine the postdeirids of L4 larvae: *cdc-14(n3444)*; *cat-2::gfp* or *cdc-14(he141Δ)*; *cat-2::gfp* animals either contained four nuclei with neuronal morphology, of which one expressed the *cat-2::gfp* cell fate reporter (62% and 57%, respectively), or contained five nuclei with neuronal morphology, of which two

expressed the *cat-2::gfp* cell fate reporter (38% and 43%, respectively; n = 16 and n = 23, respectively). No abnormalities were observed in direct observation of six developing postdeirid lineages of animals with wild-type *cdc-14* function or from examining the postdeirids of animals with wild-type *cdc-14* function using Nomarski and fluorescence optics (n=36). We conclude that in animals lacking *cdc-14* function, the presumptive PDE neuron frequently undergoes an extra round of cell division to generate two cells similar to the PDE neurons and that other cells of the postdeirid are not significantly affected by loss of *cdc-14* function.

We also examined animals lacking both *cdc-14* function and *ced-3* function. Our observations were consistent with a combination of the extra PDE division observed in *cdc-14* mutants and the dopamine expression by the "undead" PVD sisters observed in cell-death-defective animals. Specifically, of 154 postdeirids examined, 43 (28%) contained one *cat-2::gfp*-expressing cell, 84 (55%) contained two *cat-2::gfp*-expressing cells and 27 (18%) contained three *cat-2::gfp*-expressing cells. These percentages are consistent with our previous observations: we found that ~40% of PDEs divided in *cdc-14(he141Δ)* animals to generate two *cat-2::gfp*-expressing cells and approximately 50% of PVD sisters expressed *cat-2::gfp* in *ced-3(n717)* animals. We did not observe animals with four *cat-2::gfp*-expressing cells in the postdeirid, which we propose suggests that *cdc-14* function is not required to prevent the inappropriate divisions of the dopaminergic undead PVD sister cells of animals defective in programmed cell death. *cdc-14* is therefore required to prevent ectopic division of the PDE neuron and acts to promote exit from mitosis in this cell. *cdc-14* is not required in the other four cells of the postdeirid lineage, including the "undead" PVD sister, which displays a cell fate

similar to that of the PDE neuron, and *cdc-14* is not required to prevent ectopic division of the anterior ADE neurons, which are structurally and lineally related to the PDE neurons. *cdc-14* function is therefore required in a sharply defined subset of cells and not required in other cells that are closely related by cell lineage or that are specified by similar cell-lineage controls and display similar reporter expression and possess similar process morphology.

cdc-14 is required to prevent cell division for a subset of cell types

The presumptive PDE neuron, but not the other four cell types generated within the postdeirid lineage, divided in *cdc-14* mutants. We thus examined other cells to determine whether they might inappropriately divide in *cdc-14* mutants. We combined *cdc-14(he141Δ)* with a collection of *gfp* cell-fate reporters each of which is expressed in a small number of identified neurons (see Table 1). We tested nine reporters, expressed in 15 specific neurons. We detected extra expressing cells using the *lin-11::gfp*, *nmr-1::gfp*, and *tbh-1::gfp* reporters. These extra expressing cells suggest that *cdc-14* is required to prevent the division of three specific neurons – the VC neurons, the RIC neurons, and one or more from the AVA, AVD, and AVE neurons. In each of these cases, 10 to 20% of *cdc-14(he141Δ)* animals contained extra expressing cells (Table 1). No extra expressing cells were detected for the other nine neuron classes scorable using these reporters (Table 1).

Prospects for the identification of determinants by which a requirement for *cdc-14* mitotic exit function is limited to specific cells

The genetic screen for alterations in *cat-2::gfp* expression in the postdeirid lineage in which we identified the *cdc-14* mutation *n3444* was not saturated: no alleles of the cell-death genes *ced-4* or *egl-1* were isolated and only single alleles of *cdc-14*, *lin-22* and *lin-32* were isolated (see Appendix II). Further genetic screens using the *cat-2::gfp* reporter might therefore lead to the identification of genes that like *cdc-14* are required to prevent the presumptive PDE neuron from dividing, possibly including genes that promote *cdc-14* function in the PDE neuron or genes that act in parallel to *cdc-14* and explain the failure of nearly 60% of presumptive PDE neurons to divide in animals completely lacking *cdc-14* function. Genes of the latter class might also be identified by enhancer screens seeking mutations that increase the percentage of presumptive PDE neurons that divide in animals lacking *cdc-14* function. Screens seeking defects in other cells of the postdeirid in animals lacking *cdc-14* or screens seeking to identify genes redundantly required with *cdc-14* for viability could lead to the identification of mechanisms that normally restrict the requirement of *cdc-14* to the PDE neurons.

Because of the essential role of its yeast homolog in promoting exit from the cell cycle in yeast and its apparent function in cytokinesis and control of ploidy, human Cdc14A has been proposed to act as a tumor suppressor (Mailand et al. 2002). hCdc14A is frequently found to be present at abnormally low levels in cancer cell lines, especially those mutated for the tumor suppressor *p53* (Paulsen et al. 2006). Determination of cell identity within a developing *C. elegans* lineage decides at single-cell resolution whether *cdc-14* function is required to exit from the cell cycle and achieve a wild-type pattern of cell division. These differences in whether *cdc-14* function is required exist not only between different tissue types (Saito et al. 2004) but also

between cells closely related by lineage and cells possessing extremely similar cell fates, suggesting that it may be possible to change whether cells require *cdc-14* function to exit from the cell cycle without greatly disrupting other aspects of their functions. Identification of genes that determine whether *cdc-14* function is required in specific cells in *C. elegans* could lead to the identification of homologous genes that similarly determine whether human cells require hCdc14A function to control their cell cycles, and could lead to therapeutic approaches to restore normal cell-cycle control to cancerous cells that have lost hCdc14A function.

Materials and Methods

C. elegans genetics

C. elegans strains were derived from the wild-type strain N2 (Bristol, England) and cultured using standard conditions (Brenner 1974) except that the bacterial strain HB101 was used as a food source. Mutations isolated in this study on the basis of their *cat-2::gfp* expression phenotypes are listed in Table S1. Other mutations used are listed below. Mutations for which no citation is given have been described previously (Riddle et al. 1997). LGI: *dpy-5(e61)*; LGII: *bli-2(e768)*, *bwIs2 [flp-1::gfp]* (Wightman et al. 2005), *cdc-14(he141Δ)* (Saito et al. 2004), *dpy-10(e128)*, *lin-31(n301)*, *rol-6(e187)*, *rrf-3(pk1426)* (Simmer et al. 2002), *unc-4(e120)*, *vab-1(e2027)*; LGIII *ced-4(n1162)*, *gmIs12 [srb-6::gfp]* (Frank et al. 2003), *nIs107 [tbh-1::gfp]* (Alkema et al. 2005), *unc-32(e189)*, *unc-86(n846)*; LGIV *ced-3(n717)*, *jeIn2 [mec-3::lacZ]* (Way et al. 1991), *lin-22(n372)*, *unc-5(e53)*; LGV: *akIs7 [nmr-1::gfp]* (Brockie et al. 2001), *dpy-11(e224)*, *egl-1(n1084 n3082)* (Conradt and Horvitz 1998), *unc-76(e911)*, *utIs13 [dat-1::gfp]* (T. Ishihara and I. Katsura, personal communication); LGX: *bcIs24 [tph-1::gfp]* (Thellmann et al. 2003), *dpy-6(e14)*, *gmIs18 [ceh-23::gfp]* (Withee et al. 2004), *lin-15AB(n765)*, *lon-2(e678)*, *mIs6 [daf-7::gfp]* (Ren et al. 1996), *nIs106 [lin-11::gfp]* (Reddien 2002), *oxIs12 [unc-47::gfp]* (McIntire et al. 1997), *unc-9(e101)*. The *cat-2::gfp* reporters *nIs116 X* and *nIs117 X* are described below.

Mapping *cdc-14(n3444)*

We mapped *n3444* to LGII, between *vab-1* and *dpy-10* and very close to *bli-2*. We mapped *n3444* using polymorphisms essentially as described (Wicks et al. 2001).

We crossed *lin-31(n301) n3444 dpy-10(e128)*; *nIs117* hermaphrodites with *nIs117* males containing a region of LGII derived from the polymorphic Hawaiian strain CB4856. 272 Lin-non-Dpy recombinants included 15 that had recombined in an interval between 18226 on cosmid EEED8 and 19093 on cosmid K05F1 that we identified as containing *n3444*. We identified additional polymorphisms within this interval on the cosmids ZK177 (nucleotide 20884 of accession number U21321), C17G10 (11731 of U28739), F59E12 (22824 of AF003386) and F10C1 (18148 of U49831). We mapped *n3444* to the 118 kb interval between the polymorphisms on ZK177 and F59E12.

Transgenesis and generation of integrated *cat-2::gfp* reporters

Germline transformation was performed as described (Mello et al. 1991). The *cat-2::gfp* reporter plasmid EM282 was injected at 50 ng/μl with 50 ng/μl of the *lin-15* rescuing plasmid pL15EK (Clark et al. 1994) as a co-injection marker. A line giving strong expression in the postdeirid with limited formation of GFP aggregates was selected for the isolation of genomic integrants, according to an established protocol (Shaham and Horvitz 1996). From approximately 600 F_1 clones established following gamma irradiation, three integrated *cat-2::gfp* reporters were established, all mapping to LGX: *nIs116*, *nIs117*, *nIs118*. *nIs117* and *nIs118* were likely identical: strains containing either transgene appeared similar, and neither *nIs117* nor *nIs118* was observed to recombine with *lon-2(e678)*. *nIs116* mapped between *dpy-6* and *unc-9* on LGX. Cosmids C0305, C17C3, C12A7, C17G10, and C41A6 were injected at ~25 ng/μl each for rescue of *cdc-14(n3444)* using 50 ng/μl P76-16B (Bloom and Horvitz 1997) as a co-injection marker.

RNAi

dsRNA targeting *cdc-14* was made by amplifying sequences corresponding to exon 4 and sequences corresponding to exon 13 of *cdc-14* (9508 to 10065 and 5459 to 5948 of cosmid C17G10, respectively; numbers refer to nucleotides of accession number U28739) using oligonucleotides with T7 transcription sites appended 5' of their homologous sequences. PCR products were purified, RNA was transcribed, purified, denatured and annealed. RNAi was performed by injection according to established protocols (Fire et al. 1998) using *nls116* animals or RNAi-hypersensitive *rrf-3(pk1426)*; *nls116* animals.

Examination of mutant phenotypes

We used Nomarski microscopy and performed cell lineage analysis according to standard methods (Sulston and Horvitz 1977). We observed of reporter gene expression using a compound microscope (AxioSkop, Zeiss) equipped with Nomarski optics. To avoid possible confusion with the two neurons and one cell death derived from the asymmetric QL lineage generated in the vicinity of the left postdeirid, we examined only postdeirids on the right side of the animal by Nomarksi microscopy. Following lineage analysis, animals were recovered from the slide and placed on a 6 cm Petri plate containing NGM agar seeded with HB101 bacteria. We allowed the recovered animals to develop for an additional day, then placed the animals on slides to score for expression of the *cat-2::gfp* reporter; fluorescence from the reporter is not seen until hours have elapsed after the cell division is completed. We successfully

observed the developing right postdeirid lineages of 39 *cdc-14(he141Δ)*; *nls117* animals, recovered them, and scored them for *cat-2::gfp* expression. Additional animals were lost during in this process; in these animals, no cell divisions inconsistent with those shown in Figure 2 were observed.

Acknowledgments

We thank Mike Hurwitz and Dave Harris for their comments about this manuscript; Beth Castor for assistance with DNA sequence determination; Na An for assistance with strains; Robyn Lints and Scott Emmons for the *cat-2::gfp* reporter plasmid EM282; Barbara Conradt for providing *bcIs24*; Gian Garriga for providing *akIs7*, *gmIs12*, and *gmIs18*; the *Caenorhabditis* Genetics Center, which is funded by the NIH National Center for Research Resources (NCRR), for strains; and the *C. elegans* Genome Sequencing Consortium and the Genome Sequencing Center at Washington University in St. Louis for the genomic sequence of *C. elegans* and for the identification of polymorphisms in CB4856. This work was supported by NIH grant GM24663. J.V. was supported by the MIT Undergraduate Research Opportunity Program (UROP) and by the Howard Hughes Medical Institute. H.T.S. was supported in part by a David H. Koch Graduate Fellowship. H.R.H. is an Investigator of the Howard Hughes Medical Institute and is David H. Koch Professor of Biology at MIT.

References

Alkema, M.J., M. Hunter-Ensor, N. Ringstad, and H.R. Horvitz. 2005. Tyramine functions independently of octopamine in the *Caenorhabditis elegans* nervous system. *Neuron* **46**: 247-260.

Berduogo, E., M.V. Nachury, P.K. Jackson, and P.V. Jallepalli. 2008. The nucleolar phosphatase *Cdc14B* is dispensable for chromosome segregation and mitotic exit in human cells. *Cell Cycle* **7**: 1184-1190.

Bloom, L. and H.R. Horvitz. 1997. The *Caenorhabditis elegans* gene *unc-76* and its human homologs define a new gene family involved in axonal outgrowth and fasciculation. *Proc Natl Acad Sci U S A* **94**: 3414-9.

Brenner, S. 1974. The genetics of *Caenorhabditis elegans*. *Genetics* **77**: 71-94.

Brockie, P.J., D.M. Madsen, Y. Zheng, J. Mellem, and A.V. Maricq. 2001. Differential expression of glutamate receptor subunits in the nervous system of *Caenorhabditis elegans* and their regulation by the homeodomain protein UNC-42. *J Neurosci* **21**: 1510-22.

Clark, S.G., X. Lu, and H.R. Horvitz. 1994. The *Caenorhabditis elegans* locus *lin-15*, a negative regulator of a tyrosine kinase signaling pathway, encodes two different proteins. *Genetics* **137**: 987-97.

Conradt, B. and H.R. Horvitz. 1998. The *C. elegans* protein EGL-1 is required for programmed cell death and interacts with the Bcl-2-like protein CED-9. *Cell* **93**: 519-29.

D'Amours, D. and A. Amon. 2007. At the interface between signaling and executing anaphase - Cdc14 and the FEAR network. *Genes Dev* **18**: 2581-95.

Ellis, H.M. and H.R. Horvitz. 1986. Genetic control of programmed cell death in the nematode *C. elegans*. *Cell* **44**: 817-29.

Fay, D.S. 2005. The cell cycle and development: lessons from *C. elegans*. *Semin Cell Dev Biol* **16**: 397-406.

Ferguson, E.L. and H.R. Horvitz. 1985. Identification and characterization of 22 genes that affect the vulval cell lineages of the nematode *Caenorhabditis elegans*. *Genetics* **110**: 17-72.

Finney, M. and G. Ruvkun. 1990. The *unc-86* gene product couples cell lineage and cell identity in *C. elegans*. *Cell* **63**: 895-905.

Fire, A., S. Xu, M.K. Montgomery, S.A. Kostas, S.E. Driver, and C.C. Mello. 1998. Potent and specific genetic interference by double-stranded RNA in *Caenorhabditis elegans*. *Nature* **391**: 806-11.

Frank, C.A., P.D. Baum, and G. Garriga. 2003. HLH-14 is a *C. elegans* achaete-scute protein that promotes neurogenesis through asymmetric cell division. *Development* **130**: 6507-18.

Horvitz, H.R. and J.E. Sulston. 1980. Isolation and genetic characterization of cell-lineage mutants of the nematode *Caenorhabditis elegans*. *Genetics* **96**: 435-54.

Kaiser, B.K., Z.A. Zimmerman, H. Charbonneau, and P.K. Jackson. 2002. Disruption of centrosome structure, chromosome segregation, and cytokinesis by misexpression of human Cdc14A phosphatase. *Mol Biol Cell* **13**: 2289-2300.

Kimble, J. and D. Hirsh. 1979. The postembryonic cell lineages of the hermaphrodite and male gonads in *Caenorhabditis elegans*. *Dev Biol* **70**: 396-417.

Li, L., B.R. Ernsting, M.J. Wishart, D.L. Lohse, and J.E. Dixon. 1997. A family of putative tumor suppressors is structurally and functionally conserved in humans and yeast. *J Biol Chem* **272**: 29403-6.

Lints, R. and S.W. Emmons. 1999. Patterning of dopaminergic neurotransmitter identity among *Caenorhabditis elegans* ray sensory neurons by a TGFbeta family signaling pathway and a Hox gene. *Development* **126**: 5819-31.

Mailand, N., C. Lukas, B.K. Kaiser, P.K. Jackson, J. Bartek, and J. Lukas. 2002. Deregulated human Cdc14A phosphatase disrupts centrosome separation and chromosome segregation. *Nat Cell Biol* **4**: 317-22.

Malumbres, M. and M. Barbacid. 2007. Cell cycle kinases in cancer. *Curr Opin Genet Dev* **17**: 60-5.

McIntire, S.L., R.J. Reimer, K. Schuske, R.H. Edwards, and E.M. Jorgensen. 1997. Identification and characterization of the vesicular GABA transporter. *Nature* **389**: 870-6.

Mello, C. and A. Fire. 1995. DNA transformation. *Methods Cell Biol* **48**: 451-82.

Mello, C.C., J.M. Kramer, D. Stinchcomb, and V. Ambros. 1991. Efficient gene transfer in *C.elegans*: extrachromosomal maintenance and integration of transforming sequences. *Embo J* **10**: 3959-70.

Paulsen, M.T., A.M. Starks, F.A. Derheimer, S. Hanasoge, L. Li, J.E. Dixon, and M. Ljungman. 2006. The p53-targeting human phosphatase hCdc14A interacts with the Cdk1/cyclin B complex and is differentially expressed in human cancers. *Mol Cancer* **5**: 25.

Reddien, P.W. 2002. Phagocytosis promotes programmed cell death and is controlled by Rac signaling pathway in *C. elegans*. *Ph. D. Thesis, Massachusetts Institute of Technology, Cambridge, MA*.

Reddien, P.W., S. Cameron, and H.R. Horvitz. 2001. Phagocytosis promotes programmed cell death in *C. elegans*. *Nature* **412**: 198-202.

Ren, P., C.S. Lim, R. Johnsen, P.S. Albert, D. Pilgrim, and D.L. Riddle. 1996. Control of *C. elegans* larval development by neuronal expression of a TGF-beta homolog. *Science* **274**: 1389-91.

Riddle, D.L., T. Blumenthal, B.J. Meyer, and J.R. Priess. 1997. *C. elegans* II (Cold Spring Harbor Laboratory Press, Cold Spring Harbor, New York).

Saito, R.M., A. Perreault, B. Peach, J.S. Satterlee, and S. van den Heuvel. 2004. The CDC-14 phosphatase controls developmental cell-cycle arrest in *C. elegans*. *Nat Cell Biol* **6**: 777-83.

Sarin, S., M.M. O'Meara, E.B. Flowers, C. Antonio, R.J. Poole, D. Didiano, R.J. Johnston, Jr., S. Chang, S. Narula, and O. Hobert. 2007. Genetic screens for *Caenorhabditis elegans* mutants defective in left/right asymmetric neuronal fate specification. *Genetics* **176**: 2109-30.

Shaham, S. and H.R. Horvitz. 1996. Developing *Caenorhabditis elegans* neurons may contain both cell-death protective and killer activities. *Genes Dev* **10**: 578-91.

Simmer, F., M. Tijsterman, S. Parrish, S.P. Koushika, M.L. Nonet, A. Fire, J. Ahringer, and R.H. Plasterk. 2002. Loss of the putative RNA-directed RNA polymerase RRF-3 makes *C. elegans* hypersensitive to RNAi. *Curr Biol* **12**: 1317-9.

Stegmeier, F. and A. Amon. 2004. Closing mitosis: The functions of the Cdc14 phosphatase and Its regulation. *Annu Rev Genet* **38**: 203-32.

Sternberg, P.W. 1990. Genetic control of cell type and pattern formation in *Caenorhabditis elegans*. *Adv Genet* **27**: 63-116.

Sulston, J., M. Dew, and S. Brenner. 1975. Dopaminergic neurons in the nematode *Caenorhabditis elegans*. *J Comp Neurol* **163**: 215-26.

Sulston, J.E. and H.R. Horvitz. 1977. Post-embryonic cell lineages of the nematode, *Caenorhabditis elegans*. *Dev Biol* **56**: 110-56.

Sulston, J.E., E. Schierenberg, J.G. White, and J.N. Thomson. 1983. The embryonic cell lineage of the nematode *Caenorhabditis elegans*. *Dev Biol* **100**: 64-119.

Sze, J.Y., M. Victor, C. Loer, Y. Shi, and G. Ruvkun. 2000. Food and metabolic signalling defects in a *Caenorhabditis elegans* serotonin-synthesis mutant. *Nature* **403**: 560-4.

Thellmann, M., J. Hatzold, and B. Conradt. 2003. The Snail-like CES-1 protein of *C. elegans* can block the expression of the BH3-only cell-death activator gene *egl-1* by antagonizing the function of bHLH proteins. *Development* **130**: 4057-71.

Trautmann, S., B.A. Wolfe, P. Jorgensen, M. Tyers, K.L. Gould, and D. McCollum. 2001. Fission yeast Clp1p phosphatase regulates G2/M transition and coordination of cytokinesis with cell cycle progression. *Curr Biol* **11**: 931-40.

Vazquez-Novelle, M.D., V. Esteban, A. Bueno, and M.P. Sacristan. 2005. Functional homology among human and fission yeast Cdc14 phosphatases. *J Biol Chem* **280**: 29144-50.

Visintin, R., K. Craig, E.S. Hwang, S. Prinz, M. Tyers, and A. Amon. 1998. The phosphatase Cdc14 triggers mitotic exit by reversal of Cdk-dependent phosphorylation. *Mol Cell* **2**: 709-18.

Ward, S., N. Thomson, J.G. White, and S. Brenner. 1975. Electron microscopical reconstruction of the anterior sensory anatomy of the nematode *Caenorhabditis elegans*. *J Comp Neurol* **160**: 313-37.

Way, J.C., L. Wang, J.Q. Run, and A. Wang. 1991. The *mec-3* gene contains cis-acting elements mediating positive and negative regulation in cells produced by asymmetric cell division in *Caenorhabditis elegans*. *Genes Dev* **5**: 2199-211.

White, J.G., E. Southgate, J.N. Thomson, and S. Brenner. 1986. The structure of the nervous system of the nematode *Caenorhabditis elegans*. *Philos Trans R Soc Lond B Biol Sci* **314**: 1-340.

Wicks, S.R., R.T. Yeh, W.R. Gish, R.H. Waterston, and R.H. Plasterk. 2001. Rapid gene mapping in *Caenorhabditis elegans* using a high density polymorphism map. *Nat Genet* **28**: 160-4.

Wightman, B., B. Ebert, N. Carmean, K. Weber, and S. Clever. 2005. The *C. elegans* nuclear receptor gene *fax-1* and homeobox gene *unc-42* coordinate interneuron identity by regulating the expression of glutamate receptor subunits and other neuron-specific genes. *Dev Biol* **287**: 74-85.

Withee, J., B. Galligan, N. Hawkins, and G. Garriga. 2004. *Caenorhabditis elegans* WASP and Ena/VASP Proteins Play Compensatory Roles in Morphogenesis and Neuronal Cell Migration. *Genetics* **167**: 1165-76.

Zhao, C. and S.W. Emmons. 1995. A transcription factor controlling development of peripheral sense organs in *C. elegans*. *Nature* **373**: 74-8.

Table 1. Loss of *cdc-14* causes the presence of extra members only of a small number of neuron classes.

Reporter	Neurons examined	Extra expressing cells (%) 0	1	2	n	References
ceh-23::gfp	2 CANs	100	0	0	38	**1**
daf-7::gfp	2 ASIs	100	0	0	45	**2**
flp-1::gfp	2 AVKs	100	0	0	43	**3**
lin-11::gfp	4 scorable VCs[a]	**80**	**17**	**2**	**41**	**4**
nmr-1::gfp	2 AVAs, 2 AVDs, 2 AVEs	**66**	**29**	**5**	**41**	**5**
	2 PVCs	100	0	0	41	
srb-6::gfp	2 PHAs, 2 PHBs	100	0	0	46	**6**
tbh-1::gfp	RICs	**88**	**12**	**0**	**41**	**7**
tph-1::gfp	NSMs	100	0	0	41	**8,9**
unc-47::gfp	6 DDs, 13 VDs, DVB	100	0	0	25	**10**

[a] Vulval fluorescence from the *lin-11::gfp* reporter transgene *nls106* obscures the positions of two of the four VC neurons.

[b] The extra cells in *cdc-14(he141Δ)*; *akIs7* animals are in the head, close to the positions of the AVA, AVD, and AVE neurons. No extra cells were observed near the positions of the PVC neurons.

cdc-14(he141Δ) animals homozygous for the indicated transgene were scored for the presence of additional cells expressing the cell-fate reporter. The percentage of animals with zero, one, or two extra cells expressing the indicated cell-fate reporter is shown. A similar number of *cdc-14(+)* animals homozygous for each transgene were scored for each reporter as a control; no extra cells were seen in *cdc-14(+)* animals. Reporters are described in the following references: **1** (Withee et al. 2004); **2** (Ren et al. 1996); **3** (Wightman et al. 2005); **4** (Reddien et al. 2001); **5** (Brockie et al. 2001); **6** (Frank et al. 2003); **7** (Alkema et al. 2005); **8,9** (Sze et al. 2000; Thellmann et al. 2003); **10** (McIntire et al. 1997)

Figure legends

Figure 1

Expression of the dopaminergic cell fate reporter *cat-2::gfp.* The dopaminergic cell fate reporter *cat-2::gfp* is expressed in the PDE neurons of wild-type animals (a), in the PDE neurons and the undead PVD sisters of animals defective in programmed cell death (b), and in the two products of the inappropriate PDE cell division seen in animals lacking *cdc-14* function (c). Cell lineage diagrams show the cell divisions by which the V5.pa blast cell divides to generate the postdeirid, a lateral sensory structure. The X indicates the programmed cell death of the sister of the PVD neuron. The ovoid ring shapes in the center of each image are the nuclear-excluded fluorescence generated by the *cat-2::gfp* reporter. Weaker fluorescence is autofluorescence from lipid particles in the intestine. Micrographs are merged images from fluorescence and Nomarski microscopy. Ventral is down, anterior is left.

Figure 2

Cell lineages observed in *cdc-14(he141Δ)* animals homozygous for the *cat-2::gfp* dopaminergic cell-fate reporter *nIs117*. 26 of 39 animals showed a wild-type pattern of cell divisions. In 13 of 39 animals the dopaminergic PDE neuron inappropriately divided to generate two *cat-2::gfp*-expressing dopaminergic neurons. Observation of different developing lineages began at different stages of postdeirid development. For the 26 wild-type patterns, observation of 7/26 began after the V5.pa cell divided and before the V5.paa and V5.pap cells divided, and observation of 19/26 began after the V5.paa and V5.pap cells divided and before the V5.paap cell divided. For the 13 patterns in which

the PDE divided, observation of 1/13 began before the V5.pa cell divided, observation of 8/13 began after the V5.pa cell divided and before the V5.paa and V5.pap cells divided, observation of 3/13 began after the V5.paa and V5.pap cells divided and before the V5.paaa and V5.paap cells divided, and observation of 1/13 began after the V5.paa cells divided and before the V5.paaa cell divided. No other cell lineage defects were observed.

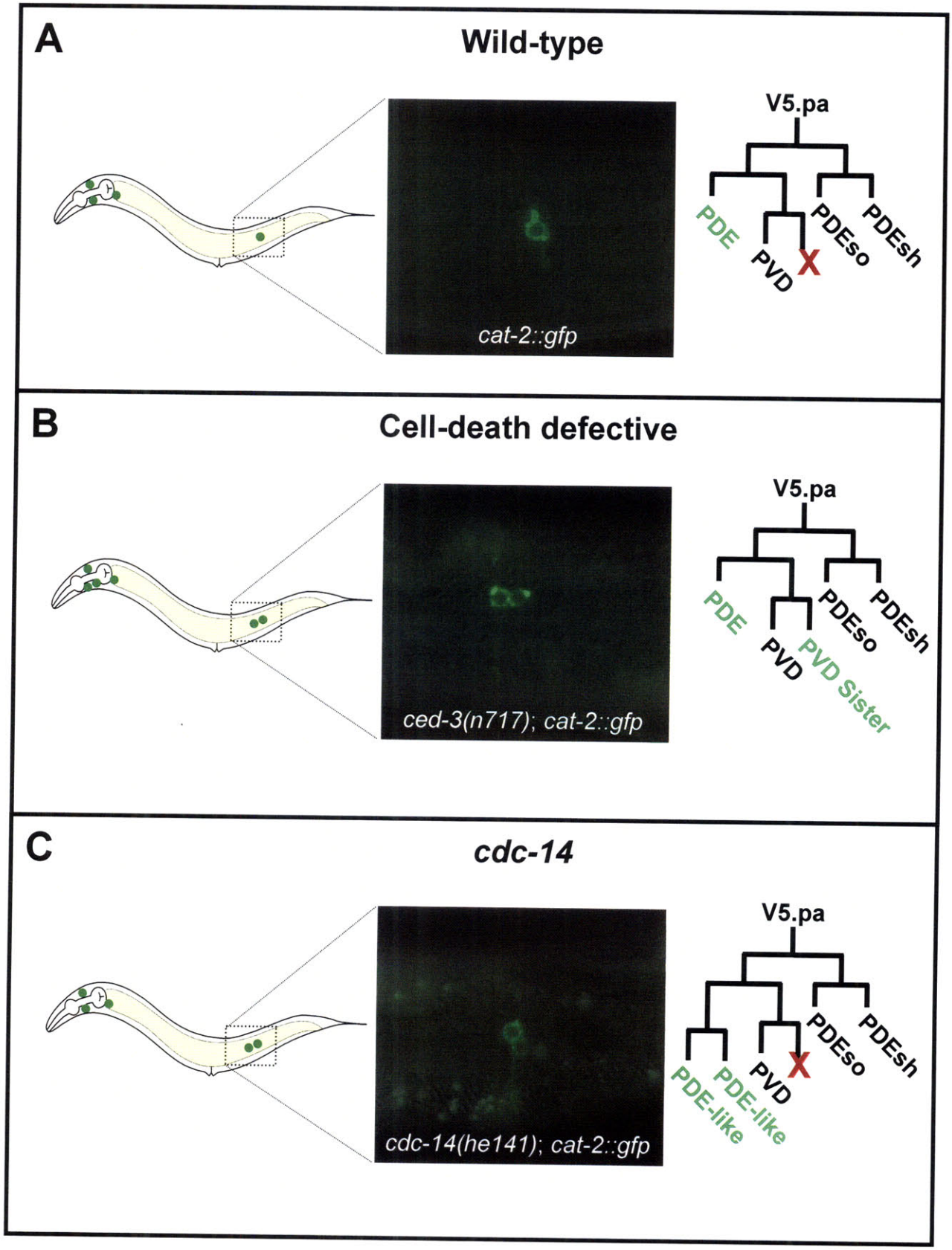
A
Wild-type
cat-2::gfp
V5.pa
PDE
PVD
PDEso
PDEsh
B
Cell-death defective
ced-3(n717); cat-2::gfp
V5.pa
PDE
PVD
PVD Sister
PDEso
PDEsh
C
cdc-14
cdc-14(he141); cat-2::gfp
V5.pa
PDE-like
PDE-like
PVD
PDEso
PDEsh

Figure 1

Postdeirid lineage in *cdc-14(he141Δ)* animals

26/39 animals:

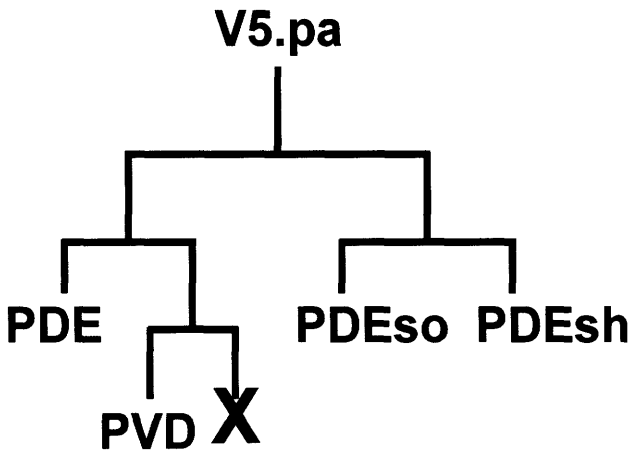

13/39 animals:

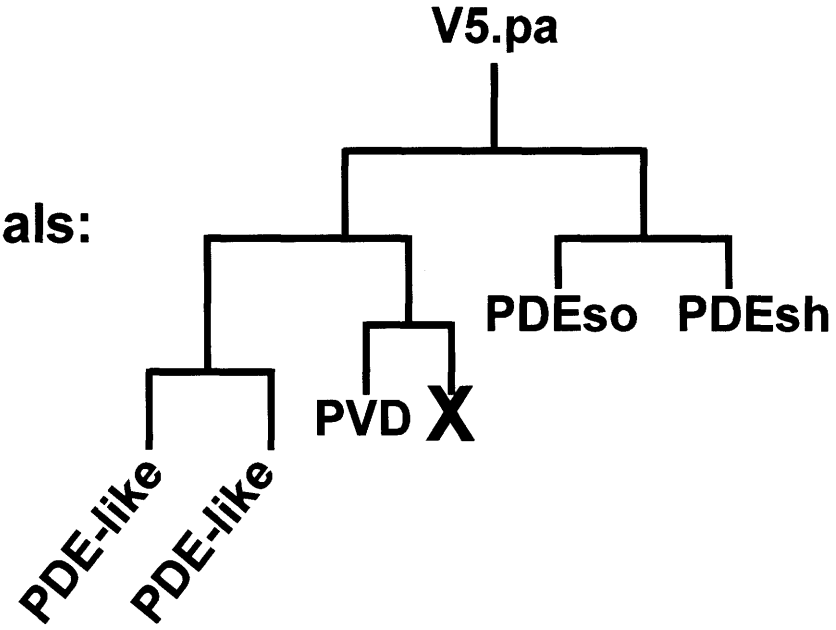

Figure 2

Chapter VI

The *C. elegans* F-box protein SEL-10 promotes female development and may target FEM-1 and FEM-3 for degradation by the proteasome

Sibylle Jäger[1, 2], Hillel T. Schwartz[3], H. Robert Horvitz[3] and Barbara Conradt[1, 4, *]

[1]Max Planck Institute of Neurobiology
Am Klopferspitz 18a
D-82152 Planegg-Martinsried, Germany

[2] Dana-Farber Cancer Institute and Department of Cell Biology
Harvard Medical School
One Jimmy Fund Way, Smith Building 956
Boston, MA 02115, U.S.A.

[3]Howard Hughes Medical Institute
Department of Biology, 68-425
Massachusetts Institute of Technology
Cambridge, MA 02139, U.S.A.

[4] Dartmouth Medical School
Department of Genetics, 7400 Remsen
Hanover, NH 03755, U.S.A.

[*] Corresponding author: Barbara Conradt, present address: Dartmouth Medical School Department of Genetics , 7400 Remsen, Hanover, NH 03755, U.S.A., Phone: (603) 650-1210, Email: Barbara.Conradt@Dartmouth.edu

Published as Jager *et al.* (2004) *PNAS* **101**: 12549-12554.

I isolated one *sel-10(gf)* mutation in a screen for hermaphrodites with surviving CEM neurons (see Chapter 2) and isolated the *sel-10* deletion *n4273*. I performed epistasis and gene dosage experiments to show that the masculinizing *sel-10* gain-of-function mutation *n3717* causes altered gene function and acts within the sex-determination pathway and mapped *sel-10(n3717)* to a 130 kb interval. Sibylle Jager and Barbara Conradt performed similar epistasis and gene dosage esperiments using the *sel-10* gain-of-function mutation *n1077*, isolated the *sel-10* loss-of-function mutation *bc189* and the *sel-10* deletion *bc243*, and used my mapping of *n3717* to clone *sel-10*. Barbara Conradt, Sibylle Jager, and I did strain constructions and assessed genetic interactions between *sel-10* mutations and mutations affecting sex-determination and Notch signaling. All of the biochemistry and mammalian cell-culture experiments were performed by Sibylle Jager.

Summary

The *Caenorhabditis elegans* F-box protein SEL-10 and its human homolog have been proposed to regulate LIN-12 Notch signaling by targeting for ubiquitin-mediated proteasomal degradation LIN-12 Notch proteins and SEL-12 PS1 presenilins, the latter of which have been implicated in Alzheimer's Disease. We found that *sel-10* is the same gene as *egl-41*, which previously had been defined by gain-of-function mutations that semidominantly cause masculinization of the hermaphrodite soma. Our results demonstrate that mutations causing loss-of-function of *sel-10* also have masculinizing activity, indicating that *sel-10* functions to promote female development. Genetically, *sel-10* acts upstream of the genes *fem-1*, *fem-2*, and *fem-3* and downstream of *her-1* and probably of *tra-2*. When expressed in mammalian cells, SEL-10 protein co-immunoprecipitates with FEM-1, FEM-2, and FEM-3, which are required for masculinization, and FEM-1 and FEM-3 are targeted by SEL-10 for proteasomal degradation. We propose that SEL-10-mediated proteolysis of FEM-1 and FEM-3 is required for normal hermaphrodite development.

Introduction

C. elegans develops either as a self-fertilizing XX hermaphrodite or as an X0 male (1). The X-to-autosome (X:A) ratio provides the primary sex-determining signal and specifies the activity of *her-1* (*her*, hermaphrodization). Downstream of *her-1*, five genes - *tra-2*, *tra-3* (*tra*, transformer), *fem-1*, *fem-2*, and *fem-3* (*fem*, feminization) - control the activity of *tra-1*, the terminal, global regulator of somatic sexual fate. In XX animals, the *her-1* gene, which encodes a secreted protein, is not expressed (2). The lack of *her-1* expression in XX animals permits the activation of the transmembrane protein TRA-2, which blocks the functions of FEM-1 (a novel protein (3)), FEM-2 (a type 2C protein phosphatase (4, 5)), and FEM-3 (an ankyrin-repeat protein (6)), possibly by directly interacting with FEM-3 (7). This block leads to the activation of the Zn-finger DNA-binding protein TRA-1 (8). Active TRA-1 represses the transcription of genes required for male development, resulting in the formation of an animal with a female soma, a hermaphrodite (9, 10). In X0 animals, the HER-1 protein is present and inhibits TRA-2 (11, 12). The FEM proteins are thus relieved from negative regulation by TRA-2, resulting in the FEM-dependent inhibition of TRA-1 and subsequent male development.

The gene *egl-41* (*egl*, egg-laying defective) was defined by three semidominantly-acting mutations, *n1069*, *n1074* and *n1077,* identified in a screen for egg-laying defective (Egl) hermaphrodites (13). Additional *egl-41* alleles were identified in screens for mutations that suppress a semidominantly-acting *tra-2* mutation (*e2055*; (14)), that cause the male-specific CEMs (cephalic companion neurons) to survive in hermaphrodites (*n3717*; H.T.S. and H.R.H., unpublished results), or that cause abnormalities in the sex-specific pattern of cell deaths in the ventral cord (*n3854*, *n4041*, *n4046*; B. Galvin and H.R.H., unpublished results). *egl-41* hermaphrodites are weakly

masculinized: for example, in *egl-41* hermaphrodites the hermaphrodite-specific neurons (HSNs) die (the HSNs normally die by programmed cell death in males and survive in hermaphrodites, in which they are required for egg laying) and the CEM neurons, which normally die in hermaphrodites, survive (13). All previously characterized *egl-41* alleles cause a semidominant phenotype. Semidominant phenotypes often are consequences of gain-of-function (gf) mutations that cause altered gene function. For this reason, previous studies could not establish whether *egl-41* normally acts in the sex-determination pathway. In this report, we describe the molecular characterization of the *egl-41* gene and the phenotype caused by the loss of *egl-41* function. Our results indicate that *egl-41* is the same gene as the previously characterized gene *sel-10* (*sel*, suppressor/enhancer of *lin-12*) and that *sel-10* normally functions in sex determination.

Materials and Methods

General methods and strains. *C. elegans* strains were maintained at 20°C unless otherwise noted. The strain N2 (Bristol) was the standard wild-type strain. For single nucleotide polymorphism (SNP) mapping, the wild-type strain CB4856 (Hawaiian) was also used. Alleles, deficiencies, and duplications used in this study are listed below and are described by Riddle et al. (15), except where noted otherwise: LGI: *him-1*(*e879*), *nIs133* (*pkd-2::gfp*, (16); H.T.S. and H.R.H, unpublished). LGII: *tra-2*(*e1875*, *e2019*, *e2021, e2531, n1106*). LGIII: *fem-2*(*b245*, *e2105*), *lin-12*(*n302*, *n676 n930*). LGIV: *fem-1*(*hc17*, *e1965*), *fem-3*(*e2006*, *e1996*), *him-8*(*e1489*), *ced-3*(*n717*). LGV: *dpy-11*(*e224*), *her-1*(*e1561*, *n695*, *hv1 y101*), *unc-42*(*e270*), *lon-3*(*e2175*), *rol-4*(*sc8*), *sel-10*(*ar41*, *n1069, n1074, n1077*, *e2055*), *sel-10*(*bc189 n1077*, *bc243*, *n4273*) (this study), *sel-10*(*n3717*) (H.T.S. and H.R.H., unpublished results), *sel-10*(*n3854*, *n4041*, *n4046*) (B. Galvin and H.R.H. unpublished results), *him-5*(*e1490*), *unc-76*(*e911*), *dpy-21*(*e428*). LGX: *sel-12*(*ar131*), *sdc-1*(*n485*). *nDf42* is a deficiency spanning the *sel-10* locus (17). *ctDp8*(*V;f*) is a free duplication spanning the *sel-10* locus (18).

Mapping of *egl-41/sel-10.* *sel-10* gf alleles had previously been mapped between *sqt-3* and *him-5* on LGV (13). The location of *n3717*gf was refined using SNP mapping and the following SNPs: *pkP5069*, *pkP5070, pkP5086, pkP5088,* F55B12 9,811, and R10D12 16,645 (19). To obtain recombinants for LGV between N2 and CB4856, the strains *nIs133*; *rol-4*(*sc8*) *sel-10*(*n3717*) *unc-76*(*e911*) or *rol-4*(*sc8*) *sel-10*(*n1077*gf) *unc-76*(*e911*) were crossed with CB4856. Recombinants were analyzed for the presence of *n3717*gf or *n1077*gf by scoring for the presence of CEMs and for an Egl

phenotype as described below, and SNPs were genotyped by performing PCR and subsequent restriction digests (19).

Isolation of *sel-10* deletion mutants. Genomic DNA pools from mutagenized animals were screened for deletions as described (20). Deletion mutant animals were identified by nested PCR, isolated from frozen stocks, and outcrossed at least three times.

Microscopic analyses of mutant and transgenic animals. The Egl phenotype of *sel-10* gf animals and the presence of HSNs were analyzed as described (21). To score for the presence of CEMs, we anesthetized L4 larvae with 50 mM sodium azide and examined all four CEM positions using Nomarski microscopy (22). In SNP mapping and in epistasis analysis with *sel-10*(*n3717*gf), we scored the presence of CEMs using the *pkd-2::gfp* reporter *nIs133*. Hermaphrodite fertility was tested by picking individual L4 hermaphrodites and analyzing 72 hr later whether progeny had been generated. Brood sizes were determined by picking individual L4 hermaphrodites, transferring them to fresh plates daily for four days and counting all progeny generated. We scored as males both animals that appeared fully male-like (most of which were presumably pseudo-males, defined as XX animals that were essentially completely masculinized) and intersexes with severely masculinized tails, as determined using a dissecting microscope (23).

Molecular analysis. pBC262 contains a 6.9 kb *Xba*I fragment of cosmid F55B12 (from 7986 to 14853; all references to F55B12 sequence refer to Genbank accession number

Z79757) ligated into Bluescript KS+. The sequences of mutant alleles of *sel-10* were determined from PCR-amplified genomic DNA. The plasmids pQNClacZ, pQNCsel-10myc and pQNCsel-10HA (17, 24) were used for transient transfections. *fem-1, fem-2,* and *fem-3* cDNAs were amplified from plasmids AS#1000, AS#1245 and AS#1197 (6) to introduce a Flag-tag or Myc-tag. The *tra-2* fragment encoding TRA-2C (25), was amplified from the plasmid pPK148. The PCR products were cloned into the expression vector pCDNA3 (Invitrogen). For construction of a plasmid driving the expression of h*sel-10* shRNA, we used appropriate oligonucleotides that were annealed and ligated into the vector pSHAG-1 (26).

Transgenic animals. Germline transformation was performed as described (27). Cosmid DNA (5-8.5 μg/ml each) was injected into *sel-10*(*n1077*gf) *unc-76*(*e911*) animals with the *unc-76* rescuing construct p76-16B (50 μg/ml) (28).

Transfections, immunoprecipitations and western analysis. For co-immunoprecipitation experiments, U2OS cells were grown to 50% confluency in Dulbecco's modified Eagle's medium (DMEM) supplemented with 10% Fetal Bovine serum (FBS) and transfected using FuGENE 6 (Roche). We added a *LacZ*-containing plasmid (pQNClacz) to keep the total amount of DNA constant. 24 hr after transfection, cells were lysed in Flag lysis buffer (50 mM Tris-HCl, pH 7.8; 137 mM NaCl; 10 mM NaF; 1 mM EDTA; 10% Glycerin, 1% Triton X-100; 0.2% Sarkosyl) and 1x complete Protease Inhibitor Cocktail (Roche). Cell lysates were incubated with anti-FlagM2 affinity gel (Sigma) or anti-Myc agarose (Santa Cruz) for 2 hr at 4°C. The beads were washed 3x with Flag-lysis-buffer and boiled in sample buffer. Precipitated proteins were

analyzed using anti-FlagM2 antibodies (Sigma) and polyclonal anti-Myc antibodies (Santa Cruz). For detection of protein steady-state levels, the expression plasmids were transfected into BOSC cells. A plasmid pSHAG-Ff1 expressing Firefly Luciferase shRNA (26) was used as a negative control (control shRNA). Cell cultures were treated 8 hr with the proteasome inhibitor Lactacystin (5 μM; Sigma). The FEM proteins were detected with anti-FlagM2 antibodies.

Results

The *egl-41* mutation *n1077* causes altered *egl-41* activity that is antagonized by wild-type *egl-41* activity

egl-41(*n1077*) semidominantly causes a cold-sensitive Egl phenotype (Table S1A and (13)). *egl-41* is not haplo-insufficient for feminization, as *nDf42*/+ hermaphrodites (*nDf42* is a deficiency that deletes the *egl-41* locus; (14)) were not Egl (Table S1B). The semidominant *egl-41* phenotype is likely not caused by an increase in wild-type *egl-41* activity: hermaphrodites carrying the duplication *ctDp8,* which spans the *egl-41* locus (+/+; *ctDp8*) (18), were non-Egl (Table S1B), and 54% of *n1077*/+ hermaphrodites but only 24% of *n1077*/+/+ hermaphrodites (*n1077*/+; *ctDp8*) were Egl (Table S1B), which also indicates that the semidominant activity of *egl-41*(*n1077*) can be antagonized by wild-type activity. However, *n1077* homozygotes had a more penetrant Egl phenotype than *n1077*/*nDf42* heterozygotes (100% and 26% penetrant for Egl, respectively; Tables S1A and S2A), which indicates that *n1077* does not simply antagonize wild-type *egl-41* activity and must cause altered gene function. We therefore refer to the eight semidominantly-acting *egl-41* alleles as gain-of-function (gf) mutations.

All eight independently isolated *egl-41*(gf) mutants carry an identical mutation in the *sel-10* open-reading frame

We mapped *egl-41*(*n3717*gf) to a 130 kb interval on linkage group V and found that the Egl phenotype of and masculinization caused by *egl-41*(*n1077*gf) could be suppressed by a 6.9 kb fragment of cosmid F55B12 (bp 7986-14853) (Fig. S1A). This fragment contains the previously characterized gene *sel-10* and the 5' region of *F55B12.4*, a gene encoding a poly (A) polymerase-like protein (Fig. S1B).

sel-10, which encodes a 587 amino acid F-box protein, was previously defined by the loss-of-function (lf) mutations *ar28* and *ar41* (17, 29). *sel-10* is a negative regulator of *lin-12* (*lin*, lineage abnormal), which encodes a Notch-like receptor. The SEL-10 protein can interact with the intracellular domain of the LIN-12 protein in mammalian cells (17), and mammalian SEL-10 interacts with the intracellular domain of mammalian Notch, N^{IC}, targeting it for ubiquitin-mediated degradation (24, 30, 31). SEL-10 also appears to be a negative regulator of the presenilin SEL-12, and mammalian SEL-10 targets the presenilin PS1, which has been implicated in Alzheimer's disease, for degradation (32-34). SEL-10 contains eight WD40 repeats, which are located in the C-terminal half of the protein (17, 35). *ar41* and *ar28* are nonsense mutations that truncate SEL-10 in WD40 repeats II and VII, respectively (17). We found that all eight *egl-41*(gf) mutants have an identical mutation leading to a glycine-to-glutamic acid substitution at position 567 in WD repeat VIII (Fig. S1C).

egl-41 and _sel-10_ are the same gene

To identify dominant suppressors of the Egl phenotype of *n1077*gf animals, we mutagenized homozygous *n1077*gf hermaphrodites and screened the F1 self-progeny for rare, non-Egl hermaphrodites. From 20,000 mutagenized haploid genomes screened, we recovered one mutation, *bc189*, that semidominantly suppressed the Egl phenotype and the masculinization caused by *egl-41*(*n1077*gf) (Table S2A, B). *bc189* is tightly linked to *egl-41* (data not shown) and is a loss-of-function allele of *sel-10*: (1) like *sel-10*(*ar41*), *bc189* is a modifier of *lin-12* and a suppressor of *sel-12*(*ar131*) (Table S3); (2) *bc189* failed to complement *sel-10*(*ar41*) for suppression of *sel-12*(*ar131*) (Table S3C); and (3) *bc189* animals have a missense mutation in *sel-10*, leading to an aspartic

acid-to-asparagine substitution at position 482 in WD40 repeat VI (Fig. S1C). We used a *cis-trans* test to determine if *sel-10*(*bc189*) is in the same gene as *egl-41*(*n1077*gf). Specifically, we used *bc189* as a *sel-10*(lf) mutation in *cis* to *egl-41*(*n1077*gf) (genotype *bc189 n1077*/+) and compared *bc189 n1077*/+ animals to animals carrying the *sel-10*(lf) mutation *ar41* in *trans* to *egl-41*(*n1077*gf) (genotype *n1077*/*ar41*) (Table S2C). *sel-10*(lf) in *cis* to *n1077*gf but not in *trans* to *n1077*gf suppressed the Egl phenotype of *n1077*, indicating that the mutations affect the same gene. Henceforth, we refer to *egl-41* as *sel-10*.

sel-10(_n1077_gf) shares selected characteristics with _sel-10_(lf) mutations

sel-10(*n1077*gf) behaved similarly to the *sel-10*(lf) mutations *ar41* and *bc189 n1077* in elevating *lin-12* function: it suppressed the two-AC (AC, anchor cell) defect caused by the weak *lin-12* lf allele *lin-12*(*n676 n930*) (29) and enhanced the Muv (Muv, multivulva) phenotype caused by the weak *lin-12* gf allele *lin-12*(*n302*) (17) (Table S3A, B). By contrast, unlike *sel-10*(lf), *sel-10*(*n1077*gf) did not suppress the *Sel-12*-Egl phenotype caused by *sel-12*(*ar131*) (29, 32, 36) (Table S3C). These findings suggest that the *sel-10*(gf) mutation affects a *sel-10* function that is involved in the regulation of LIN-12 but not of SEL-12.

The _sel-10_ null phenotype is a weak masculinization of hermaphrodites

We isolated two deletion mutations in the *sel-10* gene, *bc243* and *n4273*, which delete 851 bp (10103-10953 of F55B12) and 956 bp (10323-11278 of F55B12) and are predicted to truncate SEL-10 after amino acids 85 and 106, respectively (Fig. S1B, C). The resulting proteins should lack the F-box and all eight WD40 repeats. *bc243* and

n4273 most likely are null alleles of *sel-10*. Like *sel-10*(*ar41*) and *sel-10*(*bc189 n1077*) animals, *bc243* and *n4273* hermaphrodites appear grossly wild-type. We found that *bc243* and *n4273* suppressed *lin-12*(*n676 n930*) and *sel-12*(*ar131*) and enhanced *lin-12*(*n302*gf) to a degree similar to that seen with *sel-10*(*ar41*) (Table S3 and data not shown). Thus, as previously proposed, *ar41* represents a null allele (17).

sel-10(*n1077*gf) enhances the Tra phenotype caused by weak lf mutations of *tra-2* (13). We therefore tested whether null alleles of *sel-10* could modify the Tra phenotypes caused by a gf mutation of *her-1* or by weak lf mutations of *sdc-1* (*sdc*, sex determination and dosage compensation; *sdc-1* negatively regulates *her-1*) or *tra-2.* By several criteria, we found that *sel-10*(lf) enhanced their Tra phenotypes (Table 1A, B, C). In addition, hermaphrodites homozygous for any of the three *sel-10* null mutations exhibited defects indicative of weak masculinization, including the absence of HSNs and the presence of CEMs (Table 1B, C), albeit to a far lesser degree than seen for *sel-10*(*n1077*gf) animals (Table S2B). Thus, the *sel-10* null phenotype with respect to sex determination is a weak masculinization of hermaphrodites. We conclude that *sel-10* acts to promote hermaphrodite development.

sel-10* acts upstream of *fem-1, fem-2*, and *fem-3* and downstream of *her-1* and possibly *tra-2

To place *sel-10* function within the sex determination pathway, we examined the interactions of *sel-10* null mutations with lf mutations in *her-1, fem-1, fem-2*, and *fem-3*. To ensure detection of the weak masculinizing effects of *sel-10*(lf), we used temperature-sensitive, partial loss-of-function mutations of *her-1*, *fem-1*, *fem-2* and *fem-3* under sensitized conditions that cause a partial feminization of X0 animals.

sel-10(lf) could masculinize X0 animals feminized by *her-1*(*e1561*) but not X0 animals feminized by *fem-1*(*hc17*), *fem-2*(*b245*), or *fem-3*(*e2006*) (Table 2A, B). These results suggest that *sel-10* functions downstream of or in parallel to *her-1* and upstream of or in parallel to *fem-1*, *fem-2*, and *fem-3*. Furthermore, *sel-10*(lf) partially suppressed the Fem phenotypes caused by the dominantly-acting "enhanced gain-of-function" mutation *e2531* (11) and the "mixed character" mutations *e2019* and *e2021* (37) of *tra-2* (Table 2C, D). These findings suggest that *sel-10* acts downstream of or in parallel to *tra-2*. Results similar to those obtained with *sel-10*(lf) were obtained for the stronger masculinizing effect of the *sel-10*(gf) mutation: it has been reported previously that the Egl phenotype of *sel-10*(*e2055*gf) hermaphrodites is suppressed by a null mutation in *fem-1* (14), and we found that CEM survival caused by *sel-10*(*n3717*gf) was suppressed by null mutations in any of the three *fem* genes but was not suppressed by a null mutation in *her-1* (data not shown).

SEL-10 interacts physically with the FEM proteins

F-box proteins, which were first described as exchangeable subunits of the SCF (Skp1, Cullin, F-box) E3 ubiquitin-protein ligase complex, interact with the Skp1 subunit of the complex via their F-box domains (38, 39). Many F-box proteins contain protein-protein interaction domains, such as leucine-rich domains or WD40 repeats that recruit protein substrates for ubiquitination (38, 39).

Our epistasis studies suggest that the *fem* genes are negatively regulated by *sel-10*. We therefore tested whether the FEM proteins interact with SEL-10 by performing co-immunoprecipitation experiments using U2OS human osteosarcoma cells transiently transfected to express Flag-tagged FEM-1, FEM-2 or FEM-3 (FlagFEM-1, -2,

or -3); Myc-tagged SEL-10 (SEL-10Myc); or both a Flag-tagged FEM protein and SEL-10Myc (Fig. 1). We immunoprecipitated the Flag-tagged proteins and detected SEL-10Myc only in the precipitates from lysates expressing both SEL-10Myc and any Flag-tagged FEM protein. Similarly, the immunoprecipitation of SEL-10Myc resulted in the detection of Flag-tagged FEM proteins only in the precipitates of cell lysates expressing both SEL-10Myc and any Flag-tagged FEM protein (Fig. 1). Flag-tagged TRA-2C did not precipitate SEL-10Myc (Fig. 1). Thus, when expressed in mammalian cells, SEL-10 can physically interact with each of the three *C. elegans* FEM proteins either directly or through other proteins.

The levels of FEM-1 and FEM-3 are regulated by SEL-10 and the proteasome

The ability of SEL-10 to interact with the FEM proteins suggested that SEL-10 might target the FEM proteins for proteasomal destruction. The co-expression of MycSEL-10 and FlagFEM-1 in BOSC human embryonic kidney cells did not result in decreased FEM-1 protein levels (data not shown). However, FEM-1 protein levels were increased in the presence of Lactacystin, a proteasome inhibitor (Fig. 2). We postulated that transfected FEM-1 might be targeted by the human SEL-10 homolog hSEL-10 (FBW7), which is 46% identical to *C. elegans* SEL-10. To reduce the amount of endogenous hSEL-10, we generated specific shRNA (shRNA, short hairpin RNA) (26) against the h*sel-10* gene. We transiently transfected BOSC cells to express FlagFEM-1 and either control Firefly Luciferase shRNA or h*sel-10* shRNA. When compared to control cells, the steady-state level of FEM-1 was increased in the h*sel-10* shRNA cells to a level similar to the level of FEM-1 found in cells treated with Lactacystin (Fig. 2). In analogous experiments, Lactacystin and h*sel-10* shRNA increased the protein level of

FEM-3 but did not affect the protein level of FEM-2 (Fig. 2). Together, these results indicate that the steady-state levels of transfected FEM-1 and FEM-3 in BOSC cells are dependent on the presence of hSEL-10 and a functional proteasome.

Discussion

Our genetic analysis indicates that *egl-41* mutations cause masculinization as a result of altered function of *sel-10* and further demonstrates that *sel-10* wild-type function is required for normal hermaphrodite development. That null mutations of *sel-10* cause a weak phenotype might be explained by the fact that the genome of *C. elegans* is predicted to encode at least 326 F-box proteins (40). Hence, *sel-10* might be functionally redundant with other, similar proteins. Alternately, the sex determination processes in which *sel-10* is involved, for example the degradation of FEM-1 and FEM-3, might be redundant, i.e. pathways other than a proteasome-dependent pathway might negatively regulate the activities of the *fem* genes.

The *sel-10*(gf) mutation results in the alteration of a conserved residue in WD40 repeat VIII. We propose that rather than decreasing binding to substrate or the SCF complex, this mutation might result in the formation of stable but non-functional $SCF^{SEL\text{-}10(gf)}$ complexes. By causing the formation of such complexes, SEL-10(gf) protein could prevent wild-type SEL-10 protein as well as additional functionally redundant F-box proteins from entering SCF complexes and from mediating the ubiquitination and degradation of their substrates. This model could explain why different processes are affected to differing degrees by the *sel-10*(gf) mutation and the *sel-10*(lf) mutations. SEL-10 might be the sole or principal F-box protein responsible for regulating *lin-12* activity, which is affected similarly by *sel-10* gf and lf mutations. By contrast, in sex determination, F-box proteins in addition to SEL-10 might mediate the degradation of FEM-1 and FEM-3. In *sel-10*(lf) animals, these redundant F-box proteins could largely substitute for SEL-10 function in FEM-1 and FEM-3 degradation, resulting in a weak defect in sex determination; in *sel-10*(gf) animals, non-functional $SCF^{SEL\text{-}10(gf)}$

complexes would prevent redundant F-box proteins from substituting for SEL-10 function, leading to a stronger defect.

That *sel-12*(lf) is not suppressed by the *sel-10*(gf) mutation indicates that $SCF^{SEL\text{-}10(gf)}$ complexes might still be functional with respect to *sel-12* function. The interaction between SEL-10 and SEL-12 might therefore differ from other SEL-10-substrate interactions, a difference that may be evolutionarily conserved in the interaction of the homologous proteins hSEL-10 and PS1 in Alzheimer's Disease (32-34).

Genetically, *sel-10* wild-type function likely acts downstream of or in parallel to *tra-2* as a negative regulator of *fem-1, fem-2,* and *fem-3* (Fig. 3A). When expressed in mammalian cells, SEL-10 interacted with FEM-1, FEM-2, and FEM-3, and hSEL-10 mediated the degradation of FEM-1 and FEM-3 by the proteasome. We propose that *sel-10* promotes female development by down-regulating *fem-1* and *fem-3* activities, which are required for male development. It has been proposed that *fem-1* and *fem-3* are regulated post-transcriptionally (3, 41-43). In the germline of XX animals *fem-3* activity is downregulated at the level of translation (44). Mutations that disrupt this regulation masculinize the XX germline but do not detectably affect the sexual fate of the XX soma (45). Thus, a different or an additional mechanism must be invoked in the soma. Our data suggest that in the soma *fem-1* and *fem-3* activities are regulated at least in part at the level of protein stability, through a SEL-10-mediated process.

The direct or indirect target of the FEM proteins is the transcription factor TRA-1. One mechanism that controls TRA-1 activity seems to be the regulation of TRA-1 localization: TRA-1 is preferentially exported from the nucleus in males or masculinized

XX animals, a process that requires a functional *fem-1* gene (46). It has therefore been proposed that the FEM proteins might act to promote the export of TRA-1 from the nucleus (47). Mammalian SEL-10 has been shown to localize to and function in the nucleus (30, 31). It is possible that in XX animals SEL-10 binds to nuclearly localized FEM-1 and FEM-3 proteins and mediates their degradation, thereby preventing FEM protein-mediated export of TRA-1 and allowing TRA-1 to remain inside the nucleus and to promote female development. A model in which SEL-10 mediates the degradation specifically of nuclearly localized FEM-1 and FEM-3 could also explain the finding that the overall level of FEM-1 protein appears to be similar in XX and X0 animals (41). In X0 animals, by contrast, SEL-10 would be prevented from binding FEM-1 and FEM-3 protein, resulting in the FEM-dependent export of TRA-1 out of the nucleus and subsequent male development (Fig. 3B).

A prerequisite for substrate recognition by the SCF complex seems to be substrate phosphorylation (39). SCF^{SEL-10}-mediated degradation of FEM-1 and FEM-3 might therefore dependent on their phosphorylation. The type 2C protein phosphatase FEM-2 acts at the same step of the sex-determination pathway and its phosphatase activity is required for male development (4, 5). FEM-2 can interact with FEM-3 (5) and also with FEM-1 (48). We therefore suggest that in XX animals, FEM-1 and FEM-3 are phosphorylated by a so far unidentified protein kinase and that this phosphorylation is promoted by TRA-2 in XX animals and antagonized by FEM-2 in X0 animals (Fig. 3B).

Acknowledgments

We thank Heinke Schnabel, Simon Tuck, Craig Ceol, and Erik Andersen for comments about the manuscript, and Iva Greenwald, Jonathan Hodgkin, Patty Kuwabara, Tim Schedl, and Jochen Strayle for discussions. We thank Brendan Galvin for the *sel-10* alleles *n3854, n4041*, and *n4046*; Jonathan Hodgkin, Patty Kuwabara, and Iva Greenwald for other strains; Andrew Spence for plasmids AS#1000, 1197, and 1245; Patty Kuwabara for plasmid pPK148; Jan Kitajewski for plasmids pQNClacZ, pQNCsel-10myc, and pQNCsel-10HA; and Greg Hannon for plasmids pSHAG-1 and pSHAG-Ff1. We thank Alan Coulson and the Sanger Centre for cosmids and the *Caenorhabditis elegans* Genetics Center (CGC), which is funded by the NIH NCRR, for strains. We are grateful to Claudia Huber and Andrew Hellman for technical support and to Helma Tyrlas and Beth Castor for DNA sequence determinations. This research was supported by United States Public Health Service research grant GM24663 to H.R.H. and by funding from the Max-Planck Society, the European Molecular Biology Organization (EMBO Young Investigator Award), and the Howard Hughes Medical Institute (HHMI award #76200-560801 to Dartmouth Medical School under the Biomedical Research Support Program for Medical Schools) to B.C. H.T.S. was supported by a David H. Koch Graduate Fellowship. H.R.H. is the David H. Koch Professor of Biology at MIT and an Investigator of the Howard Hughes Medical Institute.

References

1. Madl, J. E. & Herman, R. K. (1979) *Genetics* **93**, 393-402.

2. Perry, M. D., Li, W., Trent, C., Robertson, B., Fire, A., Hageman, J. M. & Wood, W. B. (1993) *Genes Dev* **7**, 216-28.

3. Ahringer, J., Rosenquist, T. A., Lawson, D. N. & Kimble, J. (1992) *Embo J* **11**, 2303-10.

4. Pilgrim, D., McGregor, A., Jackle, P., Johnson, T. & Hansen, D. (1995) *Mol Biol Cell* **6**, 1159-71.

5. Chin-Sang, I. D. & Spence, A. M. (1996) *Genes Dev* **10**, 2314-25.

6. Spence, A. M., Coulson, A. & Hodgkin, J. (1990) *Cell* **60**, 981-90.

7. Mehra, A., Gaudet, J., Heck, L., Kuwabara, P. E. & Spence, A. M. (1999) *Genes Dev* **13**, 1453-63.

8. Zarkower, D. & Hodgkin, J. (1992) *Cell* **70**, 237-49.

9. Conradt, B. & Horvitz, H. R. (1999) *Cell* **98**, 317-27.

10. Yi, W., Ross, J. M. & Zarkower, D. (2000) *Development* **127**, 4469-80.

11. Kuwabara, P. E. (1996) *Development* **122**, 2089-98.

12. Sokol, S. B. & Kuwabara, P. E. (2000) *Genes Dev* **14**, 901-6.

13. Desai, C. & Horvitz, H. R. (1989) *Genetics* **121**, 703-21.

14. Doniach, T. (1986) *Genetics* **114**, 53-76.

15. Riddle, D. L., Blumenthal, T., Meyer, B. J. & Priess, J. R. (1997) *C. elegans II* (Cold Spring Harbor Laboratory Press, Cold Spring Harbor, New York).

16. Barr, M. M. & Sternberg, P. W. (1999) *Nature* **401**, 386-9.

17. Hubbard, E. J., Wu, G., Kitajewski, J. & Greenwald, I. (1997) *Genes Dev* **11**, 3182-93.

18. Hunter, C. P. & Wood, W. B. (1992) *Nature* **355**, 551-5.

19. Consortium, T. C. e. G. (1998) *Science* **282**, 2012-8.

20. Jansen, G., Hazendonk, E., Thijssen, K. L. & Plasterk, R. H. (1997) *Nat Genet* **17**, 119-21.

21. Conradt, B. & Horvitz, H. R. (1998) *Cell* **93**, 519-29.

22. Sulston, J. E., Schierenberg, E., White, J. G. & Thomson, J. N. (1983) *Dev Biol* **100**, 64-119.

23. Hodgkin, J. (1987) *Genes Dev* **1**, 731-45.

24. Wu, G., Lyapina, S., Das, I., Li, J., Gurney, M., Pauley, A., Chui, I., Deshaies, R. J. & Kitajewski, J. (2001) *Mol Cell Biol* **21**, 7403-15.

25. Lum, D. H., Kuwabara, P. E., Zarkower, D. & Spence, A. M. (2000) *Genes Dev* **14**, 3153-65.

26. Paddison, P. J., Caudy, A. A., Bernstein, E., Hannon, G. J. & Conklin, D. S. (2002) *Genes Dev* **16**, 948-58.

27. Mello, C. & Fire, A. (1995) *Methods Cell Biol* **48**, 451-82.

28. Bloom, L. & Horvitz, H. R. (1997) *Proc Natl Acad Sci U S A* **94**, 3414-9.

29. Sundaram, M. & Greenwald, I. (1993) *Genetics* **135**, 765-83.

30. Gupta-Rossi, N., Le Bail, O., Gonen, H., Brou, C., Logeat, F., Six, E., Ciechanover, A. & Israel, A. (2001) *J Biol Chem* **276**, 34371-8.

31. Oberg, C., Li, J., Pauley, A., Wolf, E., Gurney, M. & Lendahl, U. (2001) *J Biol Chem* **276**, 35847-53.

32. Levitan, D. & Greenwald, I. (1995) *Nature* **377**, 351-4.

33. Wu, G., Hubbard, E. J., Kitajewski, J. K. & Greenwald, I. (1998) *Proc Natl Acad Sci U S A* **95**, 15787-91.

34. Li, J., Pauley, A. M., Myers, R. L., Shuang, R., Brashler, J. R., Yan, R., Buhl, A. E., Ruble, C. & Gurney, M. E. (2002) *J Neurochem* **82**, 1540-8.

35. Orlicky, S., Tang, X., Willems, A., Tyers, M. & Sicheri, F. (2003) *Cell* **112**, 243-56.

36. Li, X. & Greenwald, I. (1997) *Proc Natl Acad Sci U S A* **94**, 12204-9.

37. Kuwabara, P. E., Okkema, P. G. & Kimble, J. (1998) *Dev Biol* **204**, 251-62.

38. Patton, E. E., Willems, A. R. & Tyers, M. (1998) *Trends Genet* **14**, 236-43.

39. Deshaies, R. J. (1999) *Annu Rev Cell Dev Biol* **15**, 435-67.

40. Kipreos, E. T. & Pagano, M. (2000) *Genome Biol* **1**, 3002.1-3002.7.

41. Gaudet, J., VanderElst, I. & Spence, A. M. (1996) *Mol Biol Cell* **7**, 1107-21.

42. Doniach, T. & Hodgkin, J. (1984) *Dev Biol* **106**, 223-35.

43. Hodgkin, J. (1986) *Genetics* **114**, 15-52.

44. Ahringer, J. & Kimble, J. (1991) *Nature* **349**, 346-8.

45. Barton, M. K., Schedl, T. B. & Kimble, J. (1987) *Genetics* **115**, 107-19.

46. Segal, S. P., Graves, L. E., Verheyden, J. & Goodwin, E. B. (2001) *Dev Cell* **1**, 539-51.

47. Goodwin, E. B. & Ellis, R. E. (2002) *Curr Biol* **12**, R111-20.

48. Tan, K. M. L., Chan, S.-L., Tan, K. O. & Yu, V. C. (2001) *J Biol Chem* **276**, 44193-44202.

Table 1. *sel-10* lf mutations have masculinizing activity

A. *sel-10* lf mutations enhance the ability of various *tra* mutations to masculinize hermaphrodites

	% Tra animals (n)							
Genotype	+/+		*sel-10(ar41)*		*sel-10(bc243)*		*sel-10(n4273)*	
+/+	0	(many)	0	(many)	0	(many)	0	(many)
sdc-1(n485)	10	(223)	52	(105)	76	(82)	73	(70)
her-1(n695gf)	28	(113)	89	(155)	ND		ND	
tra-2(n1106)	8	(266)	32	(117)	25	(101)	29	(120)
tra-2(e1875)	1	(257)	3	(152)	3	(96)	8	(101)

B. *sel-10* lf mutations enhance the ability of various *tra* mutations to cause the HSNs to undergo programmed cell death

	% HSNs missing in hermaphrodites (n)							
Genotype	+/+		*sel-10(ar41)*		*sel-10(bc243)*		*sel-10(n4273)*	
+/+	0	(many)	2	(60)	7	(60)	9	(60)
sdc-1(n485)	34	(110)	76	(50)	78	(60)	77	(60)
her-1(n695gf)	90	(50)	92	(50)	ND		ND	
tra-2(n1106)	85	(110)	86	(50)	87	(60)	83	(60)
tra-2(e1875)	32	(220)	81	(110)	60	(60)	60	(60)

C. *sel-10* lf mutations enhance the ability of various *tra* mutations to cause CEMs survival

	% CEMs present in hermaphrodites (n)							
Genotype	+/+		*sel-10(ar41)*		*sel-10(bc243)*		*sel-10(n4273)*	
+/+	0	(many)	2	(168)	4	(160)	7	(152)
sdc-1(n485)	21	(376)	46	(80)	35	(80)	39	(80)
her-1(n695gf)	80	(80)	85	(80)	ND		ND	
tra-2(n1106)	84	(160)	91	(80)	84	(80)	83	(80)
tra-2(e1875)	44	(156)	65	(80)	69	(80)	68	(80)

A. The Tra phenotype was scored as described in Materials and Methods. ND, not determined. The complete genotypes of the animals analyzed were as listed save that all strains containing *her-1(e695)* were homozygous for *dpy-11(e224)* and all strains containing *sel-10(ar41)* were homozygous for *lon-3(e2175)*.

B., C. The presence of HSNs and CEMs was scored as described in Materials and Methods. The genotypes of the animals were as in A.

Table 2. Genetic interactions between *sel-10* lf mutations and feminizing mutations

A. *sel-10(ar41)* partially suppresses the feminization of X0 animals caused by *her-1(e1561*lf)

Genotype	% males (n) 15°C	24.5°C
him-8(e1489)	30 (209)	34 (273)
him-8(e1489); her-1(e1561)	36 (270)	12 (217)
him-8(e1489); sel-10(ar41)	38 (252)	32 (93)
him-8(e1489); her-1(e1561) sel-10(ar41)	34 (291)	30 (205)
him-8(e1489); sel-10(bc243)	40 (181)	42 (186)
him-8(e1489); her-1(e1561) sel-10(bc243)	41 (207)	30 (186)
him-8(e1489); sel-10(n4273)	37 (194)	35 (221)
him-8(e1489); her-1(e1561) sel-10(n4273)	36 (114)	24 (256)

B. *sel-10(ar41)* fails to suppress the feminization of X0 animals caused by lf mutations in *fem-1, fem-2,* and *fem-3*

Genotype	% CEMs in X0 (n) +/+	*sel-10(ar41)*
+/+ [a]	91 (80)	91 (100)
fem-1(hc17) [a]	51 (100)	53 (112)
fem-2(b245) [a]	73 (100)	75 (220)
+/+ [b]	91 (80)	89 (156)
fem-3(e2006) [b]	55 (176)	55 (92)

C. *sel-10(ar41)* partially suppresses the feminization of X0 animals caused by *tra-2(e2531*eg)/+

Genotype	% CEMs present in X0 (n)
sel-10(ar41)	91 (100)
*tra-2(e2531*eg)/+	15 (120)
*tra-2(e2531*eg)/+; *sel-10(ar41)*	40 (172)

D. *sel-10(ar41)* partially suppresses the germline feminization in XX animals caused by *tra-2*(mx) mutations

Genotype	% fertile animals (n)	Average # of progeny	range	(n)
sel-10(ar41)	100 (58)	277	243-328	(6)
*tra-2(e2019*mx)	10 (102)	70	18-104	(6)
*tra-2(e2019*mx); *sel-10(ar41)*	22 (102)	127	20-180	(6)
*tra-2(e2021*mx)	13 (101)	60	7-108	(7)
*tra-2(e2021*mx); *sel-10(ar41)*	46 (101)	129	34-210	(6)

A. "Males" were identified based on the criteria described in Materials and Methods. The complete genotypes of the animals analyzed were as listed, save for the second through fourth strains as listed from top to bottom, which were: *him-8(e1489); her-1(e1561) unc-76(e911), him-8(e1489); lon-3(e2175) sel-10(ar41),* and *him-8(e1489); her-1(e1561) lon-3(e2175) sel-10(ar41) unc-76(e911).*

B. The presence of CEMs in X0 animals was scored as described in Materials and Methods. The complete genotypes of the animals analyzed were as listed save that all strains contain *him-1(e879)* and all strains containing *sel-10(ar41)* are homozygous for *lon-3(e2175).* [a] Animals were cultured at 25°C until reaching the second larval stage and then shifted to 16°C. [b] Animals were cultured at 20°C.

C. The presence of CEMs in X0 animals was scored as described in Materials and Methods. eg, enhanced gain-of-function. The complete genotypes of the animals analyzed were, from top to bottom, as follows: *him-1(e879); lon-3(e2175) sel-10(ar41), tra-2(e2531)/+, tra-2(e2531)/+; lon-3(e2175) sel-10(ar41).*

D. The number of fertile animals and the number of progeny were analyzed as described in Materials and Methods. mx, mixed character. The complete genotypes of the animals analyzed were as listed save that all strains containing *sel-10(ar41)* were homozygous for *lon-3(e2175)*.

Table S1. *n1077* is a cold-sensitive, semidominant maternal-effect mutation that causes altered *egl-41* activity, which is antagonized by wild-type activity

A. *n1077* is cold-sensitive and semidominant and shows a maternal effect

		% Egl (n)					
Genotype	Maternal genotype	15°C		20°C		25°C	
+/+	+/+	0	(many)	0	(many)	0	(many)
n1077	*n1077*	100	(93)	100	(152)	34	(161)
n1077/+	*n1077*	53	(96)	54	(114)	7	(41)
n1077/+	+/+	14	(177)	8	(211)	3	(113)

B. *n1077* causes altered *egl-41* activity, which is antagonized by wild-type activity

Genotype	% Egl (n)	
+/+	0	(many)
+/*nDf42*	1	(72)
+/+; *ctDp8*	0	(70)
n1077	97	(73)
n1077; *ctDp8*	96	(128)
n1077/+	54	(144)
n1077/+; *ctDp8*	24	(50)

A. The Egl phenotype was scored as described in Materials and methods. The complete genotypes of the animals analyzed were, from top to bottom, as follows: N2 (wild-type), *n1077, n1077 unc-76(e911)*/+, *n1077/unc-76(e911)*.

B. The Egl phenotype was scored as described in Materials and methods. *nDf42* is a deficiency that deletes the *egl-41* locus and *ctDp8* is a duplication that spans the *egl-41* locus. The complete genotypes of the animals analyzed were, from top to bottom, as follows: N2 (wild-type), +/*nT1* [*n754*]; *nT1* [*n754*]/*nDf42, unc-42(e270) him-5(e1490) dpy-21(e428); ctDp8, unc-42(e270) n1077/n1077, unc-42(e270) n1077; ctDp8, unc-42(e270) n1077*/+, *unc-42(e270) n1077/unc-42(e270) him-5(e1490) dpy-21(e438); ctDp8.* The translocation *nT1*[*n754*] was used as a balancer for the *egl-41* locus.

Table S2. *bc189* is a temperature-sensitive semidominant suppressor of *n1077*gf

A. *bc189* suppresses the Egl phenotype caused by *n1077*gf in a temperature-sensitive, semidominant manner

Genotype	% Egl (n)		
	15°C	20°C	25°C
+/+	0 (many)	0 (many)	0 (many)
n1077	100 (152)	100 (152)	34 (161)
n1077/+	14 (177)	8 (211)	3 (113)
+/nDf42	0 (73)	1 (72)	0 (62)
n1077/nDf42	43 (74)	26 (86)	14 (114)
bc189 n1077	2 (127)	1 (92)	5 (190)
bc189 n1077/+	1 (172)	0 (228)	0 (94)
bc189 n1077/n1077	90 (57)	83 (127)	17 (59)

B. *bc189 n1077* hermaphrodites have HSNs and lack CEMs

Genotype	% Egl (n)	% HSNs missing (n)	% CEMs present (n)
+/+	0 (many)	0 (many)	0 (many)
n1077	100 (152)	92 (50)	96 (80)
bc189 n1077	1 (92)	5 (48)	3 (102)

C. *bc189* and *n1077* affect the same gene: *cis-trans* test

Genotype	Maternal genotype	% Egl (n)
n1077/+	+/+	12 (139)
bc189 n1077/+	+/+	0 (54)
sel-10(ar41)	*sel-10(ar41)*	0 (153)
sel-10(ar41)/n1077	*sel-10(ar41)*	70 (168)

A. The Egl phenotype was scored as described in Materials and methods. The complete genotypes of the animals analyzed were, from top to bottom, as follows: N2 (wild-type), *n1077*, *n1077/unc-76(e911)*, *nT1* [*n754*]*/nDf42*, *n1077/nDf42*, *bc189 n1077*, *bc189 n1077/ unc-76*, *n1077 unc-76(e911)/bc189 n1077.*

B. *bc189* suppresses *n1077* for the inappropriate lack of HSNs and the inappropriate presence of CEMs in hermaphrodites. The Egl phenotype and the presence of HSNs and CEMs were scored as described in Materials and methods. The complete genotypes of the animals analyzed are listed under Genotype.

C. The Egl phenotype was scored as described in Materials and methods. The complete genotypes of the animals analyzed were, from top to bottom, as follows: *n1077/lon-3(e2175)*, *bc189 n1077/lon-3(e2175)*, *lon-3(e2175) sel-10(ar41)*, *lon-3(e2175) sel-10(ar41)/n1077.*

Table S3. Interactions of *sel-10* mutations with *lin-12* and *sel-12* mutations

A. *sel-10(bc189 n1077)* and *sel-10(n1077)* suppress the two-AC defect (AC, anchor cell) caused by *lin-12(n676 n930)*

	% animals with 2 ACs (n)					
Genotype	15°C		20°C		25°C	
+/+	0	(many)	0	(many)	0	(many)
lin-12(n676 n930)	0	(40)	21	(42)	50	(44)
lin-12(n676 n930); sel-10(ar41)	0	(25)	8	(90)	10	(40)
lin-12(n676 n930); sel-10(bc189 n1077)	0	(40)	0	(40)	4	(48)
lin-12(n676 n930); sel-10(n1077)	0	(36)	0	(40)	23	(40)
lin-12(n676 n930); sel-10(bc243)	0	(26)	0	(27)	3	(30)
lin-12(n676 n930); sel-10(n4273)	0	(30)	0	(30)	7	(30)

B. *sel-10(bc189 n1077)* and *sel-10(n1077)* cause a synthetic multivulva phenotype in *lin-12(n302*gf*)* animals

Genotype	% multivulval animals (n)	
+/+	0	(many)
*lin-12(n302*gf*)*	0	(107)
*lin-12(n302*gf*); sel-10(ar41)*	68	(59)
*lin-12(n302*gf*); sel-10(bc189 n1077)*	87	(79)
*lin-12(n302*gf*); sel-10(n1077)*	55	(150)

C. *sel-10(bc189 n1077)* but not *sel-10(n1077)* suppresses the *Sel-12*-Egl phenotype caused by *sel-12(ar131)*

Genotype	% *Sel-12*-Egl (n)	
+/+	0	(many)
sel-12(ar131)	97	(145)
sel-10(ar41)	2	(146)
sel-10(bc189 n1077)	1	(92)
sel-10(ar41); sel-12(ar131)	2	(211)
sel-10(ar41)/+; sel-12(ar131)	97	(70)
sel-10(bc189 n1077); sel-12(ar131)	13	(233)
sel-10(bc189 n1077)/+; sel-12(ar131)	90	(39)
sel-10(ar41)/sel-10(bc189 n1077); sel-12(ar131)	11	(80)
ced-3(n717); sel-10(n1077)	27	(106)
ced-3(n717); sel-12(ar131)	84	(100)
ced-3(n717); sel-10(n1077); sel-12(ar131)	80	(122)
sel-10(bc243); sel-12(ar131)	7	(160)
sel-10(n4273); sel-12(ar131)	6	(170)

A. The two anchor cell phenotype (the generation of two anchor cells rather than a single anchor cell) was analyzed as described (1, 2). The complete genotypes of the animals analyzed were, from top to bottom, as follows: N2 (wild-type), *unc-32(e189) lin-12(n676 n930), unc-32(e189) lin-12(n676 n930); lon-3(e2175) sel-10(ar41), unc-32(e189) lin-12(n676 n930); sel-10(bc189 n1077), unc-32(e189)*

lin-12(n676 n930); sel-10(n1077), unc-32(e189) lin-12(n676 n930); sel-10(bc243), unc-32(e189) lin-12(n676 n930); sel-10(n4273).

B. The multivulva phenotype was analyzed as described (1, 2). The complete genotypes of the animals analyzed were, from top to bottom, as follows: N2 (wild-type), *lin-12(n302), lin-12(n302); lon-3(e2175) sel-10(ar41), lin-12(n302); sel-10(bc189 n1077), lin-12(n302); sel-10(n1077).*

C. The *sel-12*(*ar131*) Egl phenotype, which results from multiple defects during the development of the egg-laying system rather than from the inappropriate deaths of the HSNs, and which we refer to as "*Sel-12*-Egl phenotype," was analyzed 48 hr after the animals had been picked as L4 larvae. The *Sel-12*-Egl phenotype of *sel-10*(*n1077*gf); *sel-12*(*ar131*) animals was analyzed in the presence of the *ced-3*(lf) mutation *n717* (*ced*, cell death abnormal), which blocks programmed cell death (3) and which suppresses the Egl phenotype of *sel-10*(*n1077*gf) hermaphrodites (4). The complete genotypes of the animals analyzed were, from top to bottom, as follows: N2 (wild-type), *sel-12(ar131), lon-3(e2175) sel-10(ar41), sel-10(bc189 n1077), lon-3(e2175) sel-10(ar41); sel-12(ar131), lon-3(e2175) sel-10(ar41)/+; sel-12(ar131), sel-10(bc189 n1077); sel-12(ar131), lon-3(e2175)/sel-10(bc189 n1077); sel-12(ar131), lon-3(e2175) sel-10(ar41)/sel-10(bc189 n1077); sel-12(ar131),ced-3(n717); sel-10(n1077), ced-3(n717); lon-3(e2175); sel-12(ar131), ced-3(n717); sel-10(n1077); sel-12(ar131), sel-10(bc243); sel-12(ar131), sel-10(n4273); sel-12(ar131).*

1. Greenwald, I. S., Sternberg, P. W. & Horvitz, H. R. (1983) *Cell* **34,** 435-44.
2. Sundaram, M. & Greenwald, I. (1993) *Genetics* **135,** 765-83.
3. Ellis, H. M. & Horvitz, H. R. (1986) *Cell* **44,** 817-29.
4. Desai, C. & Horvitz, H. R. (1989) *Genetics* **121,** 703-21.

Figure legends

Figure 1

The FEM proteins interact with SEL-10 in mammalian cells. Extracts from mammalian U2OS cells expressing SEL-10Myc; FlagFEM-1, -2, or -3; FlagTRA-2C; or both SEL-10Myc and the indicated Flag-tagged protein were immunoprecipitated by anti-FlagM2 or anti-Myc antibodies. The precipitated proteins were analyzed for the presence of SEL-10Myc with anti-Myc antibodies and of the Flag-tagged proteins with anti-FlagM2 antibodies.

Figure 2

FEM-1 and FEM-3 may be targeted by hSEL-10 for degradation by the proteasome. To analyze protein steady-state levels, we treated BOSC cells expressing FlagFEM-1, FlagFEM-2 or FlagFEM-3, respectively, with Lactacystin to inhibit the proteasome or with h*sel-10* shRNA to partially inactivate h*sel-10* (shRNA, short hairpin RNA). The untreated and Lactacystin-treated cells were co-transfected with a plasmid expressing control shRNA (Firefly Luciferase). Whole-cell lysates were analyzed using anti-FlagM2 antibodies. Representative data from three independent experiments are shown.

Figure 3

Genetic and molecular pathways of somatic sex determination in *C. elegans.* A. A simplified genetic pathway for sex determination in the *C. elegans* soma is shown. *sel-10* is a new gene in this pathway and acts as a negative regulator of the *fem* genes.

B. A model for the molecular interactions among SEL-10, the FEM proteins, TRA-1 and TRA-2. SEL-10 negatively regulates FEM-1 and FEM-3 by promoting the degradation of their phosphorylated forms. A negative arrow from TRA-2 to FEM-3 reflects the possibility that TRA-2 directly binds and inhibits FEM-3 (7). See text for details.

Figure S1

Mapping and cloning of *egl-41*. (*A*) Genetic and physical map. Genes and single-nucleotide polymorphisms (SNPs) (F55B12 9,811 and R10D12 16,645) used for mapping the semidominantly-acting *egl-41*(gf) mutation *n3717* are indicated. Numbers below the genetic map represent the fraction of the 120 recombination events identified between *rol-4* and *unc-76* that occurred between the loci indicated. The cosmids to which *sel-10* was mapped by using SNP mapping and that were tested for the suppression of the Egl phenotype of *sel-10*(*n1077*gf) are indicated. An asterisk indicates the cosmid F55B12, which suppressed the Egl phenotype of *sel-10*(*n1077*gf). pBC262 contains a 6.9-kb *Xba*I fragment of F55B12 that suppressed the Egl phenotype of *sel-10*(*n1077*gf). Transgenic animals carrying the indicated constructs as extrachromosomal arrays were generated, and suppression was scored as described in *Materials and Methods*. The number of lines rescued and the total number of lines obtained are indicated in parentheses. (*B*) Structure of the 6.9-kb fragment of F55B12 contained in pBC262 and the extents of the *sel-10* deletion alleles *bc243* and *n4273*. The fragment contained in pBC262 spans *sel-10* (*F55B12.3*) and also includes the 5' region of *F55B12.4*. *bc243* and *n4273* delete genomic regions corresponding to base pairs 10,103-10,953 and base pairs 10,323-11,278 of cosmid F55B12, respectively. (*C*) *egl-41/sel-10* (gf) mutations and *bc189* are missense mutations in the *sel-10* ORF. The amino acids changed as a result of the mutations *n1069*, *n1074*, *n1077*, *e2055*, *n3717*,

n3854, n4041, n4046, and *bc189* are shown in bold, and the allele numbers are shown above the protein sequence. The positions of the nonsense mutations *ar41* and *ar28* and the positions at which the deletion mutations *bc243* and *n4273* are predicted to truncate the SEL-10 protein, are indicated by asterisks and shrills, respectively, above the sequence. The F-box domain and the WD40 repeats are indicated with overhead lines and labeled.

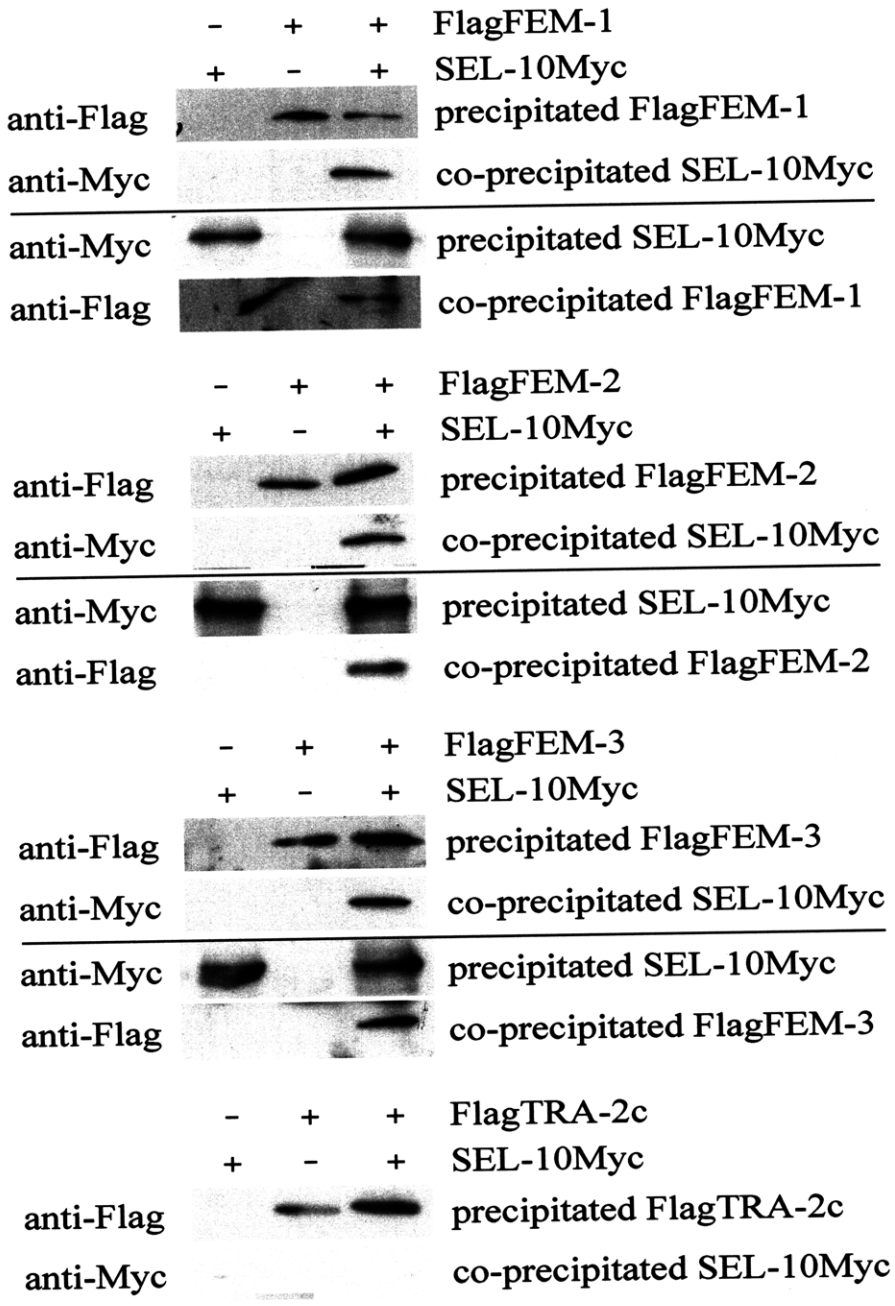
- + + FlagFEM-1
+ - + SEL-10Myc
anti-Flag precipitated FlagFEM-1
anti-Myc co-precipitated SEL-10Myc
anti-Myc precipitated SEL-10Myc
anti-Flag co-precipitated FlagFEM-1
- + + FlagFEM-2
+ - + SEL-10Myc
anti-Flag precipitated FlagFEM-2
anti-Myc co-precipitated SEL-10Myc
anti-Myc precipitated SEL-10Myc
anti-Flag co-precipitated FlagFEM-2
- + + FlagFEM-3
+ - + SEL-10Myc
anti-Flag precipitated FlagFEM-3
anti-Myc co-precipitated SEL-10Myc
anti-Myc precipitated SEL-10Myc
anti-Flag co-precipitated FlagFEM-3
- + + FlagTRA-2c
+ - + SEL-10Myc
anti-Flag precipitated FlagTRA-2c
anti-Myc co-precipitated SEL-10Myc

Figure 1

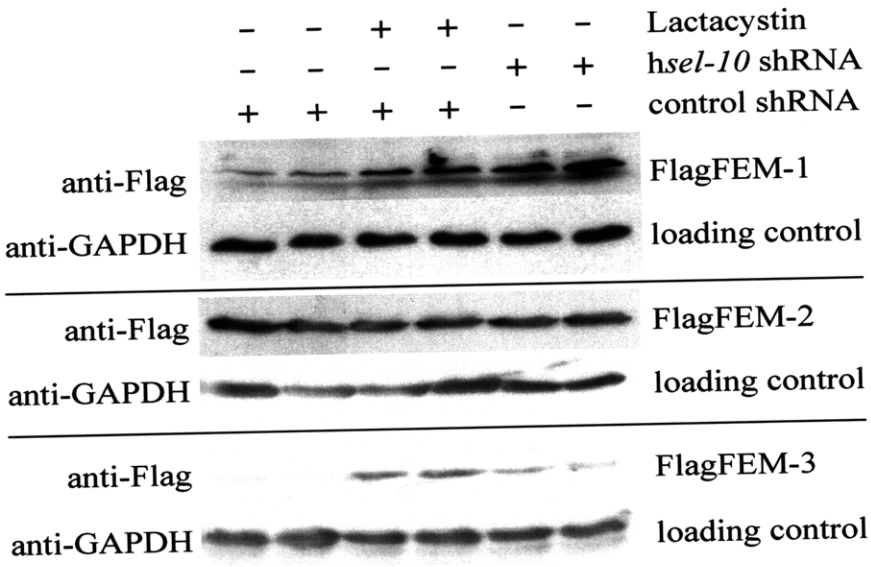
– – + + – – Lactacystin
– – – – + + hsel-10 shRNA
+ + + + – – control shRNA
anti-Flag
FlagFEM-1
anti-GAPDH
loading control
anti-Flag
FlagFEM-2
anti-GAPDH
loading control
anti-Flag
FlagFEM-3
anti-GAPDH
loading control

Figure 2

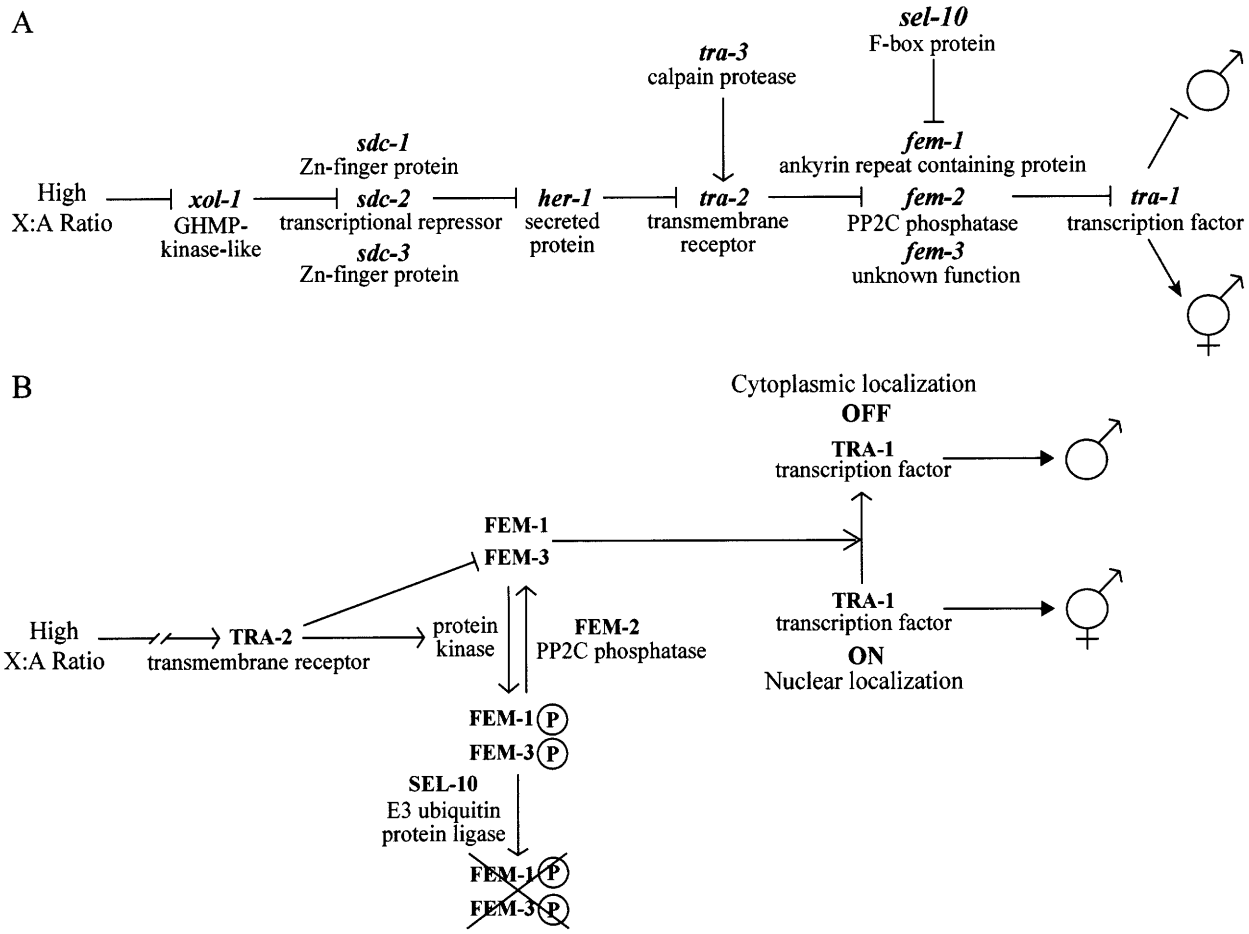
A
sel-10
F-box protein
tra-3
calpain protease
sdc-1
Zn-finger protein
fem-1
ankyrin repeat containing protein
High
X:A Ratio
xol-1
GHMP-
kinase-like
sdc-2
transcriptional repressor
sdc-3
Zn-finger protein
her-1
secreted
protein
tra-2
transmembrane
receptor
fem-2
PP2C phosphatase
fem-3
unknown function
tra-1
transcription factor
B
Cytoplasmic localization
OFF
TRA-1
transcription factor
FEM-1
FEM-3
High
X:A Ratio
TRA-2
transmembrane receptor
protein
kinase
FEM-2
PP2C phosphatase
TRA-1
transcription factor
ON
Nuclear localization
FEM-1 P
FEM-3 P
SEL-10
E3 ubiquitin
protein ligase
FEM-1 P
FEM-3 P

Figure 3

Fig. S1A

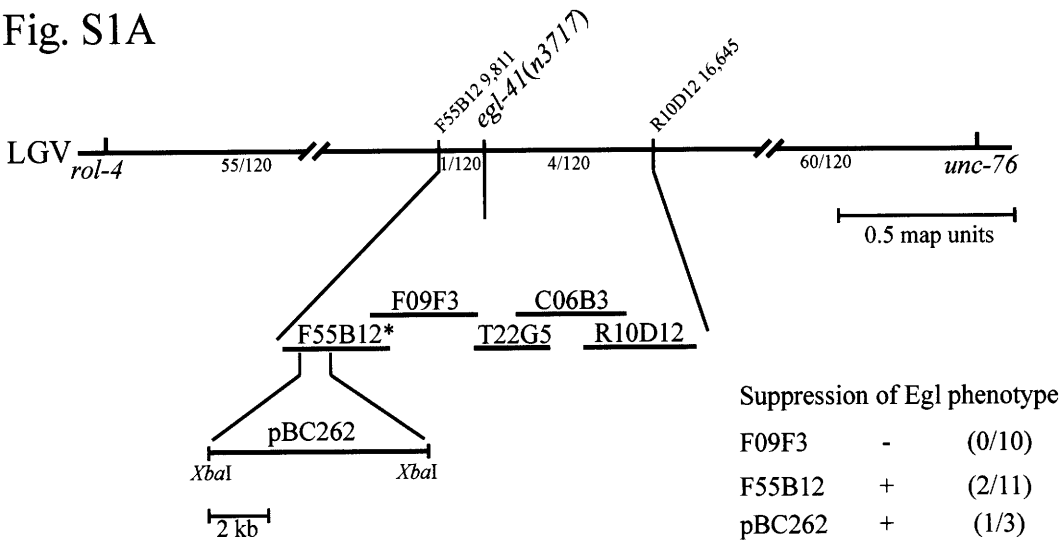

Suppression of Egl phenotype

F09F3	-	(0/10)
F55B12	+	(2/11)
pBC262	+	(1/3)

Fig. S1B

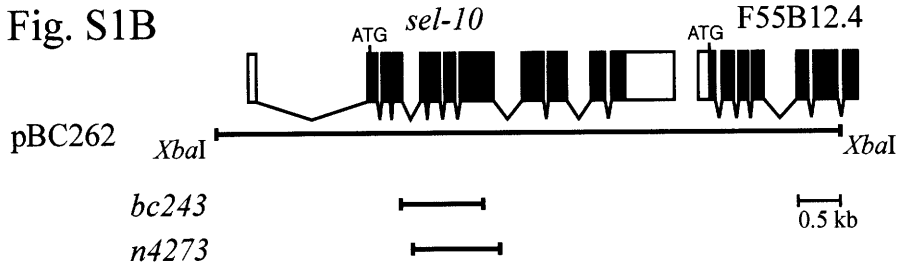

Fig. S1C

```
MWPRNDVHMD DGSMTPEDQE PVTDNDMEYN DNGEESSYSN GSSSSYNADK   50
                                          #(bc243)
LSSSRPLQHK LDLSASPSRN NDLNPRVEHL IALFKDLSSA EQMDAFTRLL  100
      #(n4273)                F-box
QESNMTNIRQ LRAIIEPHFQ RDFLSCLPVE LGMKILHNLT GYDLLKVAQV  150

SKNWKLISEI DKIWKSLGVE EFKHHPDPTD RVTGAWQGTA IAAGVTIPDH  200

IQPCDLNVHR FLKLQKFGDI FERAADKSRY LRADKIEKNW NANPIMGSAV  250
  WD I                                          WD II
LRGHEDHVIT CMQIHDDVLV TGSDDNTLKV WCIDKGEVMY TLVGHTGGVW  300
                          *(ar41)       WD III
TSQISQCGRY IVSGSTDRTV KVWSTVDGSL LHTLQGHTST VRCMAMAGSI  350
                          WD IV
LVTGSRDTTL RVWDVESGRH LATLHGHHAA VRCVQFDGTT VVSGGYDFTV  400
               WD V
KIWNAHTGRC IRTLTGHNNR VYSLLFESER SIVCSGSLDT SIRVWDFTRP  450
          WD VI                      N(bc189)
EGQECVALLQ GHTSLTSGMQ LRGNILVSCN ADSHVRVWDI HEGTCVHMLS  500
WD VII      *(ar28)                WD VIII
GHRSAITSLQ WFGRNMVATS SDDGTVKLWD IERGALIRDL VTLDSGGNGG  550
                    E(n1069, n1074, n1077, e2055, n3717, n3854, n4041, n4046)
CIWRLCSTST MLACAVGSRN NTEETKVILL DFDAVYP                587
```

Appendix I

Future Directions

Introduction

In this appendix, I suggest some of the future directions a researcher might take to extend the findings I have described in the preceding chapters.

Identifying transcriptional targets of the cell-type-specific anti-apoptotic homeodomain transcription factor CEH-30

As described in Chapter III, I identified the Bar homeodomain transcription factor gene *ceh-30* as controlling the sexually dimorphic survival of the CEM sensory neurons: in wild-type hermaphrodites, *ceh-30* expression is directly repressed by TRA-1, a Gli transcription factor required for hermaphrodite sexual identity. *ceh-30* can promote the survival of the CEM neurons in animals completely lacking *ced-9 Bcl-2* function, indicating that *ceh-30* promotes cell survival by a mechanism that differs from well-understood mechanisms in *C. elegans* and in other organisms. Transgenes that express the mouse homolog *Barhl1* can restore CEM survival to *ceh-30* mutant males, and mice lacking *Barhl1* function become progressively deaf as sensory hair cells of the inner ear disappear. It therefore seems likely that that the Bar homeodomain protein CEH-30 has an evolutionarily conserved function to protect against programmed cell death and acts by a novel and unknown mechanism. Identification of transcriptional targets of CEH-30 could reveal the nature of this mechanism.

One way to identify genes whose expression is controlled by *ceh-30* would be to do microarray studies comparing gene expression in *ceh-30* mutants to expression in wild-type animals. This could be done by collecting RNA samples from *ceh-30* gain-of-function mutant hermaphrodites for comparison to samples from wild-type

hermaphrodites, or by comparing RNA samples from *ceh-30* loss-of-function mutant males or masculinized hermaphrodites to samples from wild-type males or from otherwise wild-type masculinized hermaphrodites. In this way it might be possible to identify genes whose expression is promoted by *ceh-30* function and genes whose expression is inhibited by *ceh-30* function.

A second approach is the direct biochemical identification of candidate CEH-30 targets. This could be done by chromatin immunoprecipitation experiments by raising an antibody against CEH-30 or by using an epitope-tagged version of CEH-30, such as the *ceh-30::gfp::ceh-30* transgene already shown to rescue the CEM survival defect of *ceh-30* mutant males. Samples immunoprecipitated with CEH-30::GFP could be compared to samples immunoprecipitated from animals lacking the transgene or animals expressing GFP unlinked to CEH-30, and DNA sequences enriched in samples immunoprecipitated with CEH-30::GFP could be identified using microarray analysis. Regions of the *C. elegans* genome capable of interacting with CEH-30 could also be identified using a one-hybrid approach in yeast or by using SELEX to identify genomic fragments capable of binding CEH-30.

Whatever approaches are used to identify a candidate target of transcriptional regulation by CEH-30, it will be important to determine whether it has any detectable functional importance in the control of cell survival. A gene whose expression is controlled by CEH-30, either directly or indirectly, could be a positive or a negative regulator of cell survival, or it might do neither. Whether a candidate target of CEH-30 is involved in regulation of cell survival by CEH-30 can be assessed using deletion

mutants of these candidate targets when such are available, and otherwise by using dsRNA to target the genes for RNAi.

Homologs of CEH-30 act as transcriptional repressors; if CEH-30 is also a transcriptional repressor, then it seems likely that CEH-30 promotes CEM survival by direct transcriptional repression of genes that normally promote CEM death. Reduced function of such a target should therefore promote CEM survival in hermaphrodites. To increase the sensitivity of such an assay, it could be performed in animals partially defective in cell killing, such as the weak mutant *ced-3(n2427)*, or in hermaphrodites that show weak CEM survival as a result of partial masculinization, such as animals heterozygous for *tra-1(e1099)* or animals homozygous for *tra-2(e1875)*. If reduced function of a candidate causes CEM survival in hermaphrodites, it should be determined whether it protects the CEM neurons by weakly masculinizing the hermaprodite, or whether this effect, like the protective function of *ceh-30*, acts downstream of determination of sexual identity. This can be done by testing for CEM survival in animals lacking *ceh-30* function, which should suppress the protective effects of partial masculinization, by looking for signs of partial masculinization, or by testing for enhancement of the weakly masculinized phenotype of a mutant such as *tra-2(e1875)* or *sel-10(n1077)*.

If a gene directly or indirectly regulated by CEH-30 target normally promotes CEM neuron survival, reduction of gene function should cause decreased CEM survival in males or in masculinized hermaphrodites. To increase the sensitivity of this assay it may be helpful to use weakly masculinized hermaphrodites such as animals heterozygous for a strong loss-of-function mutation in *tra-1* or animals homozygous for

the weak *tra-2* loss-of-function mutation *e1875*. Alternatively, males homozygous for *unc-37(e262)* could be used: *unc-37(e262)* causes a weak defect in CEM survival that can be strongly enhanced by loss of *ceh-30* function, such that loss of a pro-survival gene that acts downstream of *ceh-30* may similarly enhance the *unc-37(e262)* CEM neuron survival defect. Any mutation or RNAi that causes the disappearance of CEM neurons should be tested in animals completely lacking the function of the cell-killing caspase gene *ced-3*, to determine whether the CEM neurons are thereby restored. If the CEM neurons are restored by blocking programmed cell death, the gene normally promotes CEM survival. In this case, assays should be done in animals lacking *tra-1* function to ensure that the gene does not promote CEM survival by promoting somatic masculinization. If the CEM neurons are not restored by blocking programmed cell death, then either the gene has a function in promoting CEM neuron identity other than the regulation of CEM survival, or the gene acts downstream of or in parallel to *ced-3*. As there are no epistasis tests that can determine whether *ceh-30* might act downstream of or in parallel to *ced-4* or *ced-3*, it remains possible that a target of CEH-30 might control CEM survival in animals completely lacking *ced-3* function. For more consideration of this possibility and of approaches that could be taken to examine it, see Appendix II, part D.

Further studies of the specification of CEM neuron survival

Although a large number of the isolates recovered in screens for mutant hermaphrodites defective in CEM neuron have been characterized, many screen isolates remain to be identified and important factors that control the CEM survival

decision remain unknown. Indeed, animals completely lacking *ceh-30* and the homologous gene *ceh-31* and mutant for *unc-37* still show sexual dimorphism for CEM neuron survival, indicating that at least one regulator of CEM survival remains to be identified.

The first and most obvious opportunity for further investigation of CEM neuron survival is the remaining isolates that complement mutants defective in programmed cell death, are not grossly defective in sex determination, and have not been assigned to any known gene. There are seventeen such mutants, listed in Table 3 of Chapter 2. Six of the seventeen have normal B cell morphology as L1 larvae, indicating that these six are particularly unlikely to cause CEM survival by causing sexual transformation. One mutation in particular, *n3788*, causes a relatively strong defect in CEM survival compared to the other remaining isolates and may cause a very weak defect in all programmed cell deaths.

Additional screens could be performed to recover mutant hermaphrodites defective in CEM neuron death. The screens could be made more efficient than the previous screens by using animals that lack *ceh-30* function, which should eliminate the large class of mutants in which CEM survival is caused by partial masculinization, and a second reporter could be included for the rapid identification of mutants likely to be defective in all programmed cell deaths. The identification of *cnd-1* and *vab-3* as genes in which loss-of-function mutations promote CEM death should also make it possible to rapidly eliminate a number of screen isolates from consideration through complementation tests. These genetic screens could also lead to the identification of genes that function downstream of *ceh-30* in the control of CEM survival. Screens have

also been performed to identify mutants defective in CEM survival and have recovered a large number of isolates few of which have been characterized; the results of these screens and the prospects for their future expansion are presented in Appendix II.

The finding that *vab-3* functions in parallel to *cnd-1* in the establishment of head morphology and act similarly in CEM survival has led me to propose that these two genes cooperate to promote similar effects in tissue differentiation. Further work to establish the transcriptional targets of each transcription factor, and especially to identify transcriptional targets shared between CND-1 and VAB-3, could further elucidate the functions of these genes in tissue differentiation and potentially in the control of cell survival. Approaches could be taken as described above for CEH-30; in particular, given two separate transcription factors, it may be possible to determine binding site specificities of each transcription factor *in vitro* and thereby to predict genes likely to respond to both genes. Candidate targets could be tested by causing loss-of-function and looking for effects on CEM survival and on head morphology. It may also be possible to screen for mutations or for RNAi treatments that, like weak alleles of *vab-3*, cause a strong synthetic Vab phenotype in combination with the loss of *cnd-1* function.

Molecular characterization of the green pharynx phenotype

I defined the green pharynx phenotype of transgene misexpression and extensively characterized the genetics of the green pharynx phenotype. This genetic characterization included screens likely to be saturated for loss-of-function mutations in the F_2 generation. Nonetheless, some obvious opportunities for further genetic characterization remain: two of the green pharynx genes are defined by single alleles,

one causing altered gene function and one unlikely to cause loss of gene function, suggesting that further screens might define additional genes through the identification of similar rare alleles; the green pharynx gene *hpl-2* shows maternal rescue for the green pharynx phenotype, explaining why no alleles of *hpl-2* were recovered in screens limited almost entirely to the F_2 generation; and no screens have been performed to identify suppressors of the green pharynx phenotype.

One important question remains for the green pharynx phenotype: although it appears that the green pharynx genes act to restrict the expression of selected transgenes, it has been proposed but not established that these genes similarly act to restrict the expression of a set of endogenous genes. It should be feasible to use microarray expression profiling to identify sets of genes derepressed in each of the green pharynx mutants as compared to the wild type, and to identify targets shared among these sets. As an additional control, the *lin-8* mutant *n2376* can be used; this mutant is strongly synMuv but does not cause a green pharynx phenotype. Once shared targets are identified and validated by semiquantitative RT-PCR, they will be potential molecular and biochemical tools to establish the mechanisms that the green pharynx genes use to achieve transcriptional repression.

It should be possible to identify the sequences that recruit the repressive function of the green pharynx proteins and to characterize the protein complexes involved in transcriptional repression of targets of the green pharynx proteins. Because the transgenes that are misexpressed in green pharynx mutants were generated from constructs of known sequence, modification of existing reporter transgenes that support the green pharynx phenotype should make it possible to identify sequences necessary

and sufficient for transcriptional repression by the green pharynx proteins. These sequences can then be used to purify and identify proteins that bind to sites that recruit the repressive activity of the green pharynx proteins, possibly including one or more of the green pharynx proteins. Similarly, the green pharynx proteins can be used in biochemical purifications and immunoprecipitation experiments to identify other interacting proteins and protein complexes.

Because it is known that the green pharynx proteins include homologs of chromatin modifiers and that they cause transcriptional repression of selected transgenes, the chromatin structure at these transgenes can be examined in order to understand the mechanisms that the green pharynx proteins use to establish and to maintain transcriptional repression. Chromatin immunoprecipitation experiments can be performed with antibodies against specific chromatin modifications, followed by PCR quantitation from the immunoprecipitate of transgenes known to be derepressed in green pharynx mutants. Comparisons can be made between samples from otherwise wild-type transgenic strains and from transgenic strains mutant for one or more green pharynx gene. Chromatin modifications enriched in strains with normal green pharynx function might then be modifications promoted or maintained by the green pharynx proteins.

Further studies of cell-cycle regulation by the phosphatase gene *cdc-14*

Johanna Varner and I found that the mitotic exit factor *cdc-14* is required to prevent inappropriate cell division in a highly cell-specific fashion: roughly 40% of PDE neurons undergo an inappropriate cell division in *cdc-14* mutants, but lineally related

cells and the homologous ADE neuron are not affected by loss of *cdc-14*. Further investigation could reveal genes that function to promote *cdc-14* function, genes that function in parallel with *cdc-14*, and genes that function to antagonize the function promoted by *cdc-14*.

As discussed in Chapter V, the genetic screen from which we recovered the *cdc-14* mutation *n3444* was not saturated. An expanded version of this screen might result in the identification of mutants that cause division of the presumptive PDE neuron similar to that caused by loss of *cdc-14* function, defining genes that like *cdc-14* function to prevent the inappropriate division of the presumptive PDE neuron. Such mutants might define genes that function together with *cdc-14*, or might define genes that function in parallel with *cdc-14*. Approximately 60% of presumptive PDE neurons are not affected by loss of *cdc-14*, suggesting that the existence of a mechanism that acts in parallel to *cdc-14*.

It may also be possible to identify genes that function in parallel to *cdc-14* by screening *cdc-14* animals for enhancement of the *cdc-14* PDE division defect. Screens to identify genes redundantly required with *cdc-14* for viability could also be performed, either by using mutagenesis to established mutant strains and testing them using RNAi directed against *cdc-14* or by treating *cdc-14* mutant animals with clones from an RNAi feeding library. Any of these screens intended to identify genes functioning in parallel with *cdc-14* have the potential to explain why the requirement for *cdc-14* function is restricted to a small number of specific neurons. Screens for suppressors of the PDE division defect of *cdc-14* mutants could similarly lead to the identification of genes that confer the high sensitivity of the presumptive PDE neuron to the loss of *cdc-14* function.

Acknowledgments

I would like to thank Dan Denning for his comments on this appendix.

Appendix II

Genetic screens for mutants defective in the specification of cell death and for mutants defective in transcriptional repression

Hillel Schwartz, Johanna Varner, and Dawn Wendell

As an undergraduate working under my supervision, Johanna Varner isolated 63 of the 81 mutations listed in Table 4 and performed the phenotypic characterization and epistasis tests of these isolates presented in Tables 5, 6, and 7.

As an undergraduate working under my supervision, Dawn Wendell isolated 23 of the 35 mutations listed in Table 8 and performed complementation tests and mapping experiments with many of the mutations listed in Table 8.

Summary

In this appendix I present the complete results from genetic screens that I and two undergraduate students, Johanna Varner and Dawn Wendell, performed seeking to identify mutants with cell-specific defects in the regulation of programmed cell death and mutants showing the green pharynx phenotype of transcriptional derepression. The work described in the chapters that define the main body of this thesis began with the characterization of selected mutants isolated from the screens described in this appendix.

We performed five sets of genetic screens. Some results of particular interest are highlighted:

A. Screens for lineage alterations in the postdeirid sensory structure.

1. Extended periods of developmental arrest cause lineage alterations in the postdeirid detectable using the *cat-2::gfp* dopaminergic cell fate reporter.
2. The allelic mutations *n3847* and *n3848* alter the morphology of the PDE neurons, causing an increase in nuclear size and bloating of the cell body.
3. The cell lineage mutation *n3849* causes the presence of a variable number of *cat-2::gfp*-expressing cells in the postdeirid.

B. Screens for mutant hermaphrodites in which the male-specific CEM sensory neurons failed to die.

1. The cell lineage mutation *n4743* causes a Pvl phenotype and possibly causes specific masculinization of the V5 lineage.

2. The mutation *n4753* causes the generation of an autofluorescent structure in the hermaphrodite vulva, possibly similar to the spicules of wild-type males.

C. Screens for suppressors of the CEM survival caused by masculinization.

D. Screens for suppressors of the CEM survival caused by increased function of the cell-specific anti-apoptotic transcription factor CEH-30.

1. Cell-death-defective mutants lacking *dig-1* function frequently lack *pkd-2::gfp*-expressing CEMs. This may indicate that positional cues promote the CEM neuron identity.

E. Screens for mutations causing the green pharynx phenotype of transcriptional derepression.

1. Four mutations cause lethality early in development and cause the *pkd-2::gfp* cell-fate reporter to be expressed in neurons that do not normally express the reporter.

A. Screens for lineage alterations in the postdeirid

The postdeirid is a sensory structure generated from the V5.pa blast cell during the second larval stage of *C. elegans* development (SULSTON and HORVITZ 1977; WHITE *et al.* 1986). The descendents of the V5.pa cell are five cells: the two glia-like cells PDEso and PDEsh, the dopaminergic PDE neuron, the PVD neuron, and the sister of the PVD neuron, which undergoes programmed cell death (see Figure 1) (Sulston et al. 1975; Sulston and Horvitz 1977). The transgenic cell fate reporter *mec-3::lacZ* expresses in the PVD neuron (WAY and CHALFIE 1989), but was not expressed in the "undead" PVD sisters of *ced-4(n1162)* (*ced*, cell death abnormal) animals defective in programmed cell death (data not shown). When the deaths of the PVD sisters were blocked by mutations that prevent programmed cell death, approximately 50% of "undead" PVD sisters contained dopamine like their lineal "aunts," the PDE neurons (68 of 135 postdeirids in *ced-3* mutant animals contained two dopaminergic cells) (Ellis and Horvitz 1986). The dopaminergic cell fate can be detected using markers such as expression of *cat-2*, which encodes a tyrosine hydroxylase required for production of dopamine (LINTS and EMMONS 1999). Examination of cell-death-defective (Ced) *ced-3(n717)* animals containing a *cat-2::gfp* dopaminergic cell fate reporter gave results similar to previous work staining for the presence of dopamine: 60.9% of postdeirids in *ced-3(n717)* animals grown at 25°C and 30.2% of postdeirids in *ced-3(n717)* animals grown at 20°C contained two *cat-2::gfp*-expressing cells (n = 512 and n = 665, respectively).

Two chromosomally integrated versions of the *cat-2::gfp* reporter were generated, the transgenes *nIs116* and *nIs117* (see Chapter V). Time-course

experiments examining *cat-2::gfp* reporter expression in the PDE neuron and the "undead" PVD sister cell were performed with *ced-3(n717)*; *nIs116* animals (see Figure 2). These animals were allowed to hatch in the absence of food, causing them to enter a state of developmental arrest. Following the introduction of the animals to food, animals were periodically examined for expression of *cat-2::gfp* in the PDE neuron, expression of *cat-2::gfp* in the "undead" PVD sister and for the ability to focus through the animal and visualize *cat-2::gfp* expression in both of its postdeirids. These experiments identified a period from 34 hours to 46 hours after release from larval arrest during which maximal *cat-2::gfp* expression in the "undead" PVD sister is seen and it remains feasible to visualize both postdeirids within an animal. Screens were performed under these conditions to identify mutant animals with altered *cat-2::gfp* expression in the postdeirid. *nIs116* or *nIs117* hermaphrodites were mutagenized with EMS according to standard methods (Brenner 1974). Mutagenized P_0 animals were placed on 6 cm Petri plates containing NGM agar seeded with bacteria, three to four animals per plate. Animals were tracked to identify the pool of mutagenized P_0s from which candidates originated. Plates were bleached to recover F_2 eggs, and the F_2 larvae were allowed to hatch in the absence of food and enter developmental arrest. Approximately 100 F_2 animals were screened from each pool of P_0 animals were placed on a glass slide and examined for *cat-2::gfp* expression in the postdeirid using a compound microscope. Candidates were recovered and their progeny were examined for propagation of the *cat-2::gfp* expression phenotype.

Initially very few progeny of candidate mutants displayed a phenotype of altered *cat-2::gfp* expression in the postdeirid. This high incidence of false-positives presented

difficulties in screening. The frequency of fertile false-positives was subsequently found to be directly proportional to the length of time the animals had spent in developmental arrest. For each day that animals had spent in developmental arrest prior to their being introduced to food and allowed to develop, a greater proportion developed into adults that possessed two *cat-2::gfp*-expressing cells in the postdeirid; after several days spend in developmental arrest, as many as 5% of animals developed into adults with extra *cat-2::gfp*-expressing cells in or near the postdeirid. These extra *pkd-2::gfp*-expressing cells could conceivably have resulted from a defect in the death of the PVD sister, extra division of the PDE neuron, or a cell-fate transformation or lineage alteration. The source of the extra *cat-2::gfp*-expressing cells in animals that spent long times in developmental arrest has not been determined.

Modifying the screening protocol so that animals spent no more than 18 hours in a state of developmental arrest increased the proportion of fertile candidates that re-tested, and established phenotypic mutant lines increased from approximately 2% to 50%. 24,358 *nls116* F_2 animals and 8,712 *nls117* F_2 animals were screened, for a total of approximately 16,000 homozygous mutagenized haploid genomes. An additional 2,241 F_3 *nls116* animals were screened. In total, approximately 18,000 mutagenized haploid genomes were screened for recessive effects on *cat-2::gfp* expression in the postdeirid lineage, and approximately 1,100 mutagenized haploid genomes were screened for recessive maternal-effect alteration of *cat-2::gfp* expression in the postdeirid lineage. A complete list of the 20 mutations isolated in screens for altered *cat-2::gfp* expression in the postdeirid is presented in Table 1.

Mutant strains were tested for complementation with mutations known to cause similar phenotypes. In this way, mutations that failed to complement *ced-3(n717)*, *lin-22(n372)*, *lin-32(e1926)*, and *unc-86(n846)* were identified (*lin*, abnormal cell lineage; *unc*, uncoordinated locomotion). Five screen isolates showed significant reduction in the level of *cat-2::gfp* expression. To establish that these were mutants defective in expression of the reporter transgene rather than mutants containing altered, weaker versions of the *cat-2::gfp* transgene, these strains were crossed with the wild type, and I demonstrated that outcrossed strains could be recovered in which strong expression of the *cat-2::gfp* cell-fate reporter had been restored. Two screen isolates, *n3847* and *n3848*, displayed similar phenotypes of bloated PDE cell body morphology and enlarged PDE nuclei. *n3847* and *n3848* failed to complement and mapped to LGX. Both *n3847* and *n3848* could not be separated from *nIs117 X* and therefore were not mapped. One screen isolate, *n3849*, caused the presence of a variable number of from zero to three *cat-2::gfp*-expressing cells in the postdeirid. Previously identified lineage mutations that affect the postdeirid either cause an absence of *cat-2::gfp*-expressing cells (e.g. *lin-32*) or cause an increase in the number of *cat-2::gfp*-expressing cells (e.g. *unc-86*), but no previously identified mutation causes both a reduction and an increase in the number of *cat-2::gfp*-expressing cells. The screen isolate *n3444* was determined to be an allele of the cell-cycle gene *cdc-14*. The characterization of *cdc-14* function in the postdeirid and in other cells is presented in Chapter V.

B. *pkd-2::gfp* screens for hermaphrodites with surviving CEM neurons

The CEM neurons are generated in both males and hermaphrodites. The CEMs of hermaphrodites undergo programmed cell death during embryogenesis; the CEM neurons of males survive and function in the detection of mating partners (SULSTON *et al.* 1983; CHASNOV *et al.* 2007). The cell-fate reporter *pkd-2::gfp* is expressed in the CEM neurons of males and in selected neurons of the male tail that are not generated in hermaphrodites (BARR and STERNBERG 1999). The *pkd-2::gfp* reporter is also expressed in the surviving CEMs of partially masculinized hermaphrodites and in the "undead" CEMs of hermaphrodites defective in programmed cell death (SCHWARTZ and HORVITZ 2007). *pkd-2::gfp* can therefore be used to identify hermaphrodites in which the CEM neurons have failed to die. We generated chromosomally integrated versions of the *pkd-2::gfp* cell fate reporter for this purpose (see Chapter II).

Screens were performed using the *pkd-2::gfp* transgenes *nIs128 II*, *nIs130 IV*, and *nIs133 I* to identify hermaphrodites defective in the deaths of the CEM neurons. These screens are described in detail in Chapter II. From these screens, 189 independent mutations were identified that caused *pkd-2::gfp* expression in the hermaphrodite. Of the 189, 144 caused CEM survival in hermaphrodites, and the characterization of these mutants is described in Chapter II. Of the 189, 29 caused the green pharynx phenotype of transgene misexpression, and the characterization of these mutants is described in Chapter IV. The remaining 16 screen isolates not described in Chapter II or in Chapter IV caused *pkd-2::gfp* expression in hermaphrodites distinguishable from CEM survival and from the green pharynx phenotype, and one additional isolate displayed an autofluorescence phenotype independent of the

pkd-2::gfp reporter. A complete list of mutations isolated in screens for mutant hermaphrodites with *pkd-2::gfp* expression is presented in Table 2.

The 16 screen isolates with fluorescence phenotypes distinguishable from CEM survival and from the green pharynx phenotype were as follows: seven alleles of *lin-22*, the uncharacterized lineage mutant *n4743*, six alleles of *cfi-1*, two isolates with greatly increased levels of intestinal expression from the *pkd-2::gfp* transgene, and the vulval autofluorescence mutant *n4753*. Loss of *lin-22* function causes the six pairs of bilaterally symmetric V blast cells to adopt a fate similar to that normally seen for the V5 cell (FIXSEN 1985). In the male, the V5 gives rise to two ray neurons of the male tail (SULSTON and HORVITZ 1977), including one that expresses *pkd-2::gfp* (BARR and STERNBERG 1999). The extra V5-like neuroblasts of *lin-22* mutant males generated extra lateral neurons that expressed the *pkd-2::gfp* cell-fate reporter. Weak sexual transformation of the Pn.a lineages was previously observed in *lin-22* mutant hermaphrodites (FIXSEN 1985). We found that the V5-like cells of *lin-22* mutant hermaphrodites can similarly show male-specific development at low expressivity, such that approximately one of every two *lin-22* mutant hermaphrodites has a *pkd-2::gfp*-expressing ray neuron in its body (data not shown). The uncharacterized lineage mutation *n4743* causes a completely penetrant Pvl (Protruding Vulva) phenotype. The Pvl phenotype caused by *n4743* was associated with an additional pseudovulval blip posterior to the protruding vulva, which was not seen in the Pvl phenotype sometimes seen in masculinized hermaphrodites. At low penetrance, *n4743* animals have a *pkd-2::gfp*-expressing cell whose position and morphology are consistent with weak sexual transformation of the V5 lineage, causing the generation of

a ray neuron. *n4743* did not cause apparent CEM neuron survival or apparent masculinization of the tail. Loss of *cfi-1* function has been reported to cause the URA sensory neurons to express aspects of the CEM fate, including *pkd-2::gfp* expression (SHAHAM and BARGMANN 2002). The six isolates identified as alleles of *cfi-1* had *pkd-2::gfp*-expressing neurons with positions typical for *cfi-1* mutants rather than for hermaphrodites with surviving CEMs, and these six isolates failed to complement the canonical allele *cfi-1(ky651)*. The two intestinal reporter expression mutants *n3651* and *n3652* were characterized by greatly increased levels of intestinal expression of the *pkd-2::gfp* reporter transgene. Although *pkd-2::gfp* is strongly expressed only in male-specific neurons, *pkd-2::gfp* reporters also cause weak *gfp* expression in unidentified head neurons with cell bodies in both the male and the hermaphrodite and cause weak *gfp* expression in the posterior intestine. Intestinal expression from *pkd-2::gfp* is initially weak but increases after one day of adulthood. *n3651* and *n3652* mutants show *pkd-2::gfp* reporter expression in the same cells as seen in a wild-type genetic background, but with greatly increased levels of reporter expression in the intestines of larvae and younger adults. The vulval autofluorescence seen in *n4753* mutants under UV illumination is not dependent on the *pkd-2::gfp* reporter transgene and is comparable in appearance to the autofluorescence seen in the spicules of wild-type males. The males' spicules, like the vulvas of hermaphrodites, are a copulatory structure. At least one similarity can be seen between the cells that form the hermaphrodite vulva and the cells that form the male spicules: primary vulval cells and the socket cells required for spicule formation each specifically express the cell-fate reporter *egl-17::gfp* (BURDINE *et al.* 1998; JIANG and STERNBERG 1999).

C. Screens for mutants defective in *tra-2(n1106)*-induced CEM survival

To complement my screens for mutants in which the sexually dimorphic CEM sensory neurons inappropriately survived in hermaphrodites, I screened seeking to identify mutants in which the CEM neurons inappropriately died despite their having adopted a masculine sexual identity. I performed this screen in partially masculinized self-fertile *tra-2(n1106)* hermaphrodites (*tra*, sexual transformer). *tra-2(n1106)* causes partial loss of function of *tra-2* (DESAI and HORVITZ 1989), a gene required to prevent masculinization (HODGKIN and BRENNER 1977). *tra-2(n1106)* homozygotes were self-fertile hermaphrodites with fully penetrant CEM survival (data not shown). Using masculinized hermaphrodites simplifies the screening process; screening for mutant males requires either that the screening process be done clonally, enabling the recovery of mutations from the siblings of the affected males, or that the mutant males be capable of mating, allowing recovery of the mutation from the resulting heterozygous cross-progeny.

tra-2(n1106) hermaphrodites were mutagenized with EMS according to standard methods (BRENNER 1974). Mutagenized P_0 animals were placed on each of 32 10 cm Petri plates containing NGM agar seeded with HB101 bacteria as a food source, 32 animals per plate. The plates were bleached to recover F_2 eggs; the F_2 larvae were then allowed to hatch in the absence of food and enter developmental arrest. Three aliquots of 300-400 animals from each 10 cm Petri plate were placed on seeded 6 cm Petri plates and grown at 22.5°C for four days before screening. Animals lacking *pkd-2::gfp*-expressing CEM neurons or with other recognizeable alterations in *pkd-2::gfp*

expression were picked singly to seeded Petri plates, and their progeny were tested for propagation of the mutant phenotype. All isolates were labeled so as to identify the group of mutagenized P_0s from which they originated.

I recovered 43 mutant strains were recovered: 30 lacked *pkd-2::gfp*-expressing CEM neurons in *tra-2(n1106)* hermaphrodites, 8 exhibited unusually weak *pkd-2::gfp* expression in the CEMs of *tra-2(n1106)* hermaphrodites, 4 had the green pharynx phenotype, and one mutation, *n3644*, that caused a *lin-22*-like phenotype and failed to complement *lin-22(n372)*. Characterization of the green pharynx mutations is described in Chapter IV. A complete list of mutants isolated in the screen for suppressors of *tra-2(n1106)*-induced CEM presence in hermaphrodites is presented in Table 3.

I tested some of the mutations that most strongly suppressed the presence of *pkd-2::gfp*-expressing CEM neurons in *tra-2(n1106)* hermaphrodites to determine whether they also caused the absence of *pkd-2::gfp*-expressing CEM neurons in males. This test was done by mating *nIs133* males with the suppressed strains and then in the next generation mating the resulting F_1 males with the original suppressed strain; if the suppressor mutation were autosomal, half of the males from the second cross would be homozygous for the suppressor mutation. Of the 22 mutations that were tested in this fashion, three mutations (*n4446*, *n4449*, and *n4458*) also caused the absence of CEM neurons in males (see Table 3). One mutation, *n4448*, did not cause CEM absence in males, but the CEM neurons of *n4448* males had extremely variable nuclear positions. This nuclear location defect was similar to defects previously seen in *dig-1* mutants. *dig-1* encodes a giant secreted protein of 13,100 amino acids that contains Ig, Fibronectin Type III, Sushi/Complement Control Protein (CCP), and EGF domains and

functions non-cell-autonomously to maintain nuclear architecture: in *dig-1* mutants, cell bodies and processes are initially placed correctly and become displaced over time (THOMAS *et al.* 1990; BENARD *et al.* 2006; BURKET *et al.* 2006). *n4448* failed to complement the canonical *dig-1* mutation *n1321*. Six mutations that suppressed the presence of *pkd-2::gfp*-expressing CEMs in *tra-2(n1106)* hermaphrodites were mapped against cluster linked markers on five of the six autosomes: *unc-4(e120) II*, *lon-1(e185) III*, *unc-5(e53) IV*, *dpy-11(e224) V*, and *lon-2(e678) X*. *n4455* and *n4457* showed strong linkage to *unc-4 II*. *n4446*, *n4447* and *n4480* showed strong linkage to *lon-1 III*. *n4465* showed weak linkage to *dpy-11 V* and no linkage to the other four markers.

D. Screens for suppressors of *ceh-30(n3714gf)*-induced CEM survival

The CEM-specific survival factor *ceh-30* can protect the CEM neurons from programmed cell death independently of the function of the only *C. elegans* member of the multidomain Bcl-2 family, *ced-9* (see Chapter III). Nearly every other known cell-specific regulator of apoptotic cell death in *C. elegans* functions through transcriptional regulation of *egl-1*, a negative regulator of CED-9 function, and mechanisms known to regulate apoptosis independently of the Bcl-2 superfamily in other organisms have no known correlate in the regulation of *C. elegans* apoptosis (for more information, see Chapter I). The cell-protective function of *ceh-30* is evolutionarily conserved in its mouse homolog *Barhl1*, suggesting that identification of genes acting downstream of *ceh-30* to control cell survival could inform our understanding of how cell survival is controlled in mammals. We therefore performed screens seeking seeking

mutations that suppress the CEM survival in hermaphrodites caused by *ceh-30(n3714*gf*)*. These screen were intended to identify genes that function downstream of *ceh-30* in the control of CEM survival and to provide insight into how *ceh-30* functions in parallel to *ced-9* to control CEM survival.

Two screens were performed with *ceh-30(n3714*gf*)* doubly *cis*-marked, as *unc-2(e55) ceh-30(n3714*gf*) lon-2(e678)*, primarily seeking loss-of-function alleles of *ceh-30*. These screens are described in Chapter III. In addition to the *ceh-30* loss-of-function mutation *n4111*, which is described in Chapter III, an additional 17 mutations were isolated that suppress the presence of *pkd-2::gfp*-expressing CEM neurons in *ceh-30(n3714*gf*)* animals. None of these 17 mutations were tightly linked to *ceh-30*, and they were therefore not candidates to be loss-of-function mutations in *ceh-30*.

Three additional genetic screens were performed to identify suppressors of *ceh-30(n3714*gf*)*-mediated CEM survival in hermaphrodites. In each, animals were mutagenized with EMS according to standard methods (Brenner 1974). Mutagenized P_0 animals were placed on 6 cm Petri plates containing NGM agar seeded with bacteria, three to four animals per plate. Animals were tracked to identify the pool of mutagenized P_0s from which candidates originated. In an F_2 clonal screen, F_2 progeny of mutagenized *nIs133*; *ceh-30(n3714*gf*)* hermaphrodites were placed singly on 6 cm Petri plates containing NGM agar seeded with bacteria, and their adult progeny were examined to identify plates on which few or no hermaphrodites had surviving CEM neurons. 866 F_2 animals generated viable progeny, for a total of 433 homozygous mutagenized haploid genomes screened. 27 mutant strains were recovered from this F_2

clonal screen. In two F_1 clonal screens, 832 fertile F_1 progeny of mutagenized *nIs128*; *ceh-30(n3714*gf*)* hermaphrodites and 851 fertile F_1 progeny of mutagenized *nIs133*; *ceh-30(n3714*gf*)* hermaphrodites were placed singly on 6 cm Petri plates containing NGM agar seeded with bacteria, and their progeny were examined for reduced penetrance of the *ceh-30(n3714*gf*)* CEM survival phenotype. If an F_1 animal was heterozygous for a strong *ceh-30(n3714*gf*)* suppressor, one quarter of its progeny would be homozygous for the suppressor and would therefore lack surviving CEM neurons, a significant and detectable increase over the proportion of *ceh-30(n3714*gf*)* animals normally lacking surviving CEM neurons. We recovered 41 mutant strains from these F_1 clonal screens, which totaled 3366 mutagenized haploid genomes. A complete list of all mutations recovered in screens for suppression of *ceh-30(n3714*gf*)*-induced CEM survival is presented in Table 4.

Twelve mutations were recovered that caused phenotypes other than suppression of the presence of *pkd-2::gfp*-expressing CEMs: three mutations (*n4326*, *n4327* and *n4351*) caused weak *pkd-2::gfp* expression in the CEMs, one mutation (*n4132*) blocked expression of *pkd-2::gfp* in male-specific neurons, two mutations (*n4336* and *n4338*) that caused partial or complete masculinization, one mutation (*n4379*) caused a *pkd-2::gfp* expression pattern similar to that seen in hermaphrodites lacking *lin-22* function; and four green pharynx mutants (*n4319*, *n4320*, *n4356* and *n4411*). The green pharynx mutant *n4319* is the only known allele of the class B synMuv green pharynx gene *gei-4*. Characterization of the green pharynx mutations is described in Chapter IV. Further investigation identified *n4132* as an unusual

function-specific allele of the RFX transcription factor gene *daf-19*. Characterization of *daf-19(n4132)* is described in Appendix V.

Many of the mutations that suppressed the presence of *pkd-2::gfp*-expressing CEMs in *ceh-30(n3714*gf*)* hermaphrodites were scored to determine the strengths of their *ceh-30* suppression phenotypes (see Tables 5 and 6). As was done with some mutations that suppressed the presence of *pkd-2::gfp*-expressing CEM neurons in *tra-2(n1106)* hermaphrodites, some of the stronger *ceh-30(n3714*gf*)* suppresssors were tested to determine whether they also caused the absence of *pkd-2::gfp*-expressing CEM neurons in males (see Table 7A). As seen for suppressors of *tra-2(n1106)*, a distinct minority of *ceh-30(n3714*gf*)* suppressors – three of 20 that were tested, including the *ceh-30* loss-of-function mutation *n4111* – caused the absence of CEM neurons in males. Examination of *n4499* males and complementation testing identified *n4499* as an allele of *dig-1*.

The missing *pkd-2::gfp*-expressing CEMs of suppressed *ceh-30(n3714*gf*)* hermaphrodites might be missing for three reasons: 1) the cells were never generated, 2) the cells were generated but have a fate defect that precludes expression of the *pkd-2::gfp* reporter, or 3) the cells were generated and could express the *pkd-2::gfp* reporter, but the cells failed to survive. Any mutants in this third category could define genes required for CEM survival. To identify potential mutants in this third category, strong *ceh-30(n3714*gf*)* suppressors were tested to determine whether *pkd-2::gfp*-expressing CEM neurons were seen when programmed cell death was blocked with the strong mutations *ced-3(n717)* or *ced-4(n1162)*. To obviate the need for mapping the suppressor mutations, suppressors were mated with

pkd-2::gfp; *unc-30(e191) dpy-4(e1166)*; *ceh-30(n3714*gf*)* hermaphrodites or *pkd-2::gfp*; *unc-93(e1500) dpy-17(e164)*; *ceh-30(n3714*gf*)* hermaphrodites and suppressed Dpy Unc strains were generated.

pkd-2::gfp; *ced-3(n717)*; *him-5(e1467)*; *ceh-30(n3714*gf*)* or *pkd-2::gfp*; *ced-4(n1162)*; *him-5(e1467)*; *ceh-30(n3714*gf*)* males were mated with the suppressed Dpy Unc strains: *unc-30 dpy-4* can be used to balance *ced-3(n717)* and *unc-93 dpy-17* can be used to balance *ced-4(n1162)*. Progeny homozygous for the suppressor mutations were identified while the cell-death mutations were maintined in *trans* to the *dpy* and *unc* markers, after which *ced* mutant homozygotes were identified on the basis of their having lost the *dpy* and *unc* markers. Results from testing 17 *ceh-30(n3714*gf*)* suppressors for the ability of cell-death defects to restore *pkd-2::gfp*-expressing CEMs are presented in Table 7B. Only the CEM neurons of the *ceh-30* loss-of-function mutant *n4111* were restored by mutations blocking programmed cell death. It is therefore likely that the CEM neurons of the other 16 mutants tested were not generated or failed to express the *pkd-2::gfp* reporter.

The *ceh-30(n3714*gf*)* suppressors whose CEM neurons were not restored by a defect in programmed cell death include the *dig-1* mutation *n4499*. The absence of *pkd-2::gfp*-expressing CEM neurons in masculinized *tra-2(n1106)* hermaphrodites, in *ceh-30(n3714*gf*)* hermaphrodites, and in *ced-3(n717)* cell-death-defective hermaphrodites may indicate that *dig-1* promotes the CEM identity. CEM neurons are often displaced in *dig-1* mutant males, but the remaining CEM neurons of *dig-1* mutant hermaphrodites defective in cell death usually have normal positions (data not shown). It may be that the CEM neurons receive signals from the cells that are normally

adjacent to them that promote the CEM identity. Displaced CEM neurons do not receive these signals; in cell-death-defective hermaphrodites, these displaced CEM neurons do not maintain their identity, including *pkd-2::gfp* expression. The displaced CEM neurons of males remain detectable using the *pkd-2::gfp* cell-fate reporter, suggesting that sex determination acts in parallel to these positional signals to promote CEM identity.

ceh-30 can control CEM survival downstream of or in parallel to *ced-9*, and there are no epistasis tests that can determine whether *ceh-30* might act downstream of or in parallel to *ced-4* or *ced-3*. The possibility cannot therefore be excluded that *ceh-30* acts downstream of *ced-4* and *ced-3* to promote CEM survival. In this case, mutations might suppress the *ceh-30(n3714*gf)-induced survival of the CEM neurons by promoting their deaths downstream of *ced-4* and *ced-3*, and the deaths of the CEMs caused by these *ceh-30(n3714*gf) suppressors might then not be suppressed by loss of *ced-4* or *ced-3* function. It might be possible to address this remaining question by direct observation of developing cell-death-defective embryos containing these *ceh-30(n3714*gf) suppressors, to determine whether the CEM neurons in these mutants die independently of *ced-4* and *ced-3* function.

E. Clonal screens for the green pharynx phenotype

The green pharynx phenotype, which is described in detail in Chapter IV, is a defect of transcriptional repression. The green pharynx phenotype can be seen in animals containing selected *gfp* reporters, including *pkd-2::gfp* reporters. Loss-of-function mutations in any of four synthetic multivulva (synMuv) genes, the class A synMuv gene *lin-8* and the class B synMuv genes *hpl-2*, *lin-13*, and *lin-61*, can

cause the green pharynx phenotype. The green pharynx phenotype was initially observed in a set of 29 independent mutations isolated in screens intended to recover mutant hermaphrodites in which the CEM neurons had failed to undergo programmed cell death (see Table 2).

The initial set of 29 green pharynx isolates provided an incomplete set of green pharynx mutations, including only a single allele of *lin-13* and no alleles of *lin-61*, even though animals completely lacking *lin-61* function are viable and have a green pharynx phenotype. There are at least two explanations for the incompleteness of the set of green pharynx mutants isolated in nonclonal screens: (1) the screens were performed using synchronized populations of F_2 adults, rather than the late embryos or early larvae in which the green pharynx phenotype is most easily observed, especially in *lin-61* mutants; and (2) the nature of the screens required that mutations recessively causing the green pharynx phenotype not also recessively cause sterility or lethality. One green pharynx gene, the class B synMuv gene *lin-13*, is required for viability, and strong loss-of-function mutations in *lin-13* recessively cause sterility.

To obtain a more complete set of green pharynx mutations, we performed clonal screens optimized for the detection of the green pharynx phenotype. These screens permitted the recovery of mutations causing lethality or sterility from among the heterozygous siblings of the affected homozygous animals. These screens are described in detail in Chapter IV. In addition to 31 mutations that caused the green pharynx phenotype and that are described in Chapter IV, an additional four mutations were isolated that caused embryonic or early larval lethality associated with intense expression of the *pkd-2::gfp* reporter in head neurons. A complete list of

mutations isolated in clonal screens for the green pharynx phenotype is presented in Table 8.

The neurons strongly expressing the *pkd-2::gfp* reporter in the four recessive lethal isolates appeared by morphology to be sensory neurons, with cell bodies within the head of the animal and sensory processes extending to the tip of the nose. No similar neuronal expression is seen from the *pkd-2::gfp* reporter in the wild type; the only neurons that strongly express the *pkd-2::gfp* reporter in the wild type are found only in males, and expression is seen only beginning late in the fourth (L4) larval stage. One of these four mutations, *n3851*, was characterized by lethality later in larval development than the other three, with *n3851* homozygotes frequently making it to the L3 larval stage. I mapped *n3851* to LGV, between the visible phenotypic markers *dpy-11* and *unc-76*.

Acknowledgments

I thank Daniel Denning for his comments about this appendix.

References

BARR, M. M., and P. W. STERNBERG, 1999 A polycystic kidney-disease gene homologue required for male mating behaviour in *C. elegans*. Nature **401:** 386-389.

BENARD, C. Y., A. BOYANOV, D. H. HALL and O. HOBERT, 2006 DIG-1, a novel giant protein, non-autonomously mediates maintenance of nervous system architecture. Development **133:** 3329-3340.

BRENNER, S., 1974 The genetics of *Caenorhabditis elegans*. Genetics **77:** 71-94.

BURDINE, R. D., C. S. BRANDA and M. J. STERN, 1998 EGL-17(FGF) expression coordinates the attraction of the migrating sex myoblasts with vulval induction in *C. elegans*. Development **125:** 1083-1093.

BURKET, C. T., C. E. HIGGINS, L. C. HULL, P. M. BERNINSONE and E. F. RYDER, 2006 The *C. elegans* gene *dig-1* encodes a giant member of the immunoglobulin superfamily that promotes fasciculation of neuronal processes. Dev Biol **299:** 193-205.

CHASNOV, J. R., W. K. SO, C. M. CHAN and K. L. CHOW, 2007 The species, sex, and stage specificity of a *Caenorhabditis* sex pheromone. Proc Natl Acad Sci U S A **104:** 6730-6735.

DESAI, C., and H. R. HORVITZ, 1989 *Caenorhabditis elegans* mutants defective in the functioning of the motor neurons responsible for egg laying. Genetics **121:** 703-721.

ELLIS, H. M., and H. R. HORVITZ, 1986 Genetic control of programmed cell death in the nematode *C. elegans*. Cell **44:** 817-829.

FIXSEN, W., 1985 The genetic control of hypodermal lineages during nematode development. Ph. D. Thesis, Massachusetts Institute of Technology, Cambridge, MA.

HODGKIN, J. A., and S. BRENNER, 1977 Mutations causing transformation of sexual phenotype in the nematode *Caenorhabditis elegans*. Genetics **86:** 275-287.

JIANG, L. I., and P. W. STERNBERG, 1999 Socket cells mediate spicule morphogenesis in *Caenorhabditis elegans* males. Dev Biol **211:** 88-99.

LINTS, R., and S. W. EMMONS, 1999 Patterning of dopaminergic neurotransmitter identity among *Caenorhabditis elegans* ray sensory neurons by a TGFbeta family signaling pathway and a Hox gene. Development **126:** 5819-5831.

SCHWARTZ, H. T., and H. R. HORVITZ, 2007 The *C. elegans* protein CEH-30 protects male-specific neurons from apoptosis independently of the Bcl-2 homolog CED-9. Genes Dev **21**.

SHAHAM, S., and C. I. BARGMANN, 2002 Control of neuronal subtype identity by the *C. elegans* ARID protein CFI-1. Genes Dev **16:** 972-983.

SULSTON, J., M. DEW and S. BRENNER, 1975 Dopaminergic neurons in the nematode *Caenorhabditis elegans*. J Comp Neurol **163:** 215-226.

SULSTON, J. E., and H. R. HORVITZ, 1977 Post-embryonic cell lineages of the nematode, *Caenorhabditis elegans*. Dev Biol **56:** 110-156.

SULSTON, J. E., E. SCHIERENBERG, J. G. WHITE and J. N. THOMSON, 1983 The embryonic cell lineage of the nematode *Caenorhabditis elegans*. Dev Biol **100:** 64-119.

THOMAS, J. H., M. J. STERN and H. R. HORVITZ, 1990 Cell interactions coordinate the development of the *C. elegans* egg-laying system. Cell **62:** 1041-1052.

WAY, J. C., and M. CHALFIE, 1989 The *mec-3* gene of *Caenorhabditis elegans* requires its own product for maintained expression and is expressed in three neuronal cell types. Genes Dev **3:** 1823-1833.

WHITE, J. G., E. SOUTHGATE, J. N. THOMSON and S. BRENNER, 1986 The structure of the nervous system of the nematode *Caenorhabditis elegans*. Philos Trans R Soc Lond B Biol Sci **314:** 1-340.

Table 1. Screen isolates with altered expression of the *cat-2::gfp* dopaminergic cell fate reporter in the postdeirid.

Class	Gene(s)	Isolates	Alleles
Cell death	*ced-3*	3	*n3369*[a], *n3433*[a], *n3434*[a]
Cell lineage	*cdc-14*	1	*n3444*[b]
Cell lineage	*lin-22*	1	*n3427*[b]
Cell lineage	*lin-32*	1	*n3850*[a]
Cell lineage	*unc-86*	2	*n3414*[a], *n3445*[b]
Cell lineage	Unknown	5	*n3849*[b,c], *n3911*[a,d], *n3912*[b,e], *n3913*[b,e], *n3914*[b,e]
PDE morphology	Unknown	2	*n3847 X*[b,f], *n3848 X*[b,f]
Reduced *cat-2::gfp* expression	Unknown	5	*n3428*[a,g], *n3429*[a,g], *n3430*[a,g], *n3431*[b,g], *n3432*[b,g]

[a] Isolated in a MT10336 *nIs116 X* strain background

[b] Isolated in a MT10337 *nIs117 X* strain background

[c] *n3849* mutants variably had from zero to three *cat-2::gfp*-expressing cells in the postdeirid. No strong effect on the dopaminergic ADE neurons was observed.

[d] *n3911* mutants had no *cat-2::gfp*-expressing cells in 51% of postdeirid regions (n=68). When PDEs were present, they were often abnormally placed and their axons often did not project directly to the ventral cord, unlike those of wild-type PDE neurons. No strong effect on the dopaminergic ADE neurons was observed.

[e] *n3912*, *n3913*, and *n3914* mutants had no *cat-2::gfp*-expressing cells in 5-15% of postdeirids (n>70). No strong effect on the dopaminergic ADE neurons was observed.

[f] *n3847* and *n3848* mutants showed a bloated PDE morphology, with large nuclei and large, irregular cell bodies. The two mutations map to LGX, fail to complement and could not be separated from *nIs117 X*.

[g] *n3428*, *n3429*, *n3430*, *n3431*, and *n3432* mutants showed greatly reduced levels of *cat-2::gfp* expression. For each of these mutants, strong expression could be restored by outcrossing to the wild type.

Table 2. Mutations isolated in screens for mutant hermaphrodites expressing the male-specific reporter *pkd-2::gfp.*

Class	Gene(s)	Isolates	Alleles
Cell death	*ced-3*	32	*n3452*[a], *n3453*[a], *n3454*[a], *n3458*[c], *n3534*[a], *n3546*[b], *n3547*[b], *n3548*[b], *n3549*[b], *n3570*[b], *n3571*[b], *n3574*[b], *n3575*[c], *n3576*[c], *n3577*[c], *n3578*[c], *n3579*[a], *n3580*[a], *n3612*[b], *n3614*[c], *n3615*[c], *n3616*[c], *n3618*[a], *n3619*[a], *n3695*[c], *n3820*[a], *n3821*[c], *n4079*[b], *n4699*[c], *n4706*[c], *n4707*[c], *n4727*[c]
Cell death	*ced-4*	16	*n3455*[a], *n3456*[a], *n3457*[a], *n3459*[c], *n3460*[c], *n3532*[c], *n3533*[a], *n3550*[b], *n3551*[c], *n3572*[b], *n3573*[b], *n3613*[b], *n3617*[c], *n3620*[a], *n3621*[b], *n4080*[a]
Cell death	*ced-9*	4	*n4081*[a], *n4698*[c], *n4700*[b], *n4713*[b]
CEM fate	*cnd-1*	3	*n3786*[a], *n3787*[a], *n4744*[b]
CEM fate	*vab-3*	2	*n3721*[a], *n3723*[a]
CEM-specific survival	*ceh-30*	3	*n3713*[c], *n3714*[c], *n3720*[a]
Sex determination	*sel-10*	1	*n3717*[c]
Sex determination	*tra-4*	4	*n3715*[c], *n3716*[c], *n4724*[b], *n4726*[b]
Sex determination	Unknown	62	*n3819*[a], *n4084*[a], *n4085 II*[a], *n4657*[a], *n4658*[b], *n4659*[b], *n4660*[b], *n4661*[b], *n4662*[b], *n4663*[b], *n4664*[b], *n4665*[b], *n4667*[b], *n4668*[b], *n4669*[b], *n4680*[a], *n4681*[a], *n4682*[a], *n4683*[a], *n4684*[a], *n4686*[a], *n4687*[a], *n4688*[a], *n4689*[b], *n4690*[b], *n4691*[b], *n4692*[c], *n4693*[c], *n4694*[c], *n4695*[c], *n4701*[a], *n4702 II*[c], *n4703*[b], *n4704*[a], *n4708*[c], *n4709*[c], *n4710*[c], *n4714*[c], *n4715*[c], *n4717*[a], *n4718*[a], *n4719*[c], *n4720*[c], *n4721*[c], *n4722*[a], *n4723*[c], *n4728*[c], *n4730*[a], *n4731*[c], *n4732*[c], *n4733*[a], *n4734*[b], *n4735*[c], *n4736*[c], *n4737*[a], *n4738*[a], *n4739*[b], *n4742*[c], *n4745*[c], *n4746*[a], *n4755*[b], *n4758*[a]
Undetermined CEM survival	Unknown	17	*n3788*[b], *n3793 I*[c], *n4082*[a], *n4083*[b], *n4679 V*[a], *n4685*[c], *n4697*[b], *n4711*[c], *n4712*[b], *n4740*[a], *n4741*[b], *n4748*[b], *n4749*[a], *n4750*[c], *n4752*[a], *n4756*[b], *n4757*[a]
Green pharynx	*lin-8*	24	*n3582*[a], *n3583*[a], *n3584*[a], *n3585*[a], *n3586*[a], *n3587*[a], *n3588*[a], *n3589*[a], *n3590*[a], *n3591*[a], *n3593*[a], *n3595*[a], *n3597*[a], *n3598*[a], *n3600*[b], *n3601*[b], *n3602*[b], *n3603*[b], *n3605*[b], *n3606*[b], *n3607*[b], *n3608*[c], *n3609*[c], *n3610*[c]
Green pharynx	*lnes-1*	3	*n3592*[a], *n3594*[a], *n3604*[b]
Green pharynx	*lin-13*	1	*n3596*[a]
Green pharynx	*pag-6*	1	*n3599*[a]
Cell lineage	*lin-22*	7	*n3526*[a], *n3527*[a], *n3528*[b], *n3529*[b], *n3530*[b], *n3531*[c], *n3552*[b]
Cell lineage	Unknown	1	*n4743*[a]
Cell fate	*cfi-1*	6	*n4696*[c], *n4705*[c], *n4716*[b], *n4725*[c], *n4729*[b], *n4751*[c]
Intestinal *pkd-2::gfp*	Unknown	2	*n3651*[a], *n3652*[a]
Vulval autofluorescence	Unknown	1	*n4753*[c]

[a] Isolated in a MT10729 *nIs128 II* background.
[b] Isolated in a MT10739 *nIs130 IV* background.
[c] Isolated in a MT10742 *nIs133 I* background.

Members of the cell death, CEM fate, CEM-specific survival, sex determination, and undetermined CEM survival classes are characterized by CEM survival in hermaphrodites and are discussed in Chapter II. Members of the green pharynx class are discussed in Chapter IV.

Table 3. Mutations isolated in screens for suppression of *tra-2(n1106)*-induced CEM presence in hermaphrodites.

Class	Gene(s)	Isolates	Alleles
CEMs absent	*dig-1*	1	*n4448*[a]
CEMs absent	Unknown	29	*n4446 III*[b], *n4447 III*[a], *n4449*[b], *n4450*[a], *n4451*[a,e], *n4452*[a,e], *n4453*[a,e], *n4455 II*[a], *n4457 II*[c,f], *n4458*[b,f], *n4460*[a], *n4461*[g], *n4462*[a,g], *n4464*[a,h], *n4465 V*[a,h], *n4466*[a], *n4468*[a], *n4469*[a], *n4477*, *n4478*[a], *n4479*[a], *n4480 III*[c], *n4484*[a], *n4485*, *n4486*, *n4489*[a,d], *n4490*[d], *n4497*[h], *n4498*[a,d]
pkd-2::gfp weak in CEMs	Unknown	8	*n4445*, *n4454*[i], *n4456*[a], *n4459*, *n4463*, *n4467*, *n4476*, *n4487*[c,i]
Green pharynx	*lin-8*	1	*n3686*
Green pharynx	*lnes-1*	2	*n3688*, *n3689*
Green pharynx	*lin-61*	1	*n3687*
Cell lineage	*lin-22*	1	*n3644*

[a] *pkd-2::gfp*-expressing CEM neurons are not missing in mutant males.
[b] *pkd-2::gfp*-expressing CEM neurons missing in mutant males.
[c] CEM neurons present in mutant males, but with reduced *pkd-2::gfp* expression.
[d] Mutation dominantly or semidominantly causes absence of *pkd-2::gfp*-expressing CEMs in *nls133*; *tra-2(n1106)* animals, and is linked to a recessive-inviable phenotype.
[e,f,g,h,i] Mutations that share one of these superscripts were isolated from among the progeny of the same pool of mutagenized P_0 animals and cause similar phenotypes and might therefore be repeated isolates of the same mutation.

Green pharynx isolates were recovered as F_3 green pharynx embryos trapped within the egg-laying-defective F_2 animals and are discussed in Chapter IV.

Table 4. Mutations isolated in screens for suppression of *ceh-30(n3714*gf*)*-induced CEM survival in hermaphrodites.

Class	Gene(s)	Isolates	Alleles
CEM death	*ceh-30*	1	*n4111*[a]
CEM absence	*dig-1*	1	*n4499*[b]
CEM absence	Unknown	68	*n4116*[c], *n4118*[c], *n4119*[c], *n4120*[c], *n4121*[c], *n4122*[c], *n4127*[c], *n4128*[c], *n4129*[c], *n4133*[a], *n4134*[c], *n4135*[c], *n4136*[c], *n4137*[c], *n4138*[a], *n4139*[c], *n4321*[d], *n4322*[d], *n4323*[d], *n4324*[d], *n4325*[d], *n4339*[d], *n4340*[d], *n4341*[d], *n4343*[d], *n4344*[d], *n4345*[d], *n4346*[d], *n4347*[d], *n4348*[d], *n4349*[d], *n4353*[e], *n4354*[e], *n4383*[d], *n4384*[e], *n4385*[e], *n4386*[e], *n4387*[e], *n4388*[e], *n4389*[e], *n4391*[e], *n4392*[b], *n4393*[b], *n4394*[b], *n4395*[b], *n4396*[b], *n4406*[b], *n4407*[b], *n4408*[b], *n4410*[b], *n4424*[b], *n4500*[b], *n4506*[d], *n4507*[e], *n4509*[e], *n4510*[e], *n4511*[b], *n4512*[e], *n4513*[b], *n4516*[e], *n4521*[d], *n4551*[e], *n4552*[e], *n4553*[e], *n4554*[e], *n4555*[e], *n4556*[e], *n4561*[e]
pkd-2::gfp weak in CEMs	Unknown	3	*n4326*[d], *n4327*[d], *n4351*[e]
pkd-2::gfp expression	*daf-19*	1	*n4132*[a]
Sex determination	Unknown	2	*n4336*[e,f], *n4338*[e,f]
Cell lineage	*lin-22*	1	*n4379*[e]
Green pharynx	*lin-8*	3	*n4320*[d], *n4356*[e], *n4411*[b]
Green pharynx	*gei-4*	1	*n4319*[d]

[a] Mutation recovered in F_1 clonal screen for absence of CEM survival in the progeny of *nIs133*; *unc-2(e55) ceh-30(n3714*gf*) lon-2(e678)*/+ animals.

[b] Mutation recovered in F_1 clonal screen for reduced penetrance of CEM survival in a *nIs128*; *ceh-30(n3714*gf*)* background.

[c] Mutation recovered in F_1 clonal screen for reduced penetrance of CEM survival in a *nIs133*; *unc-2(e55) ceh-30(n3714*gf*) lon-2(e678)* background.

[d] Mutation recovered in F_2 clonal screen for reduced penetrance of CEM survival in a *nIs133*; *ceh-30(n3714*gf*)* background.

[e] Mutation recovered in F_1 clonal screen for reduced penetrance of CEM survival in a *nIs133*; *ceh-30(n3714*gf*)* background.

[f] *n4336* recessively causes nearly complete masculinization. *n4338* causes an intersex phenotype, including Egl, Pvl, and *pkd-2::gfp*-expressing male tail structures

Members of the green pharynx class are discussed in chapter IV.

Table 5. Scoring CEM presence in strongly suppressed *ceh-30(n3714*gf*)* strains.

with suppressor:	None	D OR V	D AND V	n
No suppressor	5	68	25	102
*ceh-30(n4111*lf*)*	97	3	0	113
n4383	100	0	0	30
n4384	100	0	0	30
n4385	100	0	0	30
n4386	100	0	0	30
n4387	97	3	0	30
n4388	87	13	0	30
n4389	87	10	3	30
n4391	100	0	0	30
n4392	83	17	0	30
n4393	100	0	0	30
n4394	80	10	10	30
n4396	100	0	0	30
n4406	79	21	0	14
n4407	97	3	0	30
n4410	100	0	0	20
dig-1(n4499)	87	13	0	30
n4500	77	23	0	30
n4506	85	15	0	13
n4507	100	0	0	30

The presence of CEM neurons was scored using a *pkd-2::gfp* reporter. When CEM presence was scored using the dissecting microscope, the left and right ventral CEMs could not readily be distinguished from each other, and the left and right dorsal CEMs could not readily be distinguished from each other; CEM presence was therefore assessed for ventral CEMs and for dorsal CEMs. The resulting numbers were found to be reproducible and sensitive to changes in the degree of CEM death or survival. In this and in other tables, D OR V denotes animals in which dorsal or ventral CEMs, but not both, were observed and indicates animals displaying only weak CEM presence; D AND V denotes animals in which both dorsal and ventral CEMs were observed and indicates animals showing strong CEM presence. All strains were homozygous for *ceh-30(n3714*gf*)*, for the *ceh-30(n3714*gf*)* suppressor indicated and for the *pkd-2::gfp*

reporter transgene used in their isolation (for a list, see Table 4). The strain containing *n4111* was outcrossed to remove *cis* markers and was homozygous for *him-5(e1467)*. The other strains were not outcrossed. Suppressed strains for which more than 25% of hermaphrodites in a sample possessed surviving *pkd-2::gfp*-expressing CEMs were declared to show only weak or intermediate suppression of the CEM presence in hermaphrodites caused by *ceh-30(n3714*gf*)* and are listed in Table 6.

Table 6. Scoring CEM presence in weakly and intermediately suppressed *ceh-30(n3714gf)* strains.

	CEM presence in hermaphrodites (%)			
ceh-30(n3714gf) with suppressor:	None	D OR V	D AND V	n
No suppressor	5	68	25	102
n4553	15	70	15	130
n4343	16	45	39	31
n4556	16	65	19	74
n4321	17	67	17	30
n4324	17	47	37	30
n4340	17	66	17	29
n4552	17	68	14	104
n4555	18	32	50	22
n4396	20	53	27	30
n4341	21	50	29	28
n4347	21	62	17	29
n4348	23	50	27	30
n4353	23	47	20	30
n4354	24	67	10	21
n4408	24	59	18	17
n4323	25	0	75	30
n4325	25	56	19	16
n4344	27	45	27	22
n4345	27	67	7	30
n4346	27	27	47	30
n4349	30	47	23	30
n4509	33	57	10	30
n4512	33	52	15	21
n4521	33	40	27	30
n4516	36	60	3	30
n4121	48	48	4	29
n4339	50	50	0	14
n4511	50	43	7	30
n4510	56	40	4	25
n4120	57	43	0	30
n4554	68	29	3	38
n4551	69	19	13	32
n4424	70	30	0	30
n4513	72	24	1	33

CEM presence was scored as described in the legend to Table 5. All strains were homozygous for *ceh-30(n3714gf)*, for the indicated suppressor mutation and the

pkd-2::gfp reporter transgene used in their isolation (for a list, see Table 4). Strains were not outcrossed. Suppressed strains for which fewer than 25% of hermaphrodites in a sample possessed surviving *pkd-2::gfp*-expressing CEMs were arbitrarily declared to show strong suppression of the CEM presence in hermaphrodites caused by *ceh-30(n3714*gf*)* and are listed in Table 5.

Table 7. Scoring *ceh-30(n3714*gf*)* suppressors in males and in cell-death-defective hermaphrodites.

A. Testing *ceh-30(n3714*gf*)* suppressors for effects on males

Phenotype	*ceh-30(n3714*gf*)* suppressors:
Males missing CEMs	*ceh-30(n4111*lf*), n4384, n4507*
Males not missing CEMs	*n4116, n4127, n4136, n4383, n4385, n4386, n4387, n4388, n4389, n4391, n4393, n4394, n4396, dig-1(n4499), n4500, n4510, n4521*

B. Testing *ceh-30(n3714*gf*)* suppressors for effects on males

Phenotype	*ceh-30(n3714*gf*)* suppressors:
CEMs restored by *ced-3(n717)* or by *ced-4(n1162)*	*ceh-30(n4111*lf*)*
CEMs not restored by *ced-3(n717)* or by *ced-4(n1162)*	*n4116, n4120, n4121, n4383, n4384, n4385, n4386, n4387, n4388, n4389, n4391, n4393, n4394, n4396, dig-1(n4499), n4500*

A. *ceh-30(n3714*gf*)* suppressors were tested for their ability to cause the absence of *pkd-2::gfp*-expressing CEMs in males.

B. *ceh-30(n3714*gf*)* suppressors were tested to determine whether the CEMs of suppressed animals were restored by blocking programmed cell death with a loss-of-function mutation in *ced-3* or *ced-4*. The only tested *ceh-30(n3714*gf*)* suppressor for which CEMs were restored by loss of *ced-3* or *ced-4* function was the *ceh-30* loss-of-function mutation *n4111*.

Table 8. Mutations isolated in clonal screens for the green pharynx phenotype.

Class	Gene(s)	Isolates	Alleles
Green pharynx	*lin-8*	11	*n3794*[a], *n3800*[a], *n3808*[a], *n3810*[a], *n3811*[a], *n3812*[a], *n3813*[a], *n3815*[a], *n3816*[a], *n3817*[a], *n3818*[a]
Green pharynx	*lnes-1*	8	*n3795*[a], *n3796*[a], *n3803*[a], *n3814*[a], *n3822*[a], *n3917*[b], *n3919*[b], *n3921*[b]
Green pharynx	*lin-13*	8	*n3797*[a], *n3801*[a,c], *n3802*[a,c], *n3804*[a,c], *n3907*[b,c], *n3918*[b,c], *n3920*[b], *n3989*[b]
Green pharynx	*lin-61*	3	*n3807*[a], *n3809*[a], *n3922*[b]
Green pharynx	Unknown	1	*n3841*[a]
Neuronal expression	Unknown	4	*n3805*[a,c], *n3830*[a,c], *n3851 V*[a,c], *n3974*[a,c]

[a] Isolated as F_2 embryos in a clonal *sem-4(n1378)*; *nIs128* screen intended to recover mutations causing the green pharynx phenotype in embryos and larvae.
[b] Isolated as F_2 embryos in a clonal *nIs133*; *egl-1(n1084)* screen intended to recover mutations causing the green pharynx phenotype in embryos and larvae.
[c] Mutation causes sterility or lethality and cannot be maintained as a homozygote.

Members of the green pharynx class are discussed in chapter IV.

Figure legends

Figure 1

The dopaminergic cell fate reporter *cat-2::gfp* is expressed in the PDE neurons of wild-type animals and in the "undead" PVD sisters of animals defective in programmed cell death. Micrographs of each are shown, with accompanying lineage diagrams that show the cell divisions that generate the postdeirid, a lateral sensory structure. Green fluorescence in the micrographs is from the *cat-2::gfp* reporter; yellow fluorescence is from lipid particles in the intestine. A representation of the whole animal is shown, indicating the dopaminergic neurons on each side of the animal. The region shown in the photomicrographs is surrounded with a dotted rectangle.

Figure 2

Time course for optimizing the use of the *cat-2::gfp* reporter *nIs116* in screening for mutants with surviving PVD sisters. Developmentally arrested *ced-3(n717)*; *nIs116* were placed on NGM agar plates seeded with HB101 bacteria and grown at 25°C. At various time points, animals were scored using a Zeiss Axioskop compound microscope equipped with fluorescence optics for the presence of *cat-2::gfp* expression in the PDE, for the presence of *cat-2::gfp* expression in the "undead" PVD sister cell and for whether reporter expression could be scored in the postdeirids on both sides of the animal. Older animals are thicker than younger animals and adults contain eggs; both this increased thickness and the eggs can interfere with the ability to focus through the animals and detect *cat-2::gfp* reporter expression. A period from 34 to 46 hours,

indicated with a gray box, maximizes reporter expression in the "undead" PVD sister and the ability to score both sides of the animal.

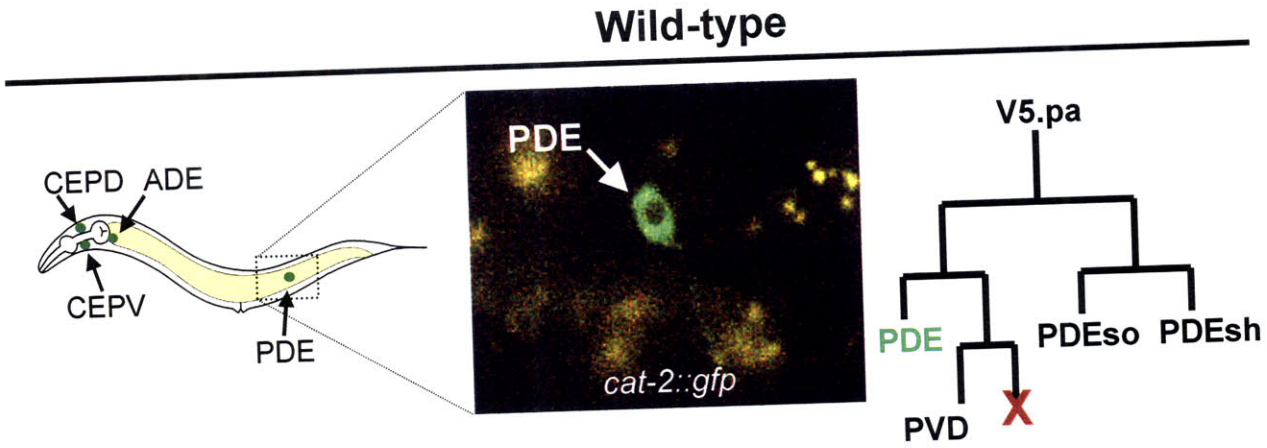
Wild-type
CEPD
ADE
CEPV
PDE
PDE
cat-2::gfp
V5.pa
PDE
PDEso
PDEsh
PVD
X

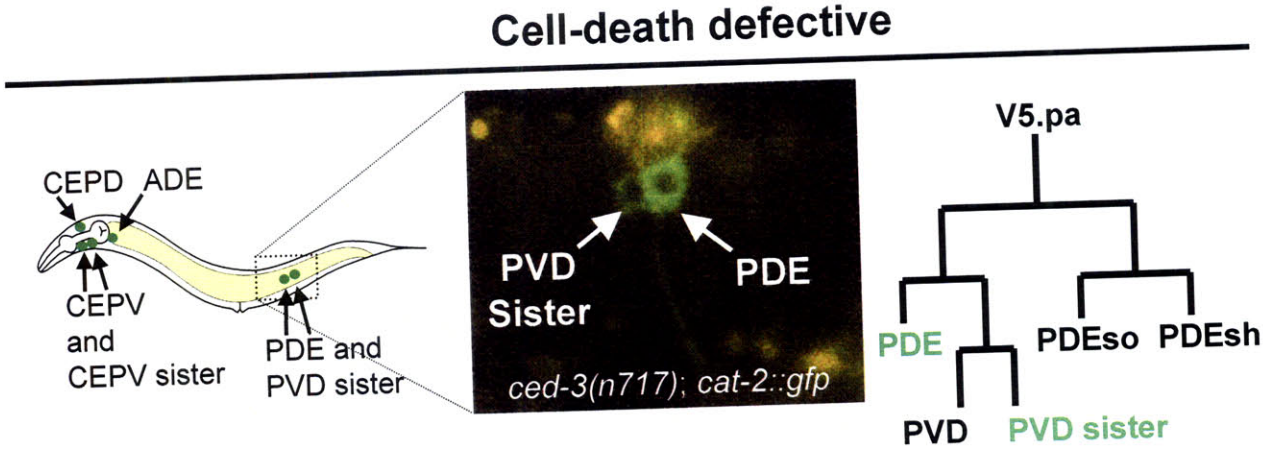
Cell-death defective
CEPD
ADE
CEPV
and
CEPV sister
PDE and
PVD sister
PVD
Sister
PDE
ced-3(n717); cat-2::gfp
V5.pa
PDE
PDEso
PDEsh
PVD
PVD sister

Figure 1

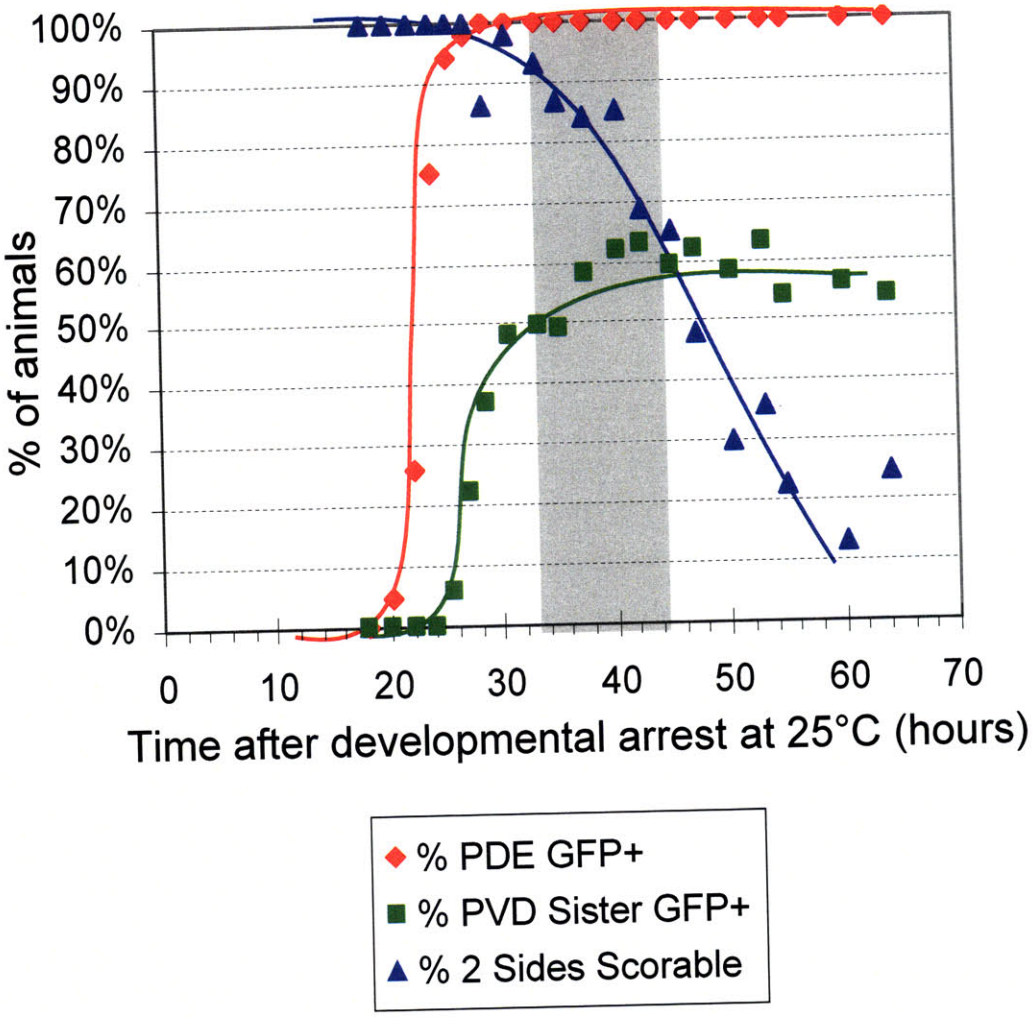
100%
90%
80%
70%
60%
50%
40%
30%
20%
10%
0%
% of animals
0
10
20
30
40
50
60
70
Time after developmental arrest at 25°C (hours)
% PDE GFP+
% PVD Sister GFP+
% 2 Sides Scorable

Figure 2

Appendix III

A protocol describing pharynx counts and a review of other assays of apoptotic cell death in the nematode worm *C. elegans*

Hillel T. Schwartz

Published as Schwartz (2007) *Nature Protocols* **2**: 705-714

Abstract

Studies of the nematode worm *C. elegans* have provided important insights into the genetics of programmed cell death, and revealed molecular mechanisms conserved from nematodes to humans. The organism continues to offer opportunities to investigate the processes of apoptosis under very well-defined conditions and at single-cell resolution in living animals. I present here a survey of the common methods used to study the process of programmed cell death in *C. elegans*. Detailed instructions are provided for one standard method -- the counting of extra cells of the anterior pharynx -- a quantitative technique that can be used to detect even very subtle alterations in the progression of apoptotic cell death.

Introduction

Programmed cell death (PCD), or apoptosis, is a process by which cells die in a controlled fashion and is important in animal development[1]. The misregulation of PCD can contribute to disease; inappropriate cell death is observed in neurodegenerative disorders[2], while the failure of cells to undergo apoptosis in response to self-antigens or to cell proliferation is seen in autoimmunity and in cancer[3,4]. Genetic pathways exist that effect or prevent cellular suicide. The first genes shown to be required for cells to undergo PCD, *ced-3* and *ced-4* (*ced*, cell death abnormal), were discovered in the nematode worm *C. elegans*[5-7]. Subsequent work in a variety of organisms has established significant knowledge regarding how cell deaths are regulated, how cells die by apoptosis, and how the dying cells are engulfed and degraded. All of these processes show a high degree of conservation from nematodes to mammals[8,9]. The

core pathway for the execution of apoptotic cell death[10-17], shown in Figure 1, is especially well conserved.

With its small size, optical transparency, rapid generation time, and defined invariant cell lineage - exactly 1090 somatic cells are generated in the hermaphrodite, of which 131 die[18,19] - the nematode *C. elegans* continues to offer an excellent system in which to study the process of programmed cell death. To supplement previously available resources[20,21], I attempt to provide here a comprehensive overview of the methods currently available for the study of PCD in *C. elegans*. In particular, I provide a discussion of and a detailed protocol for one important method for assessing the execution of apoptotic cell death -- the counting of extra cells in the anterior pharynx.

Transgenic reporters of cell survival

Several transcriptional reporters have been characterized and shown to be expressed in a small number of cells, including cells that are present only when their normal death fate has been prevented. These reporters can be used to efficiently detect the survival of these cells and have been extensively used to study the genetic programs that control the programmed deaths of specific cells[22,23]. The use of transgenic cell-fate reporters makes it feasible to assess the survival of specific cells when the stage of embryonic development or the condition of the animal makes it extremely difficult to identify these cells using other standard methods, such as recognizing these cells by their morphology or their position[24]. Transgenic reporters of cell survival have proved very popular, especially because little or no practice is needed prior to using them.

When using cell-fate reporters to assess PCD, it is important to determine if a mutation that has altered the number of cells expressing the cell-fate reporter might cause a cell-fate transformation or cell-lineage abnormality, rather than a defect in cell death. Always ensure that the extra reporter-expressing cell is in an appropriate position and has appropriate morphology for that undead cell. Additionally test whether adding mutations that block essentially all PCD cause the presence of unexpected supernumerary expressing cells; such a result would indicate that the extra expressing cell whose presence is caused by the initial mutation is different from the cell that can express the reporter if its death is prevented, indicating an alteration in cell fate or cell lineage. It is important to use multiple cell-fate reporters or to adopt other PCD assays in parallel, particularly if assessing a general defect in cell death.

Although other reporters have been useful in studies of the developmental control of specific cell deaths, one reporter, a *lin-11::gfp* transgene modified to limit its expression largely to the Pn.aap neurons[25], is particularly useful in assessing PCD execution. In the wild-type animal, 12 Pn.aap cells are generated; of these, six survive and six undergo PCD. Because *lin-11::gfp* expression can reliably be scored in up to five undead Pn.aap cells in each animal, this reporter can provide a single-animal quantitative assay of cell death. This permits the user to establish strains with a partial defect in cell death and screen for the presence of individual animals in which the cell-death-defective phenotype has been modified. When using *lin-11::gfp*, particularly in sensitized backgrounds weakly defective in PCD, some care must be taken, as it has been observed that presumably identical strains can show significantly different levels of Pn.aap neuron survival, possibly as a result of different environmental conditions or the

accumulation of spontaneous mutations (B. D. Galvin and H. R. Horvitz, personal communication). It is therefore recommended that strains under analysis be regularly re-thawed from frozen stocks and that multiply mutant strains be constructed immediately prior to analysis. *lin-11::gfp* transgenes are sometimes susceptible to alterations in their expression levels, and care should be taken to use only strongly expressing lines; it may be desirable to use only strains homozygous for the *lin-11::gfp* transgene. Because the Pn.aap lineage shows sexual dimorphism, mutations or treatments that cause Pn.aap survival should be tested to confirm that their effect is not a consequence of alterations in sex determination. This can be achieved by using additional assays of PCD, or by using a null mutation in the *fem* genes, the most downstream genes in the sex determination pathway required for masculinization[26].

A list of transgenes known to be expressed in specific cells when their programmed deaths are prevented is given in Table 1. Each of these reporters offers a resource for the study of the mechanisms controlling specific PCD. Although these reporters can be used to assess general defects in PCD in a quantitative fashion when populations are examined, only *lin-11::gfp* offers a single-animal quantitative assay.

Additional transgene-based assays of programmed cell death

The transgenic cell-fate reporter *egl-1::gfp* provides a marker for cells that adopt an apoptotic cell fate in *C. elegans*[17]. This reporter can be used to examine whether specific cells show transcriptional upregulation of the upstream activator of cell death, *egl-1*, a gene required for all somatic cell deaths[16]. *egl-1::gfp* is usually used in animals defective in PCD, such as *ced-3* mutants, so that, irrespective of whether they activate

the death program, cells will survive to be examined for upregulation of the *egl-1::gfp* reporter. This approach has been taken in several studies of the transcriptional control of specific programmed cell deaths[17,22,23,27].

When cell-killing genes such as *egl-1*, *ced-4*, or *ced-3* are transgenically overexpressed in cells that normally survive, they can cause these cells to die in a process that has morphological and genetic characteristics similar to those seen in endogenous PCD in *C. elegans*[15,16]. Similar assays can be used to test constructs for their ability to cause apoptotic cell death when overexpressed in *C. elegans*[28] and can also be used to test the effects of mutations of treatments on the susceptibility of cells to the activation of PCD; for example, such an has detected the protective function of the Bcl-2 homolog CED-9 in cells not normally induced to undergo PCD[13,15]. Similar over-expression systems have been used in models of non-apoptotic cell death, for example in studies examining the effects on cells of overexpressing a toxic polyglutamine repeat and seeking to identify genes that might mediate such effects[29,30].

Another transgene-based assay that can be used to examine apoptotic cell death is the detection of cell corpses using translational *ced-1::gfp* fusions. CED-1 encodes a protein spanning the membranes of engulfing cells that aggregates in the presence of cell corpses[31]. When translational *ced-1::gfp* fusions are appropriately expressed, cell corpses can be visualized using a dissecting microscope equipped with fluorescence optics as a ring of fluorescence surrounding the cell corpse (for an example see Figure 2). Such a reporter expressed in the somatic gonad has proven of particular use in the quantitation of apoptosis in the germline, particularly when the removal of dying cells is blocked by a loss-of-function mutation in the engulfment gene *ced-6*, which does not

interfere with CED-1::GFP clustering[32]. Fluorescently-tagged versions of other proteins that act in the engulfment and degradation of apoptotic cells, including actin, the *C. elegans* dynamin DYN-1, and the endosomal protein HGRS-1, have also been found to accumulate around cell corpses[33,34].

Lethality and visible phenotypes as assays of cell death

Alterations in genes regulating cell survival can visibly affect animals' survival, appearance, or behavior. Suppression of the phenotypic consequences of inappropriate cell death has been used to isolate and to characterize mutants defective in cell killing since the first studies of genes required for *C. elegans* PCD[5]. By such approaches it has been possible to recover extremely weak alleles of known cell-death genes and loss-of-function mutations in genes, such as *ced-8*, that contribute to the efficient process of cell killing but are not normally required for cells to die[35-37]. Selected alterations in cell death that can cause visible phenotypic effects are described in Table 2.

Histological assays of programmed cell death

All of the assays discussed thus far are microscopy assays performed on untreated living animals. In addition, a broad range of histological assays exist that can provide insight into the process of PCD in *C. elegans*. Of these, one of the first used[38] and one of the most powerful is electron microscopy. Electron microscopy is of particular importance in the characterization of mutations causing the persistence of cell corpses, as it provides the only definitive assay for determining whether cell corpse

persistence is due to defects in engulfment of dying cells, in degradation of the engulfed dead cell, or some combination of the two[34,39-41].

DNA dyes can be used to detect the condensed morphology of the DNA of apoptotic cells and the undigested DNA of incompletely degraded dead cells. In addition to DAPI[42] or Feulgen[43] stains, which require fixation of the sample for their use, the vital dye Syto 11 can be used to visualize the DNA of apoptotic and normal cells in living animals[44]. A different vital dye, Syto 12, has been reported to preferentially label the DNA of apoptotic germ cells in *C. elegans*, even after they have ceased to be readily identifiable using Nomarski microscopy[45]. The vital dye acridine orange has also been found to be useful in labeling apoptotic germ cells[45].

Beyond assessing the persistence of the DNA of apoptotic cells, histological assays provide useful tools in studying the process of engulfment and degradation of apoptotic cells. In *C. elegans* as in other organisms, the process of apoptosis is characterized by the generation of reactive DNA 3' hydroxyl ends, which can be detected by the use of TUNEL (terminal transferase dUTP nick end labeling)[44,46]. TUNEL assays in *C. elegans* have been used to assess the functions of genes reported to be involved in DNA degradation and nuclear remodeling[47-49] and to identify candidate nucleases potentially involved in apoptosis[50]. The process by which apoptotic cells are recognized and engulfed by their neighbors can, as discussed above, be examined in part through the localization of transgenically expressed fluorescently tagged versions of proteins that normally function in this process; the endogenous localization of at least one of these proteins, actin, can also be examined histologically, through the use of phalloidin[33]. Another reagent, the monoclonal antibody F2-P3E3, has been found to

specifically recognize an unidentified epitope present in organelles, likely phagosomes, of cells that respond to the presence of neighboring apoptotic cells[51].

Histological assays are of particular use in examining the function of the mitochondria in PCD in *C. elegans*. Much of the work characterizing apoptosis in mammalian systems has centered on the role of the mitochondria[52]; less is known about the role of the mitochondria in *C. elegans* PCD. The Apaf-1 homolog CED-4 localizes to the mitochondria in a CED-9-dependent fashion, and activation of PCD by the BH3-only protein EGL-1 can release CED-4 from mitochondrial localization[53]. Similar EGL-1-induced release of a fluorescently tagged version of the mitochondrial protein WAH-1 to the nucleus and cytoplasm has been reported[48]. Either of these phenomena might provide an indirect assay of the state of mitochondrial protection from programmed cell death. More recently, the effects of PCD on mitochondrial fission and fusion have been more directly assessed in *C. elegans*, using the mitochondria-specific dye Mitotracker Red[24,54].

Assessing programmed cell death using Nomarski microscopy

Programmed cell death was first observed in *C. elegans* by direct observation of the developing animal using Nomarski microscopy, and Nomarski-based assays remain among the most useful methods for studying PCD in *C. elegans*. Unlike transgene-based assays of cell survival, which often require minimal training prior to their use, Nomarski-based assays of PCD cannot be properly used without first practicing and accustoming one's self to the assay.

Nomarski microscopy allows for the observation and quantitation of dying cells and cell corpses. This is commonly done in investigating mutants defective in the engulfment and removal of cell corpses. The counting of persistent cell corpses in such mutants has been used as an assay of the overall level of programmed cell death[11]. Cell corpses usually appear as flat, raised disks with uniform and high refractility[41] (see Figure 3). When counting cell corpses, care should be taken to use a defined developmental timepoint and to count the cell corpses within a defined area. Most commonly, persistent cell corpses are counted in the heads (defined as the area between the anterior tip of the nose and the anterior end of the intestine) of first-stage (L1) larval hermaphrodites; wild-type larvae have no corpses in their heads[5]. To maximize the reproducibility of this assay, it is recommended to use young L1 larvae, either by identifying animals whose gonadal precursors and germ cells are comprised of only four cells[31,39] or by using animals within 1.5 hours of their hatching[55]. For reasons that are unclear, different investigators have reported significantly different corpse counts for the same strains[31,33,55,56]. Although these investigators may have used L1 larvae of different ages within the first larval stage, it has been shown that some mutants defective in the removal of dead cells, such as *ced-5(n1812)*, do not show a significant decrease in the number of persistent cell corpses from the first to the second larval stages[56]. Thus, other differences in procedure, possibly of culture conditions or in the identification of cell corpses, must account for the discrepancies. Numbers obtained using this assay should therefore be considered only as relative values and should not be compared to results another investigator has obtained.

The developmental temporal profile of PCD can be examined by counting visibly apoptotic cells at various stages of embryonic development. This assay is easy to perform and has provided important insights into gene function[36]; however, the data that it provides can be difficult to interpret, as it cannot always readily be determined whether changes reflect alterations in the efficient progression of programmed cell death, in the engulfment and removal of apoptotic corpses, or in the generation and fate determination of cells programmed to die. As with counting cell corpses in the heads of larvae, different investigators have reported significantly different numbers using this assay, although the developmental pattern of cell death that these numbers are intended to reflect is invariant[18,19,36,47,57]. This may reflect that the identification of embryonic stages can be somewhat arbitrary and that each of these stages of embryonic development lasts longer than any individual dying cell is likely to persist.

Perhaps the assay that most powerfully uses the power of Nomarski microscopy and the optical transparency of *C. elegans* to study PCD is the direct observation of the process of cell death *in vivo*. This approach, which can be done by manual observation of developing animals[18,43] or by using an automated 4D system[58], can provide a wealth of information, including how soon after their generation cells begin to show signs of programmed cell death, how rapidly they adopt a completely apoptotic morphology, and how long the cell corpses persist before they are removed. If this approach is linked to a knowledge of the cells' identities, derived from the invariant cell lineage of *C. elegans*, yet further information can be obtained, particularly as to whether any observed effects are general or show biases with regard to specific cells.

The presence of selected cells that normally undergo programmed death can, with only limited practice, be assessed using Nomarski microscopy. When the deaths of the two bilaterally symmetric PVD sisters [V5(l/r).paapp] are prevented, each can become part of a postdeirid, an isolated lateral posterior structure that normally contains two neurons and two glial cells, whose nuclei as visualized with Nomarski microscopy possess morphology similar to that commonly seen for neurons (small and stippled; see Figure 4). In the vicinity of the left postdeirid, the migrating QL neuroblast gives rise to two neurons and one cell that undergoes programmed cell death. These QL-derived cells have variable positions that make counting more difficult; this, as well as the extra cell death, means that results from counting the extra cells of the left and right postdeirid regions should not be conflated. The cell bodies of the HSN (hermaphrodite-specific neuron) neurons, which die in males and in many masculinized hermaphrodites, have a distinctive and isolated position, lateral and posterior to the vulva, that facilitates their observation using Nomarski microscopy (see Figure 5A - C). The CEM (cephalic male) neurons, which die in hermaphrodites and survive in males, have an unusual morphology by Nomarski microscopy: unlike most neuronal nuclei, which have a speckled appearance, the nuclei of CEM neurons appear relatively clear and contain a single large raised dot (see Figure 5D, E). In learning to recognize the CEMs using Nomarski microscopy, it may be helpful to use a cell-fate reporter that specifically expresses in the CEM neurons, such as *pkd-2::gfp*[59], to identify the CEMs of males of the fourth larval stage (L4) until the CEMs can be recognized by their distinctive morphology without resort to fluorescence.

The anterior pharynx (the pharynx is the feeding organ of *C. elegans*) is a contained region with a highly reproducible anatomy that contains a large number of cells that normally undergo PCD. Counting the number of extra nuclei in the anterior pharynx provides a single-animal quantitative assay that can be used to detect subtle defects in the execution of programmed cell death[13]. This can be the most sensitive and reproducible assay of non-cell-specific effects on the execution of programmed cell death. In animals strongly defective in programmed cell death, there can be up to 16 extra "undead" cells in the anterior pharynx; in wild-type animals, extra cells are very rare (averaging ~one extra cell per ten animals). Because the undead cells whose presence is being scored in pharynx counts represent at least ten distinguishable cell fates, this assay can readily distinguish between cell-specific and general defects in programmed cell death. By coupling the quantitative power of this assay with sensitized genetic backgrounds weakly defective in programmed cell death, it has been possible to detect cell-killing defects in mutants that in a wild-type genetic background do not show any obvious defect in cell killing[25,36,60]. A detailed protocol for learning to perform this assay is provided below.

Reagents

- S Basal Medium (see REAGENT SETUP)
- Agarose (see REAGENT SETUP)
- 20mM Sodium Azide in S Basal (see REAGENT SETUP.
- Immersion oil for microscope objective (Zeiss Immersol 518F)

Equipment

- Glass test tubes (Catalog number VWR 89000-480)
- Test tube clamp (Catalog number VWR 21770-028)
- Parafilm (Catalog number VWR 52858-032)
- Pipet bulbs (Catalog number VWR 82024-556)
- Pasteur pipets (Catalog number VWR 14673-010)
- Platinum wire (Catalog number VWR 66260-068)
- Worm pick, made with Pasteur pipet and platinum wire
- Glass microscope slides (Catalog number VWR 16004-368)
- Cover glasses, 25 mm. (Catalog number VWR 48366-089)
- Lab tape (Catalog number VWR 36425-045)
- Heat block for glass test tubes (Catalog numbers VWR 12621-104, 13259-130)
- Bunsen burner (Catalog number VWR 17911-002)
- Dissecting microscope
- Nomarski microscope
- Microwave oven

REAGENT SETUP

S Basal Medium: 0.1 M NaCl, 0.05 M KCl, pH 6.0, 0.005 mg/ml cholesterol

Agarose: Prepare 50ml of 4% (weight/volume) agarose in S Basal by boiling in microwave. Aliquot 1-2 ml into each glass test tube. Seal test tubes with Parafilm; can be stored for up to two years at 4°C.

20 mM Sodium Azide in S Basal: Prepare stock solution of 1M sodium azide in S Basal; this stock can be stored for years at 4°C. Dilute small amounts to 20 mM for a working solution. Working solution can be stored at room temperature for at least six months. CAUTION: wear gloves when handling azide, especially the stock solution.

Procedure

CRITICAL: Culture animals according to standard protocols[61].

1. Set heat block to 70°C. Carefully boil one glass test tube of 4% agarose in S Basal over a Bunsen burner, trying not to scorch glass. Place test tube in heat block to keep the agarose molten.
2. Place three microscope slides beside each other on bench next to dissecting microscope. Place one layer of lab tape on each of the outer two slides. For a diagram of this and the next three steps, see Figure 6.
3. Use a Pasteur pipet to place one drop of 4% agarose on central slide and immediately place a fourth slide face-down on the spot of agarose, perpendicular to the three slides. Press this fourth slide down until it rests on the tape on the two neighboring slides, raised slightly by this tape above the central slide. Try to minimize bubbles. The resulting agarose pad will be used to mount the animals.

4. Load 3 μl 20 mM azide solution in a pipetman; set aside, close to hand. Load worm pick with several L3 or very early L4 animals in a glob of bacteria using dissecting microscope (these can be identified by their size and the first signs of vulval morphogenesis; for images of the vulva at late L3 and early L4 larvae, see Figure 2 of Herman, Hartwieg, and Horvitz[62]).
5. Quickly, so animals on pick do not dry out, pull out the center slide with its agarose pad and place on the stage of the dissecting microscope, pipet the 20 mM azide solution onto the agarose pad, and swirl the worm pick in the puddle of liquid until animals are off the pick and the glob of bacteria has broken up. Gently place cover glass on slide, trying to minimize bubbles. Sodium azide will immobilize the animals; animals can be recovered from the slide later if desired using a worm pick with a large moist glob of bacteria, and will recover if placed on a normal NGM agar plate seeded with bacteria.

CRITICAL: When making each agarose pad, place the agarose drop onto the slide that was pressed down to flatten the agarose pad of the previous slide, with the side that contacted the agarose facing upward to receive the new drop of agarose solution. This appears to help prevent the agarose pad from slipping away when its slide is pulled out.

6. Place slide on Nomarski microscope. Examine anterior pharynx using Figures 7 and 8 as a reference. The nuclei of interest are essentially arranged in three planes placed rotationally around the central axis of the animal. These nuclei can be recognized by their stereotyped positions and by their smallish sizes and stippled appearances using Nomarski optics. The nuclei of undead cells, if

present, will usually be nearby to and morphologically similar to the nuclei of closely related cell present in the wild type; care should be taken to ensure that any undead cells that are in slightly different focal planes are noticed. The relevant nuclei of the dorsal pharynx, which are present on only one side and are arrayed almost in a line, tend to present few difficulties, but at least one of the two ventral planes will usually be oriented so as to require some reconstruction within the mind of the user. When beginning to count an animal's pharynx, it is often helpful to determine the positions and orientations of the two ventral planes by looking for the readily recognizable triangular arrangement of the NSM, I2, and MC neuronal nuclei. Practice with animals in which one of the two ventral planes, as defined by the arrangement of these three nuclei, happens to be roughly parallel to the plane of focus should familiarize the user sufficiently that, when they encounter ventral planes that are oblique to the plane of focus, they can reconstruct these planes in their mind while focusing through the animal.

7. Count the extra cells of the anterior pharynx; this is easier than counting the total cells and later subtracting the expected cells. At least ten animals should be examined of each genotype, more if required to achieve statistical significance to establish or to disprove a small effect on PCD.

CRITICAL: The pharynges of strains strongly defective in PCD can be disorganized and therefore difficult to count. Users are encouraged to familiarize themselves with the assay through extensive practice first with the wild-type strain N2 and then with strains weakly defective in PCD before attempting to score strains strongly defective in programmed cell death. Recommend strains weakly defective in programmed cell death

include the weak *ced-3* allele *ced-3(n2427)*, which normally averages approximately 1.5 extra cells per anterior pharynx, and then the intermediate *ced-3* allele *ced-3(n2436)*, which normally averages approximately 6 extra cells per anterior pharynx. The user should practice until they can reliably obtain numbers consistent with those previously reported[35]. In this fashion, one can learn the common positions and shapes of the undead cells. This will provide good preparation before attempting to score animals more strongly defective in programmed cell death.

Timing

Once the technique has been learned, it should be feasible to prepare a slide and count the pharynges of ten animals within fifteen minutes. Learning the technique can typically require several practice sessions, each lasting two to four hours.

Troubleshooting

Troubleshooting advice can be found in Table 3.

Anticipated results

Between zero and sixteen extra cells will be observed, depending on the strength of the cell death defect. The pharynges of control strains should be counted in parallel, to ascertain that the results obtained are consistent with previous results. Note should be taken of which cells survive, to distinguish between general effects on PCD and possible cell-specific protective effects.

Acknowledgments

I would like to thank H. Robert Horvitz, Brendan Galvin and Daniel Denning for their comments on the manuscript, Brian Harfe and Andrew Fire for providing the unpublished *egl-17::gfp* reporter and information on its expression in the M4 neuron, Brendan Galvin for discussions regarding the use of *lin-11::gfp*, Maureen Barr and Paul Sternberg for *pkd-2::gfp*, Robyn Lints and Scott Emmons for *cat-2::gfp*, Catherine Branda and Michael Stern for *egl-17::gfp*, and Mike Hurwitz for the *ced-1(e1735)*; *bcIs39* strain. This work was supported by a David H. Koch Graduate Fellowship and by funding from the Howard Hughes Medical Institute to H. Robert Horvitz.

COMPETING INTERESTS STATEMENT

The author declares that he has no competing financial interests.

References

1. Jacobson, M. D., Weil, M. & Raff, M. C. Programmed cell death in animal development. *Cell* **88**, 347-354 (1997).
2. Benn, S. C. & Woolf, C. J. Adult neuron survival strategies - slamming on the brakes. *Nat Rev Neurosci* **5**, 686-700 (2004).
3. Bidere, N., Su, H. C. & Lenardo, M. J. Genetic disorders of programmed cell death in the immune system. *Annu Rev Immunol* **24**, 321-352 (2006).
4. Fesik, S. W. Promoting apoptosis as a strategy for cancer drug discovery. *Nat Rev Cancer* **5**, 876-85 (2005).
5. Ellis, H. M. & Horvitz, H. R. Genetic control of programmed cell death in the nematode *C. elegans*. *Cell* **44**, 817-29 (1986).
6. Horvitz, H. R. Worms, life, and death (Nobel lecture). *Chembiochem* **4**, 697-711 (2003).
7. Yuan, J. & Horvitz, H. R. A first insight into the molecular mechanisms of apoptosis. *Cell* **116**, S53-6, 1 p following S59 (2004).
8. Lettre, G. & Hengartner, M. O. Developmental apoptosis in *C. elegans*: a complex CEDnario. *Nat Rev Mol Cell Biol* **7**, 97-108 (2006).
9. Metzstein, M. M., Stanfield, G. M. & Horvitz, H. R. Genetics of programmed cell death in *C. elegans*: past, present and future. *Trends Genet* **14**, 410-6 (1998).
10. Yuan, J., Shaham, S., Ledoux, S., Ellis, H. M. & Horvitz, H. R. The *C. elegans* cell death gene *ced-3* encodes a protein similar to mammalian interleukin-1 beta-converting enzyme. *Cell* **75**, 641-52 (1993).
11. Yuan, J. & Horvitz, H. R. The *Caenorhabditis elegans* cell death gene *ced-4* encodes a novel protein and is expressed during the period of extensive programmed cell death. *Development* **116**, 309-20 (1992).
12. Zou, H., Henzel, W. J., Liu, X., Lutschg, A. & Wang, X. Apaf-1, a human protein homologous to *C. elegans* CED-4, participates in cytochrome c-dependent activation of caspase-3. *Cell* **90**, 405-13 (1997).
13. Hengartner, M. O., Ellis, R. E. & Horvitz, H. R. *Caenorhabditis elegans* gene *ced-9* protects cells from programmed cell death. *Nature* **356**, 494-9 (1992).
14. Hengartner, M. O. & Horvitz, H. R. *C. elegans* cell survival gene *ced-9* encodes a functional homolog of the mammalian proto-oncogene *bcl-2*. *Cell* **76**, 665-76 (1994).
15. Shaham, S. & Horvitz, H. R. Developing *Caenorhabditis elegans* neurons may contain both cell-death protective and killer activities. *Genes Dev* **10**, 578-91 (1996).
16. Conradt, B. & Horvitz, H. R. The *C. elegans* protein EGL-1 is required for programmed cell death and interacts with the Bcl-2-like protein CED-9. *Cell* **93**, 519-29 (1998).
17. Conradt, B. & Horvitz, H. R. The TRA-1A sex determination protein of *C. elegans* regulates sexually dimorphic cell deaths by repressing the *egl-1* cell death activator gene. *Cell* **98**, 317-27 (1999).
18. Sulston, J. E. & Horvitz, H. R. Post-embryonic cell lineages of the nematode, *Caenorhabditis elegans*. *Dev Biol* **56**, 110-56 (1977).

19. Sulston, J. E., Schierenberg, E., White, J. G. & Thomson, J. N. The embryonic cell lineage of the nematode *Caenorhabditis elegans*. *Dev Biol* **100**, 64-119 (1983).
20. Ledwich, D., Wu, Y. C., Driscoll, M. & Xue, D. Analysis of programmed cell death in the nematode *Caenorhabditis elegans*. *Methods Enzymol* **322**, 76-88 (2000).
21. Shaham, S., ed. WormBook: Methods in Cell Biology (January 2, 2006), WormBook, ed. The *C. elegans* Research Community, WormBook, doi/10.1895/wormbook.1.49.1, http://www.wormbook.org
22. Liu, H., Strauss, T. J., Potts, M. B. & Cameron, S. Direct regulation of *egl-1* and of programmed cell death by the Hox protein MAB-5 and by CEH-20, a *C. elegans* homolog of Pbx1. *Development* **133**, 641-650 (2006).
23. Thellmann, M., Hatzold, J. & Conradt, B. The Snail-like CES-1 protein of *C. elegans* can block the expression of the BH3-only cell-death activator gene *egl-1* by antagonizing the function of bHLH proteins. *Development* **130**, 4057-71 (2003).
24. Jagasia, R., Grote, P., Westermann, B. & Conradt, B. DRP-1-mediated mitochondrial fragmentation during EGL-1-induced cell death in *C. elegans*. *Nature* **433**, 754-760 (2005).
25. Reddien, P. W., Cameron, S. & Horvitz, H. R. Phagocytosis promotes programmed cell death in *C. elegans*. *Nature* **412**, 198-202 (2001).
26. Hodgkin, J. Exploring the envelope. Systematic alteration in the sex-determination system of the nematode *Caenorhabditis elegans*. *Genetics* **162**, 767-80 (2002).
27. Hoeppner, D. J. et al. *eor-1* and *eor-2* are required for cell-specific apoptotic death in *C. elegans*. *Dev Biol* **274**, 125-38 (2004).
28. Yang, C. et al. RNA aptamers targeting the cell death inhibitor CED-9 induce cell killing in *Caenorhabditis elegans*. *J Biol Chem* **281**, 9137-9144 (2006).
29. Faber, P. W., Voisine, C., King, D. C., Bates, E. A. & Hart, A. C. Glutamine/proline-rich PQE-1 proteins protect *Caenorhabditis elegans* neurons from huntingtin polyglutamine neurotoxicity. *Proc Natl Acad Sci U S A* **99**, 17131-6 (2002).
30. Faber, P. W., Alter, J. R., MacDonald, M. E. & Hart, A. C. Polyglutamine-mediated dysfunction and apoptotic death of a *Caenorhabditis elegans* sensory neuron. *Proc Natl Acad Sci U S A* **96**, 179-84 (1999).
31. Zhou, Z., Hartwieg, E. & Horvitz, H. R. CED-1 is a transmembrane receptor that mediates cell corpse engulfment in *C. elegans*. *Cell* **104**, 43-56 (2001).
32. Schumacher, B. et al. *C. elegans ced-13* can promote apoptosis and is induced in response to DNA damage. *Cell Death Differ* **12**, 153-161 (2005).
33. Kinchen, J. M. et al. Two pathways converge at CED-10 to mediate actin rearrangement and corpse removal in *C. elegans*. *Nature* **434**, 93-99 (2005).
34. Yu, X., Odera, S., Chuang, C. H., Lu, N. & Zhou, Z. *C. elegans* dynamin mediates the signaling of phagocytic receptor CED-1 for the engulfment and degradation of apoptotic cells. *Dev Cell* **10**, 743-757 (2006).
35. Shaham, S., Reddien, P. W., Davies, B. & Horvitz, H. R. Mutational analysis of the *Caenorhabditis elegans* cell-death gene *ced-3*. *Genetics* **153**, 1655-71 (1999).

36. Stanfield, G. M. & Horvitz, H. R. The *ced-8* gene controls the timing of programmed cell deaths in *C. elegans*. *Mol Cell* **5**, 423-33 (2000).
37. Speliotes, E. K. *C. elegans* BIR-1 acts with the Aurora-like kinase AIR-2 to affect chromosomes and the spindle midzone. *Ph. D. Thesis, Massachusetts Institute of Technology, Cambridge, Massachusetts.* (2000).
38. Robertson, A. M. G. & Thompson, J. N. Ultrastructural study of cell death in *Caenorhabditis elegans*. *J Embryol Exp Morphol* **67**, 89-100 (1982).
39. Ellis, R. E., Jacobson, D. M. & Horvitz, H. R. Genes required for the engulfment of cell corpses during programmed cell death in *Caenorhabditis elegans*. *Genetics* **129**, 79-94 (1991).
40. Zhou, Z., Caron, E., Hartwieg, E., Hall, A. & Horvitz, H. R. The *C. elegans* PH domain protein CED-12 regulates cytoskeletal reorganization via a Rho/Rac GTPase signaling pathway. *Dev Cell* **1**, 477-89 (2001).
41. Hedgecock, E. M., Sulston, J. E. & Thomson, J. N. Mutations affecting programmed cell deaths in the nematode *Caenorhabditis elegans*. *Science* **220**, 1277-9 (1983).
42. Fixsen, W. The genetic control of hypodermal lineages during nematode development. *Ph. D. Thesis, Massachusetts Institute of Technology, Cambridge, Massachusetts.* (1985).
43. Sulston, J. E. Post-embryonic development in the ventral cord of *Caenorhabditis elegans*. *Philos Trans R Soc Lond B Biol Sci* **275**, 287-97 (1976).
44. Wu, Y. C., Stanfield, G. M. & Horvitz, H. R. NUC-1, a *Caenorhabditis elegans* DNase II homolog, functions in an intermediate step of DNA degradation during apoptosis. *Genes Dev* **14**, 536-48 (2000).
45. Gumienny, T. L., Lambie, E., Hartwieg, E., Horvitz, H. R. & Hengartner, M. O. Genetic control of programmed cell death in the *Caenorhabditis elegans* hermaphrodite germline. *Development* **126**, 1011-22 (1999).
46. Gavrieli, Y., Sherman, Y. & Ben-Sasson, S. A. Identification of programmed cell death *in situ* via specific labeling of nuclear DNA fragmentation. *J Cell Biol* **119**, 493-501 (1992).
47. Parrish, J. et al. Mitochondrial endonuclease G is important for apoptosis in *C. elegans*. *Nature* **412**, 90-4 (2001).
48. Wang, X., Yang, C., Chai, J., Shi, Y. & Xue, D. Mechanisms of AIF-mediated apoptotic DNA degradation in *Caenorhabditis elegans*. *Science* **298**, 1587-92 (2002).
49. Parrish, J. Z., Yang, C., Shen, B. & Xue, D. CRN-1, a *Caenorhabditis elegans* FEN-1 homologue, cooperates with CPS-6/EndoG to promote apoptotic DNA degradation. *Embo J* **22**, 3451-60 (2003).
50. Parrish, J. Z. & Xue, D. Functional genomic analysis of apoptotic DNA degradation in *C. elegans*. *Mol Cell* **11**, 987-96 (2003).
51. Eisenhut, R. J., Knox, D. & Hermann, G. J. Characterization of a conserved apoptotic marker expressed in *Caenorhabditis elegans* phagocytic cells. *Biochem Biophys Res Commun* **335**, 1231-1238 (2005).
52. Green, D. R. & Kroemer, G. The pathophysiology of mitochondrial cell death. *Science* **305**, 626-629 (2004).

53. Chen, F. et al. Translocation of *C. elegans* CED-4 to nuclear membranes during programmed cell death. *Science* **287**, 1485-9 (2000).
54. Delivani, P., C., A., Taylor, R. C., Duriez, P. J. & Martin, S. J. Role for CED-9 and EGL-1 as regulators of mitochondrial fission and fusion dynamics. *Mol Cell* **21**, 761-773 (2006).
55. Wu, Y. C. & Horvitz, H. R. The *C. elegans* cell corpse engulfment gene ced-7 encodes a protein similar to ABC transporters. *Cell* **93**, 951-60 (1998).
56. Wu, Y. C. & Horvitz, H. R. *C. elegans* phagocytosis and cell-migration protein CED-5 is similar to human DOCK180. *Nature* **392**, 501-4 (1998).
57. Sugimoto, A. et al. Many genomic regions are required for normal embryonic programmed cell death in *Caenorhabditis elegans*. *Genetics* **158**, 237-52 (2001).
58. Thomas, C., DeVries, P., Hardin, J. & White, J. Four-dimensional imaging: computer visualization of 3D movements in living specimens. *Science* **273**, 603-7 (1996).
59. Barr, M. M. & Sternberg, P. W. A polycystic kidney-disease gene homologue required for male mating behaviour in *C. elegans*. *Nature* **401**, 386-9 (1999).
60. Hengartner, M. O. & Horvitz, H. R. Activation of *C. elegans* cell death protein CED-9 by an amino-acid substitution in a domain conserved in Bcl-2. *Nature* **369**, 318-20 (1994).
61. Brenner, S. The genetics of *Caenorhabditis elegans*. *Genetics* **77**, 71-94 (1974).
62. Herman, T., Hartwieg, E. & Horvitz, H. R. *sqv* mutants of *Caenorhabditis elegans* are defective in vulval epithelial invagination. *Proc Natl Acad Sci U S A* **96**, 968-73 (1999).
63. Aspock, G., Ruvkun, G. & Burglin, T. R. The *Caenorhabditis elegans* ems class homeobox gene *ceh-2* is required for M3 pharynx motoneuron function. *Development* **130**, 3369-78 (2003).
64. Sze, J. Y., Victor, M., Loer, C., Shi, Y. & Ruvkun, G. Food and metabolic signalling defects in a *Caenorhabditis elegans* serotonin-synthesis mutant. *Nature* **403**, 560-4 (2000).
65. Lints, R. & Emmons, S. W. Patterning of dopaminergic neurotransmitter identity among *Caenorhabditis elegans* ray sensory neurons by a TGFbeta family signaling pathway and a Hox gene. *Development* **126**, 5819-31 (1999).
66. Alkema, M. J., Hunter-Ensor, M., Ringstad, N. & Horvitz, H. R. Tyramine functions independently of octopamine in the *Caenorhabditis elegans* nervous system. *Neuron* **46**, 247-260 (2005).
67. Burdine, R. D., Branda, C. S. & Stern, M. J. EGL-17(FGF) expression coordinates the attraction of the migrating sex myoblasts with vulval induction in *C. elegans*. *Development* **125**, 1083-93 (1998).
68. Desai, C., Garriga, G., McIntire, S. L. & Horvitz, H. R. A genetic pathway for the development of the *Caenorhabditis elegans* HSN motor neurons. *Nature* **336**, 638-46 (1988).
69. Desai, C. & Horvitz, H. R. *Caenorhabditis elegans* mutants defective in the functioning of the motor neurons responsible for egg laying. *Genetics* **121**, 703-21 (1989).
70. Shaham, S. & Horvitz, H. R. An alternatively spliced *C. elegans ced-4* RNA encodes a novel cell death inhibitor. *Cell* **86**, 201-8 (1996).

71. Driscoll, M. & Chalfie, M. The *mec-4* gene is a member of a family of *Caenorhabditis elegans* genes that can mutate to induce neuronal degeneration. *Nature* **349**, 588-93 (1991).
72. Ferguson, E. L. & Horvitz, H. R. Identification and characterization of 22 genes that affect the vulval cell lineages of the nematode *Caenorhabditis elegans*. *Genetics* **110**, 17-72 (1985).
73. Joshi, P. & Eisenmann, D. M. The *Caenorhabditis elegans pvl-5* gene protects hypodermal cells from *ced-3*-dependent, *ced-4*-independent cell death. *Genetics* **167**, 673-85 (2004).

Table 1. Transgenic reporters of cell survival in *C. elegans*

Promoter	Reporter expresses in:	
	Normal cells	Undead cells
lin-11[25]	Pn.aap neurons, vulval cells	Pn.aap neurons
pkd-2[59]	Male-specific neurons: CEM, HOB, Ray neurons	CEM neurons in hermaphrodites
ceh-2[23,63]	Pharyngeal cells: NSM, M3, and I3 neurons, m2 muscles, and e2 epithelial cells	NSM sisters
tph-1[23,64]	Serotonergic neurons: NSM, ADF, HSN, male-specific CP, sometimes AIM and RIH	NSM sisters, potentially HSN neurons in males
cat-2[65]	Dopaminergic neurons: CEPD, CEPV, ADE, PDE	CEPV sisters, PVD sisters
tdc-1[66]	Tyraminergic cells: RIM and RIC neurons, gonad sheath cells, and UV1 uterine cells	RIM sisters, RIC sisters
tbh-1[66]	Octopaminergic cells: RIC neurons and gonad sheath cells	RIC sisters
ceh-28	M4 neuron	M4 sister
egl-17[67]	M4 neuron and P6.p-derived vulval cells	M4 sister

Transgene expression patterns in normal cells are from descriptions in the referenced publications, except for *ceh-28*, which is from a personal communication by B. D. Harfe and A. Fire. Expression patterns in the undead cells of animals defective in apoptotic cell death are from descriptions in the referenced publications (*lin-11*, *ceh-2*, *tph-1*, *tdc-1*, *tbh-1*) or from unpublished observations (*pkd-2*, *cat-2*, *ceh-28*, *egl-17*).

Table 2. Visible phenotypes as assays of cell death

Gene(s)	Alteration	Phenotype	Comments
ced-9	Strong loss of function[13]	Maternal-effect lethality Loss of male tail rays	Phenotype results from loss of the protective function of *ced-9*, and is suppressible by loss of *ced-3* or *ced-4* function.
ced-9	Partial loss of function[13,68,69] or Partially suppressed strong loss of function[60]	Egg-laying defect Reduced brood size Uncoordinated	Seen in maternally rescued *ced-9(lf)* homozygotes, in *ced-9(n1653ts)* animals at the permissive temperature, and in animals completely lacking *ced-9* and weakly defective in cell killing, such as *ced-9(n2812)* animals also homozygous for the weak allele *ced-3(n2427)*. Phenotype depends on the strengths of the *ced-9* and cell-killing defects.
ced-4, *ced-9*	Allele-specific genetic interaction[70]	Lethality	Allele-specific interaction between *ced-9(n1653)* and the splice-site mutation *ced-4(n2273)*. Can be suppressed by mutations causing very weak defects in PCD[37].
egl-1	Gain of function[17]	Egg-laying defect	Inappropriate expression of the BH3-only cell-killing gene *egl-1* in the HSN neurons of hermaphrodites. The HSN neurons are required for egg laying.
mec-4 or *deg-1*	Gain of function[71]	Insensitivity to light touch	Channel hyperactivation in touch neurons results in their cell deaths with necrotic characteristics.
lin-24 or *lin-33*	Gain of function[72]	Vulvaless	Mutations cause the atypical, nonapoptotic cell deaths of the Pn.p hypodermal blast cells that give rise to the vulva.
pvl-5	Presumed loss of function[73]	Vulvaless Loss of male tail rays	*pvl-5* mutations cause atypical *ced-3*-dependent cell death.

Some mutations cause inappropriate cell deaths, resulting in phenotypic alterations visible using a dissecting microscope. For more information, see the references indicated.

Table 3: Troubleshooting

Step	Problem	Solution
6	One of the three rotationally arranged planes is difficult to see as a result of orientation or obscuration by intervening tissue	Increased practice will help, but some animals cannot readily be scored and should be disregarded as necessary. To maximize efficiency, ensure all three planes are visible before beginning to count an animal's anterior pharynx.
6	Poor images using Nomarski microscopy	Check that condenser is properly focused and if necessary heat immersion oil to solubilize crystals that may have formed. Nomarski images from anesthetized animals progressively degrade as the animals remain on the slide; slides should be prepared fresh and used within fifteen minutes to, at most, half an hour.
6	Difficulty locating I1 neuron nuclei	The I1 neuron nuclei have a distinctive position at the pharyngeal lumen immediately anterior to the anterior bulb of the pharynx, but their flattened morphology and proximity to the lumen can make them difficult to spot. Undead I1 sister cells are typically less flattened, farther from the lumen, and easier to recognize.
6	Difficulty locating ventral m1 muscle nuclei or counting extra cells near to ventral m1 muscle nuclei	The ventral m1 muscle nuclei and nearby undead cells are positioned more variably than are other nuclei of interest but are reliably positioned between the MC and the I1 nuclei on the anterior/posterior axis. It can help to identify the M3, NSM, MC, I2, and I1 nuclei, and then to count all other nuclei in the area. The number of extra nuclei in this area can then be determined by subtracting the two m1 nuclei present in the wild type.
6	Difficulty finding the undead sisters of the NSM neurons	Undead cells can be in slightly different focal planes than normally surviving cells. The nuclei of the undead NSM sisters in particular can be in focal planes especially different from those of other nuclei. All focal planes in the ventral anterior bulb of the pharynx should be examined.
6	Difficulty finding the undead sister of the M4 neuron	The nucleus of the undead M4 sister is often located in the posterior bulb of the pharynx or in the isthmus between the two bulbs of the pharynx. Only those undead M4 sister cells whose nuclei can be seen near to the M4 or in the isthmus need be counted.

Figure legends

Figure 1

A conserved core pathway for the execution of programmed cell death. The *C. elegans* and *H. sapiens* versions of this pathway are shown. In *C. elegans*, this pathway consists of *egl-1* (*egl*, egg laying defective), *ced-9*, *ced-4*, and *ced-3*. CED-3 is a caspase (cysteine aspartate-specific protease). CED-3 activity is positively regulated by CED-4, a functional homolog of the mammalian protein Apaf-1. CED-4 killing activity is regulated by the Bcl-2 homolog CED-9, a critical negative regulator of cell death that also contributes to the deaths of cells programmed to die. CED-9 activity in somatic cells is controlled by transcriptional regulation of *egl-1*, which encodes a member of the BH3-only family of cell-killing proteins.

Figure 2

CED-1::GFP surrounds apoptotic cell corpses. **A)** A composite Nomarski microscopy image showing part of the gonad of a *ced-1(e1735)*; *bcIs39* adult hermaphrodite. Regions of two focal planes are combined to show all relevant nuclei. *bcIs39* is an integrated transgene driving *ced-1::gfp* expression in the somatic gonad as a tool for the visualization of apoptotic germline cells. In these and in all other images, anterior is left and ventral is down. Two apoptotic germline cells in the distal gonad are labeled as "Germline corpse"; the apoptotic germ cell on the right is visibly cellularized and shows a raised morphology differing from that seen for normal germline nuclei; a representative germline nucleus is indicated for comparison. The apoptotic germ cell on the left has less distinctive morphology. **B)** GFP from the *bcIs39 ced-1::gfp* transgene

forms rings around the two germline cell corpses. Apoptotic germline cells that may be difficult to identify using Nomarski microscopy, such as the apoptotic germline cell on the left in part A, can readily be recognized using *ced-1::gfp*.

Figure 3

A) A Nomarski microscopy image of the head of a young wild-type L1 stage larva. No apoptotic cell corpses are visible. **B)** A Nomarski microscopy image of the head of a young *ced-1(e1735)* L1 stage larva. *ced-1(e1735)* animals are defective in the engulfment of cell corpses. Three persistent apoptotic cell corpses visible in this focal plane are indicated with arrowheads. The raised disk morphology seen here is typical of somatic cell corpses, but differs from that of germline cell corpses, as seen in Figure 2A.

Figure 4

A) A composite Nomarski microscopy image showing the right postdeirid of a wild-type early L4 stage larval hermaphrodite. The four postdeirid nuclei are indicated. Regions of two focal planes are combined to show all relevant nuclei. **B)** A Nomarski microscopy image of another focal plane of the same animal as in part A showing the turn of the posterior gonad, to provide a reference indicating where in the animal the postdeirid can be found. **C)** A representation of the relevant features of parts A and B; the postdeirid nuclei are shown with black ovals and the posterior gonad is gray. **D)** A composite Nomarski microscopy image showing the right postdeirid of a *ced-3(n717)* early L4 stage larval hermaphrodite. Regions of two focal planes are combined to show all relevant nuclei. This postdeirid contains a fifth nucleus, of an undead cell that has

survived because of the *ced-3(n717)* defect in apoptotic cell death. The five postdeirid nuclei are indicated. **E)** A Nomarski microscopy image of another focal plane of the same animal as in part D showing the turn of the posterior gonad, to provide a reference indicating where in the animal the postdeirid can be found. **F)** A representation of the relevant features of parts D and E; the postdeirid nuclei are shown with black ovals and the posterior gonad is gray.

Figure 5

Using Nomarski microscopy to identify cells sexually dimorphic for PCD. **A)** A Nomarski microscopy image showing the nucleus of one HSN neuron of a wild-type L4 stage larval hermaphrodite. This HSN nucleus is the only lateral neuronal nucleus in this area. **B)** A Nomarski microscopy image of a different focal plane of the same animal showing the vulva, to provide a reference indicating the position of the HSN. The HSN nuclei are positioned lateral to and slightly posterior of the vulva. **C)** A representation illustrating the relevant features of parts A and B. The HSN and vulva are labeled. **D)** A Nomarski microscopy image of part of the head of a wild-type L4 stage larval male. The nucleus of a ventral CEM neuron is labeled; some other nuclei in the same focal plane that possess more typical neuronal morphology are indicated with arrowheads. The CEM nucleus contains a single large raised dot and is otherwise clear, while nuclei with more typical neuronal morphology are stippled in appearance, each containing several small dots. **E)** A Nomarski microscopy image of the head of a *ced-3(n717)* L4 stage larval hermaphrodite. *ced-3(n717)* animals are defective in apoptotic cell death. The nucleus of a ventral CEM neuron, which would have died in a wild-type hermaphrodite, is

labeled; some other nuclei in the same focal plane that possess more typical neuronal morphology are indicated with arrowheads.

Figure 6

Diagrams illustrating the preparation of agarose pads for mounting *C. elegans* for Nomarski microscopy. **A)** Three microscope slides are placed in a row, with a single layer of lab tape on each of the two outer slides. A drop of 4% agarose in S basal is placed on the center slide. **B)** A fourth microscope slide is rested on the lab tape on top of the two outer slides and used to flatten the agarose on the center slide. **C)** The center slide is slid out. **D)** 3μl of 20 mM azide in S basal are pipetted onto the agarose pad and animals are picked into the azide. A cover slip is placed atop the animals.

Figure 7

A) A composite Nomarski microscopy image of the anterior pharynx of a wild-type L3 stage larval hermaphrodite; regions from thirteen focal planes are combined to represent examples of all nuclei whose positions should be learned. Note that these nuclei are arranged essentially in three rotational planes: one for the dorsal nuclei and two nearly identical planes for the ventral nuclei. The dorsal nuclei and one set of ventral nuclei can be seen. The animal is positioned with dorsal up and anterior to the left. **B)** Annotated version of the image in part A. Relevant nuclei are circled and labeled. Nuclei of cells whose sister cells normally undergo programmed cell death are filled in dark grey; nuclei of cells whose sister cells and "aunts" both normally undergo programmed cell death are filled in black. The MC neuron is half-filled to indicate

asymmetry: the sister of the left MC neuron dies, but the sister of the right MC neuron survives. When a cell fails to die, the surviving nucleus is often found near to the position of a closely related cell that normally lives.

Figure 8

A) A composite Nomarski microscopy image of the anterior pharynx of one *ced-3(n717)* L3 stage larval hermaphrodite. *ced-3(n717)* causes a strong defect in the execution of programmed cell death. Regions from sixteen focal planes are combined to represent examples of all relevant nuclei in the dorsal and left ventral rotational planes. Note that in each mutant animal, some undead cells are not found; in this example, eight of the ten undead cell nuclei possible in these planes are present. The possible undead cells that are not present are the sister of the left I1 and one cell whose nucleus would be in the left ventral anterior bulb. The animal is positioned with dorsal up and anterior to the left. **B)** Annotated version of the image in part A. Relevant nuclei are circled. Nuclei of undead cells are filled in black.

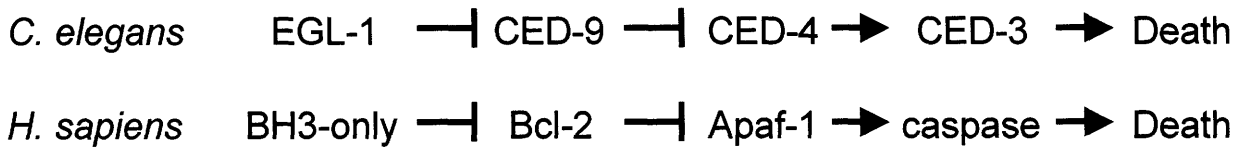
C. elegans
EGL-1
CED-9
CED-4
CED-3
Death
H. sapiens
BH3-only
Bcl-2
Apaf-1
caspase
Death

Figure 1

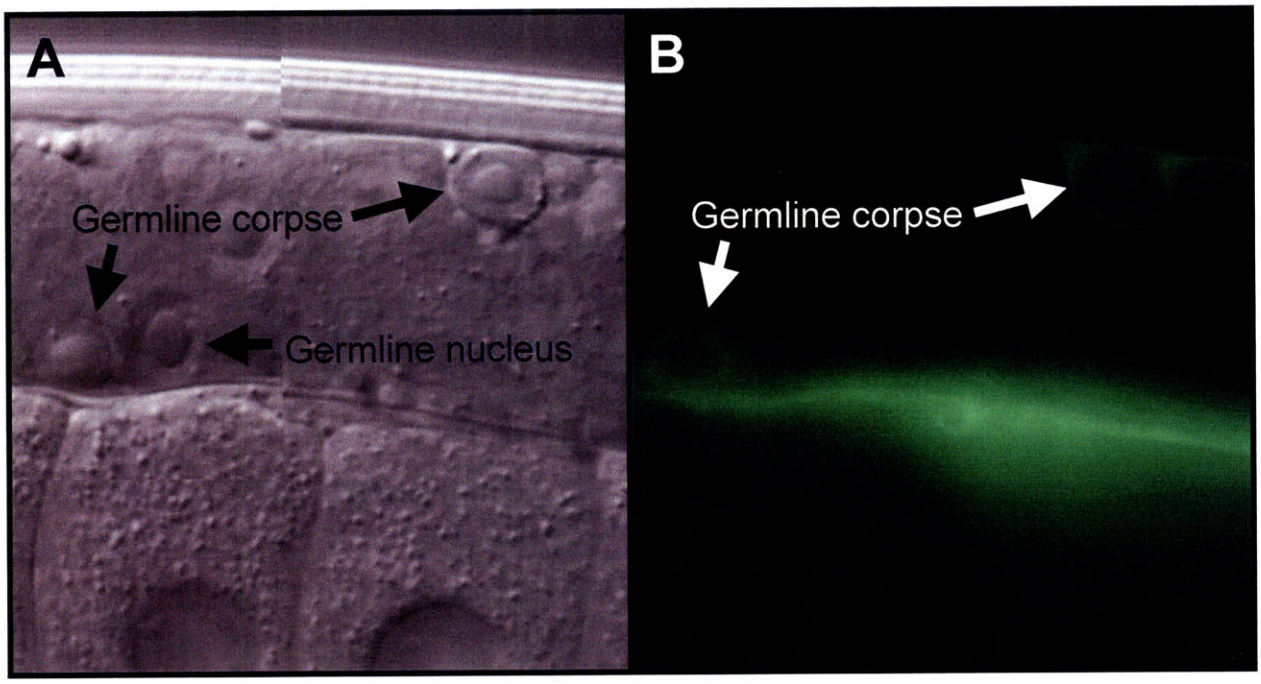

Figure 2

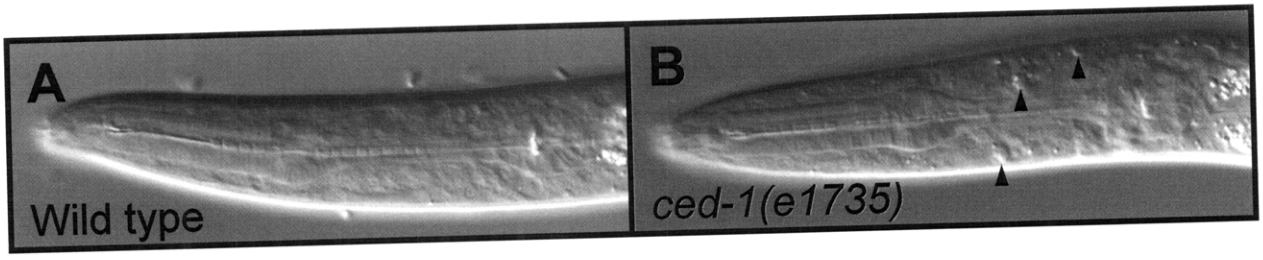

Figure 3

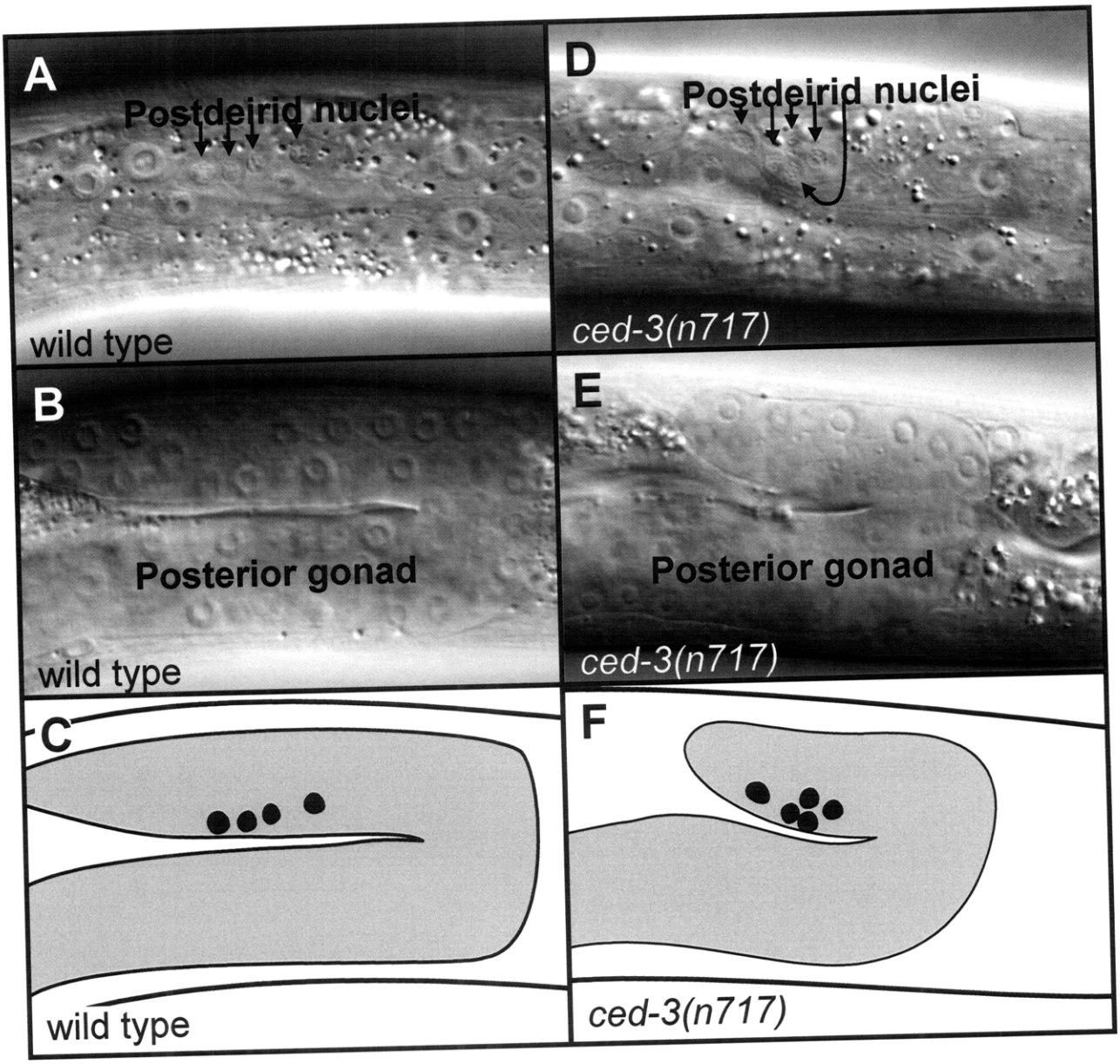
A
Postdeirid nuclei
wild type
D
Postdeirid nuclei
ced-3(n717)
B
Posterior gonad
wild type
E
Posterior gonad
ced-3(n717)
C
wild type
F
ced-3(n717)

Figure 4

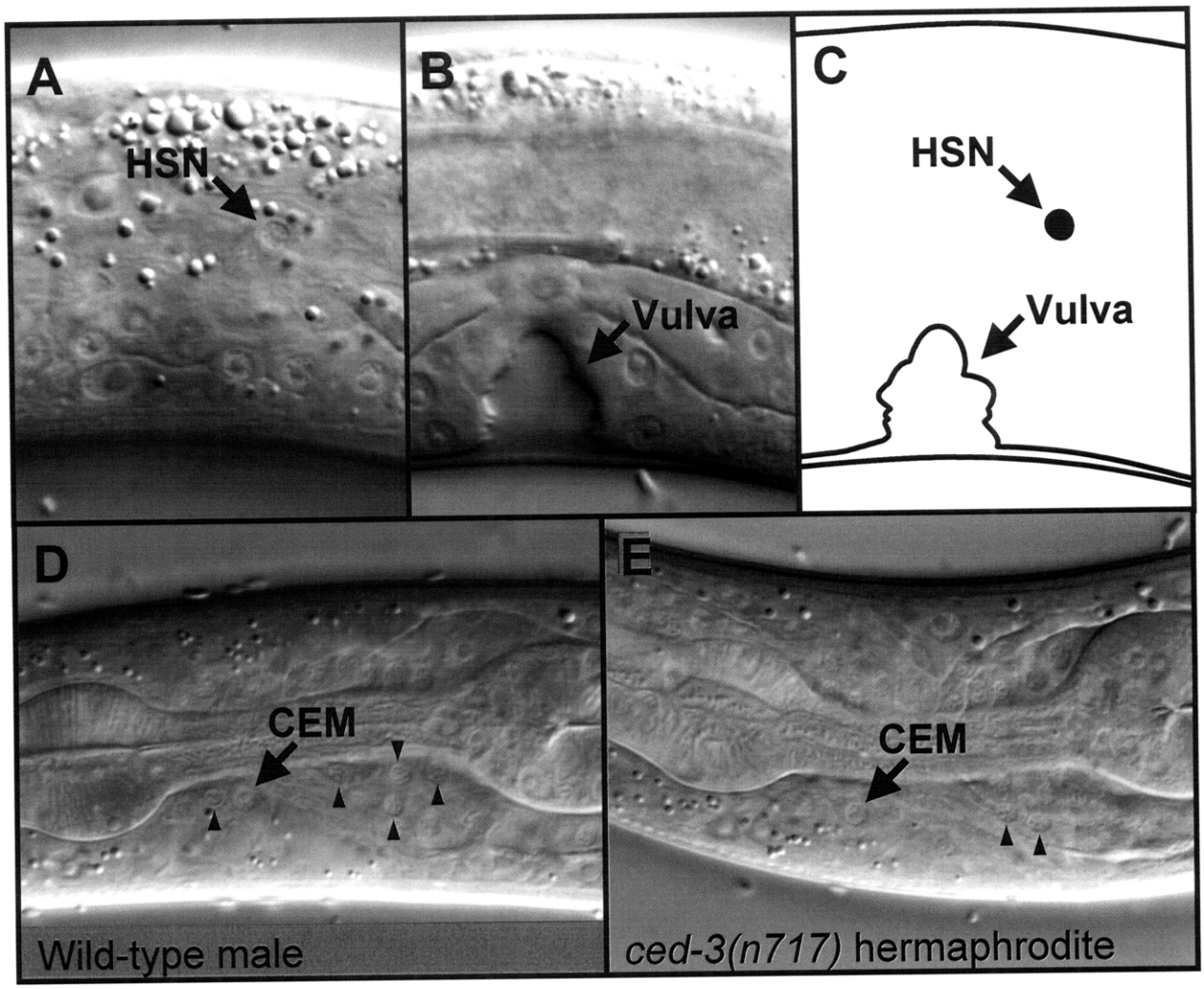
A
HSN
B
Vulva
C
HSN
Vulva
D
CEM
Wild-type male
E
CEM
ced-3(n717) hermaphrodite

Figure 5

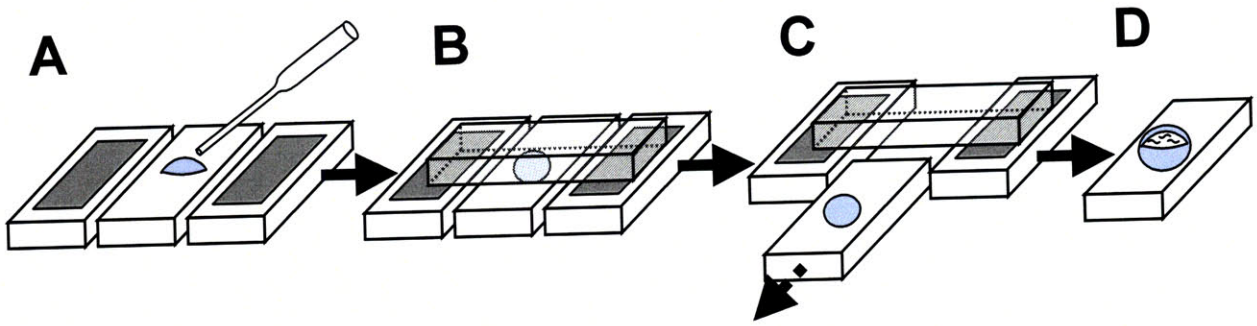

Figure 6

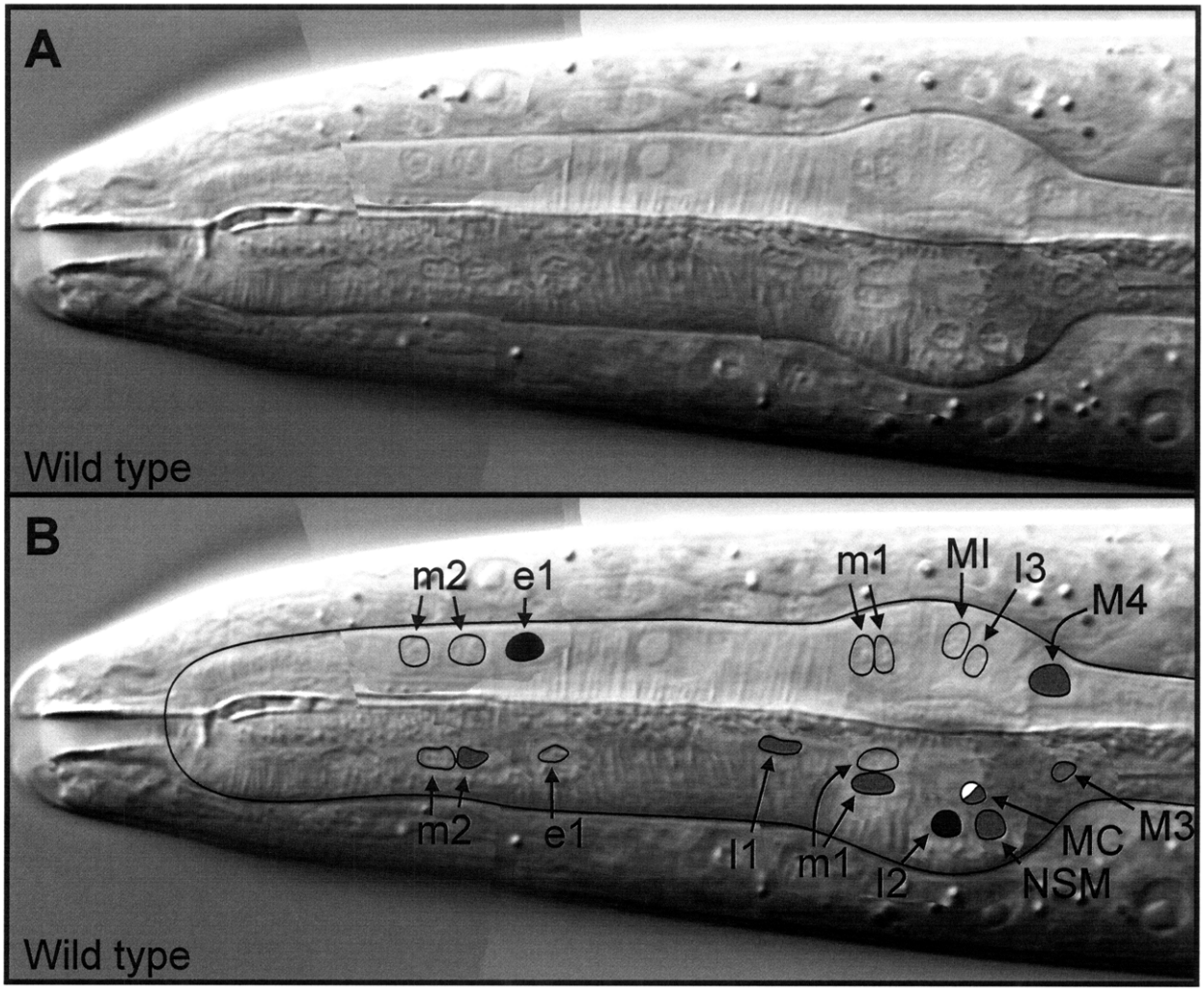

Figure 7

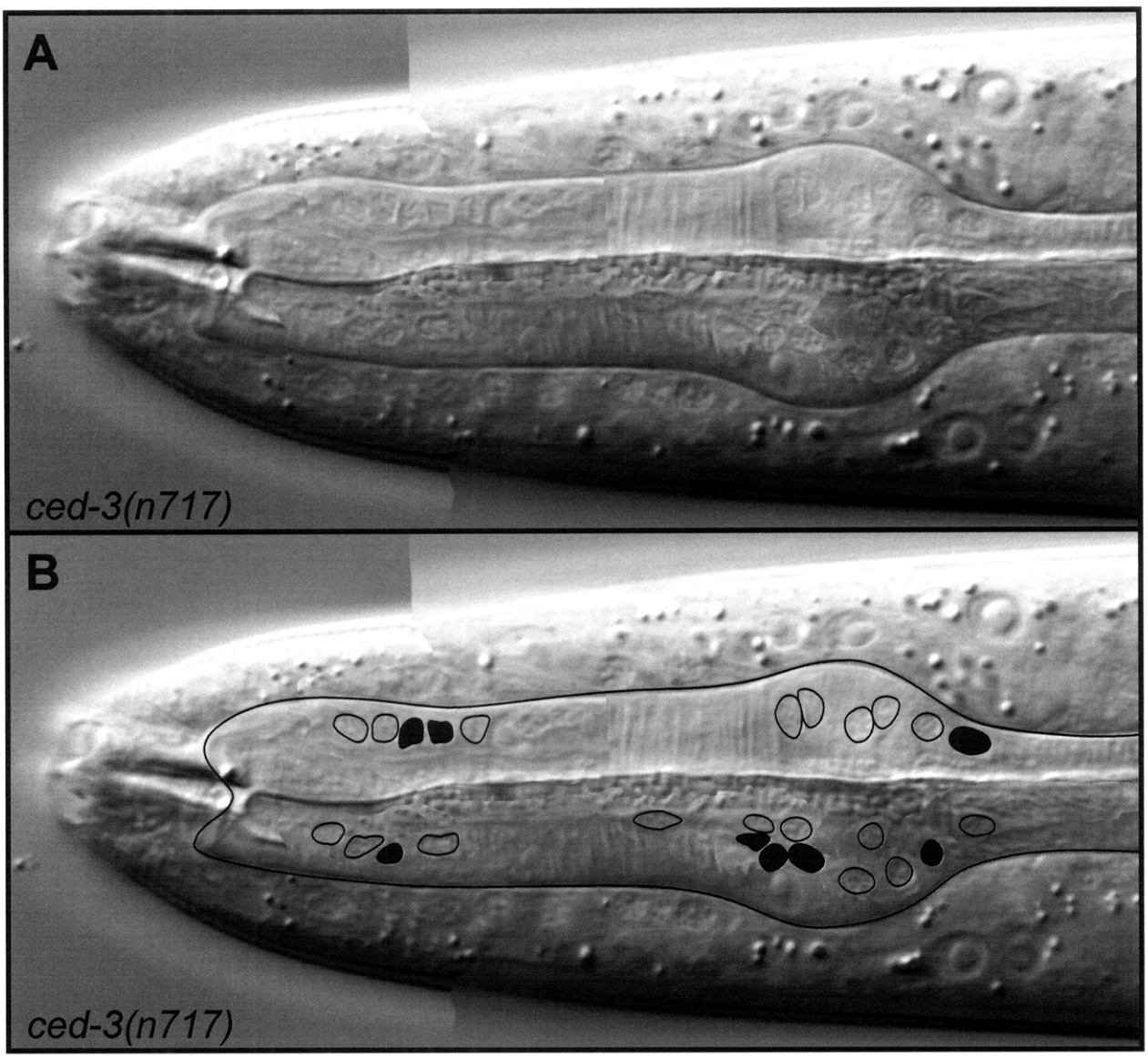

Figure 8

Appendix IV

New Genes that Interact with *lin-35 Rb* to Negatively Regulate the *let-60 ras* Pathway in *Caenorhabditis elegans*

Jeffrey H. Thomas[1,2], Craig J. Ceol[2], Hillel T. Schwartz and H. Robert Horvitz

Howard Hughes Medical Institute, Department of Biology,
Massachusetts Institute of Technology, Cambridge, Massachusetts 02139

[1]Current address: Dept. of Molecular Biology, Princeton University, Princeton, NJ 08544

[2]These authors contributed equally to this work

Published as Thomas *et al.* (2003) *Genetics* **164**: 135-151.
Jeffrey Thomas performed the genetic screens and mapped and characterized the screen isolates. I identified the mutation *n770* as being an allele of *lin-13* and mapped and performed complementation tests with all of the *lin-13* alleles using the green pharynx phenotype caused by these mutations. Craig Ceol confirmed these results using the synMuv phenotype caused by these mutations, determined the *lin-13* sequence alterations in these mutants and molecularly identified *lin-52*.

Abstract

Previous studies have shown that a synthetic multivulva phenotype results from mutations in genes that antagonize the *ras*-mediated intercellular signaling system responsible for vulval induction in *Caenorhabditis elegans*. Synthetic multivulva mutations define two classes of genes, A and B, and a mutation in a gene of each class is required to produce the multivulva phenotype. The ectopic vulval tissue in multivulva animals is generated by vulval precursor cells that in the wild type do not generate vulval tissue. One of the class B synthetic multivulva genes, *lin-35*, encodes a protein similar to the retinoblastoma (Rb) protein. In this paper, we describe the isolation and characterization of 50 synthetic multivulva mutations, the identification of new components of both the class A and class B *lin-35 Rb* pathway, and the cloning of *lin-52*, a class B gene that may have a conserved role in Rb-mediated signaling.

Introduction

A receptor tyrosine kinase (RTK) and Ras-mediated signal transduction pathway induces vulval cell fates during the development of the vulva of the *Caenorhabditis elegans* hermaphrodite (AROIAN *et al.* 1990; BEITEL *et al.* 1990; HAN and STERNBERG 1990). Little is known about how the activities of such pathways can be negatively regulated. The synthetic multivulva (synMuv) genes act as negative regulators of vulval development (HORVITZ and SULSTON 1980; SULSTON and HORVITZ 1981; FERGUSON and HORVITZ 1985, 1989). One of the synMuv genes, *lin-35*, is a member of the Rb gene family; one member of this family, Rb, acts as tumor suppressor gene in mammals. Another synMuv gene, *lin-53*, shows similarity to RbAp48, an Rb-binding protein (LU and HORVITZ 1998). Thus, the synMuv genes provide an opportunity to analyze genetically a pathway containing an Rb-like gene, to define additional components of this pathway, and to elucidate the mechanism by which an Rb-like protein antagonizes a process stimulated by a Ras protein.

The hermaphrodite vulva of *C. elegans* is formed from the descendants of three hypodermal blast cells, P5.p, P6.p and P7.p (SULSTON and HORVITZ 1977). These cells are members of the vulval equivalence group, P(3-8).p, a set of six cells with the potential to adopt either of two vulval fates (1° or 2°) or a nonvulval fate (3°) (SULSTON and WHITE 1980; KIMBLE 1981; STERNBERG and HORVITZ 1986). These cell fates are specified by cell interactions. The gonadal anchor cell induces the nearest P(3-8).p cells to adopt vulval fates. (KIMBLE 1981; STERNBERG and HORVITZ 1986; THOMAS *et al.* 1990). Another signal, apparently from the nearby hypodermal syncytium, hyp7, acts to inhibit the adoption of vulval fates (HERMAN and HEDGECOCK 1990). It is likely that the anchor cell signal overrides this inhibitory signal to induce the cells nearest to the anchor cell to adopt vulval fates.

Genetic analysis of vulval development has led to the identification and characterization of numerous genes involved in different aspects of this process (for reviews, see HORVITZ and STERNBERG 1991; KORNFELD 1997; STERNBERG and HAN 1998). Reduction-of-function mutations in genes encoding signaling proteins reduce the output of the anchor cell signaling pathway and result in a vulvaless (Vul) phenotype in which the vulva is not formed. By contrast, some mutations result in a multivulva (Muv) phenotype in which ectopic vulval tissue is produced. The Muv phenotype of certain mutant strains results from the interaction of two different mutations (HORVITZ and SULSTON 1980; SULSTON and HORVITZ 1981; FERGUSON and HORVITZ 1985, 1989). The mutations that interact to produce such a synthetic multivulva (synMuv) phenotype fall into two classes, A and B. Animals carrying both a class A and a class B mutation have a Muv phenotype. Animals that carry mutations in a single class have a wild-type vulval phenotype. FERGUSON and HORVITZ (1989) proposed that the synMuv genes encode the components of two functionally redundant pathways that negatively regulate vulval development.

Systematic mutagenesis of strains carrying either the class A mutation *lin-8(n111)* or the class B mutation *lin-9(n112)* as well as the mutagenesis of another strain carrying a previously undetected class A synMuv mutation allowed the identification of additional class A and class B mutations (FERGUSON and HORVITZ 1989). Both class A and class B alleles, as well as class AB alleles (which are Muv as a consequence of a single mutation), were identified for a locus named *lin-15*, indicating that *lin-15* is a complex locus with distinct class A and class B functions (FERGUSON and HORVITZ 1985; 1989). Molecular analyses of *lin-15* revealed that it consists of two adjacent genes that encode two nonoverlapping transcripts to control the A and B functions; the class AB alleles affect both genes (CLARK *et al.* 1994; HUANG *et al.* 1994). These genetic analyses resulted in the identification and characterization of three class A genes (*lin-8*, *lin-15*A, and *lin-38*) and five class B genes (*lin-9*, *lin-15*B,

lin-35, *lin-36*, and *lin-37*). Three additional class B mutations (*n770*, *n771*, *n833*) were identified, but were neither further characterized nor given gene names (FERGUSON and HORVITZ 1989).

SynMuv mutants in which the anchor cell has been ablated nonetheless still display a Muv phenotype (FERGUSON *et al.* 1987). This result suggests that in the absence of synMuv gene activity, the P(3-8).p cells do not require the anchor cell signal to adopt vulval cell fates. However, reduction-of-function mutations in genes known to be involved in inductive signal transduction, *let-23 rtk*, *sem-5*, *let-60 ras*, and *lin-45 raf*, are epistatic to synMuv mutations (FERGUSON *et al.* 1987; BEITEL *et al.* 1990; HAN *et al.* 1990, CLARK *et al.* 1992; HAN *et al.* 1993; HUANG *et al.* 1994; LU and HORVITZ 1998; THOMAS and HORVITZ 1999). Thus, the activity of the RTK signal transduction cascade, but not the anchor cell-derived RTK ligand itself, is required for the adoption of vulval cell fates by P(3-8).p cells in the absence of inhibitory synMuv gene activity. Genetic mosaic analyses indicate that both *lin-15*AB and *lin-37* act non-cell autonomously and most likely in hyp7 (HERMAN and HEDGECOCK 1990; HEDGECOCK and HERMAN 1995) while *lin-36* likely acts cell autonomously in the Pn.p cells (THOMAS and HORVITZ 1999). These observations led to the suggestion that the synMuv genes encode the components of two signaling systems by which hyp7 prevents P(3-8).p cells from adopting vulval fates. When both redundant signaling systems are disabled, P(3-8).p cells adopt vulval fates and produce a Muv phenotype.

The molecular natures of several synMuv genes have been determined. Two class B genes, *lin-15*B and *lin-36*, and one class A gene, *lin-15*A, have been cloned and shown to encode novel proteins (CLARK *et al.* 1994; HUANG *et al.* 1994; THOMAS and HORVITZ 1999). The class B gene *lin-9* encodes a protein with sequence similarity to the *Drosophila* Aly protein, which regulates the meiotic cell cycle and spermatogenesis (BEITEL *et al.* 2000; WHITE-COOPER *et al.* 2000). The class B gene *lin-35* encodes a protein with sequence similarity to the Rb protein, and the class B gene *lin-53* encodes

a protein with sequence similarity to RbAp48, an Rb-binding protein (LU and HORVITZ 1998). The class B gene *dpl-1*, the discovery of which is described in this manuscript, encodes a protein similar to DP, an Rb-regulated transcription factor that regulates the G1-to-S phase transition of the cell cycle. The class B gene *efl-1* encodes a protein similar to E2F, a component of the DP/E2F heterodimeric transcription factor (CEOL and HORVITZ 2001). Another gene with class B activity, *tam-1*, encodes a RING finger and B-box protein involved in modulating gene expression (HSIEH *et al.* 1999). *lin-13*, a gene which has class B and possibly also class A synMuv activity, encodes a protein with an Rb binding motif (MELÉNDEZ and GREENWALD 2000). Genetic analysis of *let-418/chd-4*, which encodes a chromodomain helicase protein, indicates that it is a class B synMuv gene (VON ZELEWSKY *et al.* 2000). *mep-1*, which encodes a zinc-finger protein that interacts with LET-418, has class B synMuv activity (UNHAVAITHAYA *et al.* 2002). RNAi experiments suggest that *hda-1* and *hpl-2*, which encode a protein similar to class I histone deacetylases and a protein similar to heterochromatin protein 1, respectively, may have some synMuv activity (LU and HORVITZ 1998; COUTEAU *et al.* 2002). DUFOURCQ *et al.* (2002) reported that *hda-1/gon-10(e1795)* does not have class B synMuv activity but other results using stronger class A synMuv mutations suggest that *hda-1/gon-10(e1795)* does have class B synMuv activity (C. J. CEOL, E. C. ANDERSEN and H. R. HORVITZ, unpublished results). Many of these genes are known as components of a nucleosome remodeling and histone deacetylase (NuRD) complex, and the class B synMuv genes have been proposed to remodel chromatin and repress transcription of genes important for vulval cell fate specification (LU and HORVITZ 1998; VON ZELEWSKY *et al.* 2000). Some of the class B synMuv genes are involved in the promotion of early larval P3.p fusion and G1-to-S phase progression of the cell cycle (CHEN and HAN 2001; BOXEM and VAN DEN HEUVEL 2002).

In this paper, we identify and characterize 50 new synMuv mutations. Some of these mutations define new class A and new class B loci. *lin-52*, one of the new class B loci, encodes a protein that is similar to mammalian and *Drosophila* proteins of unknown function. Because *lin-52* has genetic properties similar to *lin-35* Rb, LIN-52 homologs may act in an Rb pathway in mammals.

MATERIALS AND METHODS

Strains and general techniques: *Caenorhabditis elegans* var. Bristol strain N2 was the wild-type strain used in this study. To map *lin-52*, we used the strain RW7000, which contains the polymorphism *stP127* (WILLIAMS *et al.* 1992). Mutations were described by HODGKIN *et al.* (1988) unless otherwise noted.

LGI: *bli-3(e767)*; *sup-11(n403)*; *dpy-5(e61)*; *lin-35(n745)*; *unc-29(e1072)*; *dpy-14(e188)*; *unc-13(e1091)*; *lin-11(n566)*; *unc-75(e950)*; *unc-101(m1)*; *unc-54(e1092)* (WATERSTON *et al.* 1980).

LGII: *lin-8(n111)*; *lin-31(n301)*; *unc-85(e1414)*; *bli-2(e768)*; *dpy-10(e128)*; *rol-6(e187)*; *let-23(n1045, mn23, mn216)* (HERMAN 1978; SIGURDSON *et al.* 1984; FERGUSON and HORVITZ 1985); *let-240(mn209)*; *unc-4(e120)*; *unc-53(e569)*; *rol-1(e91)*; *lin-38(n751)*; *unc-52(e444)*; *mnDf67* (SIGURDSON *et al.* 1984); *mnDf85* (SIGURDSON *et al.* 1984); *mnDf46* (SIGURDSON *et al.* 1984); *mnC1[dpy-10(e128) unc-52(e444)]*.

LGIII: *dpy-1(e1)*; *unc-93(e1500)*; *dpy-27(y57)* (PLENEFISCH *et al.* 1989); *unc-79(e1068)*; *dpy-17(e164)*; *lon-1(e185)*; *sma-3(e491)*; *lin-37(n758)*; *egl-5(n945)*; *lin-36(n766)*; *nDf40* (HENGARTNER *et al.* 1992); *unc-36(e251)*; *dpy-19(e1259)*; *lin-9(n112)*; *sqv-3(n2842)*; *unc-32(e189)*; *unc-16(e109)*; *unc-47(e307)*; *unc-69(e587)*; *unc-25(e156)*; *unc-49(e382)*; *dpy-18(e364)*; *qC1[dpy-19(e1259) glp-1(q339)]* (AUSTIN and KIMBLE 1989; GRAHAM and KIMBLE 1993).

LGIV: *dpy-9(e12)*; *egl-18(n162)*; *lin-1(e1275)*; *unc-17(e245)*; *unc-5(e53)*; *dpy-20(e1282)*; *unc-22(e66)*; *unc-30(e191)*; *lev-1(x22)*; *ced-3(n717)*; *unc-26(e205)*; *dpy-4(e1166)*.

LGV: *unc-34(e566)*; *dpy-11(e224)*; *unc-51(e369)*.

LGX: *lon-2(e678)*; *unc-3(e151)*; *lin-15(n433, n744, n765, n767)* (FERGUSON and HORVITZ 1989).

In addition, we used strains containing the chromosomal aberration *eT1(III;V)* (ROSENBLUTH and BAILLIE 1981). Methods for the culture and genetic manipulation of *C. elegans* have been described by BRENNER (1974). Genetic nomenclature was described by HORVITZ *et al.* (1979). Nomenclature used for synMuv strains is as used by FERGUSON and HORVITZ (1989).

Mutagenesis of class A and class B mutants: Screens for new synMuv strains were conducted essentially as described by FERGUSON and HORVITZ (1989) using EMS as a mutagen, according to BRENNER (1974). Only one Muv strain was selected from each group of mutagenized P_0 hermaphrodites for subsequent analysis to ensure each mutation was independently derived. N2 males were crossed with the Muv strains, and the F_2 progeny were scored for the Muv phenotype. The segregation of 1/16 or fewer Muv F_2 progeny indicated candidate synMuv strains. In no case did the Muv phenotype of a strain in which the original mutation was autosomal result from a synthetic interaction with a second mutation on the same linkage group, based upon either of two criteria: (1) failure of the new Muv mutation to complement a known Muv mutation, or (2) failure of the Muv phenotype to show linkage to the chromosome containing the parental mutation. In mutagenesis experiments in which the original mutation was a *lin-15* allele, strains that segregated 1/4 or fewer Muv F_2 progeny were also retained for further analysis since new *lin-15* mutations would be tightly linked to the parental mutation. All candidate synMuv strains were backcrossed to their strain of origin two to five times.

To isolate class B mutations, a *lin-8(n111)* homozygous strain and a *lin-15(n433)* homozygous strain were mutagenized. FERGUSON and HORVITZ (1989) previously mutagenized *lin-8(n111)* and *lin-15(n767)* animals to isolate class B mutations. After the mutagenesis of *lin-8(n111)* animals, we screened approximately 6,000 haploid genomes and isolated 15 synMuv strains. After the mutagenesis of *lin-15(n433)* animals, we screened approximately 10,000 haploid genomes and isolated 15 synMuv strains. To isolate class A mutations, a *lin-36(n766)* homozygous strain and a *lin-15(n744)* homozygous strain were mutagenized. FERGUSON and HORVITZ (1989) previously mutagenized *lin-9(n112)* animals to isolate class A mutations. After the mutagenesis of *lin-36(n766)* animals, we screened approximately 10,000 haploid genomes and isolated five synMuv strains. After the mutagenesis of *lin-15(n744)* animals, we screened approximately 13,000 haploid genomes and isolated 14 synMuv strains.

The *lin-52* mutation *n3718* was isolated following mutagenesis of a *lin-15(n767)* homozygous mutant strain (C. J. CEOL, F. STEGMEIER, M. M. HARRISON and H. R. HORVITZ, unpublished results). Other results of this screen will be described elsewhere.

Molecular analysis of *lin-15*AB lesions: Genomic DNA was purified, essentially using standard methods, from *lin-15*AB strains isolated after the mutageneses of *lin-15(n744)* and *lin-15(n433)* animals (SULSTON and HODGKIN 1988). DNA was digested by *Eco*RI, separated by agarose gel electrophoresis, and probed with ^{32}P-labeled *lin-15* plasmid DNA (SAMBROOK *et al.* 1989; CLARK *et al.* 1994). Some samples of genomic DNA that showed a lesion were digested with *Eco*RI and either *Eag*I, *Sac*I, *Msc*I, *Bgl*I, *Mlu*I or *Nru*I, and probed with ^{32}P-labeled *lin-15* plasmid DNA.

Molecular analysis of *lin-13* and *lin-52* lesions: N2, *lin-13* and *lin-52* strains were lysed and the coding regions and adjacent noncoding regions of the *lin-13* and

lin-52 genes were amplified using the polymerase chain reaction (PCR). The sequences of the PCR products were determined using an automated ABI 373A cycle sequencer (Applied Biosystems, Foster City, CA). The sequence of each mutation was confirmed using an independently derived PCR product.

Nomarski observation and P(3-8).p cell lineage analysis of *lin-54* animals: P(3-8).p cells and their descendants in *lin-8(n111); lin-54(n2231)* animals were observed using Nomarski optics at different times during vulval development as described by SULSTON and HORVITZ (1977). The nomenclature and criteria of STERNBERG and HORVITZ (1986, 1989) were used to describe and assign 1°, 2° and 3° cell fates.

Construction of strains homozygous for newly isolated synMuv mutations: Strains carrying a single homozygous synMuv mutation were constructed and their genotypes confirmed essentially as described by FERGUSON and HORVITZ (1989). In these experiments, *unc-79 dpy-27* balanced *lin-13(n770)*, *unc-69* balanced *lin-52(n771)*, *unc-29* balanced *lin-53(n833)*, *unc-22 ced-3 unc-26* balanced *lin-54(n2231)*, and *rol-6 unc-4* balanced both *dpl-1(n2994)* and *lin-56(n2728).*

Construction of unlinked synMuv double mutants: Class A; class A or class B; class B double mutants carrying a new mutation and a *lin-15* mutation of the same class were constructed essentially as described by FERGUSON and HORVITZ (1989). Class B; class B double mutants carrying a new mutation and an autosomal mutation of the same class were also constructed essentially as described by FERGUSON and HORVITZ (1989). To ensure that mutations were not lost by recombination, several independent lines were isolated for each strain.

In these constructions, *lin-15(n767)* and *lin-15(n744)* were used as the class A and class B *lin-15* alleles, respectively. The autosomal class B mutation used was *lin-36(n766)*. This allele was marked in *cis* by *unc-32*. The following markers were linked in *cis* to the new mutations: *unc-32* to *lin-13(n770)*, *unc-32* to *lin-52(n771)*, *dpy-5*

to *lin-53(n833)*, *dpy-20* to *lin-54(n2231)*, *rol-6* to *dpl-1(n2994)*, and *rol-6* to *lin-56(n2728)*.

Construction of linked synMuv double mutants: To construct a class B class B double mutant between *lin-13(n770)* and *lin-36,* hermaphrodites of genotype *lin-13* + + *unc-32/+ egl-5 lin-36* +; *lin-15*A were generated. The frequency of recombination between *lin-13* and *egl-5* is greater than that between *lin-36* and *unc-32* and much greater than that between *egl-5* and *lin-36*. Muv non-Unc non-Egl recombinant progeny were isolated; from these animals, Egl Muv progeny were selected and the *lin-15*A mutation crossed out, yielding animals of putative homozygous genotype *lin-13 egl-5 lin-36*. This genotype was confirmed by crossing with another class A mutation and performing complementation tests with *lin-13* and with *lin-36* to show that the strain contained both class B mutations.

A class B class B double mutant between *lin-36* and *lin-52(n771)* was constructed in a manner similar to that for the construction of the double between *lin-13* and *lin-36*. Hermaphrodites of genotype + *lin-36 unc-36 +/sma-3* + + *lin-52; lin-15*A were generated. The frequency of recombination between *unc-36* and *lin-52* is greater than that between *sma-3* and *lin-36* and much greater than that between *lin-36* and *unc-36*. Muv non-Sma recombinant progeny were isolated and used to generate Unc Muv progeny of putative genotype *lin-36 unc-36 lin-52; lin-15*A. *lin-15*A was removed to generate animals of homozygous genotype *lin-36 unc-36 lin-52*. This genotype was confirmed by crossing with another class A mutation and performing complementation tests with *lin-52* and with *lin-36* to show that the strain contained both class B mutations.

To construct a class A class A double mutant between *lin-8* and *lin-56(n2728)*, animals of genotype *lin-8 unc-85 dpy-10* + +/+ + + *rol-6 lin-56; lin-15*B/+ were constructed. From these animals, Unc non-Dpy non-Muv recombinant animals that did not segregate Muv progeny were isolated; these animals segregated Rol Unc animals

of putative genotype *lin-8 unc-85 rol-6 lin-56*. This genotype was confirmed by conducting complementation tests, in the presence of a class B mutation, with *lin-8* and *lin-56* to show that the strain was homozygous for both class A mutations.

Transgenic animals: Germline transformation was performed as described by MELLO et al. (1991) by injecting cosmid (5-10 ng/μL) or plasmid (50-80 ng/μL) DNA into *lin-52(n771); lin-15(n767)* animals. pRF4, which causes a dominant Rol phenotype, was used as a coinjection marker.

***lin-52* cDNA isolation and RNA-mediated interference:** We obtained a partial *lin-52* cDNA clone (kindly provided by YUJI KOHARA), yk253b12, that included 249 nucleotides of the *lin-52* open reading frame and also included the 3' untranslated region and a polyA tail. We used the 5' RACE system v2.0 (GIBCO-BRL) to determine the 5' end of the *lin-52* transcript. *lin-52* 5' RACE products were *trans*-spliced to the SL2 leader sequence. Consistent with our observations, ZORIO *et al.* (1994) previously found that an SL2 oligonucleotide could be used to PCR amplify gene sequence corresponding to ZK632.13, the predicted gene we have identified as *lin-52*. RNA-mediated interference (RNAi) was conducted as described by FIRE *et al.* (1998), using double-stranded RNA corresponding to the full-length *lin-52* cDNA.

RESULTS

Isolation of new synMuv strains: To identify new class A mutations, we used EMS to mutagenize class B *lin-36(n766)* or class B *lin-15(n744)* homozygotes, which display wild-type vulval development. The vulval morphology of synMuv strains can be readily distinguished from that of Muv strains mutant in *lin-1* or *lin-31*. SynMuv animals usually have a vulva with wild-type morphology and have a few regularly spaced pseudovulvae. By contrast, *lin-1* animals frequently have abnormal and distinctively

protruding vulvae, and *lin-31* animals are often egg-laying defective, have incomplete vulvae and have a variable number of small pseudovulval protrusions that are distinctive in number and morphology. A Muv phenotype that segregated as 1/16 or less in the F_2 generation after crossing with wild-type males was considered a candidate for being synMuv, as was a strain obtained in a *lin-15* background that segregated either as 1/16 or 1/4 because new *lin-15* mutations would be linked to the parental *lin-15* mutation. We obtained five synMuv strains from the mutagenesis of *lin-36(n766)* animals and 14 synMuv strains from the mutagenesis of *lin-15(n744)* animals. A total of 19 new class A mutations were identified (Table 1).

To identify new class B mutations, we used EMS to mutagenize animals homozygous for the class A mutations *lin-8(n111)* or *lin-15(n433)*. Muv strains were tested to determine if their phenotypes depended upon two unlinked loci as described for the isolation of class A mutations. We obtained 15 synMuv strains from the mutagenesis of *lin-8(n111)* animals and 15 synMuv strains from the mutagenesis of *lin-15(n433)* animals. A total of 30 new class B mutations were identified in these screens (Table 1).

An additional class B mutation, *n3718*, was obtained in a screen for synMuv mutants following the mutagenesis of *lin-15(n767)* animals (C. J. CEOL, F. STEGMEIER, M. M. HARRISON and H. R. HORVITZ, unpublished results).

Linkage and complementation: SynMuv mutations already shown to segregate as two unlinked loci were expected to display linkage to two loci: the parental locus and the new locus (FERGUSON and HORVITZ 1989). Mutations caused by most of the candidate synMuv strains displayed linkage to the parental locus and to another linkage group. A few *lin-15* strains, discussed below, did not display linkage to a new location (Table 1).

Newly isolated synMuv mutations were tested for complementation with alleles of the then known synMuv genes: *lin-8*, *lin-9*, *lin-15*A, *lin-15*B, *lin-35*, *lin-36*, *lin-37*, *lin-38*

and *lin(n770)*, *lin(n771)*, and *lin(n833)*, three previously identified but not extensively characterized synMuv mutations (FERGUSON and HORVITZ 1989). Mutations that complemented all known synMuv complementation groups were tested against each other after strains carrying identical parental mutations of the opposite class were constructed.

Mutations were assigned to the same complementation group only if hermaphrodites of genotype *a; b1/b2*, where *a* is the background mutation required for the synthetic interaction and *b1* and *b2* are the two mutations being tested, were Muv and segregated only Muv progeny. As described by FERGUSON and HORVITZ (1989), this approach was necessary to distinguish intragenic noncomplementation from the intergenic noncomplementation observed in some doubly heterozygous synMuv strains. Several combinations of genotype *a; b1/+; b2/+* displayed intergenic noncomplementation; in most cases, the penetrance and expressivity of the Muv phenotype produced by intergenic noncomplementation was lower than that produced by homozygosity at either of the two loci that displayed intergenic noncomplementation. Thus, animals lacking the activity of a synMuv gene of one class and having reduced doses of two genes of the other class as well as no maternal activity from one of these genes were occasionally Muv. This observation suggests that the synMuv genes are dose-sensitive. *lin-53(n833)* (see below) was notable in that it showed very strong intergenic noncomplementation with other class B mutations, consistent with the observation that this mutation causes dominant-negative activity (LU and HORVITZ 1998).

A total of 38 mutations failed to complement alleles of known synMuv genes. These mutations included eight *lin-8* alleles, eight *lin-15*A alleles, 10 *lin-15*B alleles, six *lin-35* alleles, three *lin-36* alleles, one *lin-37* allele, and two *lin-38* alleles. Another six mutations failed to complement *n770* or *n833*, mutations that had previously been isolated but not extensively characterized. The mutations that defined the *n770*

complementation group failed to complement *lin-13* for class B activity. We named the other gene, defined by *n833*, *lin-53*. Our new mutations included five *lin-13* class B alleles and one *lin-53* allele. We obtained no new alleles of *lin-9*. *n771*, another mutation that had been previously isolated but not extensively characterized, defined the gene we named *lin-52*. We obtained one new *lin-52* mutation in a separate screen. Another four mutations defined three new complementation groups, which we named *lin-54*, *dpl-1*, and *lin-56*. (The name *dpl-1* was assigned after studies by CEOL and HORVITZ (2001) showed the DPL-1 protein to be similar to mammalian DP.) There were two *lin-54* alleles, one *dpl-1* allele, and one *lin-56* allele (Table 1).

Identification of *lin-15*AB double mutants: The mutations of several Muv strains isolated in a *lin-15*A or *lin-15*B background did not segregate as two loci yet displayed a Muv phenotype similar to that of synMuv strains. These strains included five isolated in a *lin-15(n433)* background and seven isolated in a *lin-15(n744)* background. The Muv phenotype of these strains showed linkage only to *unc-3 X*, which marked the parental *lin-15* mutation, and failed to complement *lin-15(n765)*, a *lin-15* allele defective in both class A and class B activities. Thus, the new strains are defective in both *lin-15*A and *lin-15*B activities and they carry new *lin-15* alleles.

Six of the seven *lin-15* Muv mutants that have been isolated as single mutants and analyzed - all but *lin-15(n765)* - have gross mutations that disrupt both *lin-15* mRNAs (CLARK *et al.* 1994; HUANG *et al.* 1994). *lin-15(n765)* is a deletion in the class B gene and presumably also has a point mutation in the class A gene. Several *lin-15*A and *lin-15*B mutations have been analyzed molecularly; each specifically affects only one of the two genes (CLARK *et al.* 1994).

To determine whether the Muv phenotype of each of the *lin-15*AB mutants isolated in these screens is the result of the newly induced mutation alone or rather the result of an interaction between the newly induced mutation and the parental mutation, we used Southern hybridization to analyze the *lin-15* locus in these strains. Four of the

12 mutant strains showed polymorphisms, three of which were confined to only the A or only the B region. Specifically, the *lin-15(n2993 n433)* strain has a loss of an *Eco*RI site in the B region of *lin-15*, the *lin-15(n744 n2733)* strain has a small deletion of 0.3 kb in the A region, and the *lin-15(n744 n2735)* strain has a larger deletion of several kilobases in the A region.

By contrast, the *lin-15(n744 n2726)* strain has a deletion of about 0.9 kb in an *Eco*RI-*Sac*I restriction fragment containing both A and B sequences. This region includes both the start of the class A mRNA and the end of the class B mRNA. The deletion probably eliminates the 5' end of the class A mRNA, and may eliminate some of the 3' end of the class B mRNA. This deletion may be sufficient to cause a class B defect, and the Muv phenotype of this strain may result entirely from the new mutation, *n2726*.

Polymorphisms were not detected in the other *lin-15* strains. Since the parental mutation of these strains is either a *lin-15*A or a *lin-15*B point mutation, and EMS produces predominantly point mutations (ANDERSON 1995), it is likely that the Muv phenotype of most if not all of these *lin-15*AB strains is the result of a synthetic interaction between *lin-15* class A and class B point mutations.

Identification of *lin-13* mutations: Five newly identified putative class B mutations and *lin(n770)* failed to complement *lin-13(n387)* in a class A mutant background. *lin-13(n387)*, which causes a sterile Muv phenotype at 25°, had been shown to behave as a class B synMuv at 15° (FERGUSON and HORVITZ 1989). No class A mutations in *lin-13* were isolated.

Unlike *lin-15*, which encodes two nonoverlapping transcripts, *lin-13* encodes a single transcript encoding a nuclear protein predicted to contain 24 C2-H2 zinc fingers, one C4 zinc finger and an LXCXE potential Rb-binding motif (MELÉNDEZ and GREENWALD 2000). Sterile Muv mutations of *lin-13*, *n387* and *n388*, have been shown to be nonsense mutations at residues S524 and R857, respectively. The mutant

gene products are predicted to be truncated proteins with either two or five complete zinc fingers (MELÉNDEZ and GREENWALD 2000). To determine the molecular natures of the *lin-13* mutations we isolated, we used PCR to amplify DNA from the mutants and determined the sequence changes in these strains. Three mutants carry *lin-13* nonsense mutations: *lin-13(n770)*, *lin-13(n2238)* and *lin-13(n2985)* (Table 2). These alleles are all predicted to encode truncated proteins, albeit ones longer than those generated by *lin-13(n387)* and *lin-13(n388)*. It is notable that the *lin-13(n2238)* predicted protein product of 995 amino acids is only slightly longer than the *lin-13(n388)* predicted protein product of 856 amino acids and has only one additional undisrupted zinc finger domain. Three other mutants carry *lin-13* missense mutations. *lin-13(n2988)* and *lin-13(n2981)* each encode a cysteine-to-tryptophan change in the first cysteine of the first and fifth zinc fingers, respectively (Table 2). The first zinc finger may play a more important role than the fifth zinc finger, since *lin-13(n2988)* is notably stronger at low temperature than is *lin-13(n2981)* (Table 1). The remaining missense mutation, *lin-13(n2984)*, encodes a glycine-to-glutamic acid change in the residue immediately preceding the first cysteine of the first zinc finger (Table 2). The bulky negatively charged mutant residue may partially interfere with the ability of the first cysteine to act in the coordination of zinc. Consistent with this hypothesis, the phenotype of *lin-13(n2984)* is weaker than that of *lin-13(n2988)* at lower temperatures (Table 1).

Phenotypes of newly isolated synMuv strains: Many of the newly isolated synMuv strains displayed a temperature-sensitive effect on vulval development such that the penetrance of the Muv defect increased at higher temperatures (Table 1). Similar observations were made by FERGUSON and HORVITZ (1989). The synMuv strains also often showed temperature-sensitive growth characteristics. Many strains showed a reduced growth rate or, in some cases, lethality at 25° (Table 1). Similar observations also were made by FERGUSON and HORVITZ (1989). Although there

were some differences among strains in growth at 20°, the differences were much greater at 15° and 25°. Rare synMuv animals displayed a protruding excretory pore. Some animals ruptured as adults at the vulva or, rarely, at a pseudovulval protrusion. Strains isolated in the screen in which *lin-15(n744)* was used as the parental mutation had a fairly high percentage of rupture, often exceeding 50% of adults (data not shown).

Animals homozygous for the *lin-52(n3718)* mutation were sterile. The sterility of these animals is likely caused by a loss of *lin-52* gene function, as we always observed its cosegregation with the *lin-52* synMuv phenotype. Furthermore, animals heterozygous for *lin-52(n771)* in *trans* to *nDf40*, a deficiency that removes the *lin-52* locus, have diminished brood sizes and display maternal-effect lethality, indicating that a reduction of *lin-52* function leads to reduced fertility.

Strains carrying *lin-54* mutations differed from other synMuv strains in that a greater proportion of these animals had a ventral protrusion that was further posterior to the vulva than was the case for most synMuv mutants. Also, a number of these strains had two ventral protrusions posterior to the vulva, a rare occurrence for other synMuv strains. This phenomenon was observed with both alleles of *lin-54*. Among *lin-8(n111); lin-54(n2231)* animals, 13% had a relatively far posterior ventral protrusion, and 11% had two posterior ventral protrusions (n=126). Among *lin-54(n2231); lin-15(n767)* animals, 26% had a ventral protrusion further posterior than ususal, and 19% had two ventral protrusions (n=75). Among *lin-54(n2990); lin-15(n433)* animals, 13% had a ventral protrusion further posterior than usual, and 10% had two ventral protrusions (n=112).

To determine the origin of these unusually far posterior pseudovulvae and two posterior pseudovulvae in *lin-54* animals, we used Nomarski optics to observe the P(3-8).p cells and their descendants in *lin-8(n111); lin-54(n2231)* animals. Our observations established that, as in the wild type, in these animals there are only six

potential vulval precursor cells: P(3-8).p divided to give 1°, 2° and 3° cell fates, as in the wild type, and other Pn.p cells, such as P9.p, which lies posterior to P8.p, were not transformed into potential vulva precursor cells (as seen in "superMuv" mutants, which have extra pseudovulval protrusions in a *lin-15* background; CLARK 1992). Cell lineage analysis revealed that in *lin-8; lin-54* animals, the functional vulva sometimes formed from P(4-6).p rather than from P(5-7).p (data not shown). In these cases, the P5.p nucleus did not lie directly beneath the anchor cell nucleus; instead, the P5.p and P6.p nuclei were located to either side of and below the anchor cell nucleus (data not shown). This phenomenon has been observed in other synMuv strains, but is rare (FERGUSON *et al.* 1987, THOMAS and HORVITZ 1999). In animals in which the functional vulva was formed from the descendants of P(4-6).p, P7.p and P8.p and their descendants were posterior to the developing vulva. These cells adopted vulval fates in the mutant animals and formed either two posterior pseudovulvae or one posterior pseudovulva at a greater relative distance from the misplaced vulva than a pseudovulva formed from only P8.p relative to a properly positioned functional vulva. In one case, the vulva was observed to derive from the descendants of P5.p, P6.p and part of P7.p. The descendants of P7.p were spread over a greater distance than usual; some joined a number of P8.p descendants to form a pseudovulva, while other P8.p descendants formed a second posterior pseudovulva. Thus, the P(3-8).p cells and the anchor cell seem to be occasionally displaced relative to each other in *lin-54* animals. In some animals in which the anchor cell was located over P6.p, the descendants of P7.p and P8.p were spread over a wider distance than in the wild type. These data suggest that the posterior members of the vulval equivalence group are displaced posteriorly in a significant number of *lin-54* animals.

Analysis of synMuv genes: We mapped three new synMuv genes, *lin-52*, *lin-54* (class B) and *lin-56* (class A) and three previously described synMuv genes, *lin-13*,

lin-53 and *dpl-1* (all class B), using multi-factor crosses and deficiencies (Table 3; Figure 1).

dpl-1 mapped to the same linkage group II deficiency interval as *let-23*, which encodes a receptor tyrosine kinase involved in inductive vulval signaling (FERGUSON and HORVITZ 1987; AROIAN *et al.* 1990). To determine if *dpl-1(n2994)* is allelic to *let-23*, we performed complementation tests against *let-23(mn23)*, *let-23(mn216)* and *let-23(n1045)*. These *let-23* alleles were chosen because *mn23* and *mn216* represent putative null alleles, and *n1045* is a viable reduction-of-function allele that causes both a Vul and a hyperinduced phenotype (Hin; P(3-8).p cells immediately adjacent to the developing vulva often adopt vulval fates, producing an abnormal vulva with adjacent Muv-like protrusions; FERGUSON and HORVITZ 1985; AROIAN and STERNBERG 1991). *dpl-1(n2994)* complemented *let-23* for all phenotypes: synMuv, Vul, Hin, and lethal (Let). The allele used in these tests, *dpl-1(n2994)*, is predicted to fail to complement a loss-of-function allele for the synMuv phenotype, since *dpl-1(n2994)/mnDf67; lin-15*A animals are Muv (Table 3).

The class B synMuv gene *dpl-1* was represented by only one mutant allele in these screens. To test whether the phenotype produced by this allele is weaker than that expected from a null phenotype, this mutation was tested in *trans* to a deficiency (Table 3). Animals of genotype *dpl-1(n2994)/mnDf67; lin-15(n433)* had a Muv phenotype and an incidence of sterility similar to those of animals of genotype *dpl-1(n2994); lin-15(n433)* when both were progeny of a mother of genotype *dpl-1(n2994)/mnDf67; lin-15(n433)*. However, the fertile animals of genotype *dpl-1(n2994)/mnDf67; lin-15(n433)* had a much greater incidence of maternal-effect lethality than did animals of genotype *dpl-1(n2994); lin-15(n433)* when both were progeny of a mother of genotype *dpl-1(n2994)/mnDf67; lin-15(n433)*. Animals of both of these genotypes had a stronger Muv phenotype and were less fertile than animals of genotype *dpl-1(n2994); lin-15(n433)* when descended from animals of genotype

dpl-1(n2994); lin-15(n433). These results suggest that *dpl-1(n2994)* is a weak allele of a locus that has a stronger, possibly sterile and maternal-effect lethal, null phenotype. CEOL and HORVITZ (2001) have subsequently isolated a putative null allele of *dpl-1*, which causes sterility.

To demonstrate formally that *lin-52*, *lin-53*, *lin-54*, *dpl-1* and *lin-56* are indeed synMuv genes, we conducted tests similar to those used by FERGUSON and HORVITZ (1989). First, we separated an allele of each gene from its parental mutation and showed that strains that carried only the isolated allele in homozygous condition displayed wild-type vulval development at the level of resolution of the dissecting microscope (Table 4). Double mutants were then constructed between alleles of the new synMuv genes and alleles of previously defined synMuv genes. Double mutants carrying class A and class B mutations were Muv; double mutants carrying two class A mutations or two class B mutations were wild-type for vulval development (Table 4). *lin-13(n770)* has also been shown to behave as a class B synMuv mutation by these criteria (Table 4 and data not shown).

Maternal rescue of the synMuv phenotype depends on both class A and class B genes: Many of the new synMuv strains displayed maternal rescue of the Muv phenotype, such that animals of genotype *a/a; b/b* descended from animals of genotype *a/+; b/+* had lower penetrance and reduced expressivity compared to animals of genotype *a/a; b/b* descended from animals of *a/a*; *b/b* genotype (Table 5). Similar results have been shown for other synMuv strains (FERGUSON and HORVITZ 1989). To determine whether this maternal rescue was conferred by only one of the two classes, we compared the Muv phenotypes of animals of genotype *a/a; b/b* descended from animals of genotypes *a/+; b/+* versus *a/a; b/+* versus *a/+; b/b*. Several different combinations of synMuv mutations were tested. In many cases, neither class alone produced significant maternal rescue compared to that produced by both classes together. We concluded that maternal rescue displayed in synMuv strains is the result

of a synergistic interaction between genes of the two classes rather than the result of the maternal contribution of genes of just one class (Table 5).

Molecular identification of *lin-52*: We further characterized the class B synMuv gene *lin-52*. Using standard three- and four-factor mapping techniques, we localized *lin-52* to a small genetic interval between *sqv-3* and the Tc1 transposon polymorphism *stP127* (Figure 2). We generated transgenic animals using DNA clones from this interval and found that the overlapping cosmids ZK630 and C26C12 and subclones of DNA common to both of these cosmids rescued the Muv phenotype of *lin-52(n771); lin-15(n767)* mutants. Typically greater than 70 percent of transgenic animals in the first generation of a stable transgenic line (*i.e.* in the transgenic F_2 progeny of an injected animal) were rescued. However, transgenic lines containing these cosmids or their subclones displayed a progressive reduction in the penetrance of rescue in each subsequent generation. The reason for this trend is unknown; we speculate that it may have resulted from transgene silencing. Such generation-dependent transgene silencing occurs in the *C. elegans* germline and is thought to be caused by the preferential recruitment of silencing factors to repetitive stretches of DNA (KELLY *et al.* 1997).

Because two complete predicted genes, ZK632.9 and ZK632.13, were present on the minimal rescuing fragment, we performed further experiments to define *lin-52* (Figure 2). Into the minimal rescuing fragment we cloned a small double-stranded oligonucleotide that is predicted to introduce an in-frame stop codon into the ZK632.13 gene. This altered subclone was unable to rescue the Muv phenotype of *lin-52(n771); lin-15(n767)* mutants, whereas a subclone in which the oligonucleotide was removed, thereby restoring the ZK632.13 open reading frame, rescued like the clones described above. In addition, we found that RNA-mediated interference of ZK632.13 in a *lin-15(n767)* background resulted in a highly penetrant Muv phenotype. Finally, we determined the sequence of ZK632.13 in *lin-52(n771)* and *lin-52(n3718)* mutants.

lin-52(n771) mutants contain a missense mutation that is predicted to substitute a positively-charged lysine in place of a negatively-charged glutamate, and *lin-52(n3718)* mutants contain a nonsense mutation that is predicted to truncate the ZK632.13 protein after 30 amino acids (Figure 3). These results identify ZK632.13 as *lin-52*.

We assembled a cDNA clone of *lin-52* (Figure 3A; see MATERIALS AND METHODS). This clone contains a 5' SL2 splice leader sequence and a polyA tail, indicating that it is full-length. An SL2 leader sequence is often *trans*-spliced upstream of genes that are initially transcribed as downstream genes of an operon (ZORIO *et al.* 1994). The SL2 leader sequence and the proximity of *lin-52* to the gene immediately upstream of it suggest that *lin-52* is transcribed as part of a polycistronic operon. The large open reading frame of this cDNA is predicted to encode a 161 amino acid protein that is similar to uncharacterized proteins predicted by human, mouse and *Drosophila* cDNA and genomic sequences (Figure 3B; C. J. CEOL and H. R. HORVITZ, unpublished observations). LIN-52 is most similar to these proteins in a short carboxy-terminal domain. Over a stretch of 28 amino acids, LIN-52 is 50% identical and 75% similar to the human predicted protein LOC91750. This region of similarity may represent a functional domain within the LIN-52 protein.

DISCUSSION

In this paper we describe the isolation and characterization of 50 new synMuv mutants. We define and describe two new genes, *lin-54* and *lin-56*, describe two other newly named genes, *lin-52* and *lin-53*, of which one allele each had been previously isolated, describe the initial identification and characterization of a previously described gene, *dpl-1*, and identify class B synMuv alleles of *lin-13*. In sum, at least four class A genes (*lin-8*, *lin-15*A, *lin-38*, *lin-56*) and at least 14 class B genes (*lin-9*, *lin-13*, *lin-15*B,

lin-35 Rb, *lin-36*, *lin-37*, *lin-52*, *lin-53, lin-54*, *dpl-1*, *tam-1*, *let-418*, *efl-1*, *hda-1*, *mep-1)* are now known (Table 6). We showed that the maternal rescue of the synMuv phenotype is dependent on a synergistic interaction between the wild-type alleles of both classes. We also cloned the *lin-52* gene and found that it encodes a small protein that may be evolutionarily conserved.

Null phenotypes of synMuv genes: The null phenotype of most synMuv genes has not been rigorously established. Most likely, not all synMuv genes have the same null phenotypes (Table 6). Several synMuv genes are likely to have a synMuv null phenotype. The class A mutation *lin-15(n767)* is a likely null allele by molecular criteria: it is a deletion in the middle of the coding sequence with a small insertion producing a frameshift in the class A transcript (HUANG *et al.* 1994). *lin-15(n767)* mutants display a class A synMuv phenotype and are viable and fertile. The *lin-15* class B gene is also likely to have a synMuv null phenotype. The *lin-15*AB mutations *lin-15(n309)* and *lin-15(e1763)* are deletions of most of the DNA of the locus and are therefore molecular nulls for both A and B *lin-15* transcripts (CLARK *et al.* 1994; HUANG *et al.* 1994). These mutants are Muv, viable and fertile, indicating that the *lin-15* class B gene also has a synMuv null phenotype. *lin-36* is also likely to have a synMuv null phenotype: nonsense mutations isolated in a non-complementation screen are synMuv, viable and fertile (THOMAS and HORVITZ 1999).

Several other synMuv genes have a null phenotype that is either lethal or sterile. *lin-13* Muv mutants carry nonsense mutations and have a zygotic sterile and maternal effect larval arrest phenotype (MELÉNDEZ and GREENWALD 2000). It is likely that the null phenotype of *lin-9* is sterile. A non-complementation screen for *lin-9* mutants led to the isolation of *lin-9* alleles that were sterile and behaved as synMuv mutations (FERGUSON and HORVITZ 1989). These sterile *lin-9* mutations were shown to be nonsense mutations (BEITEL *et al.* 2000). Similarly, we found that the *lin-52(n3718)* mutation causes a sterile and synMuv phenotype and is a nonsense mutation that is

predicted to severely truncate the LIN-52 protein. Therefore, the *lin-52* null phentoype is likely sterile. The class B mutation *dpl-1(n2994)* was tested in *trans* to a deficiency that spanned the locus. *dpl-1(n2994)* mutants have a stronger Muv phenotype, are less fertile, and have a greater incidence of maternal-effect lethality when they and their mothers are *trans*-heterozygotes for a deficiency of this locus. This observation suggests that *dpl-1(n2994)* is probably a reduction-of-function mutation rather than a complete loss-of-function mutation. A null mutation of *dpl-1* isolated by CEOL and HORVITZ (2001) causes the sterile phenotype predicted by the analysis described here.

The screens described in this paper were not designed to isolate synMuv mutations that caused lethality or sterility (*lin-52(n3718)* was isolated in a separate screen that allowed the identification of lethal or sterile mutations. However, the other mutants isolated in this screen are not described in this manuscript, and for this reason this screen is not considered in the following discussion.). Thus, complete loss-of-function alleles of loci with such null phenotypes were not isolated. However, viable and fertile reduction-of-function mutations in such loci could have been isolated. Mutations in complementation groups with few alleles are candidates for being such reduction-of-function mutations. Loci that are not readily mutated to a viable synMuv phenotype may not have been identified.

From our general screens, we isolated mutations in different complementation groups at different frequencies. Class A mutations fell into either a frequently isolated group, *lin-8* and *lin-15*A (eight alleles each), or an infrequently isolated group, *lin-38* and *lin-56* (one or two alleles each). Class B mutations included 10 alleles of *lin-15*B, six of *lin-35*, five of *lin-13*, three of *lin-36*, two of *lin-54*, one each of *lin-37*, *lin-53*, *dpl-1*, and no alleles of *lin-9*, *lin-52*, *tam-1*, *let-418*, *efl-1*, *hda-1* or *mep-1*. Given the number of haploid genomes screened and the expected frequency of mutation of the average *C. elegans* gene by EMS, 5×10^{-4}, we expected to isolate about nine alleles of each

gene with a synMuv null phenotype (BRENNER 1974; GREENWALD and HORVITZ 1980), suggesting that *lin-8*, *lin-15*A, *lin-15*B and *lin-35* are such genes. In contrast to these results, class B alleles of *lin-13*, which are not null alleles, were isolated at a relatively high frequency. *lin-13*, which encodes a protein of 2248 amino acids (MELÉNDEZ and GREENWALD 2000), may provide a large mutagenic target.

There are several reasons why mutations may have been isolated at a lower frequency than $5x10^{-4}$. Some of the genes may have a sterile or lethal loss-of-function phenotype, so that only rare reduction-of-function mutations were isolated. We probably failed to isolate any *lin-9* alleles for this reason. Mutations in such genes should be easily obtained in screens that allow the isolation of sterile and lethal mutants. Other genes may provide a small mutagenic target. Only one allele of *lin-37* was isolated in the screens described in this paper. This gene is physically small, and the allele we isolated is consistent by molecular criteria with its being a loss-of-function allele (X. LU, personal communication). Mutations affecting *lin-52* were likewise difficult to isolate, probably because of the likely sterile loss-of-function phenotype and the small physical size of *lin-52*. In addition, there may have been a bias in our experiments as a consequence of the parental mutations we used in our screens. The class A mutations *lin-8(n111)* and *lin-15(n433)* do not produce highly penetrant Muv phenotypes in conjunction with some class B mutations, which may have resulted in a lower frequency of isolation of alleles of certain genes.

Many Class A and class B synMuv genes probably act in distinct pathways: Most genes isolated in the screens described here or by FERGUSON and HORVITZ (1989) seem to be distinctly a member of either the class A or the class B pathway. With the exception of *lin-15* alleles, no class A and class B mutations mapped to the same site. However, the *lin-15* locus consists of two adjacent genes, a class A gene and a class B gene (CLARK *et al.* 1994; HUANG *et al.* 1994). These results suggest that most synMuv genes act in only one of the two pathways.

Genetic evidence suggests that *lin-13* may act in both pathways. It was previously shown that at 25° the *lin-13(n387)* mutation produces a Muv phenotype similar to that of the synMuv double mutants but acts like a class B synMuv at 15° (FERGUSON and HORVITZ 1989; MELÉNDEZ and GREENWALD 2000). We have identified a class B allele of *lin-13, n770*. Thus, all described mutations in *lin-13* either cause a Muv phenotype or a class B synMuv phenotype. The Muv phenotype of certain *lin-13* alleles may be caused either by the elimination of both class A and class B activities of *lin-13* or by the elimination of another activity of *lin-13* that is independent of the synMuv pathways. If *lin-13* has both class A and class B activities, why might it be difficult to isolate class A alleles of *lin-13*? Particular regions of *lin-13* may be required for class A and class B activities, and class B regions may provide a larger or easier target for mutagenesis. Alternatively, some regions, possibly certain zinc fingers, are required for only class B activity while others are required for both, but none is required solely for class A activity. It is possible that *lin-13* mutations that cause a class A phenotype are not fertile or viable; however, no other class A mutations exhibit these phenotypes (Table 6). It is also possible that weaker *lin-13* alleles show only a class B synMuv phenotype. Either the class B pathway may be more sensitive to disruption or *lin-13* may play a more vital role in the class B pathway; if so, it would be impossible to get a mutation strong enough to exhibit class A activity without concomitantly exhibiting class B activity.

Synthetic phenotypes: Synthetic phenotypes are produced by combinations of mutations in different genes. Many synthetic lethal phenotypes have been studied in yeast, affecting such processes as cytoskeletal organization and secretion (HUFFAKER *et al.* 1987, KAISER and SCHEKMAN 1990). Often, a synthetic phenotype is indicative of functional redundancy. There are several genes that are functionally redundant for various developmental processes in metazoa. In *Drosophila*, *achaete* and *scute* are functionally redundant for the specification of larval sense organs; however, individually

each of these genes is required for the specification of a specific group of adult bristles (reviewed by GHYSEN and DAMBLY-CHAUDIERE 1991). In *C. elegans*, *lin-12* and *glp-1* are molecularly similar and functionally redundant for some aspects of development, since double mutants exhibit defects not found in either single mutant (LAMBIE and KIMBLE 1991). Partial functional redundancy also is seen among *C. elegans* genes that function in the engulfment of cell corpses during programmed cell death; there are two classes of genes, such that animals carrying mutations in both classes have a more severe defect in engulfment than do animals carrying mutations in only one class (ELLIS *et al.* 1991). The three *C. elegans* genes that encode Rac-like proteins, *ced-10*, *mig-2* and *rac-2/3*, function redundantly in axon guidance and subsets of these genes function redundantly in certain cell migrations (LUNDQUIST *et al.* 2001). Whereas many synMuv genes are individually necessary for fertility or viability, others are not known to be individually required in any process other than vulval development. In contrast to lone mutations in many partially functionally redundant genes that have slight defects in a particular process, lone mutations in the synMuv genes do not have any discernable defects in vulval development (FERGUSON and HORVITZ 1989; THOMAS and HORVITZ 1999).

Functional redundancy at the genetic level suggests that two sets of genes implement the same biological effect, *e.g.* the negative regulation of vulval induction. The precise molecular mechanisms by which these genes act can be completely distinct, and the two classes of synMuv genes need not act at the same point in the pathway for vulval development. At what point(s) in the vulval pathway might the synMuv genes act? Mutations in the LET-23 receptor tyrosine kinase produce a Vul phenotype that is epistatic to the Muv phenotype caused by synMuv mutations, indicating that for the synMuv phenotype to be expressed *let-23* gene function is needed. If the Muv phenotype were caused by mutation in a single gene, this gene could act either parallel to or upstream of *let-23*. However, the synMuv phenotype is

instead caused by mutations in two genes. Thus, if the effects of mutation in either of these two genes is blocked by a *let-23* mutation, the synMuv phenotype would be suppressed. These considerations indicate that at least one of the two classes of synMuv genes (A or B) must act parallel to or upstream of *let-23*, but the other class of synMuv gene could act parallel to, upstream of or downstream of *let-23*. Specific models of how the class B synMuv genes may act in parallel to the *let-23* signal transduction pathway have been discussed by LU and HORVITZ (1998) and THOMAS and HORVITZ (1999).

Class B synMuv genes including *lin-52* define an Rb-mediated pathway: *lin-35*, a member of the class B synMuv pathway, encodes a protein similar to the mammalian tumor suppressor pRb (LU and HORVITZ 1998). Other genes with class B synMuv activity encode DP (*dpl-1*), E2F (*efl-1*), RbAp48 (*lin-53*), histone deacetylase (*hda-1*) and HP1 family proteins (*hpl-2*) (LU and HORVITZ 1998; CEOL and HORVITZ 2001; COUTEAU *et al.* 2002). In addition to their role in vulval development, many class B genes have been shown to regulate G1-to-S phase progression in the cell cycle. These genes include *dpl-1*, *efl-1*, *lin-9*, *lin-15*B, *lin-35* and *lin-36*; other class B genes, *hda-1*, *let-418*, *lin-37*, *lin-53* and *tam-1*, do not appear to be involved in cell cycle control (BOXEM and VAN DEN HEUVEL 2001, 2002). Even among the subgroup of class B genes that are involved in cell cycle control, *lin-35* and *lin-15*B have been shown to have partially nonoverlapping functions (BOXEM and VAN DEN HEUVEL 2002). These results suggest that the class B synMuv genes either act differently in vulval development and cell cycle control or that we have not yet distinguished more subtle differences in their roles in vulval development.

Mammalian homologs of some of these class B synMuv proteins are known to functionally, and in some cases physically, interact with pRb. These and other parallels indicate that the class B synMuv pathway is an analog of Rb pathways in other organisms, particularly those pathways in which Rb is involved in chromatin remodeling.

Consequently, additional class B synMuv genes may have homologs with analogous functions in other organisms. One such gene is *lin-52*. *lin-52* encodes a small protein, portions of which are conserved in similarly small proteins predicted by the human, mouse and *Drosophila* genome sequences. The further analysis of *lin-52* and other synMuv genes should help elucidate the mechanisms of action of Rb-like proteins and their regulators and effectors. The determination of how the class B synMuv genes negatively regulate the vulval induction process should provide insight concerning the antagonistic actions of Rb-mediated and Ras-mediated pathways.

Acknowledgments

We thank BETH CASTOR for expert technical assistance. We thank EWA DAVISON and XIAOWEI LU for sharing unpublished data. We thank current and former members of the Horvitz laboratory, especially GREG BEITEL, KERRY KORNFELD and SHAI SHAHAM, for helpful discussions during the course of this work. We thank GREG BEITEL, BRENDAN GALVIN, KERRY KORNFELD and XIAOWEI LU for critically reading this manuscript. We thank the *Caenorhabditis* Genetics Center (supported by the National Institutes of Health National Center for Research Resources) for providing some of the strains used in this work. We thank Jonathan Hodgkin for providing the *hda-1(e1795)* strain. We also thank Yuji Kohara for providing a *lin-52* cDNA clone. This work was supported by National Institutes of Health grant GM24663 to H.R.H. J.H.T. was a Predoctoral Fellow of the Howard Hughes Medical Institute. C.J.C and H.T.S were Koch Graduate Fellows. H.R.H. is an Investigator of the Howard Hughes Medical Institute.

LITERATURE CITED

ANDERSON, P., 1995 Mutagenesis, pp. 31-58 in *Caenorhabditis elegans*: Modern Biological Analysis of an Organism. *Methods Cell Biol.* 48, edited by H. F. EPSTEIN and D. C. SHAKES. Academic Press, New York.

AROIAN, R. V., M. KOGA, J. E. MENDEL, Y. OSHIMA, and P. W. STERNBERG, 1990 The *let-23* gene necessary for *Caenorhabditis elegans* vulval induction encodes a tyrosine kinase of the EGF receptor subfamily. Nature **348:** 693-699.

AROIAN, R. V., and P. W. STERNBERG, 1991 Multiple functions of *let-23*, a *Caenorhabditis elegans* receptor tyrosine kinase gene required for vulval induction. Genetics **128:** 251-267.

AUSTIN, J., and J. KIMBLE, 1989 Transcript analysis of *glp-1* and *lin-12*, homologous genes required for cell interactions during development of *C. elegans*. Cell **58:** 565-571.

BEITEL, G. J., S. G. CLARK, and H. R. HORVITZ, 1990 *Caenorhabditis elegans ras* gene *let-60* acts as a switch in the pathway of vulval induction. Nature **348:** 503-509.

BEITEL, G. J., E. J. LAMBIE, and H. R. HORVITZ, 2000 The *C. elegans* gene *lin-9*, which acts in an Rb-related pathway, is required for gonadal sheath cell development and encodes a novel protein. Gene **254:** 253-263.

BELFIORE, M., L. D. MATHIES, P. PUGNALE, G. MOULDER, R. BARSTEAD, J. KIMBLE and A. PUOTI, 2002 The MEP-1 zinc-finger protein acts with MOG DEAH box proteins to control gene expression via the *fem-3* 3' untranslated region in *Caenorhabditis elegans*. RNA **8:** 725-739.

BOXEM, M., and S. VAN DEN HEUVEL, 2001 *lin-35* Rb and *cki-1* Cip/Kip cooperate in developmental regulation of G1 progression in *C. elegans*. Development **128:** 4349-4359.

BOXEM, M., and S. VAN DEN HEUVEL, 2002 *C. elegans* class B synthetic multivulva genes act in G1 regulation. Curr. Biol. **12:** 906-911.

BRENNER, S., 1974 The genetics of *Caenorhabditis elegans*. Genetics **77:** 71-94.

CEOL, C. J., and H. R. HORVITZ, 2001 *dpl-1* DP and *efl-1* E2F act with *lin-35* Rb to antagonize Ras signaling in *C. elegans* vulval development. Mol. Cell **7:** 461-473.

CHEN, Z., and M. HAN, 2001 *C. elegans* Rb, NuRD, and Ras regulate *lin-39*-mediated cell fusion during vulval cell fate specification. Curr. Biol. **11:** 1874-1879.

CLARK, S. G., 1992 Intercellular Signaling and Homeotic Genes Required during Vulval Development in *C. elegans*. Ph. D. Thesis, Massachusetts Institute of Technology.

CLARK, S. G., X. LU, and H.R. HORVITZ, 1994 The *Caenorhabditis elegans* locus *lin-15*, a negative regulator of a tryrosine kinase signaling pathway, encodes two different proteins. Genetics **137:** 987-997.

CLARK, S. G., M. J. STERN, and H. R. HORVITZ, 1992 *Caenorhabditis elegans* cell-signalling gene *sem-5* encodes a protein with SH2 and SH3 domains. Nature **356:** 340-344.

COUTEAU, F., F. GUERRY, F. MÜLLER, and F. PALLADINO, 2002 A heterochromatin protein 1 homologue in *Caenorhabditis elegans* acts in germline and vulval development. EMBO Rep. **3:** 235-241.

DUFOURCQ, P., M. VICTOR, F. GAY, D. CALVO, J. HODGKIN, and Y. SHI, 2002 Functional requirement for Histone Deacetylase 1 in *Caenorhabditis elegans* gonadogenesis. Mol. Cell. Biol. **22:** 3024-3034.

DESAI, C., G. GARRIGA, S. L. MCINTIRE, and H. R. HORVITZ, 1988 A genetic pathway for the development of the *Caenorhabditis elegans* HSN motor neurons. Nature **336:** 638-646.

ELLIS, R., D. M. JACOBSON, and H. R. HORVITZ, 1991 Genes required for the engulfment of cell corpses during programmed cell death in *Caenorhabditis elegans*. Genetics **129:** 79-94.

FERGUSON, E. L., and H. R. HORVITZ, 1985 Identification and genetic characterization of 22 genes that affect the vulval cell lineages of the nematode *Caenorhabditis elegans*. Genetics **110:** 17-72.

FERGUSON, E. L., and H. R. HORVITZ, 1989 The Multivulva phenotype of certain *Caenorhabditis elegans* mutants results from defects in two functionally redundant pathways. Genetics **123:** 109-121.

FERGUSON, E. L., P. W. STERNBERG, and H. R. HORVITZ, 1987 A genetic pathway for the specification of the vulval cell lineages of *Caenorhabditis elegans*. Nature **326:** 259-267.

FIRE, A., S. XU, M. K. MONTGOMERY, S. A. KOSTAS, S. E. DRIVER and C. C. MELLO, 1998. Potent and specific genetic interference by double-stranded RNA in *Caenorhabditis elegans*. Nature **391:** 806-811.

GHYSEN, A., and C. DAMBLY-CHAUDIERE, 1988 From DNA to form: the *achaete-scute* complex. Genes Dev. **2:** 495-501.

GRAHAM, P. L., and J. KIMBLE, 1993 The *mog-1* gene is required for the switch from spermatogenesis to oogenesis in *Caenorhabditis elegans*. Genetics **133:** 919-931.

GREENWALD, I. S., and H. R. HORVITZ, 1980 *unc-93(e1500)*: a behavioral mutant of *Caenorhabditis elegans* that defines a gene with a wild-type null phenotype. Genetics **96:** 147-164.

HAN, M., A. GOLDEN, Y. HAN, and P. W. STERNBERG, 1993 *C. elegans lin-45 raf* gene participates in *let-60 ras*-stimulated vulval differentiation. Nature **363:** 133-140.

HAN, M., and P. W. STERNBERG, 1990 *let-60*, a gene that specifies cell fates during *C. elegans* vulval induction, encodes a ras protein. Cell **63:** 921-931.

HEDGECOCK, E. M., and R. K. HERMAN, 1995 The *ncl-1* gene and genetic mosaics of *Caenorhabditis elegans*. Genetics **141:** 989-1006.

HENGARTNER, M. O., R. E. ELLIS and H. R. HORVITZ, 1992 *Caenorhabditis elegans* gene *ced-9* protects cells from programmed cell death. Nature **356:** 494-9.

HERMAN, R. K., 1978 Crossover suppressors and balanced recessive lethals in *Caenorhabditis elegans*. Genetics **88:** 49-65.

HERMAN, R. K., and E. M. HEDGECOCK, 1990 Limitation of the size of the vulval primordium of *Caenorhabditis elegans* by *lin-15* expression in the surrounding hypodermis. Nature **348:** 169-171.

HILL, R. J., and P. W. STERNBERG, 1992 The gene *lin-3* encodes an inductive signal for vulval development in *C. elegans*. Nature **358:** 470-476.

HODGKIN, J., M. EDGLEY, D. L. RIDDLE, and D. G. ALBERTSON, 1988 Appendix 4: Genetics, pp. 491-584 in The Nematode *Caenorhabditis elegans*, edited by W. B. WOOD and the Community of *C. elegans* Researchers. Cold Spring Harbor Press, Cold Spring Harbor, New York.

HORVITZ, H. R., S. BRENNER, J. HODGKIN, and R. K. HERMAN, 1979 A uniform genetic nomenclature for the nematode *Caenorhabditis elegans*. Mol. Gen. Genet. **175:** 129-133.

HORVITZ, H. R., and P. W. STERNBERG, 1991 Multiple intercellular signalling systems control the development of the *Caenorhabditis elegans* vulva. Nature **351:** 535-541.

HORVITZ, H. R., and J. E. SULSTON, 1980 Isolation and genetic characterization of cell-lineage mutants of the nematode *Caenorhabditis elegans*. Genetics **96:** 435-454.

HSIEH, J., J. LIU, S. A. KOSTAS, C. CHANG, C, P. W. STERNBERG, and A. FIRE, 1999 The RING finger/B-Box factor TAM-1 and a retinoblastoma-like protein

LIN-35 modulate context-dependent gene silencing in *Caenorhabditis elegans*. Genes Dev. **13:** 2958-2970.

HUANG, L. S., P. TZOU, and P. W. STERNBERG, 1994 The *Caenorhabditis elegans lin-15* locus encodes two negative regulators of vulval development. Mol. Biol. Cell **5:** 395-412.

HUFFAKER, T. C., M. A. HOYT, and D. BOTSTEIN, 1987 Genetic analysis of the yeast cytoskeleton. Ann. Rev. Genet. **21:** 259-284.

KAISER, C. A., and R. SCHEKMAN, 1980 Distinct sets of *SEC* genes govern transport vesicle formation and fusion early in the secretory pathway. Cell **61:** 723-733.

KIMBLE, J., 1981 Alterations in cell lineage following laser ablation of cells in the somatic gonad of *Caenorhabditis elegans*. Dev. Biol. **87:** 286-300.

KORNFELD, K., 1997 Vulval development in *Caenorhabditis elegans*. Trends Genet. **13:** 55-61.

KORNFELD, K., K-L. GUAN, and H. R. HORVITZ, 1995a The *Caenorhabditis elegans* gene *mek-2* is required for vulval induction and encodes a protein similar to the protein kinase MEK. Genes Dev. **9:** 756-768.

KORNFELD, K., D. B. HOM, and H. R. HORVITZ, 1995b The *ksr-1* gene encodes a novel protein kinase involved in Ras-mediated signaling in *C. elegans*. Cell **83:** 903-913.

LACKNER, M. R., K. KORNFELD, L. M. MILLER, H. R. HORVITZ, and S. K. KIM, 1994 A MAP kinase homologue, *mpk-1*, is involved in ras-mediated induction of vulval cell fates in *Caenorhabditis elegans*. Genes Dev. **8:** 160-173.

LAMBIE, E., and J. KIMBLE, 1991 Two homologous regulatory genes, *lin-12* and *glp-1*, have overlapping functions. Development **112:** 231-240.

LUNDQUIST, E. A., P. W. REDDIEN, E. HARTWIEG, H. R. HORVITZ, and C. I. BARGMANN, 2001 Three *C. elegans* Rac proteins and several alternative Rac

regulators control axon guidance, cell migration and apoptotic cell phagocytosis. Development **128:** 4475-4488.

LU, X., 1999 Molecular analyses of the class B synthetic multivulva genes of *Caenorhabditis elegans*. Ph.D. Thesis, Massachusetts Institute of Technology, USA.

LU, X., and H. R. HORVITZ, 1998 *lin-35* and *lin-53*, two genes that antagonize a *C. elegans* Ras pathway, encode proteins similar to Rb and its binding protein RbAp48. Cell **95:** 981-991.

MELÉNDEZ, A., and I. GREENWALD, 2000 *Caenorhabditis elegans lin-13*, a member of the LIN-35 Rb class of genes involved in vulval development, encodes a protein with zinc fingers and an LXCXE motif. Genetics **155:** 1127-1137.

MELLO, C. C., J. M. KRAMER, D. STINCHCOMB and V. AMBROS, 1991 Efficient gene transfer in *C. elegans*: extrachromosomal maintenance and integration of transforming sequences. EMBO J. **10:** 3959-70.

PAGE, B. D., S. GUEDES, D. WARING, and J. R. PRIESS, 2001 The *C. elegans* E2F- and DP-related proteins are required for embryonic asymmetry and negatively regulate Ras/MAPK signaling. Mol. Cell **7:** 451-460.

PLENEFISCH, J. D., L. DELONG, and B. J. MEYER, 1989 Genes that implement the hermaphrodite mode of dosage compensation in *Caenorhabditis elegans*. Genetics **121:** 57-76.

ROSENBLUTH, R. E., and D. L. BAILLIE, 1981 The genetic analysis of a reciprocal translocation, *eT1(III; V)*, in *Caenorhabditis elegans*. Genetics **99:** 415-28.

SAMBROOK, J., E. F. FRITSCH, and T. MANIATIS, 1989 Molecular Cloning: A Laboratory Manual. Cold Spring Harbor Press, Cold Spring Harbor, New York.

SIGURDSON, D. C., G. J. SPANIER, and R. K. HERMAN, 1984 *Caenorhabditis elegans* deficiency mapping. Genetics **108:** 331-345.

STERNBERG, P. W., and M. HAN, 1998 Genetics of RAS signaling in *C. elegans*. Trends Genet. **14:** 466-472.

STERNBERG, P. W., and H. R. HORVITZ, 1986 Pattern formation during vulval development in *C. elegans*. Cell **44:** 761-772.

STERNBERG, P. W., and H. R. HORVITZ, 1989 The combined action of two intercellular signalling pathways specifies three cell fates during vulval induction in *C. elegans*. Cell **58:** 679-693.

SULSTON, J., and J. HODGKIN, 1988 Methods, pp. 587-606 in *The Nematode* Caenorhabditis elegans, edited by W. B. WOOD and the Community of *C. elegans* Researchers. Cold Spring Harbor Press, Cold Spring Harbor, New York.

SULSTON, J. E., and H. R. HORVITZ, 1977 Postembryonic cell lineages of the nematode *Caenorhabditis elegans*. Dev. Biol. **56:** 110-156.

SULSTON, J. E., and H. R. HORVITZ, 1981 Abnormal cell lineages in mutants of the nematode *Caenorhabditis elegans*. Dev. Biol. **82:** 41-55.

SULSTON, J. E., and J. G. WHITE, 1980 Regulation and cell autonomy during postembryonic development of *Caenorhabditis elegans*. Dev. Biol. **78:** 577-597.

THOMAS, J. H., and H. R. HORVITZ, 1999 The *C. elegans* gene *lin-36* acts cell autonomously in the *lin-35 Rb* pathway. Development **126:** 3449-3459.

THOMAS, J. H., M. J. STERN, and H. R. HORVITZ, 1990 Cell interactions coordinate the development of the *Caenorhabditis elegans* egg-laying system. Cell **62:** 1041-1052.

TRENT, C., N. TSUNG, and H. R. HORVITZ, 1983 Egg-laying defective mutants of the nematode *Caenorhabditis elegans*. Genetics **104:** 619-647.

UNHAVAITHAYA, Y., T. H. SHIN, N. MILIARAS, J. LEE, T. OYAMA and C. C. MELLO, 2002 MEP-1 and a Homolog of the NURD complex componenet Mi-2 act together to maintain germline-soma distinction in *C. elegans*. Cell **111:** 991-1002.

VON ZELEWSKY, T., F. PALLADINO, K. BRUNSCHWIG, H. TOBLER, A. HAJNAL, and F. MÜLLER, 2000 The *C. elegans* Mi-2 chromatin-remodelling proteins function in vulval cell fate determination. Development **127:** 5277-5284.

WATERSTON, R. H., J. N. THOMSON, and S. BRENNER, 1980 Mutants with altered muscle structure in *Caenorhabditis elegans*. Dev. Biol. **77:** 271-301.

WHITE-COOPER, H., D. LEROY, A. MACQUEEN, and M. T. FULLER, 2000 Transcription of meiotic cell cycle and terminal differentiation genes depends on a conserved chromatin associated protein, whose nuclear localization is reulated. Development **127:** 5463-5473.

WILLIAMS, B. D., B. SCHRANK, C. HUYNH, R. SHOWNKEEN and R. H. WATERSTON, 1992 A genetic mapping system in *Caenorhabditis elegans* based on polymorphic sequence-tagged sites. Genetics **131:** 609-24.

WU, Y., and M. HAN, 1994 Suppressors of activated Let-60 Ras protein defines a role of *Caenorhabditis elegans* Sur-1 MAP kinase in vulval differentiation. Genes Dev. **8:** 147-159.

WU, Y., M. HAN, and K-L. GUAN, 1995 MEK-2, a *Caenorhabditis elegans* MAP kinase kinase, functions in Ras-mediated vulval induction and other developmental events. Genes Dev. **9:** 742-758.

ZORIO, D. A., N. N. CHENG, T. BLUMENTHAL and J. SPIETH, 1994 Operons as a common form of chromosomal organization in *C. elegans*. Nature **372:** 270-2.

TABLE 1

Origins, chromosomal linkages and phenotypes of new synthetic Multivulva strains

	Penetrance of Muv phenotype		Strain Growth		
Genotype	15˚	20˚	15˚	20˚	25˚
lin-8(n111) II; lin-13(n2238) III	65% (n=391)	100% (n=74)	Very slow	Slow	Inviable
lin-8(n111) II; lin-15(n2230) X	20% (n=254)	93% (n=376)	Slow	WT	Slow
lin-8(n111) II; lin-15(n2233) X	100% (n=235)	100% (n=385)	Slow	WT	Slow
lin-8(n111) II; lin-15(n2241) X	100% (n=130)	100% (n=238)	Slow	WT	Inviable
lin-8(n111) II; lin-15(n2244) X	91% (n=128)	99.6% (n=280)	WT	WT	Slow
lin-8(n111) II; lin-15(n2245) X	6% (n=202)	98% (n=306)	WT	WT	WT
lin-35(n2232) I; lin-8(n111) II	100% (n=200)	99.9% (n=942)	Inviable	WT	Inviable
lin-35(n2236) I; lin-8(n111) II	99% (n=96)	100% (n=97)	Inviable	Slow	Inviable
lin-35(n2239) I; lin-8(n111) II	100% (n=197)	100% (n=290)	Inviable	WT	Slow
lin-35(n2242) I; lin-8(n111) II	N.D.	100% (n=278)	Inviable	Slow	Very slow
lin-8(n111) II; lin-36(n2235) III	13% (n=279)	79% (n=313)	WT	WT	WT
lin-8(n111) II; lin-36(n2240) III	7% (n=189)	79% (n=373)	WT	WT	WT
lin-8(n111) II; lin-36(n2243) III	51% (n=115)	94% (n=593)	WT	WT	WT
lin-8(n111) II; lin-37(n2234) III	96% (n=192)	100% (n=278)	WT	WT	Inviable
lin-8(n111) II; lin-54(n2231) IV	39% (n=334)	99% (n=164)	Very slow	WT	Slow
lin-13(n2981) III; lin-15(n433) X	0% (n=237)	84% (n=241)	WT	WT	Inviable
lin-13(n2984) III; lin-15(n433) X	1% (n=217)	97% (n=239)	WT	WT	Inviable
lin-13(n2985) III; lin-15(n433) X	2% (n=229)	94% (n=213)	WT	WT	Slow
lin-13(n2988) III; lin-15(n433) X	33% (n=247)	97% (n=261)	Slow	Slow	Inviable
lin-15(n2980 n433) X[a]	2% (n=209)	99% (n=252)	WT	WT	Slow
lin-15(n2983 n433) X[a]	2% (n=232)	99% (n=227)	WT	WT	Slow
lin-15(n2987 n433) X[a]	0% (n=207)	91% (n=267)	WT	WT	WT
lin-15(n2989 n433) X[a]	0% (n=238)	100% (n=235)	WT	WT	WT
lin-15(n2991 n433) X[a]	2% (n=226)	100% (n=216)	WT	WT	WT
lin-15(n2993 n433) X[a]	0% (n=205)	79% (n=201)	WT	WT	WT
lin-35(n2977) I; lin-15(n433) X	8% (n=257)	100% (n=234)	Slow	WT	Slow
lin-35(n2996) I; lin-15(n433) X	18% (n=216)	100% (n=202)	Slow	Slow	Slow
lin-53(n2978) I; lin-15(n433) X	0% (n=211)	59% (n=203)	WT	WT	WT
lin-54(n2990) IV; lin-15(n433) X	4% (n=199)	95% (n=216)	WT	WT	Slow
dpl-1(n2994) II; lin-15(n433) X	4% (n=246)	78% (n=234)	WT	WT	Slow

lin-52(n3718) III; lin-15(n767) X	100% (n=41)	100% (n=82)	_b	_b	_b
lin-8(n2376) II; lin-36(n766) III	18% (n=382)	96% (n=189)	WT	WT	WT
lin-8(n2378) II; lin-36(n766) III	19% (n=456)	100% (n=125)	WT	WT	WT
lin-8(n2403) II; lin-36(n766) III	48% (n=402)	99% (n=549)	WT	WT	WT
lin-36(n766) III; lin-15(n2375) X	0% (n=544)	82% (n=675)	WT	WT	Slow
lin-38(n2402) II; lin-36(n766) III	28% (n=643)	99.7% (n=667)	WT	WT	WT
lin-8(n2724) II; lin-15(n744) X	100% (n=211)	100% (n=126)	Slow	Slow	Slow
lin-8(n2731) II; lin-15(n744) X	100% (n=217)	100% (n=167)	Slow	Slow	Slow
lin-8(n2738) II; lin-15(n744) X	100% (n=128)	100% (n=140)	Slow	Slow	Very slow
lin-8(n2739) II; lin-15(n744) X	100% (n=158)	100% (n=97)	Slow	Slow	Slow
lin-8(n2741) II; lin-15(n744) X	100% (n=157)	100% (n=155)	WT	Slow	Slow
lin-15(n744 n2725) X[a]	100% (n=152)	100% (n=177)	Slow	Slow	Very slow
lin-15(n744 n2726) X[a]	100% (n=141)	100% (n=145)	Slow	Slow	Very slow
lin-15(n744 n2733) X[a]	100% (n=193)	100% (n=140)	Slow	Slow	Inviable
lin-15(n744 n2734) X[a]	100% (n=124)	100% (n=159)	Slow	Slow	Slow
lin-15(n744 n2735) X[a]	100% (n=132)	100% (n=176)	Slow	Slow	Very slow
lin-15(n744 n2737) X[a]	99% (n=199)	100% (n=121)	Slow	Slow	Inviable
lin-15(n744 n2742) X[a]	100% (n=121)	100% (n=173)	Slow	Slow	Very slow
lin-38(n2727) II; lin-15(n744) X	100% (n=201)	100% (n=165)	Slow	Slow	Slow
lin-56(n2728) II; lin-15(n744) X	100% (n=214)	100% (n=163)	Slow	Slow	Slow

New synMuv mutations were mapped to linkage groups using strains carrying the markers *bli-3 I*; *dpy-5 I*; *unc-54 I*; *unc-85 II*; *bli-2 II*; *mnC1 dpy-10 unc-52 II*; *unc-52 II*; *dpy-1 III*; *unc-32 III*; *unc-25 III*; *dpy-9 IV*; *egl-18 IV*; *unc-5 IV*; *dpy-4 IV*; *unc-34 V*; *dpy-11 V*; *unc-51 V*; *lon-2 X* and *unc-3 X*. in a manner similar to that described previously (TRENT *et al.* 1983; FERGUSON and HORVITZ 1989).

The penetrance of the Muv phenotype of each synMuv strain was determined at 15° and 20° after growth at the indicated temperature for two or more generations. Several strains displayed a temperature-dependent reduction in viability. This reduction in viability was tested in an assay similar to that of FERGUSON and HORVITZ (1989)

but differing in that exactly 10 eggs laid by hermaphrodites of the indicated genotype grown at 20° were placed on each of the four assay plates (each with a 2 cm diameter lawn of bacteria) used at each temperature. The plates were checked daily to determine when the bacterial lawn was consumed. The data are presented according to the following criteria; at 15°, WT, 8.5-14 days; Slow, 14-24 days; Very slow, 24-28 days; Inviable, lethal or more than 28 days. At 20°, WT, 5.5-9 days; Slow, 9-17 days; Very slow, 17-28 days; Inviable, lethal or more than 28 days. At 25°, WT, 5-7.5 days; Slow, 7.5-15 days; Very slow, 15-28 days; Inviable, lethal or more than 28 days. The last value of the range described was included in that category. The data obtained from the wild-type (WT) strain N2 was: 15°: 10 days, 20°: 6 days, 25°: 5 days. N. D., not determined because the strain was lethal at the listed temperature.

[a] The mutations in these strains displayed linkage only to *unc-3 X*. Linkage of the new mutation to *unc-3 X* is assumed since the mutations in these strains segregated as single locus Muv mutations and failed to complement *lin-15(n765) X*.

[b] As the *lin-52(n3718)* mutation causes recessive sterility, the growth rate of *lin-52(n3718)* mutants derived from *lin-52(n3718)* homozygous parents could not be measured.

TABLE 2

Sequences of *lin-13* class B mutations

Allele	Wild-type sequence	Mutant sequence	Substitution
n770	CAG	TAG	Q1988amber
n2238	CAA	TAA	Q996ochre
n2981	TGC	TAC	C814Y
n2984	GGA	GAA	G360E
n2985	CAA	TAA	Q1717ochre
n2988	TGT	TAT	C361Y

Wild-type and mutant codons are shown with the mutated nucleotide underlined. All mutations were GC-to-AT transitions as expected for EMS-induced mutations (ANDERSON 1995). Amino acid substitutions are shown as wild-type residue identity, residue number, and predicted mutant residue.

TABLE 3

Three- and four-factor crosses

Gene	Genotype of heterozygote	Phenotype of selected recombinants	Genotype of selected recombinants (with respect to unselected markers)
lin-13			
	lin-13 unc-32+ +/+ + unc-49 dpy-18; lin-15(n767)	Unc-32	0/2 *unc-49 dpy-18/+ +*
		Dpy	7/7 *lin-13 unc-32/+ +*
		Unc-49	0/1 *lin-13 unc-32/+ +*
	+ + lin-13/unc-93 dpy-27 +; lin-15(n767)	Unc	30/30 *lin-13/+*
	+ + lin-13/unc-93 dpy-17 +; lin-15(n767)	Unc	8/8 *lin-13/+*
		Dpy	0/3 *lin-13/+*
	+ lin-13 +/dpy-17 + unc-32; lin-15(n767)	Dpy	1/8 *lin-13/+*
		Unc	5/10 *lin-13/+*
lin-52			
	+ + unc-32 lin-52/lon-1 sma-3 + +; lin-15(n767)	Lon	1/1 *lin-52 unc-32/ + +*
		Sma	0/4 *lin-52/+*
		Muv	7/7 *lon-1/+*
	+ + lin-52/sma-3 unc-32; lin-15(n767)	Sma	3/3 *lin-52/+*
		Unc	0/13 *lin-52/+*
	+ lin-52 +/dpy-19 + unc-69; lin-15(n767)	Dpy	17/31 *lin-52/+*
		Unc	2/11 *lin-52/+*
	+ lin-52 +/unc-16 + unc-49; lin-15(n767)	Unc-16	0/2 *lin-52/+*
		Unc-49	13/16 *lin-52/+*
	+ lin-52 + / unc-16 + unc-47; lin-15(n767)	Unc-47	7/9 *lin-52 / +*
	lin-52 + unc-69 / + stP127 +; lin-15(n767)	Muv	3/12 *stP127 / +*
	sma-3 + lin-52 + / + sqv-3 + unc-69; lin-15(n767)	Sma	9/9 *sqv-3 / +*
		Muv	1/27 *sqv-3 / +*
		Unc	14/16 *lin-52 / +*
lin-53			
	dpy-5 lin-53 + +/+ + lin-11 unc-75; lin-15(n767)	Dpy	7/7 *lin-11 unc-75/+ +*
		Muv	0/12 *lin-11 unc-75/+ +*
		Vul	0/10 *dpy-5 lin-53/+ +*
		Unc	8/8 *dpy-5 lin-53/+ +*
	+ lin-53 +/unc-29 + lin-11; lin-15(n767)	Unc	1/3 *lin-53/+*
		Vul	11/19 *lin-53/+*

lin-54			
	lin-8; + + lin-54/unc-22 unc-30 +	Unc-22	19/19 *lin-54/+*
		Unc-30	0/15 *lin-54/+*
	lin-8; + lin-54 +/unc-30 + dpy-4	Unc	2/11 *lin-54/+*
		Dpy	21/22 *lin-54/+*
	lin-54 + +/+ lev-1 unc-26; lin-15(n433)	Lev	0/25 *lin-54/+*
dpl-1			
	+ dpl-1 +/dpy-10 + unc-53; lin-15(n433)	Dpy	6/9 *dpl-1/+*
		Unc	6/11 *dpl-1/+*
	+ dpl-1 +/rol-6 + unc-4; lin-15(n433)	Rol	6/14 *dpl-1/+*
		Unc	9/14 *dpl-1/+*
	dpl-1 + +/+ let-240 unc-4; lin-15(n433)	Unc	25/25 *dpl-1/+*
lin-56			
	+ + lin-56/unc-85 dpy-10 +; lin-15(n744)	Unc	4/4 *lin-56/+*
		Dpy	0/6 *lin-56/+*
	+ lin-56 +/dpy-10 + unc-53; lin-15(n744)	Dpy	5/10 *lin-56/+*
		Unc	6/11 *lin-56/+*
	+ + lin-56/rol-6 unc-4 +; lin-15(n744)	Rol	16/16 *lin-56/+*
		Unc	0/9 *lin-56/+*

Deficiency heterozygotes

Gene	Genotype of heterozygote	Phenotype of heterozygote
dpl-1		
	dpy-10 dpl-1(n2994) +/+ mnDf46 unc-4; lin-15(n433)	wild-type
	dpy-10 dpl-1(n2994) +/+ mnDf85 unc-4; lin-15(n433)	wild-type
	dpy-10 dpl-1(n2994) +/+ mnDf67 unc-4; lin-15(n433)	Muv
lin-52		
	unc-36 lin-52 +/+ nDf40 dpy-18; lin-15(n767)	Muv

Three and four-factor crosses were performed as described previously (BRENNER 1974; FERGUSON and HORVITZ 1989). Deficiency heterozygotes were constructed, and the vulval phenotype was scored. The presence of the deficiency was confirmed in each animal based upon the segregation of 1/4 dead eggs or larvae.

TABLE 4

Phenotypes of single and double mutants

			Double mutant with Class A		Double mutant with Class B	
	New Mutation	Single mutant	*lin-8(n111)*	*lin-15(n767)*	*lin-36(n766)*	*lin-15(n744)*
Class A						
	lin-56(n2728)	WT	WT	WT	Muv	Muv
Class B						
	lin-13(n770)	WT	Muv	Muv	WT	WT
	lin-52(n771)	WT	Muv	Muv	WT	WT
	lin-53(n833)	WT	Muv	Muv	WT	WT
	lin-54(n2231)	WT	Muv	Muv	WT	WT
	dpl-1(n2994)	WT	Muv	Muv	WT	WT

Mutations in new genes were separated from the original mutation present in the synMuv strain as described in MATERIALS AND METHODS. Double mutants carrying mutations in these new genes and mutations in previously known class A or class B genes were constructed as described in MATERIALS AND METHODS. WT, animals had wild-type vulval morphology as observed using a dissecting microscope, *i.e.* 0% Muv ($n > 500$). Muv, animals had a Muv phenotype of greater than 50% penetrance ($n \geq 100$). *lin-13*, *lin-52* and *lin-54* animals displayed a weaker Muv phenotype in double mutants with *lin-8(n111)* than with *lin-15(n767)*. *dpl-1* animals displayed a weaker Muv phenotype in a *lin-15(n433)* background than in a *lin-15(n767)* background.

TABLE 5

Maternal rescue of synMuv phenotype

Class A mutation	Class B mutation	Penetrance of the Muv phenotype in animals of *a/a; b/b* genotype descended from animals of maternal genotype			
		a/+; b/+	*a/+; b/b*	*a/a; b/+*	*a/a; b/b*[b]
lin-8(n111)	*lin-9(n112)*	72% (n=57)[a]	83% (n=141)[a]	100% (n=183)	100% (n=165)
lin-8(n111)	*lin-35(n745)*	45% (n=65)[a]	N. D.	97% (n=149)	100% (n=209)
lin-8(n111)	*lin-36(n766)*	14% (n=93)[a]	23% (n=216)[a]	84% (n=300)	98% (n=207)
lin-8(n111)	*lin-37(n758)*	31% (n=69)[a]	98% (n=133)[a]	85% (n=188)	100% (n=161)
lin-15(n433)	*lin-54(n2231)*	9% (n=89)[a]	N. D.	21% (n=211)	99% (n=164)
lin-15(n767)	*lin-13(n770)*	58% (n=64)[a]	97% (n=238)[a]	90% (n=220)	95% (n=230)
lin-15(n767)	*lin-52(n771)*	83% (n=98)[a]	103% (n=225)[a]	90% (n=294)	100% (n=211)
lin-15(n767)	*lin-53(n833)*	103% (n=76)[a]	N. D.	100% (n=64)	100% (n=116)
lin-15(n433)	*dpl-1(n2994)*	11% (n=95)[a]	75% (n=125)[a]	50% (n=298)	78% (n=234)
lin-38(n751)	*lin-9(n112)*	81% (n=65)[a]	100% (n=146)	99% (n=189)[a]	100% (n=165)
lin-56(n2728)	*lin-15(n744)*	93% (n=92)[a]	99% (n=200)	N. D.	100% (n=163)

The contribution of class A and class B genes to the maternal rescue of the synMuv phenotype of doubly homozygous animals descended from either singly or doubly heterozygous mothers was determined by counting the number of Muv animals of phenotype R, where R is the phenotype produced by the *cis* marker *r*. Doubly heterozygous mothers were obtained by mating N2 males with marked doubly homozygous hermaphrodites. Singly heterozygous mothers were obtained by mating males homozygous for one of the synMuv mutations with marked doubly homozygous hermaphrodites. A strain homozygous for *lin-35* was obtained by the general procedure used for the isolation of strains homozygous for single synMuv mutations. *dpy-14* was used to balance *lin-35*. The *lin-8; lin-9* strain was marked with *lon-1*. The *lin-35; lin-8* strain was marked with *unc-13*. The *lin-8; lin-36* strain was marked with *unc-32*. The *lin-8; lin-37* strain was marked with *lon-1*. The *lin-38; lin-9* strain was marked with *unc-52*. The *lin-13; lin-15(n767)* strain was marked with *unc-93* or *unc-32*. The *lin-52;*

lin-15(n767) strain was marked with *sma-3*. The *lin-53; lin-15(n767)* strain was marked with *dpy-5* or *lin-11*. The *lin-54; lin-15(n433)* strain was marked with *dpy-20*. The *dpl-1; lin-15(n433)* strain was marked with *rol-6*. The *lin-56; lin-15(n744)* strain was marked with *rol-6*.

[a]These data were obtained by estimating the penetrance and by assuming that the number of doubly homozygous animals were 1/4 of the R progeny.

[b]These data are from Table 1 of FERGUSON and HORVITZ (1989).

TABLE 6

SynMuv genes and alleles

	Gene	No. of alleles	Mutant alleles	Probable null phenotype (evidence)
Class A				
	lin-8	9	*n111*, *n2376*, *n2378*, *n2403*, *n2724*, *n2731*, *n2738*, *n2739*, *n2741*	SynMuv[a] (no. alleles)
	*lin-15*A	13	*n433*, *n749*, *n767*, *n2375*, *n2725*, *n2726*, *n2733*, *n2734*, *n2735*, *n2737*, *n2742*, *sy211*, *sy212*	SynMuv (molecular data[b], no. alleles)
	lin-38	4	*n751*, *n761*, *n2402*, *n2727*	Unknown
	lin-56	1	*n2728*	Unknown
Class B				
	lin-9	3	*n112*, *n942*, *n943*	SynMuv, sterile (molecular data[c], non-complementation screen[d])
	lin-13	8	*n770*, *n2238*, *n2981*, *n2984*, *n2985*, *n2988*, (*n387* and possibly *n388* at 15°C[d])	SynMuv, sterile, maternal-effect lethal[a] (molecular data[e])
	*lin-15*B	14	*n374*, *n743*, *n744*, *n2230*, *n2233*, *n2241*, *n2244*, *n2245*, *n2980*, *n2983*, *n2987*, *n2989*, *n2991*, *n2993*	SynMuv (molecular data[b], no. alleles)
	lin-35	8	*n373*, *n745*, *n2232*, *n2236*, *n2239*, *n2242*, *n2977*, *n2996*	SynMuv (molecular data[f], no. alleles)
	lin-36	13	*n747*, *n750*, *n766*, *n772*, *n2235*, *n2240*, *n2243*, *n3090*, *n3093*, *n3094*, *n3095*, *n3096*, *n3097*	SynMuv (molecular data[g], non-complementation screen[g])
	lin-37	2	*n758*, *n2234*	SynMuv (molecular data[h])
	lin-52	2	*n771*, *n3718*	SynMuv, sterile (molecular data[i])
	lin-53	3	*n833*, *n2978*, *n3368*[j]	SynMuv, sterile, protruding vulva (molecular data[j], *n833* and *n2978* are dominant negative[k])
	lin-54	2	*n2231*, *n2990*	Unknown
	dpl-1	4	*n2994*, *n3316*, *n3643*, *zu355*	SynMuv, sterile, maternal-effect lethal (phenotype enhanced by Df, molecular data[l], *zu355* isolated in maternal-effect lethal screen[m])
	tam-1[n]	18	*cc566*, *cc567*, *cc587*, *sy272* and 14 others	synMuv (molecular data[o], no. alleles[o], phenotype not enhanced by Df[o])
	let-418	3	*ar113*, *ar114*, *s1617*	SynMuv, sterile, maternal-effect lethal, everted vulva (molecular data[p], phenotype not enhanced by Df[p])

efl-1	3	*n3318*, *n3639*, *se1*	SynMuv, sterile, maternal-effect lethal[q](molecular data[l], *se1* isolated in maternal-effect lethal screen[m])
hda-1	1	*e1795*[r]	SynMuv, protruding vulva, gonad development abnormal and sterile (molecular data[s])
mep-1	1	*q660*	SynMuv[t,u], sterile[t,v], protruding vulva[t,v], larval lethal[v] (molecular data[t,v])

Mutant alleles not described in the text are described by HORVITZ and SULSTON (1980), FERGUSON and HORVITZ (1985, 1989), DESAI *et al.* (1988), HUANG *et al.* (1994), THOMAS and HORVITZ (1999), HSIEH *et al.* (1999), VON ZELEWSKY *et al.* (2000), CEOL and HORVITZ (2001), PAGE *et al.* (2001). Probable null phenotype is given at 20°; see Table 1. Under evidence, no. alleles indicates that a high number of mutations were isolated in the screens described in the text, consistent with the hypothesis that some of these alleles are null alleles.

[a]See FERGUSON and HORVITZ (1985) for possibly contradictory deficiency data.

[b]CLARK *et al.* (1994), HUANG *et al.* (1994).

[c]BEITEL *et al.* (2000).

[d]FERGUSON and HORVITZ (1989).

[e]MELÉNDEZ and GREENWALD (2000).

[f]LU and HORVITZ (1998).

[g]THOMAS and HORVITZ (1999).

[h]LU (1999).

[i]Text.

[j]X. LU and H. R. H. (personal communication).

[k]Text and LU and HORVITZ (1998).

[l]CEOL and HORVITZ (2001).

[m]PAGE *et al.* (2001).

[n]This gene does not act as a class B synMuv in double mutants with *lin-8*, but does with *lin-15*A and *lin-38* (HSIEH *et al.* 1999). Such an interaction had not been previously observed for the synMuv genes, but *lin-8(n111)* synMuv double mutants have occasionally been observed to be weaker than corresponding synMuv double mutants carrying other class A mutations. (THOMAS and HORVITZ 1999).

[o]HSIEH *et al.* (1999).

[p]VON ZELEWSKY *et al.* (2000).

[q]PAGE *et al.* (2001), C. J. CEOL and H. R. HORVITZ (unpublished results).

[r]*hda-1* is also known as *gon-10* (DUFOURCQ *et al.* 2002). The *hda-1(e1795)* mutation alone causes a weakly penetrant Muv phenotype (DUFOURCQ *et al.* 2002), but in combination with the class A mutation *lin-15(n767)* this phenotype is fully penetrant and displays stronger expressivity (C. J. CEOL, E. C. ANDERSEN and H. R. HORVITZ, unpublished results).

[s]DUFOURCQ *et al.* (2002).

[t](C. J. CEOL, F. STEGMEIER, M. M. HARRISON and H. R. HORVITZ, unpublished results).

[u]UNHAVAITHAYA *et al.* (2002).

[v]BELFIORE *et al.* (2002).

Figure legends

Figure 1. Partial genetic map of *C. elegans* showing the locations of newly identified or newly characterized synMuv genes and the markers that were used to position these genes on the map. New synMuv genes are shown above the line representing the linkage group; marker genes are shown below the line. Deficiencies are drawn below the line and indicate which genes are deleted.

Figure 2. Molecular cloning of *lin-52*. The top panel shows the genetic map location of *lin-52* on linkage group III. The dashed portion of *nDf40* indicates that the left endpoint of this deficiency is not precisely known but maps between *emb-30* and *sqv-3*. The middle and bottom panels show the rescuing cosmids ZK630 and C26C12 and subclones assayed for *lin-52* rescue. The restriction sites used to generate subclones are indicated. "+", a majority of transgenic lines were rescued in the first generation of establishing the line. When rescue was observed, typically greater than 70% of transgenic animals in a line were rescued in this generation. Arrows indicate the direction of transcription. Coding sequences of predicted genes are shaded. An oligonucleotide encoding an in-frame stop codon was inserted into (arrowhead) and subsequently removed from (arrowhead with "X") the ZK632.13 predicted gene.

Figure 3. *lin-52* gene structure and predicted protein sequence

(A) *lin-52* gene structure as derived from cDNA and genomic sequences. Exons (closed boxes), 5' and 3' untranslated regions (open boxes), predicted translational start and stop codons, SL2 splice leader sequence and polyA tail are indicated. Arrows indicate the locations of the *n771* and *n3718* mutations.

(B) Alignment of the predicted LIN-52, human LOC91750 and *Drosophila* CG15929 proteins. Solid boxes indicate identities and shaded boxes indicate similarities. Arrowheads indicate the positions of *lin-52* mutations.

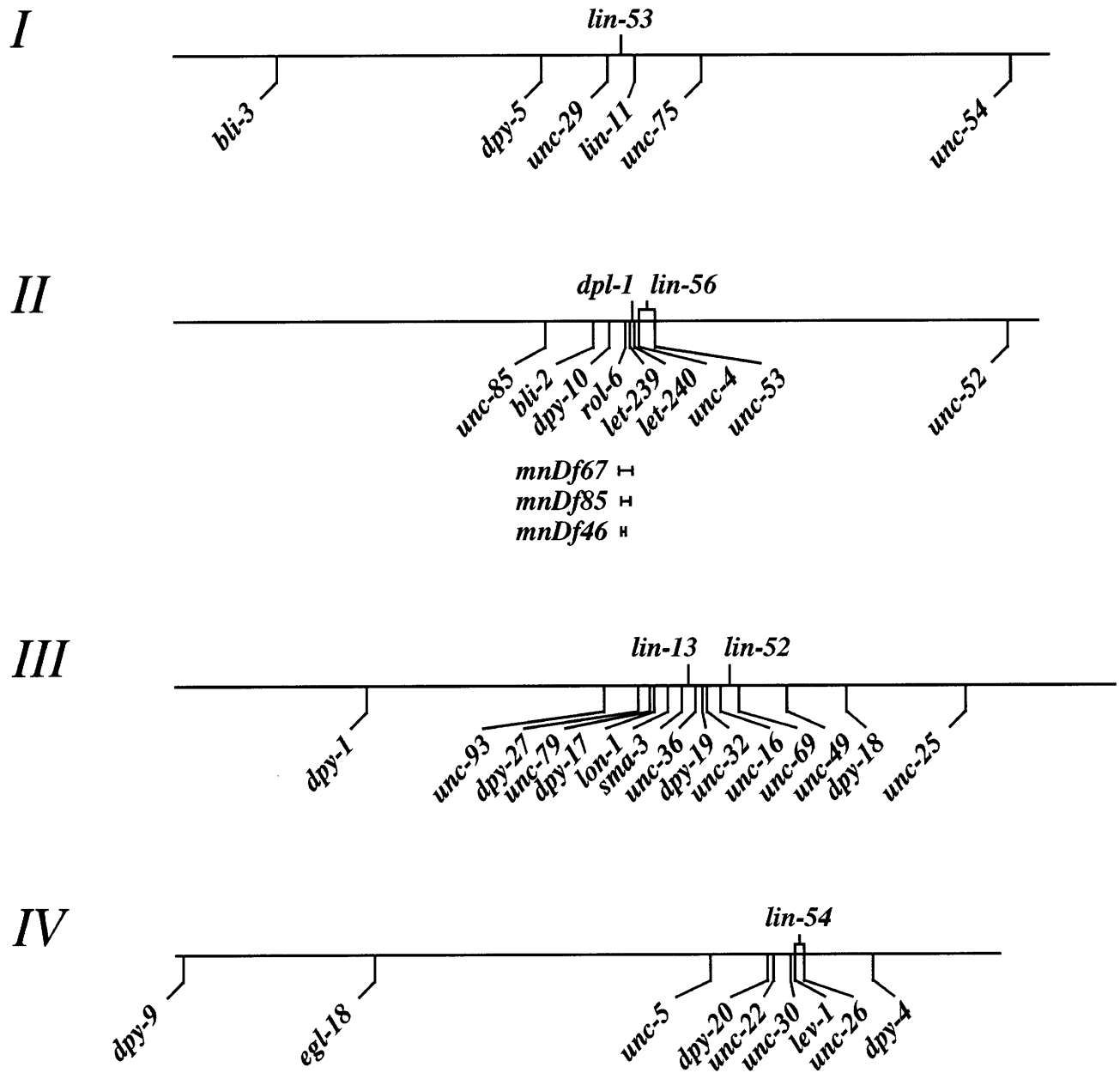
I
lin-53
bli-3
dpy-5
unc-29
lin-11
unc-75
unc-54
II
dpl-1
lin-56
unc-85
bli-2
dpy-10
rol-6
let-239
let-240
unc-4
unc-53
unc-52
mnDf67
mnDf85
mnDf46
III
lin-13
lin-52
dpy-1
unc-93
dpy-27
unc-79
dpy-17
lon-1
sma-3
unc-36
dpy-19
unc-32
unc-16
unc-69
unc-49
dpy-18
unc-25
IV
lin-54
dpy-9
egl-18
unc-5
dpy-20
unc-22
unc-30
lev-1
unc-26
dpy-4
= 10 map units

Figure 1

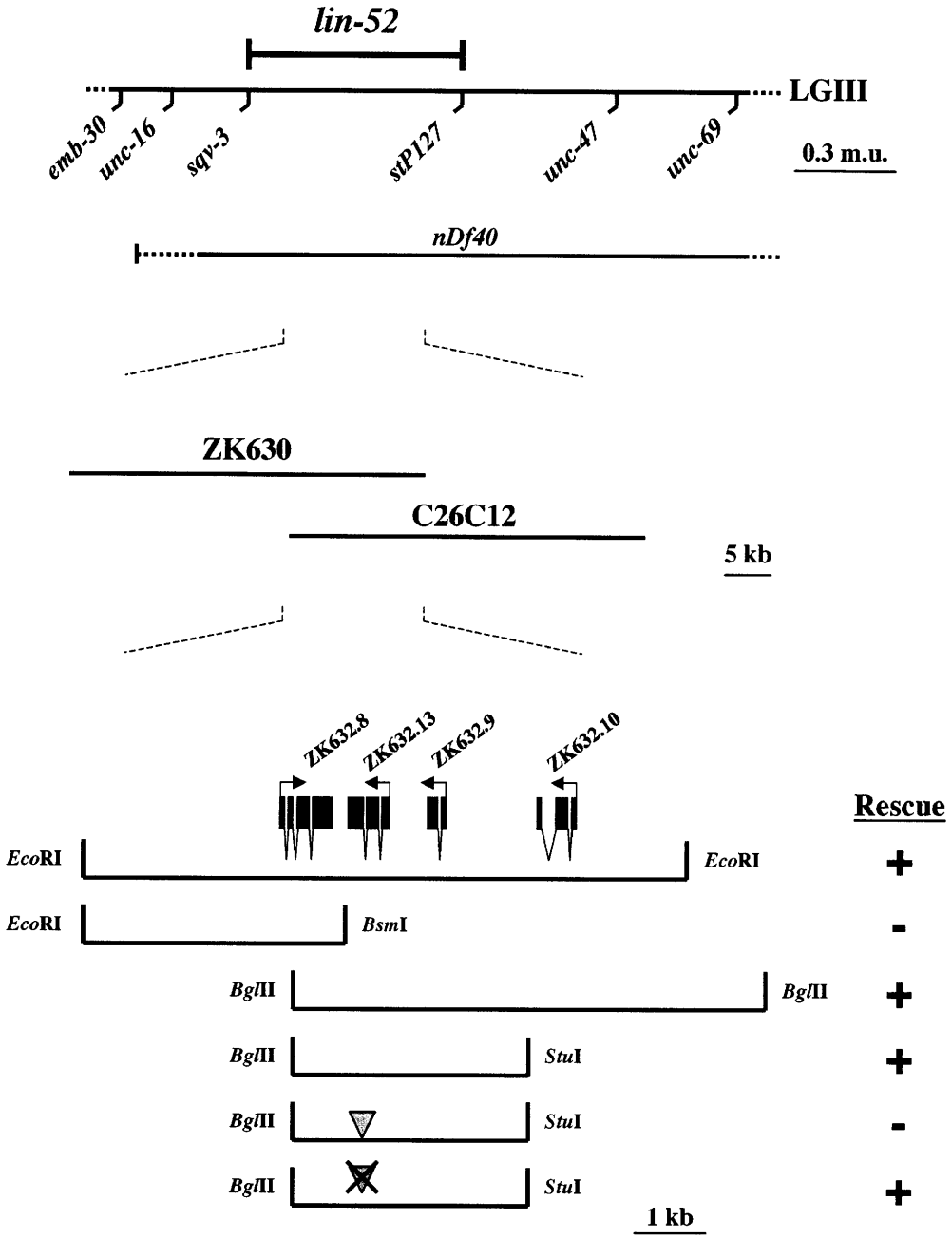
lin-52
LGIII
emb-30
unc-16
sqv-3
stP127
unc-47
unc-69
0.3 m.u.
nDf40
ZK630
C26C12
5 kb
ZK632.8
ZK632.13
ZK632.9
ZK632.10
Rescue
EcoRI
EcoRI
+
EcoRI
BsmI
-
BglII
BglII
+
BglII
StuI
+
BglII
StuI
-
BglII
StuI
+
1 kb

Figure 2

Figure 3

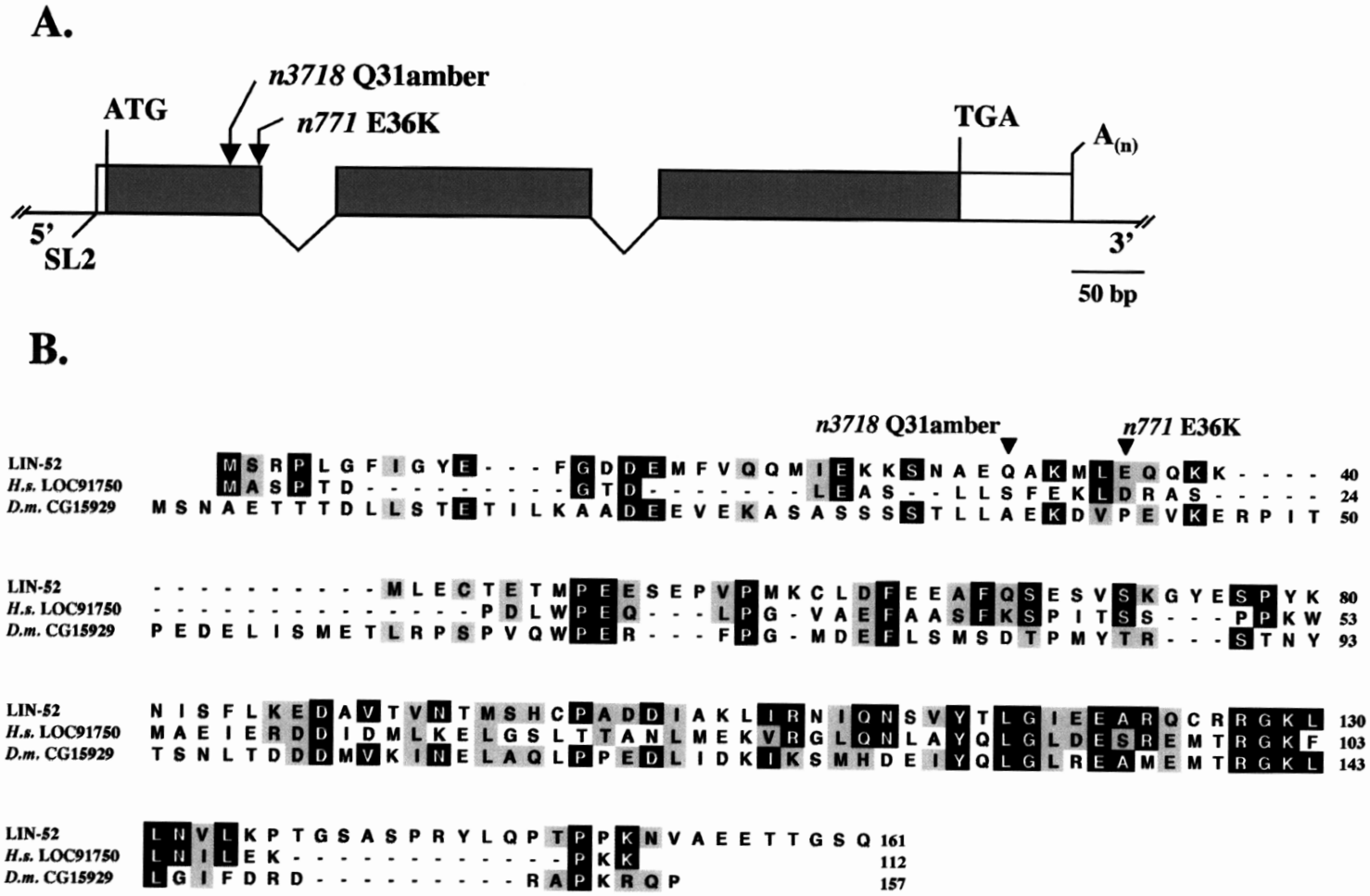
A.
n3718 Q31amber
n771 E36K
ATG
TGA
A(n)
5'
SL2
3'
50 bp
B.
n3718 Q31amber
n771 E36K
LIN-52
H.s. LOC91750
D.m. CG15929
MSNAETTTDLLSTETILKAADEEVEKASASSSSTLLAEKDVPEVKERPIT
MLECTETMPEESEPVPMKCLDFEEAFQSESVSKGYESPYK
PEDELISMETLRPSPVQWPERFPG-MDEFLSMSDTPMYTR
NISFLKEDAVTVNTMSHCPADDIAKLIRNIQNSVYTLGIEEARQCRRGKL
MAEIERDDIDMLKELGSLTTANLMEKVRGLQNLAYQLGLDESREMTRGKF
TSNLTDDDMVKINELAQLPPEDLIDKIKSMHDEIYQLGLREAMEMTRGKL
LNVLKPTGSASPRYLQPTPPKNVAEETTGSQ
LNILEK
LGIFDRD
RAPKRQP
40
24
50
80
53
93
130
103
143
161
112
157

Appendix V

Transcriptional control and patterning of adult sexual behaviors in *C. elegans*

Juan Wang[1], Hillel T. Schwartz[2], and Maureen M. Barr[1]

[1]Department of Genetics, Rutgers, The State University of New Jersey
145 Bevier Road, Piscataway, NJ 08884
[2]Department of Biology, Massachusetts Institute Of Technology
77 Massachusetts Avenue, Cambridge, MA 02139

Corresponding author: Maureen M. Barr
Phone (732) 445-1639, Fax (732) 445-1147
barr@biology.rutgers.edu

Submitted for publication to *PNAS* in July 2008.
I identified *n4132* and found that it prevented expression of a *pkd-2::gfp* reporter. All subsequent analysis was performed by Juan Wang and Maureen Barr.

Abstract

Sexual behaviors are evoked by a wide variety of sensory cues and generated by specialized sensory neurons that sense mate-derived signals. Male sexual behaviors in *C. elegans* are driven by long- and short-range chemical and contact-based signals from a potential mate. 21 "B-type" male-specific neurons control several aspects of sexual sensory behaviors. CEM neurons modulate chemotaxis to sex-pheromones, RnB ray neurons are required for response to contact with the hermaphrodite, and the HOB hook neuron is essential for vulva location. These B-type neurons share similar ciliary ultrastructure and express a unique repertoire of sensory molecules, herein referred to as the autosomal dominant polycystic kidney disease (ADPKD) gene battery. RFX transcription factors are master regulators of ciliogenesis in nematodes, *Drosophila*, zebrafish, and mammals. The molecular mechanisms that program B-type ciliated sensory neurons for sexually dimorphic functions or any specialized ciliated cell type are not well understood. Here we identify a mutation in the *daf-19* RFX transcription factor that destroys ADPKD gene battery expression and male mating functions of B-type neurons without affecting expression of ciliogenic genes or cilia formation. The *daf-19(n4132)* allele specifically disrupts *daf-19m* (for function in mating behavior), an isoform expressed solely in B-type neurons and regulated by distinct promoter and enhancer elements. Hence a single gene acts as a master regulator of both cilia development and adult male sexual behaviors.

Introduction

Sexual behaviors are genetically programmed. Human courtship, mate selection, and reproductive behaviors are presumably under polygenic controls. By contrast, animal models demonstrate that a single gene mutation may have profound consequences on sexual behaviors (reviewed by (1)). In mice, the transient receptor potential channel TRPC2 is required in males for sex discrimination and aggression and in females for maternal aggression and lactation behavior (2, 3). In *Drosophila*, the fruitless transcription factor controls sexually dimorphic behaviors via unidentified downstream target genes. In the nematode *Caenorhabditis elegans*, the TRP polycystin receptor-channel unit LOV-1 and PKD-2 directs three male sexual behaviors: chemotaxis to females of a closely related species, response to contact with a potential mate, and vulva location (4-6).

C. elegans male mating behavior involves a sequential set of sensory inputs and motor outputs. Long and short-range cues from the adult hermaphrodite attract the adult male, a behavior that requires ciliated sensory neurons (4, 7, 8). Once in close proximity to a mate, the male uses distinct sets of sensory neurons in the tail to respond, locate the vulva, insert his copulatory spicules, and transfer sperm into the uterus (9). This complex copulatory ritual is wired into a simple nervous system, comprised of 294 core and 89 male-specific neurons, thus providing a simple animal model to study the cellular, genetic, and molecular basis of sexual behaviors.

More than half of male-specific nervous system is comprised of ciliated neurons (10). Ciliogenic mutants are defective in multiple sensory behaviors, including male mating behaviors (5, 7, 8, 11, 12). A subset of 21 male-specific ciliated neurons may be

defined by their unique ultrastructural anatomy, functional properties, and gene expression profiles. Four CEM cephalic, one HOB hook, and 16 ray neurons (RnB where n= rays 1 through 9, but not ray 6) possess B-type cilia that are exposed to the environment and lie adjacent to A-type cilia embedded in the cuticle (10, 13, 14). The CEMs, HOB, and RnB neurons are implicated in chemotaxis to mates, response, and vulva location, respectively (4, 5, 8, 9). These male-specific neurons express the autosomal dominant polycystic kidney disease (ADPKD) gene homologs *lov-1* and *pkd-2*, the kinesin-like protein gene *klp-6*, and four co-expressed with polycystin (*cwp*) genes, herein called the "ADPKD gene battery" (5, 6, 15, 16). Only ray R6B does not possess an exposed cilium or express the ADPKD gene battery. Consistent with sensory function in RnB and HOB neurons, *lov-1*, *pkd-2*, and *klp-6* mutant males are response (Rsp) and location of vulva (Lov) defective.

Six IL2 core neurons possess B-type sensory cilia and express *klp-6*, yet are among the few *C. elegans* neurons with no assigned function (11). We collectively refer to IL2, CEM, HOB, and RnB (except 6) sensory cells as "B-type neurons." Although B-type neurons have several features in common, they are also individually specified via distinct lineage-driven mechanisms and also express unique repertoires of neurotransmitters and neuropeptides (17-23). This raises the question of how the shared traits of the B-type neurons are patterned and how the ADPKD gene battery is regulated to generate sexual behaviors.

Previous studies showed that a null allele of *daf-19* disrupted *pkd-2* expression (17). *daf-19* encodes an evolutionarily conserved regulatory factor X (RFX) transcription factor that regulates X-box promoter element containing genes, which are

essential for ciliogenesis in core and sex-specific neurons (25-27). Accordingly, *daf-19* null mutants fail to express many ciliogenic genes, lack all cilia, and are defective in many sensory behaviors (11, 24-27). Here, we identify a *cis*-regulatory mutation in the *daf-19* locus that produces Rsp, Lov, and ADPKD gene battery expression defects without affecting ciliogenesis. *daf-19(n4132)* disrupts *daf-19m*, a *daf-19* isoform required for male mating and that specifically acts in B-type ciliated neurons. These studies reveal how the complex genomic architecture of an RFX transcription factor enables a single gene to program cilia development in the core and sex-specific nervous system and post-developmental sensory functions of the adult male nervous system.

Results

The *n4132* mutation disrupts expression of the ADPKD genes and male sexual behaviors

To study the mechanisms by which sexually dimorphic behaviors are genetically programmed, we characterized the mutant *n4132*, which was isolated based on the loss of P*pkd-2*::GFP expression in male-specific CEM head neurons. We find that *n4132* is also required for expression of the ADPKD gene battery in head and tail neurons. *n4132* mutant males do not express *lov-1*, *pkd-2,* or *klp-6* GFP reporters in the male-specific CEMs, HOB and RnBs (Fig. 1D, E, H, I, Table 1). *n4132* also disrupts KLP-6::GFP expression in the core IL2 neurons of males and hermaphrodites at all developmental stages (Table 1). Four *cwp* (co-expressed with polycystin) genes share an identical expression pattern with *lov-1* and *pkd-2* (15). A full length CWP-1::GFP translational fusion is also expressed in IL2 neurons (Table 1). *n4132* completely abolishes CWP-1::GFP expression (Table 1). *n4132* disrupts expression of the neuropeptide *nlp-8* GFP reporter in HOB while leaving expression in non-B-type neurons intact (Table 1). The TRPV channel *osm-9* is expressed in B-type neurons as well as other ciliated neuron types including the amphids and phasmids (43, 44). In *n4132* animals, *osm-9* expression is disrupted only in B-type neurons (Fig. 1L, M, Table 1).

To determine if *n4132* broadly affects gene expression in ciliated sensory neurons, we examined a battery of GFP reporters. *n4132* does not affect ciliogenic gene expression of *osm-5, osm-6, bbs-1, bbs-2, bbs-5*, and *daf-10* in B-type neurons

and other sensory neurons (Fig. 1R, S, Table 1). The odorant receptor *odr-10* and guanylate cyclase (*gcy-5* and *gcy-32*) genes are not affected by the *n4132* mutation (data not shown). We conclude that the *n4132* mutation specifically disrupts expression of sensory signaling genes in B type neurons (*pkd-2*, *lov-1*, *klp-6*, *cwp-1*, *nlp-8* and *osm-9*) without affecting genes required for ciliogenesis or acting in other sensory neurons.

Like *pkd-2*, *lov-1*, and *klp-6* mutants, *n4132* males exhibit Rsp and Lov defects (Fig. 2A). The response efficiency of *n4132* males is not significantly different from the *lov-1*; *pkd-2* double mutant (approximately 35% of mutant males respond to contact with a hermaphrodite compared to 95% of wild-type males, Fig. 2A). However, *n4132* males exhibit significantly more severe Lov defects than *lov-1*; *pkd-2* mutants (Fig. 2A). *n4132* mutant animals are able to sire cross progeny in 24 hour mating efficiency assays; however, their mating efficiency is lower than *lov-1; pkd-2* double mutant males (Fig. 2B). We conclude that *n4132* affects polycystin-dependent and polycystin-independent pathways required for *C. elegans* male mating.

n4132* is a hypomorphic allele of *daf-19

We mapped *n4132* to a small region near the *daf-19* locus on chromosome II (Fig. 3A). Rescue of the PKD-2::GFP expression, Rsp, and Lov defects was obtained by transforming *n4132* animals with cosmid F33H1 or ORF F33H1.1, which contains the RFX transcription factor gene *daf-19* (Fig. 3A). To identify the molecular lesion in *daf-19*, we sequenced *n4132* genomic DNA including 3 kb upstream and 1 kb downstream non-coding regions. The *n4132* allele is a 504 bp deletion within the fifth

intron of the *daf-19* genomic clone (Fig. 3A). In contrast, the *daf-19(m86)* null reference allele introduces a stop codon in exon 7 before all functionally conserved domains, including the DNA binding domain (DBD) and DNA dimerization (DIM) domain (Fig. 3A) (27).

daf-19(m86) null animals resemble *n4132* mutants in that *pkd-2::gfp* expression in B-type neurons and *nlp-8::gfp* expression in HOB are abolished ((17); data not shown). However, *n4132* is distinct from other *daf-19* alleles (*m86*, *sa190*, *sa232*), which do not express ciliogenic genes like *osm-6* and do not form cilia. The *daf-19* alleles *m86*, *sa190* and *sa232* also result in constitutive formation of dauer larvae (Daf-c) (27). By contrast, *n4132* mutants are not Daf-c (data not shown). *n4132* amphid and phasmid cilia are also intact, as judged by lipophilic fluorescent dye uptake (200/200 animals normal in dye-filling assays) and visualization of an OSM-6::GFP reporter in amphid, phasmid, and male-specific sensory cilia (Fig. 1 compare panels P, Q with R, S). *daf-19(m86)* but not *n4132* abolishes the expression of ciliogenic genes that contain X-box promoter elements, including *osm-6*, *osm-5*, and *bbs-2* (Table 1, (27, 28)).

To genetically confirm that *n4132* is an allele of *daf-19*, we performed complementation tests between *n4132* and the *daf-19* Daf-c alleles *sa190, sa232,* and *m86* (Table 2 and data not shown). The *daf-19* alleles *m86, sa190*, and *sa232* failed to complement *n4132* PKD-2::GFP expression defects (Table 2). Conversely, *n4132* complements the Daf-c phenotypes of *m86, sa190*, and *sa232* (Table 2). We conclude that the *n4132* mutation disrupts a particular aspect of *daf-19* function by affecting gene expression specifically in ADPKD sensory neurons, but not acting globally in all ciliated cell types.

n4132 specifically disrupts the *daf-19m* isoform

The predicted *daf-19* gene encodes two isoforms, DAF-19^{A} and DAF-19^{B}, with alternative splicing resulting in an additional exon in *daf-19b* (Fig. 3A). We identified a third cDNA isoform by RT-PCR using mRNA from mixed-stage *him-5* animals (Fig. 3C) (accession no. EU812221). We refer to this new isoform as *daf-19m* for its apparent function in regulating mating behavior and ADPKD gene expression. *daf-19m* starts with a novel exon containing a 166 bp 5' UTR and 11 amino acid (aa) coding region not present in other isoforms, followed by exon 6 and the rest of the DNA sequence shared between all *daf-19* isoforms (Fig. 3C). All three *daf-19* isoforms contain the same DNA binding and DNA dimerization domains. *daf-19m* encodes a predicted 622 aa protein (Fig. 3C). In the *daf-19(n4132)* background, the *daf-19m* but not *daf-19a* or *daf-19b* cDNA is absent (Fig. 3C). We conclude that *daf-19(n4132)* specifically disrupts *daf-19m*, a specific isoform of *daf-19* required for ADPKD gene battery expression and male mating behaviors.

To determine how the *n4132* molecular lesion affects *daf-19m*, we defined a minimal sized fragment capable of phenotypic rescue. PCR2, a PCR amplicon that lacks the predicted promoter and exons 1 to 2 of *daf-19a/b*, fully rescues the *n4132* PKD-2::GFP expression defects in the head (CEMs) and tail (HOB and RnB) as well as Rsp and Lov defects (Fig. 3B). A shorter fragment (PCR3) lacking all coding and non-coding regions of *daf-19a/b* to intron 5, rescues PKD-2::GFP expression in tail but not head neurons. Interestingly, PCR3 rescues *n4132* Lov but not Rsp defects, suggesting that expression of the ADPKD gene battery in both the head CEM and tail

RnB neurons is necessary for response behavior. Introducing the *n4132* molecular lesion into PCR3 to generate PCR4 does not rescue any *n4132* defects, indicating that those deleted elements are required to activate PKD-2::GFP expression. RFX type transcription factors can activate gene expression without a DNA dimerization (DIM) domain (27, 29). A *daf-19*$^{a/b}$ genomic clone lacking its DIM domain rescues ciliogenesis in *daf-19(m86)* null animals (27). Likewise, we find that a *daf-19*^{m} genomic clone without a DIM domain rescues PKD-2::GFP expression in *daf-19(n4132)* animals (data not shown), indicating that DIM domain plays a regulatory but not activating function, and that this phenomenon conserved among *daf-19* isoforms.

daf-19m is expressed in ADPKD neurons via distinct promoter and enhancer elements

Why does the 13 kb *daf-19* PCR2 fragment rescue PKD-2::GFP expression in both head and tail neurons, while the 11 kb *daf-19* PCR3 fragment rescues only in tail neurons? One possibility is that PCR2 and PCR3 both contain a regulatory element that drives *daf-19m* expression in the HOB and RnB tail neurons, but only PCR3 possesses an enhancer for CEM head neuron expression. We therefore examined *daf-19m* expression patterns by fusing various intronic regions of the *daf-19* genomic locus to a GFP reporter (Fig. 4). We fused the putative *daf-19m* promoter, a 1 kb intron 5 fragment, to GFP to construct P*daf-19m*::GFP1 (Fig. 4B). P*daf-19m*::GFP1 is specifically expressed in the male tail HOB and RnB neurons but not male-specific CEM head neurons nor in any other ciliated neurons. This result is consistent with PCR3 rescue of PKD-2::GFP expression in tail but not head neurons.

To identify the CEM enhancer of *daf-19m*, we fused 2 kb of the 5' region of PCR2 to P*daf-19*^{m}::GFP1 and observed GFP expression in the male-specific CEM head neurons and HOB and RnB tail neurons as well as the IL2 head neurons in wild-type and *n4132* animals (data not shown). These results are consistent with a role for *daf-19m* in the regulation of *klp-6* and *cwp-1* expression in the IL2s, and also indicate that *daf-19m* does not regulate its own expression. We conclude that this 2 kb fragment of PCR2 contains the *daf-19m* CEM/IL2 enhancer element.

Bioinformatics is an effective method to study gene regulation. The genomes of three *Caenorhabditis* species (*elegans*, *briggsae*, and *remanei*) contain *daf-19*, *lov-1*, *pkd-2* and *klp-6*. Interspecific comparisons of non-coding regions enable identification of cis-acting regulatory elements that control gene expression and that are evolutionarily constrained. By comparing the 2 kb CEM/IL2 enhancer region of the *daf-19* genomic sequence of *C. elegans, C. briggsae* and *C. remanei*, we identified a 22 bp conserved sequence (Fig. 4A). Adding this 22 bp element to P*daf-19m*::GFP1 (generating P*daf-19m*::GFP3) drives GFP expression in the male-specific CEM, HOB and RnB and core IL2 ciliated neurons (Fig. 4 C, D, G). We conclude that this 22 bp sequence acts as the *daf-19m* CEM/IL2 enhancer element. *daf-19*(*n4132)* animals have a mutation in the HOB/RnB promoter region but retain the CEM/IL2 enhancer; however, *n4132* animals do not express the ADPKD genes in both head and tail neurons. This data indicates that the CEM/IL2 enhancer depends upon the HOB/RnB promoter.

To identify the essential HOB/RnB promoter element, the 504 bp *n4132* molecular lesion was introduced to P*daf-19m*::GFP1, generating P*daf-19*^{m}::GFP2. This lesion abolished HOB and RnB expression (P*daf-19m*::GFP2 in Fig. 4B). To define the

HOB/RnB enhancer, we compared this 504 bp region between *C. elegans, C. briggsae* and *C. remanei* and identified a 13 bp conserved element (Fig. 4A) that is essential for HOB and RnB expression of *daf-19m* (P*daf-19m*::GFP4 in Fig. 4B). The CEM/IL2 enhancer is also dependent on this 13 bp promoter element (P*daf-19m*::GFP5 in Fig. 4E, F, H). In summary, we identified two elements that confer precise spatial regulation to *daf-19*.

Discussion

In this study, we identify the *daf-19m* isoform that directs mating functions of the B-type neurons by spatial patterning of the ADPKD gene battery and show that the sexual behaviors of response and vulva location require this spatial organization. Expression of the *daf-19m* isoform is spatially regulated within B-type neurons by two hierarchal *cis* regulatory elements. One promoter activates *daf-19m* expression in RnB and HOB neurons after ray and hook sensilla development. A distal enhancer causes the tail promoter to drive *daf-19m* expression in IL2 and CEM head neurons. By coordinating the expression of the ADPKD gene battery in the head and tail, *daf-19m* acts to pattern multiple behaviors required for sexual reproduction.

Cilia are highly specialized for functions in signal transduction, development, or motility (30). On the other hand, all cilia and flagella are built by the evolutionarily conserved intraflagellar transport (IFT) machinery, which was first identified in the alga *Chlamydomonas* (31). RFX transcription factors perform an evolutionarily conserved role in ciliogenesis (27, 32-36). Interestingly, the *Chlamydomonas* genome does not encode a DAF-19 RFX transcription factor. By contrast, ciliogenesis in multicellular

animals such as *C. elegans*, *Drosophila*, zebrafish, and mammals depends on RFX transcription factors, hinting at a role in ciliary specialization. This provides the first evidence that a specific RFX isoform, *daf-19m*, governs sensory perception ("sensorigenesis") but not ciliogenesis. *C. elegans* diversifies gene function by second promoters that generate spatial-temporal specific isoforms (37). DAF-19^{M} shares the conserved DBD and DIM domains with known DAF-19 isoforms, suggesting that homo- or hetero-dimer formation may transcriptionally activate different sets of genes according to cell-type specific functional requirements. Promoters of the ADPKD gene battery do not contain X-boxes but do share a short motif (J.W. and M.M.B., in preparation). Hence, it is unlikely that a canonical RFX transcription factor directly activates the ADPKD gene battery. The identity of *daf-19m* direct targets and ADPKD gene battery direct regulators will reveal how ciliated sensory neurons are molecularly programmed to generate the behavioral complexity needed for sexual reproduction in *C. elegans*.

Materials and Methods

Strains, plasmids and PCR products. Growth and culture of *C. elegans* strains were carried out as described (38). All strains were grown at 20°C unless otherwise stated. Strains used for this study are listed in Supplemental Table ST1. *daf-19* genomic DNA fragments were generated by PCR and described in supplemental table ST2. *cwp-1* and *osm-9* reporters were made by PCR-SOE (Splice by overlap extension)(39), as described in Supplemental Table ST2.

Determining gene expression pattern. All expression analysis was carried out using transgenic GFP reporters. *daf-19(n4132)(II); pha-1(e2123ts)(III); him-5(e1490), myIs4 [PKD-2::GFP+ccGFP]* worms were transformed by injection of *daf-19* DNA from PCR or plasmids. *n4132* rescue was scored by visualizing the integrated *myIs4* PKD-2::GFP transgene.

Behavioral assays. Response and Location of vulva efficiency assays were carried out according to (9). Mating efficiency assays were carried out as described by (40).

Mapping of *n4132*. Three-factor mapping placed *n4132* on chromosome II to the right of *unc-4*. Deficiency strains were used to map *n4132* to the 1.99-2.35 region. *mnDf83* and *mnDf29* failed to complement *n4132*, while *mnDf71, mnDf25, mnDf28, mnDf12, mnDf22* and *mnDf27*complemented *n4132.* PCR amplified genomic DNA was used in *n4132* rescue experiments. *n4132* genomic DNA including 2 kb upstream and 1 kb

down stream of *daf-19* gene was sequenced. A deletion flanking "CACAAGCCACAAGCTA……GCCACCGCCGAGCCA" in the fifth intron of *daf-19b* was identified in *n4132*.

***daf-19m* cDNA isolation and functional confirmation.** The cDNA corresponding to *daf-19m* was generated from oligo dT primed first-strand cDNA by using SuperScript III First-Strand Synthesis System for RT-PCR (Invitrogen, Carlsbad, CA), followed by amplification with 5' primer JWatg6 5' cctgtcgacatgagaagagtgtacgaaacg 3' and 3' primer JWc4 5' cttaccggtgacctgcaggatgatgacg a 3'. The resulting cDNA was subcloned into the *Sal*I and *Age*I sites in pPD95.75. The 2.4 kb *unc-119* promoter (41) flanked by *Pst*I sites was inserted into this construct. *daf-19m* cDNA function was confirmed by transforming the resulting construct to *n4132* mutant for rescuing PKD-2::GFP expression (data not shown).

The 5' primer used to amplify *daf-19m* was determined by using primers started at all possible start codon in the shortest rescuing *daf-19* genomic fragments, paired with 3' primer JWc4, to amply genomic DNA of *daf-19* and testing function by expressing with *unc-119* promoter. The six primers were used: JWatg1, 5' aatgtcgacatgcgcaccactgagcgttc 3'; JWatg2 5'ccggtcgacatggcaagtagcaatgaatttatc 3'; JWatg3, 5' ccagtcgacatgaatagtcgctgg gtgct 3'; JWatg4, 5' cccgtcgacatgtacaggttcgttagagga 3'; JWatg5, 5' caagtcgacatggctttttttg gcgttttgc 3' and JWatg6, 5' cctgtcgacatgagaagagtgtacgaaacg 3'

Bioinformatics. Family Relationship II (42) was used to identify conserved DNA

sequences among *Caenorhabditis* species.

Microscopy and Image Analysis. Live worms were mounted on 2% agarose pads with 10 mM levamisol as described previously (12). Fluorescence images were obtained with an Axioplan 2 (Carl Zeiss MicroImaging [Oberkochen, Germany]) microscope equipped with a digital CCD camera (Photometrics Cascade 512B; Roper Scientific), captured with Metamorph software (Universal Imaging [West Chester, PA]), and then deconvolved with AutoDeblur 1.4.1 (Media Cybernetics, Inc.). Photoshop (Adobe) was used for image rotation, cropping, brightness/contrast.

Acknowledgements

We thank Dr. H.R. Horvitz, in whose lab the *n4132* mutant was isolated; Drs. P. Swoboda and G. Senti for sharing unpublished data and stimulating discussions; Drs. P. Anderson, J. Kimble, Q. Mitrovich, and P.W. Sternberg for critical intellectual input in the early stages of this work; Barr and Swoboda lab members for constructive criticism of the manuscript; Drs. A. Hart, M. Leroux, P.W. Sternberg, and the *Caenorhabditis* Genetics Center, which is funded by the NIH National Center for Research Resources (NCRR). for strains. This research was supported by grants from the PKD Foundation (to J.W.) and NIH/NIDDK (to M.M.B.).

References

1. Manoli DS, Meissner GW, Baker BS (2006) Blueprints for behavior: genetic specification of neural circuitry for innate behaviors. *Trends Neurosci* 29: 444-451.
2. Stowers L, *et al.* (2002) Loss of sex discrimination and male-male aggression in mice deficient for TRP2. *Science* 295: 1493-1500.
3. Kimchi T, Xu J, Dulac C (2007) A functional circuit underlying male sexual behaviour in the female mouse brain. *Nature* 448: 1009-1014.
4. Chasnov JR, So WK, Chan CM, Chow KL (2007) The species, sex, and stage specificity of a *Caenorhabditis* sex pheromone. *Proc Natl Acad Sci U S A* 104: 6730-6735.
5. Barr MM, Sternberg PW (1999) A polycystic kidney-disease gene homologue required for male mating behaviour in *C. elegans*. *Nature* 401: 386-389.
6. Barr MM, *et al.* (2001) The *Caenorhabditis elegans* autosomal dominant polycystic kidney disease gene homologs *lov-1* and *pkd-2* act in the same pathway. *Curr Biol* 11: 1341-1346.
7. Simon JM, Sternberg PW (2002) Evidence of a mate-finding cue in the hermaphrodite nematode Caenorhabditis elegans. *Proc Natl Acad Sci U S A* 99: 1598-1603.
8. White JQ, *et al.* (2007) The sensory circuitry for sexual attraction in *C. elegans* males. *Curr Biol* 17: 1847-1857.
9. Liu KS, Sternberg PW (1995) Sensory regulation of male mating behavior in *Caenorhabditis elegans. Neuron* 14: 79-89.

10. Sulston JE, Albertson DG, Thomson JN (1980) The *Caenorhabditis elegans* male: postembryonic development of nongonadal structures. *Dev Biol* 78: 542-576.

11. Perkins LA, Hedgecock EM, Thomson JN, Culotti JG (1986) Mutant sensory cilia in the nematode *Caenorhabditis elegans*. *Dev Biol* 117: 456-487.

12. Bae YK, *et al.* (2006) General and cell-type specific mechanisms target TRPP2/PKD-2 to cilia. *Development* 133: 3859-3870.

13. Ward S, Thomson N, White JG, Brenner S (1975) Electron microscopical reconstruction of the anterior sensory anatomy of the nematode *Caenorhabditis elegans*. *J Comp Neurol* 160: 313-337.

14. Jauregui AR, Nguyen KC, Hall DH, Barr MM (2008) The *Caenorhabditis elegans* nephrocystins act as global modifiers of cilium structure. *J Cell Biol* 180: 973-988.

15. Portman DS, Emmons SW (2004) Identification of *C. elegans* sensory ray genes using whole-genome expression profiling. *Dev Biol* 270: 499-512.

16. Peden EM, Barr MM (2005) The KLP-6 Kinesin Is Required for Male Mating Behaviors and Polycystin Localization in *Caenorhabditis elegans*. *Current Biology* 15: 394-404.

17. Yu H, Pretot RF, Burglin TR, Sternberg PW (2003) Distinct roles of transcription factors EGL-46 and DAF-19 in specifying the functionality of a polycystin-expressing sensory neuron necessary for *C. elegans* male vulva location behavior. *Development* 130(21):5217-27.

18. Shaham S, Bargmann CI (2002) Control of neuronal subtype identity by the *C. elegans* ARID protein CFI- 1. *Genes Dev* 16: 972-983.

19. Peden E, *et al.* (2007) Control of sex-specific apoptosis in *C. elegans* by the BarH homeodomain protein CEH-30 and the transcriptional repressor UNC-37/Groucho. *Genes Dev* 21: 3195-3207.

20. Schwartz HT, Horvitz HR (2007) The *C. elegans* protein CEH-30 protects male-specific neurons from apoptosis independently of the Bcl-2 homolog CED-9. *Genes Dev* 21: 3181-3194.

21. Lints R, Emmons SW (1999) Patterning of dopaminergic neurotransmitter identity among *Caenorhabditis elegans* ray sensory neurons by a TGFbeta family signaling pathway and a Hox gene. *Development* 126: 5819-5831.

22. Lints R, *et al.* (2004) Axial patterning of *C. elegans* male sensilla identities by selector genes. *Dev Biol* 269: 137-151.

23. Nathoo AN, Moeller RA, Westlund BA, Hart AC (2001) Identification of neuropeptide-like protein gene families in *Caenorhabditis elegans* and other species. *Proc Natl Acad Sci U S A* 98: 14000-14005.

24. Collet J, *et al.* (1998) Analysis of *osm-6,* a gene that affects sensory cilium structure and sensory neuron function in *Caenorhabditis elegans. Genetics* 148: 187-200.

25. Efimenko E, *et al.* (2005) Analysis of *xbx* genes in *C. elegans*. *Development* 132: 1923-1934.

26. Chen N, *et al.* (2006) Identification of ciliary and ciliopathy genes in *Caenorhabditis elegans* through comparative genomics. *Genome Biol* 7: R126.

27. Swoboda P, Adler HT, Thomas JH (2000) The RFX-type transcription factor DAF-19 regulates sensory neuron cilium formation in *C. elegans*. *Mol Cell* 5: 411-421.

28. Ansley SJ, *et al.* (2003) Basal body dysfunction is a likely cause of pleiotropic Bardet-Biedl syndrome. *Nature* 425: 628-633.

29. Reith W, *et al.* (1990) MHC class II regulatory factor RFX has a novel DNA-binding domain and a functionally independent dimerization domain. *Genes Dev* 4: 1528-1540.

30. Marshall WF, Nonaka S (2006) Cilia: tuning in to the cell's antenna. *Curr Biol* 16: R604-614.

31. Kozminski KG, Johnson KA, Forscher P, Rosenbaum JL (1993) A motility in the eukaryotic flagellum unrelated to flagellar beating. *Proc Natl Acad Sci U S A* 90: 5519-5523.

32. Dubruille R, *et al.* (2002) Drosophila regulatory factor X is necessary for ciliated sensory neuron differentiation. *Development* 129: 5487-5498.

33. Laurencon A, *et al.* (2007) Identification of novel regulatory factor X (RFX) target genes by comparative genomics in *Drosophila* species. *Genome Biol* 8: R195.

34. Liu Y, Pathak N, Kramer-Zucker A, Drummond IA. (2007) Notch signaling controls the differentiation of transporting epithelia and multiciliated cells in the zebrafish pronephros. *Development* 134:1111-22.

35. Bonnafe E, *et al.* (2004) The transcription factor RFX3 directs nodal cilium development and left-right asymmetry specification. *Mol Cell Biol* 24: 4417-4427.

36. Ait-Lounis A, *et al.* (2007) Novel function of the ciliogenic transcription factor RFX3 in development of the endocrine pancreas. *Diabetes* 56: 950-959.

37. Choi J, Newman AP (2006) A two-promoter system of gene expression in *C. elegans. Dev Biol* 296: 537-544.

38. Brenner S (1974) The genetics of *Caenorhabditis elegans. Genetics* 77: 71-94.

39. Hobert O (2002) PCR fusion-based approach to create reporter gene constructs for expression analysis in transgenic *C. elegans. Biotechniques* 32: 728-730.

40. Hodgkin J (1983) Male phenotypes and mating efficiency in *Caenorhabditis elegans. Genetics* 103: 43-64.

41. Maduro M, Pilgrim D (1995) Identification and cloning of *unc-119*, a gene expressed in the *Caenorhabditis elegans* nervous system. *Genetics* 141: 977-988.

42. Brown CT, Xie Y, Davidson EH, Cameron RA (2005) Paircomp, FamilyRelationsII and Cartwheel: tools for interspecific sequence comparison. *BMC Bioinformatics* 6: 70.

43. Colbert HA, Smith TL, Bargmann CI. (1997) OSM-9, a novel protein with structural similarity to channels, is required for olfaction, mechanosensation, and olfactory adaptation in *Caenorhabditis elegans. J Neurosci* 17:8259-69.

44. Knobel KM, Peden EM, Barr MM. (2008) Distinct protein domains regulate ciliary targeting and function of *C. elegans* PKD-2. *Exp Cell Res* 314: 825-33.

Table 1. Comparison of reporter expression patterns in B-type neurons of wild-type and *daf-19(n4132)* animals.

Reporter	Expression pattern		Genotype (% worm with reporter expression)	
	Hermaphrodite	Male	WT	*daf-19(n4132)*
LOV-1::GFP		CEM	100	0
		HOB	100	0
		RnB	100	0
PKD-2::GFP		CEM	100	0
		HOB	100	0
		RnB	100	0
KLP-6::GFP	IL2		100	24
		IL2	100	0
		CEM	100	0
		HOB	100	0
		RnB	100	2
CWP-1::GFP	IL2		100	0
		IL2	100	0
		CEM	100	0
		HOB	100	0
		RnB	100	0
P*nlp-8*::GFP		HOB	100	0
P*osm-9*::GFP	IL2		100	0
	Amphid&phasmid		100	99
		IL2	96	0
		CEM	98	0
		HOB	98	47
		RnB	96	40
		Amphid & phasmid	96	98
P*osm-5*::GFP	All ciliated sensory neurons		100	100
OSM-6::GFP	All ciliated sensory neurons		100	100

n4132 disrupts expression of genes required for ciliated B-type neuron sensory function but not cilia development. In male-specific B-type neurons, *n4132* disrupts expression of the ADPKD gene battery, which includes *lov-1, pkd-2*, *klp-6*, and *cwp-1*. In *n4132* males, *osm-9* expression is abolished in CEMs and reduced in HOB and RnB tail

neurons. In the IL2 core B-type neurons, *n4132* also affects *klp-6*, *cwp-1*, and *osm-9* expression. *n4132* abolishes *nlp-8* expression in HOB but not in other core neurons. *n4132* does not affect the expression of *osm-9* in amphids or phasmids, the sensory genes *odr-10*, *gcy-5*, and *gcy-32*, or the expression of ciliogenesis genes *osm-6*, *osm-5.* *n4132* animals are also not defective in expression of the ciliary structural genes *daf-10*, *bbs-1*, or *bbs-2* (not shown). Numbers refer to the percentage of neurons expressing the reporter. For each genotype, at least 20 animals (or 80 CEM, 120 IL2, 20 HOB, and 320 RnB neurons) were scored.

Table 2. Complementation tests between *n4132* and other *daf-19* alleles.

genotype	PKD-2::GFP expression	Daf-C
n4132/n4132	-	non Daf-C
m86/m86	-	Daf-C
n4132/m86	-	non Daf-C
n4132/sa190	-	non Daf-C
n4132/sa232	-	non Daf-C

daf-19(n4132) does not express PKD-2::GFP and does not form dauers constitutively (non Daf-C), while *daf-19* alleles *m86, sa190, sa232* alleles do not express PKD-2::GFP and are Daf-C. *n4132* complements the Daf-C but not PKD-2::GFP expression defect, indicating that the *n4132* mutation is hypomorphic allele of *daf-19*.

Supplemental Table 1. List of transgenic and mutant strains used in this study.

Strain	Description	Ref
MT13057	*nIs133 I; daf-19(n4132) II; him-5(e1467ts) V*	This study
PT1727	*daf-19(n4132) II; him-5(e1490) V*	This study
PT1725	*daf-19(n4132) II; pha-1(e2123ts) III; him-5(e1490) V*	This study
PT1726	*daf-19(n4132) II; pha-1(e2123ts) III; myIs4[PKD-2::GFP + ccGFP] him-5(e1490) V*	This study
PT1770	*daf-19(n4132) II; pha-1(e2123ts) III; him-5(e1490) V; syEx301[lov-1::GFP1 + pBX1]*	This study
PT1771	*daf-19(n4132) II; pha-1(e2123) III; him-5(e1490) V; myEx256[Posm-5::gfp + pBX1]*	This study
PT1772	*daf-19(n4132) II; pha-1(e2123) III; him-5(e1490) V; myEx4[DAF-10::GFP + pBX1]*	This study
PT1773	*daf-19(n4132) II; him-5(e1490) V; nxEx1[Pbbs-1::GFP + dpy-5(+)]*	This study
PT1774	*daf-19(n4132) II; him-5(e1490) V; nxEx2[Pbbs-2::GFP + dpy-5(+)]*	This study
PT1734	*daf-19(n4132) II; him-5(e1490), mnIs17[OSM-6::gfp + unc-36(+)] V*	This study
PT1731	*daf-19(m86) II; him-5(e1490) V*	This study
PT1777	*daf-19 (n4132) II;him-5(e1490) V; rtEx277 [Pnlp-8::GFP + lin-15(+)]*	This study
PT1778	*daf-19 (n4132) II; chIs1200[ceh-26::GFP + dpy-20(+)]* III; *him-5(e1490)V; Is[ceh-26::GFP]*	This study
PT1750	*daf-19(n4132) II; pha-1(e2123ts) III; myIs4 him-5(e1490) V; myEx633[PCR1 + pBX1]*	This study
PT1779	*daf-19(n4132) II; pha-1(e2123ts) III; myIs4 him-5(e1490) V; myEx634[PCR2 + pBX1]*	This study
PT1780	*daf-19(n4132) II; pha-1(e2123ts)III; him-5(e1490), myIs4V; myEx635[PCR3 + pBX1]*	This study
PT1781	*daf-19(n4132) II; pha-1(e2123ts) III; myIs4 him-5(e1490) V; myEx636[PCR4 + pBX1]*	This study
PT1783	*pha-1(e2123) III; him-5(e1490) V; myEx637[Pdaf-19m::GFP1 + pBX1]*	This study
PT1784	*pha-1(e2123) III; him-5(e1490) V; myEx638[Pdaf-19m::GFP2 + pBX1]*	This study
PT1785	*pha-1(e2123) III; him-5(e1490) V; myEx639[Pdaf-19m::GFP3 + pBX1]*	This study
PT1786	*pha-1(e2123) III; him-5(e1490) V; myEx640[Pdaf-19m::GFP4 + pBX1]*	This study
PT1787	*pha-1(e2123) III; him-5(e1490) V; myEx641[Pdaf-19m::GFP5 + pBX1]*	This study
PT1764	*him-5(e1490) V; myEx642[Posm-9::GFP + ccGFP]*	This study
PT1766	*daf-19(n4132) II; him-5(e1490) V; myEx642[Posm-9::GFP + ccGFP]*	This study
PT1768	*daf-19(m86)II; him-5(e1490) V; myEx642[Posm-9::GFP + ccGFP]*	This study
PT1788	*daf-19(n4132)II; him-5(e1490) V; lin-15(n765) X; adEx1262[gcy-5::GFP + lin-15(+)]*	This study
PT1789	*daf-19(n4132) II; him-5(e1490) V; lin-15(n765) X; adEx1295[gcy-32::GFP + lin-15(+)]*	This study

General strains

PT658	*lov-1(sy582) II; pkd-2(sy606) IV; him-5(e1490) V*	Barr 1999
PS622	*dpy-17(e164) III; him-5(e1490) V*	Brenner 1974
PS3149	*pha-1(e2123ts) III; him-5(e1490) V; syEx301[lov-1::GFP1 + pBX1]*	Barr 1999
CB444	*unc-52(e444) II*	Brenner 1974
PT2	*pha-1(e2123ts) III; him-5(e1490) V; myEx256(Posm-5::gfp)*	Qin 2001
PT26	*pha-1(e2123ts) III; him-5(e1490) V; myEx4[pBX1 + DAF-10::GFP]*	Qin 2001
MX1	*dpy-5(e907) I; nxEx1 [Pbbs-1::GFP + dpy-5(+)]*	Michel Leroux
MX2	*dpy-5(e907) I; nxEx2[Pbbs-2::GFP + dpy-5(+)]*	Michel Leroux
DR103	*dpy-10(e128) unc-4(e120) II*	Varkey 1993
CB4077	*eDf21 / mnC1 [dpy-10(e128) unc-52(e444)] II*	Shen 1988
SP354	*unc-4(e120) mnDf71 / mnC1 [dpy-10(e128) unc-52(e444)] II*	Sigurdson 1984
Sp429	*mnDf25 / mnC1 [dpy-10(e128) unc-52(e444)] II*	Sigurdson 1984
SP540	*mnDf27 / mnC1 [dpy-10(e128) unc-52(e444)] II*	Sigurdson 1984
SP542	*mnDf29 / mnC1 [dpy-10(e128) unc-52(e444)] II*	Sigurdson 1984
MB5	*him-5(e1490) V; lin-15(n765ts) X; rtEx277[Pnlp-8::GFP + lin-15(+)]*	Yu 2003
JT190	*daf-19(sa190ts) II*	Swoboda 2000
JT6824	*daf-19(sa232ts) II*	Swoboda 2000
DR431	*daf-19(m86) / mnC1 [dpy-10(e128) unc-52(e444)] II*	Swoboda 2000
PS3380	*him-5(e1490), mnIs17[OSM-6::gfp+unc-36(+)] V*	Collet 1998
TB1225	*chIs1200[ceh-26::GFP + dpy-20(+)]III; him-5(e1490)V*	Yu 2003
DA1262	*lin-15(n765) X; adEx1262[gcy-5::GFP + lin-15(+)]*	Yu 1997
DA1295	*lin-15(n765) X; adEx1295[gcy-32::GFP + lin-15(+)]*	Yu 1997

Supplemental Table 2. Primers, templates, vectors used for PCR fragments and plasmids in this study.

	5' primer	3' primer	template
CWP-1::GFP	5'-catgacgacaaagcggatca-3'	5'-ttctcctttactgaatttctta gaggcgagaaggc-3'	*him-5* genomic DNA
	5'-ctctaagaaattcagtaaag gagaagaacttttcac-3'	5'-caaacccaaaccttcttccg-3'	pPD95.75
P*osm-9*::GFP	5'-aaagtcgaggcttgctccc-3'	5'-gagtcgacctgcaggcatagag ccaagatatgggcgg-3'	B0229
	5'-ccgcccatatcttggctcta tgcctgcaggtcgactct-3'	5'-gccatcgccaattggagtat-3'	pPD95.75
PCR1	5'-gattccgacgttggctttcg-3'	5'-caagatggaacgggagac-3'	F33H1 cosmid
PCR2	5'-gcgtttcgtagaacaactac-3'	5'-caagatggaacgggagac-3'	F33H1 cosmid
PCR3	5'-cacctgacaccgttttgagc-3'	5'-caagatggaacgggagac-3'	F33H1 cosmid
PCR4	5'-cacctgacaccgttttgagc-3'	5'-caagatggaacgggagac-3'	*n4132* genomic DNA
P*daf-19m*::GFP1	5'-gaatgcatgcggttcacaa ctaacctggatag-3'	5'-gaagtcgacaagccac ctgctctcgggtt-3'	F33H1 cloned to pPD95.75
P*daf-19m*::GFP2	5'-gaatgcatgcggttcacaa ctaacctggatag-3'	5'-gaagtcgacaagccac ctgctctcgggtt-3'	*n4132* DNA cloned to pPD95.75
P*daf-19m*::GFP3	5'-cagaattcttaatttttttataat tgcagccatcacaagccaca-3'	5'-caaacccaaaccttcttccg-3'	P*daf-19m*::GFP1
P*daf-19m*::GFP4	5'-gaatgcatgcggttcacaact aacctggatag-3'	5'-cggtgatgagtcccgagcgcgc ccatagtttcaacaag-3'	P*daf-19m*::GFP1
	5'-cttgttgaaactatgggcgcgct cgggactcatcaccg-3'	5'-caaacccaaaccttcttccg-3'	P*daf-19m*::GFP1
P*daf-19m*::GFP5	5'-cagaattcttaatttttttataattg cagccatcacaagccaca-3'	5'-caaacccaaaccttcttccg-3'	P*daf-19m*::GFP4

To make the PCR-SOE reporter, primer 1 and 2 were paired with template 1, primer 3 and 4 were paired with template 2; in the second round, primer 1 and 4 were paired with template made by mixing same molar concentration of products of the two first round PCR.

Supplemental references:

1. Barr MM, Sternberg PW (1999) A polycystic kidney-disease gene homologue required for male mating behaviour in *C. elegans*. *Nature* 401: 386-389.

2. Brenner S (1974) The genetics of *Caenorhabditis elegans*. *Genetics* 77, 71-94.

3. Qin H, Rosenbaum JL, Barr MM (2001) An autosomal recessive polycystic kidney disease gene homolog is involved in intraflagellar transport in *C. elegans* ciliated sensory neurons. *Curr Biol.* 11: 457-61.

4. Yu S, Avery L, Baude E, Garbers DL (1997) Guanylyl cyclase expression in specific sensory neurons: a new family of chemosensory receptors. *Proc Natl Acad Sci U S A.* 94: 3384-7.

5. Varkey JP, Jansma PL, Minniti AN, Ward S (1993) The *Caenorhabditis elegans spe-6* gene is required for major sperm protein assembly and shows 2nd site noncomplementation with an unlinked deficiency. *Genetics* 133: 79-86.

6. Shen MM, Hodgkin J (1988) *mab-3*, a gene required for sex-specific yolk protein expression and a male-specific lineage in *C. elegans. Cell* 54: 1019-31.

7. Sigurdson DC, Spanier GJ and Herman RK (1984) *C. elegans* deficiency mapping. *Genetics* 108: 331-345.

8. Yu H, Pretot RF, Burglin TR, Sternberg PW (2003) Distinct roles of transcription factors EGL-46 and DAF-19 in specifying the functionality of a polycystin-expressing sensory neuron necessary for *C. elegans* male vulva location behavior. *Development.* 130: 5217-27.

9. Swoboda P, Adler HT, Thomas JH (2000) The RFX-type transcription factor DAF-19 regulates sensory neuron cilium formation in *C. elegans*. *Mol Cell* 5: 411-421.

10. Collet J, Spike CA, Lundquist EA, Shaw JE, Herman RK (1998) Analysis of *osm-6*, a gene that affects sensory cilium structure and sensory neuron function in *Caenorhabditis elegans. Genetics.* 148: 187–200.

Figure Legends

Figure 1. *daf-19(n4132)* disrupts B-type neuronal expression of *lov-1, pkd-2* and *osm-9* but not *osm-6*. (A) Cartoon shows the cell body positions of the B-type male-specific (CEM, HOB, and RnB), core B-type (IL2), and core amphid neurons in an adult male. (B-C, F-G) In wild type, LOV-1::GFP and PKD-2::GFP are expressed in four CEM, one HOB and 16 RnB (n=1-9 but not 6) neurons. (D-E, H-I) In *n4132* males, LOV-1::GFP and PKD-2::GFP expression is completely abolished. In the male tail, autofluorescence is observed in the sclerotized hook and spicule structures. (G-K) *osm-9* is expressed more broadly in sensory neurons, including B-type neurons, amphids, and phasmids (43, 44). (L-M) In *daf-19(n4132)* males, *osm-9* is not expressed in IL2 and CEM neurons and expressed in approximately 50% of HOB and RnB neurons (see also Table 1). (L-M) *daf-19(n4132)* does not affect *osm-9* expression in amphids or phasmids. (N-O) In *daf-19(m86)* null males, *osm-9* expression is completely abolished. (P-Q, R-S) In wild-type and *n4132* males, the *osm-6* ciliogenic gene is expressed in all ciliated neurons, including the A- and B-type, amphid, and phasmid neurons. Ciliary transition zones and ciliary axonemes are visible in wild-type and *daf-19(n4132)* males (arrows). In *daf-19(m86)* males, *lov-1, pkd-2* and *osm-6* expression is completely abolished in all sensory neurons (17, 27).

Figure 2. *daf-19(n4132)* males are response, Lov (location of vulva), and mating efficiency defective. (A) Response and location of vulva efficiency was scored for each genotype. *n4132* males exhibit behavioral efficiency defects compared to wild type ($p<0.001$ for both Response efficiency and Location of vulva efficiency assay).

n4132 and *lov-1;pkd-2* have comparable response efficiencies. *n4132* males have a more severe Lov defect than *lov-1; pkd-2* double mutants. (B) *n4132* males are able to sire progeny, but mating efficiency is significantly lower than *lov-1*; *pkd-2* double mutant ($p<0.001$). Error bars indicate s.e.m. An asterisk marks wherever the data are significantly different between *n4132* and *lov-1; pkd-2* (*P <0.01). ns = not significantly different. Statistical analyses were performed by nonparametric Mann-Whitney tests with two-tailed *P*-value.

Figure 3. *n4132* is a hypomorphic allele of *daf-19* that specifically disrupts *daf-19m*, an isoform of the RFX transcription factor required for male mating behaviors. (A) Genetic map and genomic structure of the locus mutated in *n4132*. *n4132* maps to chromosome II and is a molecular deletion in the *daf-19* gene (F33H1.1). The published and predicted *daf-19* genomic structure includes two isoform that differ in the inclusion of a 4th exon in *daf-19b* (shown here). The *daf-19(m86)* null allele introduces a stop codon immediately upstream of the DBD (DNA binding domain) and DIM (dimerization) domain. The *daf-19(n4132)* hypomorphic allele is a deletion in the 5th intron of the *daf-19b* predicted structure. Light blue boxes are exons, light gray regions are UTRs (untranslated regions). (B) Transgenic rescue data of PKD-2::GFP expression and male mating behavior (RE = response efficiency; LE = location efficiency). *daf-19* genomic fragments, with exons numbered according to *daf-19b*, were scored for the ability to rescue *n4132* PKD-2::GFP expression defects in male-specific B-type neurons and behavioral defects (restoration of RE and ME). Both PCR1 and PCR2 fully rescue PKD-2::GFP expression. PCR2 is lacking the promoter and two exons of *daf-19a/b*. PCR2 also rescues *n4132* Response and Lov defects

(normal RE and LE). The shorter PCR3 fragment rescues PKD-2::GFP expression in tail (HOB and RnB) but not head (CEM) neurons (normal LE, abnormal RE). PCR3 rescues *n4132* Lov but not response defects (not shown). PCR4, made by introducing the *n4132* molecular lesion to PCR3, fails to rescue *n4132* (abnormal RE and LE). (C) Diagram of *daf-19m* genomic and cDNA structure compared to the *daf-19b* isoform. *daf-19m* uses an alternative promoter (in the 5th predicted intron) and a distal upstream enhancer (in the 2nd predicted intron) but shares the DBD and DIM domain with *daf-19a/b*. RT-PCR shows *daf-19m* cDNA in wild type but not *n4132*. In contrast, *daf-19a/b* cDNA is present in both wild type and *n4132*.

Figure 4. *daf-19m* is exclusively expressed in B-type neurons. (A) Discrete cis-regulatory elements regulate *daf-19m* expression in B-type head (CEM/IL2) and tail (HOB/RnB) neurons. The CEM/IL2 distal enhancer and HOB/RnB promoter elements are conserved among *Caenorhabditis* species *C. briggsae, C. elegans* and *C. remanei.* (B) Diagram of *daf-19m* promoter::GFP reporters and their relationship to *daf-19b* and the *n4132* deletion. P*daf-19*::GFP1, which contains 1 kb of intron 5 of *daf-19b*, expresses in B-type tail neurons only. Adding a 22bp upstream enhancer to generate P*daf-19*::GFP3 drives *daf-19m* expression in B-type neurons in both the head and tail (Fig. 4C, D, G). *Pdaf-19m*::GFP1 expression is completely abolished by introducing the *n4132* molecular lesion (P*daf-19m*::GFP2) or by deleting the 13bp HOB/RnB promoter element (P*daf-19m*::GFP4); P*daf-19*::GFP3 expression is also abolished by deletion of the 13bp HOB/RnB element (P*daf-19*::GFP5, Fig. 4E, F, H). (C, D) In males, *daf-19m* is expressed in core IL2 neurons and B-type male-specific CEM neurons in the head (C)

and HOB and RnB neurons in the tail (D). (E, F) *daf-19m* expression is completely abolished by deleting the 13 bp HOB/RnB promoter element. (G, H) In hermaphrodites, *daf-19m* is expressed in core IL2 neurons and abolished by deleting the HOB/RnB promoter element.

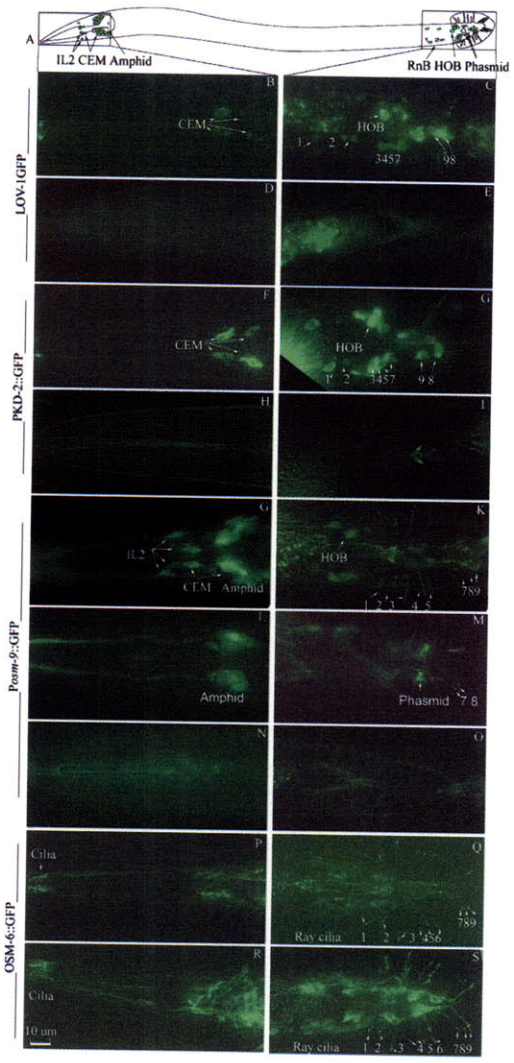
A
IL2 CEM Amphid
RnB HOB Phasmid
LOV-1GFP
PKD-2::GFP
Posm-9::GFP
OSM-6::GFP
B
CEM
C
HOB
1 2 3457 98
D
E
F
CEM
G
HOB
1 2 3457 98
H
I
J
IL2
CEM Amphid
K
HOB
1 2 3 4 5 789
L
Amphid
M
Phasmid 7 8
N
O
P
Cilia
Q
Ray cilia 1 2 3 456 789
R
Cilia
10 um
S
Ray cilia 1 2 3 4 5 6 789

Figure 1

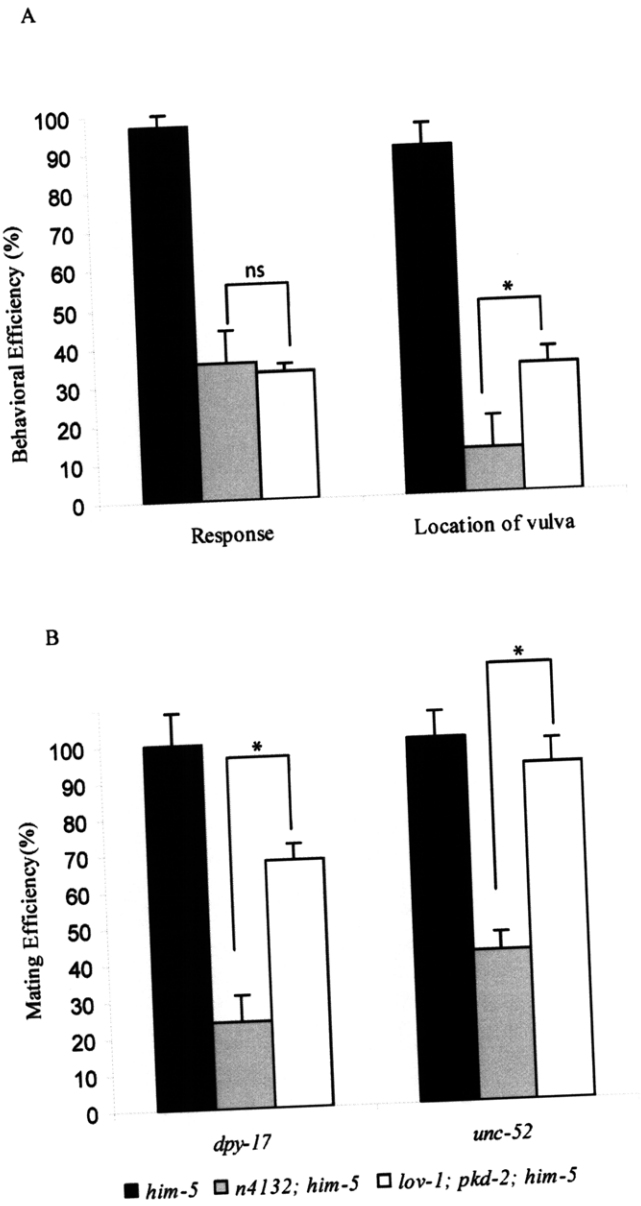
A
Behavioral Efficiency (%)
100
90
80
70
60
50
40
30
20
10
0
ns
*
Response
Location of vulva
B
Mating Efficiency(%)
100
90
80
70
60
50
40
30
20
10
0
*
*
dpy-17
unc-52
him-5
n4132; him-5
lov-1; pkd-2; him-5

Figure 2

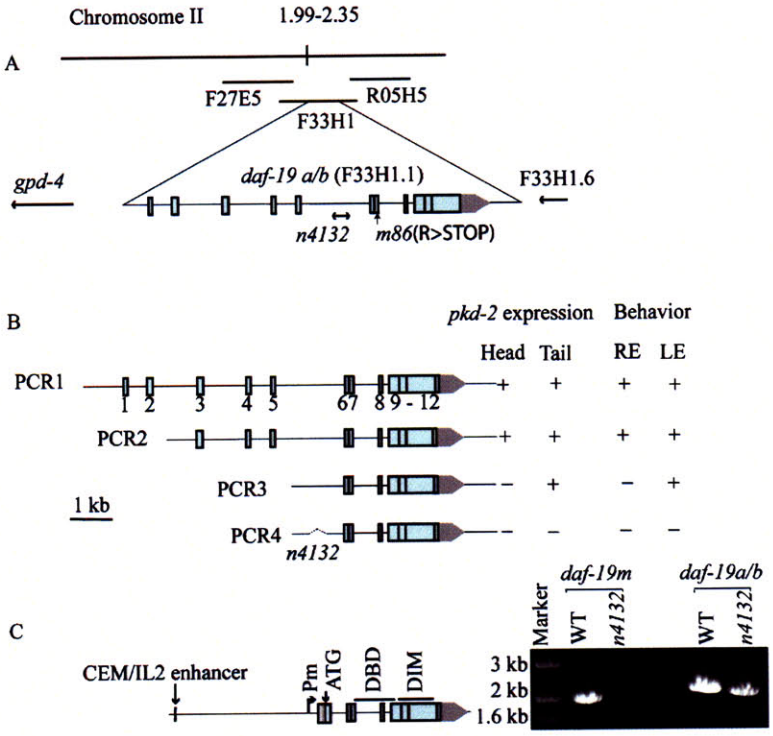
Chromosome II
1.99-2.35
A
F27E5
R05H5
F33H1
gpd-4
daf-19 a/b (F33H1.1)
F33H1.6
n4132
m86(R>STOP)
B
pkd-2 expression
Behavior
Head
Tail
RE
LE
PCR1
1 2 3 4 5 6 7 8 9 - 12
PCR2
PCR3
PCR4
n4132
1 kb
C
CEM/IL2 enhancer
Pm
ATG
DBD
DIM
daf-19m
daf-19a/b
Marker
WT
n4132
WT
n4132
3 kb
2 kb
1.6 kb

Figure 3

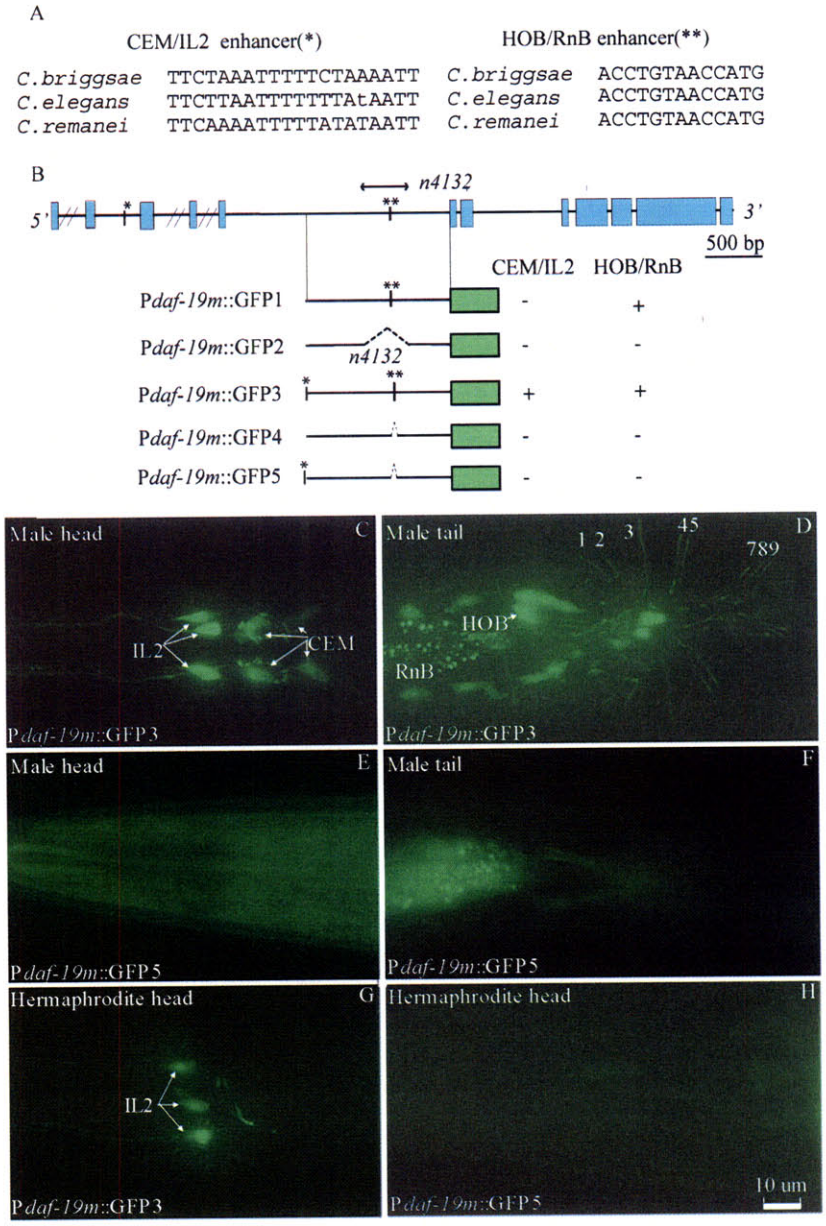
A
CEM/IL2 enhancer(*)
HOB/RnB enhancer(**)
C.briggsae TTCTAAATTTTTCTAAAATT
C.elegans TTCTTAATTTTTTTAtAATT
C.remanei TTCAAAATTTTTATATAATT
C.briggsae ACCTGTAACCATG
C.elegans ACCTGTAACCATG
C.remanei ACCTGTAACCATG
B
n4132
5'
3'
500 bp
CEM/IL2 HOB/RnB
Pdaf-19m::GFP1 - +
Pdaf-19m::GFP2 - -
n4132
Pdaf-19m::GFP3 + +
Pdaf-19m::GFP4 - -
Pdaf-19m::GFP5 - -
Male head C
IL2
CEM
Pdaf-19m::GFP3
Male tail D
1 2 3 45 789
HOB
RnB
Pdaf-19m::GFP3
Male head E
Pdaf-19m::GFP5
Male tail F
Pdaf-19m::GFP5
Hermaphrodite head G
IL2
Pdaf-19m::GFP3
Hermaphrodite head H
Pdaf-19m::GFP5
10 um

Figure 4